DECLARATION

This work has not previously been accepted in substance for any degree and is not concurrently submitted in candidature for any degree.

Signed ..K.S.Brar..... (candidate) Date ...22/2/11.....

STATEMENT 1

This thesis is being submitted in partial fulfillment of the requirements for the degree of PhD

Signed ...K.S.Brar..... (candidate) Date .....22/2/11.....

STATEMENT 2

This thesis is the result of my own independent work/investigation, except where otherwise stated.
Other sources are acknowledged by explicit references.

Signed ....K.S.Brar..... (candidate) Date ....22/2/11.....

STATEMENT 3

I hereby give consent for my thesis, if accepted, to be available for photocopying and for inter-library loan, and for the title and summary to be made available to outside organisations.

Signed ..K.S.Brar..... (candidate) Date ....22/2/11.....

GLUTAMATE REGULATION FOR BONE REPAIR

KAREN BRAKSPEAR

Cardiff University

PhD

ProQuest LLC
789 East Eisenhower Parkway
P.O. Box 1346
Ann Arbor, MI 48106-1346

ACKNOWLEDGEMENTS

I would like to begin by extending my heartfelt thanks to my supervisor Dr Debbie Mason for her guidance, friendship and unwavering belief in my abilities. That I have enjoyed a large proportion of my PhD is a great testament to her encouragement and inspiration.

I have also been lucky enough to spend 3 years in a lab with a group of people that have been invaluable in providing me with help and advice when I needed it, as well as tea and cake whether I needed it or not. So I would like to thank lab members past and present; Dr Emma Blain, Dr Sophie Gilbert, Dr Siyuan Li, Dr Rebecca Shuttleworth, Dr Cleo Bonnet, Marisol Vazquez, Dr Helen Roberts, Daisy Moore and Dr Yadan Zhang. I would also like to thank Professor Vic Duance for his support, his sense of humour and for providing the setting of our indispensable morning coffee rituals.

Thanks must also go to everyone at the Smith & Nephew Research Centre who made me feel so welcome during my 3 months spent working there, particularly my industrial supervisor Dr Philippa Parsons, who has helped me to see the bigger picture of my research, and also Dr Alan Horner and Dr Steve Fenwick for their help and advice.

Thanks must go to Dr Bronwen Evans for provision of the MG-63, SaOS-2 and primary osteoblast cell lines and Carole Elford for her cell culture expertise.

Last, but by no means least, I must thank my parents and Andy for their love and support.

This work was funded by the BBSRC and Smith & Nephew.

ABSTRACT

Mechanical loading plays a key role in the physiology of bone, allowing bone to functionally adapt to its environment. A screen for genes associated with mechanical load-induced bone formation identified the glutamate transporter GLAST, implicating the excitatory amino acid glutamate in the mechanoresponse. Bone cells express functional components from each stage of the glutamate signalling pathway.

Five high affinity Na^+-dependent excitatory amino acid transporters (EAATs) terminate glutamatergic signalling. EAAT1 (GLAST) is expressed by osteocytes and bone-forming osteoblasts *in vivo*, and may influence osteogenesis by regulating glutamate uptake, glutamate release, glutamate-gated ion channel activity or through activation of intracellular signalling pathways. The aim was to assess EAAT expression and function in osteoblasts and determine whether modulation of EAAT activities in osteoblasts influences differentiation and bone forming activity through measurement of cell number, gene expression, alkaline phosphatase (ALP) activity and mineralisation.

QRT-PCR revealed mRNA expression of EAATs 1-3 and both splice variants of EAAT1 (EAAT1a and EAAT1ex9skip) in human osteoblast-like cell lines (MG-63 and SaOS-2) and human primary osteoblasts. ^{14}C-glutamate uptake assays revealed Na^+-dependent glutamate transport in osteoblasts, consistent with functional EAAT activity. Over-expression of EAAT1a and EAAT1ex9skip in MG-63 and SaOS-2 by antisense mediated exon skipping reduced Na^+-dependent glutamate uptake, indicating decreased transport function of these variants.

EAAT activity was modulated in osteoblasts at 0μM or 500μM extracellular glutamate concentrations by inhibitors of EAATs 1-5 (*t*-PDC and TBOA), over-expression of EAAT1 splice variants and through transient transfection of expression vectors encoding competing peptides to EAAT1 intracellular domains. In the absence of glutamate, EAAT inhibitors increased osteoblast-like cell number and inhibited SaOS-2 ALP activity and mineralisation. In contrast, TBOA increased ALP activity in primary human osteoblasts cultured for 5 days in the presence of exogenous glutamate. EAAT inhibitors also significantly affected mRNA expression of osteocalcin, osteonectin, osteoprotegerin and ALP. Overexpression of EAAT1ex9skip increased SaOS-2 ALP activity at 0μM glutamate while overexpression of EAAT1a decreased SaOS-2 osteocalcin mRNA levels at both glutamate concentrations. Overexpression of EAAT1 splice variants also affected cell number of each cell line analysed and competing peptides to EAAT1 C-terminal domain increased MG-63 cell number at 500μM glutamate. Inhibition of EAAT1 intracellular interactions regulated expression of osteocalcin mRNA in both osteoblast-like cell lines and decreased OPG mRNA expression in SaOS-2 cells. Overall, specific EAAT modulation could increase both osteoblast cell number and differentiation.

These data show for the first time that EAATs are functional in human osteoblasts and that inhibition of their activity can modulate the osteoblast bone-forming phenotype. Manipulation of these mechanically regulated glutamate transporters may represent a new therapeutic approach for the treatment of fractures and disorders such as osteoporosis where the bone is biologically and structurally compromised.

GLUTAMATE REGULATION FOR BONE REPAIR

ABBREVIATIONS

aa	Amino acid
α-MEM	Alpha-minimum essential medium
ALP	Alkaline phosphatase
ALS	Amyotrophic lateral sclerosis
AMPA	DL-α-amino-3-hydroxy-5-methylisoxasole-4-propionate
ANOVA	Analysis of variance
AON	Antisense oligoribonucleotide
AP-1	Activator protein-1
ASCT	Neutral amino acid transporter
ATCC	American Type Culture Collection
ATP	Adenosine triphosphate
BBB	Blood-brain barrier
BCA	Bicinchoninic acid
(n)BLAST	(nucleotide) Basic local alignment search tool
BMD	Bone mineral density
(rh)BMP	(Recombinant human) Bone morphogenetic protein
BMU	Basic multicellular unit
BNPI	Brain-specific Na^+-dependent inorganic phosphate transporter
bp	Base pairs
Bq	Becquerels
BRC	Bone remodelling compartment
BSA	Bovine serum albumin
cAMP	Cyclic adenosine 3',5'- monophosphate
CCGIII	L-2-(carboxycyclopropyl)glycine-III
CD38	Cluster of Differentiation 38
cDNA	Complementary DNA
CGRP	Calcitonin gene-related peptide
CIA	Collagen induced arthritis
CMV	Cytomegalovirus
CNQX	6-cyano-7-nitroquinoxaline-2,3-dione
CNS	Central nervous system
CoIP	Coimmunoprecipitation
CPP	Cell penetrating peptide
Ct	Cycle threshold
Cx	Connexin
DAG	Diacylglycerol
DAPI	4,6-diamidino-2-phenylindole
DAT	Dopamine transporter
DHK	Dihydrokainic acid
Dlx5	Distal-less homeobox-5
DNase	Deoxyribonuclease
DNPI	Differentiation-associated Na^+-dependent inorganic phosphate cotransporter
dNTP	Deoxyribonucleotide triphosphate
(D)MD	(Duchenne's) Muscular Dystrophy
DMEM	Dulbecco's modified eagle's medium
DMP-1	Dentin matrix protein-1
dpm	Disintegrations per minute

DTT	Dithiothreitol
EAAC	Excitatory amino acid carrier
EAAT	Excitatory amino acid transporter
EDTA	Ethylenediaminetetraacetic acid
eNOS	Endothelial NOS
ER	Endoplasmic reticulum
ERα	Oestrogen receptor alpha
ERM	Ezrin-Radixin-Moesin
ESE	Exonic splice enhancer
FAM	5-carboxy fluorescein
FBS	Foetal bovine serum
FDA	Food and Drug Administration
FITC	Fluorescein
GABA	Gamma-aminobutyric acid
GAT-1	GABA transporter -1
GDP	Guanosine diphosphate
GEF	Guanine nucleotide exchange factor
GFAP	Glial fibrillary acidic protein
GFP	Green fluorescent protein
GLAST	Glutamate-aspartate tranporter
GLM	General linear model
GLT-1	Glutamate transporter -1
(i/m)GluR	Ionotropic/Metabotropic glutamate receptor
GPCR	G-protein coupled receptor
GPS-1	G protein pathway suppressor-1
GS	Glutamine synthetase
GSH	Glutathione
GTP	Guanosine triphosphate
GTPase	Guanosine triphosphatases
GTRAP	Glutamate transporter associated proteins
HEK	Human embryonic kidney
HEPES	N-2-Hydroxyethylpiperazine-N'-2-Ethanesulfonic Acid
HDAC	Histone deacetylase
HPLC	High-performance liquid chromatography
IGF	Insulin-like growth factor
IP3	Inositol 1,4,5-triphosphate
IPTG	Isopropyl β-D-1-thiogalactopyranoside
KA	Kainate
KRH	Krebs-Ringer HEPES
LB	Lysogeny broth
LDH	Lactate dehydrogenase
LIM	Lin-11, Isl-1 and Mec-3
LRP5/6	Low density lipoprotein receptor-related protein 5/6
MAPK	Mitogen-activated protein kinase
MEPE	Matrix extracellular phosphoglycoprotein
MCPG	α-methyl-4-carboxyphenylglycine
M-CSF	Macrophage- colony-stimulating factor
mRNA	Messenger RNA
MSC	Mesenchymal stem cell
Msx2	msh homeobox homologue-2

NET	Norepinephrine transporter
NHERF	Na^+/H^+ exchanger regulatory factor
NHOB	Normal human primary osteoblast
NF-κB	Nuclear factor-kappaB
NMDA	N-methyl-D-aspartate
NO(S)	Nitric oxide (synthase)
OA	Osteoarthritis
OPG	Osteoprotegerin
ORF	Open reading frame
Osx	Osterix
PACAP	Pituitary adenylate cyclase activating peptide
PAGE	Polyacrylamide gel electrophoresis
PBS	Phosphate buffered saline
pCi	picocuries
PCR	Polymerase chain reaction
PDGF	Platelet derived growth factor
PDZ	Postsynaptic density-95/Discs large/Zona occludens-1
PGE	Prostaglandin E
PI3K	Phosphatidylinositol-3-kinase
PICK1	Protein-interacting-with-C-kinase 1
PFA	Paraformaldehyde
PKA	Protein Kinase A
PKB	Protein Kinase B
PKC	Protein Kinase C
PM	Plasma membrane
pNP	*p*-nitrophenol
pNPP	*p*-nitrophenol phosphate
PP2	Protein phosphatase 2
(rh)PTH	(Recombinant human) Parathyroid hormone
QRT-PCR	Quantitative real time-polymerase chain reaction
RA	Rheumatoid arthritis
RANK(-L)	Receptor activator of nuclear factor κB (ligand)
rhBMP	Recombinant human bone morphogenetic protein
RNA	Ribonucleic acid
RNase	Ribonuclease
ROS	Reactive oxygen species
rpm	Revolutions per minute
RT	Reverse transcription
RT-PCR	Real time-polymerase chain reaction
Runx2	Runt-related transcription factor-2
SDS-PAGE	Sodium dodecyl sulphate polyacrylamide gel electrophoresis
SEM	Standard error mean
SERMs	Selective estrogen receptor modulators
SLC1A3	Solute carrier family 1 member 3
SLRP	Small leucine-rich proteoglycans
SNS	Sympathetic nervous system
SOST	Sclerostin
SP	Substance P
SSCC	Stretch sensitive calcium channels
T3MG	*threo*-3-Methylglutamic acid

Tat	Transcription-transactivating
TBE	Tris borate EDTA
TBOA	DL-threo-b-benzyloxyaspartic acid
TDPA	L-trans-2,3-PDC, (*RS*)-2-amino-3-(3-hydroxy-1,2,5-thiadiazol-4-yl)propionic acid
TE	Tris-EDTA
TGF-β	Transforming growth factor beta
THA	β-*threo*-hydroxy-aspartate
Tm	Melting temperature
TM	Transmembrane
***t*-PDC**	L-*trans*-Pyrrolidine-2,4-dicarboxylic acid
TRITC	Rhodamine
UTR	Untranslated region
VEGF	Vascular endothelial growth factor
VGLUT	Vesicular glutamate transporters
VIP	Vasoactive intestinal polypeptide
VSCC	Voltage stimulated calcium channels
Y2H	Yeast 2 Hybrid

List of Figures

Chapter 1

Chapter 2

Chapter 3

Chapter 4

Chapter 5

Chapter 6

List of Tables

Chapter 1: Introduction

1. Introduction

There is a pressing need to identify new targets for anabolic bone therapies. This thesis will examine the role of the glutamate signalling pathway, with specific attention to the glutamate transporters, in the regulation of bone formation, and investigate mechanisms to modulate this pathway to achieve increased bone formation. The following introduction provides an overview of bone tissue, discussing its structure, composition, formation and associated pathologies. The glutamate signalling pathway, with emphasis on the glutamate transporters, is then introduced and the literature regarding the role of glutamate in bone reviewed.

1.1 Bone physiology and function

Bones are rigid organs that form the human skeletal system and are responsible for a diverse range of functions including haematopoiesis, mineral homeostasis (most notably calcium and phosphorus), protection of the body's organs, attachment sites for muscles to generate movement and determinants of our size and shape (Dempster 2006).

The human skeleton is formed of 206 bones which are grouped into the axial and the appendicular skeletons (reviewed in (Standring 2004) and discussed below). The axial skeleton forms the long axis of the body and consists of bones of the skull, vertebral column and rib cage which are primarily responsible for support and protection. The appendicular skeleton is comprised of bones of the upper and lower limbs, and the girdles that attach the limbs to the axial skeleton. 126 bones form the appendicular skeleton and its main function is movement.

The bones within the body can be categorised into five types: long, short, flat, irregular and sesamoid. Long bones (e.g. humerus, tibia, femur, ulna, metacarpals) contain a shaft (the diaphysis) that is longer than it is wide, and these bones often work as levers in the upper and lower extremeties (Figure 1.1). They are mainly composed of compact bone with some trabecular bone and marrow within the medullary cavity. Short bones are cube-shaped and have a thin layer of compact bone surrounding a trabecular interior. Short bones are located in the wrist and ankle. Flat bones are thin and often curved, with parallel layers of compact bone sandwiching a

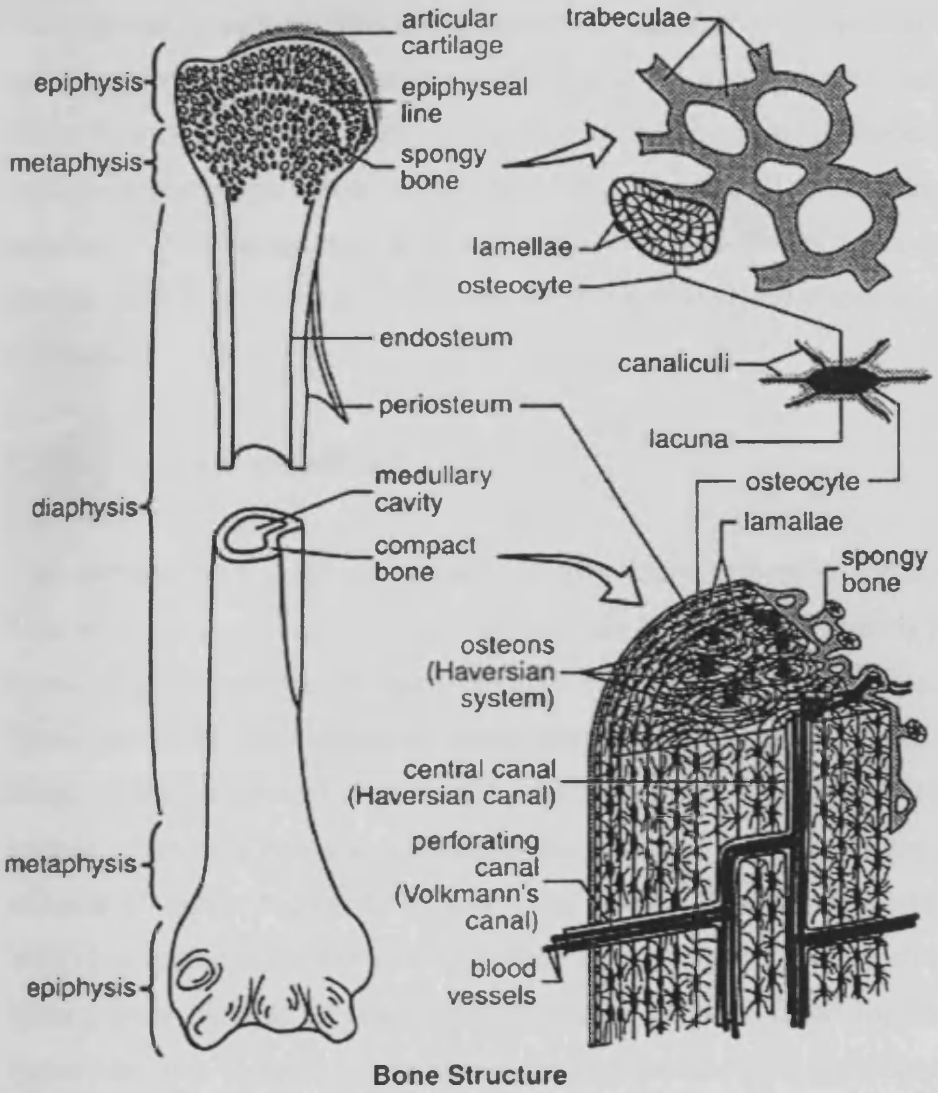

Figure 1.1. Main features of a long bone. Long bones contain a hard outer layer of cortical bone and spongy trabecular bone at the epiphysis and metaphysis. The Haversian system is the main functional unit of compact bone and comprises concentric layers of bone (lamellae) surrounding a central Harversian canal which contains nerve and blood supplies for the bone. Osteoblasts become trapped within the matrix, forming osteocytes that live within their own small space (lacuna) and connect with one another via a network of canals (canaliculi). Figure source: Anatomy and Physiology by (Pack 2001). Figure reprinted with permission of John Wiley & Sons, Inc. Copyright (John Wiley & Sons, Inc. 2010).

layer of trabecular bone. Flat bones have broad surfaces for protecting organs and the attachment of muscles and are common within the skull and the sternum. Irregular bones do not fit into the above categories; they are of varied shapes and sizes and include bones of the vertebrae, hips and some in the skull. Sesamoid bones e.g. the patella, are special types of short bone that are embedded in tendons and hold the tendon away from the joint, increasing its angle and therefore increasing the force of the muscle.

1.1.1 Bone composition

Two forms of bone exist within the human skeleton; trabecular and cortical. Cortical bone accounts for about 80% of the skeletal mass (Parfitt 1983) and is highly resistant to bending and torsion, providing strength to the skull and the shafts of long bones. Trabecular bone, also known as cancellous or spongy bone, is more porous, and is found in the epiphyseal and metaphyseal regions of long bones (Figure 1.1), the interior of short bones and constitutes the majority of the bone tissue in the axial skeleton (Johnson 1964). Trabecular bone forms 20% of the skeletal mass (Parfitt 1983) but accounts for 80% of its surface area due to its spongy structure which is formed from bundles of short, parallel strands of bone fused together (Jee 1983). Plates and rods (trabeculae) represent the two basic microarchitechtural features of trabecular bone and are important in determining its mechanical properties. Plates have a flat structure while rods are cylindrical. Trabecular plates play an important role in determining the yield strength of human trabecular bone and the arrangement of trabeculae is highly adapted to the mechanical environment (Liu et al. 2006; Stauber et al. 2006; Liu et al. 2008; Liu et al. 2009). A recent study of femoral, tibial and vertebral trabecular bone demonstrated that the majority of plates aligned with the longitudinal axis and the rods primarily aligned with the transverse plane (Liu et al. 2008). Compressive loading of vertebral trabecular bone indicates that longitudinal plates withstand the majority of axial loading and transverse rods act as links to stabilise the structure (Liu et al. 2009).

Bone is deposited first as disorganised woven bone, or primary bone, that forms quickly but is weak and contains small amounts of randomly orientated collagen fibres which convey isotropic mechanical properties to the tissue i.e. it adapts to forces from any direction in a similar fashion (Smith 1960; Su et al. 1997; Su et al.

2003). Woven bone contains a high number of cells per unit volume that are randomly arranged. In humans, woven bone is resorbed by one year of age and replaced by lamellar bone which is highly organised, stronger and contains many highly organised collagen fibres within parallel columns called osteons (Bullough 1992; Buckwalter et al. 1996a). The osteon (or Haversian system) is the main functional unit of compact bone (Figure 1.1) (Parfitt 1983; Buckwalter et al. 1996a). Compact bone tissue forms concentric layers (lamellae) surrounding a central Harversian canal which contains nerve and blood supplies for the bone. The bone-forming cells, osteoblasts, form the osteon externally to internally and some become trapped within the matrix, forming osteocytes that live within their own small space (lacuna) (Mundy 1999) and connect with one another via extended cell processes within a network of canals (canaliculi). In each lamella, the collagen fibres run parallel to one another, but at an angle to fibres within adjacent lamellae (Giraud-Guille 1988). The organised, stress-orientated alignment of collagen fibres in lamellar bone gives it anisotropic properties which allow different mechanical responses to the orientation of an applied force. Osteons are separated from one another by cement lines (Schaffler et al. 1987; Burr et al. 1988) and Volkmann's canals which run perpendicular to Harversian canals and are responsible for connecting osteons to each other and connecting the blood vessels of the Haversian canals with the periosteum

Bone is composed of primarily four types of cells; osteoblasts, osteoclasts, osteocytes and bone lining cells in conjunction with an acellular matrix (Buckwalter et al. 1996b, a).

1.1.1.1 Osteoblasts

Osteoblasts are mononucleated bone cells that differentiate from mesenchymal stem cells (MSCs) of the bone marrow. MSCs are also capable of differentiating into cells of the adipocyte, myocyte and chondrocytic lineages (Owen and Friedenstein 1988; Aubin et al. 1995; Gimble et al. 1996; Prockop 1997). The transcription factors runt-related transcription factor-2 (Runx2), distal-less homeobox-5 (Dlx5) and msh homeobox homologue-2 (Msx2) are required to direct the stem cells towards to the osteoblast lineage (Ducy et al. 1997; Komori et al. 1997; Bendall and Abate-Shen 2000). Pre-osteoblasts express type I collagen and bone sialoprotein and require the expression of Runx2, osterix (Osx) and components of the Wnt signalling pathway to

further differentiate into the mature bone-forming osteoblast phenotype (Ducy et al. 1997; Nakashima et al. 2002; Glass et al. 2005; Hu et al. 2005). Osteoblasts are morphologically characterised as plump, cuboidal cells with a prominent rough endoplasmic reticulum and Golgi complex, reflecting high metabolic activity and secretion. Mature osteoblasts are present at the bone surface where they produce the osteoid (unmineralised bone matrix) and alkaline phosphatase (ALP), an enzyme that has a role in mineralisation of bone (Robison 1923; Moss et al. 1967; Majeska and Wuthier 1975; Fallon et al. 1980; Rezende et al. 1994). Osteoblasts are also able to produce cytokines and hormones such as prostaglandins that regulate bone growth and the activity of neighbouring bone-resorbing osteoclasts (Vaes 1988; Suda et al. 1992). Mature osteoblasts have one of three fates; they may die, become embedded within the bone matrix as osteocytes, or cease bone matrix synthesis and become bone lining cells (Parfitt 1987; Miller et al. 1989).

1.1.1.2 Osteoclasts

Osteoclasts are large, multinucleated cells derived from a monocyte-cell lineage and are located on the bone surface where they form resorption pits. Fusion of mononuclear cells to form multinuclear immature pre-osteoclasts requires the presence of macrophage colony-stimulating factor (M-CSF) and a member of the tumour-necrosis factor family, the receptor activator of nuclear factor κB ligand (RANK-L) (Felix et al. 1990; Kodama et al. 1991; Suda et al. 1992; Nakagawa et al. 1998). RANK-L is expressed at the cell surface of osteoblasts and interacts with the osteoclast cell-surface receptor RANK (Fuller et al. 1998; Lacey et al. 1998). Osteoprotegerin (OPG), a soluble decoy receptor for RANK-L, is secreted by osteoblasts and competes with osteoclast RANK for binding sites (Yasuda et al. 1998a; Yasuda et al. 1998b). Osteoblasts are therefore able to regulate osteoclastogenesis both positively and negatively by altering the balance of OPG and RANK-L expression (Simonet et al. 1997; Yasuda et al. 1998b). The continued presence of osteoblast RANK-L is necessary for further osteoclast differentiation to a mature osteoclast, and regulation of its bone-resorbing activity and survival (Burgess et al. 1999; Udagawa et al. 1999). Activated pre-osteoclasts migrate and attach to the matrix, forming a compartment into which they pump hydrogen ions to solubilise the mineral substrate and secrete proteases that digest the organic component (Delaisse et

al. 1991; Blair et al. 1993; Delaisse et al. 1993; Goto et al. 1993; Wucherpfennig et al. 1994; Holliday et al. 1997). Osteoclasts are highly polarised when physiologically active, with an apical membrane at the contact with bone and a basolateral membrane at its opposite (Mulari et al. 2003). Actively resorbing osteoclasts are typified by a characteristic organisation of F-actin into a ring called the sealing zone, which restricts proton and enzyme secretions to the resorption lacuna (Vaananen et al. 2000).

1.1.1.3 Osteocytes

Osteocytes are the most abundant cell type in bone (Parfitt 1977) and are differentiated from osteoblasts that have become trapped within the bone matrix and begin to express the early osteocyte marker E11 (Wetterwald et al. 1996). Osteocytes are smaller than osteoblasts and have lost many of their cytoplasmic organelles (Jande and Belanger 1973; Irie 2000). These cells occupy non-mineralised spaces called lacunae and have a dendritic morphology with many cellular processes extending within canaliculi that reach out to meet neighbouring osteocytes, surface bone cells (Doty 1981; Menton et al. 1984; Bonewald 1999) and bone marrow (Kamioka et al. 2001), facilitating communication (Palumbo et al. 1990). Contact of osteocytes with the bone marrow gives this cell type the potential to recruit osteoclast precursors to stimulate bone resorption (Baylink et al. 1973; Zhao et al. 2002) and regulate mesenchymal stem cell differentiation (Hartmann 2006). Apoptosis of osteocytes in the vicinity of microcracks has been shown to act as an activator of osteoclastogenesis and stimulate resorption of the deteriorated bone in that area (Noble et al. 2003; Gu et al. 2005; Kurata et al. 2006; Seeman and Delmas 2006). Mature osteocytes express dentin matrix protein-1 (DMP-1), matrix extracellular phosphoglycoprotein (MEPE) and sclerostin (SOST) (Feng et al. 2003; Nampei et al. 2004; van Bezooijen et al. 2004). Proposed osteocyte functions include matrix maintainance, calcium and phosphate homeostasis (Belanger 1969; Feng et al. 2006; Lorenz-Depiereux et al. 2006) and regulation of the bones response to mechanical load (Skerry et al. 1989; Mullender and Huiskes 1995; Lanyon 1996; Noble et al. 1997; Burger and Klein-Nulend 1999; Bonewald 2006).

1.1.1.4 Bone lining cells

Bone lining cells are the second most abundant cell type in bone and cover more than 90% of the surfaces of adult bone (Parfitt 1983), connecting to osteocytes and osteoblasts via gap junctions (Doty 1981; Menton et al. 1984; Bonewald 1999). Bone lining cells have a flattened morphology with few cellular organelles suggesting that these cells do not actively produce matrix (reviewed in (Nakamura 2007)). They line bone surfaces that are not undergoing modelling or remodelling and are thought to be inactive osteoblasts which have ceased matrix synthesis (Miller et al. 1989; Miller 1992). Bone lining cells form a thin continuous sheet that may have a role regulating the movement of calcium and phosphate into and out of bone (Miller et al. 1989). Removal of bone lining cells is necessary for osteoclastic bone resorption to commence (Jones and Boyde 1976; Zambonin Zallone et al. 1984), exposing the underlying bone matrix (Chambers and Fuller 1985).

1.1.1.5 Bone matrix

The cellular component of bone makes up only a small proportion of its mass, with the rest composed of extracellular matrix. Bone matrix consists of both inorganic and organic parts. Crystalline mineral salts and calcium in the form of hydroxyapatite make up the inorganic component while type I collagen forms 95% of the organic element (Burgeson 1988). Collagen fibrils in bone are extensively cross-linked, both intra- and intermolecularly, making them highly insoluble (Glimcher and Katz 1965). Non-collagenous proteins are also present; growth factors such as transforming growth factor-beta (TGF-β) and insulin-like growth factors (IGFs), cell attachment factors, proteoglycans and serum-derived γ-carboxylated proteins that bind to the mineral component of bone (reviewed in (Heinegard and Oldberg 1989; Canalis 1993; Sommerfeldt and Rubin 2001)). Cell attachment factors include fibronectin, thrombospondin, osteopontin and bone sialoprotein (Oldberg et al. 1986; Somerman et al. 1988; Robey et al. 1989). Some of the non-collagenous proteins known to be present within bone are discussed below.

Osteopontin is a glycophosphoprotein secreted by osteoblasts, osteoclasts and osteocytes (Merry et al. 1993; Yamate et al. 1997) and is capable of binding to cells and the hydroxyapatite matrix. Osteopontin influences bone homeostasis by inhibiting

mineralisation (Hunter et al. 1996; Steitz et al. 2002; Pampena et al. 2004) and by promoting differentiation and activation of osteoclasts (Tani-Ishii et al. 1997; Faccio et al. 1998; Yoshitake et al. 1999; Ihara et al. 2001; Ishijima et al. 2001; Faccio et al. 2002; Chellaiah et al. 2003).

Bone sialoprotien is found exclusively in mineralised tissues such as bone and dentin (reviewed in (Ganss et al. 1999)) and there is much evidence to suggest bone sialoprotien is a marker of osteoblast differentiation and the onset of mineralisation (Chen et al. 1992; Chen et al. 1994; Cooper et al. 1998; Mizuno et al. 2000; Gordon et al. 2007).

Osteonectin is one of the most abundant non-collagenous proteins produced by osteoblasts and is a phosphorylated glycoprotein with a high affinity for Ca^{2+}, hydroxyapatite, collagen (Termine et al. 1981), and thrombospondin (Clezardin et al. 1988).

Osteocalcin is a γ-carboxylated protein found in bone (Glowacki and Lian 1987; Robey et al. 1989). Expression of osteocalcin is restricted to late osteoblasts and its serum level is commonly used as a marker of bone turnover in metabolic disease (Price et al. 1980; Watts 1999).

Proteoglycans comprise of a central core protein and polysaccharide side chains called glycosaminoglycans. In bone, various proteoglycans have been detected including small leucine-rich proteoglycans (SLRPs), heparan sulphate, aggregan and hyaluronic acid (reviewed in (Lamoureux et al. 2007)). In bone tissue, proteoglycans have structural roles, controlling collagen fibrillogenesis, and also act as co-receptors for some cytokines.

1.1.2 Bone formation

Two major mechanisms of osteogenesis exist and both involve the conversion of mesenchymal tissue into bone tissue. Intramembranous ossification is the direct transformation of mesenchymal tissue to bone whereas formation of endochondral bone occurs via a hyaline cartilage model that is formed by differentiated mesenchymal cells (Cancedda et al. 2000; Karsenty and Wagner 2002; Eames et al. 2003).

1.1.2.1 Intramembranous ossification

In the human body, bones formed by intramembranous ossification include flat bones of the skull, the clavicle and the pelvis. During intramembranous ossification, mesenchymal cells proliferate and condense into compact nodules (Hall and Miyake 1992; Huang et al. 1997). Some mesenchymal cells become osteoblasts that secrete bone matrix while others develop into fibroblasts and blood vessels (reviewed in (Buckwalter et al. 1996a)). As the secreted matrix calcifies, bony spicules radiate out from the point of ossification to become surrounded by compact mesenchymal cells forming the periosteum (Buckwalter et al. 1996a; Gilbert 2006). Beneath the periosteum, osteoblasts deposit matrix parallel to existing spicules, forming many layers of bone (Cohen 2006; Gilbert 2006).

1.1.2.2 Endochondral ossification

Endochondral ossification (Figure 1.2) replaces a hyaline cartilage model with bone tissue to form long bones, increase the length of long bones and represents an essential process for the healing of bone fractures (reviewed in (Erlebacher et al. 1995)). Mesenchymal tissue differentiates to form a hyaline cartilage model bordered by a perichondrium. Chondrocytes secrete a matrix rich in type II collagen and the proteoglycan aggrecan. Chondrocytes within the central region of the cartilage stop proliferating, enlarge and mature to hypertrophic chondrocytes that secrete a different extracellular matrix to that of proliferating chondrocytes i.e. a greater amount of type X collagen over type II collagen (Iyama et al. 1991). Hypertrophic chondrocytes also secrete angiogenic factors, such as vascular endothelial growth factor (VEGF) (Gerber et al. 1999), that induce sprouting angiogenesis from the perichondrium (called the periosteol bud) during the third month of human fetal development (Karsenty 1999; Olsen et al. 2000). The periosteal bud consists of lymph vessels, nerves, and blood vessels, which are a source of haematopoietic cells, osteoblasts and osteoclasts (Olsen et al. 2000; Colnot and Helms 2001). This results in the formation of primary ossification centres. The cartilage perichondrium becomes the periosteum which contains a layer of undifferentiated cells that go on to become osteoblasts (Hall and Miyake 2000; Eames et al. 2003; Colnot et al. 2004). These osteoblasts generate a collar of compact bone around the primary ossification centre.

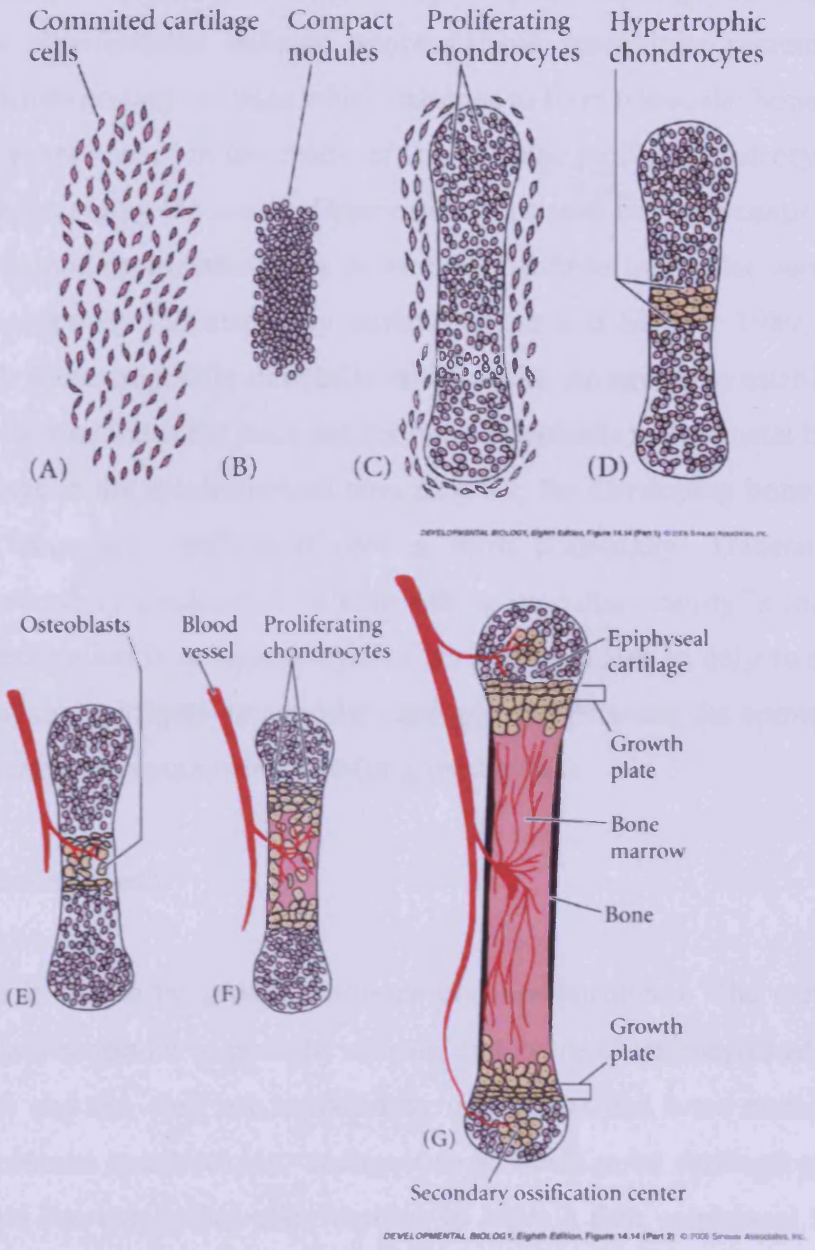

Figure 1.2. Schematic diagram of endochondral ossification. (A) Mesenchymal cells condense and commit to the chondrocyte lineage and (B) form a cartilaginous model of the bone. (C,D) Chondrocytes proliferate and the cells in the centre of the diaphysis become hypertrophic and apoptose as they mineralise their matrix. (E) Blood vessels invade the space left by the chondrocytes and provide a source of osteoblasts which attach to the cartilaginous matrix and begin to deposit osteoid. (F,G) Bone formation and growth occurs via cycles of proliferating, hypertrophic and mineralising chondrocytes. Secondary ossification centres form at the tips of bone to promote lengthening of bones. Figure source: Developmental Biology, 8th edition by (Gilbert 2006). Figure reprinted with permission of Sinauer Associates, Inc. Copyright (Sinauer Associates, Inc. 2010).

Within primary ossification centres, hypertrophic cartilage is degraded, the hypertrophic chondorcytes undergo apoptosis and osteoblasts secrete osteoid to replace the disintegrating cartilage which calcifies to form trabecular bone.
While these events occur in the centre of the cartilage mould, chondrocytes continue to proliferate, enlarging the mould. Ossification continues from the centre towards the ends of bones, and osteoclasts break down newly formed trabecular bone within the diaphysis to open up the medullary cavity (Roach and Shearer 1989; Colnot and Helms 2001). Haematopoeitic stem cells interact with the stroma to establish the bone marrow which constitutes the main site for haematopoieisis in post-natal life.
As the cartilage at the epiphysis continues to grow, the developing bone increases in length and secondary ossification centres form postnatally. Trabecular bone is retained at secondary ossification centres and no medullary cavity is formed. When secondary ossification is complete, hyaline cartilage remains in only two areas, over the surface of the epiphysis as articular cartilage and between the epiphysis and the diaphysis forming the epiphyseal plate (or growth plate).

1.1.2.3 Bone growth

Bone growth is driven by growth hormone and sex hormones. The cartilage at the epiphyseal plate continues to grow by mitosis, and as the chondrocytes adjacent to the diaphysis age and die, they are replaced by osteoblasts and bone matrix (Hunziker 1994). This process continues into adolescence at which point cartilage growth slows and stops, and the epiphyseal plate ossifies to leave a thin epiphyseal line. At this stage, bones can no longer grow in length. However, bones can continue to thicken and widen by appositional growth throughout life. Appositional growth occurs through deposition of bone by osteoblasts beneath the periosteum and degradation of bone within the medullary cavity by osteoclasts.

1.2 Bone remodelling

Bone is a dynamic tissue that is continuously self-renewing and responding to environmental cues by remodelling itself. Bone remodelling is the making of cavities by osteoclasts and the subsequent filling of these cavities by osteoblasts to maintain

skeletal integrity. At any one time, this process is occurring at multiple places throughout the skeleton. In normal young adults, equilibrium exists between bone resorption and bone formation and this depends on the coordinated differentiation and activation of osteoblasts and osteoclasts (Frost 1964). The team of cells involved in bone remodelling are collectively termed the basic multicellular unit (BMU). The BMU is a distinct, temporary, 3-dimensional form that moves along bone, with osteoclasts lining the leading edge, followed by a group of mononuclear cells that line the resorption pit during the period between resorption and formation (reversal phase) (Parfitt 1983, 1994). Rows of osteoblasts then adhere to the reversal zone and deposit layers of unmineralised bone matrix (osteoid) (Figure 1.3). The BMU is covered by a canopy of cells, which are most likely bone-lining cells connected to bone-lining cells on the quiescent bone surface (Hauge et al. 2001). Hague et al. have also shown that capillaries penetrate the canopy of bone-lining cells and presumably provide the vascular supply to the BMU as well as possibly providing the cells required for the remodeling process (Kassem et al. 1991b; Kassem et al. 1991a; Hauge et al. 2001; Eghbali-Fatourechi et al. 2005). Therefore, the BMU exists within a bone remodelling compartment (BRC) which consists of the BMU, the cell canopy and capillaries, and the BRC has been shown to exist in both cortical and cancellous bone (Hauge et al. 2001).

The resorption and formation processes are said to be coupled to one another (Frost 1964) and this coupling is a controlled process that ensures new bone is restored after old bone is removed, maintaining the bone balance (Parfitt 2000). This balance is achieved locally through the action of cytokines and growth factors such as TGF-β, bone morphogenetic proteins (BMPs), platelet-derived growth factor (PDGF), and IGF, and systemically by hormones such as oestrogen and parathyroid hormone (PTH) (Canalis 1983; Canalis et al. 1989; Canalis 1993). Within the BMU, osteoclast differentiation and resorption is also regulated by osteoblasts via the OPG/RANK/RANK-L system (Yasuda et al. 1998a; Yasuda et al. 1998b) and it is also thought that osteoclasts can enhance osteoblast differentiation and function (Martin and Sims 2005). Most skeletal disorders are caused by uncoupling of this remodelling process, favouring either bone resorption (osteoporosis) or bone formation (osteopetrosis) (Mundy et al. 2001).

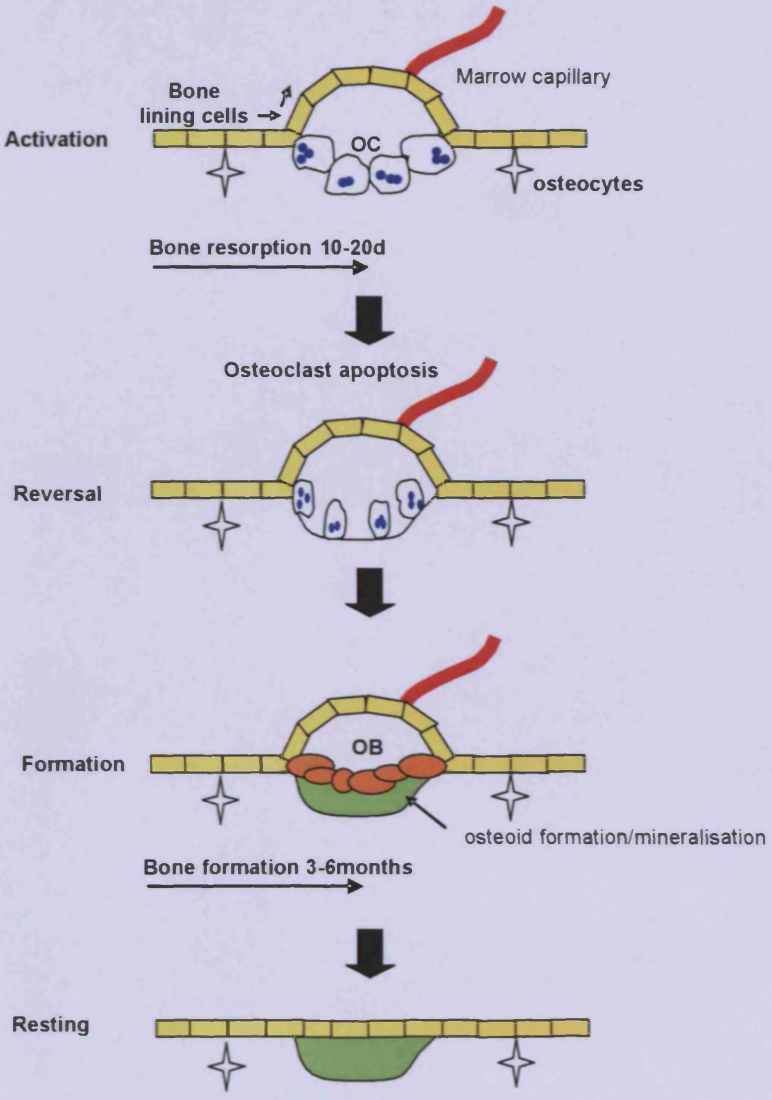

Figure 1.3. Normal bone remodelling. The bone remodelling compartment (BRC) comprises the cells of the basic multicellular unit (BMU) i.e. osteoclasts, osteoblasts and osteocytes as well as a cover of bone-lining cells and the associated vasculature (i) Activation: osteoclast precursors differentiate into mature bone-resorbing cells in response to activating factors. Osteoclasts resorb bone mineral and matrix, creating an erosion cavity. (ii) Reversal: osteoclasts apoptose and mononuclear cells prepare the bone surface for osteoblast bone formation. (iii) Formation: osteoblasts synthesise an organic matrix to fill the cavity, which is then mineralised. (iv) Resting: the bone surface is covered with flattened lining cells. OC, osteoclast; OB, osteoblast. Adapted from (Eriksen et al. 2007) and the MRC human research unit, bone and calcium metabolism webpage (last accessed 23 May 2010) <http://www.mrc-hnr.cam.ac.uk/research/bone_health/bcm.html>.

1.2.1 Uncoupled bone remodelling

Abnormalities in bone remodelling are common in many disease states such as osteopetrosis and osteoporosis (Table 1.1). A change in BMU dynamics, either activation or the speed of remodelling, can have significant effects on the bone balance. Furthermore, determining the etiology of diseases characterised by uncoupled bone remodelling may help to identify the normal factors that are responsible for controlling bone remodelling. For example, the importance of sclerostin as a negative regulator of bone formation was discovered through research into the high bone mass disorder sclerosteosis (Balemans et al. 1999; Balemans et al. 2001; Brunkow et al. 2001; Winkler et al. 2003; van Bezooijen et al. 2004).

1.2.1.1 Osteosclerosis

Sclerosing bone dysplasias are characterised by an increase in bone density and are inherited heterogeneously.

1.2.1.1.1 Osteopetrosis

Osteopetrosis is a family of sclerosing bone dysplasias characterised by defective osteoclast function and impaired bone resorption without an alteration in overall bone shape (Van Hul et al. 2001; Whyte 2002). The lethal form and several intermediate

Table 1.1. Uncoupled bone remodelling in human disorders (adapted from (Raisz 1999))

	Bone resorption	Bone formation
Osteoporosis	↑↑	↑
Disuse osteoporosis	↓	↓↓
Inflammation	↑↑	↓
Osteopetrosis	↓↓	↑
Sclerosteosis	↑	↑↑
Van Buchems	↑	↑↑

forms are inherited as autosomal recessive traits whereas the mild form is inherited as an autosomal dominant trait (Johnston et al. 1968; Beighton et al. 1979; Bollerslev and Andersen 1988). A primary abnormality in the osteoclast or its stem cell precursor has been proposed as the underlying cause of osteopetrosis (Marks 1984; Rouleau et al. 1986). Studies of mammalian osteopetrosis suggest that genetic abnormalities are present in osteoclast precursor cells (Van Slyke and Marks 1987). Experimental models of the disease have been successfully treated by bone marrow transplantation (Walker 1993), a procedure that has been translated to humans in the severest of cases (Driessen et al. 2003).

1.2.1.1.2 Sclerosteosis

Sclerosteosis is a rare bone disorder characterised by sclerosis of the skeleton, particularly the skull and mandible resulting in facial distortion, raised intracranial pressure and entrapment of cranial nerves (Beighton et al. 1976; Beighton and Hamersma 1979; Beighton 1988; Hamersma et al. 2003). Sudden death can occur as a result of impaction of raised intracranial pressure. Sclerosteosis is due to loss of function mutations in the *SOST* gene and inherited as an autosomal recessive trait with heterozygotes clinically normal (Balemans et al. 1999; Balemans et al. 2001; Brunkow et al. 2001; Winkler et al. 2003; van Bezooijen et al. 2004). Sclerosteosis is the result of increased bone formation and unaffected bone resorption leading to increased bone mass (van Bezooijen et al. 2005).

1.2.1.1.3 Van Buchem disease

Van Buchem disease is inherited as an autosomal recessive trait and clinically presents very similarly to sclerosteosis, with thickening of the skull, mandible, clavicles and diaphysis of long bones (Van Buchem et al. 1962; van Buchem 1971). However, in contrast to sclerosteosis sufferers, patients with van Buchem disease have a large stature and hand malformations (Beighton et al. 1984). Sclerosteosis and van Buchem disease are both characterised by increased bone formation and map to the same chromosomal 17q12-q21 region (Van Hul et al. 1998; Balemans et al. 1999). Patients with van Buchem disease were not found to have mutation in the *SOST* gene, but had a deletion downstream of the *SOST* gene (Balemans et al. 2002; Staehling-

Hampton et al. 2002) that was later found to include an enhancer element that drives *SOST* expression (Loots et al. 2005).

1.2.1.2 Osteoporosis

Osteoporosis is the most common metabolic disorder of the skeleton (Raisz 1997). One in two women and one in five men over the age of 50 in the UK will fracture a bone as a result of osteoporosis (van Staa et al. 2001). Osteoporosis is characterised by low bone mass and structural deterioration of bone tissue, resulting in bone fragility and increased risk of fracture. The costs of osteoporosis are both health-related and financial. In the UK, the mortality following a hip fracture is 18% (Todd et al. 1995) and osteoporosis related fractures cost the health service an annual sum of over £1 billion (Torgensen 2001; PRODIGY 2006). Osteoporotic risk is dependent upon peak bone mass which declines with age, making osteoporosis a problem that accompanies the ageing population (Maravic et al. 2005) (Figure 1.4). Indeed, the number of hip fractures worldwide is expected to increase from 1.7 million in 1990 to 6.3 million in 2050 (Johnell 1997). Peak bone mass is reached by the age of about 20, after which bone is resorbed more rapidly than it is formed. Males and females are affected differently; by old age, women tend to have lost half their trabecular bone and one third of their cortical bone whereas men typically lose one third of their trabecular bone and one fifth of cortical bone (Goldberg 2004). Bone mass in women also declines sharply for 5 years during the menopause as a result of decreased oestrogen production (Riggs et al. 1986; Wark 1993) and oestrogen deficiency is relevant to the pathogenesis of osteoporosis in both men and women (Riggs et al. 1998). Optimising peak bone mass is therefore key in reducing the risk of osteoporosis in later life.

Skeletal fragility can be the result of (1) failure to generate a skeleton of appropriate mass and strength during early development; (2) disproportionate bone resorption leading to decreased bone mass and a loss of skeletal microarchitechture; or (3) an insufficient formation response to increased bone resorption during remodelling (reviewed in (Raisz 2005)). Experimental evidence suggests that at menopause there is accelerated bone remodelling, and that while bone formation increases overall, it is insufficient to replace the bone lost by resorption (reviewed in (Raisz 2005)). This

defect in osteoblast function may be due to cellular senescence or the result of a decrease in the synthesis or activity of systemic and local growth factors (Raisz 2005).

1.2.1.3 Disuse osteoporosis

Mechanical loading of the skeleton directs bone remodelling (Robling 2006). Bone loss as a result of reduced mechanical loading of the skeleton is termed disuse osteoporosis. Disuse results in bone loss due to bone resorption exceeding formation (Weinreb et al. 1989; Bain and Rubin 1990; Zerwekh et al. 1998; Rantakokko et al. 1999; Li et al. 2005b).

Disuse osteoporosis affects astronauts and chronically immobilised patients, such as those suffering from spinal cord injury or stroke (Szollar et al. 1998; Kanis et al. 2001; Wang et al. 2001). Disuse results in an increased fracture risk (Vestergaard et al. 1998; Kanis et al. 2001) as a result of decreased mineral density (Kaneps et al. 1997; Lang et al. 2004) and a loss of trabecular architecture (Li et al. 2005a) and bone strength (Kaneps et al. 1997; Li et al. 2005b).

1.2.1.4 Treatments for osteoporosis

The majority of currently available therapeutics for osteoporosis target bone resorption. Anti-resorptives such as oestrogen, selective oestrogen receptor modulators, calcitonin and the bisphosphonates have had a major impact on osteoporosis treatment; however no dramatic increases in bone mass are achieved. Bisphosphonates are the first line of treatment for osteoporosis and this class of drugs are stable structural analogues of inorganic pyrophosphate that selectively adsorb to mineral surfaces (Jung et al. 1973). Bisphosphonates are internalised by bone resorbing osteoclasts and interfere with various biochemical processes within these cells to inhibit bone resorption (reviewed in (Russell 2007)). Bisphosphonates accumulate in bone, for years after treatment is discontinued (Lin 1996; Khan et al. 1997; Papapoulos and Cremers 2007), and the stored drug can be released by continued remodelling allowing for persistent metabolic effects (Rodan 1997). This chronic suppression of bone remodelling has led to concerns surrounding the long-term use of these drugs. Furthermore, there is some evidence to suggest that bisphosponate treatment is linked to osteonecrosis of the jaw (Marx 2003; Ruggiero et

al. 2004; Marx et al. 2005). Though, this has been more commonly reported for cancer patients receiving bisphosphonate treatment than patients with postmenepausal osteoporosis or Paget's disease receiving the same therapy (reviewed in (Silverman and Landesberg 2009)).

Growth hormone, PTH and the statins represent potentially important anabolic agents (Rosen and Bilezikian 2001). Teriparatide (Forteo) marketed by Eli Lilly is the only anabolic agent currently approved by the food and drug administration (FDA) for the treatment of osteoporosis. It is a recombinant portion of human PTH (rhPTH1-34) which is a major regulator of calcium and phosphate metabolism in bone and kidney. Teriparatide stimulates new bone formation (Dempster et al. 2001; Neer et al. 2001; Rubin and Bilezikian 2003; Sato et al. 2004) however it is only used for the treatment of advanced osteoporosis, requires daily injection and is very expensive. Furthermore, its use is restricted to 18 months in Europe as a result of studies in rats that indicated an increased risk of osteosarcoma, and other animal studies that have demonstrated increased growth of tumours following treatment with PTH (Vahle et al. 2004; Schneider et al. 2005; Tashjian and Gagel 2006).

Promising new anabolic agents that encourage bone formation are under development, such as antibodies to RANK-L and sclerostin (McClung 2006; Ominsky 2006; Padhi 2007).

Denosumab is a human monoclonal antibody to RANK-L that mimics the action of OPG by binding RANK-L and preventing the activation of osteoclasts. In published phase II and phase III trials, denosumab was tested for safety and efficacy in postmenopausal women with low bone density and found to inhibit bone resorption and remodelling as measured by decreased markers of bone turnover and increased bone mineral density, particularly of the lumbar spine (McClung 2006; Lewiecki et al. 2007; Bone et al. 2008; Miller et al. 2008; Brown et al. 2009).

Sclerostin is an osteocyte-specific glycoprotein and acts as a negative regulator of bone formation by inhibiting osteoblast differentiation (Winkler et al. 2003; van Bezooijen et al. 2004; Poole et al. 2005). The Wnt signalling pathway promotes the differentiation of osteoblasts and sclerostin blocks this pathway by binding to low density lipoprotein receptor-related protein 5/6 (LRP5/6) (Li et al. 2005c; Semenov et al. 2005; Semenov and He 2006). Sclereostosis and Van Buchem are diseases of very high bone mass characterised by mutations in the *SOST* gene which reduce the levels of the biologically active protein sclerostin (section 1.2.1.1.2-3) (Balemans et al.

2001; Brunkow et al. 2001). Monoclonal antibodies to sclerostin aim to mimic its down-regulation in response to conditions that promote bone formation i.e. mechanical load and PTH (Bellido et al. 2005; Keller and Kneissel 2005; Robling et al. 2006). Studies with a humanised monoclonal antibody to sclerostin in ovariectomised female rats, postmenopausal women and primates have shown anabolic bone activity and increased bone mass (Ominsky 2006; Padhi 2007; Ominsky et al. 2010).

Since teriparatide is currently the only FDA-approved anabolic therapy for osteoporosis and its window of use is limited, there is a clear clinical need for the development of new anabolic bone agents. Understanding the molecular pathways that regulate osteoblast bone formation and therefore bone density and resistance to fracture is critical for the identification of new approaches to treat osteoporosis. The glutamate signalling pathway in bone has been proposed as a novel target for anabolic bone therapies (Mason et al. 1997; Spencer et al. 2004). Glutamate signalling has been implicated in the mechanoresponse (Mason et al. 1997) and modulation of this pathway may offer the opportunity to prime the skeleton to mimic or enhance the

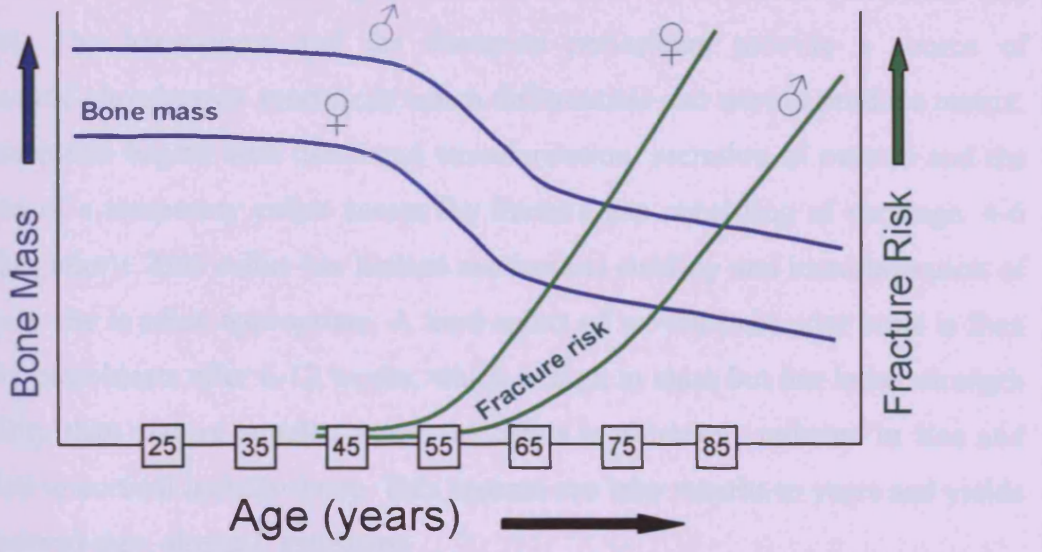

Figure 1.4. Decrease in bone mass and increase in fracture risk with age. The reduction in bone mass with age means that our ageing demographic will lead to an increased number of individuals at risk of fracture. Figure adapted from (Valsamis et al. 2006)

appropriate osteogenic response to mechanical stimulation (Mason 2004b; Spencer et al. 2004). Mechanisms to modulate the glutamate signalling pathway to this end will be addressed in the experimental portions of this thesis.

1.2.1.5 Fracture

1.2.1.5.1 Normal bone repair

During normal bone repair following fracture, the mechanisms regulating osteogenesis during embryological development are recapitulated (section 1.1.2.2) (Ferguson et al. 1999). The majority of fractures heal by indirect repair involving endochondral ossification and the formation of a callus (Einhorn 1998). There are three main phases of normal bone healing: inflammation, repair and remodelling (reviewed in (Greenbaum and Kanat 1993; Gerstenfeld et al. 2003) and summarised below). Inflammation occurs during the first two weeks after injury and is initiated after haemorrhage due to vascular injury and the formation of a haematoma. The haematoma provides a small amount of mechanical stability to the fracture site and also allows inflammatory cells and fibroblasts to infiltrate into the area. Vascularisation then occurs and granulation tissue forms at the fracture site (the procallus). The haematoma and the disrupted periosteum provide a source of osteoblast and chondrocyte precursors which differentiate and start to produce matrix. The repair phase begins with continued vascularisation, secretion of osteoid and the generation of a temporary callus across the fracture gap consisting of cartilage, 4-6 weeks after injury. This callus has limited mechanical stability and immobilisation of the fracture site is often appropriate. A hard callus of woven trabecular bone is then formed by osteoblasts after 6-12 weeks, which is high in mass but has lower strength and stability than mature lamellar bone; the callus is ultimately reduced in size and remodelled to cortical lamellar bone. This process can take months to years and yields bone of normal size, strength and shape.

1.2.1.5.2 Non-union fracture

More than one million fractures occur in the UK each year and 5-10% of these experience problems in healing (Gaston and Simpson 2007). This percentage is likely

to increase as the population ages and fragility fractures become more common (Gaston and Simpson 2007). Fractures that are slow to heal (delayed union) or fail to heal (non-union) can occur in any bone but are most likely in the tibia, talus, humerus and fifth metatarsal bone. Several factors contribute to a non-union including infection, mechanical instability, inadequate vascularity at the fracture site and systemic causes such as malnutrition, comorbidities, smoking and medications (Venkatachalapathy et al. 2007).

Non-unions are typically classified as hypertrophic or atrophic according to radiographic information. Hypertrophic non-union presents with decreased callus formation and an elephant-foot configuration at the fracture site. This type of non-union appears to have an appropriate healing response and blood supply but is linked to inadequate immobilisation (Megas 2005). Atrophic non-unions show little callus formation surrounding a fracture gap filled with fibrous tissue. Atrophic non-unions are typified by inadequate vascularisation or insufficient availability of bone forming cells or both, preventing normal bone healing from occurring (Megas 2005). This type of non-union is common following a high-energy injury, an open fracture, an infected fracture or following multiple failed internal fixation procedures (Dagrenat 2002).

1.2.1.5.2.1 Treatment for non-union fracture

Treatment of hypertrophic non-unions involves the placement of stable fixation (nail, plate, or an external fixator) to provide stability and improve the mechanical environment without disrupting the blood supply. Atrophic non-unions require both mechanical stability and an adequate biological environment at the fracture site. Autologous bone grafts are commonly employed and represent a source of MSCs, scaffolding and growth factors e.g. BMPs, to enhance bone formation (Canalis et al. 1989; Megas 2005; Phieffer and Goulet 2006). However, this strategy is restricted by donor site morbidity (Younger and Chapman 1989) and limited availability. Recombinant human BMP-2 (rhBMP-2; INFUSE® Bone Graft, Medtronic Spinal and Biologics) and BMP-7 (rhBMP-7; OP-1, Stryker) represent commercially available bone graft substitutes that are osteoinductive and have therapeutic application to treating non-union fracture. Both proteins are delivered on an absorbable collagen sponge and rhBMP-2 is currently FDA approved for use in spinal fusion, fresh tibial

fractures, and oral maxillofacial bone grafting procedures whereas BMP-7 is FDA approved for long bone non-union and spinal fusion.

Non-invasive stimulation such as low-intensity pulsed ultrasound (Heckman et al. 1994; Gebauer et al. 2005; Rutten et al. 2007) and electrical stimulation (Brighton et al. 1975; Connolly 1981) can also provide alternative treatments for non-union.

1.3 Mechanical loading

The importance of mechanical strain on the maintenance of bone architecture and adequate bone mass has been demonstrated by numerous animal and human studies. There is a dynamic relationship between bone structure and its mechanical environment allowing bone to functionally adapt. This is most notable in examples of load-bearing exercise-induced increases in bone mass (Jones et al. 1977; Smith and Gilligan 1996) and the reduction in bone mass associated with reduced load-bearing typical of astronauts in weightless environments for extended periods of time (Donaldson et al. 1970; Smith and Gilligan 1996). High strain rates and short periods of loading have been identified as the mechanical loading parameters required to achieve a maximal osteogenic response (reviewed in (Skerry 1997; Burr et al. 2002)). The mechanoresponsive signalling pathways which convert mechanical load to cellular signals to account for this biological phenomenon are unclear, although there is evidence to suggest that osteocytes are the mechosensory cells in bone (Skerry et al. 1989; Klein-Nulend et al. 1995; Mullender and Huiskes 1995; Lanyon 1996; Noble et al. 1997; Burger and Klein-Nulend 1999). Osteocytes are ideally situated to respond to mechanical load by transmitting osteogenic signals through their canalicular syncytium to cells at the bone surface which then release paracrine factors such as prostaglandins, nitric oxide (NO) and IGFs that signal progenitor cells to differentiate into bone-forming osteoblasts and inhibit osteoclastogenesis (Duncan 1995; Duncan and Turner 1995; Pitsillides et al. 1995; Burger and Klein-Nulend 1999; Ehrlich and Lanyon 2002; Rubin et al. 2003). Blockade of the gap junctions that exist between osteocytes and osteoblasts (Doty 1981) affects the response of bone to mechanical load (Li et al. 2006).

Osteocytes respond to short periods of load *in vivo* by increasing transcriptional and metabolic activities (Pead et al. 1988; Skerry et al. 1989). The physical signal that

prompts these responses is not known; strain resulting from stress or stress induced canalicular fluid flow or both might activate bone cells (Piekarski and Munro 1977; Weinbaum et al. 1994). Chicken calvarial osteocytes experimentally exposed to fluid flow stress respond by releasing prostaglandins and NO (Klein-Nulend et al. 1995; Ajubi et al. 1999; Burger and Klein-Nulend 1999). Fluid flow stress may activate stretch activated channels (i.e. potassium channels), cell surface G-protein coupled receptors (GPCRs) or integrin receptors on osteocytes to stimulate mechanotransduction pathways (Duncan 1995).

In vivo, inhibition of prostaglandin production in rats has indicated that prostaglandins represent an essential component of the mechanotransduction pathway leading to bone formation (Chow and Chambers 1994). Both primary osteocytes and the osteocyte-like MLO-Y4 cells can be mechanically induced to synthesise and release prostaglandin E_2 (PGE_2) (Ajubi et al. 1999; Cherian et al. 2005) which increases the cell surface expression of connexin (Cx) 43 protein and the formation of hemichannels (Cherian et al. 2005). PGE_2 achieves this response by signalling through the prostaglandin EP_2 receptor and the subsequent activation of cyclic adenosine 3',5'-monophosphate (cAMP)-dependent protein kinase A (PKA) (Cherian et al. 2005). Prostaglandin up-regulation in primary avian osteocytes following fluid flow stress appears to be dependent upon increased release of NO (Klein-Nulend et al. 1995). Human primary bone cell cultures constitutively express endothelial nitric oxide synthase (eNOS) (Klein-Nulend et al. 1998), and *in vivo* studies have linked increased NO production to the mechanoresponse (Fox et al. 1996; Turner et al. 1996). Expression of eNOS in endothelial cells is related to the sensitivity of these cells to blood fluid shear stress and causes NO release, up-regulated expression of prostaglandins, and induction of *c-fos* (Uematsu et al. 1995; Busse and Fleming 1998; Chien et al. 1998; Davies et al. 1999) indicating that endothelial and bone cells use similar mechanisms for sensing fluid flow stress. The *eNOS* gene contains several promoter elements that respond to shear stress and oestrogen (Hayashi et al. 1995) and expression of eNOS is upregulated in human osteoblast-like cells exposed to oestrogen (Armour and Ralston 1998). Oestrogen is known to suppress bone resorption (Christiansen et al. 1982; Wronski et al. 1988) and its loss is therefore thought to play an important role in post-menopausal osteoporosis. Oestrogen has also been implicated as a direct stimulant of osteoblast function (Samuels et al. 1999a; Tobias and Compston 1999) and its osteogenic activity can be partially suppressed by

inhibitors of NOS (Wimalawansa et al. 1996; Samuels et al. 2001) and prostaglandin synthesis (Samuels et al. 1999b). *In vivo* studies indicate that the oestrogen receptor alpha (ERα) is involved in the response of bone to mechanical strain, since primary osteoblast-like cells from ERα$^{-/-}$ mice do not proliferate in response to mechanical load and rescue of this response requires transfection of a fully functional ERα (Lee et al. 2003)

The ubiquitous amino acid glutamate has been implicated in the mechanoresponse through a gene-screening experiment designed to identify osteogenic signalling components following mechanical loading in rat ulna (Mason et al. 1997). Expression of the glutamate-aspartate transporter (GLAST) was observed to be down-regulated in osteocytes after loading (Mason et al. 1997) and during recent years the glutamate signalling pathway has received attention as a mechanism that may link mechanical loading to bone formation.

1.4 Innervation of bone

Bone marrow, mineralised bone and periosteum are densely innervated (Calvo and Forteza-Vila 1969; Bjurholm et al. 1988a; Hill and Elde 1991; Serre et al. 1999). Direct contact between nerve fibers and bone cells has been demonstrated however no typical synapses were detected (Serre et al. 1999). Some nerve fibers terminate in varicosities at the bone/periosteum interface while others run within the Haversian and Volkmann's canals of cortical bone (Hill and Elde 1991; Hukkanen et al. 1992) and are abundant along the epiphyseal trabeculae facing the growth plate and the metaphysis of long bones (Hara-Irie et al. 1996; Serre et al. 1999). Bone contains both sensory and sympathetic nerve fibers and a variety of neurotransmitters have been identified in bone by immuohistochemistry including the neuropeptides vasoactive intestinal polypeptide (VIP) (Lundberg et al. 1979; Hohmann et al. 1986; Bjurholm et al. 1988b), calcitonin gene-related peptide (CGRP) (Bjurholm et al. 1988a), pituitary adenylate cyclase activating peptides (PACAP), neuropeptide Y (Bjurholm et al. 1988b), substance P (SP) (Bjurholm et al. 1988a) and the classic neurotransmitters noradrenalin (Duncan and Shim 1977), serotonin (Bliziotes et al. 2001) and glutamate (Serre et al. 1999). Functional receptors for many of these neurotransmitters have also been detected in bone cells *in vitro* (Hohmann and Tashjian 1984; Bjurholm et al.

1992; Chenu et al. 1998; Serre et al. 1999; Westbroek et al. 2001; Elefteriou et al. 2005; Bliziotes et al. 2006). Many studies have demonstrated that the nervous system, particularly the sympathetic nervous system (SNS), influences the regulation of bone metabolism ((Takeda et al. 2002; Elefteriou et al. 2005), reviewed in (Chenu 2002; Takeda et al. 2002; Chenu 2004; Spencer et al. 2004; Elefteriou et al. 2005; Patel and Elefteriou 2007)). For example, denervation inhibits developmental skeletal growth in the rat foot (Edoff et al. 1997) and modulates the number of activated osteoclasts in the rat mandible and gerbil middle ear bulla bone (Hill and Elde 1991; Sherman and Chole 2000). Furthermore, changes in bone innervation have been associated with various skeletal pathologies including osteoarthritis, heterotopic bone formation and fracture repair (Bjurholm et al. 1990; Hukkanen et al. 1992; Hukkanen et al. 1993; Hukkanen et al. 1995; Li et al. 2001).

A central control of skeletal homeostais via the hypothalamus has been proposed (Ducy et al. 2000; Takeda et al. 2002; Elefteriou et al. 2005; Sato et al. 2007). The fat-derived hormone leptin can control bone formation through a hypothalamic relay and mice deficient in leptin display increased bone formation leading to high bone mass (Ducy et al. 2000). Binding of leptin to its hypothalamic receptor is sufficient to stimulate sympathetic nerves to release noradrenalin into the bone microenvironment and activate β2-adrenergic recpetors on osteoblasts, inhibiting their osteogenic activity and resulting in bone loss (Ducy et al. 2000; Takeda et al. 2002). Similarly, mice deficient in Y2 receptors for neuropeptide Y display a two-fold increase in trabecular bone volume and intracerebroventricular administration of neuropeptide Y leads to bone loss (Baldock et al. 2002).

However, the adaption of bone to mechanical load is highly site specific (Rubin and Lanyon 1984) and therefore unlikely to be centrally controlled (Hert et al. 1971; Pitsillides et al. 1995; Cheng et al. 1996). Innervated and denervated limbs have been shown to react to loading in the same way (Hert et al. 1971) and bone explants as well as isolated bone cells display sensitivity to mechanical stimuli, excluding the requirement of central connections (Pitsillides et al. 1995; Wada et al. 2001). Nevertheless, the expression of some of the neurotransmitter receptors in bone has been shown to be modulated by mechanical load (Chenu et al. 1998; Westbroek et al. 2001; Szczesniak et al. 2005; Bliziotes et al. 2006), supporting a role for innervation in the response of bone to mechanical stress. The direct regulation of bone by the paracrine release of neurotransmitters by nerve terminals non-synaptically is therefore

possible and gap junctions between osteoblasts and osteocytes have been proposed as a means of transmission of neuronal signals (Serre et al. 1999; Spencer and Genever 2003; Patel and Elefteriou 2007). Furthermore, bone cells are known to release glutamate in a regulated manner (Genever and Skerry 2001; Hinoi et al. 2002b) indicating that this signalling molecule might also act in an autocrine or paracrine capacity within bone.

1.5 Glutamate as a signalling mediator in bone

Functional components from each stage of the glutamate signalling pathway have been identified within bone, including proteins necessary for calcium-mediated glutamate exocytosis, receptors, transporters and signal propagation (Mason et al. 1997; Laketic-Ljubojevic et al. 1999; Gu and Publicover 2000; Genever and Skerry 2001; Hinoi et al. 2001; Gu et al. 2002; Hinoi et al. 2002b; Bhangu 2003; Mason 2004a; Takarada et al. 2004). Furthermore, glutamatergic nerves have been identified in the vicinity of bone cells expressing glutamate receptors *in vivo* (Chenu et al. 1998; Patton et al. 1998; Serre et al. 1999).

It is not yet known how a glutamate signalling event is initiated in bone or its physiological significance, however the regulation of the glutamate transporter in response to mechanical loading *in vivo* has implicated glutamate signalling in the osteogenic response to mechanical loading (reviewed in (Mason 2004a)). Glutamate signalling mechanisms are able to detect very fast stimulatory signals and self-modify, making them well-suited for responding to mechanical signalling in bone (Skerry 2002; Turner et al. 2002; Spencer and Genever 2003; Bowe and Skerry 2005). Glutamate receptor and transporter activation are modulated by previous glutamate signals, so that maximal responses can be achieved by relatively few signalling events (Gonzalez and Ortega 2000; Riedel et al. 2003; Persson et al. 2005); this potential mechanism could explain why short periods of high strain rates are all that is required for the maximal osteogenic response in bone (Skerry 1997; Burr et al. 2002).

1.5.1 Glutamatergic signalling in the central nervous system (CNS)

Upon stimulation of a pre-synaptic neuron, voltage sensitive calcium channels (VSCC) open and the ensuing Ca^{2+} influx triggers the release of glutamate into the synaptic cleft by binding to protein complexes associated with primed synaptic vesicles tethered to the pre-synaptic membrane. Glutamate acts on a variety of receptors at the post-synaptic membrane resulting in an influx of Ca^{2+} into the post-synaptic neuron and propagation of the depolarising signal. Glutamate receptors (GluRs) can be categorised into ionotropic (iGluRs) and metabotropic (mGluRs). Post-synaptic glutamate release can be inhibited by the opening of K^+ channels and the inhibitory activities of some mGluR subtypes on VSCCs. Glutamate transporters (excitatory amino acid transporters; EAATs) at the pre-synaptic and post-synaptic membrane and neighbouring glial cells terminate the signalling event by removing glutamate from the synaptic cleft. In glial cells, glutamate is converted to glutamine by glutamine synthetase (GS) for metabolic purposes or for transport to neurons where glutamine is then converted back to glutamate for excitatory signalling (Figure 1.5).

1.5.2 Glutamate signalling in peripheral tissues

There is strong evidence to suggest that glutamate signalling pathways are functional in several sites of the body besides the CNS, such as bone, skin, β-islet cells of the pancreas and megakaryocytes of the bone marrow (reviewed in (Skerry and Genever 2001; Hinoi et al. 2004)). Furthermore, expression of proteins associated with glutamatergic signalling has been identified in a variety of other tissues (e.g. intestine, heart, synovial joint, thymus, testis, kidney and lung). EAAT expression in peripheral tissues is summarised in Table 1.2.

Various iGluR and mGluR subunit mRNA has been detected in the patella, fat pad, cartilage and meniscus of the rat knee and in human articular cartilage (Salter et al. 2004; Hinoi et al. 2005b; Flood et al. 2007). Glutamate and iGluR agonists elicit increases in intracellular Ca^{2+} in fibroblast-like synoviocytes from rheumatoid arthritis (RA) patients, demonstrating functional acitivity of iGluRs (Flood et al. 2007).

Recent studies implicate peripheral glutamatergic signalling in arthritis, gout and cancer (McNearney et al. 2000; Rzeski et al. 2002; McNearney et al. 2004; Hinoi et al. 2005b; Jean et al. 2008; Sharma et al. 2009). Glutamate concentrations increase in the synovial fluid of arthritic patients (McNearney et al. 2000) and in the dialysates of osteoarthritic (OA) rat knees (Jean et al. 2005). Glutamate is present in human synovial fluid at 6μM (Plaitakis et al. 1982; McNearney et al. 2000)), however, glutamate concentrations in the synovial fluid from human patients with RA, gout and OA can reach 332.3 ± 29.3, 364.21 ± 50.19 and 240 ± 38 μM respectively (McNearney et al. 2004). EAAT1 and 2 protein expression is significantly increased

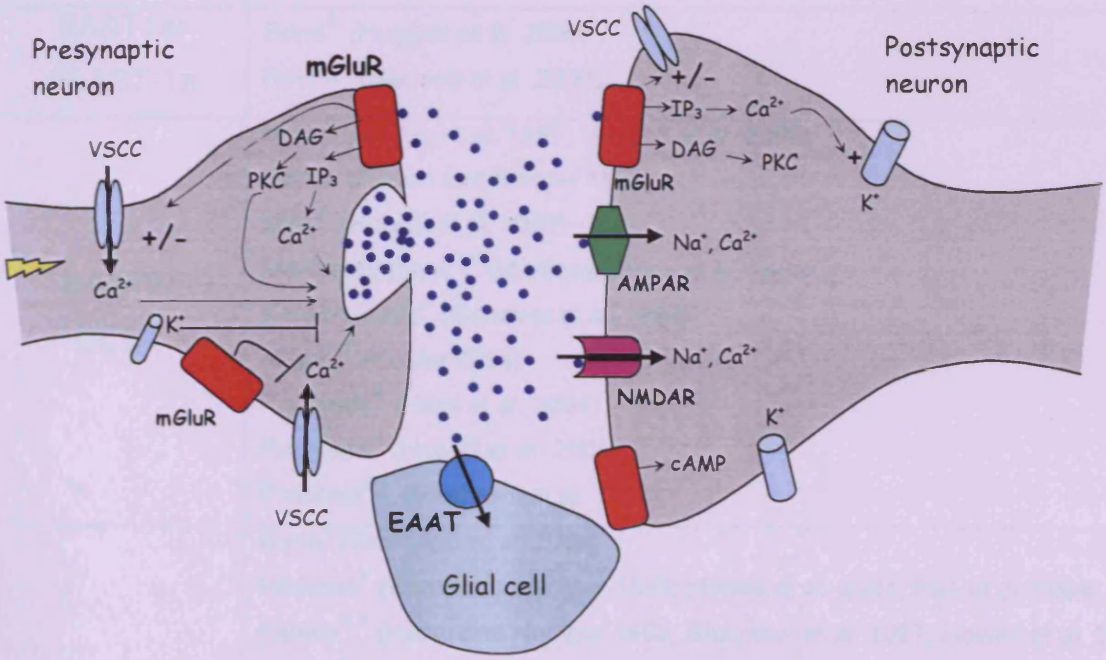

Figure 1.5. Glutamatergic signalling in the CNS. In response to depolarisation of the pre-synaptic neuron, glutamate is released into the synaptic cleft where it acts on glutamate sensitive ionotropic (NMDA, AMPA) and metabotropic receptors (mGluR) present on the post-synaptic cell. Glutamate release also triggers transporters located on the pre-synaptic cell and neighbouring glial cells, which actively remove glutamate from the synaptic cleft, terminating the signalling episode (VSCC; voltage sensitive calcium channel, EAAT; excitatory amino acid transporter, cAMP; cyclic adenosine monophosphate, DAG; diacylglycerol, PKC; protein kinase C, IP3; inositol triphosphate). Adapted from (Mason 2004a).

Table 1.2. EAAT expression in peripheral tissues. R, mRNA; P, Protein.

Transporter *Human/Rodent nomenclature*	**Tissue distribution**
EAAT1/ GLAST	Bone^{R,P} (Mason et al. 1997; Huggett et al. 2000) Retina^{R} (Rauen et al. 1996; Lehre et al. 1997; Pow and Barnett 1999) Testis^{R} (Tanaka 1993) Mammary gland^{R,P} (Martinez-Lopez et al. 1998) Placenta^{R,P} (Matthews et al. 1998) Pancreas^{R,P} (Howell et al. 2001) Heart^{R,P} (Nakayama et al. 1996; Ralphe et al. 2004) Synovial fibroblasts^{R,P} (Hinoi et al. 2005b) Cartilage^{R,P} (Hinoi et al. 2005a; Jean et al. 2008)
EAAT1a/ GLAST-1a	Bone^{R} (Huggett et al. 2000) Retina^{P} (Macnab et al. 2006)
EAAT2/ GLT-1	Bone^{R} (Mason et al. 1997; Huggett et al. 2000) Retina (Rauen and Kanner 1994) Liver^{R} (Howell et al. 2001) Mammary gland^{R,P} (Martinez-Lopez et al. 1998) Keratinocytes^{P} (Genever et al. 1999) Heart^{R,P} (Kugler 2004) Rat testis^{R} (Hinoi et al. 2004) Pancreas^{P} (Howell et al. 2001) Placenta^{R,P} (Matthews et al. 1998)
EAAT3/ EAAC1	Bone^{R} (Takarada et al. 2004) Intestine^{P} (Kanai and Hediger 1992; Howell et al. 2001; Fan et al. 2004) Kidney^{R,P} (Kanai and Hediger 1992; Shayakul et al. 1997; Howell et al. 2001) Retina^{R} (Rauen et al. 1996; Schniepp et al. 2004) Heart^{R,P} (Nakayama et al. 1996; Kugler 2004) Liver^{R,P} (Shashidharan et al. 1994; Howell et al. 2001) Mouse testis^{R} (Wagenfeld et al. 2002) Keratinocytes^{P} (Genever et al. 1999) Placenta^{R,P} (Matthews et al. 1998)
EAAT4	Placenta^{R} (Matthews et al. 1998) Bone^{R,P} (Hinoi et al. 2007; Takarada and Yoneda 2008)
EAAT5	Retina^{R,P} (Arriza et al. 1997) Liver^{R} (Arriza et al. 1997) Rat testis^{R} (Hinoi et al. 2004)

in chondrocytes of rabbit knee joints upon induction of OA (Jean et al. 2008) and EAAT uptake activity is increased in synovial fibroblasts from rats with collagen-induced arthritis (CIA) (Hinoi et al. 2005b). Cancer cell lines, including breast and prostate cancer cell lines, are known to release glutamate (Carrascosa et al. 1984; Collins et al. 1998; Sharma et al. 2009) and iGluR antagonists can inhibit tumour growth (Rzeski et al. 2001; Rzeski et al. 2002; Abdul and Hoosein 2005).

1.5.3 Glutamate signalling in bone

1.5.3.1 Glutamate release in bone

Osteoblasts express the functional components required for neuronal glutamate release including molecules involved in synaptic vesicle packaging, targeting and fusion (Bhangu et al. 2001; Bhangu 2003). Osteoblasts spontaneously release glutamate *in vitro* (Genever and Skerry 2001; Hinoi et al. 2002b) and glutamate release by rat calvarial osteoblasts is increased following depolarisation with 50mM KCl or activation of iGluRs with DL-α-amino-3-hydroxy-5-methylisoxasole-4-propionate (AMPA) (Hinoi et al. 2002b). There are some discrepancies in these studies and glutamate release appears to vary with differentiation (Bhangu et al. 2001) and the phenotype of the osteoblast-like cell (Genever and Skerry 2001). Depolarisation of the osteoblast-like cell lines MG-63 and SaOS-2 with 60mM KCl inhibits glutamate release but does not affect glutamate release by the murine calvarial-derived cell line MC3T3-E1 (Genever and Skerry 2001). The initiating stimulus for glutamate release in osteoblasts remains unclear, though a model suggested by Mason proposes that mechanical load induces opening of stretch sensitive calcium channels (SSCCs) in osteocytes, which in turn, may trigger glutamate release by osteocytes to act on receptors on surface osteoblasts (Mason 2004a).

Mature osteoclasts, but not pre-osteoclasts, release glutamate and bone degradation products from transcytotic vesicles following depolarisation with 50mM KCl and this release is dependent on extracellular Ca^{2+} (Morimoto et al. 2006).

1.5.3.2 Glutamate receptors in bone

Glutamate is the primary excitatory neurotransmitter in the central CNS and signals through glutamate receptors. These receptors can be categorised into two major groups based on sequence homologies and intracellular signalling mechanisms (Reynolds and Miller 1988; Hollmann et al. 1989; Nakanishi et al. 1999; Yoneda et al. 2001); ionotropic and metabotropic (Figure 1.6). Ionotropic GluRs can be further classified by sequence homology and agonist preference as AMPA, kainate (KA) and N-methyl-D-aspartate (NMDA) which are associated with ion channels permeable to particular cations (Wisden and Seeburg 1993; Hollmann and Heinemann 1994). Cloning studies have revealed the existence of a variety of different subtypes within each receptor family, allowing the formation of heteromeric receptors, with the precise function of the receptor being determined by its subunit composition (Monaghan et al. 1989). Furthermore, the diversity of glutamate receptor subunits is considerably increased by adenosine-to-inosine RNA editing (Higuchi et al. 1993; Bass 1995; Seeburg 1996; Seeburg et al. 1998) and alternative splicing (Pin et al. 1992; Tanabe et al. 1992; Gregor et al. 1993; Hollmann et al. 1993; Kohler et al. 1994; Pin and Duvoisin 1995; Barbon et al. 2001). This mode of regulation can yield receptor subtypes with altered expression patterns, pharmacology and signal transduction mechanisms (Sommer et al. 1990; Verdoorn et al. 1991; Burnashev et al. 1992; Kohler et al. 1993; Lomeli et al. 1994; Flor et al. 1996).

Metabotropic GluRs are G-protein coupled and are categorised into three functional groups based on their sensitivity to exogenous agonists and intracellular signalling mechanisms; group I (mGluR1 and mGluR5), group II (mGluR2 and mGluR3), and group III (mGluR4, mGluR6, mGluR7 and mGluR8) (Masu et al. 1991; Tanabe et al. 1992; Wisden and Seeburg 1993). Group I mGluRs stimulate the formation of inositol 1,4,5-triphosphate (IP3) and diacylglycerol (DAG) whereas both group II and group III mGluRs inhibit the production of intracellular cAMP. At least four splice variants have been identified for mGluR1, termed mGluR1a to mGluRd (Mary et al. 1998).

Various glutamate receptor subunits are expressed and functional in bone cells (Table 1.3). Both glutamate and NMDA elicit significant increases in membrane currents in MG-63 and SaOS-2 osteoblast-like cells (Laketic-Ljubojevic et al. 1999) and in rabbit primary osteoclasts (Espinosa et al. 1999; Peet et al. 1999), which can be inhibited by the NMDA receptor antagonist MK-801. Electrophysiological studies further

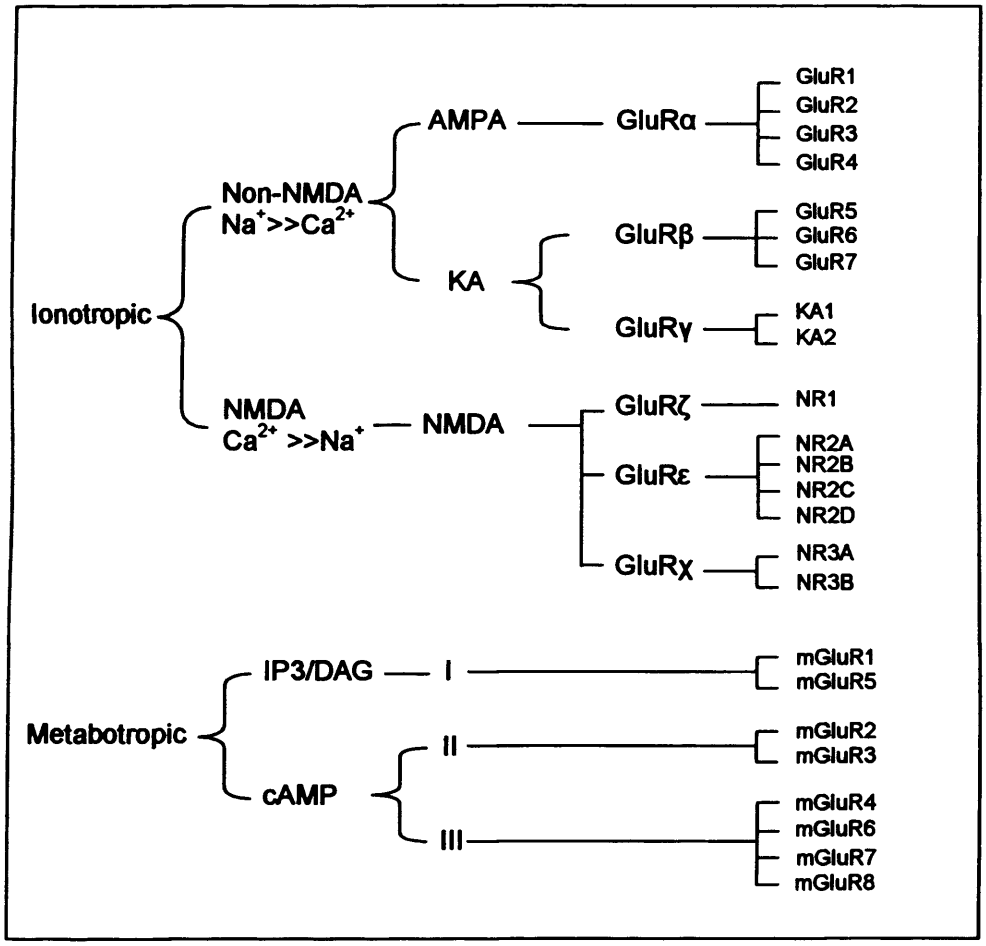

Figure 1.6. The glutamate receptor family. Glutamate receptors are classified into two major groups according to sequence homology and intracellular signalling mechanisms; ionotropic (iGluRs) and metabotropic (mGluRs). There are three subgroups of iGluRs; NMDA, AMPA and KA receptors, each of which is ion channel associated. iGluRs are divided into subtypes by sequence homology and sensitivity to exogenous agonists. mGluRs are subclassified into groups I, II and III on the basis of sensitivity to exogenous agonists and intracellular signalling mechanisms. (Adapted from (Hinoi et al. 2004)).

demonstrate that NMDA receptors are expressed and functional in primary cultures of rat osteoblasts, with electrophysiological and pharmacological characteristics similar to neuronal NMDA receptors (Gu et al. 2002). MG-63 osteoblast NMDA receptors are blocked by Mg^{2+} in a voltage-insensitive manner (Laketic-Ljubojevic et al. 1999) in contrast to primary osteoblasts, which display a 'classical' voltage sensitive Mg^{2+} block, typical of neuronal NMDA receptors (Gu et al. 2002).

Transcripts for mGluR1b have been detected in rat femoral osteoblasts (Gu and Publicover 2000) and transcripts for mGluR4 and 8 have been detected in rat calvarial osteoblasts (Hinoi 2001). Upon exposure of rat femoral osteoblasts to 1*S*,3*R*-ACPD, an mGluR agonist, elevated levels of intracelullar Ca^{2+} were observed, indicating functional group I mGluR expression (Gu and Publicover 2000). The initial phase of this response was not dependent on extracellular Ca^{2+} levels, reflecting mobilisation of Ca^{2+} from intracellular stores (Gu and Publicover 2000). In rat calvarial osteoblasts, the group III mGluR agonist L-AP4 significantly inhibited forskolin-induced cAMP accumulation in a manner that could be prevented by cotreatment with the group III mGluR antagonist CPPG, indicating functional group III mGluR expression (Hinoi 2001). Interestingly, NMDA currents in rat femoral osteoblasts that were lost upon treatment with glutamate could be restored by blockade of mGluRs with α-methyl-4-carboxyphenylglycine (MCPG), indicating that inhibitory cross talk occurs between mGluRs and NMDA receptors in osteoblasts (Gu and Publicover 2000). This crosstalk has not been demonstrated in osteoclasts indicating different glutamate-induced signalling pathways.

Expression of mGluR6 has also been detected by western blotting and RT-PCR in rat bone marrow stromal cells (Foreman et al. 2005). In these cells, treatment with glutamate resulted in inhibition of Ca^{2+} influx and subsequent membrane hyperpolarisation (Foreman et al. 2005). These effects were sensitive to the group III mGluR antagonist (s)-MAP4, suggesting that activation of mGluR6 inhibits a Ca^{2+}-permeable membrane channel (Foreman et al. 2005).

1.5.3.3 Glutamate signal propagation in bone

Expression of iGluR subunits is regulated by mechanical load in bone (Szczesniak et al. 2005). Long bones (radius/ulna, tibia/fibula) of young adult rats that were subject to cyclic compressive load for four consecutive days displayed a load-induced loss of

Table 1.3. Reported expression of glutamate receptors in bone. Transcript/protein detected (black) or not detected (red) or not investigated (-).

	Osteoblast		Osteoclast		Osteocyte	
	mRNA	***Protein***	***mRNA***	***Protein***	***mRNA***	***Protein***
NMDAR1	(Patton et al. 1998; Hinoi et al. 2001; Itzstein et al. 2001; Hinoi et al. 2003)	(Chenu et al. 1998; Patton et al. 1998; Hinoi et al. 2003)	(Patton et al. 1998; Itzstein et al. 2001; Merle et al. 2003)	(Chenu et al. 1998; Patton et al. 1998)	(Patton et al. 1998)	(Chenu et al. 1998) (Patton et al. 1998)
NMDAR2A	(Itzstein et al. 2001) (Hinoi et al. 2001; Hinoi et al. 2003)	(Hinoi et al. 2003)	(Itzstein et al. 2001) (Merle et al. 2003)	(Szczesniak et al. 2005)	-	-
NMDAR2B	(Itzstein et al. 2001) (Hinoi et al. 2001; Hinoi et al. 2003)	(Hinoi et al. 2003)	(Itzstein et al. 2001; Merle et al. 2003)	(Szczesniak et al. 2005)	-	-
NMDAR2C	(Gu and Publicover 2000) (Hinoi et al. 2001; Hinoi et al. 2003)	(Hinoi et al. 2003)	(Itzstein et al. 2001)	(Szczesniak et al. 2005)	-	-
NMDAR2D	(Patton et al. 1998; Hinoi et al. 2001; Itzstein et al. 2001; Hinoi et al. 2003)	(Itzstein et al. 2001; Hinoi et al. 2003; Ho et al. 2005)	(Itzstein et al. 2001; Merle et al. 2003)	(Itzstein et al. 2001; Ho et al. 2005)	-	-
AMPA GluR1	(Hinoi et al. 2002c)	(Chenu et al. 1998)	-	(Szczesniak et al. 2005)	-	(Chenu et al. 1998)
AMPA GluR2	(Hinoi et al. 2002c)	(Chenu et al. 1998)	-	(Szczesniak et al. 2005)	-	(Chenu et al. 1998)
AMPA GluR3	(Hinoi et al. 2002c)	-	-	(Szczesniak et al. 2005)	-	-
AMPA GluR4	(Hinoi et al. 2002c)	-	-	(Szczesniak et al. 2005)	-	-

	Osteoblast		Osteoclast		Osteocyte	
	mRNA	*Protein*	*mRNA*	*Protein*	*mRNA*	*Protein*
KA1	(Hinoi et al. 2002b)	-	-	-	-	-
KA2	(Hinoi et al. 2002b)	-	-	-	-	-
Kainate GluR5	(Hinoi et al. 2002c)	-	-	(Szczesniak et al. 2005)	-	-
Kainate GluR6	(Hinoi et al. 2002c)	-	-	(Szczesniak et al. 2005)	-	-
Kainate GluR7	(Hinoi et al. 2002c)	-	-	(Szczesniak et al. 2005)	-	-
mGluR1a	(Gu and Publicover 2000)	-	-	-	-	-
mGluR1b	(Gu and Publicover 2000)	-	-	-	-	-
mGluR2	(Gu and Publicover 2000; Hinoi et al. 2001)	-	-	-	-	-
mGluR3	(Gu and Publicover 2000; Hinoi et al. 2001)	-	(Morimoto et al. 2006)	(Morimoto et al. 2006)	-	-
mGluR4	(Hinoi et al. 2001) (Gu and Publicover 2000)	-	(Morimoto et al. 2006)	(Morimoto et al. 2006)	-	-
mGluR5	(Gu and Publicover 2000; Hinoi et al. 2001)	-	(Morimoto et al. 2006)	-	-	-
mGluR6	(Gu and Publicover 2000; Hinoi et al. 2001)	-	-	-	-	-
mGluR7	(Hinoi et al. 2001)	-	-	-	-	-
mGluR8	(Hinoi et al. 2001)	-	(Morimoto et al. 2006)	(Morimoto et al. 2006)	-	-

Table 1.4. Reported expression of glutamate transporters in bone. Transcript/protein detected (black) or not detected (red) or not investigated (-).

	Osteoblast		Osteoclast		Osteocyte	
	mRNA	*Protein*	*mRNA*	*Protein*	*mRNA*	*Protein*
EAAT1/ GLAST	(Mason et al. 1997; Huggett et al. 2000; Kalariti et al. 2004; Takarada et al. 2004; Kalariti et al. 2007)	(Mason et al. 1997; Kalariti et al. 2004; Kalariti et al. 2007)	(Takarada and Yoneda 2008)	-	(Mason et al. 1997; Huggett et al. 2000)	(Mason et al. 1997)
EAAT2/ GLT-1	(Mason et al. 1997; Huggett et al. 2000; Takarada et al. 2004)	-	(Hinoi et al. 2007; Takarada and Yoneda 2008)	-	(Mason et al. 1997; Huggett et al. 2000; Hinoi et al. 2004)	-
EAAT3/ EAAC1	(Takarada et al. 2004)	-	(Takarada and Yoneda 2008)	-	-	-
EAAT4	(Takarada et al. 2004)	-	(Hinoi et al. 2007; Takarada and Yoneda 2008)	(Hinoi et al. 2007; Takarada and Yoneda 2008)	-	-
EAAT5	(Takarada et al. 2004)	-	(Takarada and Yoneda 2008)	-	-	-

immunoreactivity to GluR2/3, GluR4, GluR5/6/7 and NMDAR2A on osteoclasts and NMDAR2A, NMDAR2B, GluR2/3 and GluR4 on bone lining cells (Szczesniak et al. 2005). However, Ho et al. have reported downregulation of NMDAR1 and NMDAR2D mRNA and protein expression in osteoblasts, but not osteoclasts, in association with disuse-induced bone loss in rats following a three-week tail suspension (Ho et al. 2005). Expression of mGluR5 and the glutamate transporter EAAT1 have also been shown to be upregulated by glucocorticoid treatment in osteoblast-like cells (Kalariti et al. 2007).

The secondary signalling pathways following glutamate receptor activation of osteoblasts have not been well characterised, although activation of receptor associated protein kinases and translocation of the transcription factor activator protein-1 (AP-1) has been demonstrated (Taylor 2002; Lin et al. 2008). Antagonists to NMDA receptors down-regulate the transcription factor Runx2 and inhibit alkaline phosphatase activity and osteocalcin expression in rat primary osteoblasts (Hinoi et al. 2003; Ho et al. 2005). More recent studies have shown that the AMPA receptor antagonist 6-cyano-7-nitroquinoxaline-2,3-dione (CNQX) and the NMDA receptor antagonist MK-801 inhibit rat calvarial osteoblast activity and mineralisation in 510μM extracellular glutamate and that AMPA and NMDA up-regulate osteocalcin expression and mineralisation of osteoblasts in glutamate-free medium (Lin et al. 2008). The authors also demonstrated that injection of AMPA locally into the tibia of young rats increased bone volume and that this was antagonised by CNQX (Lin et al. 2008).

In mice treated with the AMPA receptor antagonist NBQX or the NMDA receptor antagonist AP5 by osmotic minipumps over 8 days, differences were observed in trabecular and cortical thickness (Burford et al. 2004). Trabecular thickness was reduced by 50% in NBQX-treated mice but not in AP5-treated mice whereas cortical thickness at midshaft sites was reduced by 40% in AP5-treated mice and increased by 30% in NBQX-treated mice (Burford et al. 2004), indicating different roles for NMDA and AMPA receptors in the regulation of trabecular and cortical bone mass (Burford et al. 2004; Skerry 2008). Skerry has also reported the generation of tissue specific NMDAR1 knockout mice under the control of the osteocalcin promoter (Skerry 2008). These mice fail to express functional NMDA receptors in osteoblasts and are born with stunted skeletons (Skerry 2008), indicative of a role for glutamate signalling in skeletal development.

Modulation of NMDA receptors in osteoclasts can also modify the cellular phenotype *in vitro*. In cocultures of mouse bone marrow leukocytes and osteoblasts in which osteoclasts differentiate, the NMDA receptor antagonist MK-801 suppressed osteoclast differentiation and reduced resorption pit formation in dentine (Peet et al. 1999). No significant effects of MK-801 upon mature osteoclast activity could be discerned in this study (Peet et al. 1999), although others have reported that MK-801 inhibits mature rabbit osteoclast activity (Chenu et al. 1998; Itzstein et al. 2000) and promotes apoptosis, via decreased NO production (Mentaverri et al. 2003). Glutamate and NMDA receptor agonists induced nuclear translocation of nuclear factor-kappaB (NF-κB) in osteoclast precursor cell lines, and this was inhibited by MK-801 (Merle et al. 2003) indicating that activation of this pathway is involved in osteoclastogenesis in response to glutamate receptor signalling.

1.5.3.4 Glutamate transporters

1.5.3.4.1 General overview

A variety of proteins with the capacity to transport glutamate have been described. These include the high affinity transporters, low affinity transporters, cystine/glutamate antiporters and vesicular glutamate transporters (reviewed in (Danbolt 2001)). The high affinity glutamate transporters (K_M 1-100μM) are termed excitatory amino acid transporters (EAATs) and are sodium dependent. EAATs exhibit a preference for L-glutamate, D- and L-aspartate and are classified into five subtypes in human (EAAT 1, EAAT2, EAAT3, EAAT4, and EAAT5) (Arriza et al. 1994; Fairman et al. 1995; Arriza et al. 1997). Rodent homologues to EAATs 1-3 are termed GLAST, glutamate transporter-1 (GLT-1) and excitatory amino acid carrier (EAAC1) respectively (Kanai and Hediger 1992; Pines et al. 1992; Storck et al. 1992; Tanaka 1993), and studies performed in human or rodent will be described here using the appropriate nomenclature for the species. Sodium-dependent transport systems are referred to by capital letters, which for dicarboxylic amino acid transporters such as the EAATs is 'X' (Bannai et al. 1984; Danbolt 2001). Sodium-independent uptake systems are instead referred to by lower case letters (Bannai et al. 1984; Danbolt 2001). The charge of the amino acid transported is indicated by +/- as superscript and the letters A, G or C in subscript denote the preferred substrates aspartate, glutamate

or cystine respectively. Therefore EAATs can be referred to as X^-_{AG}, while the sodium-independent cystine/glutamate antiporter is referred to as x^-_C (or x^-_{CG}). The EAAT subtypes display heterologous spatial and cellular expression profiles (Danbolt 2001) indicating a complex and finely tuned control over extracellular glutamate levels. This thesis will focus on the role of EAATs in bone and EAAT expression profiles, activity, and structure will be described in subsequent sections.

Low-affinity glutamate transporters (K_M > 500μM) (Johnston 1981) have been described as sodium-independent and sensitive to inhibition by D-glutamate (Benjamin and Quastel 1976) and L-homocysteic acid (Cox et al. 1977). These transporters may provide cells with amino acids for metabolic purposes (reviewed in (Erecinska and Silver 1990)) though the existence of these transporters as separate entities remains controversial (Wheeler 1987; Robinson et al. 1991; Robinson et al. 1993).

Cystine/glutamate antiporters are sodium-independent, chloride-dependent high-affinity glutamate transporters that have been described in a variety of tissues including bone (Bannai and Kitamura 1980, 1981; Waniewski and Martin 1984; Bannai 1986; Cho and Bannai 1990; Sato et al. 1999). The transporter is a heterodimer of the CD38 heavy chain (also called 4F2hc) and the x^-_C (referred to as xCT) light chain which determines the substrate specificity. Cystine (the dimeric form of cysteine) is necessary for the generation of the tripeptide antioxidant glutathione (γ-Glu-Cys-Gly; GSH) (reviewed in (Cooper and Kristal 1997; Dringen 2000)).

Vesicular glutamate transporters (VGLUTs) are necessary for the condensation of glutamate into vesicular compartments for exocytic release. Within the CNS, VGLUT1 (also called brain-specific Na^+-dependent inorganic phosphate transporter, BNPI) and VGLUT2 (also called differentiation-associated Na^+-dependent inorganic phosphate cotransporter, DNPI) are restricted to glutamatergic neurons (Fremeau et al. 2001; Herzog et al. 2001) and heterologous expression of either is capable of converting inhibitory neurons into excitatory ones (Takamori et al. 2000, 2001; Kaneko and Fujiyama 2002). VGLUT3 is expressed by a variety of cell types that reportedly release glutamate via exocytosis such as dopaminergic, gamma-aminobutyric acid (GABA)-ergic and serotonergic neurons and astrocytes (Fremeau et al. 2002; Schafer et al. 2002).

A sodium-dependent transporter for cystine, glutamate and aspartate has also been detected in rat alveolar type 2 cells and in astrocytes (Bukowski et al. 1995; Bender et

al. 2000) and high affinity sodium-dependent heterocarriers have been identified for glutamate and ascorbate (Grunewald 1993), for glutamate and GABA and for glutamate and glycine, however these have not been fully characterised (Levi et al. 1976; Bonanno et al. 1993; Bonanno and Raiteri 1994).

1.5.3.4.2 Role of glutamate transporters in bone

Despite EAATs being the first component of glutamatergic signalling to be identified in bone, studies elucidating their role within this tissue have been limited.

The cystine/glutamate antiporter is expressed and functionally required for the cellular differentiation of pre-osteoblasts, pre-osteoclastic RAW264.7 cells and primary osteoclasts differentiated from bone marrow precursor cells (Hinoi et al. 2007; Takarada-Iemata et al. 2010). Differentiation was inhibited by high glutamate concentrations (over 500μM) in a manner that was sensitive to inhibitors of the antiporter (Hinoi et al. 2007; Takarada-Iemata et al. 2010). High concentrations of extracellular glutamate are likely to result in cystine being released from the cell, which will result in reduced levels of cystine available to generate GSH. Reduced levels of GSH can also lead to cell death due to oxidative stress (Murphy et al. 1989; Cho and Bannai 1990). Indeed, expression of the cystine/glutamate antiporter has also been reported in MC3T3-E1 osteoblast-like cells where it is thought to mediate the suppression of proliferation following treatment with exogenous glutamate in association with decreased levels of intracellular GSH (Uno et al. 2007).

Expression of VGLUT1, but not VGLUT2, has been detected in rat calviarial osteoblasts (Hinoi et al. 2002b) and glutamate release in these cells was Ca^{2+} dependent and sensitive to AMPA antagonists (Hinoi et al. 2002b). VGLUT1 is also expressed by mature osteoclasts derived from bone marrow and is thought to accumulate glutamate into transcytotic vesicles for release, with bone degradation products, upon stimulation with 50mM KCl or ATP in a Ca^{2+} dependent manner (Morimoto et al. 2006). Glutamate released from osteoclasts by transcytosis may be autoregulatory, since agonists to osteoclastic mGluR8 inhibits secretion of glutamate and bone degradation products whereas mGluR8 antagonists stimulate bone resorption (Morimoto et al. 2006).

1.5.3.4.3 EAATs in bone

GLAST was the first glutamate transporter to be isolated from bone, leading to the hypothesis that glutamate may act as a signalling molecule in the skeleton (Mason et al. 1997). GLAST and GLT-1 are expressed in bone *in vivo* (Mason et al. 1997) and EAAT3 has been detected in rat primary osteoblasts *in vitro* (Takarada et al. 2004). Reported expression of EAAT subtypes in bone is summarised in Table 1.4.

GLAST is expressed by osteocytes and bone-forming osteoblasts *in vivo* and its expression in osteocytes is down-regulated following mechanical load (Mason et al. 1997). The GLAST proteins in bone and brain are identical in sequence and monomers have been identified of the same molecular weight in both tissues (Huggett et al. 2000; Huggett et al. 2002; Mason and Huggett 2002).

In 2001, Gray et al. reported that GLAST knockout mice displayed little difference to wild-type siblings in mandibular and long bone length and thickness at two weeks, three months and six months old. The study also claimed that long bones from knockout mice at the age of three months could not be distinguished morphologically from wild-type mice by scanning electron microscopy on the basis of trabeculation within the marrow cavity, cortical thickness, or areas of formation versus resorption on the midshaft, however these assessments were carried out on only one mouse from each genotype. High resolution x-ray tomography was used to image femora from two knockout and one wild-type mouse at the age of three months and no differences in cortical thickness, trabecular distribution or density were observed between the two genotypes. These assessments contributed to the authors' conclusion that glutamate does not play a major role in controlling bone growth. Chenu et al. and Skerry et al. argued that the lack of an abnormal bone phenotype in these knockout mice was not necessarily indicative of a minor role for glutamate in bone, and that functional studies would be more informative. One example of this would be to analyse GLAST knockout mice with reference to their mechanoresponse since glutamate has been implicated in bone cell signalling following mechanical load (Mason et al. 1997; Szczesniak et al. 2005). Furthermore, the expression of a variety of different glutamate transporters and receptors in bone suggests that several glutamatergic signalling pathways exist and so the likelihood of redundancy in this system is high (Mason et al. 1997; Gu and Publicover 2000; Itzstein et al. 2001). For example, in GLAST knockout mice, a compensatory role for GLT-1 was discovered which

resulted in a lack of neurodegeneration or a behavioural phenotype in these mice (Stoffel et al. 2004).

Various studies have shown that glutamatergic signalling can influence bone cell phenotype (Itzstein et al. 2000; Taylor 2002; Hinoi et al. 2003; Merle et al. 2003; Lin et al. 2008) and this signalling pathway has been associated with mechanically-induced osteogenesis (Mason et al. 1997; Szczesniak et al. 2005) and increased osteoblast bone-forming activity (Hinoi et al. 2003; Lin et al. 2008). While the specific role of the EAATs in bone remains controversial (Chenu et al. 2001; Gray et al. 2001; Skerry et al. 2001), the regulation of EAAT expression by mechanical load indicates that the transport system may represent a new target for anabolic bone therapies (Mason et al. 1997; Chenu 2002; Mason 2004a; Spencer et al. 2004).

1.5.3.4.4 EAAT function

In the CNS, extracellular glutamate concentrations are tightly controlled by high affinity, sodium-dependent glutamate transporters. Glutamate uptake terminates a glutamatergic signalling event and prevents glutamate reaching excitotoxic concentrations (Marcaggi and Attwell 2004). Defective EAAT function and excitotoxicity leading to neuronal cell death are thought to underlie the pathogenesis of stroke-induced ischemic brain damage (Kuwahara et al. 1992; Rossi et al. 2000), epilepsy (Meldrum 1994; Tanaka et al. 1997; Meldrum et al. 1999; Guo et al. 2010) and a number of neurodegenerative disorders of the CNS including amylotrophic lateral sclerosis (ALS) (Rothstein et al. 1995; Rothstein et al. 1996; Howland et al. 2002), Alzheimer's disease (Scott et al. 1995; Scott et al. 2002; Maragakis and Rothstein 2004) and Parkinson's disease (Blandini et al. 1996; Chase et al. 2000).

EAATs transport glutamate against its concentration gradient. Three sodium ions and one proton are co-transported with glutamate and one potassium ion is counter-transported leading to a net positive charge moving into the cell (Figure 1.7) (Zerangue and Kavanaugh 1996). Transport is therefore dependent upon the maintenance of an electrochemical gradient across the cell membrane by ion exchange pumps such as Na^+/K^+-ATPase (Schousboe and Divac 1979; Danbolt 2001). EAATs are also able to function as ion channels whereby sodium-dependent glutamate binding initiates an uncoupled anion conductance (Seal and Amara 1999; Slotboom et al. 2001b) that is physiologically measurable at some synapses (Billups

et al. 1996; Eliasof and Jahr 1996). Both Na^+ and glutamate binding is necessary for anion conductance, although transport is unecessary (Fairman et al. 1995; Wadiche et al. 1995; Billups et al. 1996; Wadiche and Kavanaugh 1998; Slotboom et al. 2001b). A chloride leak conductance has also been reported for the EAATs that is independent of glutamate and Na^+ binding (Otis and Jahr 1998; Wadiche and Kavanaugh 1998; Grewer et al. 2000). The physiological role of the glutamate- and Na^+-dependent anion conductance is unclear, though it has been suggested that it may function as a voltage clamp (Billups et al. 1996; Eliasof and Jahr 1996), whereby the flow of chloride ions may compensate for the membrane potential changes due to electrogenic glutamate uptake by EAATs. The net positive charge

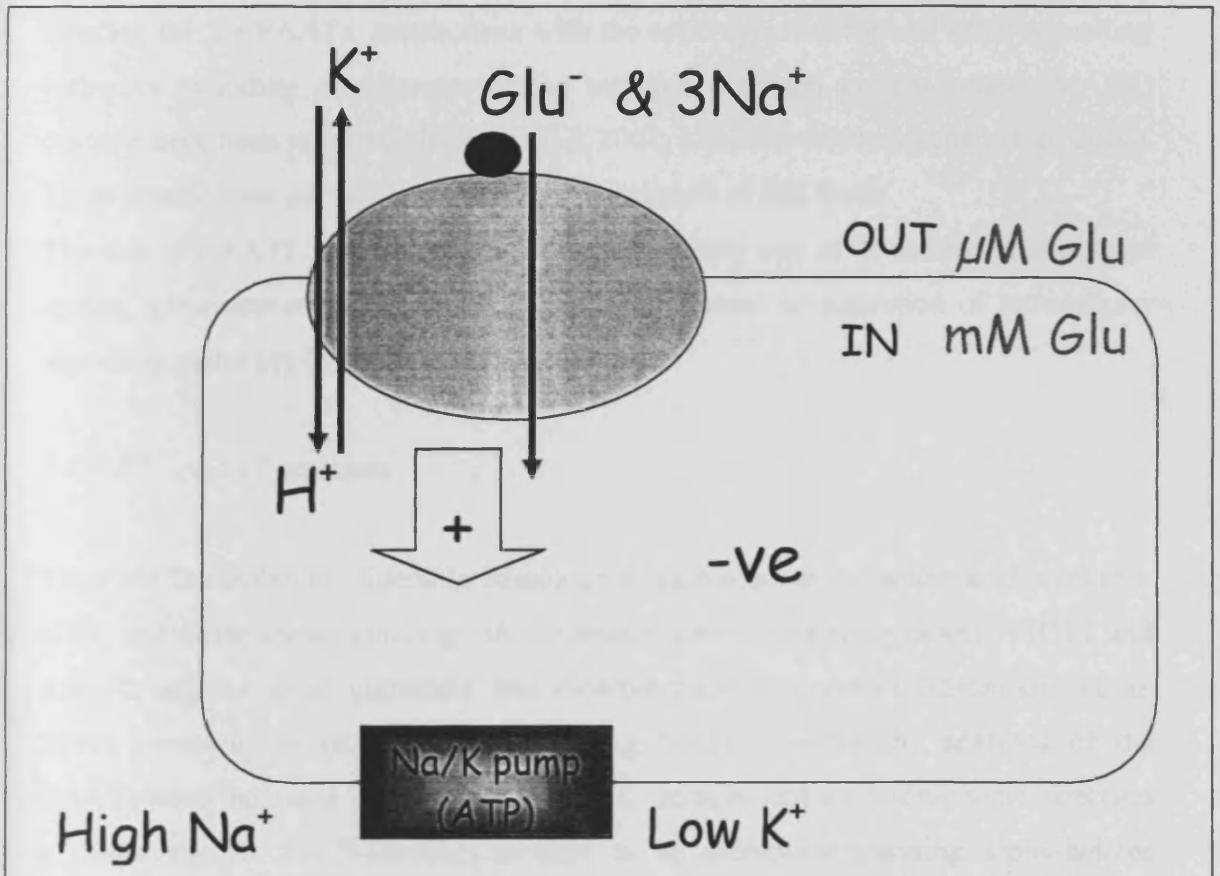

Figure 1.7. Glutamate transport by EAATs. Extracellular glutamate binds to the EAAT and is transported against its concentration gradient. Three sodium ions and one hydrogen ion are co-transported with the glutamate and one potassium ion is counter transported, resulting in a net positive charge moving into the cell. Glutamate transport is therefore driven by an electrochemical gradient across the cell membrane which is primarily maintained by the sodium/potassium ATPase pump. (Figure from (Mason 2004a)).

moving into the cell upon glutamate transport by EAATs will induce depolarisation of the cell membrane and chloride ion entry could provide a hyperpolarising influence on the cell membrane that counters this effect. The chloride conductance may also modulate glutamate receptor activity and therefore the excitatory responses of the cell or operate more like a receptor, activating intracellular signalling cascades in response to glutamate binding (Danbolt 2001; Mason and Huggett 2002). Chloride channel activity varies between different members of the EAAT family, with anion conductance particularly prominent in EAAT4 and EAAT5 and almost nonexistent in EAAT2 (reviewed in (Danbolt 2001)).

In addition to transport and ion channel activities, protein-protein interactions with both N- and C- terminal domains of the EAATs suggest a potential receptor-like function for the EAATs. Interactions with the actin cytoskeleton and other signalling pathways including components of the mitogen activated protein-kinase (MAPK) cascade have been reported (Jackson et al. 2001; Lin et al. 2001; Macnab et al. 2006). These interactions are discussed further in Chapter 6 of this thesis.

The role of EAAT1 in bone may be a function of any one of its activities; glutamate uptake, glutamate release, glutamate-gated ion channel or activation of intracellular signalling pathways (Mason 2004a).

1.5.3.4.5 EAAT structure

The EAATs display considerable homology to each other at the amino acid level (50-60%) and share some homology to the neutral amino acid transporters ASCT1 and ASCT2 and bacterial glutamate and dicarboxylate transporters ((Slotboom et al. 1999), reviewed in (Ryan and Vandenberg 2005)). Hydropathy analyses of the EAATs have indicated cytoplasmic N- and C- termini and six hydrophobic stretches of sequences at the N-terminal thought to be membrane-spanning alpha-helices (Slotboom et al. 2001a). Little is known regarding the topology of the C-terminal region, however its sequence is highly conserved and it contains a number of residues that are important for glutamate binding and ion transport (Vandenberg et al. 1995; Grunewald et al. 1998; Seal and Amara 1999; Bendahan et al. 2000; Grunewald and Kanner 2000; Seal et al. 2000; Borre et al. 2002; Ryan and Vandenberg 2002). Figure 1.8 displays a proposed transmembrane topology of the EAATs which follows the Grunewald and Kanner model of two re-entrant loops at the C-terminus that forms a

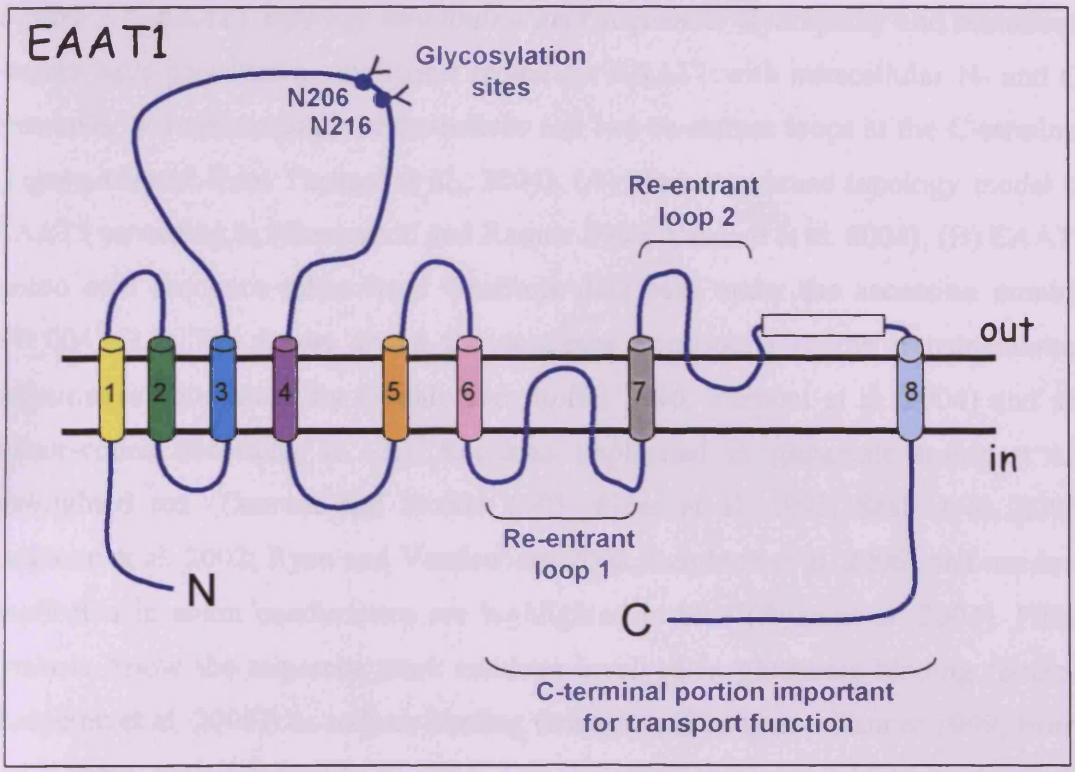


```
  1 MTKSNGEEPKMGGRMERFQQGVRKRTLLAKKKVQNITKEDVKSYLFRNAFVLLTVTAVIV
                                 *A

 61 GTILGFTLRPYRMSYREVKYFSFPGELLMRMLQMLVLPLIISSLVTGMAALDSKASGKMG
                                                    *C

121 MRAVVYYMTTTIIAVVIGIIIVIIIHPGKGTKENMHREGKIVRVTAADAFLDLIRNMFPP

181 NLVEACFKQFKTNYEKRSFKVPIQANETLVGAVINNVSEAMETLTRITEELVPVPGSVNG

241 VNALGLVVFSMCFGFVIGNMKEQGQALREFFDSLNEAIMRLVAVIMWYAPVGILFLIAGK

301 IVEMEDMGVIGGQLAMYTVTVIVGLLIHAVIVLPLLYFLVTRKNPWVFIGGLLQALITAL
                                       *C

361 GTSSSSATLPITFKCLEENNGVDKRVTRFVLPVGATINMDGTALYEALAAIFIAQVNNFE
                *C          *A          ●  ▲ ▲

421 LNFGQIITISITATAASIGAAGIPQAGLVTMVIVLTSVGLPTDDITLIIAVDWFLDRLRT
                ● ▲  ▲                                          ●

481 TTNVLGDSLGAGIVEHLSRHELKNRDVEMGNSVIEENEMKKPYQLIAQDNETEKPIDSET
                                                    *C

541 KM
```

Figure 1.8. EAAT1 topology and amino acid sequence. Hydropathy and mutational studies have proposed a topological model for EAAT1 with intracellular N- and C-terminals, 8 transmembrane alpha-helices and two re-entrant loops at the C-terminus (Figure adapted from Yernool et al., 2004). (A) Transmembrane topology model of EAAT1 according to (Grunewald and Kanner 2000; Yernool et al. 2004). (B) EAAT1 amino acid sequence taken from GenBank data base under the accession number NP_004163.3. The boxes above the sequence correspond to the transmembrane domains, as determined by (Wahle and Stoffel 1996; Yernool et al. 2004) and are colour-coded according to (A). Residues implicated in glutamate transport are highlighted red (Conradt and Stoffel 1995; Pines et al. 1995; Seal et al. 2001; Leighton et al. 2002; Ryan and Vandenberg 2002; Leighton et al. 2006) and residues implicated in anion conductance are highlighted in blue (Ryan et al. 2004). Filled symbols below the sequence mark residues involved in glutamate binding (circles; (Leighton et al. 2006)) or sodium binding (triangles; (Zhang and Kanner 1999; Borre and Kanner 2001; Yernool et al. 2004; Tao et al. 2006)). Exons 2-10 (exon 1 is fully contained within the 5' UTR) are in alternating colours and residues that overlap splice sites are in red. Potential phosphorylation sites for protein kinase C (PKC) and cAMP-dependent protein kinase (PKA) are identified by searching for consensus motifs (S/T-X-K/R for PKC and (R/K)2-X-(S/T) for PKA) and are denoted by stars with the appropriate subscript i.e. C and A respectively.

pore-like structure (Grunewald and Kanner 2000). Residues within transmembrane (TM) domain 2 are crucial for ion channel activity (Leighton et al. 2002; Ryan et al. 2004) and mutational studies of EAAT1 and structural analysis of the homologous prokaryotic amino acid transporter (Glt_{Ph}) has placed these residues in close spatial proximity to regions involved in glutamate binding (Ryan et al. 2004; Yernool et al. 2004). However, mutational studies of EAATs have also demonstrated that it is possible to influence one of the functions (transporter/ion channel) without affecting the other, suggesting that separate molecular determinants exist (Seal et al. 2000; Borre et al. 2002; Ryan and Vandenberg 2002, 2005). Freeze fracture electron microscopy indicated that the transporter functioned as a pentamer (Eskandari et al. 2000), however later molecular and biophysical analyses suggested that the transporter in fact functions as a trimer (Gendreau et al. 2004; Yernool et al. 2004; Grewer et al. 2005). The crystal structure of the glutamate transporter homologue from *Pyrococcus horikoshii* shows a bowl-shaped trimer with a solvent-filled extracellular baisin (Yernool et al. 2004) consistent with the idea that EAAT activity is exemplified by the alternating-access model (Yernool et al. 2004; Beart and O'Shea 2007).

1.5.3.4.6 EAAT splice variants

There have been reports of the existence of several splice variants of EAATs 1-3 (Lin et al. 1998; Nagai et al. 1998; Matsumoto et al. 1999; Meyer et al. 1999) and this is further discussed in chapter 5. Two splice variants of EAAT1 have been identified; GLAST-1a (EAAT1a) (Huggett et al. 2000) and EAAT1ex9skip (Vallejo-Illarramendi et al. 2005), both of which are expressed as proteins *in vivo* (Huggett et al. 2000; Vallejo-Illarramendi et al. 2005; Macnab et al. 2006; Macnab and Pow 2007a). Most EAAT2 and 3 splice variants exhibit little or no glutamate transport activity although they do interfere with the normal translation or post-translational processing of full-length EAATs (Lin et al. 1998; Nagai et al. 1998; Matsumoto et al. 1999; Meyer et al. 1999). Some studies report that aberrant RNA processing of EAAT2 is linked to the pathogenesis of ALS (Bai and Lipton 1998; Lin et al. 1998), whereas evidence also exists to dispute this and instead suggests that EAAT2 splice variants may have a physiological role (Nagai et al. 1998; Meyer et al. 1999; Honig et al. 2000; Flowers et al. 2001; Macnab and Pow 2007b) .

1.5.3.4.6.1 EAAT1a

EAAT1a is an alternatively spliced form of EAAT1 which lacks exon 3, and was first cloned from bone *in vivo* (Huggett et al. 2000). Exon 3 of the gene encoding EAAT1, solute carrier family 1 member 3 (*SLC1A3),* consists of 138 bases which encode 47 amino acids (61-107) (Figure 1.8) and its removal does not disrupt the open reading frame of the gene. GLAST-1a encodes a functional transporter (Mason, Huggett, Daniels, unpublished) but lacks residues encoded by exon 3 that are known to be important for ion channel activity (Ryan et al. 2004). GLAST-1a is expressed at low levels in brain, retina and bone *in vivo* (Huggett et al. 2000; Macnab et al. 2006) with higher levels of expression observed in MLO-Y4 osteocytes indicating an important role for the variant in this cell type (Huggett et al. 2002). A theoretical model of GLAST-1a topology proposes a reorientation of the protein in the membrane following the splice site, leading to an extracellular rather than an intracellular C-terminus (Huggett et al. 2000).

1.5.3.4.6.1 EAAT1ex9skip

EAAT1ex9skip, which lacks exon 9, is expressed at the mRNA level throughout the human brain at levels between 10% and 20% of the full-length EAAT1 form (Vallejo-Illarramendi et al. 2005). Of the brain tissues analysed, EAAT1ex9skip mRNA was present at highest levels in the hippocampus and at lowest levels within the cortex (Vallejo-Illarramendi et al. 2005). Exon 9 of *SLC1A3* comprises 135bp and its omission does not alter the RNA reading frame, yielding a predicted amino acid sequence that differs only from full length EAAT1 by 45 amino acids (430-474) located just prior to the last TM domain at the C-terminus (Figure 1.8) (Vallejo-Illarramendi et al. 2005). EAAT1ex9skip is translated in human embryonic kidney (HEK) cells into a protein that is retained in the endoplasmic reticulum (ER) and exerts a dominant negative effect over full-length EAAT1 function, possibly by protein-protein interactions at the ER which reduce the expression of full-length EAAT1 at the plasma membrane (Vallejo-Illarramendi et al. 2005). EAAT1ex9skip has also been detected by immunohistochemistry within the human brain, particularly cortical and collicular neurons (Macnab and Pow 2007a).

1.5.4 Therapeutic targeting of glutamate transport

In the CNS, glutamate excitotoxicity is linked to a variety of disorders and diseases including epilepsy, ischemic stroke, post-traumatic lesions, ALS, Parkinson's and Alzheimer's disease (reviewed in (Obrenovitch et al. 2000)). Drug discovery in the field of glutamate receptor antagonists has been very active over recent years, with the largest clinical trials for selective NMDA antagonists in stroke and traumatic brain injury (reviewed in (Muir 2006)). However both uncompetitive and competitive NMDA antagonists, which target the ion channel site and the glutamate binding site respectively, have exhibited adverse side effects including psychomimetic effects and increased blood pressure due to global effects on NMDA receptors throughout the CNS (Muir and Lees 1995; Menniti et al. 2000b; Menniti et al. 2000a; Lipton 2006).

Therapeutic targeting of the EAATs is in its early stages in contrast to glutamate receptors. However, regulating glutamate transport has the potential to limit these side effects, as it may be possible to reduce the pathological effects of high extracellular glutamate while still maintaining the physiological signalling role of glutamate.

The development of novel therapeutics capable of up-regulating transporter function has been proposed for the treatment of neurodegenerative diseases in which glutamate excitotoxicity has been implicated. Rothstein et al. discovered that β-lactam antibiotics were able to induce increases in EAAT2 protein levels of up to 6-fold (Rothstein et al. 2005). Of the antibiotics tested, ceftriaxone increased EAAT2 protein levels in a mouse model of ALS and prolonged survival of these mice compared to untreated animals (Rothstein et al. 2005).

Aberrant glutamate signalling is thought to be involved in the pathogenesis of schizophrenia and the expression of a number of proteins associated with the glutamatergic synapse have been found to be altered in the disease (McCullumsmith and Meador-Woodruff 2002). Levels of EAAT3 are decreased in response to antipsychotic medicines (Schmitt et al. 2003) and in the striatum in post-mortem studies of schizophrenic patients (McCullumsmith and Meador-Woodruff 2002), highlighting its role as a possible therapeutic target.

Targeted manipulation of EAATs has been proposed as a potential treatment for bone pathologies, such as osteoporosis or non-union fracture (Mason 2004a, b). Modulation of the glutamate signalling pathway in bone may offer the opportunity to activate mechanoresponsive bone formation in mechanically compromised tissue (Mason

2004b). Bone retains a 'strain memory' whereby maximal anabolic responses are induced by a limited number of loading cycles (reviewed in (Skerry 1997; Burr et al. 2002; Robling et al. 2002)). Proteins underlying the molecular mechanisms of memory in the CNS are also present in bone cells (Skerry 2002; Turner et al. 2002; Spencer and Genever 2003), suggesting that bone cells are capable of adapting their response to mechanically-induced glutamate signalling based on previous mechanical episodes (Spencer et al. 2001; Bowe and Skerry 2005). Modulation of glutamatergic signalling could artificially activate the cells to become more responsive to low levels of load, with clinical applications for increasing bone mass at mechanically compromised sites of the skeleton, such as fractures or osteoporotic tissues (Mason 2004a, b).

1.6 Hypothesis and Aims

Hypothesis:

Inhibition of glutamate transporter activity in bone cells can be used to mimic mechanical stimulation and enhance osteoblast differentiation and/or bone forming activity.

To investigate this hypothesis, the specific aims of the project were as follows:

1. To determine EAAT expression profile and glutamate transport activity in osteoblasts *in vitro.*
2. To determine whether inhibition of EAAT transport, ion channel, or N and C terminal interactions increases osteoblast differentiation and/or activity *in vitro.*
3. To determine whether increased expression of EAAT1a or EAAT1ex9skip mRNA splice variants increases osteoblast differentiation and/or activity *in vitro.*

Chapter 2: Materials and Methods

2. Materials and Methods

2.1 Materials

All reagents were from Sigma unless otherwise stated. All primers and oligonucleotides were synthesised and purified by MWG unless otherwise stated. GAPDH and 18S rRNA primer pairs were a kind donation from Dr Sophie Gilbert (Cardiff University, UK). All plasticware and consumables were certified ribonuclease (RNase)/deoxyribonuclease (DNase) free as appropriate. Dulbecco's modified Eagle's medium (DMEM), fetal bovine serum (FBS) and supplements were obtained from Gibco BRL (Invitrogen, Paisley, UK) unless otherwise stated. DMEM does not contain glutamate but does contain Glutamax® which is a more stable source of L-glutamine and so less likely to decompose to glutamate during storage, therefore minimising any potential source of exogenous glutamate. DMEM also contains pyruvate which has been shown to be essential for MC3T3-E1 osteoblast survival when cultured in DMEM (Hinoi et al. 2002a). Dialysed FBS (dFBS; 0.1μm filter, 10,000 MWt cut-off) to exclude exogenous glutamate was obtained from Sera Laboratories Ltd (Crawley, UK). Full composition of all solutions used can be found within Appendix 9.1.

2.2 Cell lines and cell culture

2.2.1 MG-63

MG-63 cells (ATCC CRL-1427) were a kind gift from Dr Bronwen Evans (Cardiff University, UK). The cells are derived from bone osteosarcoma of a 14-year old Caucasian male (Billiau et al. 1977) and exhibit an osteoblast phenotype with fibroblastic morphology. MG-63 propagation and subculture conditions were adapted from the American Type Culture Collection (ATCC) guidelines and DMEM was chosen as maintenance medium over the recommended Eagle's Minimum Essential Medium to ensure the presence of pyruvate and the minimisation of exogenous glutamate concentrations. MG-63 cells were routinely maintained in 75cm^2 culture flasks in DMEM containing Glutamax® and pyruvate and supplemented with

100U/ml penicillin, 100µg/ml streptomycin and 5% FBS at 37°C in 5% CO_2/95% air atmosphere. Medium was renewed twice a week. Cells were passaged once a week by rinsing the cell layer with 0.25% (w/v) trypsin and ethylenediaminetetraacetic acid (EDTA), and subsequent incubation at 37 °C for 5 min. Cells were collected by centrifugation and seeded with splitting ratios of approximately 1:5. Passages 18-35 were used for experiments.

2.2.2 SaOS-2

SaOS-2 cells (ATCC HTB-85) were a kind gift from Dr Bronwen Evans (Cardiff University, UK). The cells are derived from bone osteosarcoma of a 11-year old Caucasian female (Fogh et al. 1977) and exhibit an osteoblast phenotype with epithelial morphology. SaOS-2 propagation and subculture conditions were adapted from the ATCC guidelines and DMEM was chosen as maintenance medium over the recommended McCoy's 5a Medium Modified to ensure the presence of pyruvate and the minimisation of exogenous glutamate concentrations. SaOS-2 cells were routinely maintained in 75cm^2 culture flasks in DMEM containing Glutamax® and pyruvate and supplemented with 100U/ml penicillin, 100µg/ml streptomycin and 5% FBS at 37°C in 5% CO_2/95% air atmosphere. Medium was renewed twice a week. Cells were passaged once a week by rinsing the cell layer with 0.25% (w/v) trypsin and EDTA, and subsequent incubation at 37 °C for 5 min. Cells were collected by centrifugation and seeded with splitting ratios of approximately 1:4. Passages 18-35 were used for experiments.

2.2.3 Primary osteoblasts

Normal Human Osteoblasts (NHOBs) were a kind gift from Dr Bronwen Evans (Cardiff University, UK) (NHOB1 and NHOB3; Lonza, Walkersville, MD, US) and from Smith & Nephew (NHOB2; S&N, York, UK reference HS697/BC/01, provided by Promocell under Agreement Reference RC1341882Z). NHOBs have been named in the text to denote both cell line (NHOB1-3) and passage (NHOBP4-12). NHOBs were maintained in specialised basal media for osteoblast growth (Lonza Osteoblast Growth Medium and associated supplements and growth factors (NHOB1 and 3) and Promocell Osteoblast Growth Medium containing Promocell Osteoblast Supplement

Mix (NHOB2)) in 75cm^2 culture flasks at 37°C in 5% CO_2/95% air atmosphere. At 80% confluency, NHOBs were subcultured by rinsing the cell layer with 0.25% (w/v) trypsin and EDTA, and subsequent incubation at 37 °C for 10 min. Cells were collected by centrifugation and seeded at 5000 cells/cm^2. For experiments, NHOB1 was plated in Lonza Osteoblast Growth Medium and associated supplements and growth factors. However the specialised basal medium for osteoblast growth from both companies was subsequently found to contain glutamate, therefore experiments on NHOB2 and NHOB3 were performed in DMEM containing Glutamax® and pyruvate and supplemented with 100U/ml penicillin, 100µg/ml streptomycin and 10% FBS. Passages 4-12 were used for experiments.

2.3 RNA Preparation

RNA was extracted from cells in monolayer using RNase/DNase-free plasticware and molecular biology grade reagents.

2.3.1 Isolation of total RNA

Total RNA from cells grown in monolayer was isolated using an adaptation of (Chomczynski and Sacchi 1987) method. Cells were homogenised by pipetting up and down for 5 min with 1ml of TRIzol® reagent (Invitrogen, Paisley, UK) per 10cm^2. 0.2ml chloroform was then added per 1ml TRIzol® reagent and the samples shaken vigorously and centrifuged at 12,000g for 15 min at 4°C to separate the aqueous (RNA containing) and organic phases (protein containing). RNA from the aqueous phase was precipitated with 2-propanol (0.5ml per 1ml TRIzol® reagent) at room temperature for 10 min. The RNA precipitate was pelleted at 12,000g for 10 min at 4°C and washed once with 75% ethanol before air-drying and resuspension in 44µl RNase/DNase-free water.

2.3.2 DNase treatment

Isolated total RNA was subjected to DNAse treatment (DNA-*free*™ kit, Ambion, Huntington, UK) according to the manufacturer's protocol in order to eliminate any

residual genomic DNA. To 44µl total RNA, 5µl 10X DNase I buffer (final concentration of 10mM Tris-HCl pH 7.5, 2.5mM $MgCl_2$, 0.5mM $CaCl_2$) and 1µl recombinant DNase I were added and samples incubated at 37°C for 30 min. rDNase I was inactivated by the addition of 5µl DNase Inactivation Reagent and incubation at room temperature for 2 min with occasional mixing. Samples were centrifuged at 10,000g for 1.5 min and RNA supernatant transferred to a fresh tube.

2.3.3 Precipitation

To ensure the eradication of all organic contaminants, total RNA was re-precipitated with 0.1 volumes 3M sodium acetate (pH 5.5) and 2.5 volumes of 100% ethanol at -20°C overnight or at -80°C for 30 min. Precipitates were then centrifuged at 12,000g for 10min at 4°C and pellets washed once with 75% ethanol before air-drying and resuspension in 20µl RNase- and DNase-free molecular biology grade water. Total RNA was stored at -80°C.

2.3.4 Estimation of RNA concentration and purity

Total RNA was quantified by measuring the absorbance at 260nm in a NanoDrop® ND-1000 Spectrophotometer with associated NanoDrop 3.0.1 software (NanoDrop Technologies, UK) against a blank of molecular biology grade water. One unit of absorbance at 260nm corresponds to 40µg RNA per ml. The ratio of absorbance at 260nm and 280nm (A_{260}/A_{280}) indicates the purity of the RNA with respect to contaminants that absorb in the UV spectrum i.e. proteins. Pure RNA has a A_{260}/A_{280} ratio of ~2.0. The ratio of absorbance at 260nm and 230nm (A_{260}/A_{230}) indicates the purity of the RNA with respect to contaminants such as carbohydrates, salts, and phenol. Pure RNA has a A_{260}/A_{230} ratio of 2.0-2.2. Samples with A_{260}/A_{280} of $\geq$1.9 and A_{260}/A_{230} of $\geq$1.8 were deemed of suitable purity to continue to reverse transcription. Figure 2.1 shows a representative agarose gel of total RNA extracted by this procedure. Approximately 1µg total RNA isolated from MG-63 and SaOS-2 cells and 500ng isolated from human primary osteoblasts was resolved on a 1% agarose gel according to section 2.4.3. The 18S and 28S ribosomal RNA bands are clearly visible demonstrating that the isolated RNA has not degraded during the extraction process.

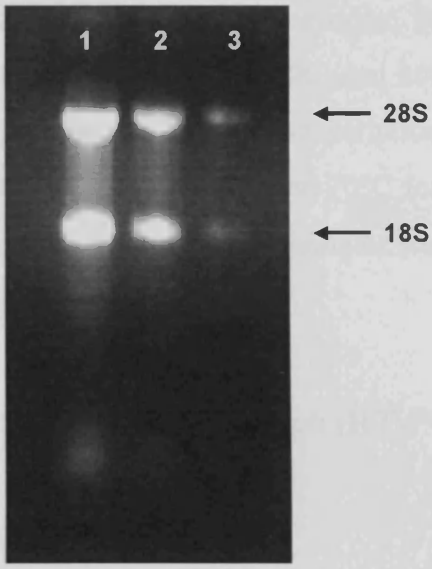

Figure 2.1. Agarose gel of RNA isolated by TRIzol® method from human osteoblasts. RNA extracted from 1. MG-63 cells (1µg), 2. SaOS-2 cells (1µg) and 3. human primary osteoblasts (500ng) was resolved on a 1% agarose gel and visualised under UV light in conjunction with SafeView nucleic acid stain. The 28S and 18S ribosomal RNA bands are clearly visible in the extracted RNA showing that no degradation had occurred during the extraction process.

2.3.5 Reverse Transcription

Total RNA was reverse transcribed to prepare complementary DNA (cDNA). The mass of RNA reverse transcribed was kept constant where possible within an experiment, but varied between experiments within a range of 100-500ng. The exact RNA mass that was reverse transcribed is detailed in the appropriate experimental chapter. Reverse transcription was carried out in a 20µl reaction volume and reaction conditions were defined by the manufacturers' protocol for SuperScript™ III reverse transcriptase (Invitrogen, Paisley, UK). Total RNA was mixed with 4µl deoxyribonucleotide triphosphate (dNTPs) (at 2.5mM) (Promega, Southampton, UK), 250ng random primers (hexadeoxynucleotides) (Promega, Southampton, UK) and water was added to 13µl. The samples were then incubated at 65°C for 5 min followed by incubation on ice for 2 min and the addition of 4µl 5X first strand synthesis buffer (to yield 1X buffer in a 20µl final reaction volume containing 50mM Tris-HCl, pH 8.3, 75mM KCl, 3mM $MgCl_2$) and 1µl dithiothreitol (DTT) (0.1M), both supplied

with the SuperScript™ III reverse transcriptase (Invitrogen, Paisley, UK). 40 units RNase inhibitor RNasin® (Promega, Southampton, UK) and 200 units SuperScript™ III reverse transcriptase were then added. Reverse transcription reaction was mixed and incubated at 25°C for 5 min, 50°C for 50 min, and 70°C for 15 min on a Techne TC-312 Thermal Cycler (Techne, Cambridge, UK). Samples were held at 4°C before storage at -20°C until cDNA was required.

2.4 Real Time-Polymerase Chain Reaction (RT-PCR)

2.4.1 Primer design

Primers were designed against known gene sequences (http://www.ncbi.nlm.nih.gov/nucleotide) using the Primer 3 web-based program (http://primer3.sourceforge.net/) to ensure similar melting temperatures (Tm), minimal internal structure (i.e. primer–dimer formation) and exclude 3' end complementation. The total gene specificity of the nucleotide sequences chosen for the primers was confirmed by nBLAST (nucleotide basic local alignment search tool) searches (GenBank database sequences). Primers were positioned in either separate exons, or at the junction between two exons to ensure specificity to cDNA and not genomic DNA sequences. Exon boundaries were viewed in Ensembl (www.ensembl.org). Primers were synthesised by MWG Biotech AG (Milton Keynes, UK). The accession number, nucleotide sequences, Tm, amplicon size (base pairs, bp) and source of the primers for housekeeping, phenotypic and glutamate transporter genes of interest are shown in Table 2.1. A diagram showing the binding sites of primers to EAAT1 and its splice variants EAAT1a and EAAT1ex9skip is shown in Figure 2.2.

2.4.2 Standard RT-PCR

Standard PCR amplification of cDNAs of interest was carried out in a reaction containing 2.5mM $MgCl_2$, 200nM of each forward and reverse primer, Go*Taq* Flexi buffer, pH 8.5, and 1 unit of Go*Taq* Flexi DNA polymerase (Promega, Southampton,

Table 2.1. Primer details for housekeeping genes (GAPDH, 18S rRNA and HPRT1), osteoblast markers (osteocalcin, osteonectin, osteoprotegerin, alkaline phosphatase, runx2 and type I collagen) and glutamate transporters (EAATs).

Gene	*Primers (5'-3')*	*Tm (°C)*	*Amplicon size (bp)*	*Source*
GAPDH NM_002046	Fwd - GGT ATC GTG GAA GGA CTC ATG A (Exon 7)	60	68	Dr Sophie Gilbert
	Rev - GGC CAT CCA CAG TCT TCT G (Exon 8)			
18S ribosomal RNA NR_003286.1	Fwd - GCA ATT ATT CCC CAT GAA CG	60	125	Dr Sophie Gilbert
	Rev - GGC CTC ACT AAA CCA TCC AA			
HPRT1 NM_000194.2	Fwd - GCA GAC TTT GCT TTC CTT GG (Exon 6)	60	80	Primer3
	Rev - GTG GGG TCC TTT TCA CCA G (Exon 7)			
Osteocalcin NM_199173.2	Fwd - GGC AGC GAG GTA GTG AAG AG (Exon 3)	60	73	Primer3
	Rev - GAT CCG GGT AGG GGA CTG (Exon 4)			
Osteonectin NM_003118.2	Fwd - AAA TAC ATC CCC CCT TGC CT (Exon6/7)	60	78	Dr Philippa Parsons
	Rev - CCA GGA CGT TCT TGA GCC AG (Exon 7)			
Osteoprotegerin NM_002546.3	Fwd - GGA AGG GCG CTA CCT TGA G (Exon 2)	60	97	Primer3
	Rev - TGT ATT TCG CTC TGG GGT TC (Exon 3)			
Runx2 NM_004348.3	Fwd - GTG GAC GAG GCA AGA GTT TC (Exon3/4)	60	107	Primer3
	Rev - TTC CCG AGG TCC ATC TAC TG (Exon 4)			
Type I Collagen NM_000088.2	Fwd - CAG CCG CTT CAC CTA CAG C (Exon 50)	60	83	(Frank et al. 2002)
	Rev - TTT TGT ATT CAA TCA CTG TCT TGC C (Exon 51)			
Alkaline Phosphatase NM_000478.2	Fwd - GGC TGG AGA TGG ACA AGT TC (Exon 4)	60	111	Primer3
	Rev - CCT TCA CCC CAC ACA GGT AG (Exon 5)			
EAAT1 (+ 1ex9skip) NM_004172	Fwd - ACC GCT GTC ATT GTG GGT A (Exon 2/3)	60	94	Primer3
	Rev - GTT CCC CAG GAA AGG AGA AG (Exon 3)			
EAAT1 (+ 1a) NM_004172	Fwd - CATTAACATGGATGGGACTGC (Exon 8)	60	119	Primer3
	Rev - CAGCTGTGGCTGTGATGC (Exon 8/9)			
EAAT1 (span exon 9) NM_004172	Fwd - CTG CCC TCT ATG AGG CTT TG (Exon 8)	60	256 (EAAT1), 121 (ex9skip)	Primer3
	Rev - TCT CCC AGT ACG TTG GTG GT (Exon 10)			
EAAT1 (span exon 3) NM_004172	Fwd – TTT GGC CAA GAA GAA AGT GC (Exon 2)	60	278 (EAAT1), 140 (EAAT1a)	Primer3
	Rev - CCA TCT TCC CTG ATG CCT TA (Exon 4)			
EAAT1a	Fwd - CGC TGT CAT TGT GGG AAT (Exon 2/4)	60	100	Primer3
	Rev - CAC AGC AAT GAT GGT GGT AG (Exon 4)			
EAAT1ex9skip	Fwd - CGG ACA AAT TAT TAC AAT CAG GGA (Exon 8/10)	60	93	Primer3
	Rev - CGT GAC AAG TGC TCC ACA AT (Exon 10)			
EAAT2 NM_004171	Fwd - ACC CTG ACG GTG TTT GGT G (Exon 2/3)	60	106	Primer3
	Rev - CCC CTG GGA AGG CTA TTA AC (Exon 3)			
EAAT3 NM_4170	Fwd - AAT TCT ACT TTG CTT TTC CTG GAG (Exon 2/3)	60	102	Primer3
	Rev - CCA GTG CAG CAA CAC CTG TA (Exon 3)			

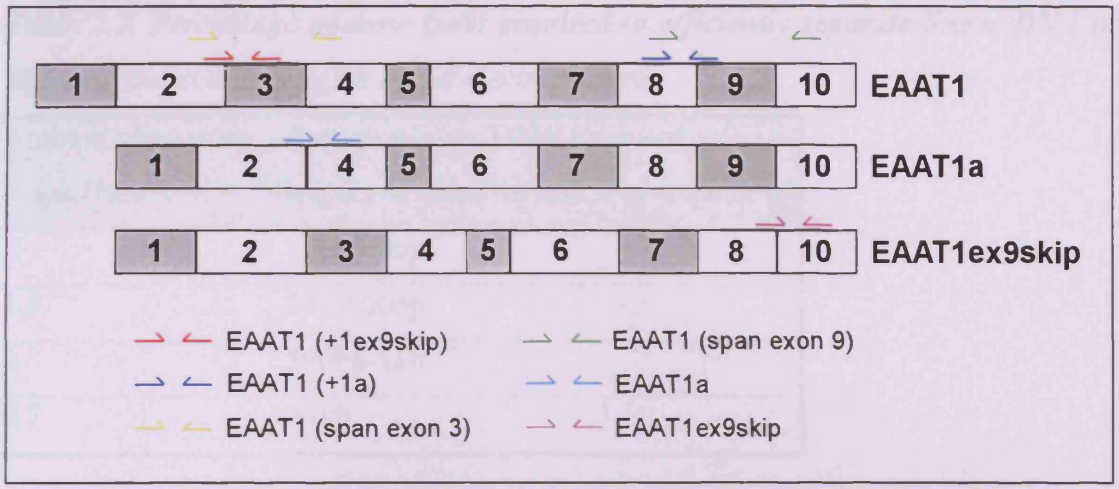

Figure 2.2. Binding sites of primers to EAAT1, EAAT1a and EAAT1ex9skip. The exons of EAAT1, EAAT1a and EAAT1ex9skip are indicated by the shaded boxes and the sites of hybridisation of the primer pairs in Table 2.1 are shown by coloured arrows.

UK) in the presence of 200nM dNTPs. Reaction volumes were scaled as appropriate to 12.5µl or 25µl. Samples were initially denatured at 95°C for 3 min then amplified for 40 cycles at 95°C for 30s, Tm for 30s (annealing, Table 2.1) and 72°C for 30s (extension) with a final extension at 72°C for 10 min. Samples were held at 4°C before analysis of products by agarose gel electrophoresis.

2.4.3 Agarose gel electrophoresis

Nucleic acid was resolved on agarose gels of the appropriate percentage agarose (Table 2.2) containing SafeView nucleic acid stain (NBS Biologicals, Cambridgeshire, UK) at 5µl/100ml. Gel electrophoresis was carried out in 1X Tris Borate EDTA (TBE) buffer (Promega, Southampton, UK) alongside a DNA ladder. DNA ladders used were a 100bp DNA ladder spanning 100-1,500bp (Promega, Southampton, UK) and a low molecular weight DNA ladder spanning 25-766bp (New England BioLabs, Herts, UK). Gels were visualised under UV light and images taken using a GelDoc system (BioRad). For densitometry of PCR products, gel pictures were scanned UMAX MagicScan DA software and bands of interest quantified by densitometry using NIH Image 6.2.

Table 2.2. Percentage agarose (w/v) required to efficiently separate linear DNA of different molecular weights by gel electrophoresis.

Amount of agarose in gel (% w/v)	Range of linear DNA fragment molecular sizes for efficient resolution
2	100-200bp
1.5	200-500bp
1	500bp-1kb
0.7	>1kb

2.4.4 Quantitative RT-PCR (QRT-PCR)

QRT-PCR assays were carried out using SYBR® Green I dye. SYBR® Green I dye specifically binds to double stranded DNA and fluorescence of the dye increases as PCR product accumulates during PCR cycles (Figure 2.3). The threshold was set so that it was in the centre of the logarithmic phase of the amplification curve for each gene and this yielded the cycle threshold value (Ct) which is defined as the cycle number at which the fluorescence curve crosses the threshold. Results were exported and either absolute (2.4.4.4) or relative (2.4.4.5) quantification was used.

2.4.4.1 Instruments and consumables

QRT-PCR assays were carried out on two separate instruments. The primer sets used, their concentrations and annealing temperatures were kept constant across instruments, as was the utilisation of SYBR® Green I dye in the assay and the employment of a dissociation thermal step to determine the melting point of the product at the end of the 40 cycles. A valid QRT-PCR assay was defined as one that generated a melt curve with a single peak (an example melt curve for each gene assay can be found in Appendix 9.2). Standard curves were assessed for each assay on each instrument and a standard curve with an efficiency of 90-110% and an R^2 of ≥ 0.99 were accepted as valid. Details of the construction of standard curves are found in section 2.4.4.2 and examples of standard curves for each instrument can be found in Appendix 9.2.

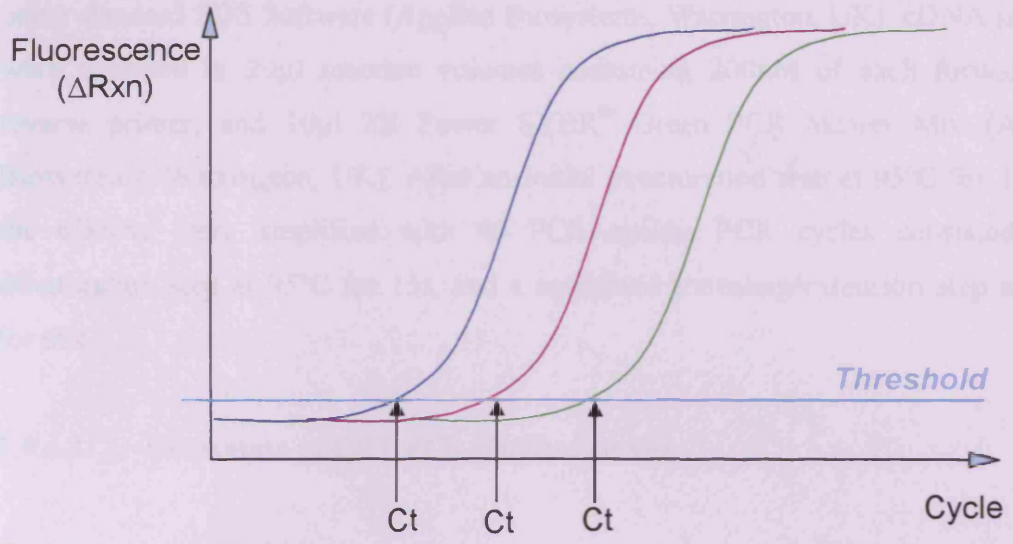

Figure 2.3. QRT-PCR amplification curves. Each amplification curve is representative of the change in fluorescence (ΔRxn) for one sample after each PCR cycle. The threshold is automatically set in the logarithmic region of all curves. The cycle threshold value (Ct) is the cycle number at which the curve crosses the threshold.

2.4.4.1.1 Stratagene (Cardiff University)

QRT-PCR reactions were performed using RNase/DNase-free 96-well plates and strip caps (both from Stratagene, Cambridge, UK) and a Stratagene MX3000P™ Real-Time PCR system and monitored using MxPro QPCR Software (Stratagene, Cambridge, UK). cDNA samples were analysed in 25µl reaction volumes containing 200nM of each forward and reverse primer, and 12.5µl 2X JumpStart™ Taq ReadyMix™ containing SYBR® Green I dye. After an initial denaturation step at 95°C for 2 min, the cDNAs were amplified with 40 PCR cycles. PCR cycles consisted of a denaturation step at 95°C for 20s, an annealing step at Tm for 40s (Table 2.1) and an extension step at 72°C for 20s.

2.4.4.1.2 Applied Biosystems (Smith & Nephew Research Centre, York)

QRT-PCR reactions were performed using RNase/DNase-free 96-well plates and ABI Prism™ optical adhesive covers (both from Applied Biosystems, Warrington, UK)

and an Applied Biosystems 7900HT Fast Real-Time PCR system and monitored using standard SDS Software (Applied Biosystems, Warrington, UK). cDNA samples were analysed in 20µl reaction volumes containing 200nM of each forward and reverse primer, and 10µl 2X Power SYBR® Green PCR Master Mix (Applied Biosystems, Warrington, UK). After an initial denaturation step at 95°C for 10 min, the cDNAs were amplified with 40 PCR cycles. PCR cycles consisted of a denaturation step at 95°C for 15s, and a combined annealing/extension step at 60°C for 60s.

2.4.4.2 Generation of QRT-PCR standard curves

To assess the efficiency and linear range of detection for the designed primers, standard curves of the cloned amplicon or a stock osteoblast cDNA sample were generated and assayed by QRT-PCR. These standard curves were also employed for quantification of expressed genes under experimental conditions by comparing the Ct values of unknowns to the standard curve.

Plasmid standard curves were used to assess linearity and efficiency of the assays on the Stratagene MX3000P™ Real-Time PCR system (section 2.4.4.1.1) whereas cDNA standard curves were used with the Applied Biosystems 7900HT Fast Real-Time PCR system (section 2.4.4.1.2). Plasmid standard curves were required for optimisation of the assays on the Stratagene MX3000P™ Real-Time PCR system because this system was used for absolute quantification (section 2.4.4.4) of EAATs in osteoblast cell lines whereas relative quantification (section 2.4.4.5) using cDNA standard curves was employed with the Applied Biosystems 7900HT Fast Real-Time PCR system which was used to assess changes in osteoblast gene expression in response to experimental treatments.

2.4.4.2.1 Plasmid standard curves

Human osteoblast cDNA samples were amplified by PCR using the primers detailed in Table 2.1 and the PCR product was resolved on an agarose gel (section 2.4.3) to confirm that a single product of the correct size was generated with each primer set. PCR products from each gene amplification assay were excised from agarose gels, purified and cloned into PGEM®-T vector (Promega, Southampton, UK).

2.4.4.2.1.1 Purification of DNA from gel

DNA bands were excised from agarose gels using sterile scalpels under UV light and weighed. The DNA was then purified from the gel using a Qiagen QIAquick gel extraction kit (Qiagen, Crawley, UK) according to the manufacturer's guidelines. DNA was eluted in 30µl molecular biology grade water.

2.4.4.2.1.2 TA cloning into PGEM®-T vector

DNA was TA cloned into 50ng PGEM®-T vector (Promega, Southampton, UK) in the presence of 3 units T4 DNA ligase (Promega, Southampton, UK) in rapid ligation buffer (containing 30mM Tris-HCl pH 7.8, 10mM $MgCl_2$, 10mM DTT, 1mM ATP, 5% polyethylene glycol) at room temperature for 3 hrs in a 10µl reaction volume. For PGEM®-T vector map and sequence of cloning site see Appendix 9.3.

2.4.4.2.1.3 Transformation into competent cells

The entire ligation reaction was transformed into 50µl ampicillin-resistant JM109 competent *Escherichia coli* (Promega, Southampton, UK) by incubation on ice for 20s followed by heat-shocking at exactly 42°C for 45s. 950µl S.O.C medium (Invitrogen, Paisley, UK) was then added and the transformation reactions incubated at 37°C for 1.5 hrs with shaking (150 revolutions per minute, rpm). 100µl of the reaction was then spread onto lysogeny broth (LB) agar plates with 100µg/ml ampicillin (Bioline, London, UK), 0.5mM Isopropyl β-D-1-thiogalactopyranoside (IPTG) and 40µg/ml X-Gal (Promega, Southampton, UK) and incubated overnight at 37°C. Recombinant (white) colonies were selected and inoculated in 5ml LB broth (containing 100µg/ml ampicillin) overnight at 37°C with shaking (150rpm).

2.4.4.2.1.4 Plasmid DNA minipreps

Plasmid DNA was extracted using Wizard® plus SV miniprep kit (Promega, Southampton, UK) according to the manufacturer's instructions. DNA was eluted in 100µl molecular biology grade water.

2.4.4.2.1.5 Sequencing

PGEM®-T vector insert DNA sequence was determined by the Cardiff University Molecular Biology Unit DNA sequencing core facility using T7 forward and SP6 reverse primers. The vector insert sequence was confirmed to be correct by displaying 100% identity with the target sequence in nBLAST.

2.4.4.2.1.6 Plasmid standard curve dilution

The concentration of plasmid DNA was measured spectrophotometrically (NanoDrop Spectrophotometer, ND-1000, NanoDrop Technologies, UK) by measuring the absorbance at 260nm. One unit of absorbance at 260nm corresponds to 50µg DNA per ml. Copy numbers were determined according to the molecular weight of the respective inserts (based on methodology from (Whelan et al. 2003) (for insert size see Table 2.1, for calculation see Appendix 9.4). Plasmids were diluted 10-fold in molecular biology grade water to generate standard curves for QRT-PCR analysis over a range of 10^1-10^8 plasmid DNA copies/µl. Stock plasmid DNA was stored at -20°C in RNase- and DNase-free no-stick microcentrifuge tubes (Alpha Laboratories, Eastleigh, UK).

2.4.4.2.2 cDNA standard curves

Stock concentrated cDNA (2-5µg RNA reverse transcribed) from osteoblasts (MG-63 or SaOS-2) was serially diluted in molecular biology grade water to generate standard curves. Standard curves generated in this way were over a narrower range than plasmid standard curves but were still able to demonstrate that the Ct values for unknown samples occurred in the linear and efficient range of the assay. For each gene assay, the stock cDNA sample and the standard curve set-up was kept constant across experiments.

2.4.4.3 Housekeeping genes

Numerous studies have reported considerable variation in housekeeping gene expression (Thellin et al. 1999; Bustin 2000; Suzuki et al. 2000; Warrington et al.

2000) and therefore validation of stable housekeeping genes should be considered for each different experimental condition. Where possible, QRT-PCR analysis was carried out in conjunction with three housekeeping genes (18S rRNA, GAPDH and HPRT1). In this case, transcript data were normalised to the most stable housekeeping gene under each condition as determined using geNorm software which compares the pair-wise variation for each housekeeping gene (Vandesompele et al. 2002). Raw expression data for each housekeeping gene in an experiment (calculated from a standard curve) were loaded into the geNorm programme and the gene expression stability measure *M* was generated. *M* is the average pair-wise variation for that gene with all other tested genes and the most stable housekeeping gene is that with the lowest *M* value. The housekeeping gene used for each experiment is stated in the appropriate experimental chapters of this thesis, as well as the relevant figure legend.

2.4.4.4 Absolute QRT-PCR

Absolute QRT-PCR analysis of experimental gene expression was carried out in conjunction with a standard curve generated from serial dilutions of plasmid vectors containing the specific amplicon under analysis (section 2.4.4.2.1). This method quantitates unknowns based on a known quantity standard curve and therefore absolute copy numbers of the transcript of interest can be determined. EAAT1 primers amplify both EAAT1 and EAAT1ex9skip, therefore the absolute copy numbers obtained for EAAT1 (+1ex9skip) were corrected by subtracting the absolute copy numbers obtained when the same samples were amplified using EAAT1ex9skip specific primers (Table 2.1). This method of determining expression levels of splice variants is only appropriate when there is near to equal abundance of the variants because the difference in Ct-values of both PCR products must be significantly higher than the inherent inter-well and inter-assay variation of real-time PCR (Vandenbroucke et al. 2001).

2.4.4.5 Relative QRT-PCR

In relative quantification, changes in expression of the gene of interest are normalised to the appropriate housekeeping gene in a given sample and expressed relative to a reference sample i.e. untreated control sample. The experimental sample group used

as the reference sample is clearly stated in the methods and figure legend for each experiment. A requirement for this method of expression analysis is that the primer set for the endogenous control and the primer set for the gene of interest are of comparable efficiencies (90-110%). Relative QRT-PCR analysis of gene expression for the housekeeping gene and gene of interest was carried out in conjunction with a plasmid standard curve (section 2.4.4.2.1) or a cDNA standard curve (section 2.4.4.2.2) to determine expression quantities. The appropriate housekeeping gene was determined (as outlined in section 2.4.4.3) and for each experimental sample, the amount of gene of interest (measured against the standard curve) was divided by the amount of the housekeeping gene (also measured against a standard curve) to obtain a normalised value. Each of the normalised values was then divided by the mean of the normalised values from the reference sample group and the relative expression levels expressed as a percentage.

2.5 Protein preparation

2.5.1 General method for cell lysis

Entire cell lysate was obtained by washing the cell monolayer with cold phosphate buffered saline (PBS) and homogenising cells in lysis buffer (cold 0.9% (v/v) Triton® X-100 in PBS containing Sigma protease inhibitor cocktail (2mM 4-(2-aminoethyl)benzenesulfonyl fluoride (AEBSF), 1mM EDTA, 130μM bestatin, 14μM E-64, 1μM leupeptin, 0.3μM aprotinin)). For analysis of cell death in the culture supernatant (section 2.5.3), the culture supernatant was incubated with 0.1 volume 9% (v/v) Triton® X-100 in PBS to ensure lysis of all dead or dying cells.

2.5.2 BCA protein assay

Protein concentration of cell lysate was determined by Bicinchoninic acid (BCA™) assay kit (Pierce, Cheshire, UK) according to the manufacturers' instructions and in comparison to a bovine serum albumin (BSA) standard curve (0-2mg/ml). Briefly, 25μl lysate/standard/lysis buffer blank was added to 200μl BCA™ working reagent (50:1, BCA™ Reagents A:B) in a 96-well plate and mixed on a plate shaker for 30s.

The plate was then covered and incubated at 37°C for 30 min and cooled to room temperature prior to measuring the absorbance at 562nm on a FLUOstar OPTIMA microplate reader (BMG Labtech, Aylesury, UK).

2.5.3 LDH assay of cell number and cell death

Cytotoxicity assay was carried out immediately on cell lysate and/or culture supernatant according to the Cytotox96 kit protocol (Promega, Southampton, UK). Lactate dehydrogenase (LDH) is an abundant intracellular enzyme (Lipton et al. 1993). LDH was quantified colourimetrically with a coupled enzymatic assay which results in the conversion of a tetrazolium salt to a red formazan dye product, using Cytotox96 (Promega, Southampton, UK) according to the manufacturer's instructions. Briefly, cell lysate or culture supernatant (diluted with distilled water if necessary to a total volume of 50µl) was incubated with 50µl Substrate Mix (prepared according to the manufacturer's instructions) for 10 min in the dark. 50µl Stop Solution was then added to each well and absorbance at 490nm measured using a FLUOstar OPTIMA microplate reader (BMG Labtech, Aylesury, UK). LDH activity in the lysed cell monolayer represents viable adherent cells whereas LDH activity in the culture supernatant represents dead or dying cells.

2.5.4 Alkaline phosphatase activity

Alkaline phosphatase (ALP) activity was quantified in cell lysates by spectrophotometric measurement of *p*-nitrophenol (pNP) release from *p*-nitrophenyl phosphate (pNPP) using Sigma Fast *p*-nitrophenyl phosphate tablet sets according to the instructions of the manufacturer. Cell lysates (diluted with distilled water if necessary to a total volume of 25µl) were incubated with 200µl pNPP substrate (1mg/ml) in alkaline buffer. Release of pNP was determined by measuring the absorbance at 405 nm after a defined incubation time (in the dark) using a FLUOstar OPTIMA microplate reader (BMG Labtech, Aylesury, UK). The incubation time varied across cell line and was chosen to ensure absorbance values were within the linear range of the spectrophotometer (5 min for SaOS-2, 1hr for primary osteoblasts). ALP activity was normalised to total cell number as determined by LDH assay

(section 2.5.3) and expressed as nmoles pNPP converted per minute per cell (see Appendix 9.5 for calculation).

2.6 Immunofluorescence of EAATs

MG-63, SaOS-2 and human primary osteoblasts (NHOB2P12) were seeded in eight-well Lab-Tek™ II Chamber Slides™ (Nunc, Naperville, IL) in normal growth medium. MG-63 and SaOS-2 cells were seeded at 2.5 x 10^4 cells/cm^2 and human primary osteoblasts were seeded at 1.25 x 10^3 cells/cm^2. At 70% confluency, cells were washed with PBS and fixed with ice cold methanol 5 min. The slides were air-dried and washed with 3 x 5 min PBS prior to 20 min incubation with 0.2% Triton® X-100 in PBS. The cells were then washed with PBS followed by 1-hour incubation at room temperature with PBS containing 5% normal goat serum and incubation overnight at 4°C with rabbit-anti-GLAST11-S (15 amino acid (aa) C-terminal epitope) at 1:500 (Alpha Diagnostics, San Antonio, TX) or rabbit-anti-EAAT3 (14aa cytoplasmic C-terminal epitope) at 6µg/ml (Alpha Diagnostics, San Antonio, TX) in PBS with 0.1% Tween®-20. Cells were washed with PBS and primary antibody localised using goat-anti-rabbit IgG-fluorescein isothiocyanate (FITC) conjugate at 1:160 or goat-anti-rabbit IgG-rhodamine isothiocyanate (TRITC) conjugate at 1:250 in PBS with 0.1% Tween®-20. Surplus antibody was removed through extensive washing with PBS containing 0.1% Tween®-20 and coverslips mounted with Vectashield mounting medium with DAPI (4,6-diamidino-2-phenylindole) (Vector Laboratories, Burlingame, CA). Labelled cells were visualised using an Olympus BX61 fluorescent microscope and attached Olympus SIS F-view digital camera (Olympus UK, London, UK) in association with AnalySIS® imaging software v3.2 (Olympus UK, London, UK). Primary negative controls were performed to confirm that staining was not a result of non-specific binding of the secondary antibody. Nonimmunoserum-only controls were not carried out.

2.7 EAAT inhibitors

L-*trans*-Pyrrolidine-2,4-dicarboxylic acid (*t*-PDC) and DL-threo-β-benzyloxyaspartic acid (TBOA) are glutamate analogues which inhibit glutamate transport in a broad range of EAATs whilst displaying weak or no affinity to glutamate receptors (Bridges

et al. 1991; Maki et al. 1994; Shimamoto et al. 1998; Bridges and Esslinger 2005). The IC_{50} values for each EAAT inhibitor with respect to specific EAAT subtypes are displayed in Table 2.3. The IC_{50} value for an inhibitor represents the inhibitor concentration at which the activity of each EAAT subtype was reduced by half. Where IC_{50} values were not available in the literature, K_i values are shown which represent the dissociation constant for inhibitor binding, or K_M values which represent the affinity of the inhibitor for the transporter.

T-PDC is a competitive transportable inhibitor of EAATs 1-4 (Arriza et al. 1994; Fairman et al. 1995) and a competitive non-transportable inhibitor of EAAT5 (Arriza et al. 1997). TBOA is a competitive non-transportable inhibitor of EAATs 1-5, displaying K_i and IC_{50} values in the range of 1-10μM (Arriza et al. 1994; Shimamoto et al. 1998; Jabaudon et al. 1999; Shigeri et al. 2001). TBOA displays similar affinities for EAAT1 and EAAT2 as *t*-PDC, but a much higher affinity for EAAT3. *T*-PDC and TBOA were purchased from Tocris Bioscience (Bristol, UK). Inhibitors were dissolved in distilled water to 10mM, frozen at -20°C and used within 8 weeks. For the structure of *t*-PDC and TBOA in comparison to glutamate, see Figure 2.4.

Table 2.3. IC_{50} (or K_i/K_M values if IC_{50} not available) for EAAT inhibitors with respect to specific EAAT subtypes. *t*-PDC; L-*trans*-Pyrrolidine-2,4-dicarboxylic acid, TBOA; DL-threo-β-benzyloxyaspartic acid.

		EAAT1	EAAT2	EAAT3	EAAT4	EAAT5
t-PDC	Transportable	IC_{50}^{U}=65[1] K_i^{U}=79[2]	IC_{50}^{U}=14[1] K_i^{U}=8[2]	K_i^{U}=61[2]	K_M^{E}=3[3]	K_i^{E}=6.2[4]
TBOA	Non-transportable	IC_{50}^{U}=67[1]	IC_{50}^{U}=5.5[1]	IC_{50}^{U}=8[5]	K_i^{E}=4[6]	K_i^{E}=3[6]

All values are expressed as mean (in μM) and assessed by electrophysiological study (E) or by uptake inhibition study (U).
[1]In EAAT expressing COS-1 kidney cell line (Shimamoto et al. 1998)
[2]In EAAT expressing COS-7 kidney cell line (Arriza et al. 1994)
[3]In EAAT expressing *Xenopus laevis* oocytes (Fairman et al. 1995)
[4]In EAAT expressing *Xenopus laevis* oocytes (Arriza et al. 1997)
[5]In EAAT expressing COS-1 kidney cell line (Shimamoto et al. 2000)
[6]In EAAT expressing *Xenopus laevis* oocytes (Shigeri et al. 2001)

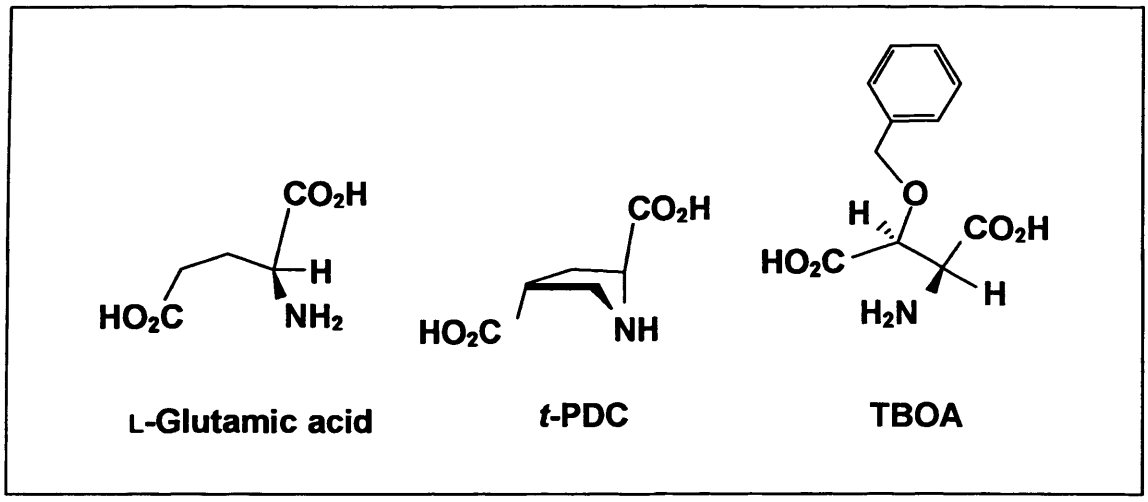

Figure 2.4. Glutamate and its analogues. Abbreviations L-*trans*-2,4-pyrrolidine dicarboxylate (*t*-PDC); DL-threo-β-benzyloxyaspartic acid (TBOA).

2.8 Radiolabelled glutamate uptake assay

Glutamate uptake assays were carried out in 24-well plates according to the described methods of (Takarada et al. 2004) to assess EAAT function. Cultured cells were washed twice with warm Krebs-Ringer HEPES (KRH) buffer (for composition see Appendix 9.1) and incubated with 250µl/well KRH buffer for 1hr at 37°C. For inhibitor experiments, KRH buffer was supplemented with 2.5µl/well of 100X EAAT inhibitor (Table 2.3) over a range of concentrations. After 1 hour, KRH buffer on cells was then replaced with 250µl of KRH buffer (± Na^+) containing a mix of cold and ^{14}C-labelled glutamate (± EAAT inhibitor for inhibitor experiments). For sodium-free experiments, sodium chloride in the KRH buffer was replaced with equimolar choline chloride. The specific activities of ^{14}C-labelled glutamate were adjusted across glutamate concentration ranges (Table 2.4) based on data from this lab (Flood, Duance and Mason, unpublished observations). Cells were incubated with ^{14}C-labelled glutamate at 37°C or 4°C for 10 min (osteoblast-like cell lines) or 20 min (primary human osteoblasts). Assay time for osteoblast-like cell lines was based on a preliminary optimisation experiment following 10µM glutamate uptake in SaOS-2 and primary human osteoblasts (NHOB2P9) over time which showed that the glutamate transporters had not reached saturation even after 30 min (Appendix 9.6). Assay time was longer for primary osteoblasts since this study indicated that these

cells transported glutamate at a slower rate than observed with osteoblast-like cells. Buffer was then aspirated and cells washed briefly with ice-cold KRH buffer containing 1.5mM unlabelled glutamate to ensure that ^{14}C-labelled glutamate accumulation is derived from uptake of labelled glutamate into cultured cells as opposed to adsorption and/or binding to the cell surface (Takarada et al. 2004). Washing with high concentrations of unlabelled glutamate had no effect on ^{3}H-labelled glutamate accumulation in cultured rat calvarial osteoblasts (Takarada et al. 2004). Cells were then lysed in 100µl 0.1M NaOH and uptake assessed by scintillation counting.

Table 2.4. Specific activity of glutamate concentrations used in glutamate uptake assays. pCi is picocuries

Final glutamate conc[a] (µM)	**Specific activity (pCi/pmol)**
0.1	100
1	50
5	20
10	20
50	10
100	10
250	4.5

2.8.1 Scintillation counting

90µl cell lysate in 0.1M NaOH from the glutamate uptake assay was added to 10ml scintillation cocktail (Emulsifier safe^{TM}, Perkin-Elmer, Beaconsfield, UK). Each sample was counted for 2 min on an LS6500 Multi-purpose scintillation counter (Beckman-Coulter, High Wycombe, UK). Radioactivity of samples is given in disintegrations per minute (d.p.m) which can be converted to pmol of ^{14}C-glutamate by the following calculations:

Becquerels (Bq) = d.p.m/60

Picocuries (pCi) = Bq x 27

Picomoles (pmol) = pCi/Specific Activity of ^{14}C-glutamate (pCi/pmol)

2.8.2 Normalisation to total protein

Protein content of lysates equivalent to the 90µl taken for scintillation counting from glutamate uptake assays was determined using parallel cultures (lysed following the methods outlined in section 2.5.1). Protein concentration was determined using a Pierce BCA™ protein assay kit in conjunction with a BSA standard curve (section 2.5.2). Glutamate uptake is expressed, where possible, as pmol of glutamate per hour per mg total protein. For calculation of sodium-dependent glutamate uptake, uptake in KRH in the absence of sodium was subtracted from uptake in KRH in the presence of sodium.

2.9 Alizarin red staining for mineralisation

Mineralisation of osteoblasts can be assessed by alizarin red S staining of calcium (Putchler 1969; Lievremont et al. 1982; Stanford et al. 1995b). Cells were washed twice with cold PBS then fixed with 70% ethanol for 1hr at 4°C before staining calcium deposits with 1mg/ml alizarin red S solution in distilled water, pH 4.2 at room temperature for 15 min with gentle agitation. Cultures were washed with tap water until excess dye had been removed. Representative images from stained wells were captured using a Canon IXUS digital camera (Canon, Japan) or by Nikon Eclipse TS100 inverted light microscope (Nikon UK ltd, UK) and attached Canon 400D digital camera (Canon, Japan) under 10X and 20X objectives. To quantify mineralisation, cells were de-stained overnight in 300µl of 5% perchloric acid and the total volume then transferred to a 96-well plate. Absorbance was measured at 450nm in conjunction with a standard curve of alizarin red S dissolved in 5% perchloric acid (an example standard curve can be found in Appendix 9.7). Bound alizarin red S was expressed in micrograms per well.

2.10 Antisense mediated exon skipping

Antisense oligoribonucleotides (AON) were used to overexpress EAAT1a and EAAT1ex9skip splice variants. AONs used here mediate exon skipping independently of RNase-H mediated degradation (Kole and Sazani 2001; Kurreck 2003). AONs can

mediate exon skipping by sterically blocking splice signals (Kole and Sazani 2001) by targeting specific sequences including the donor and acceptor splice sites, the branch point sequence and also exonic splice enhancer (ESE) sequences which are discrete sequences within exons that promote both constitutive and regulated splicing.

2.10.1 Antisense oligoribonucleotide design

AONs complimentary to EAAT1 pre-mRNA (GenBank Accession no. NM_004172, encoded by the gene *SLC1A3*) intron2/exon3 (ex3skip) and intron8/exon9 (ex9skip) boundaries were designed according to published methods (Stein 2001; Aartsma-Rus et al. 2004; Aartsma-Rus and van Ommen 2007). AONs were designed by identifying sequences positioned across the splice acceptor site i.e. 5' end of exon to be spliced out and the adjacent intronic sequence. AON length was designed to be ~ 20 nucleotides (Stein 2001). AON locations relative to full-length EAAT1 pre-mRNA sequence are depicted in Figure 2.5. The total specificity of the nucleotide sequences chosen for the AONs was confirmed by nBLAST searches (GenBank database sequences). A scrambled control oligo was generated from the ex9skip AON. nBLAST searches confirmed that the scrambled sequence was unlikely to result in non-specific effects. AONs were synthesised by MWG (high-performace liquid chromatography (HPLC) purified). All AONs were labelled with fluorescent 5-carboxy fluorescein (FAM) at the 5' end to allow for observation of transfection efficiency. AON backbone chemistry was modified to include 2'-*O*-methyl modified RNA which renders the AON RNase-H resistant and increases its affinity for target RNA (Mayeda et al. 1990; Wang and Kool 1995; Kurreck 2003). Stability of bases at each end of the AON was enhanced by phosphorothioate backbones which inhibit AON breakdown by endo- and exonucleases (Campbell et al. 1990; Sands et al. 1994). 2'-O-methyl-phosphorothioate AONs are very sensitive to mismatches in the target sequence, making them very specific (Aartsma-Rus and van Ommen 2007). AONs were dissolved in molecular biology grade water to 1µg/µl.

2.10.2 DNA transfection

Cells were transfected at 80% confluence in antibiotic-free DMEM containing 5% dFBS and 50µg/ml ascorbate. Cells were transfected with a previously optimised 5:2

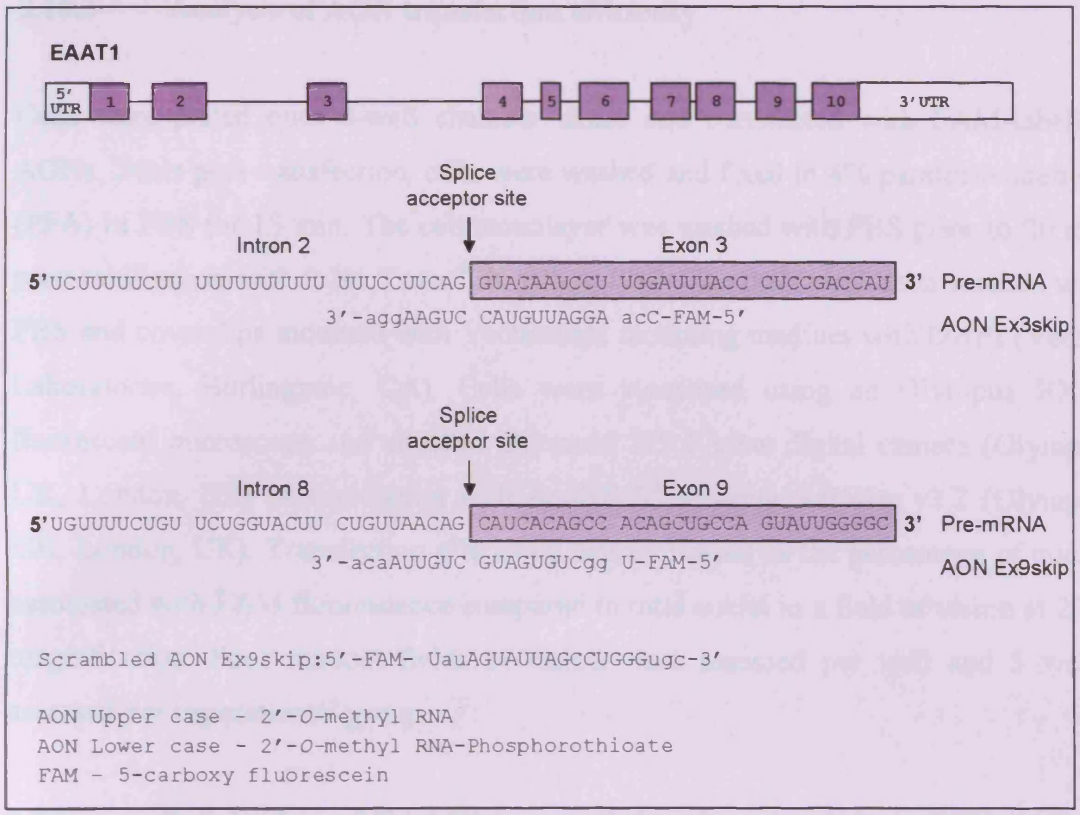

Figure 2.5. Sequences and relative binding sites of AONs. The 5' sequence of exons 3 and 9 of human EAAT1 pre-mRNA are indicated by the shaded boxes, whereas the intronic sequences neighbouring the exon are indicated by no shading. The sequence and orientation of all the AONs used in this study are indicated, except for Scrambled AON Ex9skip, which was designed not to hybridize to any known human sequence as validated by a database search.

ratio of FugeneHD transfection agent (Roche Applied Science, UK) and DNA in DMEM according to the manufacturer's protocol. Per well of a 24-well plate, 1µl FugeneHD was added to 18.6µl DMEM, mixed by flicking, then incubated at room temperature for 5 min. 0.4µg DNA was then added and mixed by flicking. Transfection mix was then incubated at room temperature for 30-45 min before being added to cells drop-wise. For smaller culture areas, the transfection mix was scaled down appropriately i.e. for 8-well chamber slides and 48-well plates, 0.4µl FugeneHD and 0.17µg DNA was combined in 8µl DMEM.

2.10.3 Analysis of AON transfection efficiency

Cells were plated onto 8-well chamber slides and transfected with FAM-labelled AONs. 24hrs post-transfection, cells were washed and fixed in 4% paraformaldehyde (PFA) in PBS for 15 min. The cell monolayer was washed with PBS prior to 20 min permeabilisation with 0.2% Triton® X-100 in PBS. The cells were then washed with PBS and coverslips mounted with Vectashield mounting medium with DAPI (Vector Laboratories, Burlingame, CA). Cells were visualised using an Olympus BX61 fluorescent microscope and attached Olympus SIS F-view digital camera (Olympus UK, London, UK) in association with AnalySIS® imaging software v3.2 (Olympus UK, London, UK). Transfection efficiency was expressed as the percentage of nuclei associated with FAM fluorescence compared to total nuclei in a field of vision at 20X magnification. Four random fields of vision were assessed per well and 3 wells assessed per experimental group.

2.11 Subcloning of EAAT1 intracellular domains into pcDNA3.1/V5-His©-TOPO® expression vector

Areas of EAAT1 were identified that may be involved in protein-protein interactions within the cell. These portions included the entire intracellular portions of the N- and C-termini and the intracellular stretch of amino acids between transmembrane domains 6 and 7 (Gegelashvili and Schousboe 1998) (Figure 1.8 and Appendix 9.8). The sequences corresponding to these domains in the EAAT1 transcript were cloned into pcDNA3.1/V5-His©-TOPO® expression vector (Invitrogen, Paisley, UK) (Figure 2.6, Appendix 9.3 for vector map and sequence of cloning site).

2.11.1 PCR and subcloning of amplicon into PGEM®-T vector

2.11.1.1 Primer design

Primers were designed to amplify sequences within the EAAT1 transcript that correspond to the intracellular domains detailed above (Table 2.5). Primers were designed by the methods outlined in section 2.4.1. Domains amplified for cloning

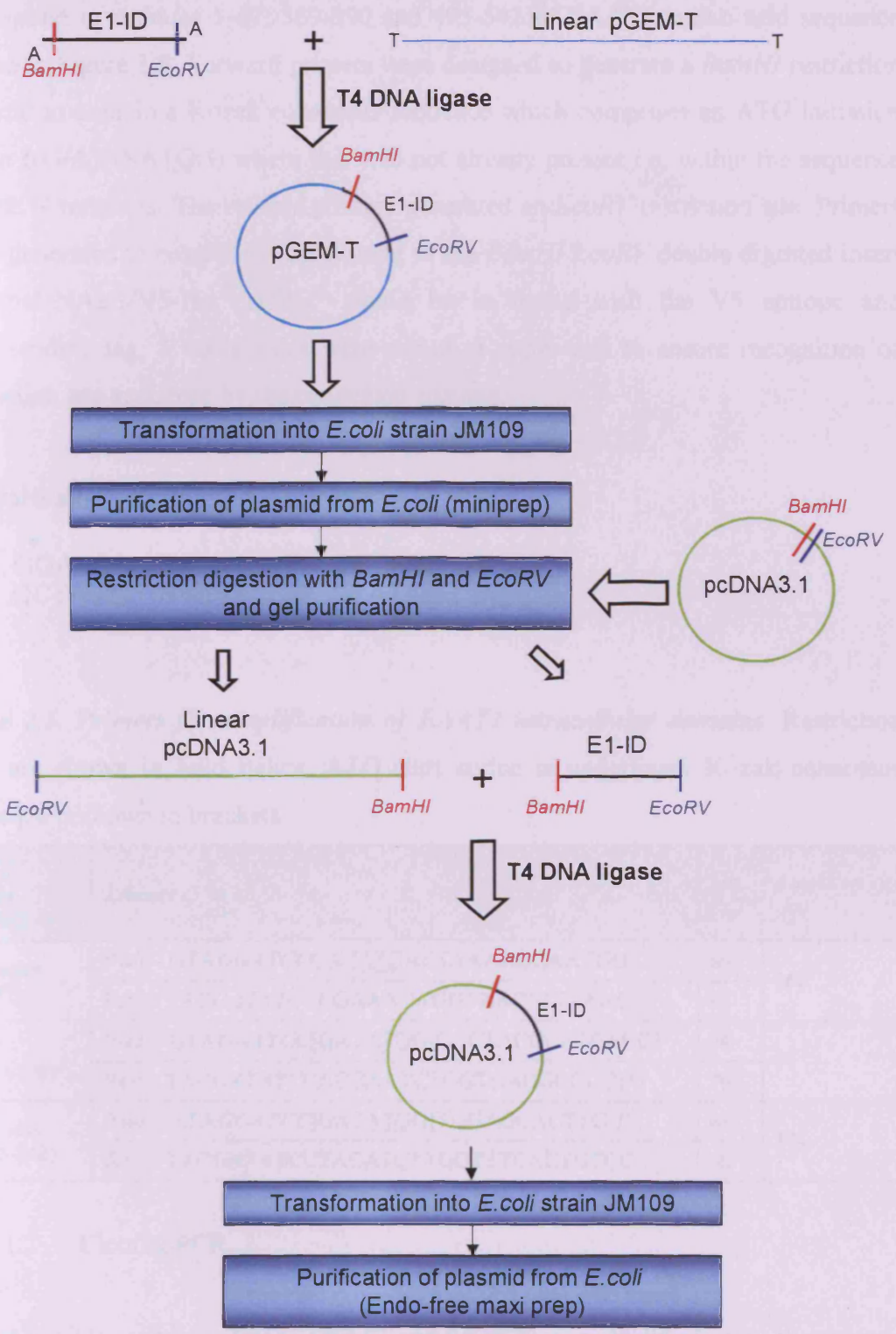

Figure 2.6 Diagramatic representation of the protocol followed to generate pcDNA3.1/V5-His©-TOPO® vector expressing EAAT1 intracellular domains (E1-ID).

correspond to residues 1-47, 369-390 and 495-542 of EAAT1 amino acid sequence shown in Figure 1.8. Forward primers were designed to generate a *BamHI* restriction site and to contain a Kozak consensus sequence which comprises an ATG initiation codon ((G/A)NNATGG) where this was not already present i.e. within the sequence for the N-terminus. The reverse primers generated an *EcoRV* restriction site. Primers were generated to ensure that subcloning of the *BamHI/EcoRV* double digested insert into pcDNA3.1/V5-His©-TOPO® would be in frame with the V5 epitope and polyhistidine tag. 3 nucleotides were added at either end to ensure recognition of restriction site sequence by the restriction enzyme.

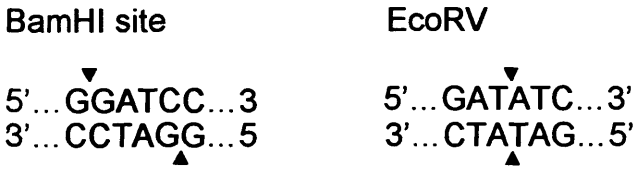

Table 2.5. Primers for amplification of EAAT1 intracellular domains. Restriction sites are shown in bold italics. ATG start codon is underlined. Kozak consensus sequence is shown in brackets.

EAAT1 domain NM_004172	***Primers (5'-3')***	***Tm (°C)***	***Amplicon size (bp)***
N-terminus (aa 1-47)	Fwd – GTA***GGATCC***GATATGACTAAAAGCAATGG	66	162
	Rev – TAC***GATATC***CCGAAACAGGTAACTTTTAAC	64	
TM6-7 (aa 369-390)	Fwd – GTA***GGATCC***[GATATGG]GCCTACCCATCACCT	74	93
	Rev – TAC***GATATC***CACGAATCTGGTGACGCGCTTG	76	
C-terminus (aa 495-542)	Fwd – ATA***GGATCC***[GATATGG]TGGAGCACTTG T	68	174
	Rev – TAC***GATATC***CTACATCTTGGTTTCACTGTCG	68	

2.11.1.2 Cloning PCR

Osteoblast-like cell line cDNA (MG-63 and SaOS-2) was amplified using the primers in Table 2.5. PCR was carried out in a 25µl reaction volume containing 2.5mM $MgCl_2$, 200nM of each forward and reverse primer, Phusion High Fidelity buffer and 0.4units Phusion High Fidelity DNA polymerase (Finnzymes, Espoo, Finland) in the presence of 200nM dNTPs. Samples were denatured for 30s at 98°C and then amplified for 40 cycles at 98°C for 10s, Tm for 30s (annealing) and 72°C for 30s

(extension) with a final extension at 72°C for 10 min. Annealing temperatures for each primer pair are shown in Table 2.6. Samples were held at 4°C before analysis of products by agarose gel electrophoresis.

Table 2.6. Cycling parameters used with primers designed for amplification of EAAT1 intracellular domains.

	Tm (°C)	*Cycles*
N-terminus	65	x 40
TM6-7	72	x 2
	70	x 2
	68	x 2
	66	x 2
	68	x 32
C-terminus	68	x 40

2.11.1.3 Purification of amplicon

PCR products were resolved on agarose gels and visualised as outlined in section 2.4.3. DNA was excised and purified from the gel as outlined in section 2.4.4.2.1.1.

2.11.1.4 Addition of A overhangs

Purified PCR products were incubated with 1 unit of Go*Taq* Flexi DNA polymerase (Promega, Southampton, UK) in the presence of 200nM dATP, 2.5mM $MgCl_2$ and Go*Taq* Flexi buffer at 72°C for 20 min. Inserts were then immediately TA cloned into PGEM®-T vector.

2.11.1.5 TA cloning into PGEM®-T vector

TA cloning, transformation, purification and sequencing of PGEM®-T plasmid minipreps containing nucleotide sequences for EAAT1 intracellular domains was carried out as outlined in section 2.4.4.2.1.2 to 2.4.4.2.1.5. Those with 100% identity

to the N-terminus, TM 6-7, and C-terminus sequences of EAAT1 were subcloned into pcDNA3.1/V5-His©-TOPO®.

2.11.2 Subcloning of amplicon into pcDNA3.1/V5His©-TOPO® vector

2.11.2.1 Restriction digests

Inserts from PGEM®-T plasmid minipreps were removed using the *BamHI* and *EcoRV* sites engineered into the forward and reverse primers respectively. Plasmid DNA was digested in a 20µl reaction with 5 units of *BamHI* and *EcoRV* (Promega, Southampton, UK), and 2µg acetylated BSA in the presence of 1X Multi-Core restriction enzyme buffer (containing 25mM Tris-Acetate, pH 9.5, 100mM potassium acetate, 10mM magnesium acetate, 1mM DTT) (Promega, Southampton, UK). Reactions were incubated at 37°C for 2hrs. The expression vector pcDNA3.1/V5-His©-TOPO® was digested using the same protocol.

2.11.2.2 Purification of excised inserts

Digest reactions were resolved on 2% (for excision of insert) or 0.7% (for excision of pcDNA3.1/V5-His©-TOPO®) agarose gels and visualised under UV exposure as outlined in section 2.4.3. Expected sizes of digested inserts are detailed in Table 2.7. Digested inserts and pcDNA3.1/V5-His©-TOPO® were excised and purified as outlined in section 2.4.4.2.1.2.

Table 2.7. Expected size of digested insert.

	Digested insert (bp)
N-terminus	152
TM6-7	83
C-terminus	164

2.11.2.3 Ligation into pcDNA3.1/V5-His©-TOPO® vector

Digested vector and insert were ligated at a ratio of 1:3 vector:insert based on the strength of the DNA bands using agarose gel electrophoresis (section 2.4.3). Purified digested insert was incubated at 65°C for 5 min in the presence of purified digested pcDNA3.1/V5-His©-TOPO® vector to reduce self-association. 3 units of T4 DNA ligase (Promega, Southampton, UK) and rapid ligation buffer (containing 30mM Tris-HCl pH 7.8, 10mM $MgCl_2$, 10mM DTT, 1mM ATP, 5% polyethylene glycol) were then added in a 10µl reaction volume and incubated at room temperature for 3hrs. Ligated plasmids were transformed into JM109 chemically competent cells following the manufacturers (Promega, Southampton, UK) instructions (as per section 2.4.4.2.1.3). Transformations were grown overnight on LB agar plates containing 100µg/ml ampicillin (Bioline, London, UK) at 37°C.

2.11.2.4 Screening for recombinant clones and determination of insert orientation

Positive colonies were identified by direct PCR of bacterial colonies using primers to pcDNA3.1/V5-His©-TOPO® vector (Table 2.8 and binding sites shown in Appendix 9.3) and the primers used to generate the insert (Table 2.5). Colonies were amplified using either vector forward primer and insert reverse primer, or vice versa, to confirm the presence of insert and correct orientation. Samples were denatured for 5-10 min at 95°C to lyse the cells prior to PCR amplification (section 2.4.2). Annealing temperatures, cycling parameters and expected product sizes are outlined in Table 2.9. Positive colonies with correct orientation were cultured overnight in 5ml LB broth (containing 100µg/ml ampicillin) at 37°C with shaking (150rpm).

Table 2.8. pcDNA3.1/V5-His©-TOPO® vector primers spanning the cloning site.

	Primers (5'-3')	*Tm (°C)*	*Position in vector sequence*
pcDNA3.1/V5-His©-TOPO® vector	Fwd - GAACCCACTGCTTACTGGCTTATCG	66	834-858
	Rev - ACTAGAAGGCACAGTCGAGGCTGAT	66	1,106-1,130

Table 2.9. Cycling parameters and expected product sizes for each primer combination used to screen for recombinant clones of pcDNA3.1/V5-His©-TOPO® vector containing N-terminus, TM 6-7 or C-terminus DNA insert.

			Vector fwd + Insert rev	*Insert fwd + Vector rev*	*Vector fwd + Vector rev*
EAAT domain	***Tm (°C)***	***Cycles***	***Product size (bp)***	***Product size (bp)***	***Product size (bp)***
N-terminus (entire)	66	x 40	245	315	398
TM6-7	75	x 2	176	246	329
	73	x 2			
	71	x 2			
	69	x 2			
	67	x 2			
	66	x 30			
C-terminus (entire)	66	x 40	257	327	410
Self ligated *BamHI/EcoRV* dbl digested vector	66	x 40	-	-	246

2.11.2.5 Endo-free Plasmid DNA purification

Plasmid DNA was extracted using Endo-free plasmid maxiprep kit (Qiagen, Crawley, UK) according to the manufacturer's instructions. DNA was eluted in 500µl endotoxin-free tris-EDTA (TE) buffer. DNA was quantified by measuring the absorbance at 260nm in a NanoDrop® ND-1000 Spectrophotometer with associated NanoDrop 3.0.1 software (NanoDrop Technologies, UK) against a blank of buffer TE. One unit of absorbance at 260nm corresponds to 50µg DNA per ml. The ratio of absorbance at 260nm and 280nm (A_{260}/A_{280}) indicates the purity of the DNA with respect to contaminants that absorb in the UV spectrum i.e. proteins. Pure DNA has a A_{260}/A_{280} ratio of ~1.8. The ratio of absorbance at 260nm and 230nm (A_{260}/A_{230}) indicates the purity of the DNA with respect to contaminants such as carbohydrates, salts, and phenol. Pure DNA has a A_{260}/A_{230} ratio of 2.0-2.2. Plasmid maxipreps with A_{260}/A_{280} of $\geq$1.7 and A_{260}/A_{230} of $\geq$1.8 were deemed of suitable purity to continue to transfection.

2.11.2.6 Sequencing

Insert DNA sequence of pcDNA3.1/V5-His©-TOPO® vector was determined by the Cardiff University Molecular Biology Unit DNA sequencing core facility using T7 forward primers.

2.11.2.7 Empty vector control

Control cells were treated with a self-ligated pcDNA3.1/V5-His©-TOPO® vector that was sequenced and found not to contain an ATG initiation codon and therefore will not express a peptide within the cell.

2.14 Statistical analysis

All statistical comparisons were performed using Minitab 15 software. Results are presented graphically as the mean ± S.E.M of replicate samples. The number of experimental samples and replicates is indicated in the relevant figure legend. Outliers were identified as data points that were >2 standard deviations away from the mean and discounted from the analysis. Data were analysed for normality (Anderson-Darling) and equal variance (Bartletts and Levenes tests) to satisfy the assumptions of a one-way analysis of variance (ANOVA) or General Linear Model (GLM; for unbalanced two-factor tests). Data that violated these assumptions were transformed (log transform or rank). Data with significant *P*-values for the ANOVA or GLM were analysed by a post-hoc Fisher's comparison test (one-way ANOVA) or Tukey's comparison test (GLM). Non parametric tests were applied (Kruskal-Wallis in place of one-way ANOVA or Shierer-Ray test in place of GLM) when data could not be normalised and if significant *P*-values obtained, 2-tailed Mann-Whitney U tests were employed for post-hoc pair-wise comparisons. Data are significantly different at $P<0.05$.

Much of the data from primary human cells are from single preliminary experiments and in these cases, statistical analyses were carried out to identify trends in the data set for comparison with cell lines, however increased repeats would be necessary to statistically validate any effects of the experimental treatments on these cells.

Chapter 3: Investigation of EAAT expression and function in human osteoblasts

3. Investigation of EAAT expression and function in human osteoblasts

3.1 Background

Glutamate mediates excitatory signalling in the CNS. However, there is now considerable evidence to suggest that glutamate may also act as a signalling molecule in several peripheral tissues, including bone (Skerry and Genever 2001; Hinoi et al. 2004).

Full length mRNA for GLAST and the splice variant GLAST-1a have been cloned from rat tibia (Huggett et al. 2000) and western blotting has revealed bands of ~69kDa corresponding to the molecular weight for GLAST in rat long bone (Huggett et al. 2000). Transcript and protein expression for EAAT1 have also been detected in human MG-63 osteoblast-like cells (Kalariti et al. 2004) and EAAT1 and EAAT1a transcripts have been detected in human SaOS-2 osteoblast-like cells (Huggett et al. 2002). Expression of transcripts for GLAST, GLT-1 and EAAC1, but not EAAT4 or EAAT5 have been demonstrated in primary cultured rat calvarial osteoblasts and, although expression of the corresponding proteins could not be confirmed by immunoblotting, temperature- and sodium- dependent glutamate uptake was observed, indicative of functional EAAT expression (Takarada et al. 2004). EAATs transport glutamate in a sodium dependent manner (reviewed in more detail in section 1.5.3.4.4) and thus far, sodium-dependent glutamate uptake activity has only been reported for osteoblasts in one instance (Takarada et al. 2004). Accumulation of radiolabelled glutamate in primary cultured rat calvarial osteoblasts was found to consist of a single kinetic component within a substrate range of 1-250μM with a K_M of 26μM and 42μM a V_{max} of 960 pmol/min/mg protein and 290 pmol/min/mg protein in osteoblasts cultured for 7 and 21 days respectively (Takarada et al. 2004). Furthermore, glutamate uptake was inhibited by the EAAT inhibitors L-(-)-*threo*-3-hydroxyaspartic acid (THA), *t*-PDC and (2S,1'S,2'R)-2-(carboxycyclopropyl)glycine (CCGIII) at 1μM-1mM and the glutamate receptor agonists kainate and NMDA at 1mM (Takarada et al. 2004).

3.1.1 Aims

EAAT function comprises both sodium-dependent glutamate uptake and anion conductance. Glutamate uptake activity can be measured *in vitro* by adding extracellular radiolabelled glutamate and monitoring movement of the labelled glutamate into the cell. The objectives of the experiments described in this chapter were to profile EAAT expression at the mRNA and protein level in human primary osteoblasts and human osteoblast-like cell lines and also to determine the sodium-dependence, kinetic components and pharmacological profile of glutamate uptake in these cells.

3.2 Methods

3.2.1 RT-PCR analysis of EAAT mRNA expression

Total RNA was extracted from MG-63 and SaOS-2 osteoblast-like cells, primary human osteoblasts (NHOB1P5 and NHOB2P7), and human bone obtained from total knee replacements (with informed consent and full ethical approval). Extracted RNA (50-500ng) was reverse transcribed in a 20µl volume which was subsequently diluted to 100µl with RNase- and DNase-free molecular biology grade water. Human cerebellum total RNA (2µg) (Clontech, Oxford, UK) was reverse transcribed by Dr Cleo Bonnet in 20µl volume which was subsequently diluted to 100µl with RNase- and DNase-free molecular biology grade water. 5µl cDNA was then used in each RT-PCR reaction using primers against EAAT1+EAAT1ex9skip, EAAT1+EAAT1a, EAAT2, EAAT3, EAAT1ex9skip and EAAT1a (Table 2.1 and Figure 2.2). RNA extraction, reverse transcription, RT-PCR and resolution of PCR products by agarose gel electrophoresis was carried out as outlined in section 2.3, 2.4.2 and 2.4.3. PCR product cloning and sequencing was carried out as outlined in section 2.4.4.2.1.

3.2.1.1 QRT-PCR analysis of EAAT mRNA expression

500ng MG-63 and SaOS-2 RNA and 50ng primary human osteoblast (NHOB1P5) RNA was reverse transcribed in 20µl volume which was subsequently diluted to

100µl with RNase- and DNase-free molecular biology grade water. 5µl cDNA was then used in each QRT-PCR reaction. Transcript expression levels of EAAT1+EAAT1ex9skip, EAAT1ex9skip, and the housekeeping gene 18S rRNA were quantified in each cell line by absolute QRT-PCR (section 2.4.4.4). Expression of EAAT3 was also quantified in MG-63 and SaOS-2 cells. Expression levels of EAAT1 were calculated by subtracting the absolute copy numbers obtained when the same samples were amplified using EAAT1ex9skip specific primers from the absolute copy numbers obtained for EAAT1 + EAAT1ex9skip. QRT-PCR was carried out using the Stratagene MX3000P™ Real-Time PCR system (section 2.4.4.1.1) in conjunction with plasmid standard curves (section 2.4.4.2.1). Absolute copy numbers of EAAT transcripts were normalised to 18S rRNA transcript copy numbers.

3.2.1.2 Effect of extracellular glutamate concentration on EAAT mRNA expression

MG-63 cells were seeded at 2.6 x 10^4 cells/cm^2 of a 24-well plate and SaOS-2 cells were seeded at 4.2 x 10^4 cells/cm^2 of a 24-well plate in normal growth medium (section 2.2.1 and 2.2.2) and allowed to adhere overnight. Cells were then incubated with DMEM, 5% dFBS, and 50µg/ml ascorbate in the presence or absence of 500µM glutamate for 24hrs. Medium was then aspirated, cells rinsed with cold PBS and homogenised with 0.2ml TRIzol® reagent per well for 5 min. The plates were stored at -80°C until RNA extractions, reverse transcription and absolute QRT-PCR for EAAT1+EAAT1ex9skip, EAAT1ex9skip, and EAAT3 expression was carried out in conjunction with the housekeeping gene 18S rRNA as outlined above (section 3.2.1.1).

3.2.2 Immunofluorescent staining of EAATs

MG-63 and SaOS-2 osteoblast-like cells and primary human osteoblasts (NHOB2P12) were immunostained for expression of EAAT1 and EAAT3 using specific antibodies (section 2.6).

3.2.3 Glutamate uptake

EAAT activity was assessed in MG-63 and SaOS-2 osteoblast-like cells and primary osteoblasts (NHOB2P9) (section 2.8).

3.2.3.1 Kinetics of glutamate uptake in osteoblasts

Cells were pre-incubated with KRH buffer (+ Na^+) for 1hr. The buffer was then aspirated and replaced with KRH buffer (± Na^+) containing a mix of labelled ^{14}C-glutamate and unlabelled glutamate over a concentration range of 1-250μM (Table 2.4) for 10 min (MG-63 and SaOS-2) or 20 min (primary human osteoblasts). Lineweaver-Burk graphs were plotted (Lineweaver and Burk 1934). Briefly, the reciprocal of glutamate uptake rate was plotted against the reciprocal of glutamate concentration to yield a straight line when data conforms to Michaelis-Menten kinetics. The y-intercept is equivalent to the inverse of V_{max} and the x-intercept is equivalent to $-1/K_M$, however this plot can distort the errors in measurement. Therefore, K_M and V_{max} values were also determined where possible by non-linear regression analysis of the uptake saturation curves using a curve fitting program followed by the application of a one-site or two-site binding (hyperbola) equation to the data, using GraphPad Prism 2 software (GraphPad Prism Software Inc, San Diego, CA).

3.2.3.2 Effect of EAAT inhibitors on Na^+-dependent glutamate uptake

Cells were pre-incubated with KRH buffer (+ Na^+) supplemented with EAAT inhibitors (*t*-PDC and TBOA) over a concentration range of 1μM to 1mM for 1hr. After the pre-incubation period, KRH buffer was replaced with KRH buffer (± Na^+) containing a mix of labelled ^{14}C-glutamate and unlabelled glutamate and the inhibitor at the appropriate concentration for 10 min.

3.2.3.2.1 EAAT inhibitors

EAAT inhibitors (section 2.7) were added to KRH to yield concentrations in the range of 1μM to 1mM. These concentrations were chosen to span the IC_{50} and Ki values

reported in the literature (Table 2.3). Inhibitors were dissolved in water and diluted in each well with KRH buffer.

3.2.3.3 Effect of extracellular glutamate concentration on Na^+-dependent glutamate uptake

MG-63 cells were seeded at 2.6 x 10^4 cells/cm^2 of a 24-well plate and SaOS-2 cells were seeded at 4.2 x 10^4 cells/cm^2 of a 24-well plate in normal growth medium (section 2.2.1 and 2.2.2) and allowed to adhere overnight. Cells were then incubated with DMEM, 5% dFBS, and 50μg/ml ascorbate in the presence or absence of glutamate (10 or 500μM). After 24hrs, medium was replaced with KRH buffer (+ Na^+) in the presence or absence of glutamate (10 or 500μM) for a further 1 hour. Some cells were incubated with glutamate for the 1 hour pre-incubation period only in order to observe both the short-term (1hr) and long-term (24hrs) effect of extracellular glutamate on EAAT activity. After the pre-incubation period, KRH buffer was replaced with KRH buffer (± Na^+) containing a mix of labelled ^{14}C-glutamate and unlabelled glutamate at 10μM for 10 min.

3.3 Results

3.3.1 Expression of EAAT transcripts in human osteoblasts

Total RNA was extracted from MG-63 and SaOS-2 osteoblast-like cells, primary human osteoblasts, human bone and human cerebellum for subsequent analysis by RT-PCR using primers against specific EAAT sequences. Transcripts for EAATs 1-3 and the splice variants of EAAT1 - EAAT1a and EAAT1ex9skip - were detected in all samples and sequencing verified the correct RT-PCR amplification products for each primer pair in MG-63 and SaOS-2 cells (Figure 3.1).

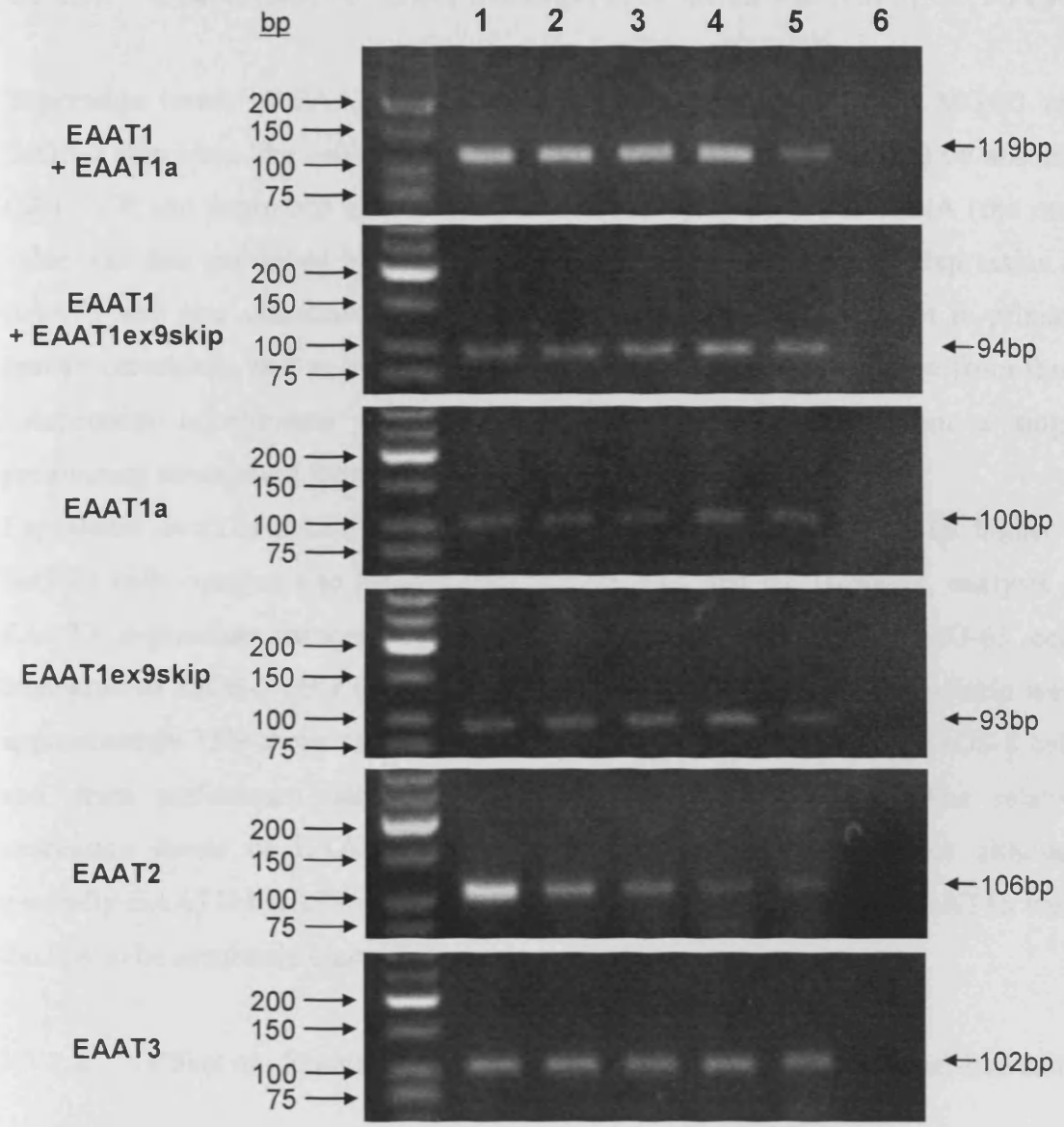

Figure 3.1. Various EAATs are expressed in human bone and brain. Expression of EAATs 1-3 and both EAAT1 splice variants (EAAT1a and EAAT1ex9skip) was shown to be expressed by RT-PCR in human brain, primary osteoblasts, osteoblast-like cells (MG63 and SaOS-2) and bone tissue. 1. Human cerebellum, 2. Human primary osteoblast (NHOB2P7), 3. MG-63, 4. SaOS-2, 5. Human bone, 6. Water blank.

3.3.1.1 Quantification of EAAT transcripts in osteoblast-like cells by QRT-PCR

Expression levels of EAAT1 and EAAT1ex9skip were quantified in MG-63 and SaOS-2 osteoblast-like cells and primary human osteoblasts (NHOB1P5) by absolute QRT-PCR and expressed as a ratio of the housekeeping gene 18S rRNA (the ratio value was then multiplied by 10^8 to yield whole numbers) (Figure 3.2). Expression of EAAT3 was also quantified in MG-63 and SaOS-2 osteoblasts but not in primary human osteoblasts due to inadequate sample quantity. Presented data are from three independent experiments where n=4 (MG-63 and SaOS-2) or from a single preliminary experiment where n=4 (NHOB1P5).

Expression levels of EAAT1 and its splice variant EAAT1ex9skip were far higher in SaOS-2 cells compared to MG-63 cells (Figure 3.2A and B). However, analysis of EAAT3 expression showed higher expression of the transcript in MG-63 cells compared to SaOS-2 cells (Figure 3.2C). Expression levels of EAAT1ex9skip were approximately 13% those of full length EAAT1 in MG-63 cells, 2% in SaOS-2 cells and, from preliminary data, 12% in primary human osteoblasts. The relative expression levels of EAATs varied for each osteoblast-like cell line although generally EAAT1>EAAT3>EAAT2. The expression of EAAT2 and EAAT1a were too low to be accurately quantified by this method.

3.3.1.2 Effect of glutamate on EAAT transcript expression in osteoblast-like cells

MG-63 and SaOS-2 osteoblast-like cells were incubated for 24hrs in the presence or absence of 500μM glutamate and expression levels of EAAT1, EAAT1ex9skip, EAAT3 were quantified by absolute QRT-PCR, normalised to the housekeeping gene 18S rRNA and expressed as a percentage of control expression for each EAAT, i.e. expression of cells at 0μM glutamate (Figure 3.3). Presented data are from three independent experiments where n=4.

Exposure of MG-63 and SaOS-2 cells to 500μM glutamate for 24hrs did not significantly affect expression of EAAT1 (in MG-63 Kruskal-Wallis P=0.525; in SaOS-2 one-way ANOVA with log data P=0.982), EAAT1ex9skip (in MG-63 one-way ANOVA P=0.703; in SaOS-2 one-way ANOVA P=0.430) or EAAT3 (in MG-63 one-way ANOVA with log data P=0.150; in SaOS-2 Kruskal-Wallis P=0.902). MG-63 cells did however show a trend toward increasing EAAT3 expression in response

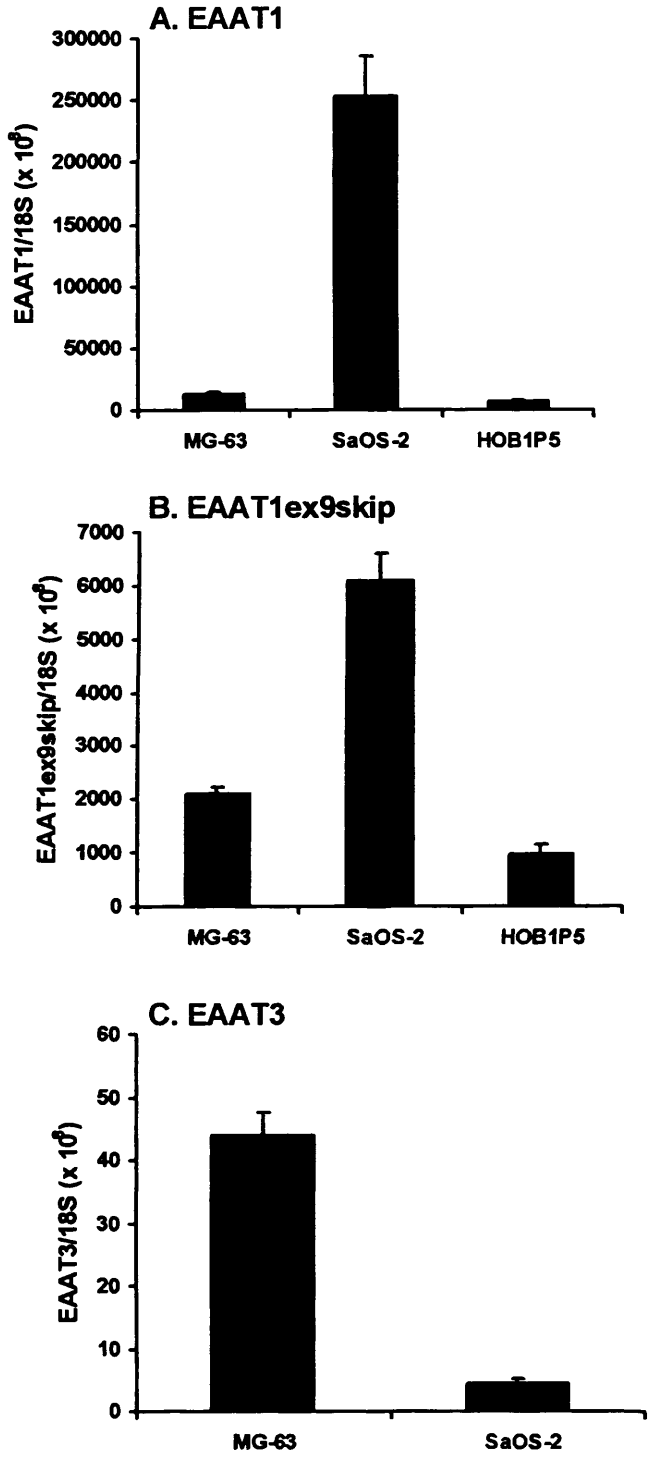

Figure 3.2. MG-63, SaOS-2 and primary human osteoblasts express EAATs at differential levels. Expression of (A) EAAT1, (B) EAAT1ex9skip and (C) EAAT3 were analysed by QRT-PCR, normalised to 18S rRNA expression and expressed as a ratio ($x10^8$). Values are mean ± S.E.M from three independent experiments, n=4 (MG-63 and SaOS-2) or a single preliminary experiment, n=4 (NHOB1P5). Expression of EAAT3 was not assessed by QRT-PCR in primary human osteoblasts.

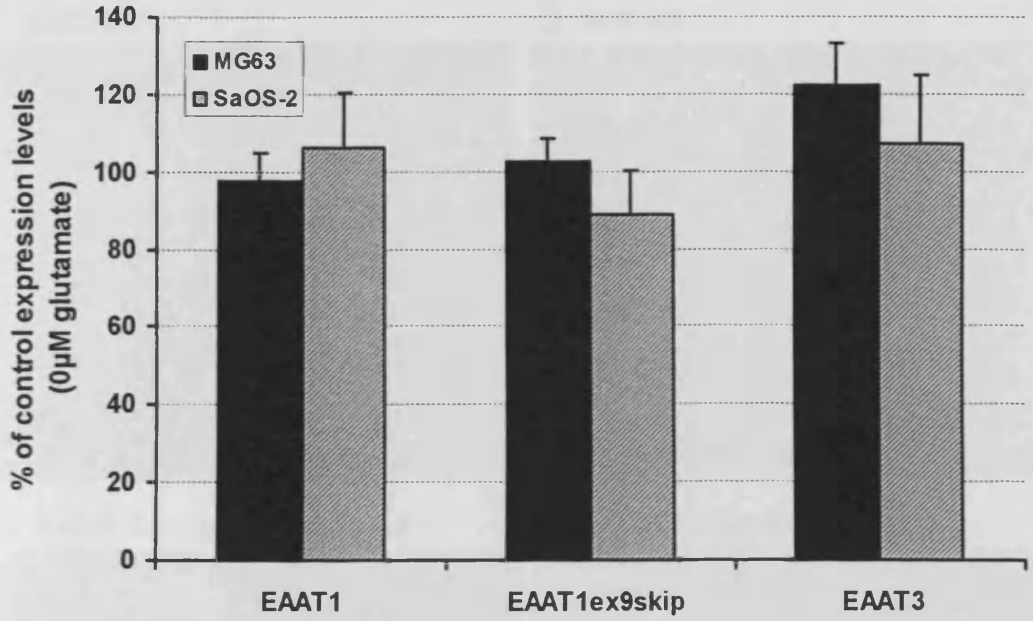

Figure 3.3. 24hr incubation with 500µM glutamate does not significantly affect EAAT transcript levels in MG-63 and SaOS-2 osteoblasts. EAAT expression was analysed by QRT-PCR in each cell line following 24hr culture at 0 and 500µM glutamate, normalised to 18S rRNA expression and expressed as the mean percentage of expression in control cells (0µM glutamate) ± S.E.M from three independent experiments, n=4.

to 24hrs pre-incubation with 500µM glutamate. Under these conditions mean EAAT3 mRNA levels were increased to 122 ± 11 % of untreated control cells.

3.3.2 Expression of EAAT protein in human osteoblasts

3.3.2.1 Immunofluorescence

MG-63, SaOS-2 and human primary osteoblasts (NHOB2P12) were immunostained for EAAT1 (Figures 3.4 and 3.6) and EAAT3 (Figures 3.5 and 3.6) expression using specific antibodies. Primary negative control tests displayed negligible non-specific staining with either the FITC-conjugated (Figure 3.4C,D; Figure 3.5C,D; Figure 3.6B) or the TRITC-conjugated (Figure 3.6D) goat-anti-rabbit secondary antibody under

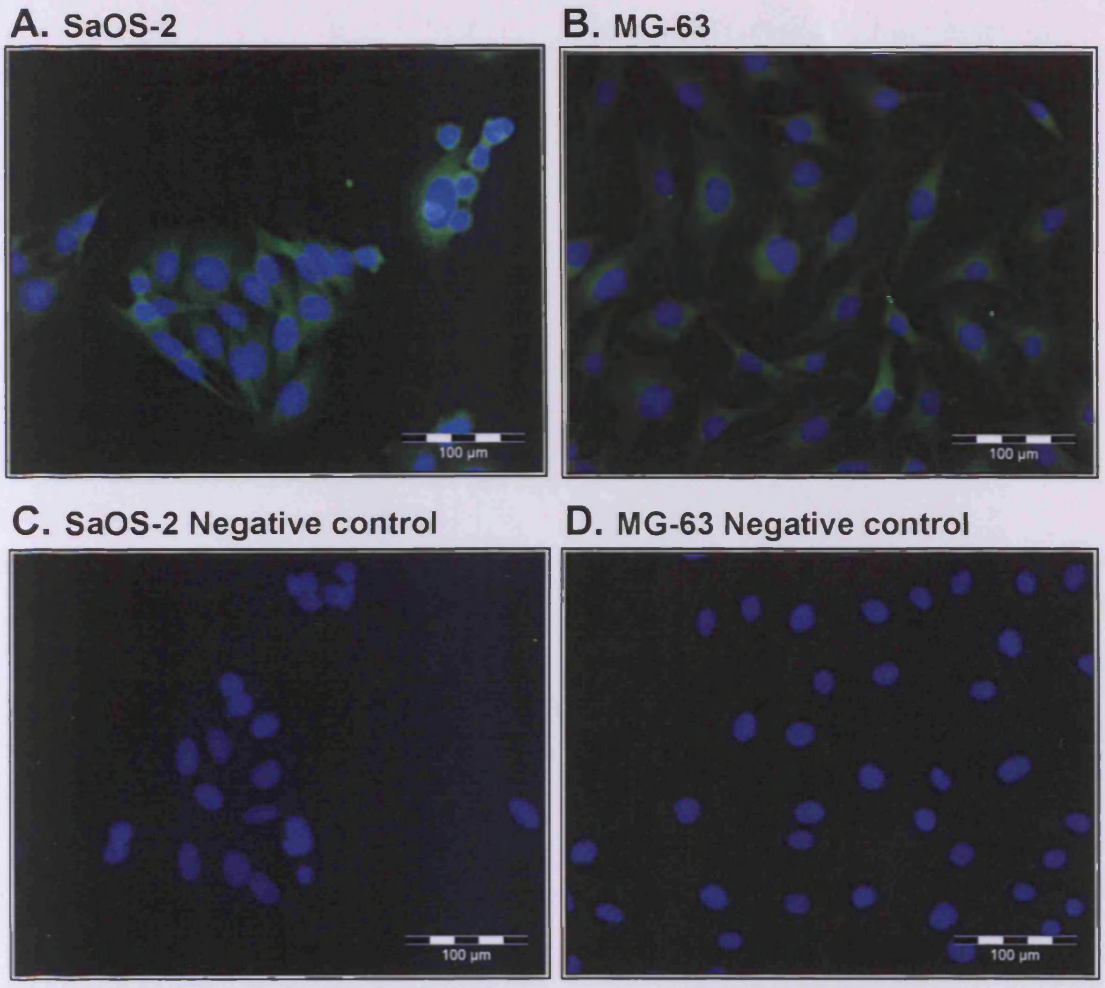

Figure 3.4. Immunofluorescence of EAAT1 in human osteoblast-like cell lines. MG-63 and SaOS-2 cells were immunofluorescently probed with rabbit-anti-EAAT1 antibody and a corresponding FITC tagged goat-anti-rabbit secondary antibody. Control cells (C,D) were probed with secondary antibody alone to determine levels of non-specific staining. Pictures were taken under 800ms exposure.

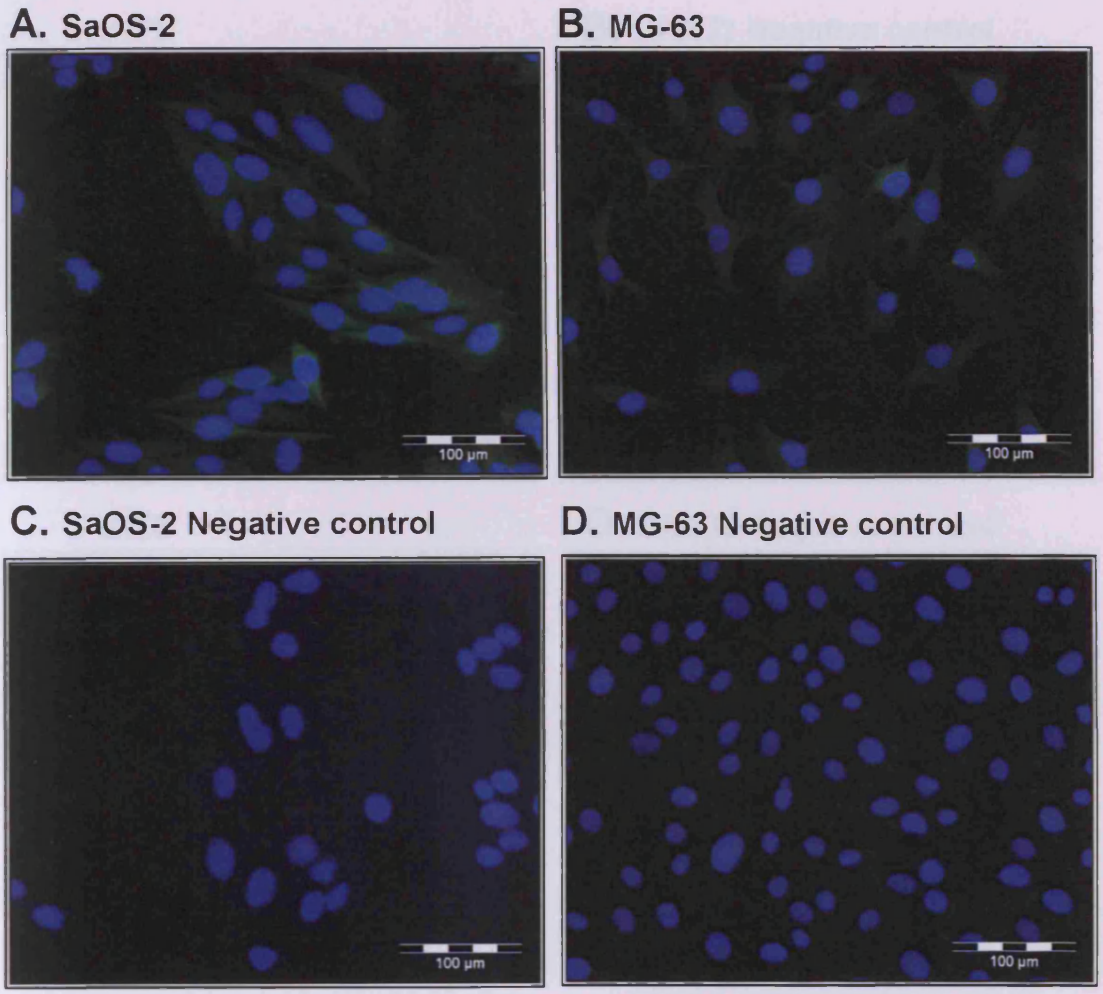

Figure 3.5. Immunofluorescence of EAAT3 in human osteoblast-like cell lines. MG-63 and SaOS-2 cells were immunofluorescently probed with rabbit-anti-EAAT3 antibody and a corresponding FITC tagged goat-anti-rabbit secondary antibody. Control cells (C,D) were probed with secondary antibody alone to determine levels of non-specific staining. Pictures were taken under 1s exposure.

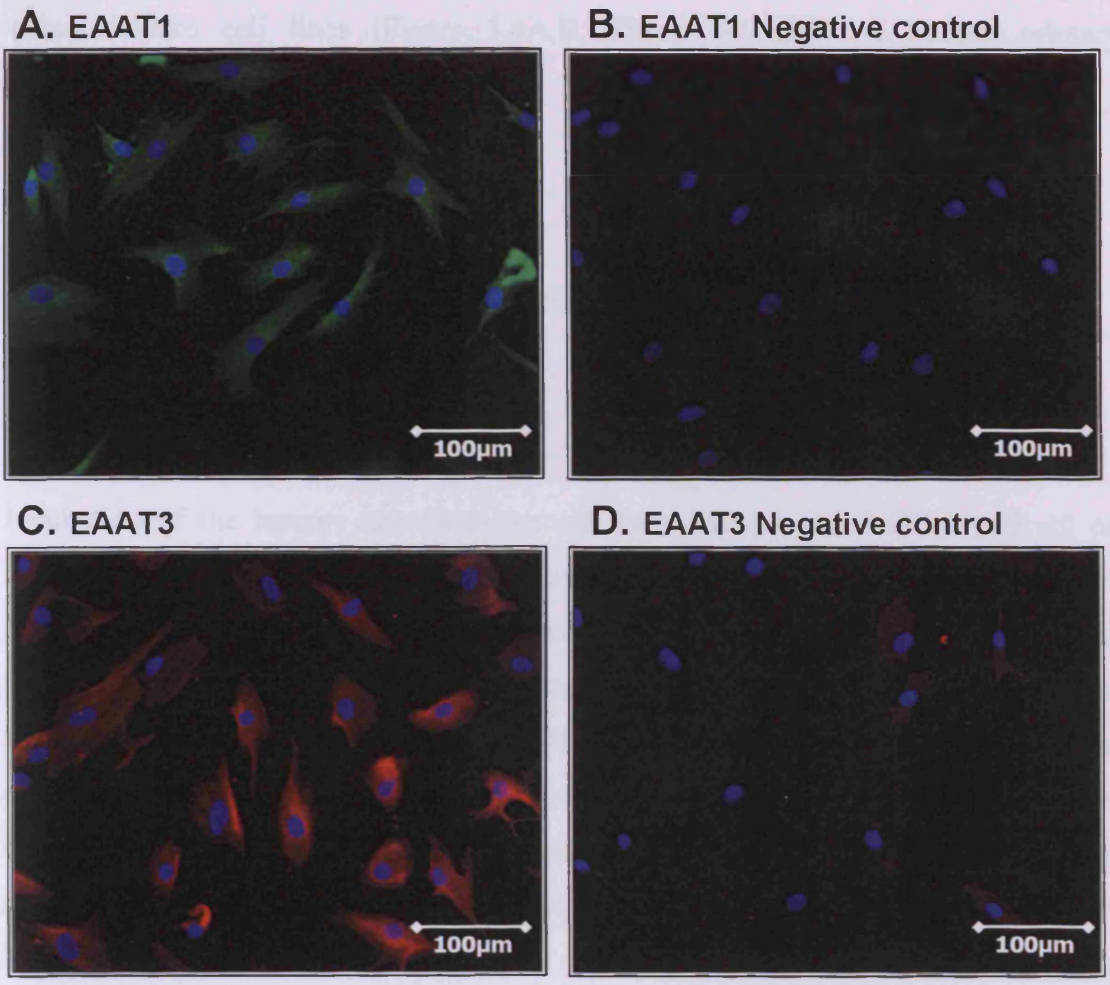

Figure 3.6. Immunofluorescence of EAAT1 and EAAT3 in primary human osteoblasts (NHOB2P12). Cells were immunofluorescently probed with specific primary antibodies (A, rabbit-anti-EAAT1; C, rabbit-anti-EAAT3) and the corresponding fluorescently tagged goat-anti-rabbit secondary antibodies (A, FITC; C, TRITC). Control cells (B,D) were probed with goat-anti-rabbit secondary antibody alone to determine levels of non-specific staining (B, FITC; D, TRITC). Pictures were taken under 1.3s (A,B) and 1.6s (C,D) exposure.

the same conditions. EAAT1 and EAAT3 specific staining was detectable in both osteoblast-like cell lines (Figure 3.4A,B; Figure 3.5A,B) and human primary osteoblasts (Figure 3.6A,C).

3.3.3 Glutamate uptake

3.3.3.1 Na^+-dependent glutamate uptake

3.3.3.1.1 Osteoblast-like cells

Incubation of the human osteoblast-like cell lines MG-63 and SaOS-2 with 10 or 250μM mix of radiolabelled and unlabelled glutamate at 37°C for 10 min in KRH (+ Na^+) buffer led to the accumulation of glutamate in these cells (Figure 3.7A and Table 3.1). Presented data are from three independent experiments where n=4. MG-63 cells accumulated 10μM glutamate at a rate of 4087 ± 274 pmol/hr/mg and 250μM at a rate of 49941 ± 4795 pmol/hr/mg. Replacement of sodium chloride with choline chloride significantly reduced MG-63 glutamate uptake by ~35%, to 2739 ± 227 pmol/hr/mg at 10μM (one-way ANOVA P=0.001) and by ~30% to 35944 ± 5157 pmol/hr/mg at 250μM, however this was not significant (one-way ANOVA P=0.059). In SaOS-2 cells, 10μM glutamate was accumulated at a rate of 32190 ± 1185 pmol/hr/mg and 250μM glutamate at a rate of 102922 ± 3971 pmol/hr/mg. Replacement of sodium chloride with equimolar choline chloride significantly reduced glutamate accumulation by ~90% (to 3355 ± 158 pmol/hr/mg) at 10μM (one-way ANOVA P<0.001) and by ~50% (to 53191 ± 2965 pmol/hr/mg) at 250μM (one-way ANOVA P<0.001).

These graphs show that both cell lines display Na^+-dependent glutamate uptake activity, characteristic of EAATs, and that compared to MG-63 cells, SaOS-2 cells display 8-fold greater Na^+-dependent glutamate uptake activity at 10μM glutamate but only 2-fold greater Na^+-dependent glutamate uptake activity at 250μM glutamate.

3.3.3.1.2 Primary osteoblasts

Human primary osteoblasts (NHOB2P9) were incubated with 10μM mix of radiolabelled and unlabelled glutamate at 37°C for 20 min in KRH buffer containing

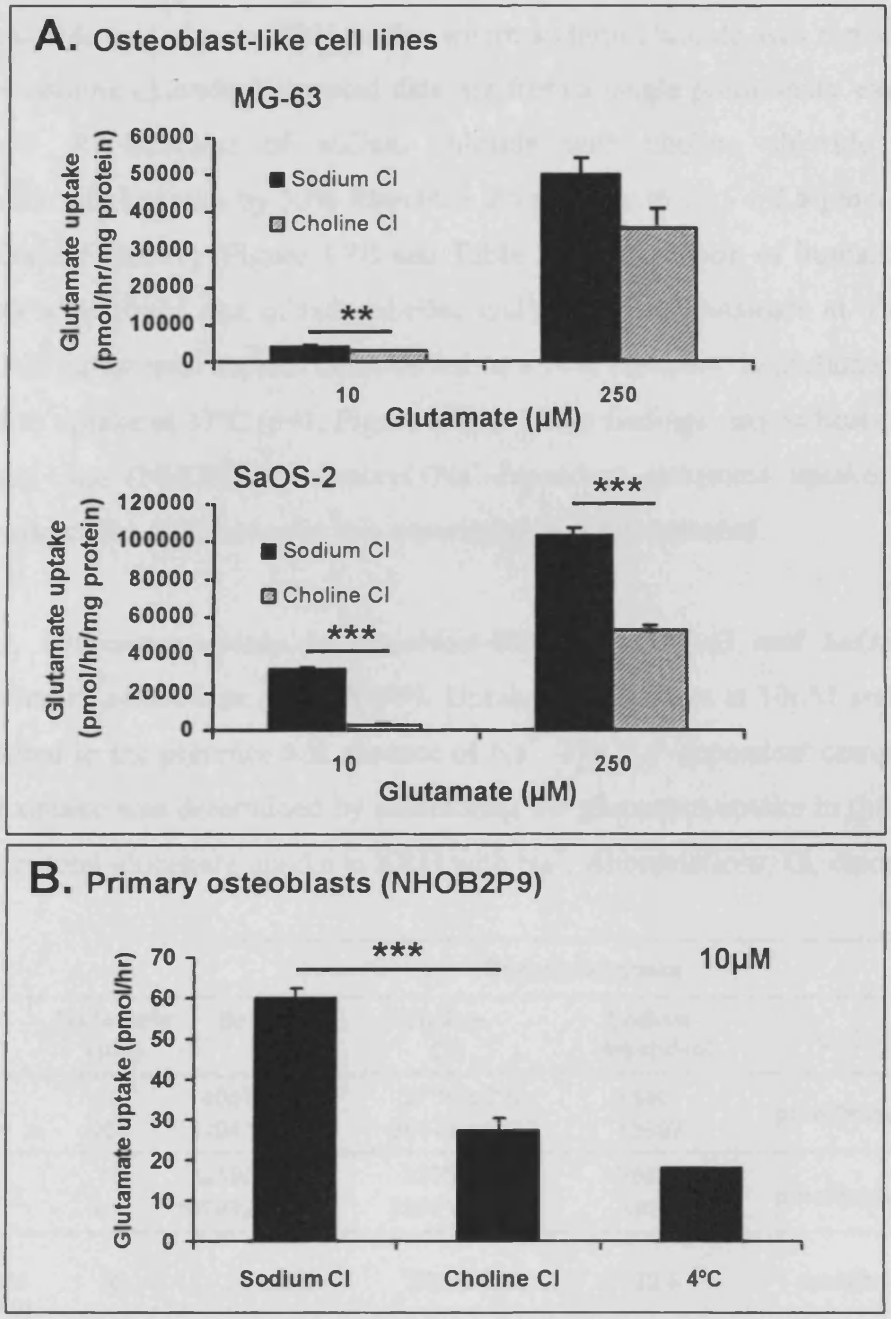

Figure 3.7. Glutamate accumulation in cultured (A) human osteoblast-like cell lines and (B) human primary osteoblasts (NHOB2P9). Osteoblasts were incubated with 10 or 250μM ^{14}C-glutamate at 4 or 37°C for 10 min (in A) or 20 min (in B) in KRH buffer, followed by aspiration of buffer and rinsing with cold KRH containing 1.5mM unlabelled glutamate. To determine the Na^+-dependent component of glutamate uptake, sodium chloride was replaced with equimolar choline chloride. Values are mean ± S.E.M from three independent experiments, n=4 in (A) or a single preliminary experiment, n=4 in (B). $^{**}P<0.01$, $^{***}P<0.001$ significantly different from control value obtained with normal KRH buffer (containing Na^+) shown by one-way ANOVA. Abbreviations: Cl, chloride.

sodium chloride and also in KRH buffer where sodium chloride was replaced with equimolar choline chloride. Presented data are from a single preliminary experiment where n=4. Replacement of sodium chloride with choline chloride reduced accumulation of glutamate by 50% from 60 ± 2.5 pmol/hr to 27.5 ± 2.8 pmol/hr (one-way ANOVA $P<0.001$) (Figure 3.7B and Table 3.1). Incubation of human primary osteoblasts with 10μM mix of radiolabelled and unlabelled glutamate at 4°C for 20 min in KRH buffer with sodium chloride led to a 70% reduction in glutamate uptake compared to uptake at 37°C (n=1, Figure 3.7B). These findings may indicate that this NHOB cell line (NHOB2P9) displays Na^+-dependent glutamate uptake activity, characteristic of EAATs, however this experiment was not repeated.

Table 3.1. Glutamate uptake in osteoblast-like cells (MG-63 and SaOS-2) and human primary osteoblasts (NHOB2P9). Uptake of glutamate at 10μM and 250μM was measured in the presence and absence of Na^+. The Na^+-dependent component of glutamate uptake was determined by subtracting the glutamate uptake in the absence of Na^+ from total glutamate uptake in KRH with Na^+. Abbreviations; Cl, chloride.

		Glutamate uptake			
Cell line	Glutamate (μM)	Sodium Cl	Choline Cl	Sodium-dependent	Unit
MG-63	10	4087 ± 274	2739 ± 227	1348	pmol/hr/mg
	250	49941 ± 4795	35944 ± 5157	13997	
SaOS-2	10	32190 ± 1185	3355 ± 158	28835	pmol/hr/mg
	250	102922 ± 3971	53191 ± 2965	49731	
Primary osteoblasts (NHOB2P9)	10	60 ± 2.5	27.5 ± 2.8	32.5	pmol/hr

3.3.3.2 Kinetics of Na^+-dependent glutamate uptake

3.3.3.2.1 Osteoblast-like cells

Osteoblast-like cell lines were incubated with 1-250μM mix of radiolabelled and unlabelled glutamate at 37°C for 10 min in KRH buffer (± Na^+) for kinetic characterisation of glutamate uptake (Figures 3.8 and 3.9). Presented data are from three independent experiments where n=4.

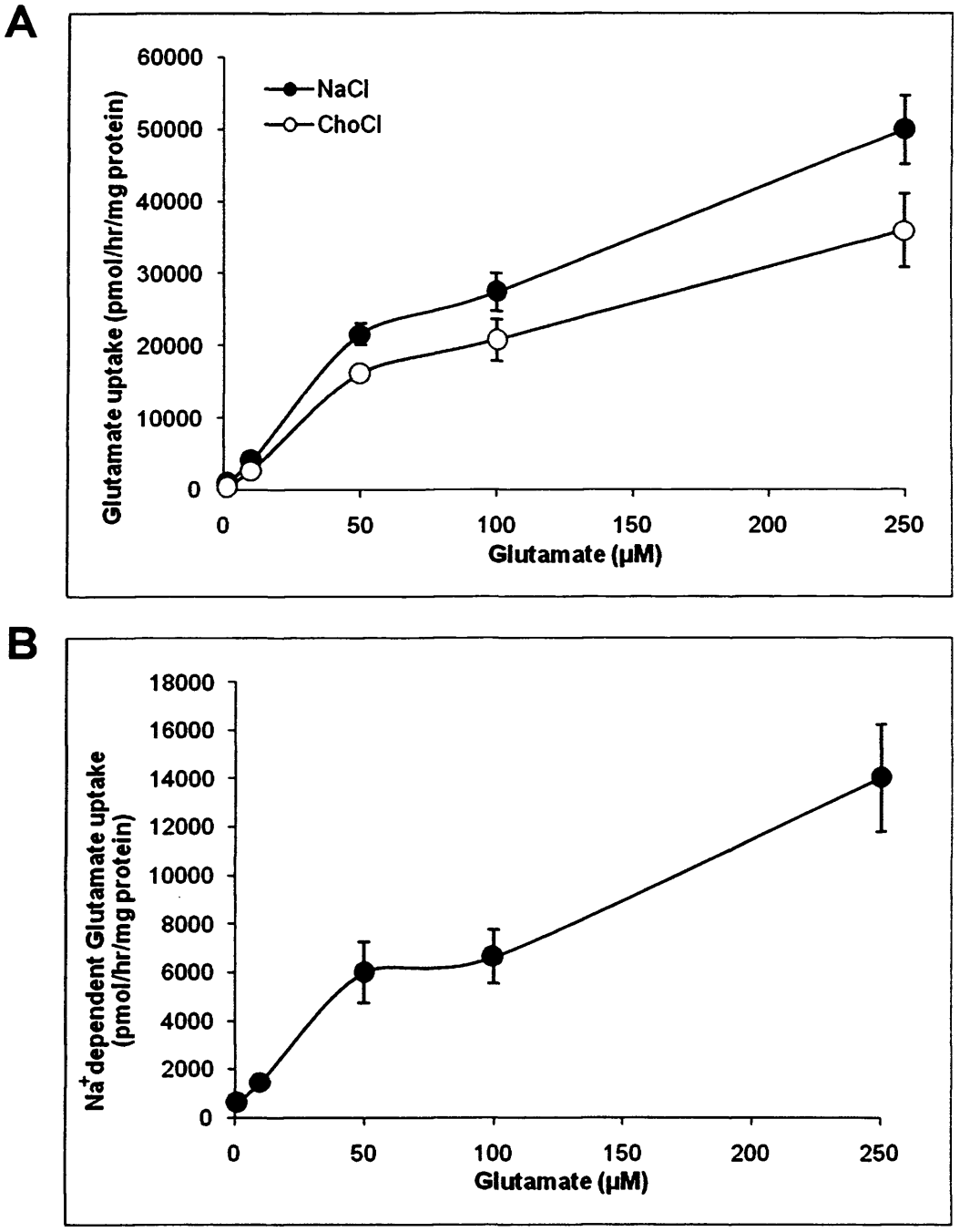

Figure 3.8. Glutamate accumulation in MG-63 cells. (A) MG-63 cells were incubated with 1-250μM mix of radiolabelled and unlabelled glutamate at 37°C for 10 min in KRH buffer ± Na^+, followed by aspiration of buffer and rinsing with cold KRH containing 1.5mM unlabelled glutamate. (B) Sodium-dependent glutamate uptake was determined by subtracting the glutamate uptake in the absence of sodium from total glutamate uptake in KRH with sodium. Values are mean ± S.E.M from three independent experiments, n=4. Abbreviations: ChoCl, choline chloride.

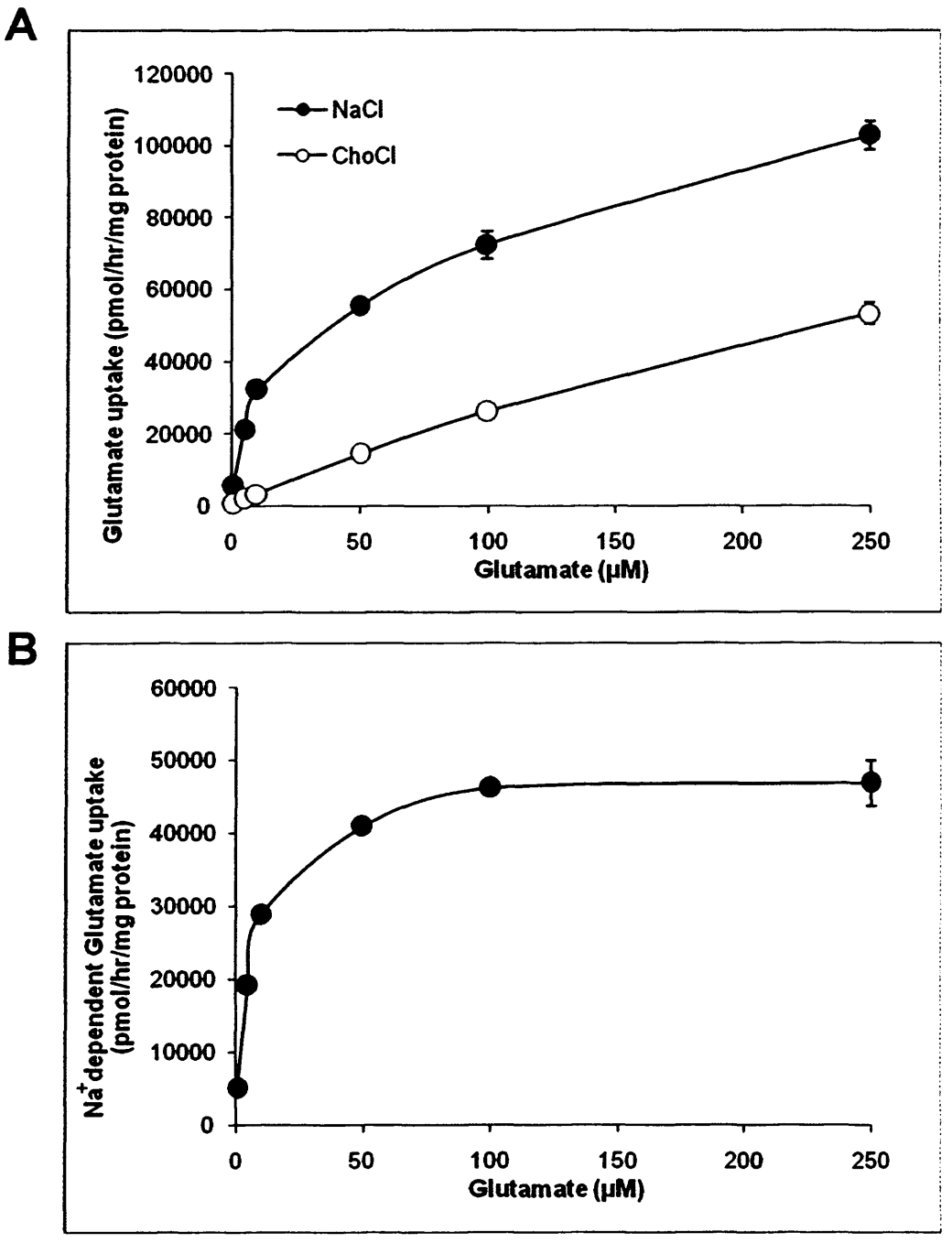

Figure 3.9. Glutamate accumulation in SaOS-2 cells. (A) SaOS-2 cells were incubated with 1-250μM mix of radiolabelled and unlabelled glutamate at 37°C for 10 min in KRH buffer ± Na^+, followed by aspiration of buffer and rinsing with cold KRH containing 1.5mM unlabelled glutamate. (B) Sodium-dependent glutamate uptake was determined by subtracting the glutamate uptake in the absence of sodium from total glutamate uptake in KRH with sodium. Values are mean ± S.E.M from three independent experiments, n=4. Abbreviations: ChoCl, choline chloride.

In MG-63 cells, glutamate uptake increased as the concentration of glutamate was increased, however no point of saturation was observed up to 250μM glutamate, both in the presence and absence of Na^+ (Figure 3.8A). Na^+-dependent glutamate uptake also increased dose-dependently in MG-63 cells and uptake was not saturated by 250μM glutamate (Figure 3.8B). Interestingly, Na^+-dependent glutamate uptake appeared to saturate between 50μM and 100μM glutamate before then continuing to increase between 100μM and 250μM glutamate suggesting that there may be two components to the Na^+-dependent glutamate uptake curve in MG-63 cells.

In SaOS-2 cells, glutamate accumulation increased as glutamate concentration increased, both in the presence and absence of sodium (Figure 3.9A). On analysis of the Na^+-dependent component of glutamate accumulation, a typical saturation curve was observed (Figure 3.9B). SaOS-2 cells increased Na^+-dependent glutamate uptake as the glutamate concentration increased, followed by saturation at a concentration above 50μM within a concentration range of up to 250μM.

3.3.3.2.1.1 Determination of kinetic constants

Lineweaver-Burk plots graphically display kinetic data and when this plot yields a straight line the data conforms to Michaelis-Menten kinetics. When this is the case, the y-intercept is equivalent to the inverse of V_{max} (the maximal glutamate uptake rate) and the x-intercept is equivalent to $-1/K_M$ (-1/the affinity of the glutamate transporter).

Na^+-dependent glutamate accumulation in MG-63 cells does not yield a typical saturation curve (Figure 3.8B) and a Lineweaver-Burk plot of these data does not generate a straight line, as shown by a goodness of fit value (R^2) of 0.7747 (Figure 3.10A), further indicating that Na^+-dependent glutamate accumulation in MG-63 cells does not adhere to typical Michaelis-Menten kinetics.

Since Lineweaver-Burk analysis can distort errors in the data, non-linear regression analysis was also carried out using a curve fitting program with GraphPad Prism software. The shape of the uptake curve in Figure 3.8B suggests that there may be two components to Na^+-dependent glutamate uptake in MG-63 cells since uptake appears to saturate between 50μM and 100μM glutamate before then continuing to increase between 100μM and 250μM glutamate. These components may represent a low- and a high-affinity transporter. However, there are too few data points in each

A. Lineweaver-Burk plot of MG-63 Na^+-dependent glutamate uptake

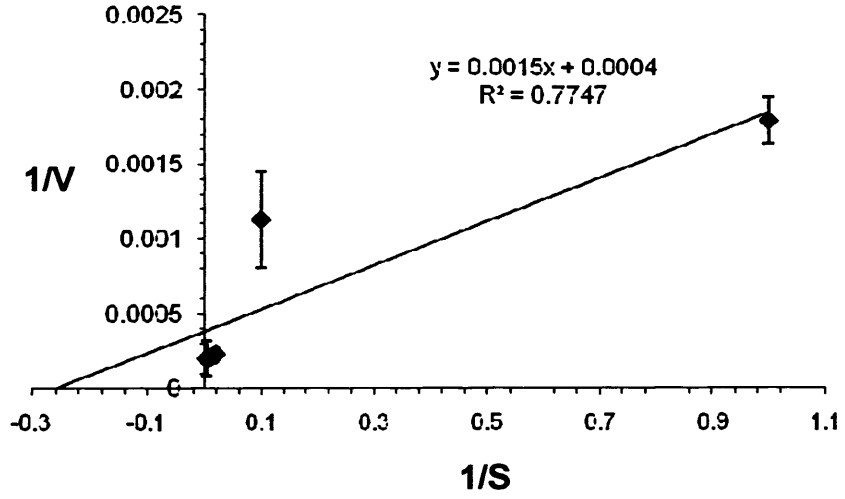

B. Curve fitting of MG-63 Na^+-dependent glutamate uptake by GraphPad Prism to a (i) one-site or (ii) two-site binding equation

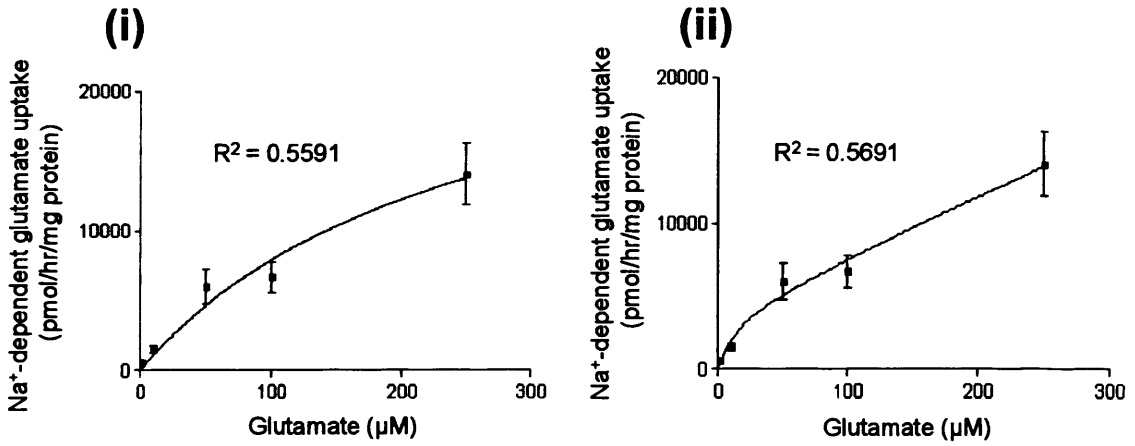

Figure 3.10. Kinetic analysis of Na^+-dependent glutamate accumulation in MG-63 cells. (A) Lineweaver-Burk analysis was carried out using data from Figure 3.8B. The reciprocal of glutamate uptake rate (in pmol/hr/mg protein) was plotted against the reciprocal of glutamate concentration (in μM). The goodness of fit (R^2) value generated by Microsoft Excel (0.7747) shows that these data do not yield a straight line indicating that the data deviates from Michaelis-Menten kinetic principles. (B) The data from Figure 3.8B was fitted to (i) one-site and (ii) two-site binding equations by GraphPad Prism software. The R^2 values generated are presented on the graph. Both curves deviate from the data points and have similarly poor R^2 values ((i) 0.5591 and (ii) 0.5691). Values are mean ± S.E.M from three independent experiments, n=4.

component for them to be analysed separately, therefore to investigate this hypothesis, GraphPad Prism was used to fit the data to either a one-site or two-site binding equation and compare the goodness of fit to these two models (Figure 3.10B). The curves generated in both cases do not pass through all data points and display similarly poor R^2 values, i.e. 0.5591 for a one-site binding hypothesis (Figure 3.10B(i)) and 0.5691 for a two-site binding hypothesis (Figure 3.10B(ii)). However, F-test comparison by GraphPad Prism indicated that a one-site binding model was the best fit to the data. Using this model, non-linear regression analysis of Na^+-dependent uptake in MG-63 cells by GraphPad Prism indicated that glutamate was accumulated with a K_M of 241 ± 151 μM and a V_{max} of 26,940 ± 9,804 pmol/hr/mg (Table 3.2). The large errors associated with these constants and the fact that the data does not strongly conform to a known model indicates that these results must be interpreted with caution. Repeating the experiment over a more comprehensive range of glutamate concentrations, particularly within the 100-250μM range, might help reveal the best kinetic model to fit the data.

In contrast, Lineweaver-Burk plot analysis indicated that Na^+-dependent glutamate accumulation in SaOS-2 cells (using data from Figure 3.9B) consisted of a single component within a substrate concentration of 1-250μM with a straight line R^2 value of 0.99 (Figure 3.11A). Using this graph to estimate kinetic constants resulted in a K_M of 10μM and a V_{max} of 50,000 pmol/hr/mg.

Comparison of a one-site or two-site binding (hyperbola) model by F-test using GraphPad Prism recommended that a one-site binding model is the best fit to the data with a R^2 value of 0.795 (Figure 3.11B). The curve fitted to this model by passing through every data point. Non-linear regression analysis of Na^+-dependent uptake in SaOS-2 cells by GraphPad Prism indicated that glutamate was accumulated with a K_M of 7.4 ± 1.2 μM and a V_{max} of 48,510 ± 1,700 pmol/hr/mg (Table 3.2).

Table 3.2. Kinetic components of glutamate uptake in osteoblast-like cells.

	K_M (μM)	Vmax (pmol/hr/mg)
MG-63	241 ± 151	26,940 ± 9,804
SaOS-2	7.4 ± 1.2	48,510 ± 1,700

A. Lineweaver-Burk plot of SaOS-2 Na^+-dependent glutamate uptake

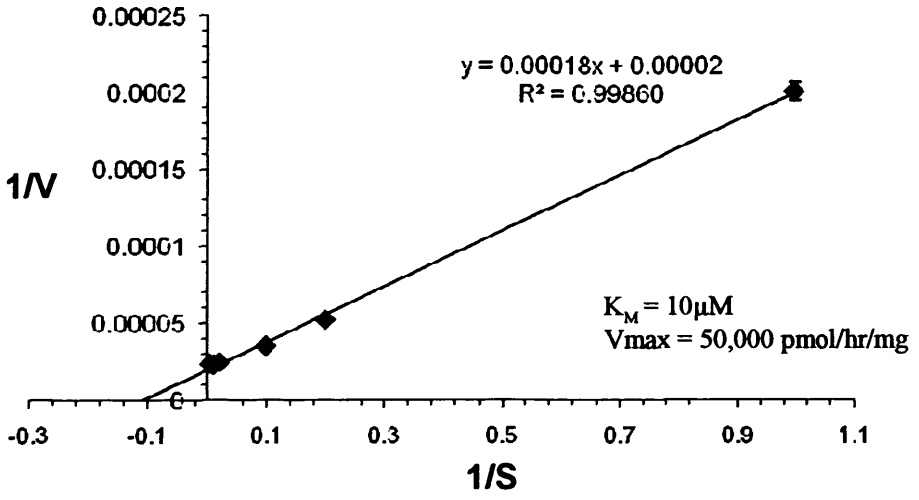

B. Curve fitting of SaOS-2 Na^+-dependent glutamate uptake by GraphPad Prism to a one-site binding equation

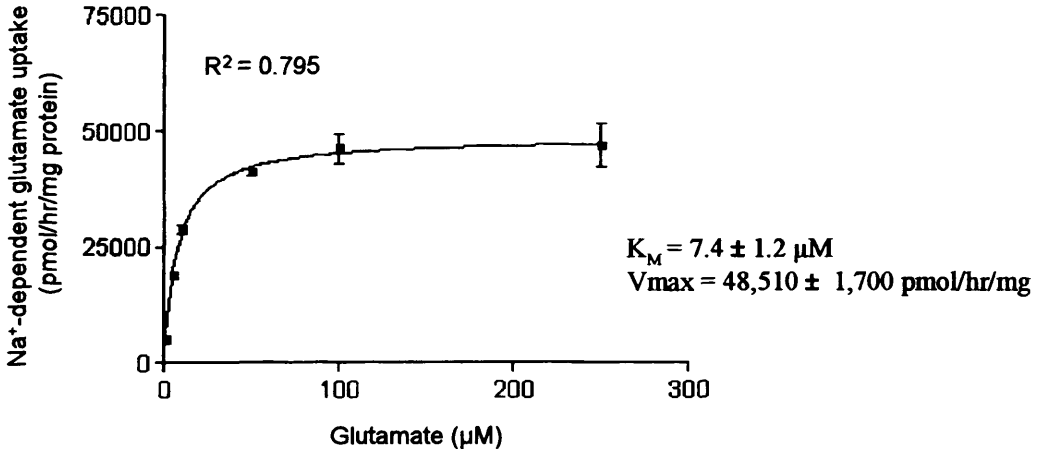

Figure 3.11. Kinetic analysis of Na^+-dependent glutamate accumulation in SaOS-2 cells. (A) Lineweaver-Burk analysis was carried out using data from Figure 3.9B. The reciprocal of glutamate uptake rate (in pmol/hr/mg protein) was plotted against the reciprocal of glutamate concentration (in μM). The goodness of fit (R^2) value generated by Microsoft Excel (0.9986) shows that these data yield a straight line indicating that the data conforms to Michaelis-Menten kinetic principles. The y-intercept of the plot is equivalent to the inverse of V_{max} and the x-intercept is equivalent to $-1/K_M$ (shown inset). (B) The data from Figure 3.9B was fitted to a one-site binding equation by GraphPad Prism software. The curve fits all the data points with a good R^2 value (0.795). GraphPad Prism estimates the kinetic parameters (K_M and V_{max}) from the data (shown inset). Values are mean ± S.E.M from three independent experiments, n=4.

3.3.3.2.2 Primary osteoblasts

Primary human osteoblasts (NHOB2P9) were incubated with 1-500μM mix of radiolabelled and unlabelled glutamate at 37°C for 20 min in KRH buffer (+ Na^+) (Figure 3.12). Presented data are from a single preliminary experiment where n=4. In these cells, glutamate uptake increased as the concentration of glutamate was increased. Due to insufficient cell number, parallel cultures could not be used for Na^+-free uptake controls or for assaying protein content and therefore uptake is expressed as pmol/hr rather than pmol/hr/mg. Since there were no experimental treatments, all uptake values would be normalised to the same protein concentration, thus the trends are unaffected by lack of protein normalisation. The lack of Na^+-free uptake controls unfortunately prevents the calculation of the Na^+-dependent component of glutamate uptake and therefore the data represent a total of all glutamate uptake systems in these cells.

3.3.3.3 Pharmacology of glutamate uptake in osteoblast-like cells

MG-63 and SaOS-2 cells were pre-incubated with KRH buffer (+ Na^+) containing EAAT inhibitors (*t*-PDC or TBOA) at a concentration range of 1μM to 1mM for 1hr at 37°C. These concentrations were chosen to span the IC_{50} and Ki values reported in the literature (Table 2.3). Glutamate uptake was then determined by supplementing the buffer with 10μM (MG-63) or 1μM (SaOS-2) mix of radiolabelled and unlabelled glutamate in KRH (± Na^+) to determine the effect of EAAT inhibitors on the Na^+-dependent component of uptake. Glutamate uptake is expressed as a percentage of control uptake (no EAAT inhibitor) over a range of inhibitor concentrations (Figure 3.13 and 3.14). Presented data are from a single experiment where n=4. GraphPad Prism 2 was used to determine IC_{50} values for each inhibitor (Table 3.3). TBOA, a competitive inhibitor of a wide range of EAATs, was the most potent inhibitor of glutamate uptake (IC_{50}=0.92μM and 7.4μM in MG-63 and SaOS-2 cells respectively) and the competitive EAAT inhibitor *t*-PDC was a less potent inhibitor (IC_{50}=318.6μM and 51.6μM in MG-63 and SaOS-2 cells respectively).

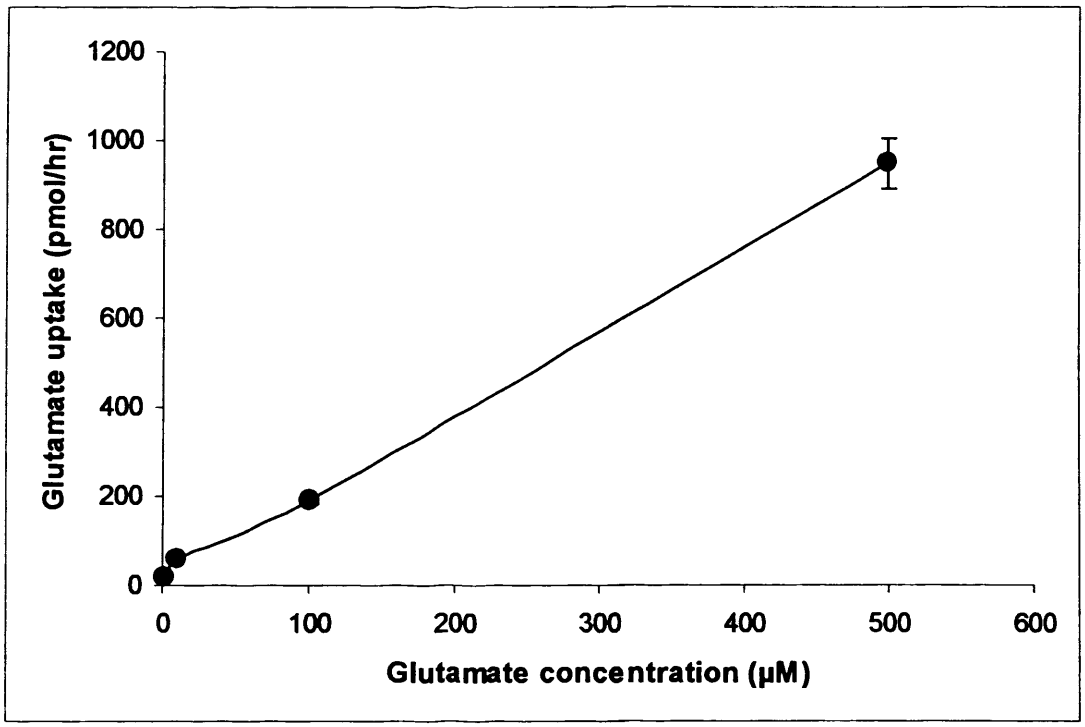

Figure 3.12. Glutamate accumulation in cultured human primary osteoblasts. Human primary osteoblasts (NHOB2P9) were incubated with 1-500µM mix of radiolabelled and unlabelled glutamate at 37°C for 20 min in KRH buffer + Na^+, followed by aspiration of buffer and rinsing with cold KRH containing 1.5mM unlabelled glutamate. Values are mean ± S.E.M from a single preliminary experiment, n=4.

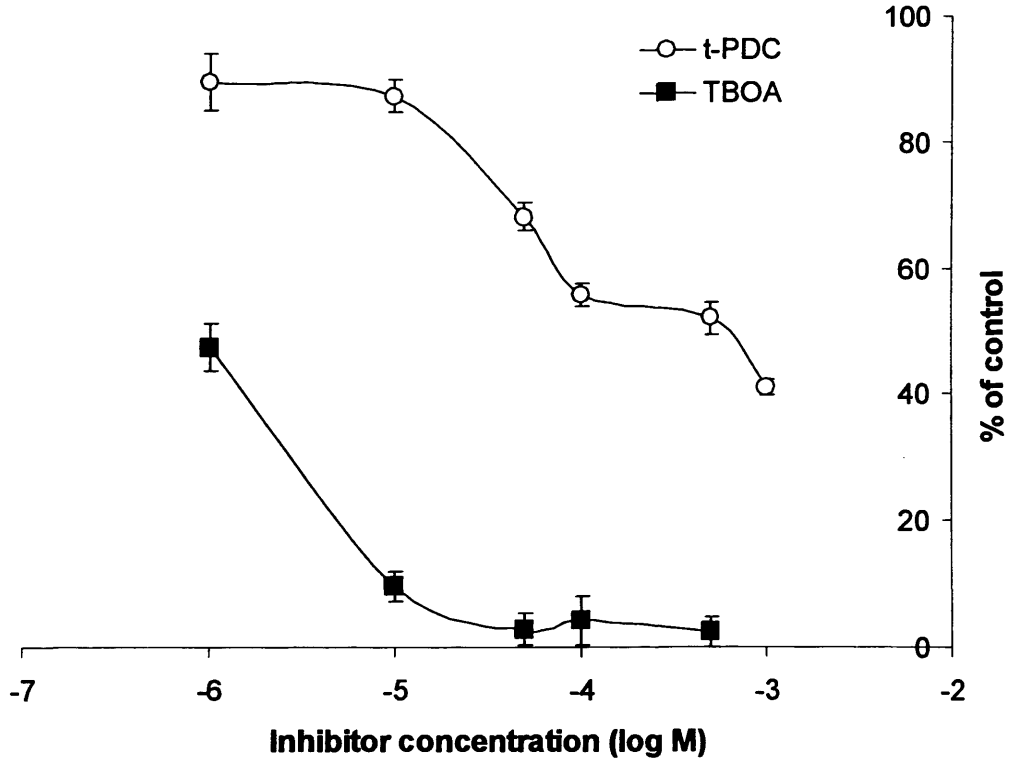

Figure 3.13. Pharmacological inhibition of glutamate accumulation in MG-63 osteoblasts. MG-63 osteoblasts were pre-incubated with KRH buffer + Na^+ in the presence and absence of 1μM-1mM EAAT inhibitor for 1hr. Osteoblasts were then incubated with 10μM mix of radiolabelled and unlabelled glutamate at 37°C for 10 min in KRH buffer ± Na^+, followed by aspiration of buffer and rinsing with cold KRH containing 1.5mM unlabelled glutamate. To determine the sodium-dependent component of glutamate uptake, sodium chloride was replaced with equimolar choline chloride. Values represent sodium-dependent uptake as a percentage of sodium-dependent uptake in untreated control cells. Values are mean ± S.E.M from a single experiment, n=4. *t*-PDC; L-*trans*-Pyrrolidine-2,4-dicarboxylic acid, TBOA; DL-threo-b-benzyloxyaspartic acid.

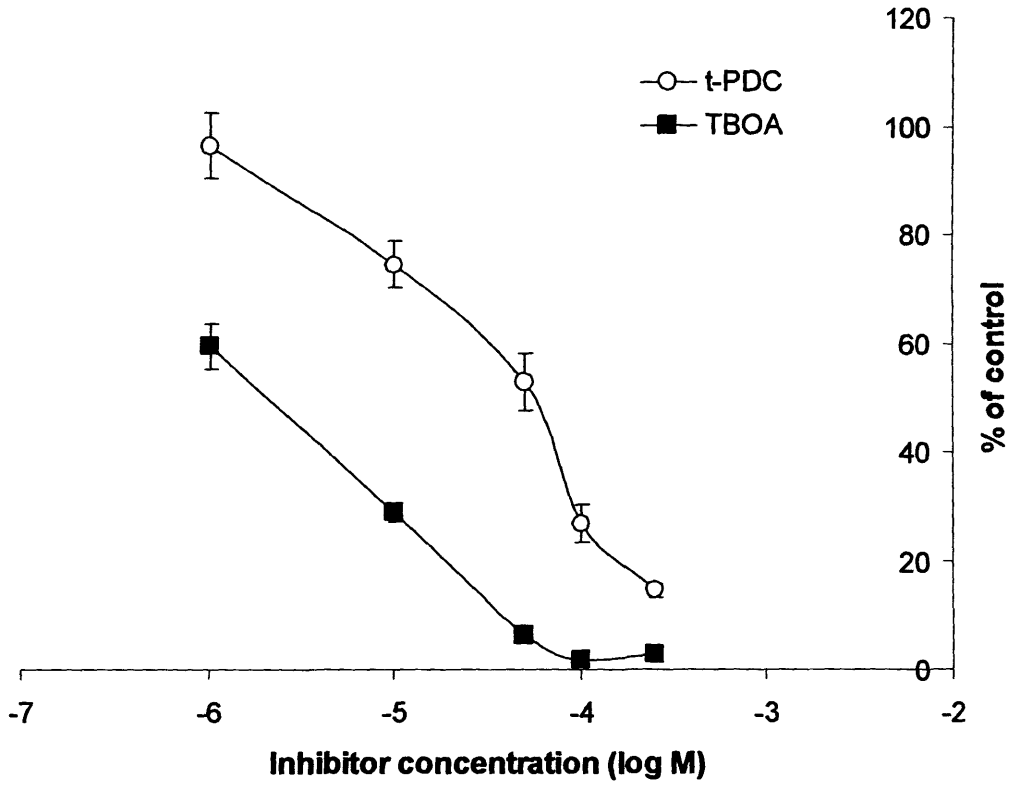

Figure 3.14. Pharmacological inhibition of glutamate accumulation in SaOS-2 osteoblasts. SaOS-2 osteoblasts were pre-incubated with KRH buffer + Na^+ in the presence and absence of 1μM-250μM EAAT inhibitor for 1hr. Osteoblasts were then incubated with 1μM mix of radiolabelled and unlabelled glutamate at 37°C for 10 min in KRH buffer ± Na^+, followed by aspiration of buffer and rinsing with cold KRH containing 1.5mM unlabelled glutamate. To determine the sodium dependent component of glutamate uptake, sodium chloride was replaced with equimolar choline chloride. Values represent sodium-dependent uptake as a percentage of sodium-dependent uptake in untreated control cells. Values are mean ± S.E.M from a single experiment, n=4. *t*-PDC; L-*trans*-Pyrrolidine-2,4-dicarboxylic acid, TBOA; DL-threo-b-benzyloxyaspartic acid.

Table 3.3. IC_{50} values and confidence intervals for the effect of EAAT inhibitors on Na^+-dependent glutamate uptake in MG-63 and SaOS-2 cells. *t*-PDC; L-*trans*-Pyrrolidine-2,4-dicarboxylic acid, TBOA; DL-threo-b-benzyloxyaspartic acid

Cell line	Inhibitors	IC_{50} (μM)	IC_{50} 95% confidence intervals (μM)
MG-63	-O- t-PDC	318.6	202 – 502
	-■- TBOA	0.92	0.73 – 1.16
SaOS-2	-O- t-PDC	51.6	25.3 – 105.1
	-■- TBOA	7.4	4.9 – 11.4

3.3.3.4 The effect of glutamate on Na^+-dependent glutamate uptake in osteoblast-like cells

The effect of short-term (1hr) and long-term (24hr) pre-treatment with glutamate on Na^+-dependent glutamate uptake was assessed in MG-63 and SaOS-2 osteoblast-like cells. Pre-incubations were carried out at both physiological (10μM) and pathological (500μM) glutamate concentrations (section 1.5.2). Na^+-dependent glutamate uptake is expressed as a percentage of control Na^+-dependent glutamate uptake measured in cells that were incubated in glutamate-free medium/KRH buffer (Figure 3.15 and 3.16). Presented data are from three independent experiments where n=4.

Na^+-dependent glutamate uptake in MG-63 cells was not significantly affected by 1hr or 24hr pre-incubation with 10μM or 500μM glutamate (Figure 3.15) as shown by Shierer-Ray test for the effect of pre-incubation time (P=0.300), glutamate concentration (P=0.667) and interaction effects (P=0.104).

Na^+-dependent glutamate uptake in SaOS-2 cells was significantly affected by pre-incubation time (P<0.001), glutamate concentration (P<0.001) and interaction effects (P<0.001) as shown by GLM (Figure 3.16). Post-hoc pair-wise Tukey's comparisons revealed that Na^+-dependent glutamate uptake was not significantly affected by 1hr pre-incubation with 10μM glutamate (P=0.7742); however a significant reduction in Na^+-dependent glutamate uptake was detectable after 1hr pre-incubation with 500μM glutamate to 85 ± 2 % of control cells (P=0.0014). 24hr pre-incubation with 10μM glutamate did not significantly affect Na^+-dependent glutamate uptake (P=0.8931),

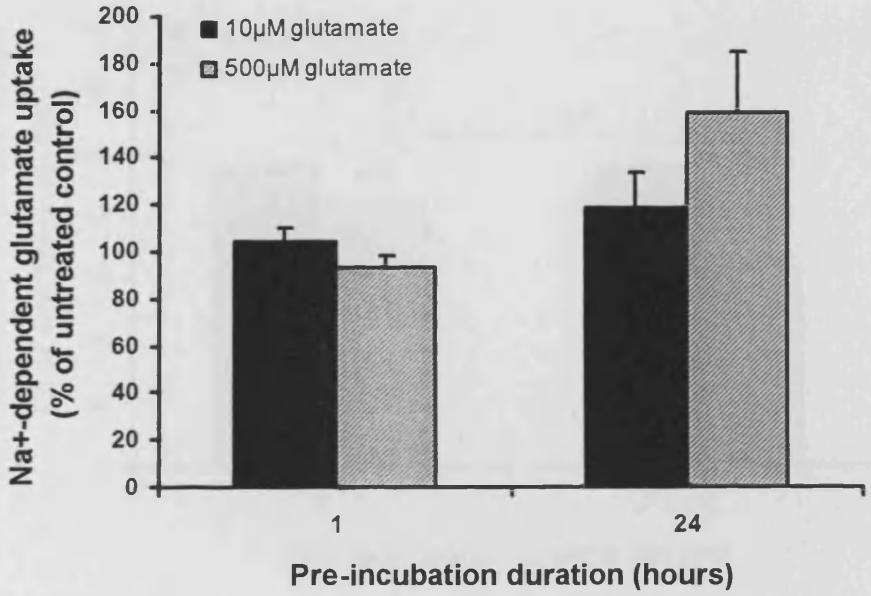

Figure 3.15. Effect of glutamate pre-incubation on Na^+-dependent glutamate uptake in MG-63 cells. MG-63 cells were pre-incubated with 0, 10 or 500μM unlabelled glutamate for 1 or 24hrs. MG-63 cells were then incubated with 10μM mix of radiolabelled and unlabelled glutamate at 37°C for 10 min in KRH buffer ± Na^+, followed by aspiration of the buffer and rinsing with cold KRH containing 1.5mM unlabelled glutamate. Na^+-dependent glutamate uptake was normalised to total cellular protein (mg) and expressed as a percentage of untreated cells (no pre-incubation with glutamate). Values are mean ± S.E.M from three independent experiments where n=4. Na^+-dependent glutamate uptake in MG-63 cells was not significantly affected by 1hr or 24hr pre-incubation with 10μM or 500μM glutamate (Shierer Ray test).

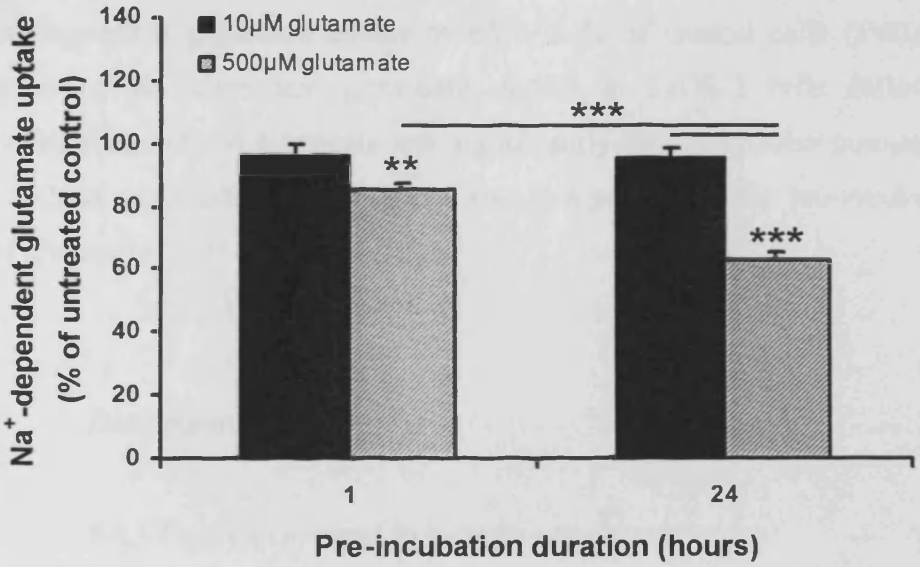

Figure 3.16. Effect of glutamate pre-incubation on Na^+-dependent glutamate uptake in SaOS-2 cells. SaOS-2 cells were pre-incubated with 0, 10 or 500μM unlabelled glutamate for 1 or 24hrs. SaOS-2 cells were then incubated with 10μM mix of radiolabelled and unlabelled glutamate at 37°C for 10 min in KRH buffer ± Na^+, followed by aspiration of the buffer and rinsing with cold KRH containing 1.5mM unlabelled glutamate. Na^+-dependent glutamate uptake was normalised to total cellular protein (mg) and expressed as a percentage of untreated cells (no pre-incubation with glutamate). Values are mean ± S.E.M from three independent experiments where n=4. Na^+-dependent glutamate uptake in SaOS-2 cells was significantly affected by pre-incubation time ($P<0.001$), glutamate concentration ($P<0.001$) and interaction effects ($P<0.001$) as shown by GLM. Post-hoc Tukey's tests revealed that Na^+-dependent glutamate uptake was significantly decreased following 1hr and 24hr pre-incubation with 500μM glutamate compared to untreated cells and cells incubated with 10μM glutamate for 24hrs. This decrease was significantly greater at 24hrs compared to 1hr. $^{**}P<0.01$, $^{***}P<0.001$ significantly different from untreated cells or from values indicated by lines.

however 24hr pre-incubation with 500μM glutamate resulted in a significant decrease in Na^+-dependent glutamate uptake to 63 ± 2 % of control cells ($P<0.001$). The reduction of Na^+-dependent glutamate uptake in SaOS-2 cells following pre-incubation with 500μM glutamate was significantly greater at 24hrs compared to 1hr with 500μM glutamate ($P<0.001$) and also compared to 24hr pre-incubation with 10μM glutamate ($P<0.001$).

3.4 Discussion

3.4.1 EAATs are expressed in human osteoblasts

The experiments presented in this chapter have shown that transcripts for EAATs 1-3 and two splice variants of EAAT1 (EAAT1a and EAAT1ex9skip) are expressed in human bone, human primary osteoblasts and human osteoblast-like cell lines. Furthermore, expression of EAAT1 and EAAT3 protein has been confirmed by immunofluoresence in human primary osteoblasts and human osteoblast-like cell lines. Since both splice variants of EAAT1 are expressed as proteins *in vivo* (Huggett et al. 2000; Vallejo-Illarramendi et al. 2005; Macnab et al. 2006; Macnab and Pow 2007a) and the antibody used here detects a 15aa C-terminal epitope, a sequence common to EAAT1, EAAT1a and possibly EAAT1ex9skip, it is likely that the immunostaining shown here for EAAT1 represents a pool of the 3 known EAAT1 variants. Expression of EAAT1 protein has been previously described for MG-63 cells (Kalariti et al. 2004; Kalariti et al. 2007) and bone-forming osteoblasts *in vivo* (Mason et al. 1997) and EAAT1 mRNA has been previously detected in SaOS-2 cells (Huggett et al. 2002; Mason and Huggett 2002).

Expression of EAAT-1a mRNA has been detected at low levels in bone *in vivo,* and also in SaOS-2 osteoblasts and MLO-Y4 osteocytes (Huggett et al. 2002). However, this is the first reported detection of EAAT1ex9skip in human bone, human primary osteoblasts and human osteoblast-like cells. In the human brain, EAAT1ex9skip mRNA is expressed at levels of 10-20% of full-length EAAT1 and acts in a dominant negative capacity over full-length EAAT1 glutamate transport function in transiently transfected HEK293 cells (Vallejo-Illarramendi et al. 2005). In MG-63 osteoblast-like

cells and primary human osteoblasts, the expression levels of EAAT1ex9skip relative to full-length EAAT1 are 13% and 12% respectively, which is comparable to the proportion of the variant in human brain. However quantitative analysis of primary human osteoblast EAAT expression was not repeated. Expression of EAAT1ex9skip was far lower in SaOS-2 osteoblast-like cells (2%). Interestingly, the experiments in this chapter have shown that MG-63 cells have a reduced capacity for Na^+-dependent glutamate compared to SaOS-2 cells (Figure 3.7). The higher proportion of the dominant negative splice variant EAAT1ex9skip in MG-63 cells compared to SaOS-2 cells may play a role in reducing Na^+-dependent transport activity. High expression levels of the EAAT1ex9skip transcript in MG-63 cells and human brain suggest a possible physiological role for this splice variant in glutamate homeostasis or signalling. EAAT1ex9skip has been detected by immunohistochemistry within the human brain, particularly cortical and collicular neurons, in contrast to the primarily glial expression of full-length EAAT1 (Macnab and Pow 2007a). Furthermore, EAAT1ex9skip is expressed in neurons and in regions that are susceptible to damage in the hypoxic pig brain, such as the CA1 region of the hippocampus, supporting the suggestion that expression of EAAT1ex9skip may indicate neurons that are subject to abnormal glutamate-mediated excitation and at risk of dying in response to insult (Sullivan et al. 2007a). A provisional patent for the use of EAAT1ex9skip (also referred to as GLAST1b) as a biomarker for the detection of hypoxia-induced neuronal damage was filed in 2008 (Pow 2008). Information regarding the regulation of EAAT1ex9skip expression in osteoblasts will be important for elucidating the role of this variant in bone.

Expression of GLT-1 and EAAC1 transcripts have previously been detected in rat calvarial osteoblasts (Takarada et al. 2004) and GLT-1 protein expression has been detected in mononuclear cells from rat bone marrow, though EAAC1 protein could not be detected in bone *in vivo* (Mason et al. 1997). However, transcript expression for EAAT2 and EAAT3 has not previously detected in human bone, human primary osteoblasts or human osteoblast-like cells.

3.4.1.1 EAATs are expressed at differential levels in human osteoblasts

Differences in EAAT expression levels observed between the osteoblast-like cell lines may reflect altered regulation of the transporters during osteoblast differentiation

since SaOS-2 cells represent a more mature phenotype compared to MG-63 cells (Jukkola et al. 1993; Chaudhary and Avioli 1994; Pautke et al. 2004; Shapira and Halabi 2009). EAATs 1-3 act as high-affinity glutamate transporters and function in the CNS to rapidly clear synaptically released glutamate (reviewed in (Danbolt 2001)). EAATs also function as glutamate gated ion channels and the anion permeability of EAATs 1-3 decreases in the order EAAT1>EAAT3>EAAT2 (Wadiche et al. 1995). The anion conductance of EAATs may therefore be of relevance to osteoblasts since the data presented here demonstrate that transcript levels for EAATs in human osteoblast-like cell lines decrease in magnitude in the order of EAAT1>EAAT3>EAAT2.

EAAT1 and EAAT2 are expressed by astrocytes in the CNS (Kanai and Hediger 2004), with EAAT1 displaying strong expression in Bergmann glia of the cerebellum and EAAT2 predominantly expressed in astrocytes of the cerebral cortex and hippocampus (Kanai and Hediger 2004). EAAT3 is primarily expressed in neurons and epithelial cells (Kanai and Hediger 1992). In the brain, EAAT3 is strongly expressed in neurons in the cerebral cortex, striatum, hippocampus, superior colliculus, olfactory bulb, and thalamus (Rothstein et al. 1994; Kanai et al. 1995b; Berger and Hediger 1998). Interestingly, despite EAAT1 and EAAT2 being expressed by the same astrocyte cells in the CNS (Kanai and Hediger 2004), they have been reported to display different distribution patterns in rat peripheral tissues at both the transcript and protein level (Berger and Hediger 2006). GLAST expression was most commonly found in epithelial cells of tissues including the tongue, urinary bladder, ovaries and prostate gland whereas GLT-1 localised primarily to glandular tissues such as mammary glands, salivary glands and lacrimal glands (Berger and Hediger 2006). These observations are consistent with the low expression of EAAT2 found in osteoblast-like cell lines and primary human osteoblasts compared to high expression levels of EAAT1.

3.4.1.2 Extracellular glutamate does not significantly affect EAAT mRNA expression in human osteoblasts

Expression levels of EAAT1, EAAT1ex9skip and EAAT3 were not changed following 24hrs exposure to 500μM glutamate in MG-63 or SaOS-2 osteoblasts. The glutamate-mediated regulation of EAAT1 expression has been previously investigated

in astrocytes of the CNS but not in cells of the peripheral tissues where glutamate signalling has been implicated. Gegelashvili et al. found that 7 day incubation of murine primary cortical astrocytes with 1mM glutamate had no effect on GLAST mRNA levels (Gegelashvili et al. 1996). Glutamate concentrations can reach as high as 3mM in the small volume of the synaptic cleft following neuronal depolarisation and glutamate release (Clements 1996; Diamond and Jahr 1997), however the glutamate concentration rapidly decreases as a result of diffusion and through binding and/or transport by EAATs (Diamond and Jahr 1997; Wadiche and Jahr 2005). In the absence of a signalling event, extracellular glutamate concentrations within the CNS are maintained at a low nanomolar range (Zerangue and Kavanaugh 1996; Herman and Jahr 2007). Therefore this study reflects the prolonged incubation of cells at glutamate concentrations typical of a synaptic signalling event i.e. pathological situation and no assessments of GLAST mRNA expression were made at earlier time-points in this study.

Other studies have observed that long-term exposure (6-24hrs) of chick cerebellar Bergmann glia to glutamate (1-1000μM) results in a reduction of GLAST transcription, which can be mimicked by AMPA and kainate and is sensitive to inhibition of PKC, suggesting that transcriptional regulation of GLAST is AMPA/kainate receptor-mediated (Lopez-Bayghen et al. 2003; Lopez-Bayghen and Ortega 2004; Rosas et al. 2007). Glutamate receptor activation increases DNA binding of the transcription factor AP-1 in neurons and glia (Gallo and Ghiani 2000) and partial analysis of the murine GLAST gene promoter has identified an AP-1 consensus sequence (Hagiwara et al. 1996) suggesting one mechanism whereby extracellular glutamate could regulate EAAT transcription in chick Bergmann glia. Interestingly the activation of AP-1 has been shown to be regulated by iGluR activity in osteoblasts in a similar manner to that observed in neurons (Taylor 2002).

These reported studies in chick Bergmann glia most closely resemble the experimental conditions used here with human osteoblasts. The differences in findings are likely to be the result of the different cell types studied. Astrocytes express EAAT1 and EAAT2 whereas human osteoblast-like cells express quantifiable levels of EAAT1 and EAAT3 but unquantifiable levels of EAAT2 (section 3.3.1). Furthermore, there are likely to be differences in glutamate receptor activation between the two cell types since extracellular glutamate concentrations within the CNS are maintained within a low nanomolar range (Zerangue and Kavanaugh 1996;

Herman and Jahr 2007) and glutamate is present in human synovial fluid at 6μM (Plaitakis et al. 1982; McNearney et al. 2000) suggesting that bone cells might be exposed to higher basal levels of glutamate than cells within the CNS.

Long term regulation of EAAT expression can occur at the level of the gene promoter or by alternative splicing of mRNA transcripts. The regulation of EAAT1ex9skip transcription has not been previously investigated in any cell type and the results shown here indicate that in osteoblasts, long-term exposure to 500μM glutamate does not significantly affect expression of this splice variant. Interestingly, 5 days exposure of SaOS-2 cells to 10μM glutamate, but not 1, 100 or 1000μM glutamate, has been shown to increase expression of EAAT1a relative to full-length EAAT1 (Huggett et al. 2002). Expression levels of full-length EAAT1 were not significantly affected by long-term exposure to 500μM glutamate in the experiments shown in this thesis, however this does not mean that the ratio of EAAT1 to EAAT1a was unaffected since this cannot be determined without also quantifying EAAT1a expression, which is very low in these cells.

EAAT3 expression appeared to be slightly up-regulated in MG-63 cells, but not SaOS-2 cells, following 24hrs exposure to 500μM glutamate, however this was not significant. This increase in expression may represent a compensatory change in response to increased extracellular glutamate. Glutamate transport activity does appear to be increased in MG-63 cells following 24hrs exposure to 500μM glutamate (Figure 3.15), although this also did not reach significance. However EAAT3 is expressed in MG-63 cells at much lower levels than EAAT1 and EAATex9skip, so a small, but significant, change in transcription seems unlikely to have a major effect on glutamate uptake activity.

3.4.2 EAATs are functional in human osteoblasts

MG-63 and SaOS-2 cells displayed Na^+-dependent glutamate uptake, consistent with functional EAAT activity. Prelimary findings also indicated Na^+-dependent glutamate uptake activity in human primary osteoblasts, however these experiments were not repeated. This is the first report of functional EAATs in human osteoblasts. Replacement of sodium chloride with equimolar choline chloride reduced 10μM glutamate uptake by 50% in human primary osteoblasts, by 35% in MG-63 cells and by 90% in SaOS-2 cells revealing the existence of a Na^+-dependent component of

glutamate uptake in these cells. At 250μM glutamate, uptake was reduced in MG-63 cells by 30% and in SaOS-2 cells by 50% following removal of sodium. These differences indicate that glutamate uptake in SaOS-2 cells occurs primarily via Na^+-dependent mechanisms whereas the majority of glutamate uptake in MG-63 cells appears to be Na^+-independent.

Na^+-dependent glutamate uptake activity has previously been reported in cells from various peripheral and musculoskeletal tissues including rat calvarial osteoblasts (Takarada et al. 2004), rat costal chondrocytes (Hinoi et al. 2005b), and human synovial fibroblasts (unpublished data, Flood, Duance and Mason). Replacement of sodium chloride with choline chloride almost entirely abolished glutamate uptake in rat calvarial osteoblasts and chondrocytes (Takarada et al. 2004; Hinoi et al. 2005b). The higher levels of Na^+-independent glutamate transport reported in this thesis in MG-63 cells may be due to variances in the assay protocol or due to increased activity of a Na^+-independent glutamate transporter such as the cystine/glutamate antiporter which has been reported to be expressed in MC3T3-E1 osteoblast-like cells (Uno et al. 2007) or the poorly characterised Na^+-independent low-affinity glutamate transporter (reviewed in (Erecinska and Silver 1990; Danbolt 2001)). Interestingly the majority of glutamate uptake in MG-63 osteoblasts appears to occur independently of sodium indicating that the dominant glutamate transport machinery in these cells is Na^+-independent. Therefore it is possible that in these cells the other potential EAAT functions besides glutamate transport, i.e. ion channel and receptor-like function, may have a more prominent role. The differences observed in the proportion of Na^+-dependent to Na^+-independent glutamate transport are clearly cell type, species and differentiation stage specific and an important consideration in the context of modulating glutamatergic signalling for therapeutic effect in human musculoskeletal disorders.

Glutamate uptake in primary osteoblasts also appeared to be temperature-dependent, in agreement with previous studies of glutamate transporters (Stallcup et al. 1979), suggesting that the transport mechanism involves steps that must overcome large energy barriers such as conformational transitions of the transporter and/or the requirement of energy for the maintenance of the Na^+/K^+ membrane gradients (Grunewald and Kanner 1995; Wadiche and Kavanaugh 1998).

3.4.2.1 Kinetic characterisation of glutamate uptake in human osteoblast-like cells

Kinetic characterisation of the osteoblast cell lines provides information relating to the affinity of the EAATs expressed for glutamate (K_M) as well as the maximum capacity of these cells to transport glutamate (V_{max}). These constants can then be used to detect differences associated with the phenotypic maturity of the cell lines.

Na^+-dependent glutamate uptake in SaOS-2 cells displayed a typical saturation curve with a high affinity for glutamate (K_M = 7.4 ± 1.2μM) and a large maximal uptake capacity (V_{max} = 48,510 ± 1,700 pmol/hr/mg). SaOS-2 cells express much higher levels of EAAT1 mRNA than any other EAAT expressed in this cell type (section 3.3.1), indicating that this transporter subtype might be responsible for the bulk of glutamate uptake in these cells.

In contrast, Na^+-dependent glutamate uptake in MG-63 cells does not display a typical saturation curve. It is possible that this reflects the presence of a low- and a high-affinity transporter; and similar uptake curves have been previously reported for glutamate uptake in human platelets (Mangano and Schwarcz 1981) and for endogenous Na^+-dependent glutamate uptake in *Xenopus Laevis* oocytes (Steffgen et al. 1991). However statistical comparison of a one- and two-site binding model indicated that the MG-63 uptake data fitted a one-site binding model better, despite both models fitting the data poorly. It is still plausible that the shape of the curve represents two components from two different transporters or differential regulation of the same transporter at increasing substrate concentrations, and that this is not mathematically detectable because transport was not measured across a broad enough range of glutamate concentrations. If this is the case then the second component transports glutamate with a high V_{max} but a low affinity which is not characteristic of the EAATs. EAATs transport glutamate with K_M values ranging from 18-42μM in *Xenopus oocytes* and HEK293 cells (Arriza et al. 1994; Jensen and Brauner-Osborne 2004), which fit better to the first component of the curve. A number of other Na^+-dependent glutamate transporters have been identified which might be responsible for the second component in the curve, however these are poorly characterised and none have been studied in osteoblasts to date (Levi et al. 1976; Bonanno et al. 1993; Bonanno and Raiteri 1994; Bukowski et al. 1995; Bender et al. 2000).

It is also possible that the non-hyberbolic shape of the curve can be explained by some glutamate-mediated effects on glutamate transporter activity and/or expression

that are occurring in MG-63 cells within the 10 min incubation period. Section 3.3.3.4 shows that 1hr pre-incubation with 10μM or 500μM glutamate had no effect on uptake of 10μM glutamate in MG-63 cells, however the effect of the same pre-incubations on uptake of higher concentrations of glutamate (i.e. 250μM) were not studied.

K_M values for glutamate uptake in HEK293 cells stably expressing human EAAT1, EAAT2, and EAAT3 were 20 ± 3 μM, 25 ± 3 μM, and 42 ± 13 μM respectively (Jensen and Brauner-Osborne 2004) and similar values were obtained in *Xenopus Laevis* oocytes expressing EAAT1, 2 and 3 (20 ± 3 μM, 18 ± 3 μM, and 28 ± 6 μM respectively) (Arriza et al. 1994). The K_M value for SaOS-2 cells observed here is ~3-fold lower than those detected in HEK293 cells or oocytes, whereas the K_M value for MG-63 cells is ~10-fold higher. These variations could be attributed to differences between experimental systems testing a single EAAT, and the combined values that arise from osteoblasts expressing different EAATs that are, in turn, likely to be differentially regulated within the cell.

In rat calvarial osteoblasts cultured for 7 or 21 days, the observed K_M values for glutamate uptake were 26 ± 6 μM and 42 ± 11 μM respectively and the V_{max} values were 57,600 ± 7320 pmol/hr/mg protein and 17,400 ± 1980 pmol/hr/mg protein respectively (Takarada et al. 2004). These findings suggest that as osteoblasts mature in culture, their maximal capacity to transport glutamate and the affinity of the transporters for glutamate decreases. The phenotype of the osteoblast-like cells used in the experiments presented in this thesis are widely accepted to reflect that of a pre-osteoblast (MG-63) and a late osteoblast (SaOS-2) (Jukkola et al. 1993; Chaudhary and Avioli 1994; Pautke et al. 2004; Shapira and Halabi 2009). In these studies, the more mature osteoblast (SaOS-2) in fact exhibits a much higher maximal glutamate capacity and higher affinity over the less mature osteoblast (MG-63) in contrast to the published findings with rat calvarial osteoblasts (Takarada et al. 2004). These inconsistencies might be attributable to species-specific differences, differences in the cell phenotypes used or simply a reflection of the short-comings of using cell lines in contrast to primary cells. However Takarada et al. maintained calvarial osteoblasts in medium containing glutamate at 510μM, a concentration which we have shown can decrease EAAT activity in a short- and long-term capacity in SaOS-2 cells (Figure 3.16). The authors also mentioned as a point of discussion that the possibility that radiolabelled glutamate might be unable to gain access to EAATs due to

mineralisation during maturation had not been ruled out (Takarada et al. 2004). It is also relevant to note that calvarial osteoblasts do not exhibit the same responses to mechanical stimulation as osteoblasts from load bearing regions of the body i.e. ulna (Rawlinson et al. 1995), and so regulation of glutamate signalling in these cells, a signalling pathway that has been implicated in the mechanoresponse, may not be comparable to osteoblasts from other sources.

3.4.2.2 Pharmacology of glutamate uptake in human osteoblast-like cells

Na^+-dependent glutamate uptake in MG-63 and SaOS-2 cells was dose-dependently inhibited by the non-selective competitive EAAT inhibitors TBOA and *t*-PDC (Figures 3.13 and 3.14). Na^+-dependent glutamate uptake was most potently inhibited by TBOA (IC_{50}=0.92 μM and 7.4 μM in MG-63 and SaOS-2 cells respectively) and to a lesser extent by *t*-PDC (IC_{50}=318.6 μM and 51.6 μM in MG-63 and SaOS-2 cells respectively). Both EAAT1 and EAAT3 are expressed in MG-63 and SaOS-2 cells and the lack of an EAAT1- or EAAT3-selective uptake inhibitor makes it difficult to discern if a single EAAT subtype is responsible for glutamate accumulation in these cell lines.

Inhibition of EAAT activity by *t*-PDC in MG-63 cells appeared to generate a biphasic dose-response curve suggesting the presence of more than one Na^+-dependent glutamate transporter responsible for glutamate uptake activity, consistent with kinetic findings of glutamate uptake in these cells (section 3.3.3.2.1). Table 2.3 shows the reported inhibition constants for *t*-PDC across the EAATs and these values indicate that the inhibitor is more potent for EAAT2, EAAT4 and EAAT5 than for EAAT1 and EAAT3. MG-63 cells express quantifiable levels of EAAT1 and EAAT3 mRNA but these EAATs have similar IC_{50} values for *t*-PDC (Arriza et al. 1994; Shimamoto et al. 1998) so it is unlikely that they are responsible for the two phases of the dose-response curve, unless post-translational regulation of the transporters modulates their sensitivity to inhibition by *t*-PDC. MG-63 cells express unquantifiable levels of EAAT2 mRNA and expression levels of EAAT4 and EAAT5 mRNA were not assessed. To determine whether any of these EAATs might be responsible for Na^+-dependent glutamate uptake in MG-63 cells, specific inhibitors could be used such as the EAAT2-specific inhibitor dihydrokainic acid.

Repeating the experiments over a wider range of inhibitor concentrations would also be advantageous in revealing more accurate IC_{50} values, since the determined IC_{50} values for TBOA in MG-63 and SaOS-2 cells are at concentrations below or in the lower range of those measured. Furthermore, a more comprehensive view of the dose-response curves for TBOA in each cell line would reveal any deviations from a simple sigmoidal curve. TBOA is 10X less potent for EAAT1 than for other EAATs (Table 2.3) so a biphasic dose-response curve for TBOA might indicate that more than one EAAT is responsible for glutamate uptake.

These experiments have however confirmed the presence of functional EAATs in osteoblast-like cell lines and informed decisions for further experiments assessing the effects of EAAT inhibitors on osteoblast bone-forming activity, which form the basis of chapter 4 of this thesis.

3.4.2.3 Extracellular glutamate regulates EAAT activity in human osteoblasts

Short-term (1hr) and long-term (24hr) pre-incubation of SaOS-2 cells with pathological (500μM) concentrations of glutamate significantly decreased Na^+-dependent glutamate uptake in these cells. The same pre-incubation periods with physiological concentrations of glutamate (10μM) had no effect on Na^+-dependent glutamate uptake. No significant effects upon Na^+-dependent glutamate uptake were observed following any of these pre-incubations in MG-63 cells.

These data may indicate that uptake is inhibited in SaOS-2 cells that are subject to excessive glutamate concentrations. The concentrated glutamate uptake activity occurring in SaOS-2 cells treated with 500μM glutamate, compared to those treated with 10μM glutamate, may result in depolarisation of the cell membrane due to the net positive charge moving into the cell which would then result in a reduction in the electrochemical gradients that drive transport, and so eventually slowing the rate of transport. Alternatively, the substrate-induced decrease in SaOS-2 Na^+-dependent glutamate uptake rate may be due to feedback signalling mechanisms via the receptors or transporters themselves.

Other studies have demonstrated a substrate induced inhibition of transport activity in microglial cultures expressing GLT-1 but not GLAST (12hrs with 0.1 and 1mM glutamate) (Persson et al. 2005) and in chick Bergmann glia expressing high levels of GLAST (30-60 min with 0.2 and 1mM glutamate) (Gonzalez and Ortega 2000). In

Bergamnn glia, inhibition was found to be due to a reduction in affinity of the transporter rather than a loss of available transporters at the cell surface, and was independent of receptor activation but sensitive to PKC inhibition (Gonzalez and Ortega 2000). This is in contrast to the effects of glutamate on EAAT transcription in Bergmann glia which are thought to be dependent upon AMPA/kainate receptor activation (Lopez-Bayghen et al. 2003; Lopez-Bayghen and Ortega 2004; Rosas et al. 2007). PKC phosphorylation has previously been shown to have an inhibitory effect upon GLAST activity (Conradt and Stoffel 1997; Gonzalez and Ortega 1997); yet PKC regulates GLT-1 and EAAC1 to increase transport (Casado et al. 1991; Dowd and Robinson 1996), suggesting that the response to pre-incubation with glutamate will alter depending on which EAAT subtypes are expressed and will therefore be cell-type specific.

Pre-incubation of primary astrocyte cultures and human platelets with 100μM glutamate for 1hr significantly increased glutamate uptake activity and increased GLAST protein expression (Duan et al. 1999; Begni et al. 2005) and this substrate-induced increase in transporter activity was also found to occur independently of receptor activation (Duan et al. 1999; Gonzalez and Ortega 2000; Munir et al. 2000; Begni et al. 2005). Long-term pre-incubation (7 days) of murine primary cortical astrocytes with 1mM glutamate also significantly increased glutamate uptake activity and increased GLAST protein expression (Gegelashvili et al. 1996). Pre-incubation of 'astrocyte-poor' neuronal cultures with 100μM glutamate for 30 min significantly increased glutamate uptake activity but had no detectable effects on transporter protein levels or cell surface expression (Munir et al. 2000).

The regulation of transporter activity by its substrate is not limited to the EAATs. The transport of norepinephrine is down-regulated by the long-term application (3 days) of the transporter antagonist, desipramine (Zhu *et al.* 1998) and the function of the GABA transporter is up-regulated by extracellular GABA (at 100μM for 1hr) in a receptor-independent fashion (Bernstein and Quick 1999).

The activity of expressed EAATs can be regulated at several levels, including phosphorylation (Casado et al. 1991; Conradt and Stoffel 1997) and intracellular protein-protein interactions (discussed further in chapter 6 of this thesis). Kinetic characterisation of Na^+-dependent glutamate uptake in SaOS-2 cells pre-incubated with glutamate would reveal whether the reduction in glutamate uptake was the result of decreased transporter expressed at the plasma membrane (decreased V_{max}) or a

decrease in transporter affinity for glutamate (increased K_M). Furthermore, pre-incubation of osteoblast-like cells with glutamate in the presence of receptor, transporter or kinase inhibitors may elucidate whether the substrate-induced inhibition of transporter activity observed in SaOS-2 cells is receptor-, transporter- and/or kinase-mediated. Alternatively, conducting the same pre-incubation conditions but in the absence of sodium would indicate whether transport of glutamate was necessary for the observed effects.

3.4.3 Knowledge of EAAT expression and function in human osteoblasts can inform methods to therapeutically target EAATs for bone repair

The experiments presented here have profiled EAAT expression and function in human osteoblasts, and provided some insight into the regulation of these transporters. In order to understand the role EAATs play in modulating the glutamate signalling pathway in bone, particularly during the mechanoresponse, and how these proteins can be therapeutically targeted, it is important to ascertain information regarding the expression and activity of the EAAT family in this tissue. Furthermore, these data have been important for informing and interpreting experiments presented in this thesis where EAAT activity has been modulated in osteoblasts.

These experiments have shown that EAATs are differentially expressed and regulated in cell lines that reflect early and late stages of osteoblast differentiation, suggesting that these cell lines will not respond similarly to modulation of EAAT activity. Therefore, methods to therapeutically modulate EAAT activity may differ depending on which stage of osteoblast maturation towards bone formation represents the most appropriate target. Analysis of EAAT expression and activity during osteoblastic differentiation of MSCs would be particularly informative in this respect.

These studies have also validated the use of osteoblast-like cell lines to compensate for primary human osteoblasts, which are expensive to obtain and can be variable. MG-63 and SaOS-2 cells display a similar EAAT expression pattern to primary human osteoblasts and both osteoblast-like cells and primary human osteoblasts exhibit Na^+-dependent glutamate uptake suggesting that these cell lines represent appropriate models to investigate the role of EAATs in osteoblasts.

3.4.4 Summary

In summary, the experiments shown here have demonstrated that human osteoblasts express EAATs 1-3 at differential levels, including two splice variants of EAAT1. Human osteoblasts transport glutamate in a Na^+-dependent manner that is sensitive to pharmacological inhibition of EAATs. An essential step towards understanding the contribution of EAATs to the modulation of glutamate signalling in osteoblasts is the analysis of the regulation of their activity. These experiments have shown that glutamate regulates its own uptake in osteoblast cell lines through effects on EAAT activity, suggestive of feedback mechanisms via either the transporter or receptors present at the cell surface. Differences exist between MG-63 cells and SaOS-2 cells in EAAT expression levels and the kinetics of Na^+-dependent glutamate uptake, as well as the glutamate-mediated regulation of these processes indicating differentiation specific influences. Such differences may be used to inform therapeutic targeting of glutamate uptake in bone since pre-osteoblast differentiation and mature osteoblast bone formation are likely to be regulated differentially by glutamate.

Chapter 4: Pharmacological inhibition of EAATs in human osteoblasts

4. Pharmacological inhibition of EAATs in human osteoblasts

4.1 Background

4.1.1 Pharmacological EAAT inhibitors

A number of pharmacological molecules have been developed to investigate and modulate properties of the glutamate transporters. Most of the compounds developed to date are competitive transportable substrate inhibitors (Gegelashvili and Schousboe 1998), generating a transport current and a substrate-dependent anion conductance (Shigeri et al. 2004). Competitive substrate inhibitors can also induce an efflux of glutamate due to heteroexchange, increasing the extracellular glutamate concentration (Nicholls and Attwell 1990; Dunlop et al. 1992; Blitzblau et al. 1996; Koch et al. 1999). Heteroexchange occurs when the addition of one substrate e.g. *t*-PDC stimulates the efflux of a second substrate that has been accumulated within the cell e.g. glutamate (Koch et al. 1999). Therefore, substrate inhibitors are able to mimic reversed operation of the transporter. The transporters are driven by ionic gradients across the membrane (K^+, Na^+) which are maintained by the sodium pump which requires ATP for activity. ATP levels drop in ischemia and the electrochemical gradients cannot be maintained, leading to reversed operation of the transporter and glutamate release (Rossi et al. 2000). This is a major contributor to neurotoxicity associated with stroke-induced ischemic brain damage (Kuwahara et al. 1992; Rossi et al. 2000), transportable EAAT inhibitors have consequently been used to investigate the role of reversed glutamate uptake in ischemia (Danbolt 2001; Maragakis and Rothstein 2004; Re et al. 2006).

L-*trans*-2,4-pyrrolidine dicarboxylate (*t*-PDC) is a conformationally restricted glutamate analogue and functions as an inhibitor of EAATs 1-5, exhibiting little cross-reactivity with iGluRs (Bridges et al. 1991; Garlin et al. 1995) and no reported cross-reactivity with mGluRs. *T*-PDC is transported slowly by EAATs 1-4 (Sarantis et al. 1993) but is a non-transportable inhibitor of EAAT5 and acts most potently on EAATs 2, 4, and 5 (Bridges et al. 1999). *T*-PDC activates the uncoupled anion conductance in EAATs 1-4 (Wadiche and Kavanaugh 1998; Shigeri et al. 2004).

A number of non-transportable EAAT inhibitors have been developed more recently including dihydrokainic acid (DHK) and DL-threo-β-benzyloxyaspartic acid (TBOA), allowing distinction between binding and translocation of the transporter. DHK is a derivative of the glutamate receptor agonist kainate and acts as a non-transportable, EAAT2 selective inhibitor of L-glutamate uptake and also binds to kainate receptors with low affinity (Arriza et al. 1994; Shimamoto et al. 1998). TBOA is an *O*-substituted hydroxyaspartate and is a non-transportable inhibitor of EAATs 1-5 with K_i and IC_{50} values in the 1-10μM range (Table 2.3). TBOA inhibits glutamate transport and also glutamate gated anion conductance (Shimamoto et al. 1998; Seal et al. 2001; Ryan and Vandenberg 2002). Non-transportable inhibitors of the EAATs, such as TBOA (and *t*-PDC with respect to EAAT5), are substrate analogues but do not by themselves elicit anion conductance (Arriza et al. 1997; Shimamoto et al. 1998; Seal et al. 2001; Ryan and Vandenberg 2002) and yet it is known that conductance is independent of substrate transport (Fairman et al. 1995; Wadiche et al. 1995; Billups et al. 1996; Wadiche and Kavanaugh 1998; Seal et al. 2001; Slotboom et al. 2001b). Seal et al. suggest that the EAAT bound substrates might undergo additional steps to activate anion conductance and that non-transportable inhibitors stabilise the transporter in a conformation that prevents the entrance into this anion conducting state (Seal et al. 2001). Indeed, lithium can support the transport of glutamate by EAAC1, but not the substrate gated anion conductance, suggesting that different conformations of the transporter are required for anion conductance and glutamate transport (Borre and Kanner 2001).

Most of the subtype selective EAAT inhibitors developed to date are specific to EAAT2, possibly due to the use of synaptosomal model systems which express high levels of EAAT2 (Koch et al. 1999). EAAT2 selective inhibitors include DHK, L-trans-2,3-PDC, (*RS*)-2-amino-3-(3-hydroxy-1,2,5-thiadiazol-4-yl)propionic acid (TDPA), L-anti-endo-3,4-PDC and WAY-855 (Arriza et al. 1994; Bridges et al. 1994; Bridges et al. 1999; Dunlop et al. 1999; Brauner-Osborne et al. 2000; Campiani et al. 2003). Selective inhibitors for the other EAATs are not available; however 4-methylglutamate and L-serine-O-sulfate are EAAT1 specific substrates with low potency (Arriza et al. 1994; Vandenberg et al. 1998).

4.1.2 Inhibition of EAATs *in vitro*

4.1.2.1 EAAT inhibitors in the CNS

In the CNS, EAATs rapidly clear glutamate from the synaptic cleft, terminating glutamatergic signalling. Therefore, inhibition of EAATs has the potential to increase the concentration of extracellular glutamate available for receptor binding (Tovar et al. 2009) and modulate the amplitude and duration of the signal. In organotypic hippocampal cultures, TBOA treatment resulted in a rapid build up of extracellular glutamate (Jabaudon et al. 1999). EAAT inhibition can cause cell death in hippocampal neurons and slices (Bonde et al. 2003; Himi et al. 2003; Guiramand et al. 2005), cerebellar granule neurons (Estrada-Sanchez et al. 2007) and retinal Müller cells (Izumi et al. 2002) in a manner sensitive to NMDA and non-NMDA antagonists, indicative of a role for EAATs in the prevention of excitotoxicity. A build up of extracellular glutamate can also lead to activation of pre-synaptic inhibitory mGluRs, which would normally be prevented by active removal of glutamate from the synaptic cleft (Maki 1994).

4.1.2.2 EAAT inhibitors and the cystine/glutamate antiporter

Inhibition of glutamate transporters can prevent the build up of intracellular glutamate, therefore affecting its concentration gradient across the cell membrane. The glutamate concentration gradient, in turn, drives cystine uptake via the cystine/glutamate antiporter (Bannai and Kitamura 1980), which provides the cell with cystine required to form the antioxidant GSH (Meister 1983). Inhibition of this mechanism has been proposed to cause cell death following EAAT inhibition due to the increased presence of reactive oxygen species (ROS) (Kato et al. 1992; Mawatari et al. 1996; Reichelt et al. 1997; Himi et al. 2003). Transportable inhibitors such as *t*-PDC can also induce an efflux of glutamate due to heteroexchange, exacerbating the build up of ROS by increasing extracellular glutamate concentrations (Griffiths et al. 1994; Volterra et al. 1996). Incubation of astrocytes and hippocampal cultures with *t*-PDC has led to cell death, in association with GSH depletion and an increase in ROS (Himi et al. 2003; Re et al. 2003; Guiramand et al. 2005).

4.1.2.3 EAAT inhibitors in osteoblasts

The role of the cystine/glutamate antiporter in osteoblasts has been highlighted by studies showing that the survival of rat calvarial osteoblasts in glutamate-free medium was significantly improved by the addition of pyruvate or cystine during the proliferative phase, and also by supplementation with GSH (Hinoi et al. 2002b). Furthermore, high concentrations of glutamate can suppress osteoblast differentiation of mouse bone marrow stromal cells through inhibition of the cystine/glutamate antiporter and depletion of GSH production (Takarada-Iemata et al. 2010).
EAAT inhibition by *t*-PDC in rat calvarial osteoblasts has also been reported to prevent bone formation *in vitro* and shift the cells from an osteoblastic to a more adipocytic phenotype (Taylor 2002).

4.1.2.4 EAAT inhibitors in chondrocytes

Cultured rodent chondrocytes express EAAT1 and EAAT2 mRNA and protein and transport glutamate in a temperature-, sodium- and time-dependent manner (Hinoi et al. 2005a; Piepoli et al. 2009). Incubation of rodent chondrocytes with EAAT inhibitors at 0.1μM-1mM for 5 min demonstrated that EAAT2 selective inhibitors (*threo*-3-Methylglutamic acid (T3MG) and DHK) were more potent in inhibiting 1μM glutamate uptake than the non-selective inhibitors CCGIII and β-*threo*-hydroxy-aspartate (THA). This demonstrated that EAAT2 plays a more prominent role in mediating glutamate uptake in these cells than EAAT1 (Hinoi et al. 2005a).

4.1.2.5 EAAT inhibitors in synovial fibroblasts

In rat synovial fibroblasts (normal and with collagen-induced arthritis (CIA)), mRNA for EAATs 1-3 was detected and functional EAAT activity was confirmed by sodium-dependent glutamate uptake assays (Hinoi et al. 2005b). EAAT uptake activity was increased in CIA rats, most drastically at 7 days post-immunisation with type II collagen and declining up to 28 days despite second and third immunisations (Hinoi et al. 2005b). Incubation of rat synovial fibroblasts with EAAT inhibitors at 100μM for 20 min demonstrated that the non-selective EAAT inhibitors (THA, CCGIII and *t*-PDC) were more potent in inhibiting 1μM glutamate uptake than the EAAT2-

selective inhibitors T3MG and DHK in both normal and CIA rats, indicating that EAAT2 does not play a dominant role in mediating glutamate uptake in rat synovial fibroblasts (Hinoi et al. 2005b). Over 24hrs, 500μM glutamate significantly increased proliferation of synovial fibroblasts from CIA rats but not normal rats, and this was inhibited by co-incubation with the non-selective EAAT inhibitors THA and CCGIII at 100μM (Hinoi et al. 2005b). The authors suggest that intracellular glutamate accumulated through increased EAAT activity may prime the cellular proliferation in synovial fibroblasts, that leads to synovial hyperplasia, early in CIA rats (Hinoi et al. 2005b).

4.1.3 Aims

The objectives of the experiments described in this chapter were to assess the importance of glutamate transport by EAATs in osteoblast differentiation and activity using small molecule inhibitors of EAATs. Since EAAT1 is the most highly expressed mRNA in human osteoblasts (section 3.3.1) and GLAST expression is regulated by osteogenic mechanical loading *in vivo* (Mason et al. 1997), the use of an EAAT1 selective inhibitor would be favourable, however to date there are no potent EAAT1 specific inhibitors available. The non-selective inhibitors, *t*-PDC and TBOA target a broad range of EAATs, including EAAT1, with differing potencies and Chapter 3 showed that TBOA and *t*-PDC inhibit glutamate uptake in MG-63 and SaOS-2 osteoblast-like cells (section 3.3.3.3). These inhibitors were chosen due to their ability to target EAAT1 (Table 2.3) and their differing effects on EAAT anion conductance, allowing the importance of the EAAT ion channel to also be assessed. The transportable inhibitor *t*-PDC inhibits EAAT glutamate uptake but activates EAAT anion conductance (in EAATs 1-4) (Shigeri et al. 2004) in contrast to the non-transportable inhibitor TBOA which inhibits both EAAT uptake and anion conductance activities (Shimamoto et al. 1998).

4.2 Methods

4.2.1 EAAT inhibitors

In cell culture experiments where the inhibitor concentration was kept constant, a concentration of 100μM was chosen since *t*-PDC and TBOA are effective inhibitors of each EAAT subtype at 100μM (section 2.7 and Table 2.3). 100μM TBOA inhibits Na^+-dependent glutamate uptake by ~100% in MG-63 and SaOS-2 cells (Figures 3.13 and 3.14). 100μM *t*-PDC inhibits Na^+-dependent glutamate uptake by 40% in MG-63 and by 70% in SaOS-2 cells (Figures 3.13 and 3.14). The differences in the potency of these inhibitors are due to the nature of inhibition – TBOA is a potent EAAT blocker whereas *t*-PDC is a competitive glutamate analogue and so will be a less effective inhibitor at the same concentration.

4.2.2 Inhibition of EAATs in human osteoblast-like cells

MG-63 and SaOS-2 cells were incubated with the transporter inhibitors *t*-PDC and TBOA at 100μM ± 500μM glutamate in DMEM containing 5% dFBS and 50μg/ml ascorbate. Cells were treated with inhibitors for 1hr prior to the addition of glutamate to ensure glutamate uptake was inhibited to the levels reported in section 3.3.3.3.

4.2.2.1 Effect of EAAT inhibitors on cell number and alkaline phosphatase (ALP) activity

MG-63 osteoblasts were seeded at 2.6 x 10^4 cells/cm^2 in 96-well plates and SaOS-2 cells were seeded at 4.2 x 10^4 cells/cm^2 in 96-well plates. Cells were allowed to adhere overnight before treatments were begun (cells were ~80% confluent). Cells were incubated with inhibitors ± 500μM glutamate for 24-72hrs and assayed for cell number (LDH Cytotox96 assay) and ALP activity (SaOS-2 cells only) at 24, 48 and 72hrs (sections 2.5.3 and 2.5.4). Cells were also incubated with 1-1000μM EAAT inhibitor in the absence of glutamate and assayed for cell number and ALP activity at 24hrs. At each time-point, medium was removed and cells were lysed with 80μl/well of lysis buffer (section 2.5.1) and 25μl of lysate was taken for each of the above

assays. Cell death was not assayed in these cultures; however previous analyses (not shown) indicated that cell death represented no more than 10% of total LDH activity in untreated cells and in cells treated with EAAT inhibitors ± 500μM glutamate over 24hrs.

4.2.2.2 Effect of EAAT inhibitors on gene expression

MG-63 osteoblasts were seeded at 2.6 x 10^4 cells/cm^2 in 24-well plates and SaOS-2 cells were seeded at 4.2 x 10^4 cells/cm^2 in 24-well plates. Cells were allowed to adhere overnight before treatments were begun (cells were ~80% confluent). Cells were incubated with inhibitors ± 500μM glutamate for 24hrs. The medium was then aspirated, cells rinsed with cold PBS and homogenised with 0.2ml TRIzol® reagent per well for 5 min. The plates were stored at -80°C until RNA extractions and reverse transcription were carried out (section 2.3). 500ng total RNA was reverse transcribed in a 20μl reaction which was then diluted to 100μl with RNase/DNase-free molecular biology grade water and 1μl taken for QRT-PCR amplification. QRT-PCR was carried out (section 2.4.4) using primers against Runx2, osteocalcin, type I collagen, osteonectin, osteoprotegerin (OPG) and ALP in conjunction with the housekeeping genes 18S rRNA, GAPDH and HPRT1 (Table 2.1). Gene expression for MG-63 and SaOS-2 cells was normalised to GAPDH and HPRT1 respectively, the most stable housekeeping genes of the three as determined using geNorm software for each experiment (Vandesompele et al. 2002). Relative QRT-PCR (section 2.4.4.5) was carried out using the Applied Biosystems 7900HT Fast Real-Time PCR system (section 2.4.4.1.2) in conjunction with cDNA standard curves (section 2.4.4.2.2). All values were expressed relative to untreated cells (0μM inhibitor, 0μM glutamate).

4.2.2.3 Effect of EAAT inhibitors on mineralisation

SaOS-2 cells were seeded at 4.2 x 10^4 cells/cm^2 in 24-well plates. Cells were allowed to adhere overnight before treatments were begun (cells were ~80% confluent). Cells were incubated with inhibitors ± 500μM glutamate for 10 days in the presence of 2mM β-glycerophosphate and treatments were refreshed every 2-3 days. SaOS-2 osteoblasts were assessed for mineralisation by alizarin red staining (section 2.9).

Parallel cultures were assayed for cell number (LDH Cytotox96 assay, section 2.5.3). Medium was removed from these cultures and cells were washed with cold PBS prior to cell lysis with 100µl/well of lysis buffer (section 2.5.1) and 5µl taken for assay of cell number.

4.2.3 Inhibition of EAATs in human primary osteoblasts

Human primary osteoblasts (NHOB1-3) were seeded at 2 x 10^4 cells/cm^2 in 24-well plates and cultured until 70% confluent. Cells were serum starved for 24hrs and then treated for a further 24hrs with 100µM glutamate transport inhibitors *t*-PDC and TBOA ± 500µM glutamate. For all experiments exceeding 24hrs, cells were incubated with fresh growth medium containing 5% dFBS, 50µg/ml ascorbate and supplemented with inhibitors ± glutamate. Medium was refreshed every 2-3 days.

4.2.3.1 Effect of EAAT inhibitors on cell number and ALP activity

The effect of EAAT inhibitors on cell number (NHOB1P5, NHOB2P7 and NHOB3P5) and ALP activity (NHOB1P5) of human primary osteoblasts was assessed at 24hrs and 5 days. At each time-point, medium was removed from cells and retained, and cells were washed with cold PBS prior to lysis with 100µl/well of lysis buffer (section 2.5.1). 5µl cell lysate was assayed for adherent cell number (section 2.5.3) and 25µl cell lysate was assayed for ALP activity (section 2.5.4). Dead and dying cells in the culture supernatant from each medium change were also lysed according to methods outlined in section 2.5.1 and 50µl culture supernatant from each medium change was assayed for cell death (section 2.5.3). Values obtained for cell death in culture supernatant from each medium change over 5 days were combined to indicate total cell death over the 5 day period.

4.2.3.2 Effect of EAAT inhibitors on gene expression

The effect of EAAT inhibitors on gene expression of human primary osteoblasts (NHOB2P7) was assessed at 24hrs and 5 days. The medium was aspirated, cells rinsed with cold PBS and homogenised with 0.2ml TRIzol® reagent per well for 5 min. The plates were stored at -80°C until RNA extractions and reverse transcription

were carried out (section 2.3). 100ng (24hrs) and 450ng (5 days) total RNA was reverse transcribed in a 20µl reaction which was then diluted to 100µl with RNase/DNase-free molecular biology grade water and 5µl taken for QRT-PCR amplification. QRT-PCR was carried out (section 2.4.4) using primers against Runx2, osteocalcin and osteonectin in conjunction with the housekeeping genes 18S rRNA, GAPDH and HPRT1 (Table 2.1). Absolute QRT-PCR was carried out with the Stratagene MX3000P™ Real-Time PCR system (section 2.4.4.1.1) in conjunction with plasmid standard curves generated from cloned template sequences (section 2.4.4.2.1). Transcript copy numbers were normalised to 18S rRNA as this was the most stable housekeeping gene of the three as determined using geNorm software for this experiment (Vandesompele et al. 2002), and expressed relative to untreated cells (0µM inhibitor, 0µM glutamate).

4.2.3.3 Effect of EAAT inhibitors on mineralisation

2mM β-glycerophosphate and 10^{-7}M dexamethasone was added to experimental medium throughout the culture period for mineralisation experiments. Medium was changed every 2-3 days and primary osteoblasts (NHOB2P11) were assessed for mineralisation by alizarin red staining after 21 days (section 2.9).

4.3 Results

4.3.1 Viability of cells treated with different concentrations of EAAT inhibitors

MG-63 and SaOS-2 osteoblasts were treated with the inhibitors *t*-PDC and TBOA at 1µM-1mM in the absence of exogenous glutamate for 24hrs and adherent cell number determined by LDH activity in the lysed cell monolayer (Figure. 4.1). Presented data are from three independent experiments where n=4.

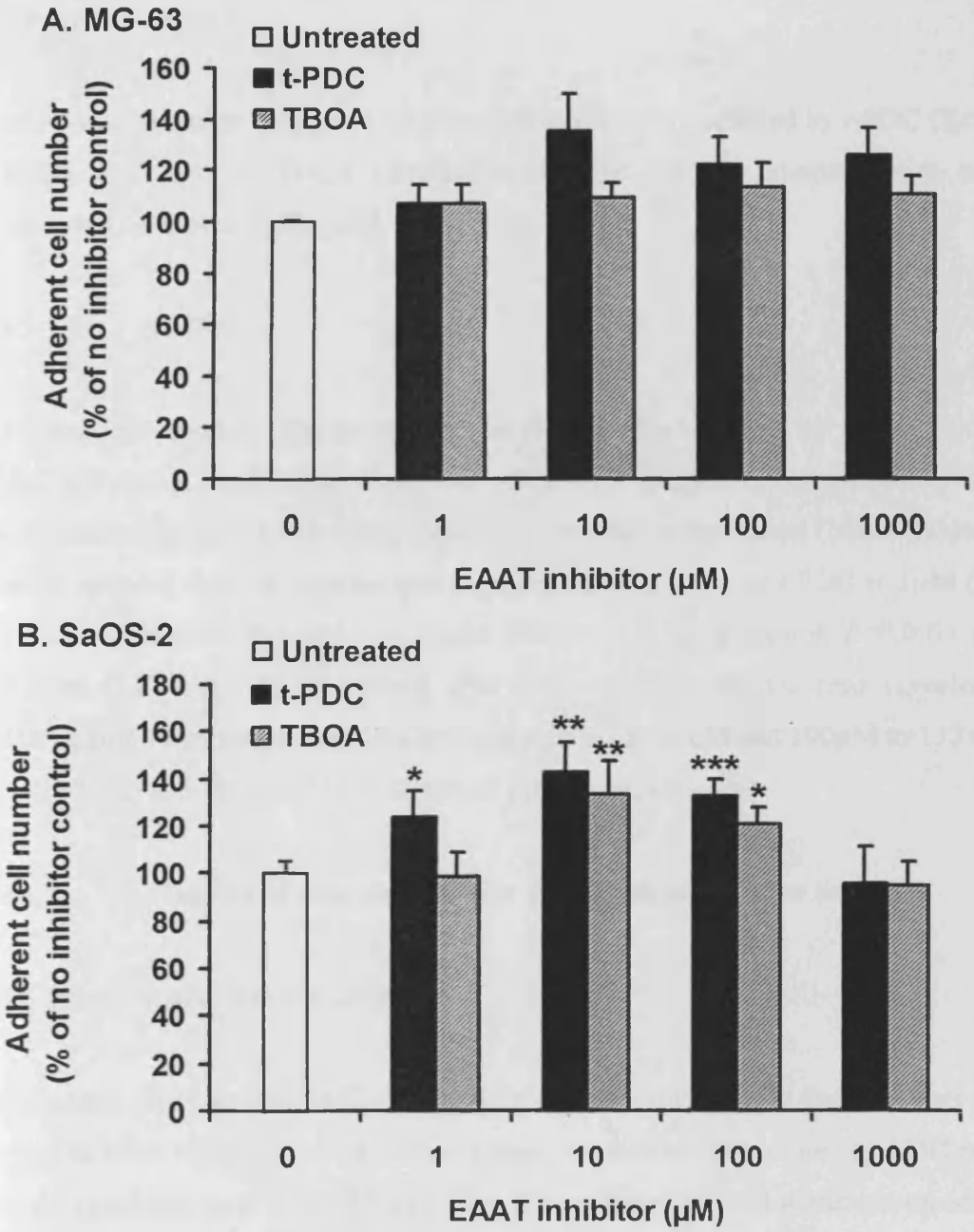

Figure 4.1. Effect of 24hr incubation with 1-1000μM EAAT inhibitor at 0μM glutamate on adherent cell number in (A) MG63 and (B) SaOS-2 osteoblasts. LDH released upon total lysis of viable adherent cells is shown as the mean percentage of LDH activity of viable adherent control cells (no inhibitor) ± S.E.M from three independent experiments, n=4. MG-63 cell number was not significantly affected by inhibitors (Kruskal-Wallis test). SaOS-2 cell number was significantly increased by 1μM, 10μM, and 100μM *t*-PDC (Kruskal-Wallis test with post-hoc Mann-Whitney U comparisons) and 10μM and 100μM TBOA (one-way ANOVA with post-hoc Fisher's comparisons). **P*<0.05, ***P*<0.01, ****P*<0.001 compared to untreated control cells.

4.3.1.1 MG-63

MG-63 cell number (Figure. 4.1A) was not significantly affected by *t*-PDC (Kruskal-Wallis P=0.214) or TBOA (Kruskal-Wallis P=0.294) in comparison to control untreated cells over 1μM-1mM.

4.3.1.2 SaOS-2

SaOS-2 cell number (Figure. 4.1B) was significantly affected by *t*-PDC (Kruskal-Wallis P<0.001) and TBOA (one-way ANOVA P=0.012) in comparison to control untreated cells over 1μM-1mM. Post-hoc pair-wise comparisons (Mann Whitney U tests) revealed that cell number was significantly increased by *t*-PDC at 1μM (124 ± 11.5 % of control, P=0.015), at 10μM (143 ± 12.9 % of control, P=0.003) and at 100μM (133 ± 6.8 % of control, P<0.001). Fisher's post-hoc tests revealed that TBOA significantly increased SaOS-2 cell number at 10μM and 100μM to 133 ± 14.7 % (P<0.01) and 121 ± 7.3 % (P<0.05) of control respectively.

4.3.2 Viability of cells treated with EAAT inhibitors over time

4.3.2.1 Osteoblast-like cells

Osteoblast-like cell lines (MG-63 and SaOS-2) were treated with the inhibitors *t*-PDC and TBOA at 100μM for 72hrs and adherent cell number determined by LDH activity in the lysed cell layer at 24, 48 and 72hrs. The effect of 500μM glutamate on adherent cell number was also assessed in these cells in the presence and absence of EAAT inhibitors. Presented data are from three independent experiments where n=4.

4.3.2.1.1 MG-63

Although MG-63 cell number was not significantly affected by glutamate alone (Shierer-Ray P=0.455) or by EAAT inhibitor treatment (Shierer-Ray P=0.312) at 24hrs, there was a significant interaction between these factors (Shierer-Ray P=0.047) (Figure 4.2). Post-hoc pair-wise comparisons (Mann-Whitney U tests) revealed that

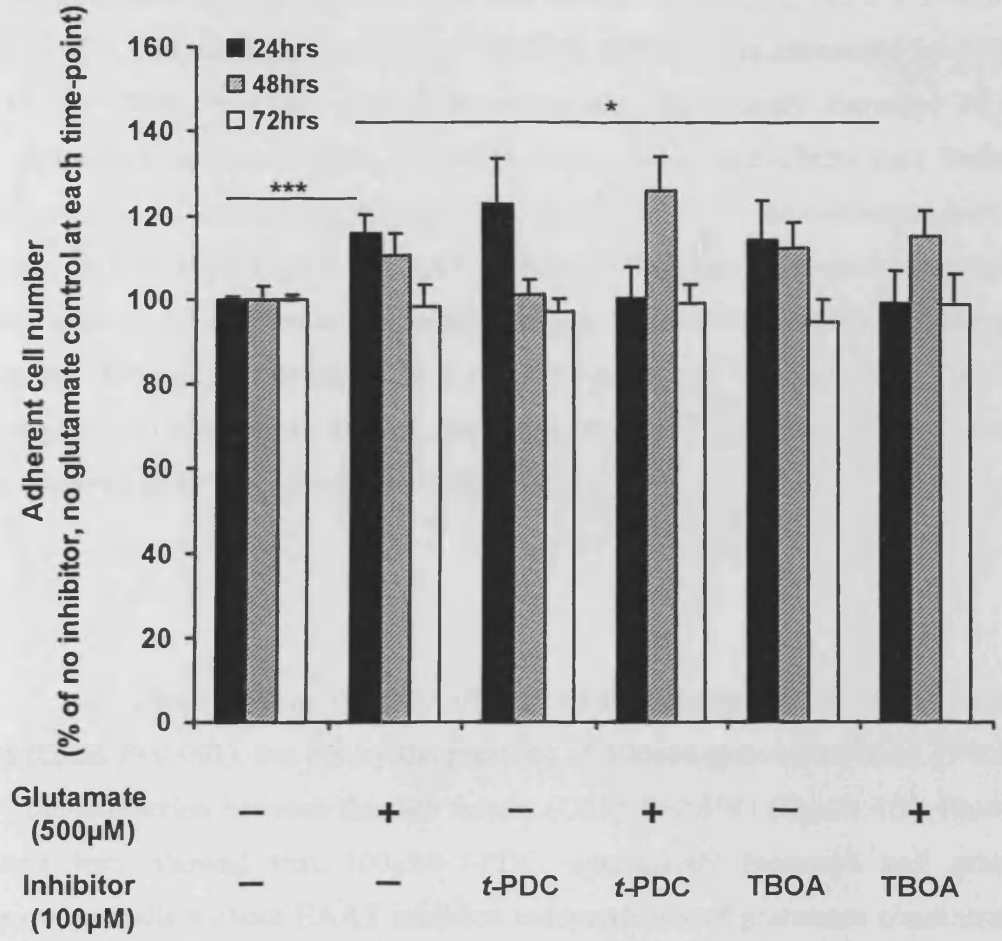

Figure 4.2. Effect of EAAT inhibitors on MG-63 osteoblast cell number over 72hrs. MG-63 cells were cultured with EAAT inhibitors ± 500µM glutamate for 72hrs and cell number was assayed by measuring LDH released upon total lysis of viable adherent cells at 24, 48 and 72hrs. LDH released is shown as the mean percentage of LDH released from viable adherent control cells (no inhibitor, no glutamate) ± S.E.M from three independent experiments, n=4. At 24hrs, there was a significant interaction between glutamate and EAAT inhibition on MG-63 cell number (Shierer-Ray P=0.047). 500µM glutamate significantly increased cell number compared to untreated control cells, and this was prevented by 100µM TBOA (post-hoc Mann-Whitney U tests). At 48hrs, 500µM glutamate also significantly increased cell number (GLM with log data P=0.014), but no post-hoc pair-wise comparisons (Tukey's test) were statistically significant. No significant effects on cell number were observed after 72hrs (Shierer-Ray test). Significance values *P<0.05, ***P<0.001.

500μM glutamate significantly increased cell number at 24hrs by 116 ± 4.9 % in the absence of EAAT inhibitor treatment (P<0.001), and this was attenuated by 100μM TBOA (P=0.046). At 48hrs, 500μM glutamate also significantly increased MG-63 cell number (GLM with log data P=0.014), but no significant effects were found in response to EAAT inhibitors (GLM with log data P=0.307) or the interaction between the two factors (GLM with log data P=0.237). Post-hoc pair-wise comparisons (Tukey's tests) did not reveal any significant pair-wise effects of 500μM glutamate, indicating that the significance was a result of an overall increase in cell number across groups in response to 500μM glutamate. No significant effects on cell number were observed after 72hrs (by Shierer-Ray test).

4.3.2.1.2 SaOS-2

SaOS-2 cell number was significantly affected by the presence of EAAT inhibitors at 24hrs (GLM P=0.001), but not by the presence of 500μM glutamate (GLM P=0.142) or by the interaction between the two factors (GLM P=0.601) (Figure 4.3). Post-hoc Tukey's tests showed that 100μM *t*-PDC significantly increased cell number compared to cells without EAAT inhibitor independently of glutamate concentration (P<0.001) and pair-wise comparisons indicated that 100μM *t*-PDC significantly increased cell number to 133 ± 6.8 % of untreated control cells at 0μM glutamate (P=0.008) and from 112 ± 8.0 % to 145 ± 8.4 % at 500μM glutamate (P=0.301). No significant effects on cell number were observed after 48hrs (by Shierer-Ray test) or 72hrs (by Shierer-Ray test).

4.3.2.2 Primary osteoblasts

Human primary osteoblasts (NHOB2P7 and NHOB3P5) were treated with the inhibitors *t*-PDC and TBOA at 100μM for 24hrs and 5 days. At each time-point, adherent cell number was determined by LDH activity in the lysed cell layer and cell death was determined by LDH activity in the lysed culture supernatant. The effect of 500μM glutamate on adherent cell number was also assessed in these cells in the presence and absence of EAAT inhibitors. Presented data are from two independent experiments where n=4. Cell number data from NHOB1P5 is not

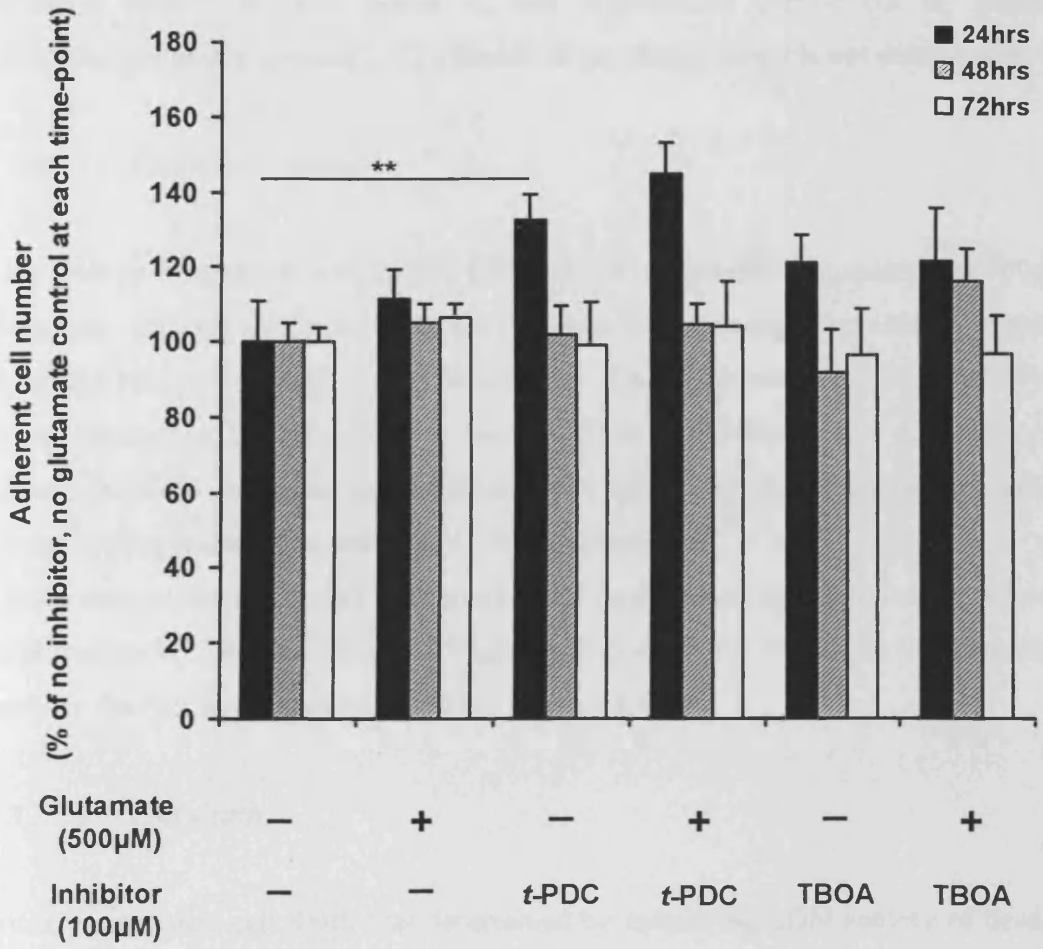

Figure 4.3. Effect of EAAT inhibitors on SaOS-2 osteoblast cell number over 72hrs. SaOS-2 cells were cultured with EAAT inhibitors ± 500μM glutamate for 72hrs and cell number was assayed by measuring LDH released upon total lysis of viable adherent cells at 24, 48 and 72hrs. LDH released is shown as the mean percentage of LDH released from viable adherent control cells (no inhibitor, no glutamate) ± S.E.M from three independent experiments, n=4. Cell number was significantly affected by EAAT inhibition at 24hrs (GLM P=0.001) and post-hoc pair-wise Tukey's comparisons revealed that 100μM *t*-PDC significantly increased cell number in the absence of glutamate. No significant effects on cell number were observed after 48hrs or 72hrs (Shierer-Ray tests). Significance values **P<0.01.

presented since cells were plated in, and experiments carried out in, medium containing glutamate (section 2.2.3), therefore the methodology is not comparable.

4.3.2.2.1 Viable cell number

After 24hrs of treatment with EAAT inhibitors in the presence or absence of 500μM glutamate, primary osteoblast cell number was significantly increased by 500μM glutamate (GLM P=0.046) but not affected by EAAT inhibition (GLM P=0.914) or by the interaction between the two factors (GLM P=0.449) (Figure 4.4). Post-hoc Tukey's tests did not reveal any significant pair-wise comparisons between treatment groups in the presence and absence of 500μM glutamate.
After 5 days treatment, primary osteoblast cell number was not significantly affected by glutamate (GLM P=0.103), EAAT inhibitors (GLM P=0.068) or by the interaction between the two factors (GLM P=0.281) (Figure 4.4).

4.3.2.2.2 Cell death

Primary osteoblast cell death was determined by measuring LDH activity of dead or dying cells in the culture supernatant and this value was expressed as a percentage of total LDH activity in the culture well (i.e. adherent cell lysate + dead or dying cells in the supernatant) (Figure 4.5). Cell death accounted for 12-14 % of total LDH activity at both 24hrs and 5 days treatment. No significant effects of glutamate, EAAT inhibitors, or the interaction between the two factors on cell death were detected at 24hrs (P=0.541, P=0.765 and P=0.885 respectively by GLM) or 5 days (P=0.142, P=0.772 and P=0.761 respectively by GLM of ranked data).

4.3.3 Effect of EAAT inhibition on osteoblast gene expression

Osteoblast-like cells and human primary osteoblasts (NHOB2P7) were incubated with 100μM *t*-PDC or TBOA in the presence and absence of 500μM glutamate for 24hrs. Expression of transcripts for Runx2, osteocalcin, type I collagen, osteonectin, OPG and ALP were determined by QRT-PCR, normalised to expression of the appropriate housekeeping gene (section 2.4.4.3) and expressed as the mean percentage change from untreated control cells (0μM inhibitor, 0μM glutamate) (Figures 4.6-4.11).

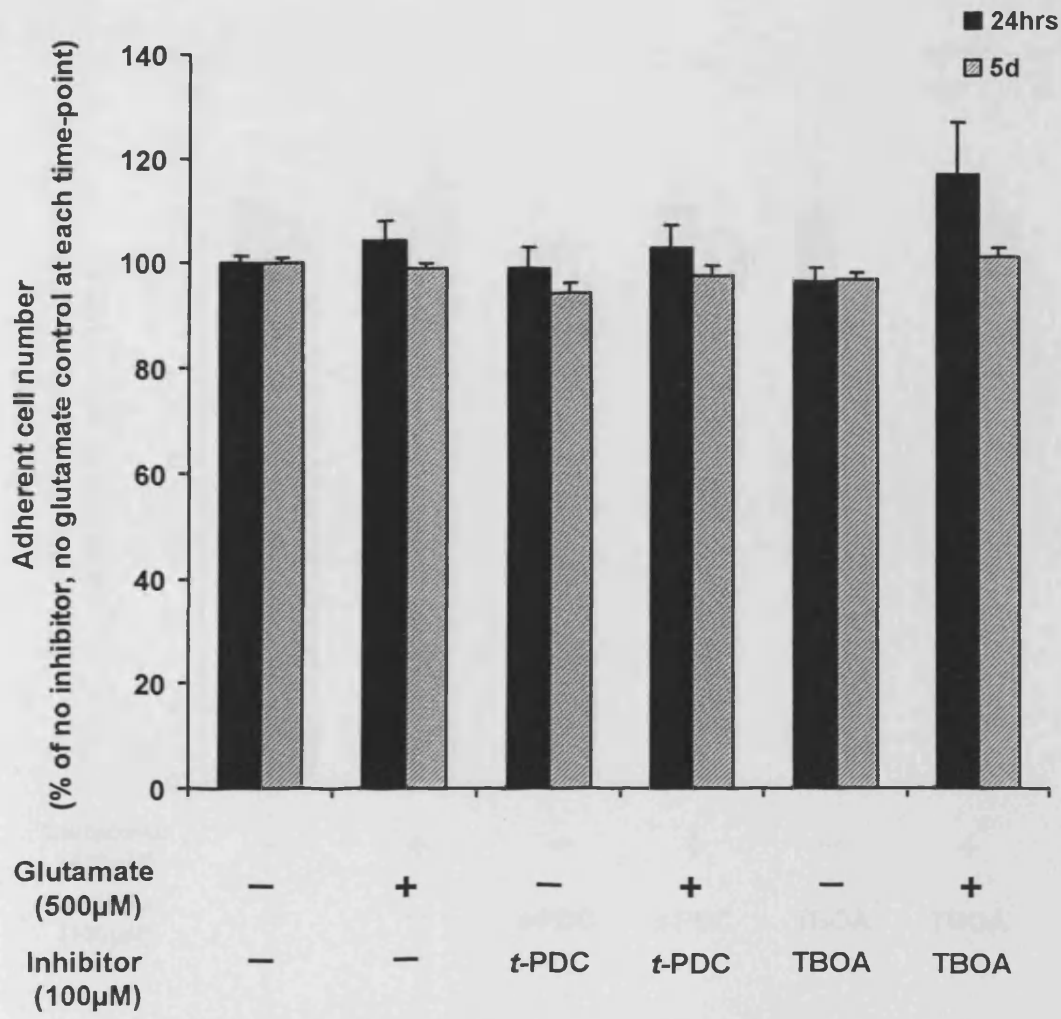

Figure 4.4. Effect of EAAT inhibitors on primary osteoblast cell number at 24hrs and 5 days. Primary osteoblasts (NHOB2P7 and NHOB3P5) were cultured with EAAT inhibitors ± 500μM glutamate and cell number was assayed by measuring LDH released upon total lysis of viable adherent cells at 24hrs and 5 days. LDH released is shown as the mean percentage of LDH released from viable adherent control cells (no inhibitor, no glutamate) at each time-point ± S.E.M from two independent experiments, n=4. At 24hrs, cell number was significantly increased by 500μM glutamate (GLM P=0.046), however post-hoc Tukey's tests did not reveal any significant pair-wise differences between individual treatment groups. No significant effects on cell number were observed at 5 days (GLM).

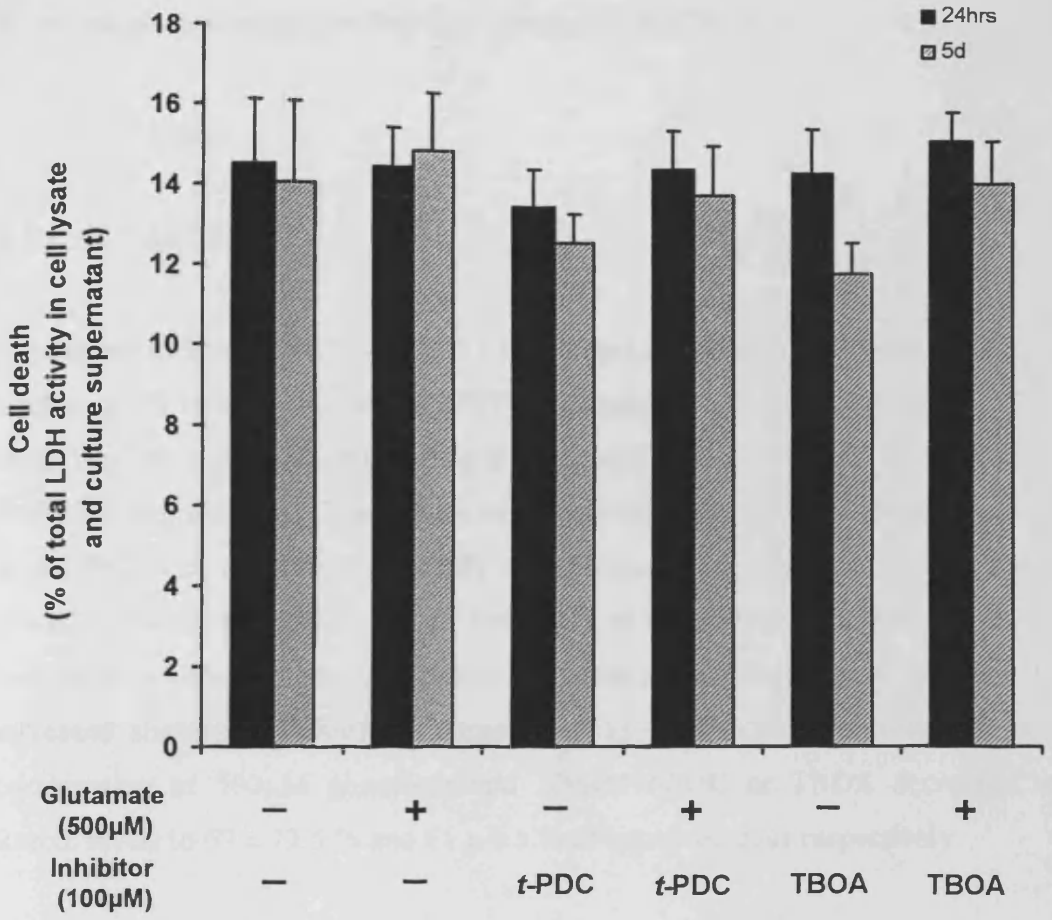

Figure 4.5. Effect of EAAT inhibitors on primary osteoblast cell death at 24hrs and 5 days. Primary osteoblasts (NHOB2P7 and NHOB3P5) were cultured with EAAT inhibitors ± 500µM glutamate and cell death assayed by measuring LDH released from dead or dying cells in the cell culture supernatant at 24hrs and 5 days. Supernatant from medium changes over 5 days was pooled. LDH activity of dead or dying cells in the supernatant is shown as the mean percentage of total LDH activity (i.e. adherent cell lysate + dead or dying cells in the supernatant) ± S.E.M from two independent experiments, n=4. Treatments had no significant effects on primary osteoblast cell death at 24hrs or 5 days (GLM).

Presented data are from three independent experiments where n=4 (MG-63 and SaOS-2) or a single preliminary experiment where n=4 (NHOB2P7).

4.3.3.1 Runx2

4.3.3.1.1 MG-63

Expression of Runx2 mRNA in MG-63 cells was not significantly affected by EAAT inhibitors (GLM with log data P=0.087), glutamate (GLM with log data P=0.071) and there was no significant interaction between the two factors (GLM with log data P=0.074) (Figure 4.6A). The effects of each of these factors were close to significant at the 5% level, and this is probably a reflection of the decrease in Runx2 mRNA levels in cells treated with EAAT inhibitors in the presence of 500μM glutamate compared to cells treated with 500μM glutamate alone. Mean Runx2 expression was increased slightly by 500μM glutamate to 113 ± 11.7 % of untreated cells. The combination of 500μM glutamate and 100μM *t*-PDC or TBOA decreased mean Runx2 levels to 69 ± 13.5 % and 61 ± 8.5 % of untreated cells respectively.

4.3.3.1.2 SaOS-2

Expression of Runx2 mRNA in SaOS-2 cells was not significantly affected by EAAT inhibitors (GLM with log data P=0.828), glutamate (GLM with log data P=0.467) and there was no significant interaction between the two factors (GLM with log data P=0.839) (Figure 4.6B).

4.3.3.1.3 Primary osteoblasts (NHOB2P7)

Preliminary findings indicated that primary osteoblast Runx2 expression was not significantly affected by EAAT inhibitors (at 24hrs GLM P=0.527; at 5 days GLM with log data P=0.106) or by the interaction between EAAT inhibitors and glutamate (at 24hrs GLM P=0.823; at 5 days GLM with log data P=0.269) (Figure 4.6C,D). However at 24hrs, glutamate significantly reduced expression of Runx2 (GLM P=0.042) and this effect was not detected after 5 days treatment (GLM with log data P=0.907). At 24hrs, 500μM glutamate decreased Runx2 mRNA levels from

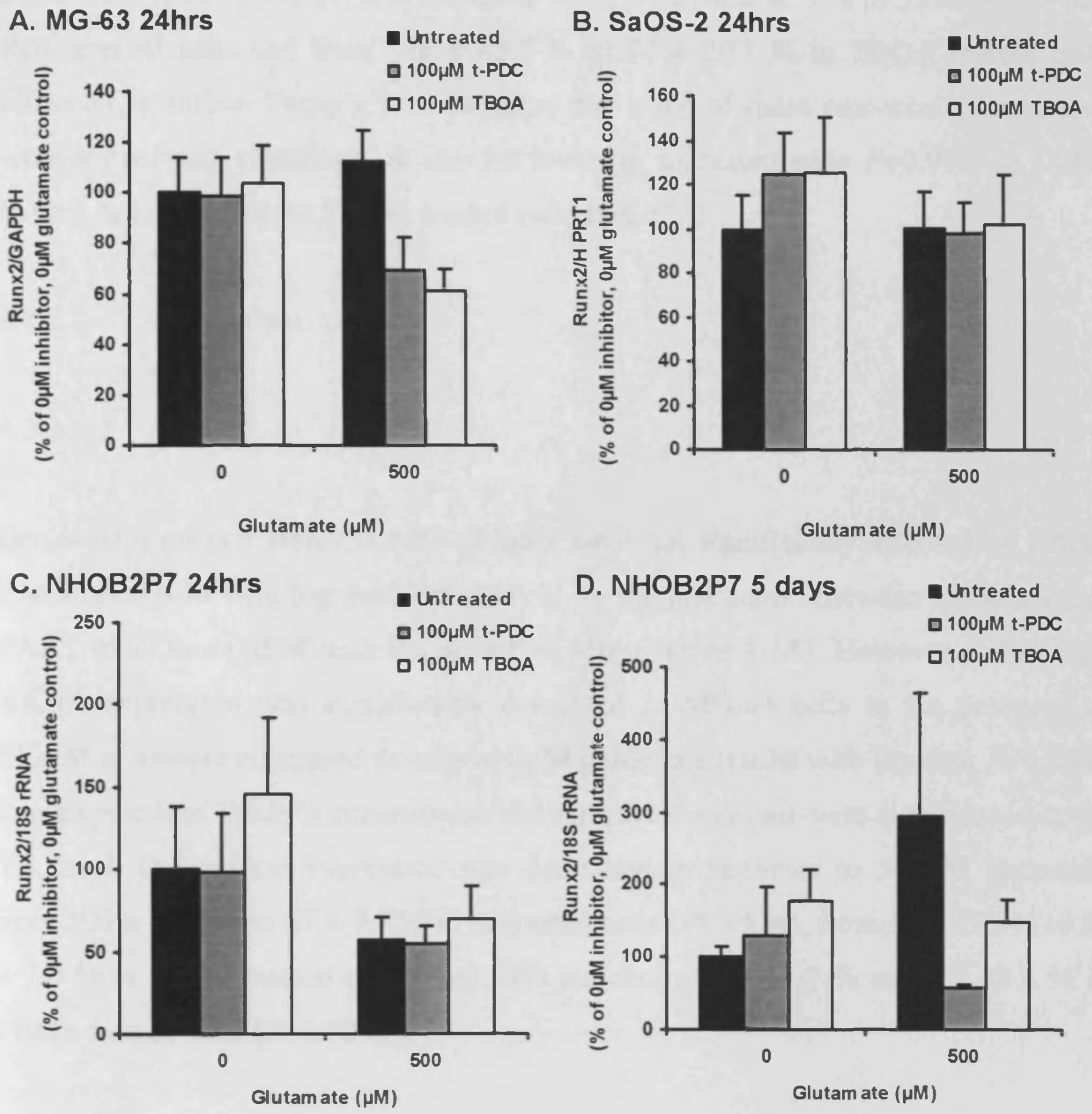

Figure 4.6. Effect of EAAT inhibitors on Runx2 mRNA expression in human osteoblasts. Human osteoblasts (A, MG-63; B, SaOS-2; C,D, NHOB2P7) were cultured with EAAT inhibitors ± 500μM glutamate for 24hrs (A-C) or 5 days (D). Runx2 expression was assessed by QRT-PCR, normalised to housekeeping gene levels and expressed as the percentage change over control cells (0μM inhibitor, 0μM glutamate). Values are mean ± S.E.M from three independent experiments, n=4 (MG-63 and SaOS-2) or a single preliminary experiment, n=4 (NHOB2P7). There were no significant effects of EAAT inhibition or glutamate on expression of Runx2 in MG-63, SaOS-2 or in NHOB2P7 at 5 days (GLM). Runx2 expression was significantly reduced in NHOB2P7 at 24hrs by 500μM glutamate (GLM P=0.042), however no pair-wise Tukey's comparisons were statistically significant.

100 ± 37.8 % to 57 ± 14.4 % in untreated cells, from 98 ± 36.3 % to 55 ± 10.5 % in *t*-PDC treated cells and from 146 ± 45.7 % to 70 ± 20.1 % in TBOA treated cells. However, post-hoc Tukey's tests revealed that none of these pair-wise comparisons were statistically significant at the 5% level (in untreated cells P=0.910; in *t*-PDC treated cells P=0.909; in TBOA treated cells P=0.503).

4.3.3.2 Osteocalcin

4.3.3.2.1 MG-63

Osteocalcin mRNA levels in MG-63 cells were not significantly affected by EAAT inhibitors (GLM with log data P=0.262) or by the interaction between glutamate and EAAT inhibitors (GLM with log data P=0.910) (Figure 4.7A). However, osteocalcin mRNA expression was significantly decreased in MG-63 cells in the presence of 500μM glutamate compared to cells at 0μM glutamate (GLM with log data P=0.004), though post-hoc Tukey's comparisons did not reveal any pair-wise significance at the 5% level. Osteocalcin expression was decreased in response to 500μM glutamate from 100 ± 14.3 % to 67 ± 7.7 % in untreated cells (P=0.514), from 129 ± 16 % to 80 ± 7.0 % in *t*-PDC treated cells (P=0.347) and from 99 ± 11.7 % to 81 ± 13.4 % in TBOA treated cells (P=0.729).

4.3.3.2.2 SaOS-2

SaOS-2 osteocalcin expression was significantly affected by EAAT inhibitors (GLM with log data P=0.032), glutamate (GLM with log data P=0.024) and the interaction between the two factors (GLM with log data P=0.039) (Figure 4.7B). Post-hoc pair-wise comparisons (Tukey's test) revealed that osteocalcin levels were significantly increased to 204 ± 28.0 % of untreated control cells by treatment with 100μM TBOA for 24hrs in the absence of glutamate (P=0.011). This increase appeared to be prevented by co-incubation with 500μM glutamate (P=0.140).

Since no other pair-wise comparisons were significant at the 5% level, the significant effect of 500μM glutamate detected by the GLM probably reflects a general trend

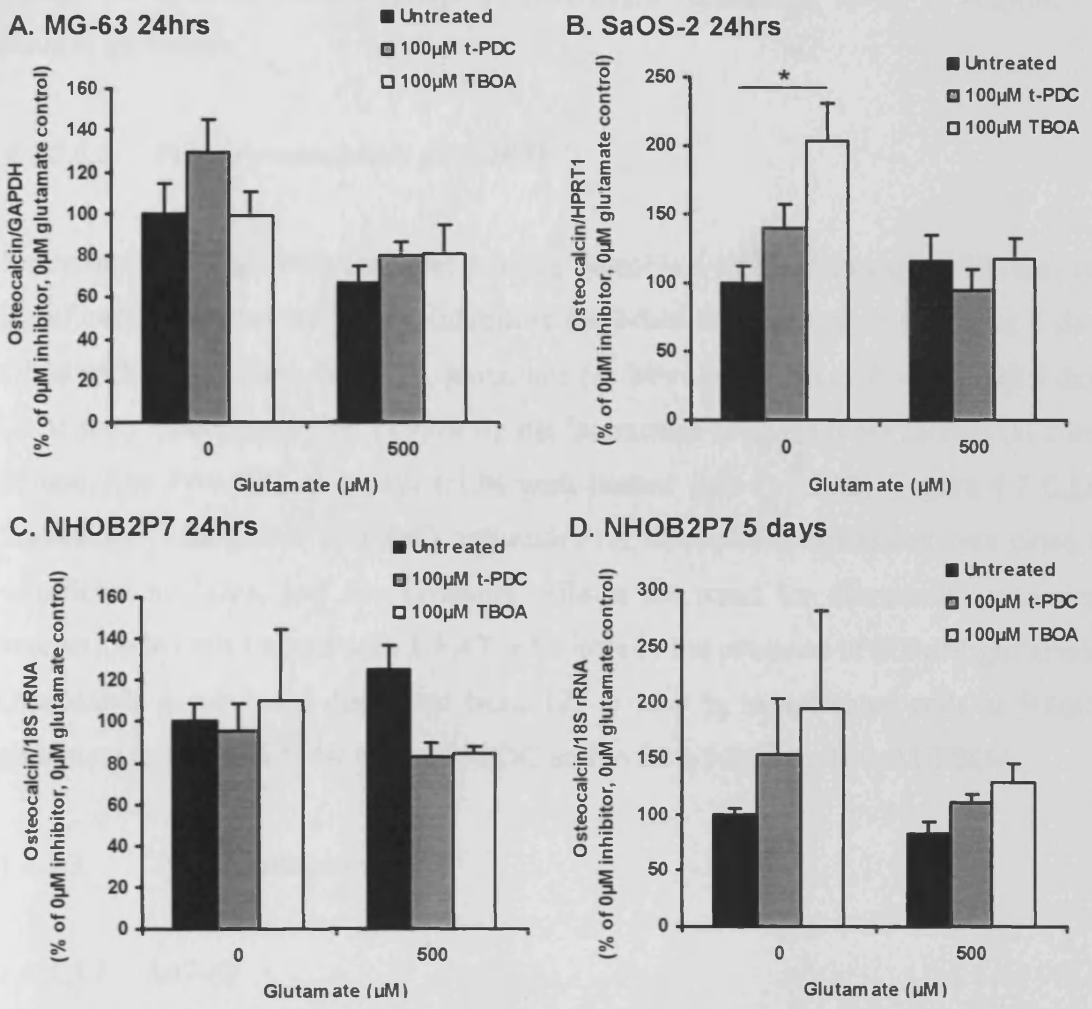

Figure 4.7. Effect of EAAT inhibitors on osteocalcin mRNA expression in human osteoblasts. Human osteoblasts (A, MG-63; B, SaOS-2; C,D, NHOB2P7) were cultured with EAAT inhibitors ± 500μM glutamate for 24hrs (A-C) or 5 days (D). Osteocalcin expression was assessed by QRT-PCR, normalised to housekeeping gene levels and expressed as the percentage change over control cells (0μM inhibitor, 0μM glutamate). Values are mean ± S.E.M from three independent experiments, n=4 (MG-63 and SaOS-2) or a single preliminary experiment, n=4 (NHOB2P7). MG-63 osteocalcin expression was significantly reduced by 500μM glutamate (GLM P=0.004). SaOS-2 osteocalcin expression was significantly affected by EAAT inhibitors (P=0.032), glutamate (P=0.024), and the two factors interacted (P=0.039) (GLM). Tukey's comparisons revealed that SaOS-2 osteocalcin levels were significantly increased by 100μM TBOA at 0μM glutamate. There were no significant effects of EAAT inhibition or glutamate on expression of osteocalcin in NHOB2P7 at 24hrs or 5 days (Shierer-Ray test and GLM respectively). Significance values *P<0.05.

across the inhibitor treated groups for decreased osteocalcin levels in response to 500μM glutamate.

4.3.3.2.3 Primary osteoblasts (NHOB2P7)

Preliminary findings indicated that primary osteoblast osteocalcin expression was not significantly affected by EAAT inhibitors (at 24hrs Shierer-Ray P=0.088; at 5 days GLM with ranked data P=0.120), glutamate (at 24hrs Shierer-Ray P=0.729; at 5 days GLM with ranked data P=0.819) or by the interaction between these factors (at 24hrs Shierer-Ray P=0.339; at 5 days GLM with ranked data P=0.852) (Figure 4.7 C,D). Interestingly, the effect of EAAT inhibitors on osteocalcin expression was close to significant at 24hrs, and this probably reflects the trend for decreased osteocalcin expression in cells treated with EAAT inhibitors in the presence of 500μM glutamate. Osteocalcin levels were decreased from 125 ± 12.0 % in untreated cells at 500μM glutamate to 83 ± 6.3 % by 100μM *t*-PDC and to 85 ± 3.2 % by 100μM TBOA.

4.3.3.3 Type I collagen

4.3.3.3.1 MG-63

Expression of type I collagen mRNA in MG-63 cells was not significantly affected by EAAT inhibitors (GLM P=0.322), glutamate (GLM P=0.797) and there was no significant interaction between the two factors (GLM P=0.290) (Figure 4.8A).

4.3.3.3.2 SaOS-2

Expression of type I collagen mRNA in SaOS-2 cells was not significantly affected by EAAT inhibitors (GLM P=0.628), glutamate (GLM P=0.376) and there was no significant interaction between the two factors (GLM P=0.246) (Figure 4.8B).

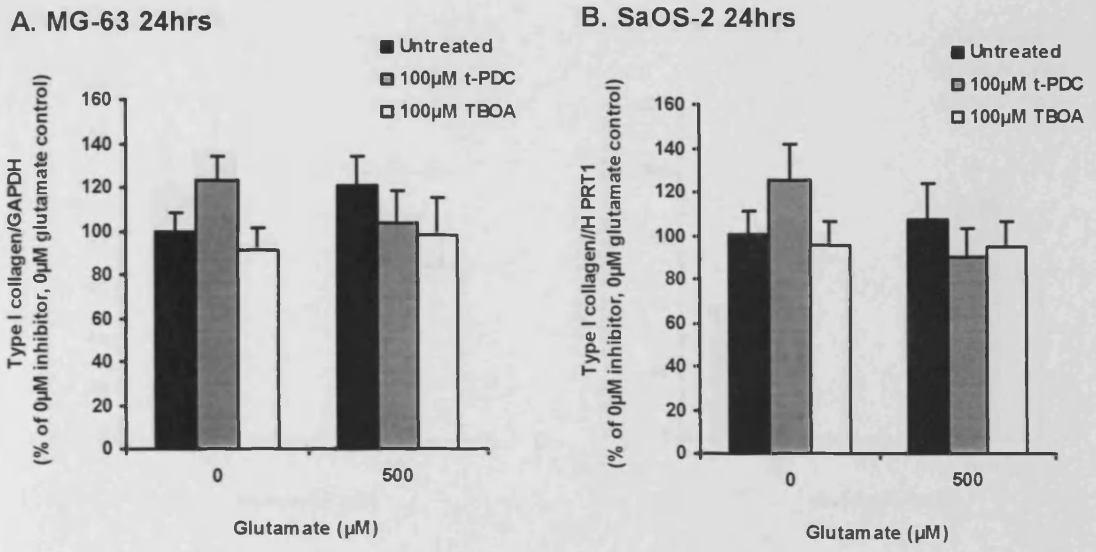

Figure 4.8. Effect of EAAT inhibitors on type I collagen mRNA expression in human osteoblasts. Human osteoblasts (A, MG-63; B, SaOS-2) were cultured with EAAT inhibitors ± 500μM glutamate for 24hrs. Type I collagen expression was assessed by QRT-PCR, normalised to housekeeping gene levels and expressed as the percentage change over control cells (0μM inhibitor, 0μM glutamate). Values are mean ± S.E.M from three independent experiments, n=4. There were no significant effects of EAAT inhibition or glutamate on expression of type I collagen in MG-63 or SaOS-2 cells (GLM).

4.3.3.4 Osteonectin

4.3.3.4.1 MG-63

MG-63 osteonectin expression was significantly affected by EAAT inhibitors (GLM with log data P=0.002), but not by glutamate (GLM with log data P=0.139) or by the interaction between these factors (GLM with log data P=0.702) (Figure 4.9A). Post-hoc Tukey's tests revealed that 100μM TBOA significantly reduced expression of osteonectin independently of glutamate concentration (P=0.010) and pair-wise comparisons revealed that 100μM TBOA decreased osteonectin expression from 100 ± 9.8 % to 77 ± 7.1 % at 0μM glutamate (P=0.071) and from 95 ± 7.2 % to 70 ± 9.3 % at 500μM glutamate (P=0.035).

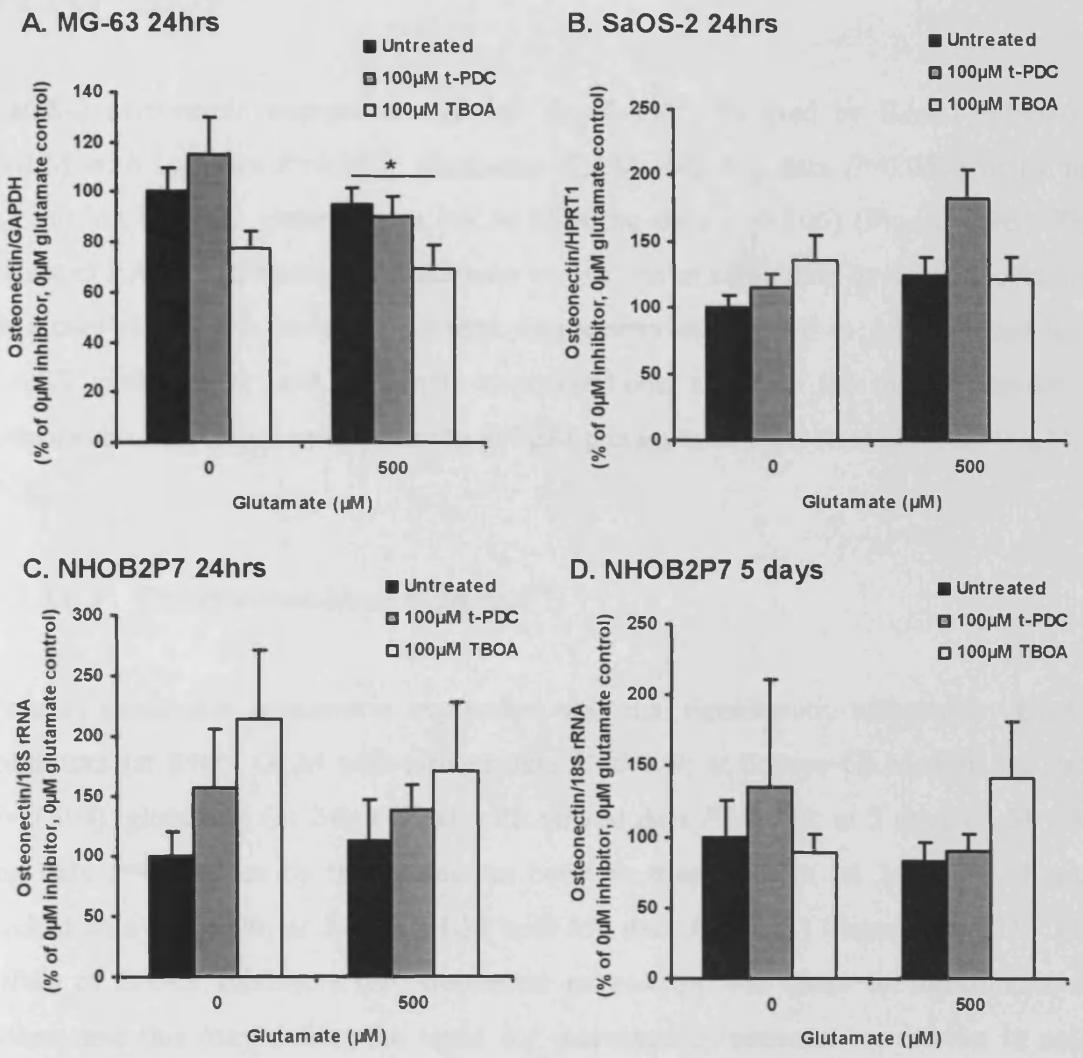

Figure 4.9. Effect of EAAT inhibitors on osteonectin mRNA expression in human osteoblasts. Human osteoblasts (A, MG-63; B, SaOS-2; C,D, NHOB2P7) were cultured with EAAT inhibitors ± 500μM glutamate for 24hrs (A-C) or 5 days (D). Osteonectin expression was assessed by QRT-PCR, normalised to housekeeping gene levels and expressed as the percentage change over control cells (0μM inhibitor, 0μM glutamate). Values are mean ± S.E.M from three independent experiments, n=4 (MG-63 and SaOS-2) or a single preliminary experiment, n=4 (NHOB2P7). MG-63 osteonectin expression was significantly reduced by EAAT inhibitors (GLM P=0.002) and pair-wise Tukey's comparisons revealed that TBOA significantly reduced osteonectin expression in the presence of 500μM glutamate. There were no significant effects of EAAT inhibition or glutamate on expression of osteonectin in SaOS-2 cells or in NHOB2P7 at 24hrs and 5 days (GLM). Significance values *$P<0.05$.

4.3.3.4.2 SaOS-2

SaOS-2 osteonectin expression was not significantly affected by EAAT inhibitors (GLM with log data P=0.069), glutamate (GLM with log data P=0.059) or by the interaction between these factors (GLM with log data P=0.106) (Figure 4.9B). The effect of EAAT inhibitors and glutamate were close to significant at the 5% level and this may reflect the increase in mean osteonectin expression in cells treated with EAAT inhibitors at both glutamate concentrations, and also the mean increase in osteonectin expression in response to 500μM glutamate in cells treated with 100μM *t*-PDC.

4.3.3.4.3 Primary osteoblasts (NHOB2P7)

Primary osteoblast osteonectin expression was not significantly affected by EAAT inhibitors (at 24hrs GLM with ranked data P=0.079; at 5 days GLM with log data P=0.808), glutamate (at 24hrs GLM with ranked data P=0.722; at 5 days GLM with log data P=0.809) or by the interaction between these factors (at 24hrs GLM with ranked data P=0.600; at 5 days GLM with log data P=0.651) (Figure 4.9C,D). The effect of EAAT inhibitors on osteonectin expression was close to significance at 24hrs, and this may reflect the trend for increased osteonectin expression in cells treated with EAAT inhibitors at both concentrations of glutamate.

4.3.3.5 OPG

4.3.3.5.1 MG-63

MG-63 OPG expression was not significantly affected by EAAT inhibitors (GLM P=0.094), glutamate (GLM P=0.549) or by the interaction between these factors (GLM P=0.291) (Figure 4.10A).

4.3.3.5.2 SaOS-2

SaOS-2 OPG expression was not significantly affected by EAAT inhibitors (GLM with log data P=0.249) or by glutamate (GLM with log data P=0.290) (Figure 4.10B).

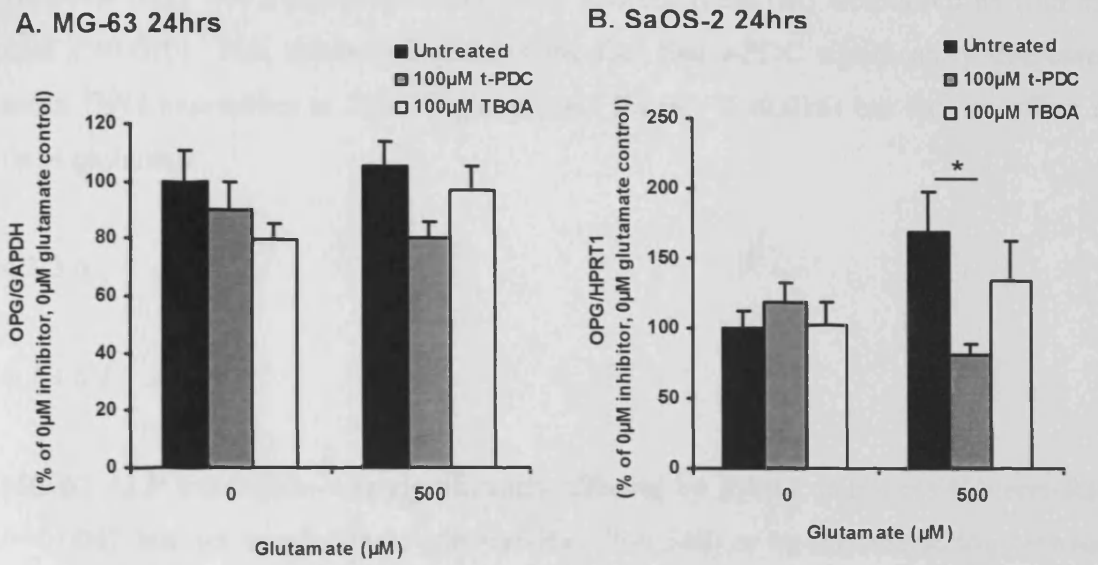

Figure 4.10. Effect of EAAT inhibitors on OPG mRNA expression in human osteoblasts. Human osteoblasts (A, MG-63; B, SaOS-2) were cultured with EAAT inhibitors ± 500μM glutamate for 24hrs. OPG expression was assessed by QRT-PCR, normalised to housekeeping gene levels and expressed as the percentage change over control cells (0μM inhibitor, 0μM glutamate). Values are mean ± S.E.M from three independent experiments, n=4. There were no significant effects of EAAT inhibition or glutamate on expression of OPG in MG-63 cells (GLM). SaOS-2 OPG levels revealed a significant interaction between EAAT inhibition and glutamate concentration (GLM P=0.010). Pair-wise Tukey's comparisons revealed that OPG expression was significantly reduced by *t*-PDC in the presence of 500μM glutamate but not at 0μM glutamate. Significance values *P<0.05.

However there was a significant interaction between these two factors (GLM with log data P=0.010). This interaction reflects the fact that *t*-PDC significantly decreased mean OPG expression at 500μM glutamate (Tukey's P=0.016) but had no effect at 0μM glutamate.

4.3.3.6 ALP

4.3.3.6.1 MG-63

MG-63 ALP expression was significantly affected by EAAT inhibitors (Shierer-Ray P=0.004), but not by glutamate (Shierer-Ray P=0.340) or by the interaction between the two factors (Shierer-Ray P=0.154) (Figure 4.11A). Post-hoc pair-wise comparisons (Mann-Whitney U tests) revealed that ALP expression was significantly decreased by EAAT inhibitors at 500μM glutamate, but not at 0μM glutamate. At 500μM glutamate, ALP levels were decreased from 133 ± 18.1 % in untreated cells to 62 ± 8.5 % by 100μM *t*-PDC (P=0.006) and to 77 ± 5.7 % by 100μM TBOA (P=0.030).

4.3.3.6.2 SaOS-2

SaOS-2 ALP expression was not significantly affected by EAAT inhibitors (GLM with log data P=0.876), glutamate (GLM with log data P=0.115) or by the interaction between these factors (GLM with log data P=0.253) (Figure 4.11B).

4.3.4 ALP activity of cells treated with different concentrations of EAAT inhibitors

SaOS-2 osteoblasts were treated with the inhibitors *t*-PDC and TBOA at 1μM-1mM at 0μM glutamate for 24hrs and ALP activity was determined and normalised to total cell number (total LDH activity within the adherent cell lysate) (Figure. 4.12). Presented data are from three independent experiments where n=4. ALP activity was significantly affected by both inhibitors over this concentration range (one-way ANOVA P=0.009 (*t*-PDC) and P=0.028 (TBOA). Post-hoc pair-wise comparisons

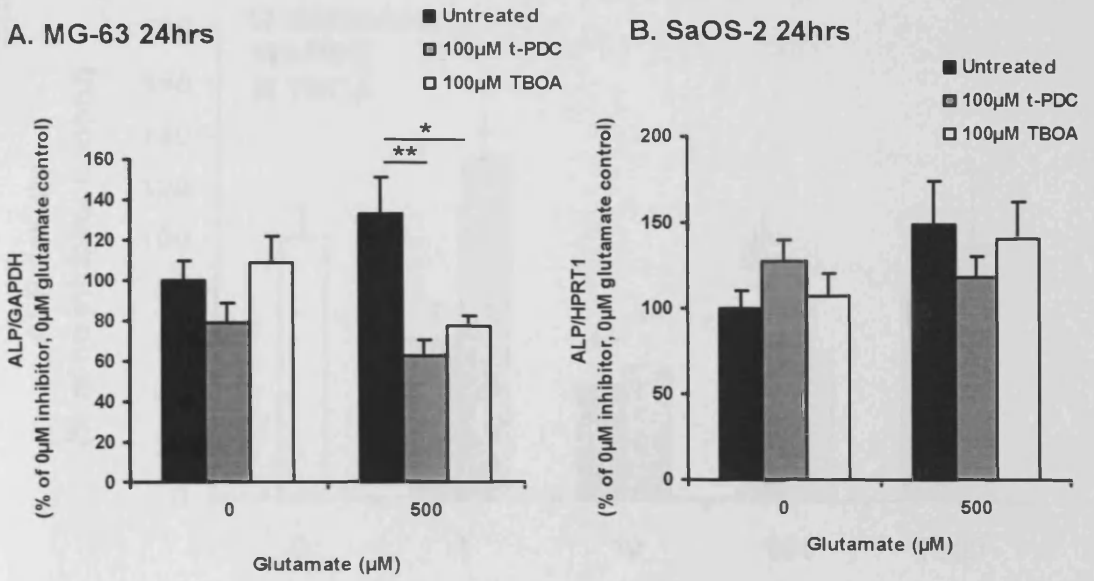

Figure 4.11. Effect of EAAT inhibitors on ALP mRNA expression in human osteoblasts. Human osteoblasts (A, MG-63; B, SaOS-2) were cultured with EAAT inhibitors ± 500μM glutamate for 24hrs. ALP expression was assessed by QRT-PCR, normalised to housekeeping gene levels and expressed as the percentage change over control cells (0μM inhibitor, 0μM glutamate). Values are mean ± S.E.M from three independent experiments, n=4. MG-63 ALP expression was significantly reduced by EAAT inhibitors (Shierer-Ray P=0.002) and pair-wise Mann-Whitney U tests revealed that both *t*-PDC and TBOA significantly reduced ALP expression in the presence of 500μM glutamate. There were no significant effects of EAAT inhibition or glutamate on expression of ALP in SaOS-2 cells (GLM). Significance values *P<0.05, **P<0.01.

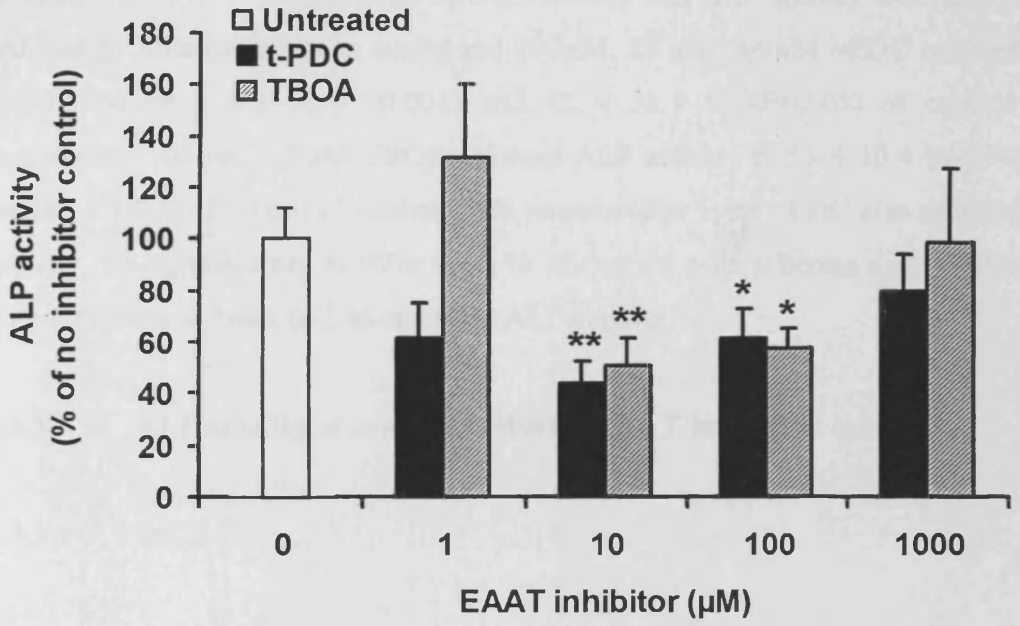

Figure 4.12. Effect of 24hr incubation with 1-1000µM EAAT inhibitor at 0µM glutamate on SaOS-2 ALP activity. Enzyme activity was measured colourimetrically and normalised to cell number (as measured by total cellular LDH activity). ALP activity is expressed as the mean percentage of ALP activity of control cells (no inhibitor) ± S.E.M from three independent experiments, n=4. ALP activity was significantly affected by both inhibitors over this concentration range (one-way ANOVA P=0.009 *(t*-PDC) and P=0.028 (TBOA)). Post-hoc pair-wise comparisons (Fisher's tests) revealed that ALP activity was significantly decreased in cells treated with 10 and 100µM *t*-PDC and TBOA. *P<0.05, **P<0.01 significantly different from control cells (no inhibitor).

(Fisher's tests) with the untreated control revealed that ALP activity was significantly reduced by both inhibitors at 10μM and 100μM. 10 and 100μM *t*-PDC reduced ALP activity to 44 ± 8.2 % ($P<0.001$) and 62 ± 11.1 % ($P<0.05$) of control cells respectively. 10 and 100μM TBOA reduced ALP activity to 51 ± 10.4 % ($P<0.001$) and 58 ± 7.9 % ($P<0.05$) of control cells respectively. 1μM *t*-PDC also reduced ALP activity non-significantly to 62 ± 13.5 % of control cells whereas 1μM TBOA and both inhibitors at 1mM had no effect on ALP activity.

4.3.5 ALP activity of cells treated with EAAT inhibitors over time

4.3.5.1 SaOS-2

ALP activity was assayed in SaOS-2 cell lysates following culture with 100μM EAAT inhibitors in the presence and absence of 500μM glutamate at 24, 48 and 72hrs treatment (Figure 4.13). Enzyme activity was normalised to total cell number (total LDH activity within the adherent cell lysate). Presented data are from three independent experiments where n=4.

At 24hrs, ALP activity was significantly affected by EAAT inhibitors (GLM with log data $P=0.011$), but not by glutamate (GLM with log data $P=0.378$) or by the interaction between the two factors (GLM with log data $P=0.372$). Post-hoc pair-wise comparisons (Tukey's tests) revealed that ALP activity was significantly reduced by 100μM *t*-PDC ($P=0.018$) and 100μM TBOA ($P=0.028$) compared to untreated cells in the absence of glutamate. EAAT inhibition did not significantly affect ALP activity compared to untreated cells at 500μM glutamate, given that 500μM glutamate alone also decreased ALP activity (to 79 ± 10.0 % of untreated control cells). At 48hrs, glutamate concentration significantly influenced ALP activity (GLM with ranked data $P=0.019$). This reflects a reduction in ALP activity when inhibitors are combined with 500μM glutamate, although no post-hoc pair-wise comparisons (Tukey's tests) were statistically significant. EAAT inhibition (GLM with ranked data $P=0.559$) and the interaction between glutamate and EAAT inhibitors (GLM with ranked data $P=0.161$) had no significant effects on ALP activity at 48hrs. ALP activity was not significantly affected at 72hrs by EAAT inhibition (GLM with ranked data $P=0.767$), glutamate (GLM with ranked data $P=0.991$) or the interaction of the two factors (GLM with ranked data $P=0.394$).

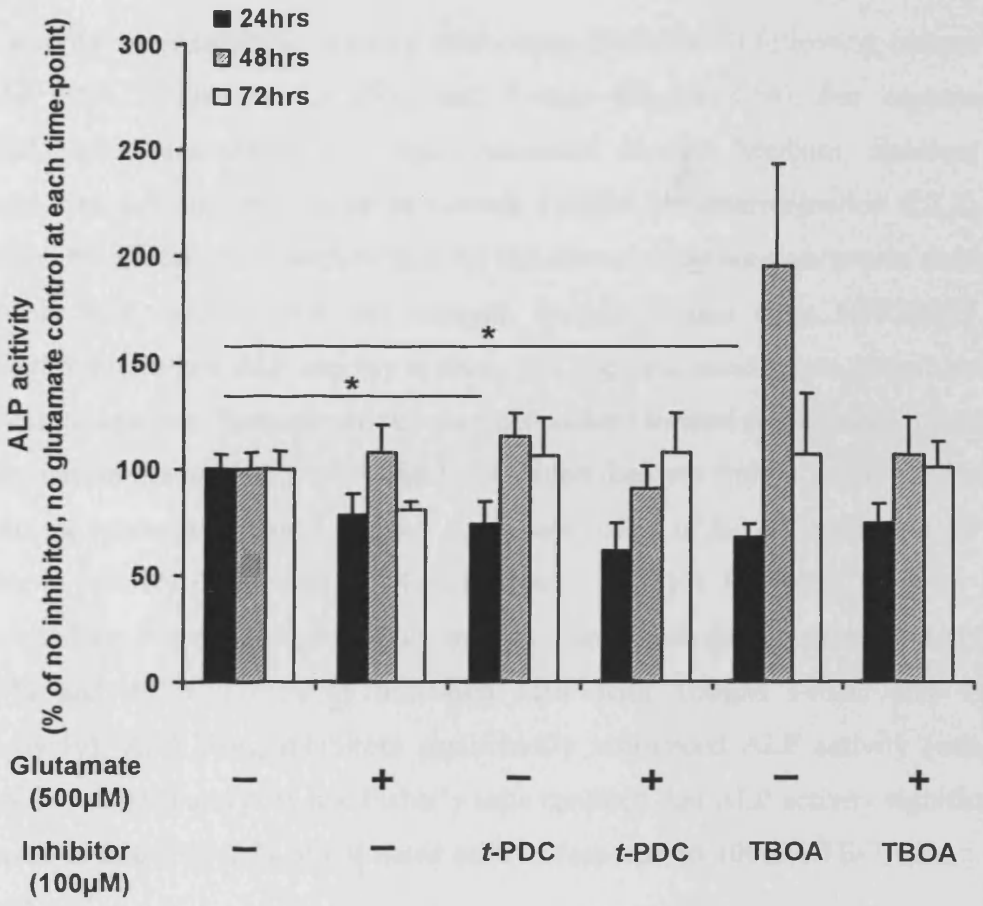

Figure 4.13. Effect of EAAT inhibitors on SaOS-2 osteoblast ALP activity over 72hrs. SaOS-2 cells were cultured with EAAT inhibitors ± 500μM glutamate for 72hrs. ALP activity was measured colourimetrically and normalised to cell number (as measured by total cellular LDH activity) at 24, 48 and 72hrs. ALP activity is expressed as the mean percentage of ALP activity in control cells (no inhibitor, no glutamate) at each time-point ± S.E.M from three independent experiments, n=4. ALP activity was significantly affected by EAAT inhibition at 24hrs (GLM P=0.011) and post-hoc Tukey's tests revealed reduced ALP activity in cells treated with 100μM *t*-PDC and TBOA in the absence of glutamate. At 48hrs, ALP activity was significantly decreased across all groups by 500μM glutamate (GLM P=0.019), but no post-hoc pair-wise comparisons were statistically significant at the 5% level. ALP activity at 72hrs was not significantly affected by experimental treatments. Significance values *P<0.05.

4.3.5.2 Primary osteoblasts (NHOB1P5)

ALP activity was assayed in primary osteoblasts (NHOB1P5) following culture with 100μM EAAT inhibitors for 24hrs and 5 days (Figure 4.14). For experiments, NHOB1 cells were plated in Lonza Osteoblast Growth Medium, however this medium was subsequently found to contain 510μM glutamate (section 2.2.3), and therefore the effects of the inhibitors in the absence of exogenous glutamate cannot be observed. ALP activity was not assayed in cell lysates from NHOB2P7 and NHOB3P5 due to low ALP activity in these cell lines and insufficient sample volume for accurate analysis. Enzyme activity was normalised to total cell number (total LDH activity within the adherent cell lysate). Presented data are from a single preliminary experiment where n=4. There was no significant effect of EAAT inhibitors on ALP activity in primary osteoblasts at 24hrs (one-way ANOVA P=0.076), however there was a trend for decreased ALP activity in cells treated with the EAAT inhibitors (79 ± 11.6 % and 49 ± 7.7 % of untreated cells with 100μM *t*-PDC and TBOA respectively). At 5 days, inhibitors significantly influenced ALP activity (one-way ANOVA P=0.037) and post-hoc Fisher's tests revealed that ALP activity significantly increased to 256 ± 52.2 % of untreated cells in response to 100μM TBOA for 5 days (P<0.05).

4.3.6 Alizarin red staining of mineralisation

4.3.6.1 SaOS-2

Mineralisation was determined in SaOS-2 cells following 10 days culture with EAAT inhibitors in the presence or absence of 500μM glutamate (Figure. 4.15). Representative pictures from stained wells are shown in Figure 4.15. The number of mineralised nodules stained by alizarin red appeared to be slightly reduced in cells treated with 500μM glutamate alone and strongly reduced in cells treated with either *t*-PDC or TBOA in the presence and absence of 500μM glutamate. To confirm this, bound alizarin red (μg) was extracted in 5% perchloric acid (section 2.9) and quantified against a standard curve (Figure 4.16A). Presented data are from three independent experiments where n=4. Alizarin red staining was significantly reduced by EAAT inhibitors (Shierer-Ray P<0.001) but not affected by glutamate (Shierer-

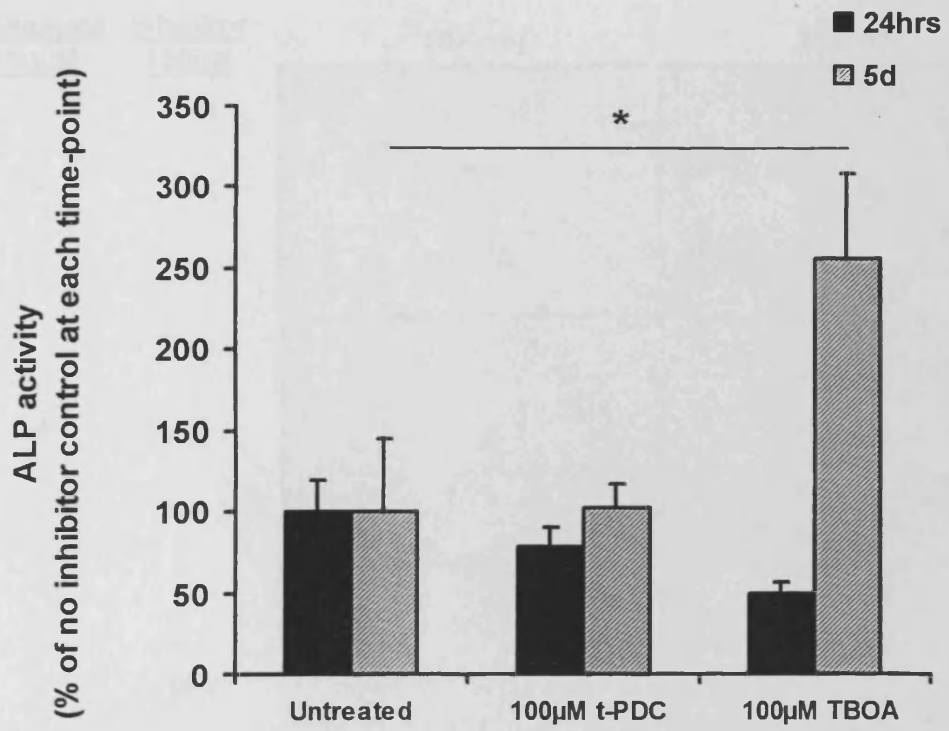

Figure 4.14. Effect of EAAT inhibitors on primary osteoblast ALP activity at 24hrs and 5 days. Primary osteoblasts (NHOB1P5) were cultured with EAAT inhibitors at 100µM in medium containing 510µM glutamate and ALP activity measured colourimetrically and normalised to cell number (as measured by total cellular LDH activity) at 24hrs and 5 days. ALP activity is shown as the mean percentage of ALP activity of control cells (no inhibitor) ± S.E.M from a single preliminary experiment, n=4. ALP activity was not significantly affected by EAAT inhibitors at 24hrs, but was significantly increased by 100µM TBOA at 5 days (one-way ANOVA P=0.037). Significance values *P<0.05.

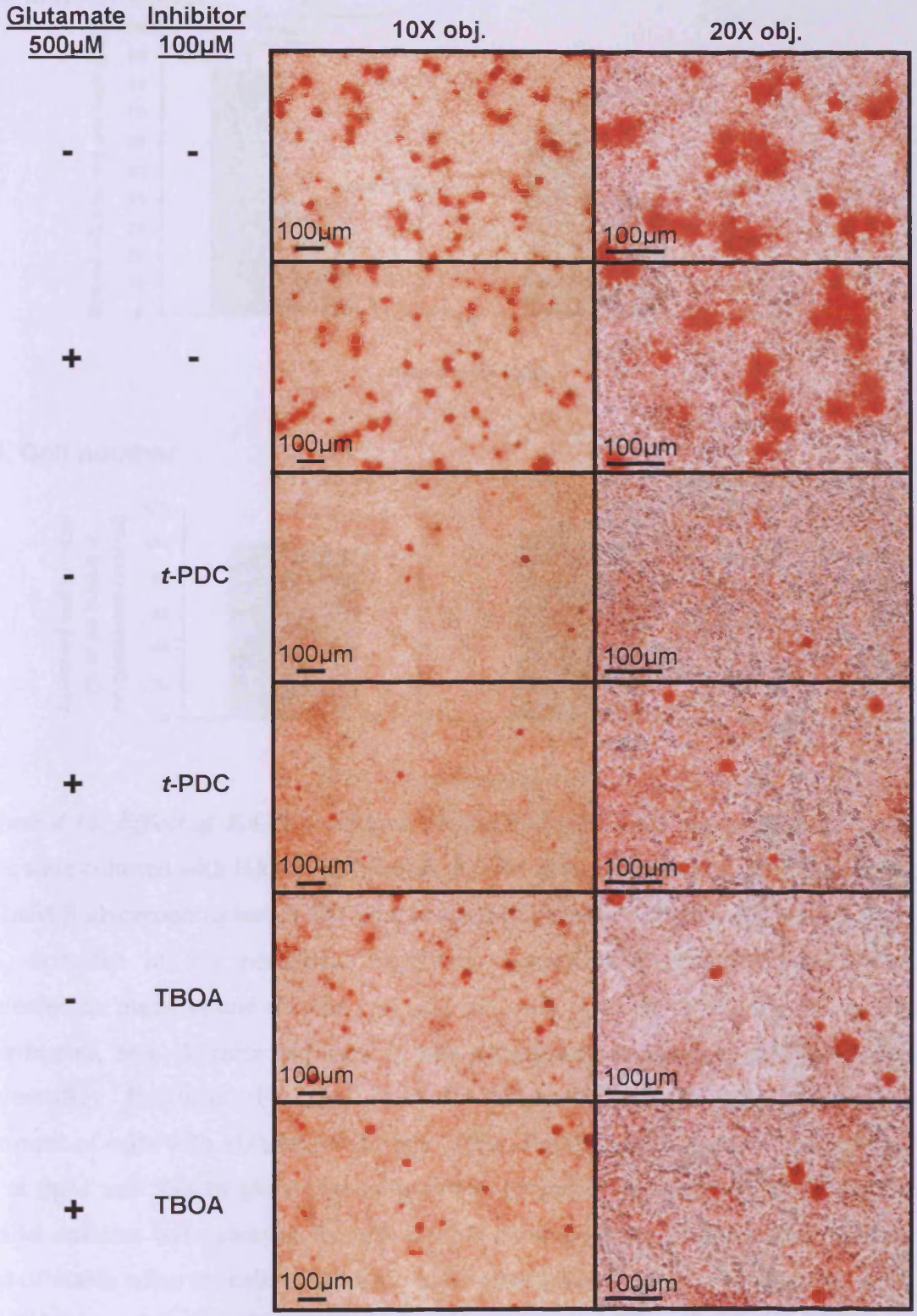

Figure 4.15. Effect of EAAT inhibition on SaOS-2 osteoblast mineralisation. SaOS-2 cells were cultured with EAAT inhibitors ± 500μM glutamate for 10 days in the presence of 2mM β-glycerophosphate and stained with alizarin red. Pictures were taken of stained cells under 10X and 20X objectives.

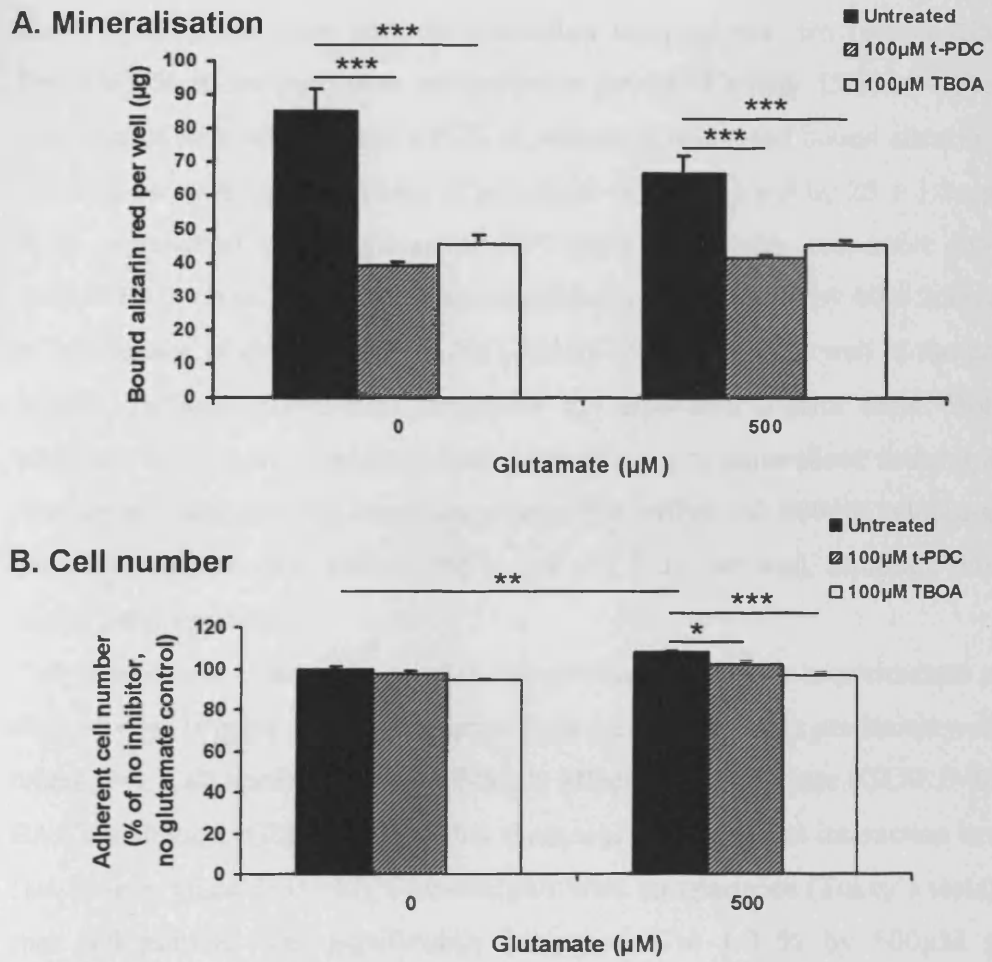

Figure 4.16. Effect of EAAT inhibition on SaOS-2 osteoblast mineralisation. SaOS-2 cells were cultured with EAAT inhibitors ± 500μM glutamate for 10 days in the presence of 2mM β-glycerophosphate. (A) Cultures were stained with alizarin red. Bound alizarin red, extracted in 5% perchloric acid, was quantified spectrophotometrically and expressed as mean bound alizarin red (μg) per well ± S.E.M from three independent experiments, n=4. Alizarin red staining was significantly reduced by EAAT inhibitors (Shierer-Ray $P<0.001$). Post-hoc pair-wise Mann-Whitney U tests revealed that treatment of cells with 100μM *t*-PDC and TBOA significantly decreased bound alizarin red at 0μM and 500μM glutamate compared to respective control cells. (B) Cells from parallel cultures were assayed for cell number by measuring LDH released upon total lysis of viable adherent cells at 10 days. LDH released is shown as the mean percentage of LDH released from viable adherent control cells (no inhibitor, no glutamate) ± S.E.M from a single experiment, n=4. Cell number was significantly affected by glutamate ($P<0.001$) and EAAT inhibition ($P<0.001$) (GLM). Post-hoc Tukey's tests revealed a significant increase in cell number in response to 500μM glutamate, and this was prevented by EAAT inhibition. Significance values *$P<0.05$, **$P<0.01$, ***$P<0.001$.

Ray P=0.935) and there was no interaction between the two factors (Shierer-Ray P=0.476). Post-hoc pair-wise comparisons (Mann-Whitney U tests) revealed that treatment of cells with 100μM *t*-PDC significantly decreased bound alizarin red by 45 ± 0.9 μg per well in the absence of glutamate (P<0.001) and by 25 ± 1.2 μg per well in the presence of 500μM glutamate (P<0.001) compared to respective control cells. 100μM TBOA also significantly decreased bound alizarin red by 40 ± 2.5 μg per well in the absence of glutamate (P<0.001) and by 19 ± 1.4 μg per well in the presence of 500μM glutamate (P<0.001) compared to respective control cells. Both EAAT inhibitors consistently inhibited alizarin red staining of mineralised nodules in SaOS-2 monolayers and this appeared to mimic the effect of 500μM glutamate which decreased mean bound alizarin red by 18 ± 5.5 μg per well, although this was not statistically significant.

Cell number was assayed in parallel cultures under the same experimental conditions after 10 days (Figure 4.16B). Presented data are from a single preliminary experiment where n=4. Cell number was significantly affected by glutamate (GLM P<0.001) and EAAT inhibition (GLM P<0.001) but there was no significant interaction between the two factors (GLM P=0.140). Post-hoc pair-wise comparisons (Tukey's tests) revealed that cell number was significantly increased 8 ± 1.0 % by 500μM glutamate (P=0.006) and that this was prevented by *t*-PDC (P=0.048) and TBOA (P<0.001).

A trend for reduced SaOS-2 mineralisation upon treatment with EAAT inhibitors ± glutamate has been observed in 7 independent experiments and this has been found to be independent of cell passage (P18-30), cell confluence at initiation of treatment (50-100%), presence or absence of antibiotics (1% penicillin/streptomycin), presence or absence of dexamethasone (10^{-7}M), pH changes associated with the treatments (tested by supplementing the medium with HEPES buffer during the 10 days treatment) or frequency of treatment replenishment (data not shown). However a further 3 independent experiments have shown contrasting results and the possible variations in methodology responsible for this are investigated in the discussion of this chapter. These 3 experiments were not included in the replicates presented in this chapter since they did not conform exactly to the uniform experimental protocol.

4.3.6.2 Primary osteoblasts (NHOB2P11)

Alizarin red staining of human primary osteoblasts (NHOB2P11) treated with EAAT inhibitors in the presence and absence of 500μM glutamate for 21 days is expressed as mean bound alizarin red (μg) per well (Figure. 4.17). Presented data are from a single preliminary experiment where n=4. 500μM glutamate significantly increased bound alizarin red (GLM with log data P=0.044), however no post-hoc pair-wise comparisons (Tukey's test) were significant at the 5% level. In this preliminary experiment, bound alizarin red was increased by 500μM glutamate from 6 ± 2.0 μg to 7 ± 1.2 μg in untreated cells (no inhibitor) (P=0.942), from 5 ± 0.9 μg to 7 ± 1.1 μg in *t*-PDC treated cells (P=0.905), and from 5 ± 0.8 μg to 11 ± 3.1 μg in TBOA treated cells (P=0.470). EAAT inhibition at 0 or 500μM glutamate did not significantly affect mineralisation (GLM with log data P=0.782), and there was no interaction between the two factors (GLM with log data P=0.774).

4.4 Discussion

4.4.1 Background

Glutamate is present in human serum within the low micromolar range (Plaitakis et al. 1982), detected to be 28.3 ± 2.5 μM by HPLC (Mally et al. 1996). Increased serum glutamate levels have been associated with autism (89.2μM) (Shinohe et al. 2006) and essential tremor (89.6μM) (Mally et al. 1996). Glutamate is present in human synovial fluid at 6μM (Plaitakis et al. 1982; McNearney et al. 2000) and glutamate concentrations in the synovial fluid from human patients with rheumatoid arthritis (RA), gout and osteoarthritis (OA), can reach 332.3 ± 29.3, 364.21 ± 50.19 and 240 ± 38 μM respectively (McNearney et al. 2004). An experimental concentration of 500μM glutamate was chosen here to reflect these pathological concentrations in the joint that osteoblasts may be exposed to. Glutamate-free medium was used as a control, however it is unlikely that the extracellular milieu remained glutamate-free for the duration of the experiment since osteoblasts (MG-63, SaOS-2, MC3T3-E1, primary mouse and human osteoblasts) spontaneously release glutamate

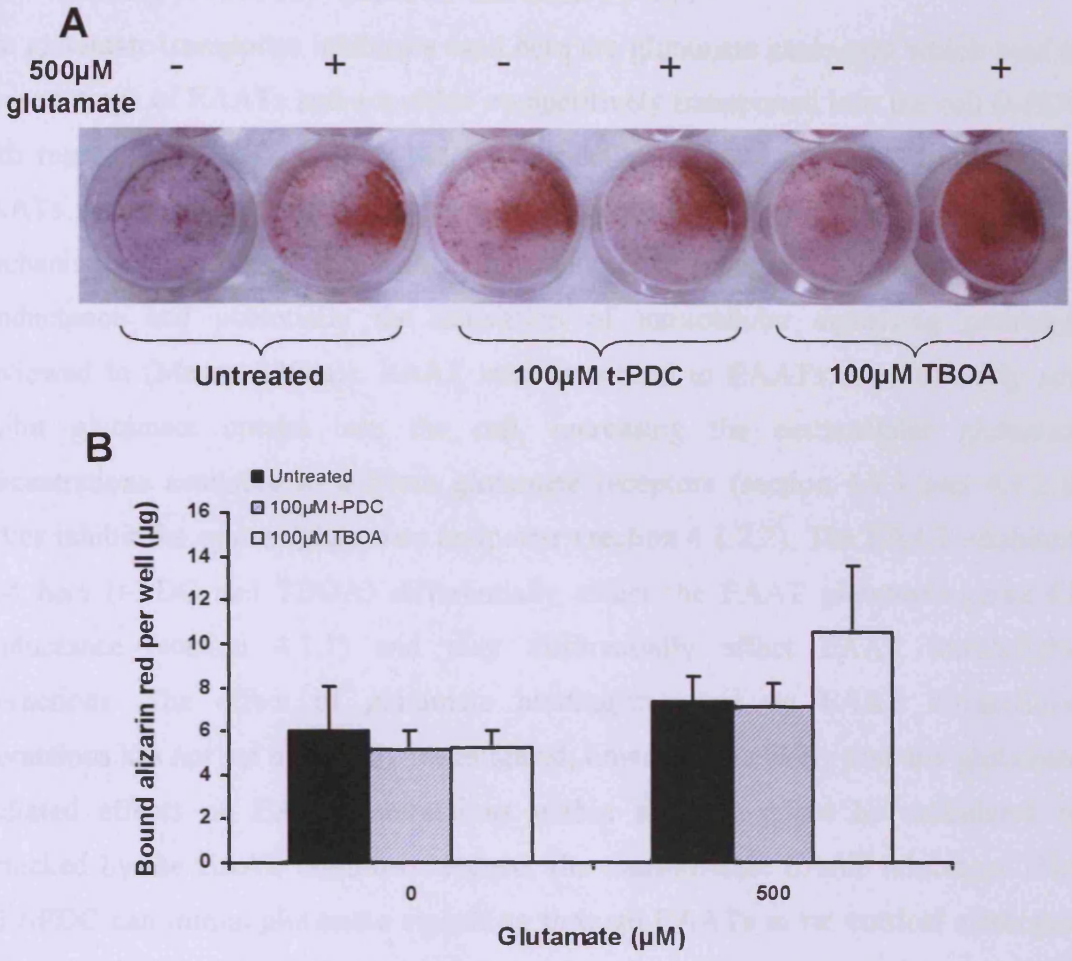

Figure 4.17. Effect of EAAT inhibition on primary osteoblast mineralisation. Osteoblasts (NHOB2P11) were cultured with EAAT inhibitors ± 500µM glutamate for 21 days in the presence of 2mM β-glycerophosphate and 10^{-7}M dexamethasone and stained with alizarin red (A). Bound alizarin red, extracted in 5% perchloric acid, was quantified spectrophotometrically and is expressed as mean bound alizarin red (µg) per well ± S.E.M from a single preliminary experiment, n=4 (B). 500µM glutamate significantly increased bound alizarin red (GLM P=0.044) however no pair-wise Tukey's comparisons were significant.

(~2–7 nmol/mg protein/day) (Genever and Skerry 2001).

The glutamate transporter inhibitors used here are glutamate analogues which bind to a broad range of EAATs and are either competitively transported into the cell (*t*-PDC with respect to EAATs 1-4) or block transport completely (TBOA). Inhibition of EAATs in osteoblasts has the potential to influence bone formation by a variety of mechanisms since EAAT activities include glutamate transport, glutamate gated Cl^- conductance and potentially the activation of intracellular signalling pathways (reviewed in (Mason 2004a)). EAAT inhibitors bind to EAATs extracellularly and inhibit glutamate uptake into the cell, increasing the extracellular glutamate concentrations available to activate glutamate receptors (section 4.1.1 and 4.1.2.1) and/or inhibit the cystine/glutamate antiporter (section 4.1.2.2). The EAAT inhibitors used here (*t*-PDC and TBOA) differentially affect the EAAT glutamate gated Cl^- conductance (section 4.1.1) and may differentially affect EAAT intracellular interactions. The effect of glutamate binding/transport on EAAT intracellular interactions has not yet been fully investigated; however it is likely that any glutamate mediated effects on EAAT interactions within the cell might be modulated or mimicked by the EAAT inhibitors. Indeed, the transportable EAAT inhibitors THA and *t*-PDC can mimic glutamate signalling through EAATs in rat cortical astrocytes leading to increased MAPK phosphorylation in a time- and concentration-dependent manner (Abe and Saito 2001).

Since EAATs display a variety of activities and, as outlined above, the EAAT inhibitors have the potential to differentially modulate these activities, the effect of inhibitors and/or glutamate in osteoblasts is unlikely to be the product of a single common pathway. A summary of the main effects of *t*-PDC and TBOA on MG-63 and SaOS-2 cells are shown in tables 4.1-3. Data from human primary osteoblasts are not included since experiments on these cells were only carried out 1-2 times; but are discussed in the following sections where appropriate for comparison with cell line data.

4.4.1.1 EAAT inhibitors in storage and culture

The half-life of the inhibitors in culture is unknown and attempts to monitor the stability of the compounds over time by HPLC were hampered by the presence of many other small compounds in DMEM which gave overlapping peaks to the

Table 4.1. Summary of the effects of 500μM glutamate on the osteoblast phenotype. Changes in the expression/activity of MG-63 (black) and SaOS-2 (grey) are shown as increases (↑), decreases (↓) or no change (-) relative to untreated cells (0μM inhibitor, 0μM glutamate). NT, not tested. Significance values *P<0.05, **P<0.01, ***P<0.001, n.s (not significant). Trends non-significant by post-hoc test but significant by ANOVA are indicated in brackets.

		Gene expression (24hrs)							
	Cell number	**Osteoblast diff^n**	**Bone extracellular matrix**			**Bone remodelling**	**Mineral-isation**	**Bone-forming activity**	
	LDH activity in cell layer (24hrs)	*Runx2*	*Osteocalcin*	*Type I collagen*	*Osteonectin*	*OPG*	*ALP*	ALP activity (24/48hrs)	Mineralisation (10d)
500μM glutamate	↑ ***	-	↓ n.s.(**)	↑ n.s.	-	-	↑ n.s.	NT	NT
	-	-	-	-	-	↑ n.s.	↑ n.s.	↓ n.s./↓ n.s.(*)	↓ n.s.

Table 4.2. Summary of the effects of pharmacological EAAT inhibition at 0μM glutamate on the osteoblast phenotype. Changes in the expression/activity of MG-63 (black) and SaOS-2 (grey) are shown as increases (↑), decreases (↓) or no change (-) relative to untreated cells (0μM inhibitor, 0μM glutamate). NT, not tested. Significance values $*P<0.05$, $***P<0.001$, n.s (not significant).

		Gene expression (24hrs)							
Inhibitor	**Cell number**	**Osteoblast diff^n**	**Bone extracellular matrix**			**Bone remodelling**	**Mineral-isation**	**Bone-forming activity**	
	LDH activity in cell layer (24hrs)	*Runx2*	*Osteocalcin*	*Type I collagen*	*Osteonectin*	*OPG*	*ALP*	ALP activity (24/48hrs)	Mineralisation (10d)
***t*-PDC**	↑ n.s. ↑ ***	-	-	↑ n.s. ↑ n.s.	-	-	↓ n.s.	NT ↓*/ -	NT ↓***
TBOA	↑ n.s. ↑ *	-	-	-	↓ n.s.	↓ n.s.	-	NT ↓*/ -	NT ↓***

Table 4.3. Summary of the effects of pharmacological EAAT inhibition at 500μM glutamate on the osteoblast phenotype. Changes in the expression/activity of MG-63 (black) and SaOS-2 (grey) are shown as increases (↑), decreases (↓) or no change (-) relative to untreated cells (0μM inhibitor, 500μM glutamate). NT, not tested. Significance values $*P<0.05$, $**P<0.01$, $***P<0.001$, n.s (not significant).

		Gene expression (24hrs)							
Inhibitor	**Cell number**	**Osteoblast diff^n**	**Bone extracellular matrix**			**Bone remodelling**	**Mineral-isation**	**Bone-forming activity**	
	LDH activity in cell layer (24hrs)	*Runx2*	*Osteocalcin*	*Type I collagen*	*Osteonectin*	*OPG*	*ALP*	ALP activity (24/48hrs)	Mineralisation (10d)
***t*-PDC**	↓ n.s. ↑ n.s.	↓ n.s. -	- -	- -	- ↑ n.s.	↓ n.s. ↓ *	↓ ** -	NT - / ↓ n.s.	NT ↓ ***
TBOA	↓ * -	↓ n.s. -	- -	- -	↓ * -	- -	↓ * -	NT - / -	NT ↓ ***

inhibitors (data not shown). High concentrations of EAAT inhibitors (333μM and 1mM), including *t*-PDC and TBOA, effectively increased extracellular glutamate concentrations in organotypic cultures of rat hippocampus after 7 days in culture without medium refreshment, however lower inhibitor concentrations had no significant effects (O'Shea et al. 2002). Lower concentrations of these inhibitors (50-200μM) were able to increase extracellular glutamate concentration when medium was replaced twice weekly over a culture period of 14 days (O'Shea et al. 2002), suggesting that the inhibitors used in this thesis (100μM) will maintain activity for the time course used. In murine astrocyte cultures, TBOA significantly reduced D-aspartate uptake over 24-72hrs, however the inhibitor was less effective after 72hrs culture compared to 24hrs (Lau et al. 2010). These studies indicate that *t*-PDC and TBOA at 100μM were able to inhibit glutamate uptake for up to 72hrs in the experiments presented here, but that effectiveness probably decreased with culture time.

Inhibitors used in these studies were dissolved in water; however the stability of the compounds during storage has not been robustly assessed. Since the stability of the stock inhibitor (10mM, stored at -20°C) over the 8 week usage period is unknown, this may represent a confounding variable in all the experiments presented in this chapter. However glutamate uptake assays have been carried out during the course of this PhD where the compounds have been shown to retain their inhibitory activity despite length of storage.

4.4.2 High concentrations of glutamate and EAAT inhibition influence osteoblast cell number

4.4.2.1 Glutamate

The addition of 500μM glutamate to the culture medium of MG-63 and human primary osteoblasts significantly increased adherent cell number in comparison to cells that were maintained in glutamate-free medium; however this experiment was only carried out twice in human primary osteoblasts and therefore needs to be further repeated to validate this finding. Increased cell number was detectable at 24hrs for both cell types and also at 48hrs for MG-63 cells and comprised a 10-20% increase in MG-63 cell number and a 5-15% increase in primary osteoblast cell number.

Glutamate at 50μM-1mM has previously been shown to increase human primary osteoblast viable cell number (by 5-15% compared to cells cultured in glutamate-free medium) over 72hrs whereas very high glutamate concentrations (10mM) resulted in a decrease in cell number (~7% compared to cells cultured in glutamate-free medium) (Genever and Skerry 2001). The authors hypothesised that glutamate in the range of 50μM-1mM may represent a survival factor since the experiments were carried out in serum-free medium. In our experiments, MG-63 and SaOS-2 cell lines were cultured in the presence of 5% dialysed serum for the duration of glutamate treatment and primary osteoblasts were cultured serum-free for only the first 24hrs of treatment, after which 10% dialysed FBS was added to the medium. Glutamate did result in a significant overall increase in primary osteoblast cell number after 24hrs in serum-free medium in our studies, in agreement with the published findings from Genever and Skerry.

Investigation of which receptor could mediate the proliferative response to glutamate have yielded contrasting results. An antagonist to NMDA receptors (MK-801) had no effect on viable cell number of rat calvarial osteoblasts over 3-28 days (Hinoi et al. 2003) suggesting that glutamate signalling through this receptor subtype does not influence cell number, however another study has shown that NMDA treatment of MC3T3-E1 osteoblast-like cells for up to 1hr could increase viable cell number (Fatokun et al. 2006).

Glutamate has been implicated in the regulation of neuronal, cancer cell, chondrocyte-like cell and synovial fibroblast proliferation (Contestabile 2000; Rzeski et al. 2001; Parada-Turska et al. 2006; Spitzer 2006; Piepoli et al. 2009). In early neuronal development, glutamate signalling is thought to play a key role in regulating proliferation of neural progenitor cells and neuronal migration (Komuro and Rakic 1993; Contestabile 2000; Spitzer 2006). Activity of iGluRs can both reduce and increase neural progenitor cell proliferation in a manner that is specific to different brain regions (LoTurco et al. 1995; Haydar et al. 2000; Bai et al. 2003). Glutamate also critically regulates neuronal survival during synaptogenesis and blockade of NMDA receptors in the developing rodent brain can trigger massive apoptotic neuronal death (Ikonomidou et al. 1999).

Antagonists to NMDA and AMPA receptors limit the proliferation of a wide variety of non-neuronal cancer cells including colon, breast, lung and thyroid carcinoma, as a result of both decreased cell division and increased cell death (Rzeski et al. 2001).

This proliferative effect of glutamate may be common to all cells but subject to altered regulation in cancer cell lines. The osteoblast-like cell lines used here, MG-63 and SaOS-2, are osteosarcoma derived and so interpretation of their proliferative responses to the modulation of glutamate signalling might be complicated by the fact that they are both osteoblast-like and a cancer cell line.

NMDA receptor antagonists and knockdown of NR1 in SW1353 human chondrosarcoma cells suppressed proliferation without affecting cell death (Piepoli et al. 2009) and a variety of ionotropic and metabotropic glutamate receptor antagonists suppressed proliferation of HIG-82 cells (Parada-Turska et al. 2006), a rabbit synoviocyte cell line that shares many characteristics of activated human synovium (Georgescu et al. 1988).

In synovial fibroblasts from rats with collagen-induced arthritis (CIA) 500μM glutamate significantly increased proliferation over 24hrs and this was attenuated by co-incubation with the non-selective EAAT inhibitors THA and CCGIII at 100μM (Hinoi et al. 2005b) indicating a role for the transporter in the proliferative activity of these cells. That an EAAT-mediated activity may underlie the proliferative response of these cells to glutamate is interesting since it is in contrast to the receptor-mediated effects of glutamate in neuronal cells, cancer cells and the chondrocyte and synoviocyte cell lines discussed above. Furthermore, the glutamate-mediated increase in MG-63 cell number at 24hrs could also be attenuated by EAAT inhibition. However EAAT inhibitors alone increased MG-63 cell number suggesting that the increase in cell number is not dependent on glutamate uptake by EAATs.

Since 500μM glutamate did not reduce cell number in any of the assayed osteoblast cell lines, nor affect cell death in human primary osteoblasts, it can be inferred that glutamate-mediated toxicity does not occur in these cells as it does in mature cell populations of the CNS (reviewed in (Obrenovitch et al. 2000)). The resistance of bone to glutamate mediated toxicity at these concentrations has been previously reported (Genever and Skerry 2001), however some studies have shown that >500μM glutamate can suppress proliferation of the pre-osteoblast mouse MC3T3-E1 cell line and the pluripotent MSC line C3H10T1/2, with no effect upon cell death (Iemata et al. 2007; Uno et al. 2007). This suppression of proliferation could be rescued by supplementation with cystine or GSH indicating that exogenous glutamate leads to retrograde operation of the cystine/glutamate antiporter and therefore reduced intracellular levels of the antioxidant GSH (Iemata et al. 2007; Uno et al. 2007). Hinoi

et al, have also shown that cysteine is important for MC3T3-E1 cell survival when cultured in DMEM (glutamate-free) compared to α-minimum essential medium (α-MEM, 510μM glutamate) (Hinoi et al. 2002a). However, the same study also showed that 1mM pyruvate could exhibit antioxidant properties and prevent the cell death associated with replacement of α-MEM with DMEM (Hinoi et al. 2002a). MG-63, SaOS-2 and primary osteoblasts used in these experiments were protected from ROS-mediated cell death by culture in DMEM medium containing pyruvate.

Glutamate had no effect on adherent cell number in MG-63 or human primary osteoblasts at later time-points (72hrs for MG-63 or 5 days for primary osteoblasts). This may be the result of extracellular glutamate depletion by EAAT activity or feedback signalling mechanisms. That SaOS-2 cell number was neither increased nor decreased by the presence of 500μM glutamate at any of the measured time-points (24-72hrs) supports the former hypothesis since these cells have much higher basal EAAT activity compared to MG-63 cells (section 3.3.3) which could result in glutamate being rapidly bound or transported from the extracellular space.

4.4.2.2 EAAT inhibitors

In the absence of extracellular glutamate, 24hrs treatment with EAAT inhibitors over a concentration range of 1-100μM increased osteoblast-like cell number. These effects were statistically significant in SaOS-2 cells for both *t*-PDC and TBOA but only an observed trend in MG-63 cells. Both inhibitors elicited the same response in SaOS-2 cells, suggesting a similar mode of action. Both *t*-PDC and TBOA inhibit EAAT glutamate transport but have differing effects on EAAT Cl^- conductance (Arriza et al. 1997; Shimamoto et al. 1998; Wadiche and Kavanaugh 1998; Seal et al. 2001; Ryan and Vandenberg 2002; Shigeri et al. 2004), suggesting that inhibition of the glutamate transport activity of EAATs is the more likely mode of action responsible for increasing cell number in these cells. EAAT inhibitors reduce glutamate uptake into the cell, preventing its intracellular accumulation and thus increasing extracellular glutamate concentrations, which we have shown can increase MG-63 cell number. This hypothesis is supported by the finding that *t*-PDC is more effective than TBOA at low concentrations in SaOS-2 cells, since *t*-PDC can also induce efflux of glutamate by heteroexchange (Nicholls and Attwell 1990; Dunlop et al. 1992; Blitzblau et al. 1996; Koch et al. 1999).

EAAT inhibitors were more effective at increasing SaOS-2 cell number compared to MG-63 cells. SaOS-2 cells have a much higher rate of EAAT activity than MG-63 cells (section 3.3.3) and a lower rate of glutamate release (Genever and Skerry 2001), suggesting that extracellular glutamate concentrations are more tightly regulated in SaOS-2 cells than in MG-63 cells. If so, SaOS-2 cells will experience the biggest change from basal conditions upon treatment with the inhibitors, providing one possible explanation as to why these are the most responsive cell line.

High concentrations of the inhibitors (1000μM) had no effect on SaOS-2 cell number and the peak increase in cell number occurred at inhibitor concentrations of 10μM, which inhibit SaOS-2 Na^+-dependent uptake of 1μM glutamate (not tested at 10μM glutamate) by 25% (*t*-PDC) and 71% (TBOA) (section 3.3.3.3, Figure 3.14). Since *t*-PDC had the greatest effect on cell number, these findings suggest that partial, as opposed to complete, inhibition of glutamate uptake in SaOS-2 cells results in increased cell number. Complete inhibition of glutamate uptake might prevent the accumulation of intracellular glutamate required metabolically or increase the extracellular glutamate concentration to such an extent that feedback signalling occurs or inhibitory GluRs are activated, thus attenuating the response. The latter theory might also explain why treatment of SaOS-2 cells with 500μM glutamate in addition to 100μM EAAT inhibitor for 24hrs does not potentiate the inhibitor-mediated increase in cell number or why the same treatment does not potentiate the glutamate-mediated increase in cell number in MG-63 cells.

EAAT inhibitors alone displayed a trend toward increasing MG-63 cell number. This effect was not observed at 48hrs, nor did EAAT inhibitors have any significant effects on MG-63 cell number at 72hrs or SaOS-2 cell number at 48 or 72hrs. The loss of EAAT-mediated effects on cell number after 24-48hrs may reflect instability of these compounds, suggesting that treatments should be regularly refreshed in long-term experiments, or that the inhibitors influence the osteoblast phenotype in a confluence-dependent manner.

The presented experiments have so far indicated that the increase in osteoblast cell number in response to EAAT inhibitors or 500μM glutamate is the result of increased concentrations of extracellular glutamate and subsequent activation of GluRs which are known to regulate proliferation of a number of different cell types, including osteoblast-like cells (Contestabile 2000; Rzeski et al. 2001; Fatokun et al. 2006; Parada-Turska et al. 2006; Spitzer 2006; Piepoli et al. 2009). From preliminary data,

EAAT inhibitors did not have any significant effects on human primary osteoblast cell number or cell death at 24hrs or 5 days, in contrast to effects observed in the osteoblast-like cell lines. Primary osteoblasts release glutamate at a lower basal rate than MG-63 and SaOS-2 cells and contain lower levels of intracellular glutamate (Genever and Skerry 2001), therefore treatment of these cells with EAAT inhibitors alone may not result in a build up of extracellular glutamate to levels comparable to that of MG-63 and SaOS-2 cell lines. However, EAAT inhibitors in the presence of 500μM glutamate might be expected to enhance the effect of glutamate on primary osteoblast cell number, and TBOA does seem to demonstrate this, though the data in this experimental group is very variable (Figure 4.4). Quantitative comparison of glutamate receptor expression in osteoblast-like cell lines and human primary osteoblasts has not previously been investigated; however since EAAT expression varies between the cell lines (section 3.3.1.1) it seems likely that differences will exist and this may represent an additional underlying factor in the proliferative response of these cells to glutamate.

4.4.3 EAAT inhibition and high concentrations of glutamate can influence markers of differentiation and bone formation in osteoblasts

4.4.3.1 Gene expression

The gene expression of a variety of markers of osteoblast differentiation, bone formation and remodelling were assessed in response to EAAT inhibition and glutamate. The proposed roles of these genes are summarised in Table 4.4 and their expression levels during osteoblast maturation are shown in Figure 4.18. Changes in the expression of a number of these genes were detected in response to the experimental treatments (Tables 4.1-4.3), revealing that modulation of the glutamate signalling pathway in osteoblasts can modify the cell phenotype. A number of the gene expression trends detected were cell line specific, suggesting that the differentiation stage of the osteoblast may regulate its response. Unfortunately, large variances in the gene expression data from primary osteoblasts and the fact that data were from a single preliminary experiment meant that significant differences were not detected in many cases. These variances were not a reflection of poor sensitivity or

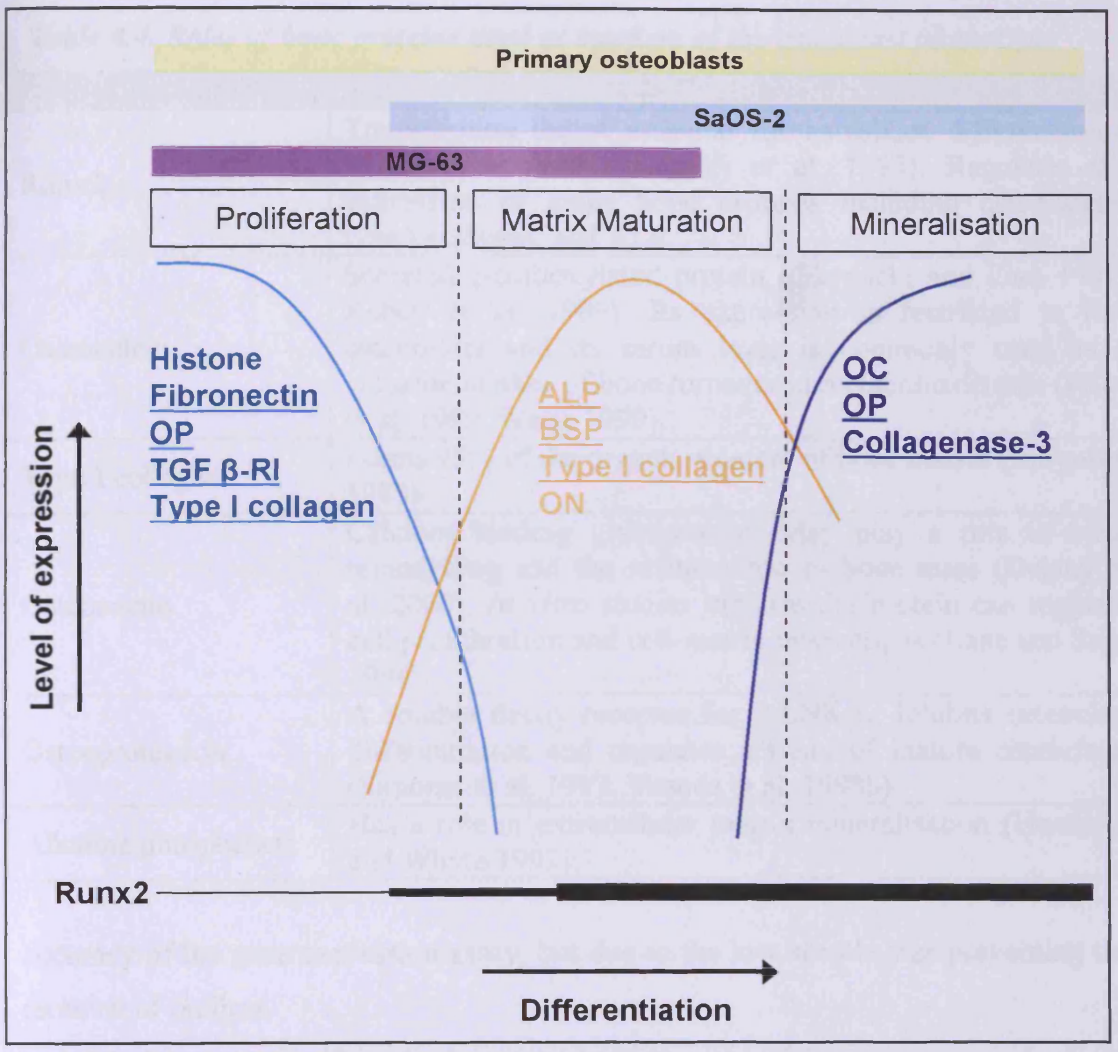

Figure 4.18. Temporal expression pattern of markers for osteoblast growth and differentiation. The growth and differentiation of osteoblasts progresses through three general stages. Osteoblast proliferation is typified by the induction of expression of various cell cycle markers including histones. Alkaline phosphatase, bone sialoprotein, type I collagen and osteonectin are expressed at high levels during the period of extracellular matrix deposition and maturation. Osteoblast matrix mineralisation is characterised by expression of osteocalcin, osteopontin and collagenase-3. Expression of many of these genes (underlined) are regulated in a Runx2-dependent manner and expression levels of Runx2 are shown at the bottom. The thickness of the line represents the expression level of Runx2 at the various stages of differentiation. The phenotypes of the osteoblast-like cell lines MG-63 and SaOS-2 and primary osteoblasts have been matched to the appropriate stage of osteoblast maturation and are shown on the diagram. Abbreviations, OP, osteopontin; ALP, alkaline phosphatase; BSP, bone sialoprotein; ON, osteonectin; OC, osteocalcin. Figure adapted from Stein et al. 2004.

Table 4.4. Roles of bone proteins used as markers of the osteoblast phenotype.

Osteoblast marker	Role
Runx2	Transcription factor essential for osteoblast differentiation (Ducy et al. 1997; Komori et al. 1997). Regulates the expression of many bone proteins including osteocalcin, type I collagen, and ALP.
Osteocalcin	Secreted γ-carboxylated protein (Glowacki and Lian 1987; Robey et al. 1989). Its expression is restricted to late osteoblasts and its serum level is commonly used as a valuable marker of bone turnover in metabolic disease (Price et al. 1980; Watts 1999).
Type I collagen	Forms 95% of the organic element of bone matrix (Burgeson 1988).
Osteonectin	Calcium binding glycoprotein. May play a role in bone remodelling and the maintenance of bone mass (Delany et al. 2000). *In vitro* studies indicate the protein can regulate cell proliferation and cell-matrix interactions (Lane and Sage 1994).
Osteoprotegerin	A soluble decoy receptor for RANK-L. Inhibits osteoclast differentiation and regulates activity of mature osteoclasts (Simonet et al. 1997; Yasuda et al. 1998b).
Alkaline phosphatase	Has a role in extracellular matrix mineralisation (Henthorn and Whyte 1992).

accuracy of the gene expression assay, but due to the low sample size preventing the removal of outliers.

500μM glutamate significantly decreased MG-63 osteocalcin expression in both the presence and absence of EAAT inhibitors indicative of a receptor-mediated effect that was not potentiated by the sustained presence of extracellular glutamate due to inhibition of uptake. Glutamate also decreased mean Runx2 expression in MG-63 cells; however this effect was only apparent in conjunction with EAAT inhibitor treatment, suggesting that either sustained exposure to extracellular glutamate was required for these effects or that the effects were mediated via glutamate transport i.e. that glutamate exerted an effect directly via the EAATs which was prevented by the inhibitors. Interestingly, preliminary data from human primary osteoblasts indicated that 500μM glutamate decreased Runx2 expression and that glutamate in conjunction with EAAT inhibitors decreased mean osteocalcin expression. The combination of 500μM glutamate and EAAT inhibitors also decreased expression of osteonectin and ALP in MG-63 cells compared to treatment with 500μM glutamate alone.

These effects on Runx2 and osteocalcin in MG-63 and primary human osteoblasts are surprising given that antagonists to NMDA receptors down-regulate the DNA binding

activity, protein and mRNA expression of Runx2 and the mRNA expression of osteocalcin in rat calvarial osteoblasts (Hinoi et al. 2003) and inhibit Runx2 mRNA expression in bone marrow stromal cells (Ho et al. 2005). Furthermore, recent studies have shown that NMDA can up-regulate osteocalcin expression in glutamate free medium (Lin et al. 2008). A variety of NMDA receptor subunits, including NR1, have been identified at the mRNA and protein level in MG-63 and primary human and rat osteoblasts (Chenu et al. 1998; Patton et al. 1998; Hinoi et al. 2001; Itzstein et al. 2001; Hinoi et al. 2003; Kalariti et al. 2004) and these receptors have been shown to be functional in MG-63 and primary rat osteoblasts (Laketic-Ljubojevic et al. 1999; Gu et al. 2002). The discrepancies between these and our studies could be a result of different treatment periods and variations in extracellular glutamate concentrations. For example, the studies from Hinoi et al. were carried out over a longer time period (7-28 days *in vitro)* than data presented in this chapter (24hrs) and the cells were cultured in α-MEM, which contains approximately 510μM glutamate, complicating a comparison with the results presented here (Hinoi et al. 2003).

In SaOS-2 cells, osteocalcin expression was significantly increased by TBOA at 0μM glutamate and this effect was prevented by 500μM glutamate which might suggest that either the response was specific to low concentrations of glutamate achievable by preventing the uptake of endogenously released glutamate, or that glutamate signalling through the transporter itself negatively regulates osteocalcin expression and that this occurred in cells treated with exogenous glutamate despite co-treatment with EAAT inhibitors due to the high glutamate concentration competing for EAAT binding sites.

SaOS-2 OPG expression was significantly reduced by *t*-PDC at 500μM glutamate and although 500μM glutamate increased the mean expression of OPG in SaOS-2 cells, these effects were not statistically significant at the 5% level. Regulation of OPG expression in SaOS-2 cells is indicative of an effect of these treatments on remodelling; however quantifying expression levels of RANKL in the same samples is necessary to confirm any such effects since it is the ratio of these two gene products that is important in the regulation of remodelling.

A similar expression pattern was observed for ALP in MG-63 cells. 500μM glutamate increased the mean expression of ALP in MG-63 cells while EAAT inhibitors in the presence of 500μM glutamate significantly decreased ALP expression. This pattern of

gene expression suggests that glutamate alone exerts an effect that is prevented by the EAAT inhibitors, suggesting that the mechanism is EAAT-mediated.

The basis for using both a transportable and a non-transportable EAAT inhibitor was to allow for the possibility that other EAAT activities besides glutamate transport might be important in osteoblasts, such as the uncoupled anion conductance or a receptor-like function. In the majority of cases, gene expression was affected in a similar manner by each inhibitor although there were some conditions where this was not the case, suggesting that EAAT activities besides glutamate uptake may be important in modulating the osteoblast phenotype. For example, TBOA but not *t*-PDC decreased MG-63 osteonectin expression and *t*-PDC but not TBOA decreased SaOS-2 OPG expression at 500μM glutamate. Differences in the effects of each inhibitor may also be a product of varying affinities for the EAAT subtypes expressed.

Overall, the effects of EAAT inhibition on osteoblast gene expression do not mimic the effects of exogenous glutamate, or potentiate these effects when added in combination. However the inhibitors alone do influence gene expression and modulate the response of the cells to 500μM glutamate suggesting that the transporters are important in regulating the osteoblast phenotype. Furthermore, different inhibitors have different effects on the same gene product, indicating the existence of more than one mechanism. Analysis of protein levels for these gene products would confirm that the changes observed at the mRNA level are translated to phenotypic changes.

4.4.3.2 ALP activity

Incubation of SaOS-2 cells with 10μM and 100μM *t*-PDC and TBOA for 24hrs significantly decreased ALP activity. The same inhibitor concentrations also significantly increased cell number. An inverse relationship between osteoblast proliferation and phenotypic maturation is well documented (Lian and Stein 1995; Karsenty 2003). Osteoblasts display a regulated pattern of gene expression (Figure 4.18) whereby the transition between proliferation and differentiation is characterised by the down-regulation of genes associated with proliferation and the up-regulation of genes associated with matrix maturation and mineralisation (Malaval et al. 1999; Karsenty 2003; Lian and Stein 2003; Stein et al. 2004). The decreased ALP activity of SaOS-2 cells treated with EAAT inhibitors may reflect prolonging of the proliferation

stage, as has been observed in primary human and rat osteoblasts subjected to dynamic cell stretching (Stanford et al. 1995a; Kaspar et al. 2000) and TGF-β (Lian and Stein 1993).

500μM glutamate decreased mean ALP activity at 24hrs and, although not statistically significant, this suggests that EAAT inhibition mimics the effects of increasing extracellular glutamate concentrations. 500μM glutamate also decreased ALP activity at 48hrs; though this was only apparent in cells that were co-incubated with EAAT inhibitors. No effect of the inhibitors or glutamate was detected at 72hrs, which might be a reflection of extracellular glutamate depletion by EAATs and/or degradation of the inhibitors. Interestingly, inhibitor effects on ALP activity or cell number in SaOS-2 cells were only effective up to 100μM suggesting that 1mM inhibitor concentrations may sustain extracellular glutamate concentrations to the extent that inhibitory glutamate receptors are activated or feedback signalling occurs, attenuating the response.

Preliminary findings indicated that primary osteoblasts also reduced mean ALP activity after 24hrs treatment with both EAAT inhibitors. Conversely, TBOA increased ALP activity after 5 days suggesting that glutamate signalling may exert differential effects depending on the stage of osteoblast maturation. Antagonists to NMDA receptors have previously been shown to inhibit ALP activity in the presence of 510μM glutamate in rat calvarial osteoblasts cultured for 28 days (Hinoi et al. 2003) and in osteoblasts derived from rat MSCs cultured for 7-11 days (Olkku and Mahonen 2008), implicating glutamate signalling through these receptors in regulating ALP activity. These findings correlate with the hypothesis that the increased ALP activity detected in human primary osteoblasts cultured with 100μM TBOA for 5 days is a result of increased extracellular glutamate levels available to activate NMDA receptors. However, the data presented here are based on a single experiment where the cells were maintained in 510μM glutamate, which is reflective of chronic pathological conditions.

4.4.3.3 Mineralisation

Mineralisation of SaOS-2 cells was reduced following incubation with 500μM glutamate for 10 days. In contrast to these findings, mineralisation of human primary osteoblasts over 21 days was increased in the presence of 500μM glutamate, however

this is preliminary data from a single experiment. Expression and activity of the glutamatergic signalling components (glutamate release, receptors and transporters) may alter as a result of time in culture in a way that differs between the SaOS-2 cell line and primary osteoblasts, providing one explanation for these contrasting effects of glutamate. The SaOS-2 cell line may be phenotypically restricted and unable to mature and regulate expression of glutamate signalling machinery in the same manner as primary osteoblasts.

The AMPA receptor antagonist CNQX and the NMDA receptor antagonist MK-801 have been shown to inhibit rat calvarial osteoblast mineralisation in the presence of 510μM glutamate over 12-18 days and that AMPA and NMDA up-regulate mineralisation over 16 days in glutamate-free medium (Lin et al. 2008). Mineralisation of osteoblasts derived from rat MSCs cultured in the presence of 510μM glutamate was also inhibited by MK-801 over 7-11 days (Olkku and Mahonen 2008). These findings are consistent with the experiments presented here in human primary osteoblasts which indicate that enhanced glutamate signalling through iGluRs may increase osteoblast mineralisation.

Mineralisation of SaOS-2 cells treated for 10 days with 100μM EAAT inhibitor ± 500μM glutamate was decreased by all treatment combinations. These changes in mineralisation occurred with very little effect on cell number (less than 10% difference in cell number in each experimental group from untreated control cells). EAAT inhibition in primary rat calvarial osteoblasts has previously been reported to prevent bone formation *in vitro* and shift the cells from an osteoblastic to a more adipocytic phenotype, however these experimental results by Spencer et al. were not published and only alluded to in a published review from the research group (Taylor 2002), so it is not possible to directly compare methodology. The inhibitory effect of long-term EAAT inhibitor treatment on SaOS-2 mineralisation is in agreement with the down-regulation of ALP activity observed in these cells at 24hrs. However, this is in contrast to the significant increase in expression of osteocalcin, a marker of late osteoblasts, in SaOS-2 cells treated with TBOA for 24hrs. Furthermore, EAAT inhibitors decreased ALP activity of primary human osteoblasts at 24hrs but long-term treatment increased ALP activity and had no effect upon mineralisation suggesting that primary osteoblasts might be differentially regulated by EAAT inhibitors during maturation in a way that does not occur in SaOS-2 cells.

Over the course of the PhD, mineralisation assays in SaOS-2 cells have had variable outcomes. Three independent experiments (n=4) were carried out according to standardised methodology, analysed and presented in this chapter. A further four independent experiments designed to test modifications to the method have displayed similar trends. However three experiments carried out in 2007 showed contrasting results, with glutamate and/or EAAT inhibitors increasing SaOS-2 mineralisation. One methodological variable that may be responsible for these differences and that has not yet been tested is β-glycerophosphate concentration. Early experiments were carried out using 10mM β-glycerophosphate as opposed to the 2mM concentration that was used in the presented experiments. The concentration of β-glycerophosphate was reduced to 2mM due to findings that concentrations above this can lead to non-physiological mineral deposition in bone cell cultures (Chung et al. 1992), which might explain some of the inconsistencies observed between experiments. However, not all experiments showing increased mineralisation in response to treatments were carried out in the presence of 10mM β-glycerophosphate; therefore other variables must be investigated.

4.4.4 Inferences from these studies regarding glutamate signalling in osteoblasts

These studies have shown that modulation of EAAT activity can regulate each stage of osteoblast differentiation including proliferation, expression of genes associated with extracellular matrix production and remodelling, and mineralisation. These effects can vary in primary osteoblasts with time in culture and between the two osteoblast-like cell lines which display pre-osteoblast and late osteoblast phenotypes, indicating that glutamate signalling may have multiple effects in osteoblasts depending on the maturation stage (discussed in section 7.3.4), which might be expected given the complexity of the glutamate receptors. In addition, EAAT inhibitors do not always mimic or potentiate the effect of extracellular glutamate, suggesting that direct EAAT-mediated effects might be important in osteoblasts.

The majority of work in the field of glutamate signalling in bone has been carried out using receptor agonists or antagonists. Such experiments investigate the effects of activation of a particular receptor subtype if and when it is expressed in bone cells. Differences are therefore to be expected between the effects of specific glutamate

receptor agonists/antagonists and the general effects of glutamate itself which have been investigated in the experiments presented here. Gu and Publicover have shown that NMDA currents in osteoblasts that were rapidly lost upon treatment with 100μM glutamate could be restored by blockade of mGluRs with MCPG, indicating inhibitory cross talk occurs between mGluRs and NMDA receptors in osteoblasts and demonstrating that the effect of glutamate can differ from the effects of specific receptor subtype activation (Gu and Publicover 2000).

4.4.5 Chemical EAAT inhibitors as a therapeutic tool in bone

The aim of this thesis was to identify a means of inhibiting EAAT activity in bone cells that would mimic mechanical stimulation and enhance bone formation with an outlook to develop an anabolic therapeutic strategy in bone. A great deal of drug development targeting components of the glutamate signalling pathway has already been carried out in the neuronal field. A common problem in designing drugs to target the CNS is the difficulty in transporting these drugs across the blood-brain barrier (BBB) (Pardridge 2003). These compounds therefore represent particularly attractive therapeutics for use in bone, since such therapeutics targeted to the glutamate signalling system in bone would not have severe non-specific effects in the CNS.
In the experiments presented in this chapter, EAAT inhibitors have increased osteoblast proliferation and mRNA expression of markers of bone formation in osteoblast-like cells, and increased mineralisation of human primary osteoblasts indicating that further investigation of these molecules as therapeutic tools for increasing bone formation is warranted. However it is also apparent that in order to clarify the effects of these inhibitors further, experiments should be carried out to determine the maturation stage that these inhibitors can most potently influence bone formation and identify a way to specifically target this.

4.4.6 Summary

EAAT inhibition was investigated in osteoblast-like cells and human primary osteoblasts as a means of mimicking osteogenic mechanical loading and enhancing osteoblast bone-forming activity. EAAT inhibitors and high concentrations of extracellular glutamate increased osteoblast proliferation and regulated the expression

of a variety of markers of osteoblast differentiation, bone formation and remodelling at the mRNA level. Mineralisation of SaOS-2 osteoblasts was inhibited by EAAT inhibitors, while preliminary data indicated that high concentrations of glutamate increased mineralisation of human primary osteoblasts, highlighting that differences exist between the osteoblast-like cell lines and primary cells in the response to long-term treatments with glutamate and/or EAAT inhibitors.

The effect of EAAT inhibition on osteoblasts has not previously been fully investigated or reported in the literature, and these studies are the first to show that EAAT inhibition can significantly modify the osteoblast phenotype. Furthermore, these experiments have provided evidence that pharmacological regulation of glutamate transporters may be important in modulating bone formation.

Chapter 5: Use of antisense mediated exon skipping to modulate EAAT1 activity in human osteoblasts

5. Use of antisense mediated exon skipping to modulate EAAT1 activity in human osteoblasts

5.1 Background

5.1.1 Splicing of glutamate transporters

Various mRNA splice variants of EAATs 1-3 have been reported (Lin et al. 1998; Nagai et al. 1998; Matsumoto et al. 1999; Meyer et al. 1999; Huggett et al. 2000; Vallejo-Illarramendi et al. 2005). Furthermore, western blotting for EAATs often identifies a number of immunoreactive fragments smaller than the EAAT monomer suggesting that alternatively spliced EAAT variants exist at the protein level and are therefore potentially of physiological relevance (Lehre et al. 1995; Haugeto et al. 1996; Huggett et al. 2000; Vallejo-Illarramendi et al. 2005; Macnab et al. 2006). Since EAATs are thought to form multimers (Yernool et al. 2004; Koch and Larsson 2005), it is possible that different EAAT variants may combine together to confer different properties to the cell (Mason 2004a).

5.1.1.1 EAAT1

EAATs are thought to consist of cytoplasmic N- and C- termini and eight membrane-spanning alpha-helices with two re-entrant loops at the C-terminus (Slotboom et al. 2001a; Yernool et al. 2004) (Figure 5.1) and the molecular weight of full-length glycosyltaed monomeric GLAST is ~ 70 kDa in rat brain (Conradt et al. 1995). Two splice variants of EAAT1 have been identified; EAAT1a (rodent nomenclature GLAST-1a) (Huggett et al. 2000) and EAAT1ex9skip (also referred to as GLAST-1b) (Vallejo-Illarramendi et al. 2005), both of which are expressed as proteins *in vivo* (Huggett et al. 2000; Vallejo-Illarramendi et al. 2005; Macnab et al. 2006; Macnab and Pow 2007a). Furthermore, detection of mRNA for an EAAT1 splice variant lacking both exons 5 and 6 in hypoxic pig brain has been reported in abstract form (Lee et al. 2008). Exon 5 and 6 comprise TM domain 4 of EAAT1 as well as part of the large, glycosylated extracellular domain between TM3 and 4 (Figure 1.8).

5.1.1.1.1 EAAT1a

5.1.1.1.1.1 Expression

EAAT1a is an alternatively spliced form of EAAT1 which lacks exon 3, and was first cloned from bone *in vivo* (Huggett et al. 2000). EAAT1a is expressed at low levels in brain and bone *in vivo* (Huggett et al. 2000) and retina (Macnab et al. 2006). Exon 3 of EAAT1 (Figure 5.1) consists of 138 bases which encode 47 amino acids (61-107) in TM1 and TM2 and its removal does not disrupt the open reading frame (ORF) of the gene. Exon 3 starts in phase 1 of the codon, between the first and second bases and the new codon formed at the exon 2/4 junction in EAAT1a does not alter the amino acid sequence.

The predicted molecular weight of EAAT1a is ~54 kDa and an immunoreactive protein of 55 kDa has been detected in rat cerebellum using a polyclonal antibody against the N-terminus of GLAST (Huggett et al. 2000) and in rat brain and retina using a GLAST-1a-specific antibody targeted against the peptide sequence across the splice site (Macnab et al. 2006). GLAST-1a was detected largely in the cerebellar Bergmann glia of the rat brain with weaker staining detected in the retinal Müller cells (Macnab et al. 2006).

5.1.1.1.1.2 Structure

Hydropathy analysis of EAAT1a topology indicates a truncation of the first and second TM domains, resulting in the formation of a single TM domain which has been proposed to re-orientate the remainder protein in the membrane (Figure 5.1B) (Huggett et al. 2000). This re-orientation would result in an extracellular rather than intracellular C-terminus and a loss of glycosylation at N206 and N216 (Conradt et al. 1995) between TM3 and 4 since these sites would no longer be presented for glycosylation in the ER (Huggett et al. 2000). A loss of glycosylation is in agreement with a molecular weight for GLAST1a of 55 kDa (Huggett et al. 2000) since glycosylation at both sites would add approximately 10 kDa (Conradt et al. 1995).

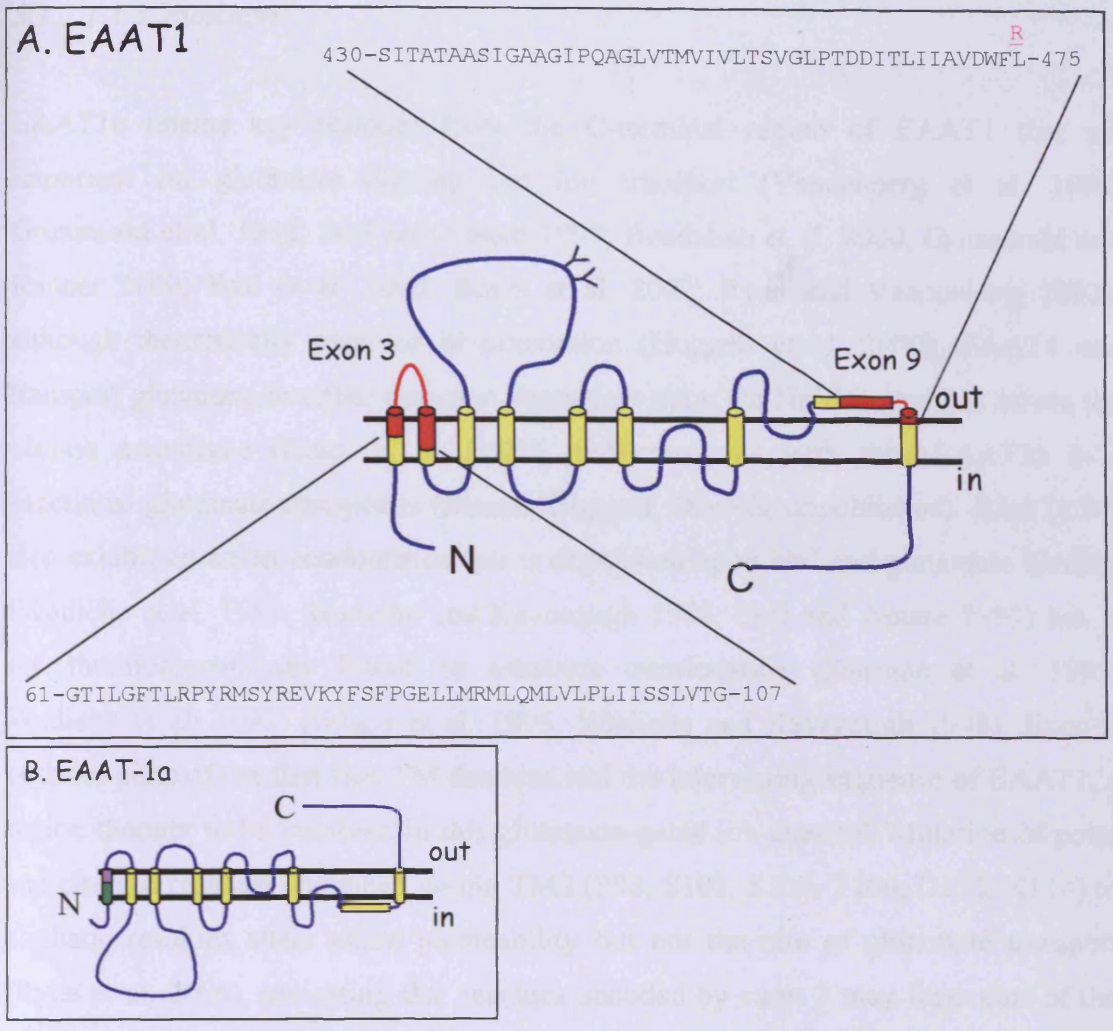

Figure 5.1. Topological model of EAAT1 and EAAT1a. (A) Regions of the EAAT1 protein encoded by exons 3 and 9 are shown in red. Amino acids 61-107 are contained within exon 3 and located in the first two transmembrane domains and the intervening extracellular sequence. Amino acids 446-475 are contained within exon 9 of EAAT1 and thought to be located extracellularly at the C-terminal region of the protein. Loss of exon 3 or exon 9 does not disrupt the open reading frame; the formation of a new codon at the exon2/4 splice boundary codes for Glycine and therefore does not alter the amino acid sequence, however Leucine 475 is converted to an Arginine in EAAT1ex9skip. Splicing of exon 3 leads to the loss of 46 amino acids and splicing of exon 9 leads to the loss of 45 amino acids (Figure adapted from Vallejo-Illarramendi et al. 2005). (B) Hydropathy analysis of EAAT1a indicates a truncation of the first and the second transmembrane domains, resulting in the formation of a single transmembrane domain which re-orientates the remainder of the protein in the membrane (Huggett et al. 2000). No topological model has been proposed for EAAT1ex9skip.

5.1.1.1.1.3 Function

EAAT1a retains key residues from the C-terminal region of EAAT1 that are important for glutamate binding and ion transport (Vandenberg et al. 1995; Grunewald et al. 1998; Seal and Amara 1999; Bendahan et al. 2000; Grunewald and Kanner 2000; Seal et al. 2000; Borre et al. 2002; Ryan and Vandenberg 2002), although theoretically reversed in orientation (Huggett et al. 2000). EAAT1 can transport glutamate in either direction dependent upon the Na^+/K^+ gradient across the plasma membrane (Rossi et al. 2000), and consistent with this, EAAT1a is a functional glutamate transporter (Mason, Huggett, Daniels, unpublished). EAATs 1-5 also exhibit an anion conductance that is dependent upon Na^+ and glutamate binding (Wadiche et al. 1995; Wadiche and Kavanaugh 1998; Seal and Amara 1999) but is not thermodynamically linked to substrate translocation (Fairman et al. 1995; Wadiche et al. 1995; Billups et al. 1996; Wadiche and Kavanaugh 1998). Exon 3 encodes parts of the first two TM domains and the intervening sequence of EAAT1, a region thought to be involved in this glutamate-gated ion channel. Mutation of polar and charged residues contained within TM2 (P98, S102, S103, T106, D112, K114) to aliphatic residues alters anion permeability but not the rate of glutamate transport (Ryan et al. 2004), indicating that residues encoded by exon 3 may form part of the chloride channel (these residues are shown in the EAAT1 sequence in Figure 1.8). Furthermore, many residues of TM2 were shown to be accessible to the external aqueous environment by sulfhydryl modification of cysteine mutants (R90, Q93, V96, L99, S102, S103), consistent with pore-lining residues of an ion channel (Ryan et al. 2004). Loss of these residues in EAAT1a as a result of exon 3 splicing may confer altered ion channel properties to the protein or ion conductance may be lost completely (Mason, Huggett, Daniels, unpublished).

Residues within TM2 have also been suggested to be involved in formation of the transporter trimerisation domain in a crystal structure of a glutamate transporter homologue from *Pyrococcus horikoshii* (Yernool et al. 2004). Eskandari et al (2000) hypothesized that EAAT monomers are capable of glutamate transport but that multimerisation of the transporter is necessary for the formation of a central pore for anion conductance, in a similar manner to multimeric ion channels (Eskandari et al. 2000; Fu et al. 2000; Murata et al. 2000). If this were the case, loss of part of TM2 in EAAT1a may prevent the variant from multimerisation and the consequent formation

of a central ion channel pore, without affecting glutamate transport activity. Furthermore, it is likely that EAAT1a is not glycosylated (Huggett et al. 2000) and there is evidence to suggest that loss of glycosylation prevents dimerisation *in vitro*, with no effect on transport activity (Conradt et al. 1995).

5.1.1.1.1.4 Bioinformatics

The structure of the gene encoding EAAT1 indicates that the potential to splice out an exon that encodes amino acids present within TM2 is retained in three other subtypes (EAAT2, EAAT3 and EAAT4) of the glutamate transporter family, lending weight to the notion that this splicing pattern is functionally significant (Mason, Huggett, Taylor unpublished). It is particularly interesting to note that EAAT5, which acts almost exclusively as an ion channel with very little transport activity (Arriza 1997), is encoded by a gene that does not retain the potential to generate a transport-only splice variant equivalent to EAAT1a (Mason, Huggett, Taylor unpublished).
Comparison of EAAT1 exon 3 to equivalent domains in EAATs 2 (amino acids 57-104), 3 (amino acids 31-78), 4 (amino acids 69-115) and 5 (amino acids 30-76) show identities of 53%, 53%, 79% and 62% respectively (Figure 5.2).

5.1.1.1.1.5 Localisation

In MLO-Y4 osteocyte-like cells and SaOS-2 osteoblasts transfected with GLAST and GLAST-1a tagged with green fluorescent protein (GFP), GLAST was localised to the plasma membrane with some accumulation within intracellular vesicles (Huggett et al. 2002; Mason and Huggett 2002). GLAST-1a was detected in internal vesicles surrounding the nucleus in MLO-Y4 osteocytes (Huggett et al. 2002) and some patchy distribution at the plasma membrane was observed in SaOS-2 osteoblasts (Mason and Huggett 2002). In MLO-Y4 osteocytes, 0.3mM extracellular glutamate redistributed GLAST into an internal expression pattern similar to GLAST-1a whereas 1.3mM extracellular glutamate appeared to increase GLAST cell surface expression (Huggett et al. 2002). In retinal Müller cells GLAST and GLAST-1a were differentially distributed within the cell, with GLAST-1a preferentially targeted to the end feet (Macnab et al. 2006).

EAAT1 exon 3

```
EAAT1 GTILGFTLRPYR-MSYREVKYFSFPGELLMRMLQMLVLPLIISSLVTG (61-107)
EAAT2 GAVCGGLLRLASPIHPDVVMLIAFPGDILMRMLKMLILPLIISSLITG (57-104)
EAAT3 GITTGVLVREHSNLSTLEKFYFAFPGEILMRMLKLIILPLIISSMITG (31-78)
EAAT4 GVSLAFALRPYQ-LTYRQIKYFSFPGELLMRMLQMLVLPLIVSSLVTG (69-115)
EAAT5 GCLLGFFLRTRR-LSPQEISYFQFPGELLMRMLKMMILPLVVSSLMSG (30-76)
```

EAAT1 exon 9

```
EAAT1 SITATAASIGAAGIPQAGLVTMVIVLTSVGLPTDDITLIIAVDWFL (430-475)
EAAT2 SLTATLASVGAASIPSAGLVTMLLILTAVGLPTEDISLLVAVDWLL (429-474)
EAAT3 SITATSASIGAAGVPQAGLVTMVIVLSAVGLPAEDVTLIIAVDWLL (398-443)
EAAT4 SITATAASVGAAGIPQAGLVTMVIVLTSVGLPTEDITLIIAVDWFL (455-500)
EAAT5 SITATAASIGAAGIPQAGLVTMVIVLTSVGLPTDDITLIIAVDWAL (409-454)
```

Figure 5.2. Amino acid alignment of EAAT1 exons 3 and 9 to homologous regions of EAATs 2-5. Amino acid residue numbers are detailed in brackets.

5.1.1.1.2 EAAT1ex9skip

5.1.1.1.2.1 Expression

EAAT1ex9skip, which lacks exon 9, was first cloned from human optic nerve and detected at the transcript level throughout the human brain at levels between 10 and 20% of full-length EAAT1 (Vallejo-Illarramendi et al. 2005). Of the tissues analysed (cerebellum, corpus callosum, hippocampus, cortex and optic nerve), EAAT1ex9skip mRNA was present at highest levels in the hippocampus and at lowest within the cortex (Vallejo-Illarramendi et al. 2005). Exon 9 of EAAT1 comprises 135 bp and its omission does not alter the RNA reading frame. The predicted amino acid sequence of EAAT1ex9skip differs from full length EAAT1 by exclusion of 45 amino acids (430-474) located extracellularly at the C-terminus (Figure 5.1) (Vallejo-Illarramendi et al. 2005). Exon 9 starts between the second and third bases of a codon (phase 2) and the new codon formed at the exon 8/10 junction results in the substitution of leucine 475 for an arginine residue (Vallejo-Illarramendi et al. 2005).

Western blotting using an EAAT1ex9skip specific antibody raised against a synthetic peptide that corresponds to the amino acids encoded by the splice site between exons 8 and 10 detected a band of 150-160 kDa, which may represent an EAAT1ex9skip trimer complex (Vallejo-Illarramendi et al. 2005; Sullivan et al. 2007a). Lower

molecular weight bands were also detected in severely damaged hypoxic pig brains of 50-55 kDa which likely represents monomeric EAAT1ex9skip and ~30 kDa which is a possible cleavage product of EAAT1ex9skip that retains immunoreactivity with EAAT1ex9skip specific antibodies and a C-terminus specific EAAT1 antibody (Sullivan et al. 2007a). Interestingly, an N-terminal specific EAAT1 antibody detected full-length EAAT1 at ~67 kDa in hypoxic pig brain but failed to detect bands at 50-55 kDa or ~30 kDa, suggesting that EAAT1ex9skip and EAAT1a may not contain the normal EAAT1 N-terminus or the specific antibody epitope, or that the antibody was not sensitive enough to detect expression of the variants (Sullivan et al. 2007a).

There is some evidence to suggest that EAAT1ex9skip mRNA or protein is unstable, since transfection of HEK293 cells with an EAAT1ex9skip expressing vector yielded less protein compared to HEK293 cells transfected with the same amount of EAAT1 expressing vector (Vallejo-Illarramendi et al. 2005).

5.1.1.1.2.2 Structure

Exon 9 is located at the C-terminus of EAAT1 (Figure 5.1). The topology of the C-terminal region of the EAATs is not confirmed, however its sequence is highly conserved across transporter subtypes and it contains a number of residues that are important for glutamate binding and transport (Vandenberg et al. 1995; Grunewald et al. 1998; Seal and Amara 1999; Bendahan et al. 2000; Grunewald and Kanner 2000; Seal et al. 2000; Borre et al. 2002; Ryan and Vandenberg 2002), many of which are encoded by exon 9 (Figure 1.8). A proposed transmembrane topology of the EAATs (Figures 1.8 and 5.1) places two re-entrant loops at the C-terminus that forms a pore-like structure (Grunewald and Kanner 2000; Yernool et al. 2004) therefore loss of exon 9 may produce a protein where the topology of second of these re-entrant loops is compromised.

5.1.1.1.2.3 Function

Within exon 9 of EAAT1, specific residues (A446-G459) have been found to be important for glutamate transport but not glutamate binding or anion conductance (Seal et al. 2001; Leighton et al. 2002; Ryan and Vandenberg 2002). Cysteine

scanning and sulphahydryl modification of amino acids 446-459 of EAAT1 (Figure 1.8) showed that access to these residues could be prevented by the presence of substrates or inhibitors (Leighton et al. 2002). Interestingly, despite the hydrophobic nature of this region, many of the residues were accessible to small, charged sulphahydryl reagents that react in an aqueous phase suggesting that this region may exist as a pore or binding pocket (Leighton et al. 2002). This region of EAAT1 has also been shown to be important in determining functional differences between EAAT1 and EAAT2 such as substrate selectivity, chloride permeability and blocker sensitivities (Mitrovic et al. 1998).

EAAT1ex9skip exerts a dominant negative effect over full-length EAAT1 as demonstrated by measuring Na^+-dependent glutamate transport in HEK293 cells transiently transfected with either the full coding sequence of EAAT1 or EAAT1ex9skip or co-transfected with both (Vallejo-Illarramendi et al. 2005). In HEK293 cells expressing only EAAT1ex9skip, no glutamate uptake activity was detected above endogenous levels, and in cells expressing EAAT1, glutamate uptake activity was dose-dependently decreased by increasing amounts of EAAT1ex9skip (Vallejo-Illarramendi et al. 2005). Furthermore, in HEK293 cells expressing both EAAT1ex9skip and EAAT1, less EAAT1 protein was detectable by western blot compared to cells expressing EAAT1 alone, suggesting that the splice variant might interfere with expression of full-length EAAT1 or target the protein for degradation (Vallejo-Illarramendi et al. 2005).

HEK293 cells transiently transfected with the coding sequence of EAAT1ex9skip expressed a protein that was retained primarily within the ER (Vallejo-Illarramendi et al. 2005). The authors speculate that this occurs due to the loss of suppression of a diarginine motif (RXR) in exon 10 which appears to function as an ER retention signal in EAAT2 and is conserved in the sequence of EAAT1 (Kalandadze et al. 2004; Vallejo-Illarramendi et al. 2005). A leucine rich region of EAAT2 that is important for normal post-translational processing and suppression of the ER retention signal (Kalandadze et al. 2004) is partially conserved in EAAT1 exon 9 and would be lost in EAAT1ex9skip leading to retention of the protein in the ER. Protein-protein interactions between EAAT1 and EAAT1ex9skip at the ER may reduce the expression of full-length EAAT1 at the plasma membrane and possibly target the complex for degradation, thus inhibiting glutamate transport activity (Vallejo-Illarramendi et al. 2005).

5.1.1.1.2.4 Bioinformatics

The amino acid sequence encoded by exon 9 of EAAT1 is highly conserved across the EAAT family indicating functional importance for this region. Exon 9 of EAAT1 and EAAT2 share 70% conserved residues (amino acids 430-475 of EAAT1, 429-474 of EAAT2), whereas comparison of EAAT1 exon 9 to equivalent domains in EAATs 3 (amino acids 398-443), 4 (amino acids 455-500) and 5 (amino acids 409-454) show identities of 83%, 96% and 98% respectively (Figure 5.2). These homologous regions of EAATs 2-5 can also be spliced out of the sequence in frame.

5.1.1.1.2.5 Localisation

HEK293 cells transiently transfected with the coding sequence of EAAT1ex9skip expressed a protein that was retained primarily within the ER, but which was also detected at the plasma membrane, whereas EAAT1 was predominantly localised at the plasma membrane (Vallejo-Illarramendi et al. 2005). EAAT1ex9skip, detected in the human brain by immunohistochemistry using EAAT1ex9skip specific antibodies (Macnab and Pow 2007a), was localised intracellularly and at the plasma membrane of cortical and collicular neurons, in contrast to the primarily glial expression of full-length EAAT1 (Macnab and Pow 2007a). The variant was found predominantly in abnormal appearing neuronal populations, suggesting that these cells were subject to abnormal glutamate-mediated excitation (Macnab and Pow 2007a). In the hypoxic pig brain, EAAT1ex9skip was detected in neurons and in regions that are susceptible to damage such as the CA1 region of the hippocampus, supporting the suggestion that expression of EAAT1ex9skip may indicate neurons that are at risk to dying in response to insult (Sullivan et al. 2007a).

5.1.1.2 EAAT2

At least 3 isoforms of GLT-1 exist as proteins and are encoded by transcripts with 3'-untranslated regions (UTRs) of different lengths: GLT-1a, GLT-1b (also called GLT-1v) and GLT-1c (Pines et al. 1992; Utsunomiya-Tate et al. 1997; Chen et al. 2002; Reye et al. 2002; Schmitt et al. 2002; Rauen et al. 2004). These splice variants differ in the sequence of their C-terminus (Figure 6.1) and also in their expression patterns.

GLT-1a and GLT-1b are expressed in glia and neurons (Chen et al. 2002; Schmitt et al. 2002; Maragakis and Rothstein 2004; Sullivan et al. 2004; Berger et al. 2005) whereas GLT-1c is expressed by photoreceptors in human and rat retina (Rauen et al. 2004). Differential targeting of GLT-1 splice variants has also been observed in astrocytes (Sullivan et al. 2004) and in retina (Reye et al. 2002). In astrocytes, expression of GLT-1b is restricted to non-synaptic locations, whereas GLT-1a is localised to astrocytic processes, which can be interposed between multiple synapses, suggesting GLT-1b may play a role in uptake of general pools of extracellular glutamate (Sullivan et al. 2004). In retina, GLT-1b was primarily localised to cone photoreceptors and subpopulations of both rod and cone bipolar cells, whereas GLT-1a was generally associated with amacrine cells, bipolar cells, and rod photoreceptor cells (Reye et al. 2002).

Alternative splicing of the 5'-UTR has been detected at the transcript level in human, mouse and rat brain tissue with the potential to generate GLT-1 with different N-termini (Utsunomiya-Tate et al. 1997; Munch et al. 2001; Munch et al. 2002; Munch et al. 2003; Rozyczka and Engele 2005). Expression of some of these variants has been shown to be increased under hypoxic conditions as well as in a transgenic model for ALS (Munch et al. 2002; Munch et al. 2003).

Other splice variants of EAAT2 have been cloned from human tissues including an exon 7 skipping variant (Honig et al. 2000), an exon 8 skipping variant (Nagai et al. 1998), an intron 7 retention variant (Lin et al. 1998), an exon 9 skipping variant (Lin et al. 1998; Meyer et al. 1998) and a variant that lacks both exons 7 and 9 (Scott et al. 2010). The exon 9 skipping variant of GLT-1 is homologous to EAAT1ex9skip, and lacks part of the glutamate translocation site of GLT-1 (Gebhardt et al. 2010). Expression of the GLT-1 exon 9 skipping variant in *Xenopus laevis* oocytes generated a protein that was expressed at the plasma membrane but was non-functional with respect to glutamate uptake (Scott et al. 2010), consistent with the loss of glutamate uptake activity detected in EAAT1ex9skip (Vallejo-Illarramendi et al. 2005).

Intron 7 retention and exon 9 skipping splice variant transcripts of EAAT2 were reported to be selectively present in brains from ALS patients (Lin et al. 1998), however other studies have shown that the variants are also present in normal brains (Meyer et al. 1999; Honig et al. 2000; Flowers et al. 2001). This was confirmed by exon-9 skipping EAAT2 protein expression in the normal adult rat brain and spinal cord (Macnab and Pow 2007b).

5.1.1.3 EAAT3

A truncated form of EAAT3 (EAAC1) termed tEAAC1 has been identified at the transcript level in the human renal carcinoma cell line, ACHN, in which EAAT3 is highly expressed (Matsumoto et al. 1999). The translated splice variant would lack amino acids G31-T77 (Matsumoto et al. 1999) which are encoded by EAAT3 exon 2; this region is homologous to exon 3 of EAAT1, therefore represents an equivalent splice variant to EAAT1a. The splice variant was detected in various human tumour cells including renal, bladder, cervical, breast and lymphoma but was not detectable in bladder carcinoma, hepatoma or glioma cells of rat origin or mammary carcinoma, hepatoma, melanoma or myeloma of mouse origin (Matsumoto et al. 1999).

5.1.2 Role of EAAT splice variants

Alternative splicing appears to be a common feature of at least 3 subtypes of the EAAT family, and protein expression for some of these splice variants has been detected (Huggett et al. 2000; Reye et al. 2002; Rauen et al. 2004; Sullivan et al. 2004; Vallejo-Illarramendi et al. 2005) suggesting physiological relevance. The two identified splice variants of EAAT1 both lack regions that have been demonstrated to contain key residues for EAAT functions (ion channel activity and glutamate transport activity) supporting the hypothesis that the variants will display different functional properties to full-length EAAT1. Furthermore, EAATs 2-4 retain the ability to splice out equivalent domains to exon 3 of EAAT1, and this has been confirmed in EAAT3 (Matsumoto et al. 1999), indicating a functional significance for the EAAT1a variant (Huggett, Taylor and Mason, unpublished data). It seems possible therefore, that splice variant expression may be a means of selectively regulating EAAT function.

5.1.3 Antisense mediated exon skipping

Antisense oligoribonucleotides (AONs) are able to interfere with RNA processing to modulate gene expression. AONs can knock down gene expression by mediating RNase H cleavage of RNA-AON duplexes (Hausen and Stein 1970; Zamecnik and Stephenson 1978) or manipulate pre-mRNA splicing by sterically hindering normal

splice signals (Kole and Sazani 2001). With respect to the latter, AONs are able to induce the skipping of specific exons to over-express a specific splice variant, or bypass frame-shift mutations and restore protein synthesis (Sierakowska et al. 1996).

5.1.4 Aims

The objectives of the experiments described in this chapter were to manipulate the splicing ratios of EAAT1 in order to ascertain the importance of the domains encoded by the spliced out exons in EAAT1a and EAAT1ex9skip. Exon 3 of EAAT1 contains a number of residues important for anion conductance, suggesting that EAAT1a may have altered or no ion channel activity. Furthermore, the potential reorientation of the transporter in the membrane will prevent any intracellular interactions downstream of the N-terminal. Exon 9 of EAAT1 encodes a portion of the transporter important for glutamate transport and expression of EAAT1ex9skip in HEK293 cells indicates that this variant exerts a dominant negative effect over full-length EAAT1 (Vallejo-Illarramendi et al. 2005). Over-expression of EAAT1a and EAAT1ex9skip will delineate the importance of each EAAT function (i.e. glutamate transport, anion conductance, intracellular interactions) in osteoblast differentiation and activity.

5.2 Methods

Design, sequence, modifications and relative binding sites of AONs (scrambled, ex3skip, ex9skip) are detailed in section 2.10 and Figure 2.5. General methods for transfection and analysis of transfection efficiency are detailed in section 2.10.2 and 2.10.3.

5.2.1 Cell culture and transfection

MG-63 osteoblasts were seeded at 2.5 x 10^4 cells/cm^2 in 48-well and 24-well plates. SaOS-2 cells were seeded at 4.4 x 10^4 cells/cm^2 in 48-well and 24-well plates. Primary human osteoblasts (NHOB2P11) were seeded at 5 x 10^2 cells/cm^2 in 24-well plates. At 80% confluence, the cells were transfected with scrambled, ex3skip or

ex9skip AONs as outlined in section 2.10.2, or left untransfected. No refreshment of culture medium was carried out post-transfection. Transfection efficiency was determined at 24hrs post-transfection (section 2.10.3).

5.2.2 Efficiency of antisense mediated EAAT1 exon 9 skipping over time

For experiments assessing the efficiency of exon 9 skipping over time, transfections were carried out glutamate-free and glutamate was not added at any subsequent time-points.

RNA was extracted and reverse transcribed from transfected cells (MG-63, SaOS-2 and human primary osteoblasts NHOB2P11) (section 2.3) and amplified using primer pairs against regions of EAAT1 spanning exon 3 or 9 (Table 2.1, Figure 2.2), as appropriate. Each primer pair yielded two products, the higher molecular weight full-length EAAT1 and the lower molecular weight splice variant.

5.2.2.1 RT-PCR

Cells were transfected in 48-well plates and RNA extractions, reverse transcription and RT-PCR were carried out as above (section 5.2.2) at 6hrs, 24hrs, 48hrs (MG-63 and SaOS-2), and 72hrs (SaOS-2 cells only) post-transfection. RT-PCR was carried out using an optimised 30 cycles of amplification (section 2.4.2) to ensure that comparison of band densities by agarose gel electrophoresis (section 2.4.3) occurred during the linear increase in PCR product and thus the ratio of EAAT1ex9skip:EAAT1 could be estimated.

5.2.2.2 QRT-PCR

MG-63, SaOS-2 and human primary osteoblasts were transfected in 24-well plates and RNA extractions were carried out as detailed in section 2.3. All cells were assayed at 24 and 48hrs post-transfection, however only MG-63 and SaOS-2 cells were also assayed at 72hrs post-transfection. 200ng (MG-63) and 400ng (SaOS-2) total RNA was reverse transcribed (section 2.3.5) in a 20µl reaction which was then diluted to 100µl with RNase/DNase free molecular biology grade water and 5µl taken for QRT-PCR amplification. As much total RNA as possible was reverse transcribed

from primary osteoblasts i.e. 8.5µl of 20µl total RNA. QRT-PCR was carried out (section 2.4.4) using primers against EAAT1 and EAAT1ex9skip in conjunction with the housekeeping gene 18S rRNA (Table 2.1). Absolute QRT-PCR was carried out with the Stratagene MX3000P™ Real-Time PCR system (section 2.4.4.1.1) in conjunction with plasmid standard curves generated from cloned template sequences (section 2.4.4.2.1). Transcript copy numbers were normalised to 18S rRNA and expressed relative to scrambled control cells.

5.2.3 Effect of antisense mediated EAAT1 exon skipping on glutamate uptake

Cells were transfected in 24-well plates. At 48hrs post-transfection, glutamate uptake activity was assayed in the presence and absence of Na^+ to determine Na^+-dependent uptake (section 2.8). Culture medium was aspirated and the cells pre-incubated with KRH buffer (+ Na^+) for 1hr and then the buffer aspirated and replaced with KRH buffer (± Na^+) containing a mix of radiolabelled and unlabelled glutamate at 10µM (Table 2.4) for 10 min. Uptake activity was normalised to total protein content determined by BCA assay from parallel cultures (sections 2.5.2 and 2.8.2).

5.2.4 Effect of antisense mediated EAAT1 exon skipping on gene expression

5.2.4.1 Human osteoblast-like cells

MG-63 and SaOS-2 cells were transfected in 24-well plates. At 24hrs post-transfection, the medium of replicate cultures was supplemented with 500µM glutamate. After a further 24hrs (i.e. 48hrs post-transfection) the medium was aspirated, cells rinsed with cold PBS and homogenised with 0.2ml TRIzol® reagent per well for 5 min. The plates were stored at -80°C for RNA extraction (section 2.3). 500ng total RNA was reverse transcribed in a 20µl reaction, diluted to 100µl with RNase/DNase-free water and 1µl taken for QRT-PCR (section 2.4.4) using primers against osteocalcin, osteonectin, osteoprotegerin (OPG), alkaline phosphatase (ALP), 18S rRNA, GAPDH and HPRT1 (Table 2.1). Gene expression for MG-63 and SaOS-2 cells was normalised to GAPDH and HPRT1 respectively, the most stable

housekeeping genes of the three as determined using geNorm software for each experiment (Vandesompele et al. 2002). Relative QRT-PCR was carried out (section 2.4.4.5) using the Applied Biosystems 7900HT Fast Real-Time PCR system (section 2.4.4.1.2) in conjunction with cDNA standard curves (section 2.4.4.2.2). All values are expressed relative to scrambled control cells at 0μM glutamate.

5.2.4.2 Human primary osteoblasts

Cells were transfected in 24-well plates at 0 and 500μM glutamate, with the addition of glutamate occurring at the point of transfection. Experimental set-up, RNA extraction and generation of cDNA are detailed in section 5.2.2.1.2. Absolute QRT-PCR was carried out using primers against osteocalcin, osteonectin and 18S rRNA (Table 2.1) on the Stratagene MX3000P™ Real-Time PCR system (section 2.4.4.1.1) in conjunction with plasmid standard curves (section 2.4.4.2.1). Transcript copy numbers were normalised to 18S rRNA, and expressed relative to scrambled control cells at 0μM glutamate.

5.2.5 Effect of antisense mediated EAAT1 exon skipping on cell number, cell death and ALP activity

5.2.5.1 Human osteoblast-like cells

MG-63 and SaOS-2 cells were transfected in 24-well plates. At 24hrs post-transfection, the medium of replicate cultures was supplemented with 500μM glutamate. After a further 24hrs (i.e. 48hrs post-transfection) the medium was aspirated and the cells lysed with 100μl/well lysis buffer (section 2.5.1). Plates were then incubated on ice for 1hr to ensure adequate cell lysis and 5μl lysate was taken for assays of adherent cell number (LDH Cytotox96 assay) and ALP activity (SaOS-2 cells only) (sections 2.5.3 and 2.5.4).

5.2.5.2 Human primary osteoblasts

Primary osteoblasts (NHOB2P11) were transfected in 24-well plates at 0 and 500μM glutamate, with the addition of glutamate occurring at the point of transfection. At 48hrs post-transfection, the medium was retained for analysis of cell death and the cells lysed with 100μl/well lysis buffer (section 2.5.1). Plates were then incubated on ice for 1hr to ensure adequate cell lysis and 5μl lysate or 50μl culture supernatant was taken for LDH assay of cell number and cell death respectively (LDH Cytotox96 assay, section 2.5.3).

5.2.6 Statistics

Cells transfected with AONs targeted against EAAT1 splice sites were compared to cells transfected with scrambled control oligoribonucleotides. Statistical comparison between untransfected and scrambled control cells was also carried out to display any non-specific effects of oligoribonucleotide transfection.

5.3 Results

5.3.1 AON transfection efficiency

MG-63 cells were transfected with scrambled control, ex3skip or ex9skip FAM-labelled AONs or left untransfected. In untransfected cells, no FAM fluorescence was observed (Figure 5.3A). In cells transfected with FAM-labelled AONs, most nuclei were surrounded by punctuate FAM fluorescence (Figure 5.3 B-D), confirming transfection of the AON into the cell. Transfection efficiency (Figure 5.3E) was 96% for scrambled AON, 94% for ex3skip AON and 94% for ex9skip AON.

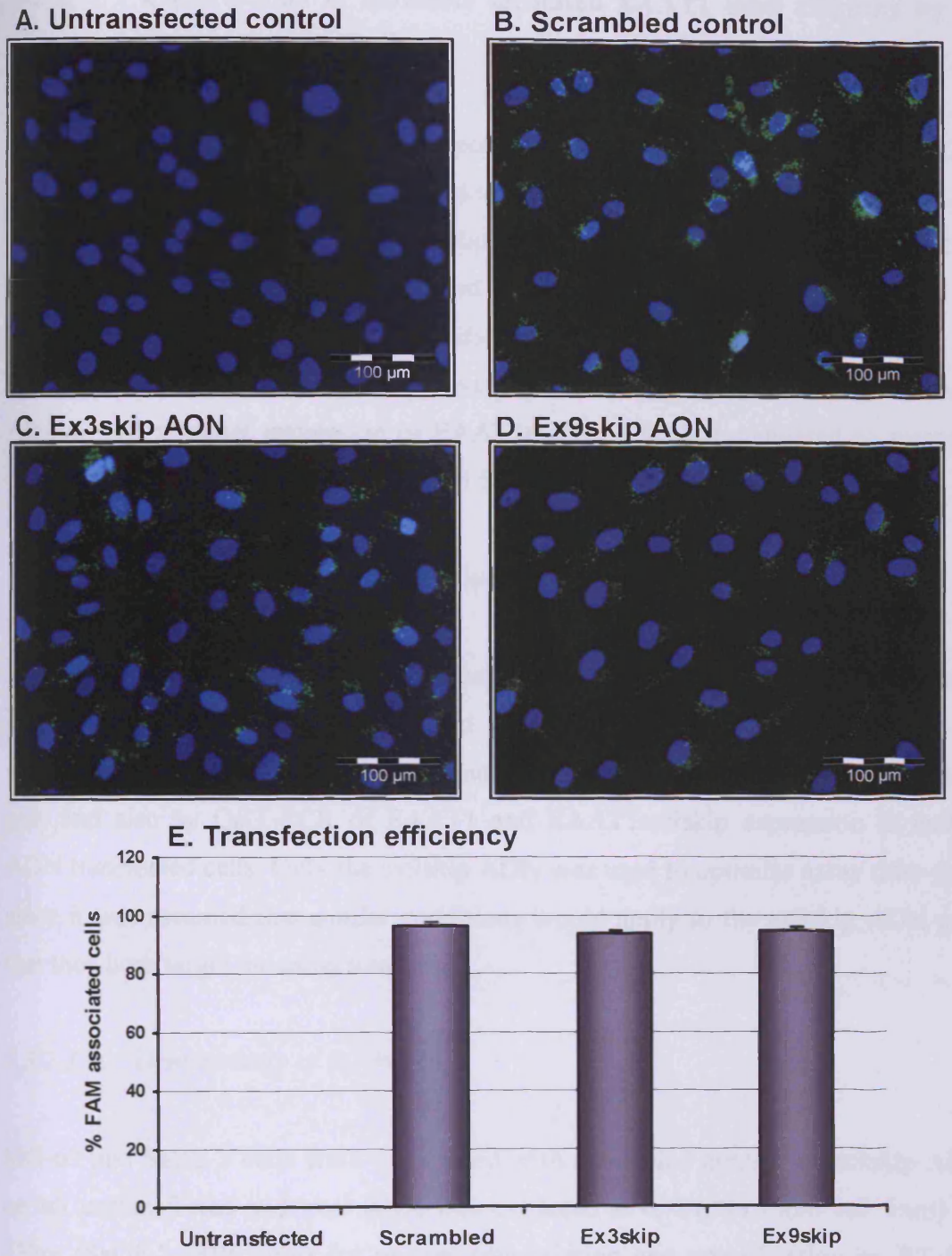

Figure 5.3. Transfection efficiency of antisense oligoribonucleotides (AONs). MG63 cells were left untransfected (A) or transfected for 24hrs with FAM labelled scrambled (B), ex3skip (C) and ex9skip (D) AONs. Nuclei were stained with DAPI and the number of FAM associated nuclei counted from four fields of view per sample using a fluorescent microscope (20X magnification) and expressed as a percentage of total nuclei (E). No significant FAM fluorescence was observed in untransfected cells. Values are mean ± S.E.M, n=3.

5.3.2 Confirmation of antisense mediated EAAT1 exon skipping by RT-PCR

Skipping of the appropriate exon was confirmed in MG-63, SaOS-2 and NHOB2P11 cells transfected with ex3skip and ex9skip AONs by RT-PCR using primers that span the skipped exon. EAAT1a levels (140bp) were increased and EAAT1 levels (218bp) decreased in ex3skip AON transfected cells compared to scrambled control and untransfected cells, in which no bands were detected for EAAT1a (Figure 5.4). Ex9skip AON transfected cells displayed a weaker band corresponding to EAAT1 (256bp) and stronger expression of EAAT1ex9skip (121bp) compared to scrambled control and untransfected cells (Figure 5.5).

5.3.2.1 Efficiency of antisense mediated EAAT1 exon 9 skipping over time

In order to define the optimum time post-transfection that assays for EAAT activity and bone formation should be carried out; the efficiency of exon skipping was observed over time by densitometric analysis of PCR products resolved on agarose gels and also by QRT-PCR of EAAT1 and EAAT1ex9skip expression in ex9skip AON transfected cells. Only the ex9skip AON was used to optimise assay time-points since it was assumed that similar conditions would apply to the ex3skip AON given that they both target the same transcript.

5.3.2.1.1 Densitometry of RT-PCR

MG-63 and SaOS-2 cells were transfected with scrambled control or ex9skip AONs or left untransfected and total RNA was extracted at 6, 24, 48 (both cell lines) and 72hrs (SaOS-2 cells only) for reverse transcription and amplification by RT-PCR using primers that span exons 8-10. Due to infection of the culture plate, no 72hr time-point was available for analysis with MG-63 cells. Products were resolved by agarose gel electrophoresis and density of DNA bands for full-length EAAT1 and EAAT1ex9skip measured. The ratio of EAAT1ex9skip:EAAT1 was determined for each experimental condition and expressed as a percentage of EAAT1ex9skip:EAAT1 ratio in scrambled control cells (Figure 5.6). No statistical analysis was carried out and the data were used merely to guide assay timings.

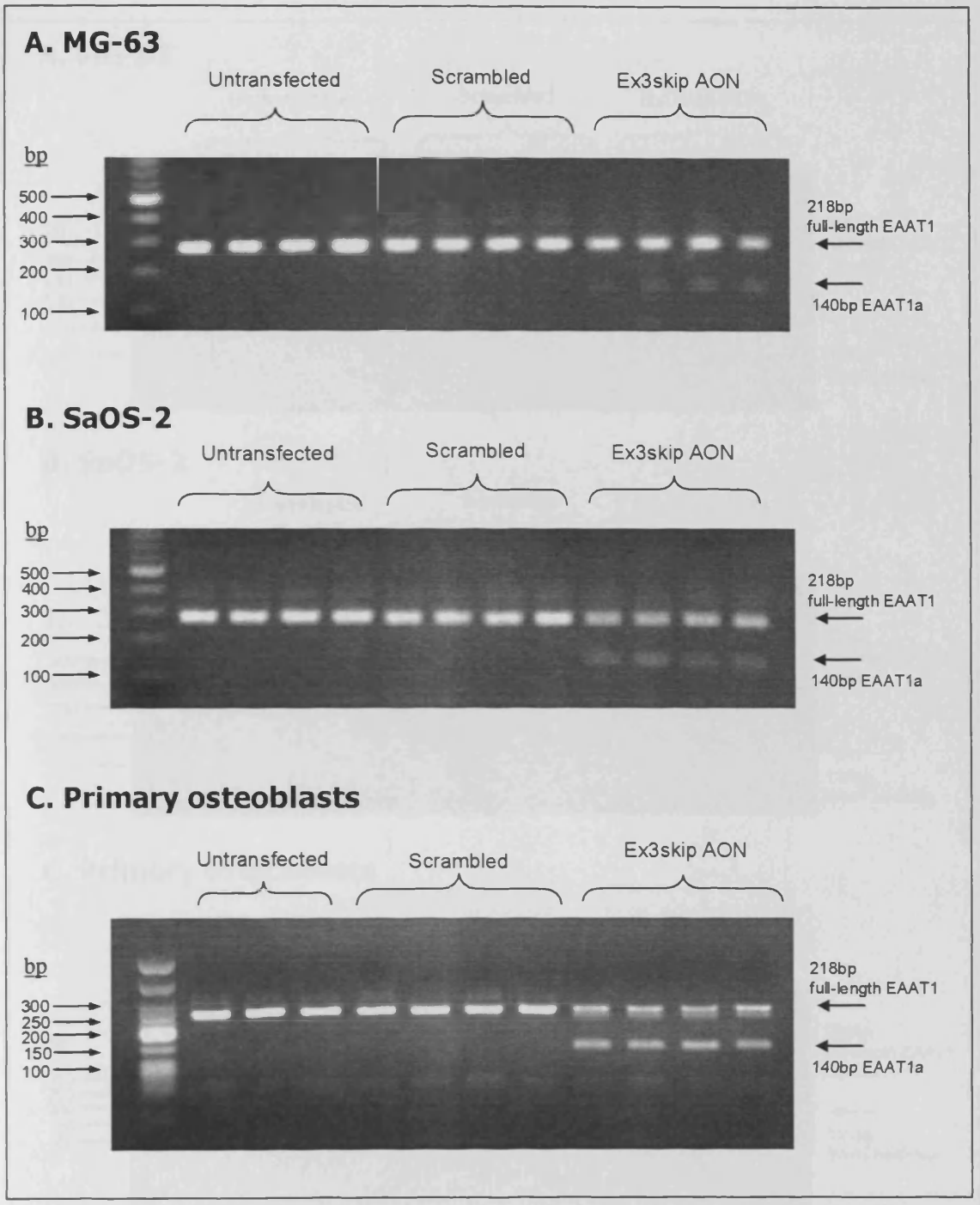

Figure 5.4. Efficiency of antisense mediated EAAT1 exon 3 skipping in human osteoblast-like cells and primary human osteoblasts. Osteoblast-like cells ((A) MG-63 and (B) SaOS-2) and (C) primary human osteoblasts (NHOB2P11) were transfected with scrambled AON, ex3skip AON or left untransfected for 48hrs and changes in splicing ratios of EAAT1 were determined by RT-PCR using primers that span exons 2-4.

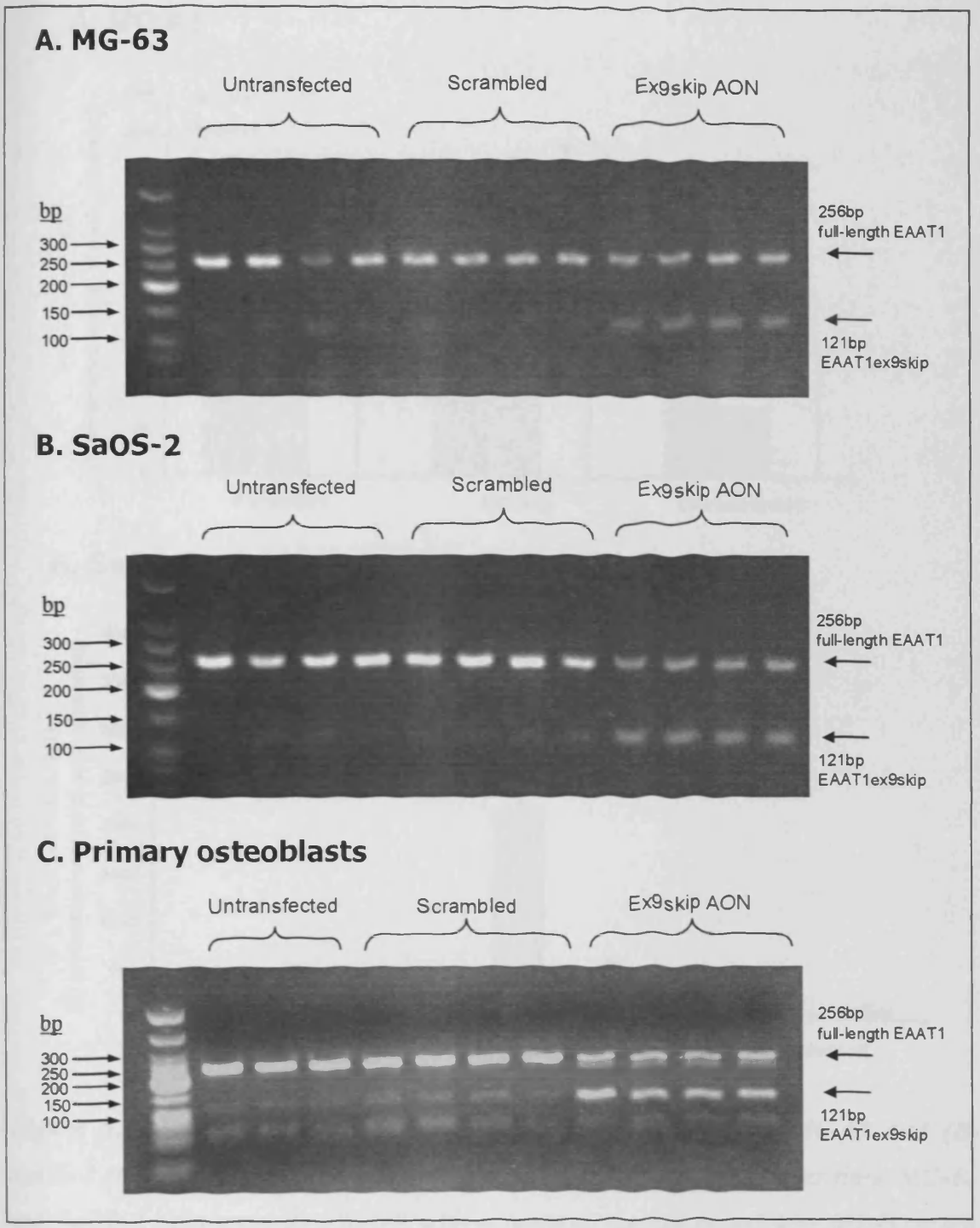

Figure 5.5. Efficiency of antisense mediated EAAT1 exon 9 skipping in human osteoblast-like cells and primary human osteoblasts. Osteoblast-like cells ((A) MG-63 and (B) SaOS-2) and (C) primary human osteoblasts (NHOB2P11) were transfected with scrambled AON, ex9skip AON or left untransfected for 48hrs and changes in splicing ratios of EAAT1 were determined by RT-PCR using primers that span exons 8-10.

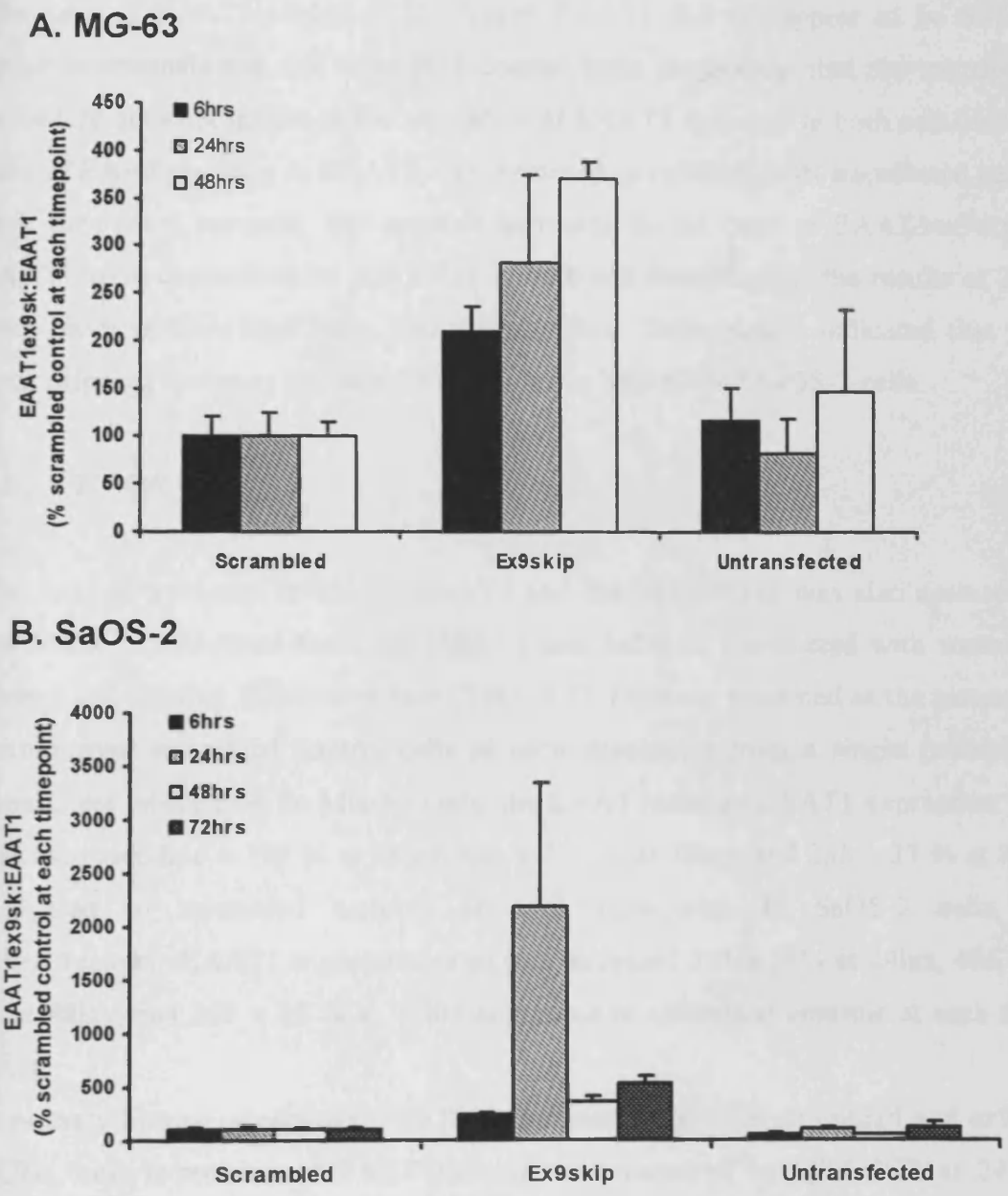

Figure 5.6. Expression ratio of EAAT1ex9skip:EAAT1 in (A) MG-63 and (B) SaOS-2 cells transfected with scrambled control or ex9skip AONs over time. MG-63 and SaOS-2 cells were transfected with scrambled control or ex9skip AONs or left untransfected and total RNA extracted at 6, 24, 48 (both cell lines) and 72hrs (SaOS-2 cells only) for reverse transcription and amplification by RT-PCR using primers that span exons 8-10. Products were resolved on an agarose gel, visualised under UV light and densitometry of DNA bands was carried out. The ratio of EAAT1ex9skip:EAAT1 is expressed as a percentage of EAAT1ex9skip:EAAT1 ratio in scrambled control cells at each time-point.

The ratio of EAAT1ex9skip to full-length EAAT1 did not appear to be different between untransfected and scrambled control cells, suggesting that the transfection procedure does not influence the regulation of EAAT1 splicing. In both cell lines, the ratio of EAAT1ex9skip to EAAT1 was increased in ex9skip AON transfected cells at each time-point assessed. The greatest increases in the ratio of EAAT1ex9skip to EAAT1 were detected at 24 and 48hrs in both cell lines, though the results at 24hrs were more variable than those detected at 48hrs. These results indicated that peak exon skipping occurs at between 24 and 48hrs in MG-63 and SaOS-2 cells.

5.3.2.1.2 QRT-PCR

The ratio of transcript levels for EAAT1 and EAAT1ex9skip was also assessed by QRT-PCR in osteoblast-like cells (MG-63 and SaOS-2) transfected with scrambled control and ex9skip AONs over time (Table 5.1). Data are presented as the percentage change over scrambled control cells at each time-point from a single preliminary experiment where n=4. In MG-63 cells, the EAAT1ex9skip:EAAT1 expression ratio was increased 856 ± 186 % at 24hrs, 646 ± 114 % at 48hrs, and 255 ± 37 % at 72hrs compared to scrambled controls at each time-point. In SaOS-2 cells, the EAAT1ex9skip:EAAT1 expression ratio was increased 381 ± 28% at 24hrs, 466 ± 58 % at 48hrs, and 208 ± 32 % at 72hrs compared to scrambled controls at each time-point.

In primary human osteoblasts (NHOB2P11) transfected with scrambled and ex9skip AONs, only expression of EAAT1ex9skip was measured by QRT-PCR at 24 and 48hrs post-transfection (Figure 5.7). In these cells, EAAT1ex9skip expression was significantly increased 1399 ± 577 % at 24hrs (Kruskal-Wallis P=0.021) and 1647 ± 391 % at 48hrs (Kruskal-Wallis P=0.021) compared to scrambled oligoribonucleotide transfected cells at each time-point.

The results of the above experiments led to the decision to assess the effect of extracellular glutamate on cells overexpressing EAAT1a and EAAT1ex9skip by adding glutamate 24hrs post-transfection, when exon skipping is high, and to assay cells at 48hrs post-transfection, when exon skipping remains high.

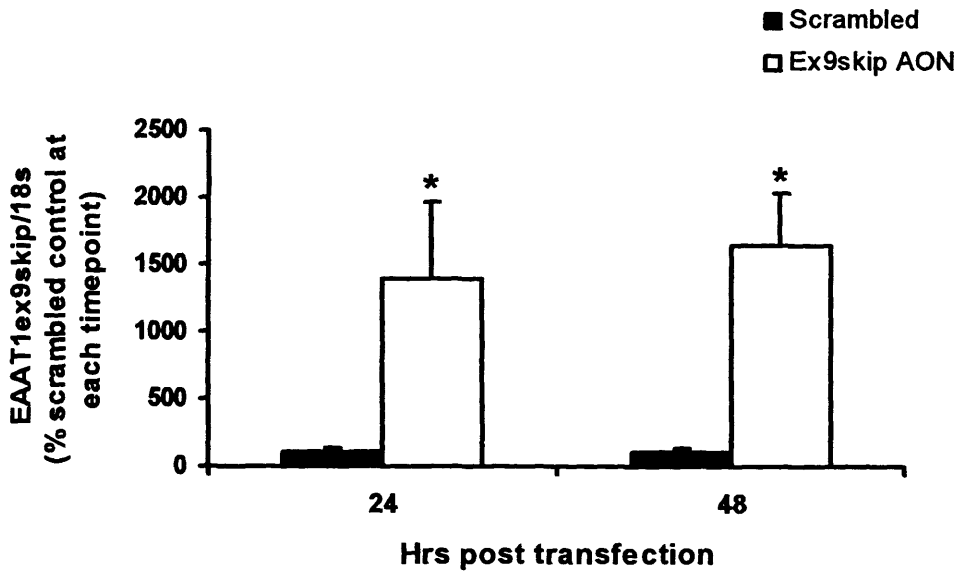

Figure 5.7. Efficiency of antisense mediated EAAT1 exon 9 skipping in primary human osteoblasts over time by QRT-PCR analysis. Osteoblasts were transfected with scrambled or ex9skip AONs and changes in expression of EAAT1ex9skip were determined by QRT-PCR at 24 and 48hrs post-transfection. Expression levels are normalised to 18S rRNA expression and shown as the percentage change over scrambled control cells at each time-point. Values are mean ± S.E.M from a single preliminary experiment where n=4. Expression of EAAT1ex9skip was significantly increased in ex9skip AON transfected cells at both time-points (Kruskal-Wallis P=0.021 (24hrs), P=0.021 (48hrs)). Significance values *P<0.05 relative to scrambled control.

Table 5.1. Efficiency of antisense mediated EAAT1 exon 9 skipping in osteoblast-like cells over time. MG-63 and SaOS-2 cells were transfected with scrambled or ex9skip AONs and changes in expression of EAAT1 and EAAT1ex9skip were determined by QRT-PCR at 24, 48 and 72hrs post-transfection. The ratio of expression levels normalised to 18S rRNA expression are shown as the percentage change over scrambled control cells at each time-point. Values are mean ± S.E.M from a single preliminary experiment where n=4.

	Hrs post-transfection	EAAT1ex9skip:EAAT1 mRNA levels in ex9skip AON transfected cells (% scrambled at each time-point)
MG-63	24	856 ± 186
	48	646 ± 114
	72	255 ± 37
SaOS-2	24	381 ± 28
	48	466 ± 58
	72	208 ± 32

5.3.3 Effect of antisense mediated EAAT1 exon skipping on Na^+-dependent glutamate uptake

Na^+-dependent glutamate uptake was measured in untransfected MG-63 and SaOS-2 osteoblast-like cells and in the same cells 48hrs post-transfection with scrambled control or antisense oligoribonucleotides. Na^+-dependent glutamate uptake was normalised to total cellular protein (mg) and expressed as a percentage of scrambled control cells. Presented data are from three independent experiments where n=3-4.

5.3.3.1 MG-63

In transfected MG-63 cells, Na^+-dependent glutamate uptake was significantly affected by overexpression of EAAT1 splice variants (Kruskal-Wallis P=0.007) (Figure 5.8). Post-hoc pair-wise comparisons (Mann Whitney U tests) revealed that Na^+-dependent glutamate uptake was significantly decreased by 23 ± 6.3 % in MG-63 cells transfected with ex3skip AON (P=0.002) and by 17 ± 6.5 % in MG-63 cells transfected with ex9skip AON (P=0.045) compared to scrambled control cells.

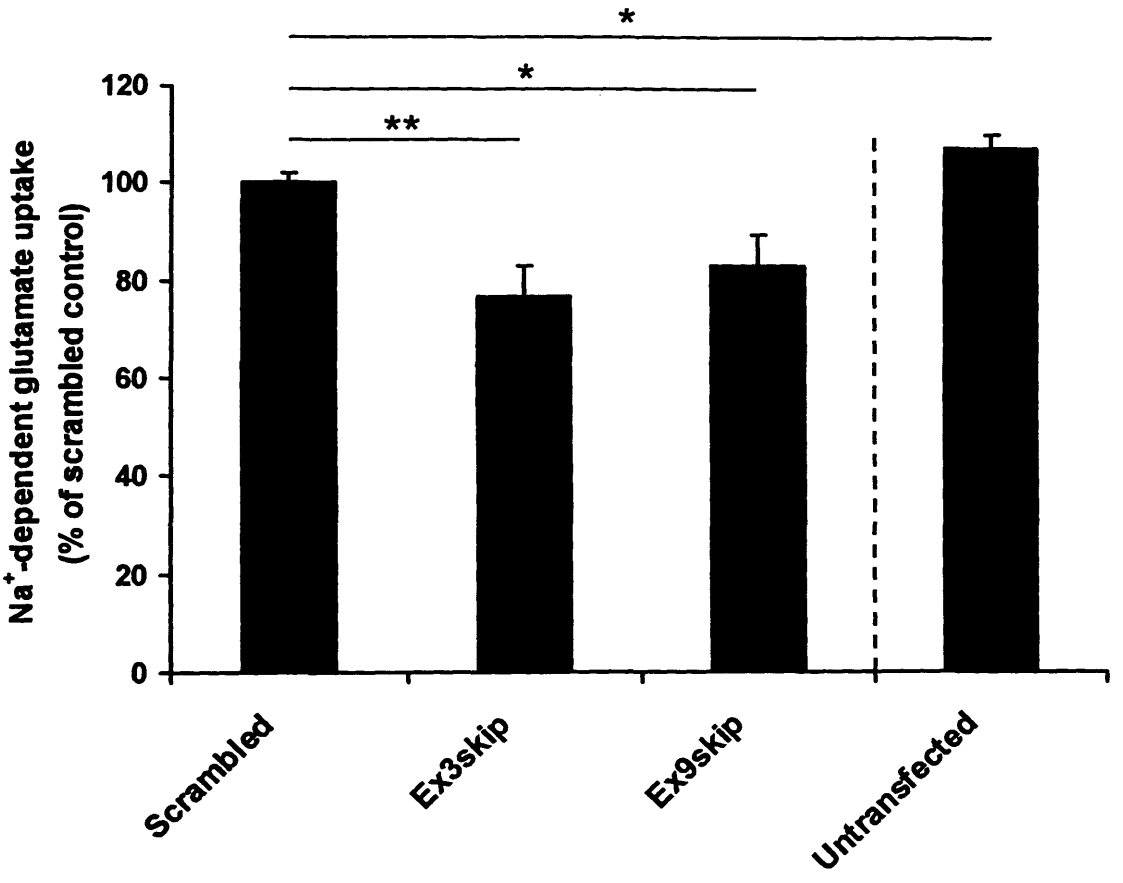

Figure 5.8. Effect of antisense mediated EAAT1 exon 3 and exon 9 skipping on Na^+-dependent glutamate uptake in MG-63 cells. MG-63 cells were transfected with scrambled control, ex3skip or ex9skip AONs for 48hrs, or left untransfected. MG-63 cells were then incubated with 10μM mix of radiolabelled and unlabelled glutamate at 37°C for 10 min in KRH buffer ± Na^+, followed by aspiration of buffer and rinsing with cold KRH containing 1.5mM unlabelled glutamate. Na^+-dependent glutamate uptake was normalised to total cellular protein (mg) and expressed as a percentage of scrambled control cells. Values are mean ± S.E.M from three independent experiments where n=3-4. Na^+-dependent glutamate uptake was significantly affected by overexpression of EAAT1 splice variants (Kruskal-Wallis P=0.007) and post-hoc pair-wise comparisons (Mann Whitney U tests) revealed that uptake was significantly decreased in cells transfected with ex3skip and ex9skip AONs compared to scrambled control cells. Na^+-dependent glutamate uptake was significantly decreased in scrambled control cells relative to untransfected cells (one-way ANOVA P=0.040). Significance values *P<0.05, **P<0.01.

Na^+-dependent glutamate uptake was significantly decreased in scrambled control cells relative to untransfected cells (one-way ANOVA P=0.040).

5.3.3.2 SaOS-2

In transfected SaOS-2 cells, Na^+-dependent glutamate uptake was significantly affected by overexpression of EAAT1 splice variants (one-way ANOVA P<0.001) (Figure 5.9). Post-hoc pair-wise comparisons (Fisher's tests) revealed that Na^+-dependent glutamate uptake was significantly decreased by 14 ± 2.1 % in SaOS-2 cells transfected with ex3skip AON (P<0.001) and by 32 ± 2.9 % in SaOS-2 cells transfected with ex9skip AON (P<0.001) compared to scrambled control cells.
Na^+-dependent glutamate uptake was significantly increased in scrambled control cells relative to untransfected cells (one-way ANOVA P=0.003).

5.3.4 Effect of antisense mediated EAAT1 exon skipping on cell number

5.3.4.1 Osteoblast-like cells

MG-63 and SaOS-2 cells were transfected with scrambled control or antisense oligoribonucleotides for 48hrs, or left untransfected. 500μM glutamate was added to replicate cultures under each condition at 24hrs post-transfection. Adherent cell number was assayed by measuring LDH released upon total lysis of viable adherent cells and expressed as a percentage of LDH activity of viable adherent control cells (scrambled, 0μM glutamate). Presented data are from two independent experiments where n=4 (MG-63) or three independent experiments where n=3 (SaOS-2).

5.3.4.1.1 MG-63

In transfected MG-63 cells, cell number was significantly affected by overexpression of EAAT1 splice variants (GLM with ranked data P=0.019) but not by 500μM glutamate (GLM with ranked data P=0.535) and there was no interaction between the two factors (GLM with ranked data P=0.144) (Figure 5.10). Post-hoc pair-wise comparisons (Tukey's tests) revealed that, compared to scrambled control cells at 0μM glutamate, cell number was significantly decreased by 5 ± 1.3 % in cells

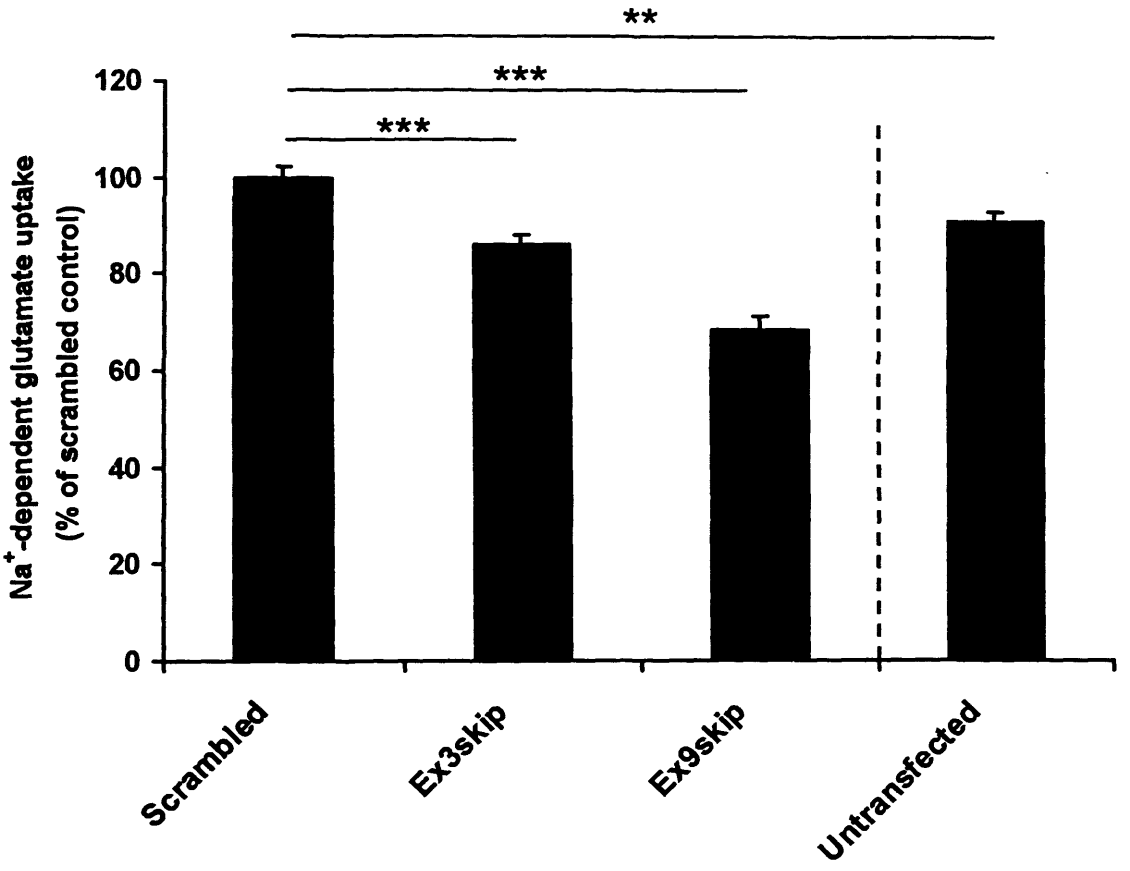

Figure 5.9. Effect of antisense mediated EAAT1 exon 3 and exon 9 skipping on Na^+-dependent glutamate uptake in SaOS-2 cells. SaOS-2 cells were transfected with scrambled control, ex3skip or ex9skip AONs for 48hrs, or left untransfected. SaOS-2 cells were then incubated with 10μM mix of radiolabelled and unlabelled glutamate at 37°C for 10 min in KRH buffer ± Na^+, followed by aspiration of buffer and rinsing with cold KRH containing 1.5mM unlabelled glutamate. Na^+-dependent glutamate uptake was normalised to total cellular protein (mg) and expressed as a percentage of scrambled control cells. Values are mean ± S.E.M from three independent experiments where n=3. Na^+-dependent glutamate uptake was significantly affected by overexpression of EAAT1 splice variants (one-way ANOVA $P<0.001$) and post-hoc pair-wise comparisons (Fisher's tests) revealed that uptake was significantly decreased in cells transfected with ex3skip and ex9skip AONs compared to scrambled control cells. Na^+-dependent glutamate uptake was significantly increased in scrambled control cells relative to untransfected cells (one-way ANOVA $P=0.003$). Significance values $^{**}P<0.01$, $^{***}P<0.001$.

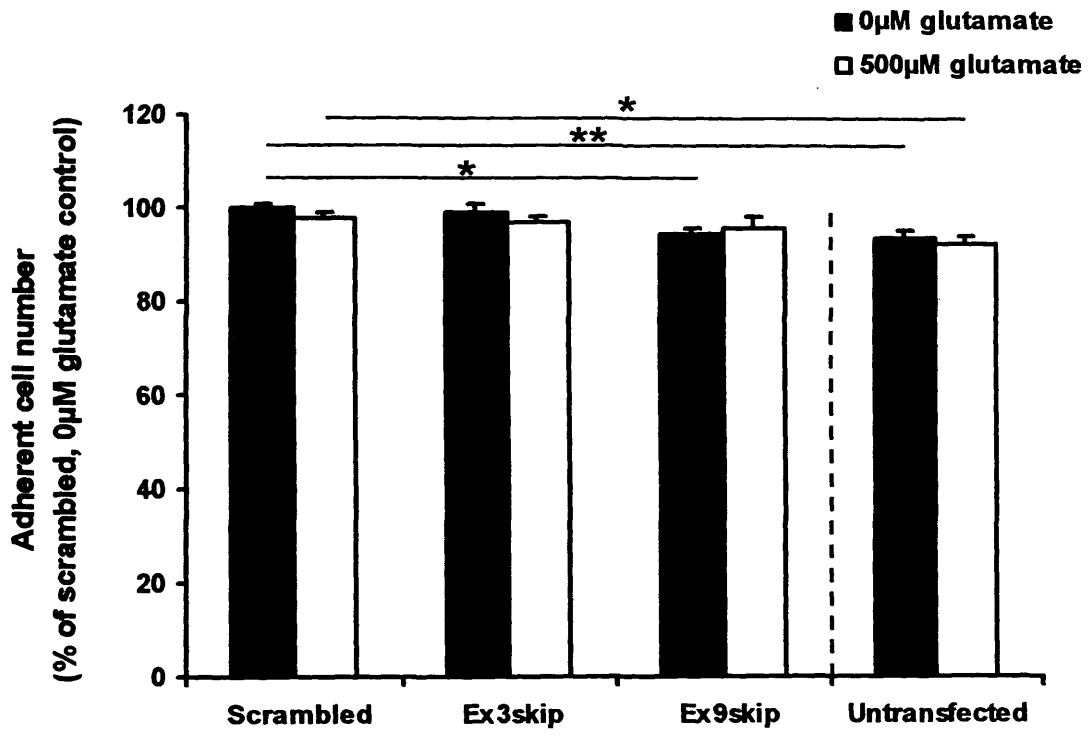

Figure 5.10. Effect of antisense mediated EAAT1 exon 3 and exon 9 skipping on MG-63 cell number at 48hrs post-transfection. MG-63 cells were transfected with scrambled control, ex3skip or ex9skip AONs for 48hrs, or left untransfected (± 500μM glutamate for last 24hrs). Adherent cell number was assayed by measuring LDH released upon total lysis of viable adherent cells and expressed as the mean percentage of LDH activity of viable adherent control cells (scrambled, no glutamate) ± S.E.M from two independent experiments, n=4. Cell number was significantly affected by overexpression of EAAT1 splice variants (GLM P=0.019) and post-hoc Tukey's tests revealed a significant reduction in cell number at 0μM glutamate in cells overexpressing EAAT1ex9skip. Cell number was significantly increased by transfection with scrambled control oligoribonucleotides compared to untransfected cells (GLM P<0.001) and this was apparent at both glutamate concentrations. Significance values *P<0.05, **P<0.01.

transfected with ex9skip AONs (P=0.016), though such a small effect is unlikely to be biologically significant. No effect of ex9skip AONs on cell number was detected at 500μM glutamate (P=0.983).

Transfection with scrambled control oligoribonucleotides significantly increased MG-63 cell number relative to untransfected cells (GLM P<0.001) and post-hoc comparisons (Tukey's tests) revealed that this occurred at both 0μM and 500μM glutamate (P=0.009 and P=0.029 respectively).

5.3.4.1.2 SaOS-2

In transfected SaOS-2 cells, cell number was significantly affected by overexpression of EAAT1 splice variants (GLM P=0.001) but not by 500μM glutamate (GLM P=0.185) and there was no interaction between the two factors (GLM P=0.070) (Figure 5.11). Post-hoc pair-wise comparisons (Tukey's tests) revealed that, compared to scrambled control cells at 500μM glutamate, cell number was significantly increased from 97 ± 1.5 % to 113 ± 2.0 % in cells transfected with ex3skip AONs (P=0.001). This increase in cell number was quite large and therefore potentially biologically significant. No effect of ex3skip AONs on cell number was detected at 0μM glutamate (P=0.879).

Transfection with scrambled control oligoribonucleotides had no significant effect on SaOS-2 cell number relative to untransfected cells (GLM P=0.156).

5.3.4.2 Primary osteoblasts

Cell number and cell death were measured in untransfected primary human osteoblasts (NHOB2P11) and in the same cells 48hrs post-transfection with scrambled control or antisense oligoribonucleotides. 500μM glutamate was added to replicate cultures under each condition at the point of transfection. Adherent cell number was assayed by measuring LDH released upon total lysis of viable adherent cells and expressed as a percentage of LDH activity in viable adherent control cells (scrambled, no glutamate) (Figure 5.12). Cell death was assayed by measuring LDH released upon lysis of dead and dying cells in the culture supernatant and expressed as the percentage of total LDH activity in the cell lysate and culture supernatant combined (Figure 5.13). Presented data are from a single preliminary experiment where n=4.

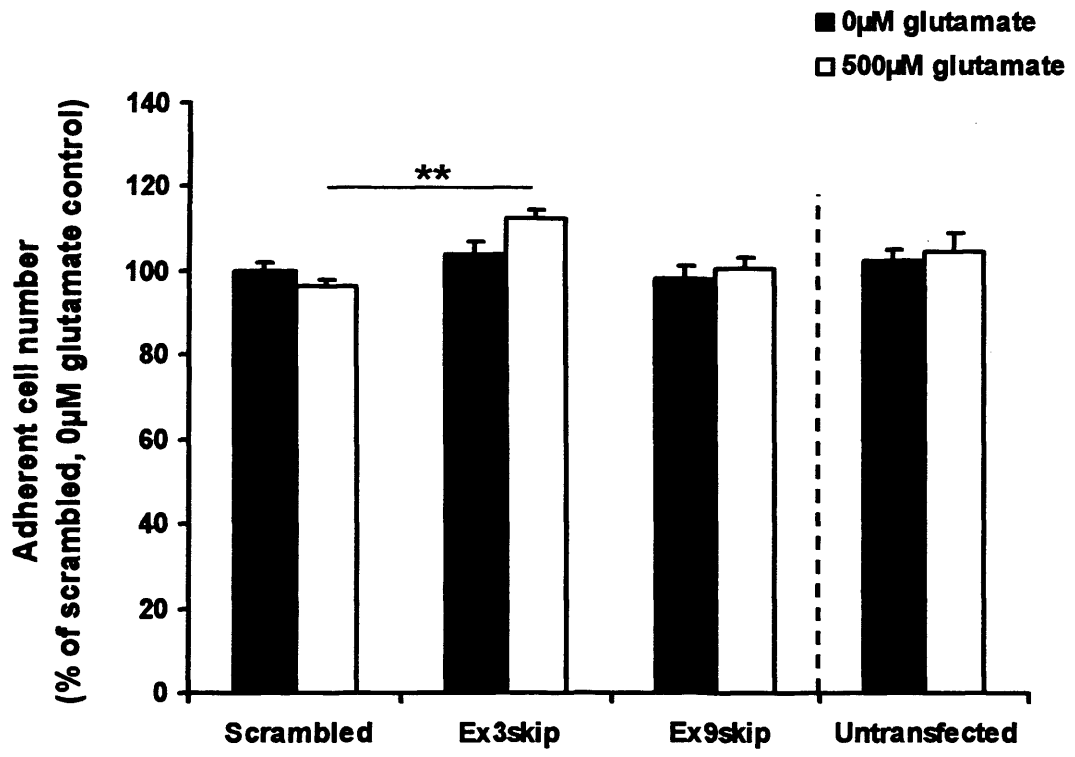

Figure 5.11. Effect of antisense mediated EAAT1 exon 3 and exon 9 skipping on SaOS-2 cell number at 48hrs post-transfection. SaOS-2 cells were transfected with scrambled control, ex3skip or ex9skip AONs for 48hrs, or left untransfected (± 500μM glutamate for last 24hrs). Adherent cell number was assayed by measuring LDH released upon total lysis of viable adherent cells and expressed as the mean percentage of LDH activity of viable adherent control cells (scrambled, no glutamate) ± S.E.M from three independent experiments, n=3. Cell number was significantly affected by overexpression of EAAT1 splice variants (GLM P=0.001) and post-hoc Tukey's tests revealed that cell number was significantly increased in cells overexpressing EAAT1a compared to scrambled control cells at 500μM glutamate. SaOS-2 cell number was not significantly different in scrambled control cells compared to untransfected cells (GLM). Significance values **P<0.01.

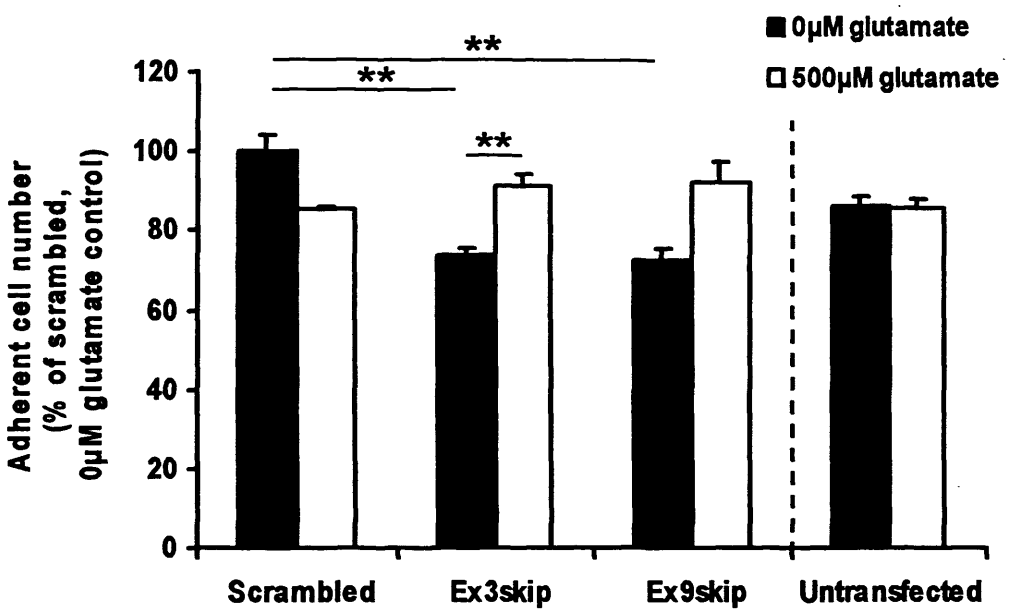

Figure 5.12. Effect of antisense mediated EAAT1 exon 3 and exon 9 skipping on primary osteoblast cell number at 48hrs post-transfection. Primary osteoblasts (NHOB2P11) were transfected with scrambled control, ex3skip or ex9skip AONs, or left untransfected ± 500μM glutamate for 48hrs. LDH released upon total lysis of viable adherent cells is expressed as a percentage of LDH activity of control cells (scrambled, no glutamate). Values are mean ± S.E.M from a single preliminary experiment, n=4. In transfected primary osteoblasts, cell number was significantly affected by overexpression of EAAT1 splice variants (P=0.006), by 500μM glutamate (P=0.004) and by the interaction between the two factors (P<0.001) (GLM). Post-hoc Tukey's tests revealed a significant decrease in cell number in cells transfected with ex3skip and ex9skip AONs, and this was significantly prevented by 500μM glutamate in ex3skip transfected cells. Transfection with scrambled control oligoribonucleotides significantly increased primary osteoblast cell number relative to untransfected cells (GLM P=0.018). Post-hoc Tukey's tests did not reveal any pair-wise significance for this effect at 0μM or 500μM glutamate. Significance values **P<0.01.

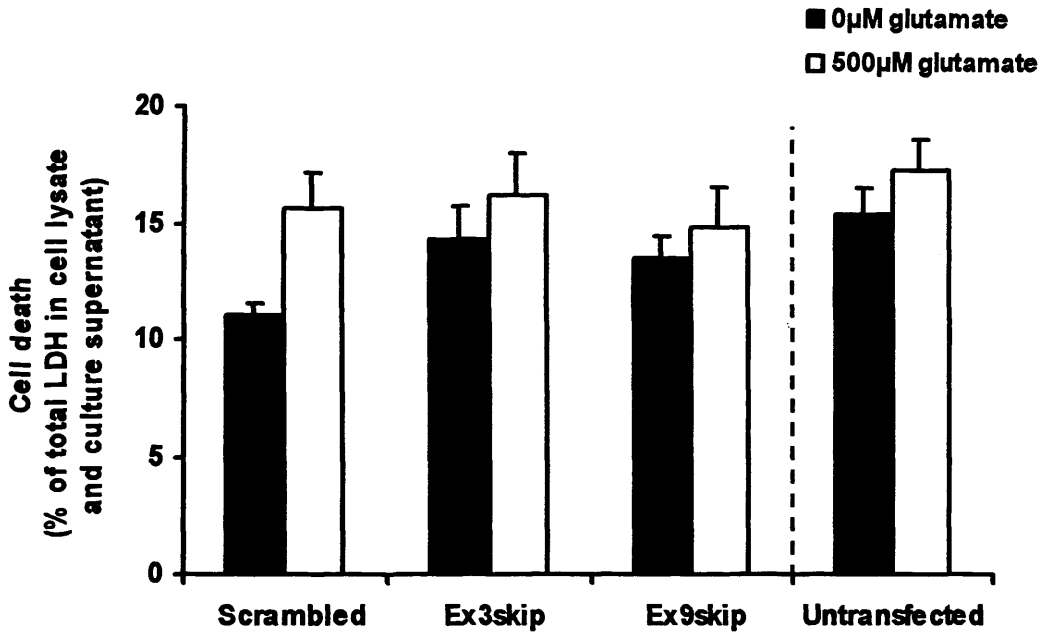

Figure 5.13. Effect of antisense mediated EAAT1 exon 3 and exon 9 skipping on primary osteoblast cell death at 48hrs post-transfection. Primary osteoblasts (NHOB2P11) were transfected with scrambled control, ex3skip or ex9skip AONs, or left untransfected ± 500μM glutamate for 48hrs. Cell death was assayed by measuring LDH released from dead or dying cells in the culture supernatant and expressed as the percentage of total LDH activity (i.e. adherent cell lysate + dead or dying cells in the supernatant). Values are mean ± S.E.M from a single preliminary experiment, n=4. In transfected primary osteoblasts, cell death was significantly increased by 500μM glutamate (GLM P=0.049), however no pair-wise significance was detected (Tukey's test). Transfection with scrambled control oligoribonucleotides significantly decreased primary osteoblast cell death relative to untransfected cells (GLM P=0.030). Post-hoc Tukey's tests did not reveal any pair-wise significance for this effect at 0μM or 500μM glutamate.

Preliminary findings from transfected primary osteoblasts demonstrated that cell number was significantly affected by overexpression of EAAT1 splice variants (GLM with ranked data P=0.006), by 500μM glutamate (GLM with ranked data P=0.004) and by the interaction between the two factors (GLM with ranked data P<0.001) (Figure 5.12). Post-hoc pair-wise comparisons (Tukey's tests) revealed a significant reduction in cell number in cells overexpressing EAAT1a and EAAT1ex9skip to 74 ± 1.7 % (P=0.001) and 73 ± 3.0 % (P=0.001) of scrambled control cells respectively at 0μM glutamate. Such a large reduction in cell number is likely to be biologically significant however these experiments need to be repeated to validate this. The presence of 500μM glutamate prevented this decrease and this was significant in ex3skip AON transfected cells (P=0.006). Transfection with scrambled control oligoribonucleotides significantly increased primary osteoblast cell number relative to untransfected cells (GLM P=0.018), but no post-hoc pair-wise comparisons (Tukey's tests) were significant.

In transfected primary osteoblasts, cell death was significantly affected by glutamate (GLM P=0.049) but not by overexpression of EAAT1 splice variants (GLM P=0.454) or by the interaction between the two factors (GLM P=0.539) (Figure 5.13). Analysis of all experimental groups showed that incubation of cells with 500μM glutamate resulted in a general increase in cell death; however post-hoc Tukey's tests did not detect any pair-wise significance. The increase in cell death was small, 4.6% at most, and therefore unlikely to be biologically significant. Transfection with scrambled control oligoribonucleotides significantly decreased primary osteoblast cell death relative to untransfected cells (GLM P=0.030), although no post-hoc comparisons (Tukey's tests) were significant.

5.3.5 Effect of antisense mediated EAAT1 exon skipping on gene expression

5.3.5.1 Osteoblast-like cells

MG-63 and SaOS-2 cells were transfected with scrambled control or antisense oligoribonucleotides for 48hrs, or left untransfected. 500μM glutamate was added to replicate cultures under each condition at 24hrs post-transfection. Expression levels of osteocalcin, osteonectin, OPG and ALP were quantified by QRT-PCR and expressed

as a percentage of expression in control cells (scrambled, 0μM glutamate). Presented data are from three independent experiments where n=3.

5.3.5.1.1 Osteocalcin

5.3.5.1.1.1 MG-63

In transfected MG-63 cells, osteocalcin expression was significantly affected by 500μM glutamate (GLM P=0.009) but not by overexpression of EAAT1 splice variants (GLM P=0.099) and there was no interaction between the two factors (GLM P=0.167) (Figure 5.14A). Post-hoc comparisons (Tukey's tests) revealed a significant decrease in osteocalcin expression of 37 ± 7.8 % in scrambled control cells at 500μM glutamate compared to cells at 0μM glutamate (P=0.037), however a similar effect was not detectable in cells overexpressing EAAT1a (P=0.848) or EAAT1ex9skip (P=0.998) at 500μM glutamate compared to 0μM glutamate. There was a trend for decreased osteocalcin expression in cells overexpressing the EAAT1 splice variants in the absence of glutamate, and this effect was significant at the 10% level. Overexpression of EAAT1a and EAAT1ex9skip decreased osteocalcin expression to 71 ± 3.5 % and 71 ± 9.7 % of scrambled control cells respectively at 0μM glutamate. The combination of transfection with oligoribonucleotides and 500μM glutamate had a significant effect on MG-63 osteocalcin expression relative to untransfected cells (GLM P=0.017). Post-hoc pair-wise comparisons (Tukey's tests) revealed that this was a reflection of the down-regulated osteocalcin expression in scrambled control cells in response to 500μM glutamate which was not apparent in untransfected cells.

5.3.5.1.1.2 SaOS-2

In transfected SaOS-2 cells, osteocalcin expression was significantly affected by overexpression of EAAT1 splice variants (GLM P=0.027) and the effect of 500μM glutamate was close to significance at the 5% level (GLM P=0.054). There was no significant interaction between the two factors (GLM P=0.477) (Figure 5.14B). Post-hoc comparisons (Tukey's tests) revealed that overall, osteocalcin expression was significantly decreased in cells transfected with ex3skip AON compared to scrambled control cells (P=0.025), however pair-wise comparisons within each glutamate

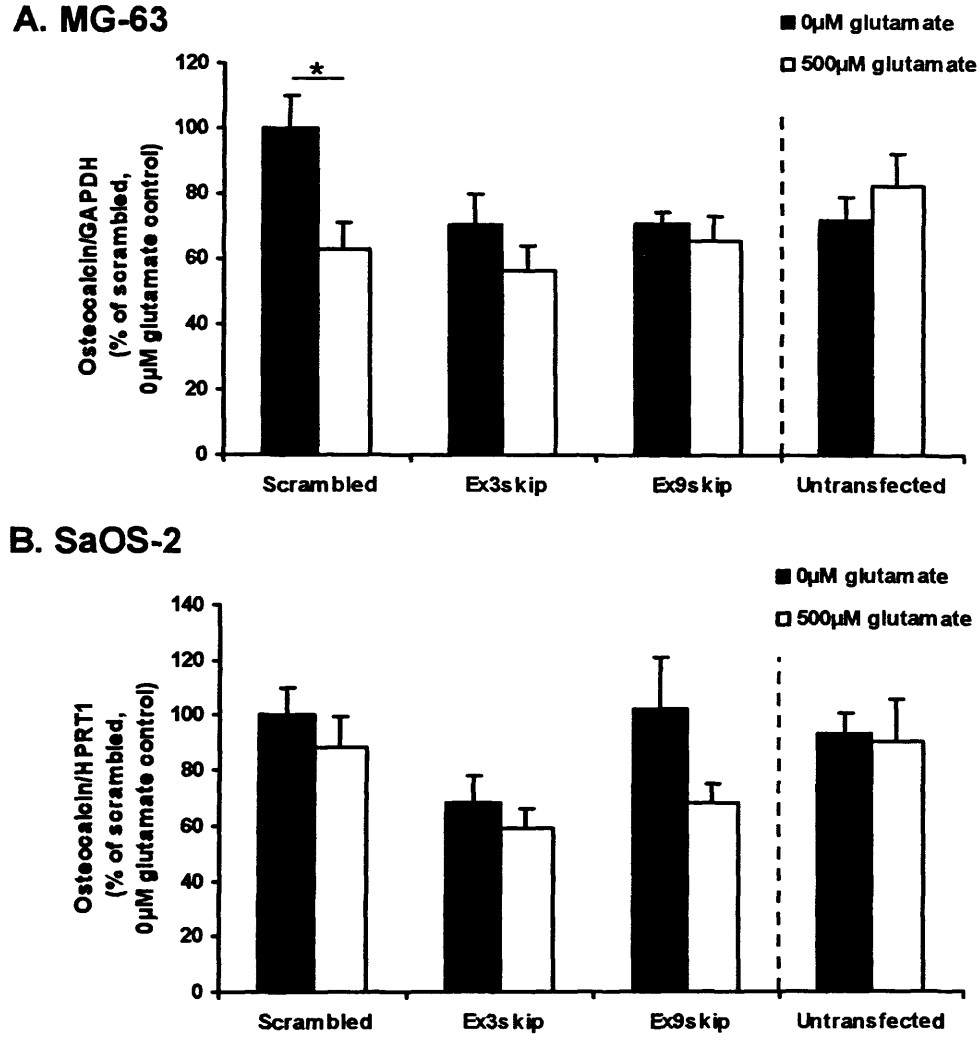

Figure 5.14. Effect of antisense mediated EAAT1 exon 3 and exon 9 skipping on osteocalcin mRNA expression in osteoblast-like cells at 48hrs post-transfection. Osteoblast-like cells (A, MG-63; B, SaOS-2) were transfected with scrambled control, ex3skip or ex9skip AONs for 48hrs, or left untransfected (± 500μM glutamate for last 24hrs). Expression of osteocalcin mRNA was assessed by QRT-PCR, normalised to housekeeping gene levels and expressed as the mean percentage change over control cells (scrambled, no glutamate) ± S.E.M from three independent experiments, n=3. MG-63 osteocalcin expression was significantly decreased by 500μM glutamate (GLM P=0.009) and this was significant in scrambled control cells but not in cells overexpressing EAAT1a or EAAT1ex9skip (Tukey's test). SaOS-2 osteocalcin expression was significantly affected by overexpression of EAAT1 splice variants (GLM P=0.027) and post-hoc Tukey's tests revealed a significant decrease in expression in cells overexpressing EAAT1a. Oligoribonucleotide transfection did not affect osteocalcin expression relative to untransfected MG-63 or SaOS-2 cells (GLM). Significance values $^{*}P<0.05$.

treatment group were not statistically significant. The effect of glutamate was close to significance reflecting the trend for decreased osteocalcin expression in cells at 500μM glutamate within each transfection group.

Transfection with oligoribonucleotides had no significant effect on SaOS-2 osteocalcin expression relative to untransfected cells (GLM P=0.845).

5.3.5.1.2 Osteonectin

5.3.5.1.2.1 MG-63

In transfected MG-63 cells, osteonectin expression was not significantly affected by overexpression of EAAT1 splice variants (GLM P=0.442) or 500μM glutamate (GLM P=0.620) and there was no interaction between the two factors (GLM P=0.279) (Figure 5.15A).

Transfection with oligoribonucleotides had no significant effect on MG-63 osteonectin expression relative to untransfected cells (Shierer Ray P=0.115).

5.3.5.1.2.2 SaOS-2

In transfected SaOS-2 cells, osteonectin expression was not significantly affected by overexpression of EAAT1 splice variants (GLM with log data P=0.753) or 500μM glutamate (GLM with log data P=0.873), and there was no interaction between the two factors (GLM with log data P=0.740) (Figure 5.15B).

Transfection with oligoribonucleotides had no significant effect on SaOS-2 osteonectin expression relative to untransfected cells (GLM P=0.071). The effect of transfection was close to significant and this appears to be a reflection of the non-specific increase in osteonectin expression in transfected cells in the absence of glutamate compared to untransfected cells.

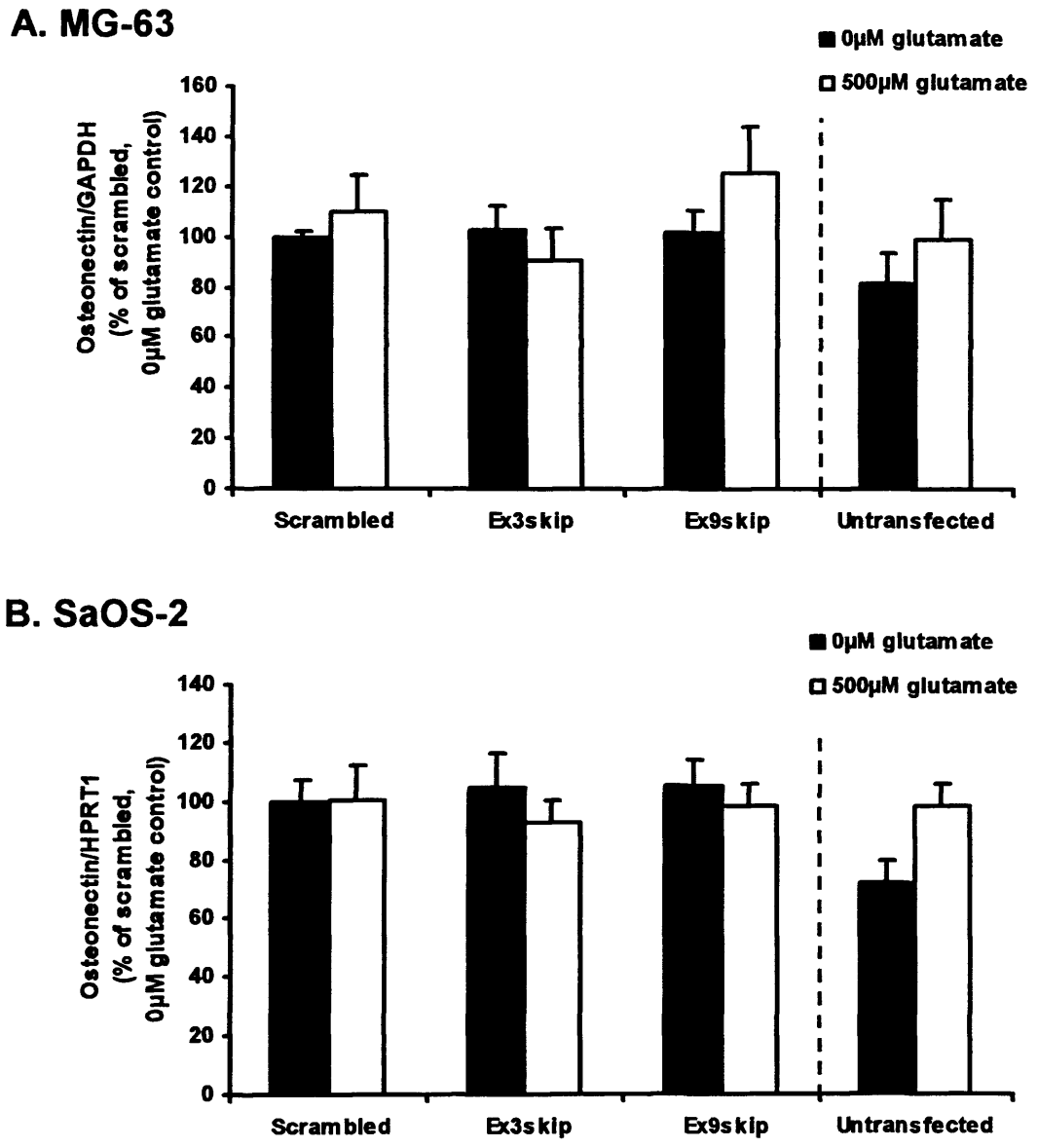

Figure 5.15. Effect of antisense mediated EAAT1 exon 3 and exon 9 skipping on osteonectin mRNA expression in osteoblast-like cells at 48hrs post-transfection. Osteoblast-like cells (A, MG-63; B, SaOS-2) were transfected with scrambled control, ex3skip or ex9skip AONs for 48hrs, or left untransfected (± 500μM glutamate for last 24hrs). Expression of osteonectin mRNA was assessed by QRT-PCR, normalised to housekeeping gene levels and expressed as the mean percentage change over control cells (scrambled, no glutamate) ± S.E.M from three independent experiments, n=3. Osteonectin expression was not significantly affected by overexpression of EAAT1 splice variants or 500μM glutamate in MG-63 or SaOS-2 cells (GLM). Oligoribonucleotide transfection did not affect osteonectin expression relative to untransfected cells in MG-63 (Shierer Ray test) or SaOS-2 cells (GLM).

5.3.5.1.3 OPG

5.3.5.1.3.1 MG-63

In transfected MG-63 cells, OPG expression was not significantly affected by overexpression of EAAT1 splice variants (GLM P=0.330) or 500μM glutamate (GLM P=0.830), and there was no interaction between the two factors (GLM P=0.390) (Figure 5.16A).
Transfection with oligoribonucleotides had no significant effect on MG-63 OPG expression relative to untransfected cells (GLM P=0.751).

5.3.5.1.3.2 SaOS-2

In transfected SaOS-2 cells, OPG expression was not significantly affected by overexpression of EAAT1 splice variants (Shierer Ray P=0.593) or 500μM glutamate (Shierer Ray P=0.206), and there was no interaction between the two factors (Shierer Ray P=0.526) (Figure 5.16B).
Transfection with oligoribonucleotides had no significant effect on SaOS-2 OPG expression relative to untransfected cells (Shierer Ray P=0.065). The effect of transfection was close to significant reflecting the non-specific increase in OPG expression in transfected cells in the absence of glutamate compared to untransfected cells.

5.3.5.1.4 ALP

5.3.5.1.4.1 MG-63

In transfected MG-63 cells, ALP expression was not significantly affected by overexpression of EAAT1 splice variants (GLM P=0.522) or 500μM glutamate (GLM P=0.783), and there was no interaction between the two factors (GLM P=0.591) (Figure 5.17A).
Transfection with oligoribonucleotides had no significant effect on MG-63 ALP expression relative to untransfected cells (GLM P=0.790).

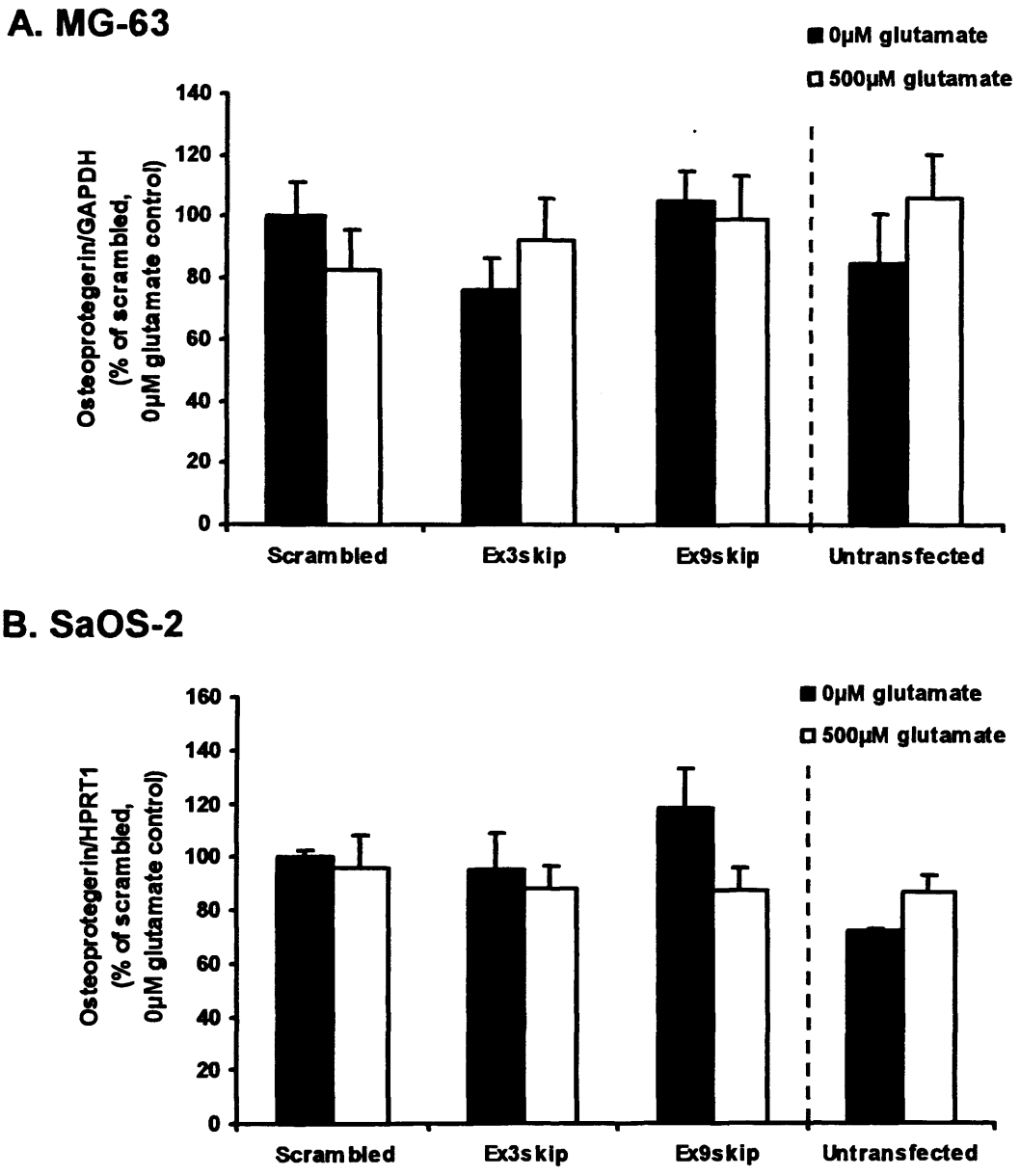

Figure 5.16. Effect of antisense mediated EAAT1 exon 3 and exon 9 skipping on osteoprotegerin (OPG) mRNA expression in osteoblast-like cells at 48hrs post-transfection. Osteoblast-like cells (A, MG-63; B, SaOS-2) were transfected with scrambled control, ex3skip or ex9skip AONs for 48hrs, or left untransfected (± 500μM glutamate for last 24hrs). Expression of OPG mRNA was assessed by QRT-PCR, normalised to housekeeping gene levels and expressed as the mean percentage change over control cells (scrambled, no glutamate) ± S.E.M from three independent experiments, n=3. OPG expression was not significantly affected by overexpression of EAAT1 splice variants or 500μM glutamate in MG-63 (GLM) or SaOS-2 cells (Shierer Ray test). Oligoribonucleotide transfection did not affect OPG expression relative to untransfected cells in MG-63 (GLM) or SaOS-2 cells (Shierer Ray test).

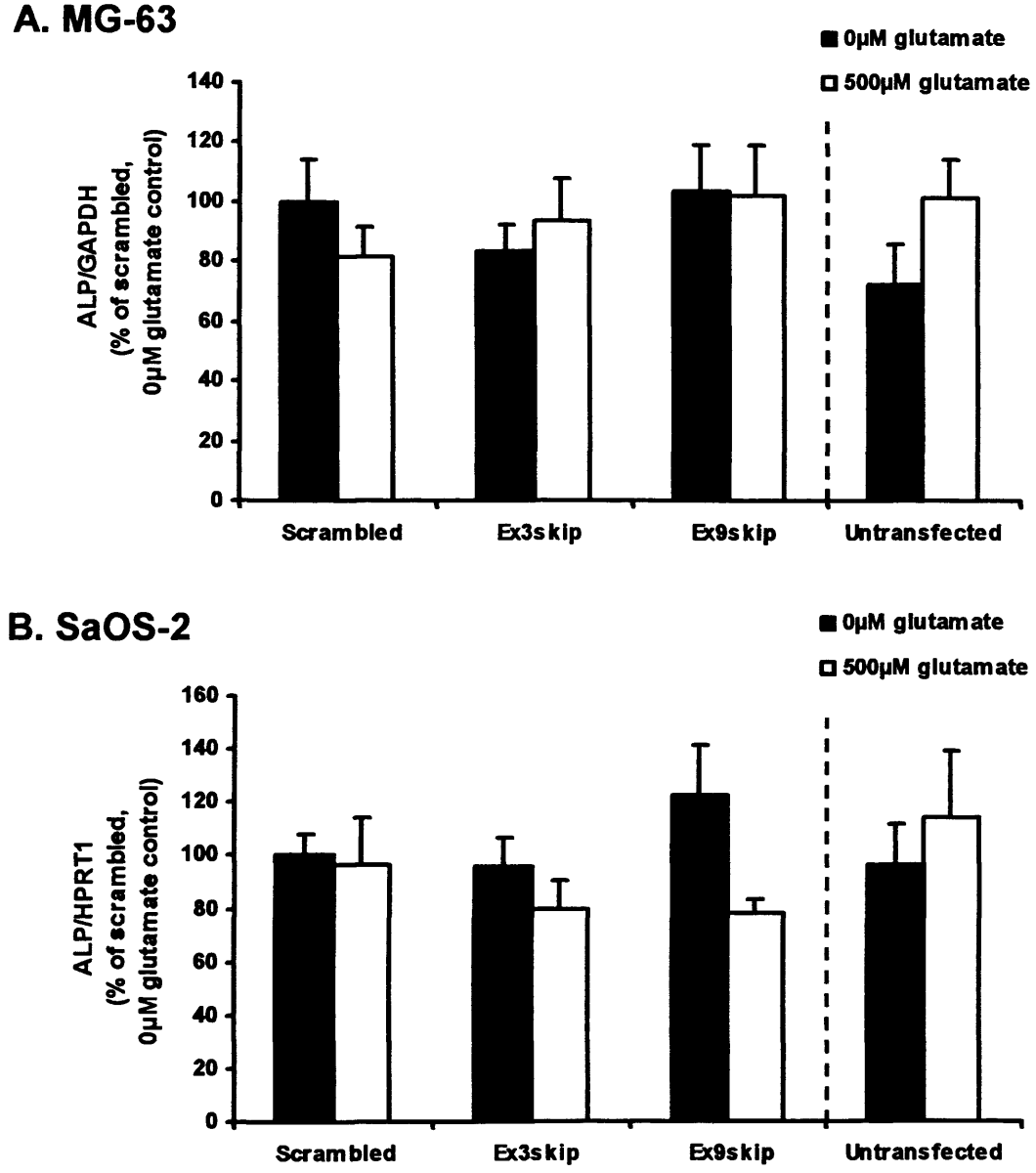

Figure 5.17. Effect of antisense mediated EAAT1 exon 3 and exon 9 skipping on ALP mRNA expression in osteoblast-like cells at 48hrs post-transfection. Osteoblast-like cells (A, MG-63; B, SaOS-2) were transfected with scrambled control, ex3skip or ex9skip AONs for 48hrs, or left untransfected (± 500μM glutamate for last 24hrs). Expression of ALP mRNA was assessed by QRT-PCR, normalised to housekeeping gene levels and expressed as the mean percentage change over control cells (scrambled, no glutamate) ± S.E.M from three independent experiments, n=3. ALP expression was not significantly affected by overexpression of EAAT1 splice variants or 500μM glutamate in MG-63 cells (GLM). SaOS-2 ALP expression was significantly decreased across transfected groups by 500μM glutamate (GLM P=0.038), however post-hoc pair-wise Tukey's tests did not reach significance. Oligoribonucleotide transfection did not affect ALP expression relative to untransfected cells in MG-63 or SaOS-2 cells (GLM).

5.3.5.1.4.2 SaOS-2

In transfected SaOS-2 cells, ALP expression was significantly affected by 500μM glutamate (GLM with log data P=0.038) but not by overexpression of EAAT1 splice variants (GLM with log data P=0.642), and there was no interaction between the two factors (GLM with log data P=0.679) (Figure 5.17B). 500μM glutamate decreased ALP expression in cells overexpressing EAAT1a and EAAT1ex9skip compared to scrambled control cells, however post-hoc pair-wise comparisons (Tukey's tests) were not statistically significant.

Transfection with oligoribonucleotides had no significant effect on SaOS-2 ALP expression relative to untransfected cells (GLM P=0.986).

5.3.5.2 Primary osteoblasts

Gene expression changes were measured in untransfected primary human osteoblasts (NHOB2P11) and in the same cells 48hrs post-transfection with scrambled control or antisense oligoribonucleotides (Figure 5.18). 500μM glutamate was added to replicate cultures under each condition at the point of transfection and remained in the culture medium for the full 48hr duration. Expression levels of osteocalcin and osteonectin were quantified by QRT-PCR and expressed as the percentage of gene expression in control cells (scrambled, no glutamate). Presented data are from a single preliminary experiment where n=4.

5.3.5.2.1 Osteocalcin

In transfected cells, osteocalcin expression was significantly decreased by 500μM glutamate (GLM P=0.047), but unaffected by overexpression of EAAT1 splice variants (GLM P=0.992) and there was no interaction between the two factors (GLM P=0.983) (Figure 5.18A). Post-hoc comparisons (Tukey's tests) did not reveal any pair-wise significance for the effect of glutamate.

Transfection with oligoribonucleotides had no significant effect on primary osteoblast osteocalcin expression relative to untransfected cells (GLM P=0.752).

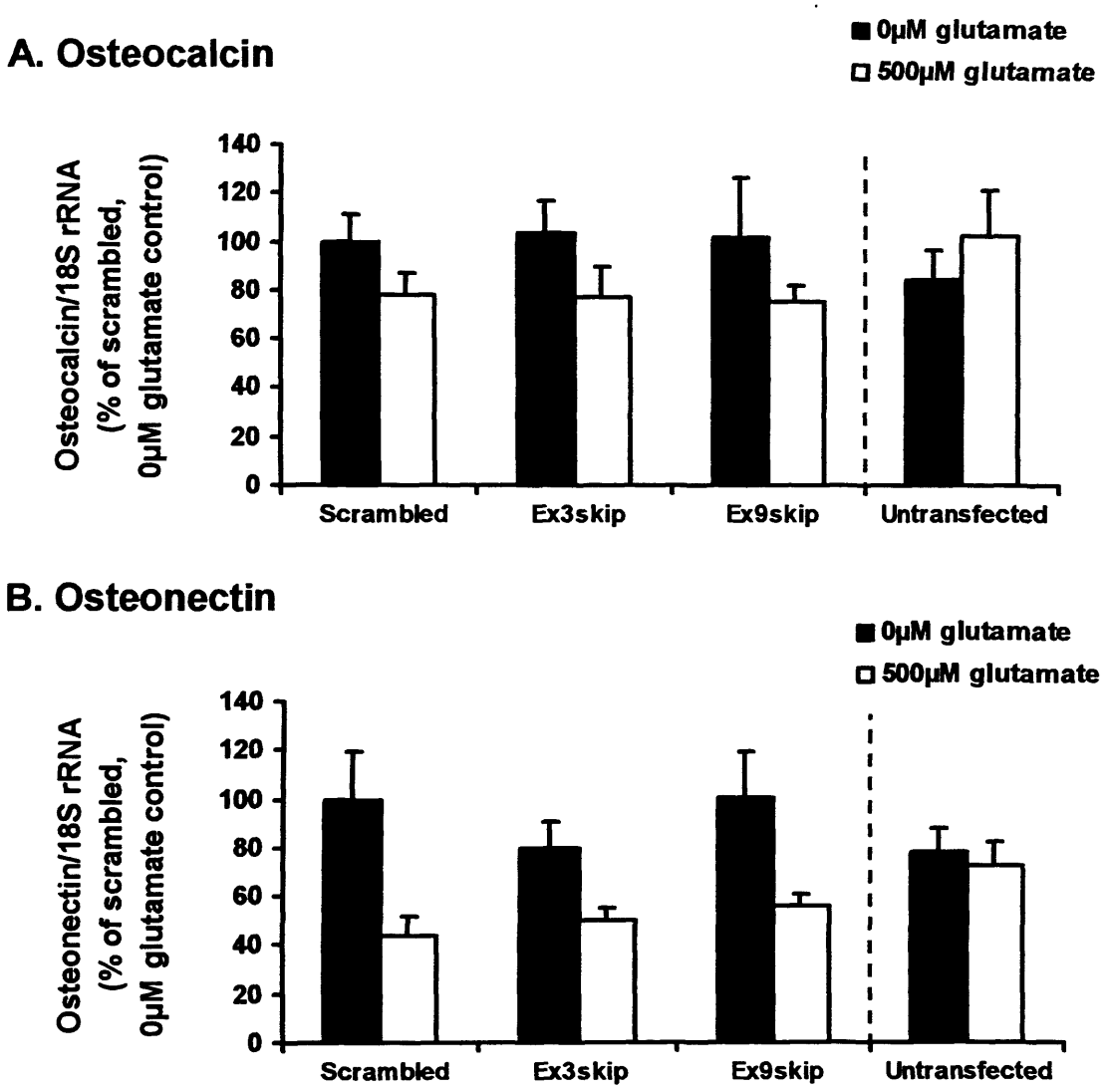

Figure 5.18. Effect of antisense mediated EAAT1 exon 3 and exon 9 skipping on gene expression in primary human osteoblasts. Primary osteoblasts (NHOB2P11) were transfected with scrambled control, ex3skip or ex9skip AONs, or left untransfected ± 500μM glutamate for 48hrs. Expression of (A) osteocalcin and (B) osteonectin mRNA was assessed by QRT-PCR, normalised to 18S rRNA levels and expressed as the mean percentage change over control cells (scrambled, no glutamate) ± S.E.M from a single preliminary experiment, n=4. In transfected primary osteoblasts, expression levels of osteocalcin and osteonectin were significantly decreased by 500μM glutamate (GLM P=0.047 and P=0.020 respectively) however no pair-wise Tukey's comparisons reached significance. Oligoribonucleotide transfection did not affect osteocalcin or osteonectin expression relative to untransfected cells (GLM).

5.3.5.2.2 Osteonectin

In transfected cells, osteonectin expression was significantly decreased by 500μM glutamate (GLM with ranked data P=0.020), but unaffected by overexpression of EAAT1 splice variants (GLM with ranked data P=0.600) and there was no interaction between the two factors (GLM with ranked data P=0.997) (Figure 5.18B). Post-hoc comparisons (Tukey's tests) did not reveal any pair-wise significance for the effect of glutamate.

Transfection with oligoribonucleotides had no significant effect on primary osteoblast osteonectin expression relative to untransfected cells (GLM with log data P=0.751).

5.3.6 Effect of antisense mediated EAAT1 exon skipping on ALP activity

ALP activity of SaOS-2 cells was measured colourimetrically at 48hrs post-transfection and normalised to total cell number (total LDH activity within the adherent cell lysate). ALP activity is shown as a percentage of ALP activity of control cells (scrambled, 0μM glutamate) (Figure 5.19). Presented data are from four independent experiments where n=3. SaOS-2 ALP activity was significantly affected by overexpression of EAAT1 splice variants (GLM with ranked data P=0.021) and by the interaction between glutamate and overexpression of the splice variants (GLM with ranked data P=0.042), however glutamate itself did not significantly affect ALP activity (GLM with ranked data P=0.378). Post-hoc pair-wise Tukey's comparisons revealed that ALP activity was significantly increased to 216 ± 38.9 % of scrambled control cells by overexpression of EAAT1ex9skip in the absence of glutamate (P=0.006). The same treatment had no effect on ALP activity compared to scrambled control cells at 500μM glutamate (P=1.000).

Comparison of scrambled control and untransfected cells revealed that oligoribonucleotide transfection did not affect ALP activity (GLM P=0.669).

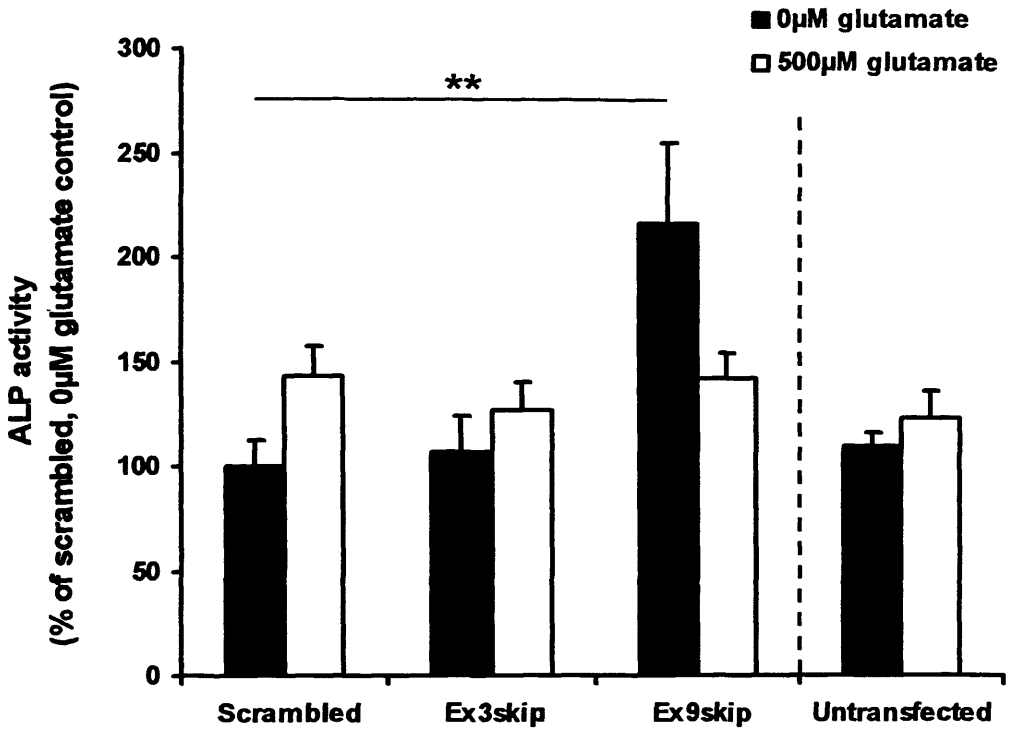

Figure 5.19. Effect of antisense mediated EAAT1 exon 3 and exon 9 skipping on SaOS-2 ALP activity over 48hrs. SaOS-2 cells were transfected with scrambled control, ex3skip or ex9skip AONs, or left untransfected, for 48hrs (± 500μM glutamate for last 24hrs). ALP activity was measured colourimetrically and normalised to cell number (as measured by total cellular LDH activity). ALP activity is shown as the mean percentage of control cell ALP activity (scrambled, no glutamate) ± S.E.M from four independent experiments, n=3. SaOS-2 ALP activity was significantly affected by overexpression of EAAT1 splice variants (GLM P=0.021) and by the interaction between glutamate and overexpression of the splice variants (GLM P=0.042). Post-hoc pair-wise Tukey's tests revealed that ALP activity was significantly increased by overexpression of EAAT1ex9skip in the absence of glutamate. Oligoribonucleotide transfection did not affect ALP relative to untransfected cells (GLM). Significance values $^{**}P<0.01$.

5.4 Discussion

5.4.1 Antisense oligoribonucleotides can be used to efficiently induce exon skipping of EAAT1 in osteoblasts

The manipulation of EAAT1 expression relative to that of its splice variants has not been previously reported. Using antisense oligoribonucleotides targeted to the splice acceptor sequences of exons 3 and 9, it has been possible to induce exon skipping and increase the expression of EAAT1a and EAAT1ex9skip relative to the full-length EAAT1 sequence. At the transcript level, both ex3skip and ex9skip AONs induced a substantial increase in EAAT1a and EAAT1ex9skip respectively in primary human osteoblasts and human osteoblast-like cell lines.

Densitometry analysis of the EAAT1ex9skip:EAAT1 expression ratio in ex9skip AON transfected cells using PCR products resolved on an agarose gel revealed that the largest increase in this ratio occurred in SaOS-2 cells, though data at the 24hr time-point was very variable and increases observed at other time-points were similar across the two osteoblast cell lines. Furthermore, densitometry was utilised here as a simple measure to ascertain the efficiency over time of exon skipping and the methodology is not quantitative. Indeed, quantitative RT-PCR indicated that the largest increase in the EAAT1ex9skip:EAAT1 ratio following ex9skip AON transfection occurred in MG-63 cells.

The increase in the ratio of EAAT1ex9skip to full-length EAAT1 transcript in response to ex9skip AON transfection is dependent upon the basal proportion of the variants in each individual cell line as well as the normal level of transcription of EAAT1. EAAT1ex9skip levels in untransfected cells are approximately 13% and 2% those of full length EAAT1 in MG-63 cells and SaOS-2 cells respectively, but SaOS-2 cells express considerably higher levels of full-length EAAT1 and EAAT1ex9skip compared to MG-63 cells (as shown by QRT-PCR analysis, section 3.3.1.1). The same quantity of AON was added to the transfection mix for each cell line, so assuming roughly equal amounts of the AON permeated the plasma membrane and were available to induce exon skipping in each cell line, the same amount of full-length EAAT1 transcripts would be converted to EAAT1ex9skip. Although exon skipping might occur to the same extent in both cell lines, the effects of this may be

much greater in MG-63 cells which express low levels of EAAT1ex9skip under normal conditions.

The lack of commercially available antibodies specific to the splice variants prevented confirmation of an increase in protein expression corresponding to the increase in variant mRNA levels. As a consequence, it is not possible to determine whether the experimental data is due to an up-regulation of splice variant protein relative to the normal EAAT1 protein, or due simply to interference with full-length EAAT1 mRNA levels. Evidence that EAAT1a and EAAT1ex9skip are translated has been provided using specific antibodies to the splice variants by western blotting and by immunohistochemistry in the rat CNS (Macnab and Pow 2007a; Sullivan et al. 2007a), but not in bone. Western blotting analysis using antibodies targeted to portions of EAAT1 present in the full-length protein as well as both splice variant proteins have identified lower molecular weight bands that may correlate with EAAT1ex9skip or EAAT1a (50-55kDa) (Huggett et al. 2000; Macnab et al. 2006; Macnab and Pow 2007a). Western blotting using such EAAT1 antibodies could be used to confirm a difference in density ratios for immunoreactive bands corresponding to EAAT1 and its splice variants following exon skipping in osteoblasts.

5.4.2 Scrambled oligoribonucleotide transfection induces non-specific effects in human osteoblasts

Transfection with scrambled control oligoribonucleotides induced some significant non-specific effects in osteoblast-like cells and primary human osteoblasts. The scrambled control oligoribonucleotide was a scrambled version of the ex9skip AON and was checked for non-specific hybridisation by BLASTN searches (GenBank database sequences), which confirmed that it was unlikely to cause non-specific effects. Thus, the non-specific effects observed are likely to be due to the transfection agent, Fugene HD.

MG-63 cells exhibited an increase in cell number in response to transfection with the scrambled control AON, indicating that the transfection agent influenced the cell cycle. This increase was very small (<10% compared to untransfected cells). Many transfection agents negatively impact cell viability and physiology (Arbab et al. 2004; Schagat and Kopish 2010). Fugene HD has been developed to limit these cytotoxic

effects (Schagat and Kopish 2010) and no increase in cell number has previously been reported in cells treated with Fugene HD.

In some cases, the response to 500μM glutamate differed between cells transfected with scrambled control oligoribonucleotides and untransfected cells. For example, in primary human osteoblasts a glutamate induced reduction in osteocalcin and osteonectin expression was observed in all transfected cells compared to untransfected cells. This effect of the transfection agent complicates interpretation of changes in cells transfected with AONs in the presence and absence of glutamate, however all comparisons were appropriately made with reference to the scrambled control.

5.4.3 Overexpression of EAAT1 splice variants decreases Na^+-dependent glutamate transport activity in osteoblast-like cells

Overexpression of EAAT1a and EAAT1ex9skip significantly reduced Na^+-dependent glutamate uptake in both MG-63 and SaOS-2 cells, indicating either a reduction in functional glutamate transporters at the plasma membrane, a reduction in affinity of the transporters for glutamate or a reduction in speed of transport. Overexpression of EAAT1a decreased Na^+-dependent glutamate uptake by approximately the same extent in both cell lines, whereas overexpression of EAAT1ex9skip decreased Na^+-dependent glutamate uptake to a greater extent in SaOS-2 than MG-63 cells. These experiments were carried out with 10μM glutamate which is close to the glutamate concentrations in serum and synovial fluid under physiological conditions (Plaitakis et al. 1982; McNearney et al. 2000) suggesting that manipulation of EAAT1 splice variant expression may be physiologically relevant to glutamate uptake in bone.

Interestingly, transfection of ex9skip AONs induced the greater increase in EAAT1ex9skip:EAAT1 ratio in MG-63 cells compared to SaOS-2 cells, yet uptake of 10μM glutamate was affected to a greater extent by this treatment in SaOS-2 cells. This may be due to the glutamate concentration used in the uptake experiments since the two cell lines exhibit very different saturation curves for glutamate uptake (section 3.3.3.2.1). Indeed, interpretation of the functionality of the splice variants would be better informed by characterisation of the kinetic constants of Na^+-dependent glutamate uptake in cells transfected with the AONs compared to those transfected with the scrambled control oligoribonucleotide. Such information would indicate whether the reduction in EAAT activity is a result of decreased affinity of the

transporter (i.e. increased K_M value) or decreased expression of the transporter at the plasma membrane (i.e. decreased V_{max} value). Possible explanations for the observed reduction in EAAT activity following overexpression of the splice variants are; (i) that the splice variant transcript or protein is unstable, resulting in a reduction of full-length functional EAAT1 transcript and protein, (ii) that the splice variant is translated but retained intracellularly, (iii) that the splice variant is translated and non-functional or (iv) that the splice variant is expressed, functional but has reduced activity compared to the full-length protein.

5.4.3.1 EAAT1a

An unstable EAAT1a transcript is in agreement with the very low mRNA levels of EAAT1a in human osteoblasts but inconsistent with detection of EAAT1a protein in the CNS (Macnab et al. 2006). Furthermore glutamate uptake assays were carried out at 48hrs post-transfection, at which point high levels of EAAT1a mRNA were detectable in AON transfected cells by RT-PCR, indicating that the transcript is stable over this time period. The stability of the EAAT1a protein has not been investigated; however its lack of glycosylation and TM2 domain may prevent the correct assembly of multimers, resulting in its retention at the ER (Conradt et al. 1995; Yernool et al. 2004).

There is some evidence to support intracellular retention of EAAT1a. In mouse MLO-Y4 osteocyte-like cells and human SaOS-2 cells transfected with GLAST-1a tagged with GFP, GLAST-1a was detected in internal vesicles surrounding the nucleus in MLO-Y4 cells (Huggett et al. 2002) and some patchy distribution at the plasma membrane was observed in SaOS-2 cells (Mason and Huggett 2002). No localisation studies of EAAT1a have been carried out in MG-63 cells or primary osteoblasts.

The proposed reorientation of EAAT1a in the plasma membrane generates an extracellular C-terminus (Huggett et al. 2000), preventing intracellular protein-protein interactions at this region as well as at any loops linking TM domains that are intracellular in the full-length protein. Interactions with the EAAT1 C-terminal domain stabilise expression of EAAT1 at the membrane (Table 6.1). Loss of such interactions might reduce the expression of EAAT1a at the cell surface. Furthermore, loss of these intracellular regions may prevent regulatory protein-protein interactions

or post-translational modifications such as phosphorylation that affect expression or activity of the transporter (discussed further in chapter 6).

Glutamate uptake has been detected in *Xenopus laevis* oocytes microinjected with cRNA encoding the ORF of GLAST-1a, demonstrating that the protein retains the functional domains required for uptake activity (Mason, Huggett and Daniels unpublished data). EAAT1a retains the C-terminal domain of EAAT1 which is highly conserved and contains a number of residues that are important for glutamate binding and transport (Vandenberg et al. 1995; Grunewald et al. 1998; Seal and Amara 1999; Bendahan et al. 2000; Grunewald and Kanner 2000; Seal et al. 2000; Borre et al. 2002; Ryan and Vandenberg 2002), predicting that the protein would be capable of glutamate transport (Huggett et al. 2000). Altered regulation of EAAT1a activity compared to full-length EAAT1 is more likely since the protein will lack crucial residues for the uncoupled anion conductance conferring altered ion channel properties to the cell (Mason, Huggett, Daniels, unpublished). The anion conductance activity of the EAATs is thought to function as a voltage clamp (Billups et al. 1996; Eliasof and Jahr 1996), which compensates for the membrane potential changes due to electrogenic glutamate uptake by EAATs. Lack of chloride entry might therefore slow glutamate transport, providing one explanation for the decreased EAAT activity in cell lines over-expressing EAAT1a.

5.4.3.2 EAAT1ex9skip

High levels of EAAT1ex9skip mRNA in human brain and osteoblasts (Vallejo-Illarramendi et al. 2005) and the detection of EAAT1ex9skip protein expression in the CNS (Macnab and Pow 2007b; Sullivan et al. 2007a) suggest that the splice variant transcript and protein are stable. However, there is evidence to indicate instability of the protein (Vallejo-Illarramendi et al. 2005), and that multimeric complexes between EAAT1 and EAAT1ex9skip at the ER might assemble incorrectly and are therefore targeted for degradation (Hurtley and Helenius 1989; Klausner and Sitia 1990).

HEK293 cells transiently transfected with the coding sequence of EAAT1ex9skip expressed a protein that was retained primarily within the ER suggesting that the splice variant is not expressed at the cell surface, however expression was also detected at the plasma membrane (Vallejo-Illarramendi et al. 2005). EAAT1ex9skip has also been detected intracellularly and at the plasma membrane of cortical and

collicular neurons using EAAT1ex9skip specific antibodies (Macnab and Pow 2007a).

No glutamate uptake activity was detected in HEK293 cells transiently transfected with the coding sequence of EAAT1ex9skip (Vallejo-Illarramendi et al. 2005). EAAT1ex9skip lacks specific residues (A446-G459) that have been found to be important for glutamate transport (Seal et al. 2001; Leighton et al. 2002; Ryan and Vandenberg 2002). The experiments presented in this chapter are consistent with a non-functional role for EAAT1ex9skip in Na^+-dependent glutamate transport, however experiments were not carried out to test the theory that EAAT1ex9skip negatively regulates the function of full-length EAAT1 (Vallejo-Illarramendi et al. 2005).

5.4.4 Overexpression of the EAAT1 splice variants has opposing effects on cell number

EAAT1 splice variants were overexpressed in osteoblasts at 0 and 500μM glutamate. It should be noted that experiments in chapter 4 demonstrated an increase in MG-63 and human primary osteoblast (NHOB2P7, NHOB3P5) cell number in response to 500μM glutamate (section 4.3.2) that was not apparent in untransfected cells here. With respect to MG-63 cells, this may reflect differences in the experimental set-up since the experiments in this chapter were carried out using different culture plates and 500μM glutamate was added 24hrs later, when cells were more confluent. This is consistent with the idea (presented in section 7.3.4) that the effect of glutamate on MG-63 cell number is confluence dependent. With respect to the human primary osteoblasts, differences observed between the experiments may also reflect an altered confluency at the time of glutamate treatment, or that a later passage of this cell line (NHOB2P11) was used.

Overexpression of EAAT1a in the presence of 500μM glutamate resulted in an increase in SaOS-2 cell number that was not apparent at 0μM glutamate. SaOS-2 cell number is not affected by 500μM glutamate over 24-72hrs, but cell number is significantly increased by chemical inhibition of EAATs (chapter 4), and this may occur via increased levels of extracellular glutamate available to activate NMDA receptors which are associated with the proliferative responses of a variety of cells, including MC3T3-E1 osteoblast-like cells, to glutamate (Contestabile 2000; Rzeski et

al. 2001; Fatokun et al. 2006; Parada-Turska et al. 2006; Spitzer 2006; Piepoli et al. 2009). Therefore, the effect of EAAT1a on SaOS-2 cell number could also be the result of an increase in extracellular glutamate concentration due to decreased glutamate uptake activity. However overexpression of EAAT1ex9skip also reduced SaOS-2 glutamate uptake, but the same effects on cell number were not observed. The effects of exon skipping on glutamate transport were only assessed at 10μM glutamate and it is unclear how transport activity might be affected by exon skipping under the pathophysiological concentration of 500μM glutamate.

Alternatively, the effect of EAAT1a on SaOS-2 cell number could be the direct result of altered anion conductance and/or intracellular interactions associated with the splice variant. The uncoupled chloride conductance of EAATs may modulate glutamate receptor activity or operate itself as a receptor, activating intracellular signalling cascades in response to glutamate binding (Danbolt 2001; Mason and Huggett 2002). The anion conductance associated with glutamate binding might negatively regulate the signalling responses that modulate cell proliferation following glutamate receptor activation under normal conditions. The potential loss of C-terminal intracellular interactions associated with the re-orientated EAAT1a protein may also modulate the proliferative responses of the cell.

Overexpression of EAAT1ex9skip reduced MG-63 cell number at 0μM glutamate, indicating that this treatment inhibits proliferation or increases apoptosis (no analysis of cell death was carried out). An inhibition of proliferation might indicate that overexpression of EAAT1ex9skip promotes the transition between the proliferation stage of osteoblast growth and differentiation, towards the matrix maturation stage (Figure 4.18). In support of this, SaOS-2 cells transfected with ex9skip AONs exhibit increased ALP activity, a marker of extracellular matrix deposition and maturation. Evidence for an inverse relationship between these stages of osteoblast growth is well documented (Lian and Stein 1995; Malaval et al. 1999; Karsenty 2003; Lian and Stein 2003; Stein et al. 2004) and a role for glutamate and/or the EAATs in this process is discussed in section 7.3.3.

Interestingly, it has been suggested that in the CNS, increased expression of EAAT1ex9skip represent neurons that are at risk of dying in response to hypoxic insult (Sullivan et al. 2007a). However the mechanism responsible for cell death in this case is glutamate-mediated excitotoxicity, which does not occur in human

osteoblast-like cells in response to 500μM glutamate (sections 4.3.2.1 and 5.3.4.1 and Genever and Skerry 2001).

Preliminary data indicated that in scrambled oligoribonucleotide transfected primary osteoblasts (NHOB2P11), 500μM glutamate decreased mean cell number and increased mean cell death. These effects were mimicked by overexpression of EAAT1a and EAAT1ex9skip in the absence of exogenous glutamate suggesting that overexpression of these splice variants increases extracellular glutamate by reducing glutamate uptake, however further repeats of this experiment are required to validate these findings. Exon skipping in the presence of 500μM glutamate had no effect on cell number or cell death in primary osteoblasts.

5.4.5 Overexpression of the EAAT1 splice variants affects osteoblast gene expression

In osteoblasts, expression of osteocalcin, osteonectin and ALP were significantly affected by 500μM glutamate, and osteocalcin mRNA levels were significantly affected by overexpression of EAAT1 splice variants.

500μM glutamate decreased MG-63 osteocalcin expression, consistent with chapter 4 (section 4.3.3.2, Figure 4.7). Preliminary data from primary human osteoblasts displayed a reduction in both osteocalcin and osteonectin expression in response to 500μM glutamate across all transfected groups, but this was not apparent in untransfected cells, suggesting that Fugene HD transfection agent modified the normal response of these cells to extracellular glutamate.

ALP expression was significantly decreased by 500μM glutamate in SaOS-2 cells across all transfection groups. No pair-wise statistical comparisons were significant, however 500μM glutamate decreased mean ALP mRNA levels to a greater extent in cells overexpressing EAAT1 splice variants in comparison to scrambled control cells. In the absence of extracellular glutamate, mean ALP mRNA levels were slightly increased by overexpression of EAAT1ex9skip, and this correlates with the significant increase in ALP activity observed in these cells. That 500μM glutamate appears to attenuate this increase in mean ALP expression, suggests that high glutamate concentrations may be able to activate inhibitory GluRs or feedback signalling pathways.

In MG-63 cells, overexpression of EAAT1a and EAAT1ex9skip in the absence of glutamate mimicked the reduced osteocalcin expression in response to 500μM glutamate, indicating a mechanism that occurs via reduced glutamate uptake. However, antagonists to NMDA receptors down-regulate the mRNA expression of osteocalcin in rat calvarial osteoblasts over 7-28 days (Hinoi et al. 2003) and NMDA and AMPA up-regulate osteocalcin expression in glutamate-free medium over 3 days (Lin et al. 2008). This discrepancy may be explained by the cell line in question, the differences in length of treatment, or the effects of a specific iGluR agonist/antagonist over the general effect of extracellular glutamate. With respect to the latter, other glutamate receptor subtypes might be expressed at the cell surface which regulate the response, such as mGluRs (further discussed in section 7.3.1).

In SaOS-2 cells, overexpression of EAAT1a at both glutamate concentrations significantly reduced osteocalcin expression. This effect was not observed in EAAT1ex9skip overexpressing cells, implicating the region of the protein lost in EAAT1a in the response. EAAT1a lacks regions important for Cl^- conductance and if re-orientated in the plasma membrane, lacks protein-protein interactions that normally occur within the cell. Therefore, one or both of these activities may normally play a role in promoting osteocalcin expression in SaOS-2 cells.

5.4.6 Overexpression of EAAT1ex9skip increases SaOS-2 ALP activity

SaOS-2 ALP activity was significantly increased by overexpression of EAAT1ex9skip and mean SaOS-2 ALP activity was also increased by 500μM glutamate in untransfected cells, and cells transfected with the scrambled or ex3skip AONs. 500μM glutamate also increased mean ALP mRNA levels in MG-63 and SaOS-2 cells in chapter 4 (section 4.3.3.6, Figure 4.11). Variability in the data may be explained by variable transfection efficiencies leading to differences in the extent of splice variant overexpression.

Overexpression of EAAT1ex9skip at 0μM glutamate may increase ALP activity in osteoblasts by decreasing glutamate uptake which in turn increases the extracellular concentration of glutamate available for glutamate receptor activation. Consistent with this, antagonists to NMDA and AMPA receptors have previously been shown to inhibit ALP activity in rat calvarial osteoblasts (Hinoi et al. 2003; Lin et al. 2008). Thus, increased concentrations of extracellular glutamate due to overexpression of

EAAT1ex9skip may activate NMDA/AMPA receptors in SaOS-2 cells leading to increased ALP activity.

Overexpression of EAAT1a also significantly reduced Na^+-dependent uptake of 10μM glutamate in SaOS-2 cells but had no effect on ALP activity. However, the reduction in uptake was much less than detected in cells overexpressing EAAT1ex9skip.

Longer term studies assessing the role of the splice variants in the regulation of mineralisation were attempted (not shown). However, Fugene HD transfection agent had an inhibitory effect on either mineralisation itself, or the staining of calcium deposits by alizarin red since mineralisation could not be detected in cells transfected with any of the AONs. Furthermore, the transient nature of exon skipping using AONs is unsuitable to the long-term nature of mineralisation studies. An alternative strategy would be to develop an expression vector for the AONs and generate a stable cell line.

5.4.7 AONs as a therapeutic tool in bone

Over recent years, antisense mediated exon skipping has shown potential therapeutic application towards Duchenne's Muscular Dystrophy (DMD), which is caused by frame-shifting mutations in the dystrophin-coding *DMD* gene that prevents production of functional dystrophin. By targeting the skipping of specific exons within the *DMD* gene using AONs, the reading frame can be restored which leads to production of an internally deleted, but largely functional, protein. This could convert the fatal DMD to the milder, Beckers MD phenotype (Dunckley et al. 1998; Wilton et al. 1999; van Deutekom et al. 2001; Mann et al. 2002), a mechanism that occurs spontaneously in some DMD patients (Aartsma-Rus et al. 2006).

Clinical trials in humans have shown that *DMD* targeted AONs injected intramuscularly can successfully restore expression of dystrophin (van Deutekom et al. 2007); however this method of delivery is unfeasible for treatment of all muscles in the body. Subcutaneous and intravenous AON delivery have been investigated in dystrophin-negative *mdx* mice and sufficient amounts of the AON reached dystrophic muscle to induce expression of functional levels of dystrophin, however the majority ended up in the liver or kidneys (Alter et al. 2006; Fletcher et al. 2007). Furthermore, the effects of chronic AON treatment have not been investigated (van Ommen et al.

2008) and toxicology as a result of non-specific hybridisation of the AON is likely to be species specific and unclear until investigated in humans (Hoffman 2007; Aartsma-Rus et al. 2009).

Therapeutic application of AONs in bone presents similar challenges. Strategies for gene therapy towards bone regeneration have investigated a number of approaches including transfection of cell populations *ex vivo* prior to implantation or injection of plasmid DNA; however none have yet reached clinical trial (reviewed in (Evans 2010)). Transfection of bone marrow stromal cells and muscle tissue-derived cells with a retrovirus encoding BMP-4 prior to seeding on a collagen sponge and implantation into a critical-sized rat femur defect has been shown to improve healing (Rose et al. 2003). Furthermore, adenoviral delivery of genes encoding BMP-2 or TGF-β into a rabbit femoral defect can stimulate bone healing (Baltzer et al. 2000). AONs could be delivered to bone via either these mechanisms, or injected intramedullary or into a defect space as oligoribonucleotides, as in the DMD studies outlined above (van Deutekom et al. 2007; Aartsma-Rus et al. 2009).

The majority of gene therapy studies in bone investigate its feasibility for improving the healing of defects such as non-union fracture rather than increasing bone mass systemically for the treatment of osteoporosis. Local delivery of gene therapy for bone healing has the advantage of not requiring chronic application, since there is no need for the activity to persist beyond the time required to achieve healing.

5.4.8 Summary

Overexpression of EAAT1 splice variants was investigated in osteoblast-like cells and primary human osteoblasts to ascertain the importance of the domains encoded by the spliced out exons in EAAT1a and EAAT1ex9skip in osteoblasts. Antisense RNA oligoribonucleotides targeted to the splice acceptor sequences of EAAT1 exons 3 and 9 efficiently induced exon skipping in osteoblasts and increased the expression of EAAT1a and EAAT1ex9skip relative to the full-length EAAT1 sequence respectively. Overexpression of both splice variants reduced Na^+-dependent glutamate uptake in osteoblast-like cells. Modulation of EAAT1 splice variants in this manner has not been previously reported in any tissue, and these are the first studies to show that altering the ratio of EAAT1 to its splice variants can have variant specific effects

on transporter function and osteoblast phenotype. Overexpression of EAAT1a increased SaOS-2 cell number and decreased osteocalcin expression in both osteoblast-like cell lines, whereas overexpression of EAAT1ex9skip reduced cell number and osteocalcin expression in MG-63 cells and increased ALP activity in SaOS-2 cells. Modulation of EAAT1a and EAAT1ex9skip expression therefore demonstrates potential for increasing osteoblast proliferation and bone-forming activity respectively, which could have therapeutic application to different stages of fracture healing.

Chapter 6: Functional effects of inhibition of EAAT1 intracellular interactions in human osteoblasts

6. Functional effects of inhibition of EAAT1 intracellular interactions in human osteoblasts

6.1 Background

6.1.1 Regulation of neurotransmitter transporter function

Within the CNS, synaptically released neurotransmitters are cleared by transporters that are selectively localised to specific membrane domains i.e. pre-synaptic, post-synaptic and astrocytic processes. A signalling event is regulated by transporter subtype, localisation, capacity and rate of transport - properties that can be modulated by protein-protein interactions within the cell and/or post-translational modification of the transporter.

6.1.1.1 Protein-protein interactions of neurotransmitter transporters

Intracellular protein-protein interactions are important for regulating the membrane trafficking and activity of neurotransmitter transporters as well as other proteins including voltage gated potassium channels and neurotransmitter receptors (Corey et al. 1994; Kim et al. 1995; Kornau et al. 1995; Dong et al. 1997; Horio et al. 1997; Tezuka et al. 1999; Yamada et al. 1999; Torres et al. 2004). Anchoring of transporters at specific regions of the membrane requires protein-protein interactions with scaffolding proteins. Many transporters contain postsynaptic density-95/discs large/zona occludens-1 (PDZ) binding regions at the extreme C-terminus, which allow for interactions with scaffolding proteins containing PDZ modules. PDZ domains are one of the most common protein motifs involved in scaffolding interactions. For example, the PDZ binding domain of the dopamine transporter (DAT) is necessary for interaction with protein-interacting-with-C-kinase (PICK) 1 which increases levels of DAT at the cell surface and increases dopamine uptake activity, possibly by anchoring DAT to the membrane (Torres et al. 2001; Bjerggaard et al. 2004). PICK1 also interacts with the C-terminus of the norepinephrine transporter (NET) and GLT-1b (Torres et al. 2001; Bassan et al. 2008).

6.1.1.2 Post-translational modifications of neurotransmitter transporters

Neurotransmitter transporters interact with a variety of intracellular proteins that directly influence their activity. PICK1 interacts with protein kinase C (PKC), a signalling molecule that modifies the properties of various neurotransmitter transporters, suggesting that PICK1 may recruit PKC to transporters such as DAT, NET and GLT-1b. Phorbol ester-mediated stimulation of PKC decreases dopamine and glycine transporter activity (Kitayama et al. 1994; Sato et al. 1995), whereas cell-surface expression and activity of the GABA transporter (GAT-1) is increased by the same treatment (Corey et al. 1994). Cell surface expression and activity of EAAT1 and EAAT3 are decreased and increased respectively by phorbol ester-mediated PKC activation (Conradt and Stoffel 1997; Gonzalez and Ortega 1997; Davis et al. 1998; Gonzalez et al. 1999; Trotti et al. 2001; Do et al. 2002; Gonzalez et al. 2002). Various other signalling molecules have been implicated in the regulation of neurotransmitter transporters including phosphatidylinositol-3-kinase (PI3K), tyrosine kinases and protein phosphatase 2 (PP2) (Vaughan et al. 1997; Bauman et al. 2000; Law et al. 2000; Apparsundaram et al. 2001; Doolen and Zahniser 2001; Zahniser and Doolen 2001; Carvelli et al. 2002). Signalling molecules such as these allow for rapid changes in activity and distribution of the transporters between the cytoplasm and the plasma membrane.

6.1.2 Regulation of EAAT function

The glutamate transporters and their splice variants display differential subcellular distribution patterns (reviewed in (Danbolt 2001)) indicating that their spatial organisation and insertion into the membrane is tightly regulated. For example, EAAT3 is preferentially distributed to apical membranes of epithelial cells and to the perisynaptic region of the post-synaptic density (Cheng et al. 2002). The amino and carboxy termini of the glutamate transporters are intracellular and large compared to other cytoplasmic regions suggesting that they may be sites for protein-protein interactions (Grunewald et al. 1998). A variety of proteins have been identified that interact with the glutamate transporters (Table 6.1), and these interactions can regulate EAAT localisation, trafficking and activity as well as intracellular signalling.

6.1.2.1 EAAT localisation/trafficking

6.1.2.1.1 C-terminal domain interactions

Human EAAT1 and rat and mouse GLAST contain a PDZ-binding motif (ETKM) at the C-terminus which is homologous to motifs found in other members of the EAAT family (Figure 6.1). In rat whole brain, GLAST coimmunoprecipitates with the Na^+/H^+ exchanger regulatory factor (NHERF) 1 and ezrin (Lee et al. 2007). NHERF1 contains two PDZ motifs and a C-terminus that binds members of the ezrin-radixin-moesin (ERM) family of membrane-cytoskeletal adaptors. The actin cytoskeleton is important in regulating the expression of GLAST at the cell surface (Duan et al. 1999). Interestingly, since actin responds to mechanical load (Vatsa et al. 2008), this interaction with GLAST may explain the first report of GLAST regulation in bone in response to mechanical load (Mason et al. 1997).

Interactions have also been demonstrated between the C-terminal tail of GLAST and an intermediate filament protein glial fibrillary acidic protein (GFAP) (Sullivan et al. 2007b). GLAST glutamate uptake was significantly increased by the presence of GFAP and NHERF1 as a result of stabilised expression of GLAST at the plasma membrane (Sullivan et al. 2007). Furthermore, expression of GFAP was found to be important for GLAST expression at the plasma membrane of astrocytes following hypoxic insult (Sullivan et al. 2007b). The interaction between GFAP and GLAST was indirect and dependent upon the presence of NHERF1 and the PDZ binding motif of GLAST, suggesting that in astrocytes, NHERF1 links an intermediate filament network beneath the plasma membrane to cell surface GLAST. The importance of GFAP in GLAST activity is demonstrated by GFAP knockout mice that display reduced glutamate clearance in the CNS and an increased sensitivity to hypoxia (Hughes et al. 2004).

Associations have also been demonstrated between the GLAST C-terminus and Sept2 and Sept4 in Bergmann glial processes surrounding axons and synapses of the mouse brain (Kinoshita et al. 2004). Sept2 and Sept4 are members of the Septin family of guanosine triphosphatases (GTPases) which form filaments in a guanosine triphosphate (GTP) -form dependent manner. Sept2 binds to GLAST in a guanosine diphosphate (GDP) -form dependent manner and constitutive expression of the GDP-

Table 6.1. Identified protein-protein interactions of the glutamate transporters. EAATs interact with a variety of proteins within the cell which regulate EAAT localisation, trafficking and activity as well as intracellular signalling processes. Abbreviations, PM, plasma membrane; CoIP, coimmunoprecipitation; Y2H, Yeast 2 Hybrid.

	Interacting protein	EAAT domain	Effect on glutamate transport	Mechanism of activity	Cell type and species	Reference	Expressed in osteoblasts?
EAAT1	GFAP	C-term	Increased	Intermediate filament protein that stabilises GLAST expression at the PM in association with NHERF1 and ezrin.	CoIP using rat and pig whole brain; activity assessed in COS7 cells	Sullivan et al. 2007	mRNA (Chipoy et al. 2004); Protein (Kasantikul and Shuangshoti 1989; Chipoy et al. 2004)
	NHERF1	C-term	Increased	PDZ adaptor protein that stabilises GLAST expression at the PM.	CoIP using rat whole brain; activity assessed in COS7 cells	Lee et al. 2007, Sullivan et al. 2007	mRNA (Schroeder et al. 2007)
	Ezrin	C-term	Not tested	Membrane-cytoskeletal adaptor protein.	CoIP using rat whole brain	Lee et al. 2007	mRNA (Khanna et al. 2001; Park et al. 2006); Protein (Park et al. 2006)
	Sept2	C-term	Decreased	Sept2 is a filament forming GTPase. Sept2 binds GLAST in a GDP-form dependent manner and the constitutively GDP-bound form causes GLAST internalisation.	CoIP using mouse brain membrane extracts and COS7 cells; activity assessed in COS7 cells and mouse Bergmann glial cells	Kinoshita et al. 2004	Not reported
	Sept4	C-term	Not tested	Sept4 is a filament forming GTPase which may hetero-complex with Sept2.	CoIP using mouse brain membrane extracts	Kinoshita et al. 2004	Not reported

Table 6.1 continued

	Interacting protein	EAAT domain	Effect on glutamate transport	Mechanism of activity	Cell type and species	Reference	Expressed in osteoblasts?
EAAT2	Ajuba	N-term	None	Cytoplasmic protein containing LIM domains. Co-expression of GLT-1 and Ajuba recruits Ajuba to the PM.	Y2H using rat hippocampal cDNA library; CoIP using rat whole brain; activity assessed in COS cells	Marie et al. 2002	Not reported
	GPS-1	C-term	Decreased	GPS-1 is a subunit of the COP9 signalosome and may be involved in the surface trafficking of GLT-1 via its leucine zipper-like motif.	Y2H (species/tissue not defined); activity assessed in HEK cells	Watanabe et al. 2003	Not reported
	PKCα	Not defined	Decreased	Phorbol ester-mediated PKC activation decreases GLT-1a expression at the PM.	CoIP using rat brain synaptosomes and GLT-1a transfected C6 glioma; activity assessed in GLT-1a transfected C6 glioma	González et al. 2005	Protein (Sanders and Stern 1996; Lampasso et al. 2002)
	PICK1	C-term	None	PDZ domain protein that interacts with PKC and GLT-1b splice variant. Co-expression of GLT-1b and PICK1 recruits PICK1 to the PM and the interaction prevents the PKC mediated decrease in GLT-1b transport activity.	Y2H using rat forebrain neuronal cDNA library; CoIP using rat whole brain and GLT-1b transfected COS7 cells; activity assessed in COS7 cells and rat forebrain neuronal cultures	Bassan et al. 2008	Not reported

Table 6.1 continued

	Interacting protein	EAAT domain	Effect on glutamate transport	Mechanism of activity	Cell type and species	Reference	Expressed in osteoblasts?
EAAT3	GTRAP3-18	C-term	Decreased	GTRAP3-18 decreases the substrate affinity of EAAC1 via a reduction of N-linked glycosylation.	Y2H using rat brain cDNA; activity assessed in HEK, COS7 and C6 glioma cells	Lin et al. 2001, Butchbach et al. 2003, Ruggiero et al. 2008	Not reported
	PKCα	Not defined	Increased	Interaction only detected after phorbol ester treatment. Phorbol ester-mediated PKC activation increases EAAC1 expression at the PM.	CoIP using C6 glioma cells	González et al. 2002, 2003	Protein (Sanders and Stern 1996; Lampasso et al. 2002)
EAAT4	GTRAP48	C-term	Increased	GTRAP48 is a Rho GEF. Interaction stabilises EAAT4 expression at the PM.	Y2H using rat whole brain cDNA library; CoIP using GTRAP48 expressing HEK cells	Jackson et al. 2001	Not reported
	GTRAP41	C-term	Increased	Possibly an actin-binding protein. Stabilises EAAT4 expression at the PM.	Y2H using rat whole brain cDNA library; CoIP using GTRAP41 expressing HEK cells	Jackson 2001	Not reported
EAAT5	PICK1	C-term	Not tested	-	-	Bassan et al. 2008	Not reported

	-3	-2	-1	0	PDZ
Human EAAT1[1]	E	T	K	M	II
Rat GLAST[2]	E	T	K	M	II
Mouse GLAST[3]	E	T	K	M	II
Human EAAT2[4]	K	R	E	K	
Human EAAT2b[5]	E	T	C	I	I
Rat GLT-1[6]	K	R	E	K	
Mouse GLT-1[7]	K	R	E	K	
Rat GLT-1b[8]/GLT-1v[9]	E	T	C	I	I
Mouse mGLT-1a[7]	K	R	E	K	
Mouse mGLT-1b[7]	E	T	C	I	I
Rat GLT-1c[10]	Q	S	W	V	I
Human EAAT3[11]	T	S	Q	F	II
Rat EAAC1[12]	T	S	Q	F	II
Mouse EAAC1[13]	T	S	Q	F	II
Human EAAT4[14]	E	S	A	M	II
Rat EAAT4[15]	E	S	V	M	II
Mouse EAAT4[16]	E	S	V	M	II
Human EAAT5[17]	E	T	N	V	I
Mouse EAAT5[18]	E	T	N	V	I
PDZ I	X	S/T	X	I/V	
PDZ II	X	φ	X	φ	

φ = hydrophobic residue

Figure 6.1. PDZ domain binding motifs in glutamate transporter C-terminal sequences. The last four amino acids from each EAAT are shown and numbered with the P0 position allocated to the extreme C-terminal amino acid of each EAAT. All known transporters except human EAAT2, and rat and mouse GLT-1 (and mouse mGLT-1a) have PDZ domain interaction motifs at their extreme C-termini, if any hydrophobic residue is allowed in the P0 position. Figure adapted from (Bassan et al. 2008). 1. (Kawakami et al. 1994), 2. (Storck et al. 1992), 3. (Tanaka 1993), 4. (Arriza et al. 1994), 5. (Maragakis and Rothstein 2004), 6. (Pines et al. 1992), 7. (Utsunomiya-Tate et al. 1997), 8. (Chen et al. 2002), 9. (Schmitt et al. 2002), 10. (Rauen et al. 2004), 11. (Smith et al. 1994), 12. (Kanai et al. 1995a), 13. (Strausberg et al. 2002), 14. (Fairman et al. 1995), 15. (Cholet et al. 2002), 16. (Yamada et al. 1997), 17. (Arriza et al. 1997), 18. (Blackshaw et al. 2004)

form of Sept2 resulted in internalisation of GLAST and a reduction in glutamate uptake (Kinoshita et al. 2004).

G protein pathway suppressor-1 (GPS-1) was identified by the Yeast-2-Hybrid (Y2H) technique using the C-terminus of GLT-1 as bait (Watanabe et al. 2003). GPS-1 is a subunit of the COP9 signalosome and may be involved in the surface trafficking of GLT-1 via its leucine zipper-like motif. Coexpression of GPS-1 with GLT-1 in HEK293 cells reduced glutamate transport activity, though it was not reported whether this effect was due to altered cell surface expression of GLT-1 (Watanabe et al. 2003).

Y2H studies using the C-terminal sequence of EAAT4 identified 'glutamate transporter associated proteins' (GTRAPs) (Jackson et al. 2001; Lin et al. 2001). The EAAT4 C-terminus associates with GTRAP48 and GTRAP41, which promote EAAT4 activity by stabilising its expression at the plasma membrane (Jackson et al. 2001). GTRAP48 is a guanine nucleotide exchange factor (GEF) for the small G-protein Rho and there is evidence to suggest that GTRAP41 is an actin-binding protein, suggesting that interaction of EAAT4 with actin filaments and Rho may be involved in stabilising EAAT4 at the membrane (Jackson et al. 2001).

6.1.2.1.2 N-terminal domain interactions

EAATs display poor homology at the N-terminus between subtypes and few interacting proteins have been identified. Ajuba, a cytoplasmic protein containing Lin-11, Isl-1 and Mec-3 (LIM) domains, is expressed in astrocytes and Bergmann glia and known to interact with the N-terminus of GLT-1. Ajuba is able to activate MAPK and may act as a scaffolding protein, linking GLT-1 to the cytoskeleton and various signalling pathways (Marie et al. 2002). Co-expression of Ajuba with GLT-1 did not alter transport activity but the presence of GLT-1 caused a redistribution of Ajuba from the cytoplasm to the plasma membrane.

6.1.2.2 EAAT activity

6.1.2.2.1 C-terminal domain interactions

Dialysis of whole-cell patch-clamped retinal glia with a competing peptide identical to the extreme 8 amino acids of the C-terminus of GLAST, containing the putative PDZ-binding domain, increased the affinity of the transporter for glutamate without affecting the maximum glutamate-evoked current (V_{max}) (Marie and Attwell 1999). The authors suggested that the C-terminal peptide disrupted an inhibitory interaction that may have been involved in slowing the removal of low concentrations of glutamate and therefore regulating the kinetics of retinal cell light responses.
Interaction of the C-terminus of EAAC1 and GTRAP3-18 (JWA in human) reduces EAAC1 mediated glutamate transport by decreasing substrate affinity via a reduction of N-linked glycosylation (Lin et al. 2001; Butchbach et al. 2003; Ruggiero et al. 2008).

6.1.2.2.2 N-terminal domain interactions

Dialysis of whole-cell patch-clamped retinal glia with a competing peptide identical to the extreme 8 amino acids of the N-terminus of GLAST had no effect upon affinity for glutamate or the maximum glutamate-evoked current of the transporter, suggesting that any protein-protein interactions at the N-terminus do not regulate GLAST transport activity in non-stimulated cells (Marie and Attwell 1999).
Identification of Ajuba, a protein that can activate MAPK signalling, at the N-terminus of GLT-1 (Marie et al. 2002) introduced the concept that EAAT protein-protein interactions may regulate downstream intracellular signalling pathways, supporting a receptor-like function for the transporters. Abe and Saito (2001) discovered that glutamate could increase MAPK phosphorylation in rat cortical astrocytes in a time- and concentration-dependent manner. This response could be mimicked by the transportable glutamate analogues THA and *t*-PDC but not by glutamate receptor agonists, suggesting that EAATs may act as receptors for changes in extracellular glutamate concentration (Abe and Saito 2001). The authors could not define the region of the protein involved in this activity and did not speculate.

6.1.2.2.3 Other interactions

The amino acid sequence of the EAATs contains putative phosphorylation sites (Figure 1.8, (Kanai et al. 1993; Conradt and Stoffel 1997)) and a number of studies have indicated that phosphorylation can regulate EAAT activity; however the results depend on the experimental model used. Furthermore, it is not yet clear if EAATs are phosphorylated directly or regulated by an associated protein that is phosphorylated. Table 6.2 summarises the findings relating to the effects of phosphorylation on EAAT activity. It is clear that rapid responses to the cellular environment can be finely tuned to regulate EAAT activity via protein kinase-dependent signalling.

Table 6.2. Protein kinase effects on EAAT transport activity. *In vitro* studies have shown that EAATs are differentially regulated by phosphorylation. Potential phosphorylation sites for PKC and PKA are shown in Figure 1.8, however PKC phosphorylation of EAAT1 occurs at a non-consensus site (Conradt and Stoffel 1997). NC, no change; NT, not tested.

EAAT	PKC	PI3K	PKA
1	↓	↑	↑
2	↓(short-term), ↑(long-term)	↑	↓
3	↑	↑	↑
4	NC	NT	NT

6.1.2.2.3.1 PKC

In *Xenopus Laevis* oocytes and HEK293 cells expressing the cloned GLAST cDNA, phorbol ester mediated activation of PKC inhibited glutamate transport activity (Conradt and Stoffel 1997). The same treatment also reduced GLAST glutamate uptake activity in GLAST-rich Bergmann glial cultures (Gonzalez and Ortega 1997) and in retinal Müller cells (Gonzalez et al. 1999).

In HEK293 cells, PKC activation by up to 1hr phorbol ester treatment did not alter plasma membrane expression of GLAST, as shown by immunohistochemistry. Expression rate and stability of the transporter were also not affected, as shown by

metabolic labelling of the protein with [^{35}S]-methionine (Conradt and Stoffel 1997). However, long-term treatment (6-24hrs) of GLAST-rich Bergmann glial cultures with phorbol esters reduced GLAST protein and mRNA levels (Gonzalez and Ortega 1997; Espinoza-Rojo et al. 2000) and phorbol ester-mediated PKC activation in retinal Müller cells reduced GLAST expression in the plasma membrane (Wang et al. 2003). Mutational studies indicate that PKC does not phosphorylate GLAST at predicted consensus PKC sites (GLAST S116, T341, T372) (Conradt and Stoffel 1997).

Phorbol ester mediated PKC activation induced a 50% increase in glial glutamate uptake from primary cultures of rat brain cerebral cortex over 3-24hrs and this was assumed to be largely due to effects of PKC on GLT-1, the predominant glial transporter in the cerebrum (Casado et al. 1991). The same group later confirmed the activation of GLT-1 following phorbol ester treatment and identified that residue Serine 113 of GLT-1 was necessary for this effect (Casado et al. 1993). However, other studies have observed a reduction in GLT-1 activity following short-term (up to 30 min) PKC activation in C6 glioma transfected with GLT-1, primary astrocyte cultures, and *Xenopus Laevis* oocytes injected with GLT-1 mRNA and the reduction in activity was thought to be the result of decreased cell surface expression of the transporter (Fang et al. 2002; Kalandadze et al. 2002; Zhou and Sutherland 2004; Gonzalez et al. 2005).

In C6 glioma, GLT-1a could be coimmunoprecipitated with the classical PKCα and the downregulation of GLT-1a cell surface expression in response to phorbol ester mediated PKC activation was sensitive to inhibitors of the classical PKC subgroup, indicating that PKCα mediates the phorbol ester-induced redistribution of GLT-1a (Gonzalez et al. 2005). Activated PKCα interacts with PICK1 (Staudinger et al. 1995; Staudinger et al. 1997; Perez et al. 2001), a PDZ domain protein that may act as an adaptor to recruit PKCα into complexes with PICK1 binding target proteins (Perez et al. 2001; Hirbec et al. 2002). PICK1 interacts with the C-terminal PDZ binding domain of GLT-1b, a splice variant of GLT-1a containing an alternative C-terminus, but does not interact with GLT-1a which lacks a PDZ binding domain (Bassan et al. 2008). GLT-1b colocalises with PICK1 in pyramidal neurons and astrocytes in the adult rat cerebral cortex (Mahadomrongkul et al. 2002) and with synaptic markers in hippocampal neurons *in vitro* (Bassan et al. 2008). Coexpression of GLT-1b and PICK1 in COS7 cells recruits PICK1 to the plasma membrane (Bassan et al. 2008). In rat forebrain neuronal cultures, where GLT-1b is expressed (Wang et al. 1998; Chen

et al. 2002), phorbol ester mediated PKC activation had no effect on glutamate transport activity. However disruption of the GLT-1b-PICK1 interaction with a competing peptide targeted to the PDZ motif of GLT-1b decreased transport activity in response to phorbol ester treatment, but did not change cell surface expression of GLT-1a or GLT-1b (Bassan et al. 2008). GLT-1c (Rauen et al. 2004). EAAT5 was also found to interact with PICK1 with comparable affinity to GLT-1b (Bassan et al. 2008), whereas GLAST, EAAC1 and EAAT4 did not show affinity for PICK1 as determined by a fluorescent polarisation assay (Bassan et al. 2008).

Phorbol ester-mediated PKC activation increased activity and cell surface expression of EAAC1 in C6 glioma cells (Davis et al. 1998; Trotti et al. 2001; Do et al. 2002; Gonzalez et al. 2002) and in EAAC1 expressing *Xenopus Laevis* oocytes (Trotti et al. 2001; Do et al. 2002). Mutational studies have shown a critical role for S465, at the C-terminal of EAAT3, in mediating this (Baik et al. 2009). Phorbol ester-mediated PKC activation in primary cortical neurons also resulted in an increase in EAAC1 cell surface expression (Gonzalez et al. 2002; Guillet et al. 2005).

Interestingly, inhibition of PI3K in EAAC1 expressing C6 glioma cells abolished the PKC-dependent increase in cell surface expression, but did not completely eliminate the increase in transport activity (Davis et al. 1998), indicating that PKC may regulate EAAC1 cell surface expression and catalytic activity independently. Gonzalez et al. found, using selective inhibitors for the PKC isoenzymes, that PKCα mediates a PKC-dependent increase in cell surface expression of EAAC1 in C6 glioma cells and that PKCε mediates a PKC-dependent increase in EAAC1 activity that is independent of changes in EAAC1 cell surface expression (Gonzalez et al. 2002). PKCα can be coimmunoprecipitated with EAAC1 in C6 glioma cells and in synaptosomes from rat cortex, cerebellum, hippocampus and midbrain, however in C6 glioma this interaction was dependent upon PKCα activation by phorbol ester treatment (Gonzalez et al. 2003). Confocal microscopy indicated that EAAC1 colocalises with phorbol ester-activated PKCα at the plasma membrane of C6 glioma cells (Gonzalez et al. 2003).

In *Xenopus laevis* oocytes expressing rat EAAT4, phorbol ester treatment enhanced the glutamate gated chloride conductance of this transporter without altering transport activity (Fang et al. 2006). This effect was only partially inhibited by the PKC inhibitors staurosporine, chelerythrine and calphostin C (Oishi and Yamaguchi 1994; Fang et al. 2006). The authors of this study did not speculate as to which residues of EAAT4 might be subject to PKC phosphorylation.

6.1.2.2.3.2 PI3K

PI3K has also been implicated in EAAT regulation. The V_{max} of GLAST in chick Bergmann glial cells was increased by treatment with IGF-I and this activation was sensitive to inhibition of PI3K, a downstream effector of IGF-I (Gamboa and Ortega 2002). IGF-I increased GLAST activity in this system in a manner that was not dependent on *de novo* protein synthesis, indicating translocation of the transporter to the plasma membrane as opposed to increased protein expression of the transporter (Gamboa and Ortega 2002).

In primary cortical neuron-enriched cultures from rats, inhibition of PI3K by wortmannin decreased cell surface levels of GLT-1 and EAAC1 (Guillet et al. 2005) and inhibited transport activity in EAAC1 expressing C6 glioma cells (Davis et al. 1998).

6.1.2.2.3.3 PKA

In primary cortical neuron-enriched cultures from rats, inhibition of PKA by H89 decreased cell surface expression of GLAST and EAAC1, but increased cell surface expression of GLT-1 (Guillet et al. 2005). In contrast, Adolph et al. detected an increase in GLAST transport activity in rat primary glial cells treated with the PKA inhibitor H89 (Adolph et al. 2007). This enhanced uptake activity was sensitive to chemical blocking of actin polymerisation by cytochalasin-B, indicating that inhibition of PKA results in increased translocation of GLAST to the plasma membrane (Adolph et al. 2007).

6.1.3 Aims

A number of proteins have been identified that interact with or phosphorylate the EAAT1 C-terminus; however no interacting proteins have yet been identified for the EAAT1 N-terminus or the intracellular loops connecting the transmembrane domains. Furthermore, none of the interacting proteins identified and discussed above have been assessed for their effects on the ion channel activity of the EAATs. The intracellular stretch of amino acids between transmembrane domains 6 and 7 of EAAT1 has been noted to show homology to a motif required for binding of IGF-II

and α-adrenergic receptors to different classes of Gα subunits of heterotrimeric G proteins (Gegelashvili and Schousboe 1998). The objectives of the experiments presented in this chapter are to modify EAAT activity and/or localisation in human osteoblasts using peptides that mimic the intracellular N- and C-termini and the stretch of intracellular amino acids between transmembrane domains 6 and 7. These peptides are expected to compete with full-length EAAT1 for phosphorylation or binding with interacting proteins, and therefore inhibit the effect of intracellular proteins on EAAT1 localisation and/or activity. The effect of these competing peptides on glutamate transport will be assessed by radiolabelled glutamate uptake assay and the effects on bone forming activity will be assessed by measuring cell number, gene expression analysis and ALP activity assay.

6.2 Methods

Sequences of EAAT1 corresponding to N-terminal, transmembrane 6-7 (TM6-7), and C-terminal intracellular domains that were subcloned into pcDNA3.1/V5-His©-TOPO® expression vector (from here on referred to as pcDNA3.1) are detailed in section 2.11 and appendix 9.8. The sequences for EAAT1 N-terminus and C-terminus were cloned into pcDNA3.1 in frame with the vector V5 and His epitope tags (appendix 9.3). The nucleotide sequence of the EcoRV restriction site mutated during cloning of EAAT1 TM6-7, taking the sequence out of frame of the V5 and His epitope tags. The mutation had no effect on the translated sequence of the TM6-7 peptide and introduced new stop codons (shown in appendix 9.3). The general method for transfection of pcDNA3.1 expression vector is detailed in section 2.10.2.

6.2.1 Cell culture and transfection

MG-63 osteoblasts were seeded at 2.6 x 10^4 cells/cm^2 in 96-well plates, 48-well plates, 8-well chamber slides, and 24-well plates. SaOS-2 cells were seeded at 4.2 x 10^4 cells/cm^2 in 96-well plates, 48-well plates, 8-well chamber slides and 24-well plates. At 80% confluence, the cells were transfected with empty pcDNA3.1 vector or pcDNA3.1 vector expressing N-terminal, TM6-7 or C-terminal domains of EAAT1

(section 2.10.2), or left untransfected in DMEM containing 5% dFBS and 50μg/ml ascorbate.

During optimisation, the transfection medium was supplemented with sodium butyrate to increase expression of the peptides (section 6.2.2.2.2). However sodium butyrate alone was found to inhibit EAAT glutamate uptake activity (section 6.3.1.4.3), so was not used in experiments where the effect of inhibiting EAAT1 intracellular domains on EAAT glutamate uptake activity, gene expression, cell number or alkaline phosphatase (ALP) activity was assessed.

6.2.2 Confirmation of transfection

6.2.2.1 mRNA expression

RNA was extracted and reverse transcribed from transfected cells (section 2.3) and amplified (section 2.4.2) using primers against pcDNA3.1 vector that span the cloning site (Table 2.8). These primers yield different sized products depending on the size of the DNA insert (Table 2.9).

6.2.2.1.1 Efficiency of pcDNA3.1 vector expression over time

Cells were transfected in 48-well plates. At 6, 24, 48, and 72hrs post-transfection the medium was aspirated, the cells rinsed with cold PBS and homogenised with 0.1ml TRIzol® reagent per well for 5 min. The plates were stored at -80°C until RNA extractions, reverse transcription and RT-PCR were carried out. RT-PCR (section 6.2.2.1) was carried out using an optimised 25 cycles of amplification to ensure that comparison of band densities by agarose gel electrophoresis (section 2.4.3) occurred during the linear increase in PCR product.

6.2.2.2 Protein expression

6.2.2.2.1 Immunofluorescence

Cells were seeded and transfected in eight-well chamber slides. At 48hrs post-transfection, the cells were washed with PBS and fixed with 4% paraformaldehyde

(appendix 9.1) for 15 min. The cells were then washed for 3 x 5 min with PBS prior to 10 min incubation with 0.2% Triton® X-100 in PBS. Staining and visualisation of the cells was as detailed in section 2.6, substituting mouse-anti-V5 (Invitrogen, Paisley, UK) as the primary antibody at 1:250 in PBS/0.1% Tween®-20 and goat-anti-mouse IgG-FITC conjugate as the secondary antibody at 1:160 in PBS/0.1% Tween®-20. One additional difference to the methodology was that fixed cells were incubated with the primary antibody for 1hr at room temperature as opposed to overnight at 4°C. Primary negative controls were performed to confirm that staining was not a result of non-specific binding of the secondary antibody.

6.2.2.2.2 Induction of expression using sodium butyrate

Since no immunoreactive proteins were detected using an antibody against the V5 epitope, sodium butyrate, a histone deacetylase (HDAC) inhibitor (Davie 2003) that can enhance gene expression controlled by mammalian promoters, such as cytomegalovirus (CMV), in various different cell types (Cockett et al. 1990; Laubach et al. 1996; Shimizu et al. 1997; Chang et al. 1999; Lai et al. 2009) was used.

6.2.2.2.2.1 Effect of sodium butyrate on viable adherent cell number

Since sodium butyrate can significantly induce apoptotic cell death in various cell types (Chang et al. 1999), the effect of sodium butyrate on viable adherent cell number was assessed. To assess the cytotoxic effects of sodium butyrate, cells were incubated with varying concentrations of sodium butyrate for 48hrs. Cells were seeded in 96-well plates and at 80% confluence; cells were incubated with sodium butyrate (0-100mM) in antibiotic-free DMEM containing 5% dFBS and 50µg/ml ascorbate. After 48hrs, the medium was aspirated and the cells rinsed with cold PBS prior to lysis with 100µl/well lysis buffer (section 2.5.1). 50µl of lysate was taken for LDH assay of cell number (section 2.5.3).

6.2.2.2.2.2 Effect of sodium butyrate on Na^+-dependent glutamate uptake

To determine the effect of sodium butyrate on endogenous EAAT activity, cells were seeded in 24-well plates and at 80% confluence; cells were incubated with 10mM

sodium butyrate in antibiotic-free DMEM containing 5% dFBS and 50μg/ml ascorbate. Cells were cultured for 48hrs in total, however medium was changed in replicate cultures at 8 and 24hrs and replaced with fresh antibiotic-free DMEM containing 5% dFBS and 50μg/ml ascorbate but lacking sodium butyrate. At 48hrs, glutamate uptake activity was assayed in the presence and absence of Na^+ to determine Na^+-dependent uptake (section 2.8 and section 6.2.3 below) and activity was compared to control cells cultured for 48hrs in the absence of sodium butyrate.

6.2.3 Effect of inhibition of EAAT1 intracellular interactions on Na^+-dependent glutamate uptake

Cells were transfected in 24-well plates (section 2.10.2 and 6.2.1). At 48hrs post-transfection, glutamate uptake activity was assayed in the presence and absence of Na^+ to determine Na^+-dependent uptake (section 2.8). Culture medium was aspirated and the cells pre-incubated with KRH buffer (+ Na^+) for 1hr and then the buffer aspirated and replaced with KRH buffer (± Na^+) containing a mix of radiolabelled and unlabelled glutamate at 10μM (Table 2.4) for 10 min. Uptake activity was normalised to total protein content determined by BCA assay from parallel cultures (section 2.5.2 and 2.8.2).

6.2.4 Effect of inhibition of EAAT1 intracellular interactions on gene expression

Cells were transfected in 24-well plates (section 2.10.2 and 6.2.1). At 24hrs post-transfection, the medium of replicate cultures was supplemented with 500μM glutamate. After a further 24hrs (i.e. 48hrs post-transfection) the medium was aspirated, cells rinsed with cold PBS and homogenised with 0.2ml TRIzol® reagent per well for 5 min. The plates were stored at -80°C until RNA extractions, reverse transcription and QRT-PCR amplifications were carried out (section 2.3 and 2.4.4) using primers against osteocalcin, osteonectin, osteoprotegerin (OPG), alkaline phosphatase (ALP), 18S rRNA, GAPDH and HPRT1 (Table 2.1). Gene expression for MG-63 and SaOS-2 cells was normalised to GAPDH and HPRT1 respectively, the most stable housekeeping genes of the three as determined using geNorm software for this experiment (Vandesompele et al. 2002). Relative QRT-PCR was carried out

(section 2.4.4.5) using the Applied Biosystems 7900HT Fast Real-Time PCR system (section 2.4.4.1.2) in conjunction with cDNA standard curves (section 2.4.4.2.2). All values were expressed relative to control cells transfected with the empty vector at 0μM glutamate.

6.2.5 Effect of inhibition of EAAT1 intracellular interactions on cell number and ALP activity

Cells were transfected in 24-well plates (section 2.10.2 and 6.2.1). At 24hrs post-transfection, the medium of replicate wells was supplemented with 500μM glutamate. After a further 24hrs (i.e. 48hrs post-transfection) the medium was aspirated and the cells rinsed with cold PBS prior to lysis with 100μl/well lysis buffer (section 2.5.1). 5μl of lysate was taken for assays of cell number (LDH Cytotox96 assay) and ALP activity (SaOS-2 cells only) (sections 2.5.3 and 2.5.4).

6.2.6 Statistics

Cells transfected with pcDNA3.1 vector expressing EAAT1 intracellular domains were compared to empty vector control cells. Statistical comparison between untransfected and empty vector control cells was also carried out to display any non-specific effects of vector transfection

6.3 Results

6.3.1 Confirmation of pcDNA3.1 vector transfection

6.3.1.1 mRNA expression

RNA isolated from MG-63 cells transfected with empty pcDNA3.1 vector or the same vector expressing EAAT1 C-terminal, N-terminal or TM6-7 intracellular domains for 6, 24 and 48hrs was reverse transcribed and amplified with primers against pcDNA3.1 vector that span the cloning site. Transfection and expression of the appropriate vector was confirmed by the presence of the correct sized transcript at each time-point (Figure 6.2).

6.3.1.2 Efficiency of pcDNA3.1 vector expression over time

In order to define the optimum time post-transfection for osteoblast phenotypic assays to be carried out; the efficiency of vector expression was observed over time (6-72hrs) by limited cycle RT-PCR and resolution of DNA products using agarose gels (Figure 6.3). Only MG-63 and SaOS-2 cells transfected with the empty vector were used to assess expression over time since it was assumed that similar conditions would apply to all the expression vectors cloned.

Expression of the vector was detected at all time-points assayed and the highest expression appeared to be at 24 and 48hrs post-transfection, consistent with the time-points of maximum exon skipping observed in optimisation experiments in chapter 5 (section 5.3.2.1). These results and the desire to design an experiment that would be directly comparable to the experiments in chapter 5 led to the decision to assay cells at 48hrs post-transfection and to assess the effect of extracellular glutamate on transfected cells by adding glutamate 24hrs post-transfection, when vector expression is likely to be high.

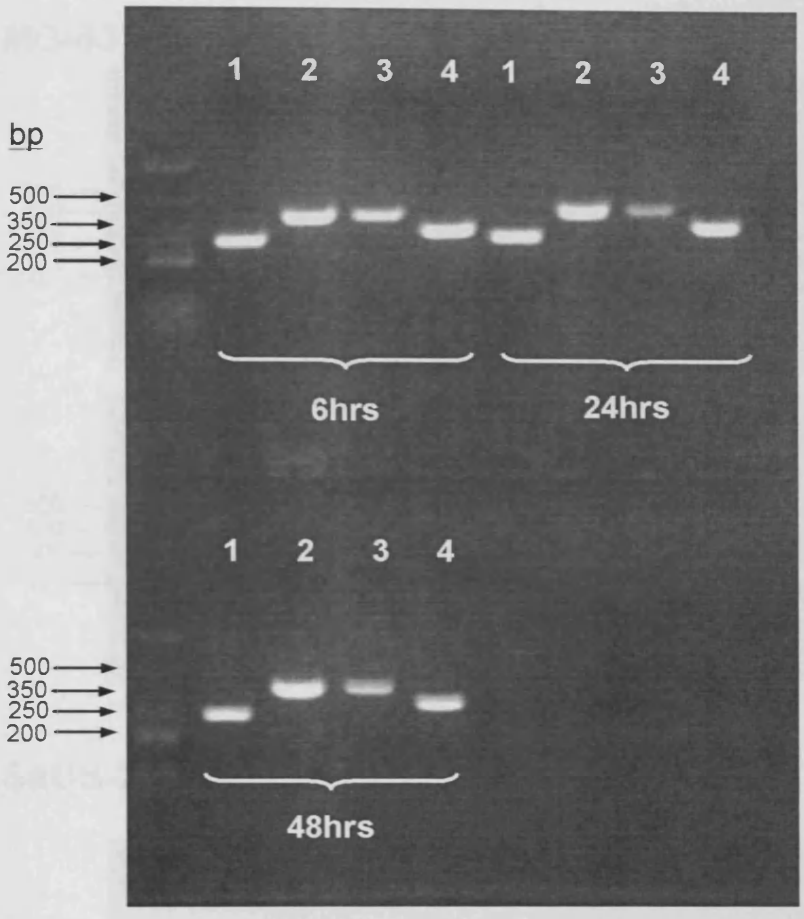

Figure 6.2. Expression of pcDNA3.1 vector in MG-63 cells. Empty pcDNA3.1 and pcDNA3.1 vector containing EAAT1 N-terminal, C-terminal and TM6-7 intracellular domains were transfected into MG-63 cells and RNA extracted at 6, 24 and 48hrs for reverse transcription and amplification by RT-PCR using primers that span the vector cloning site. Products were resolved on an agarose gel alongside a low molecular weight DNA ladder. 1. Empty vector (246bp), 2. N-terminal (398bp), 3. C-terminal (410bp), 4. TM6-7 (329bp).

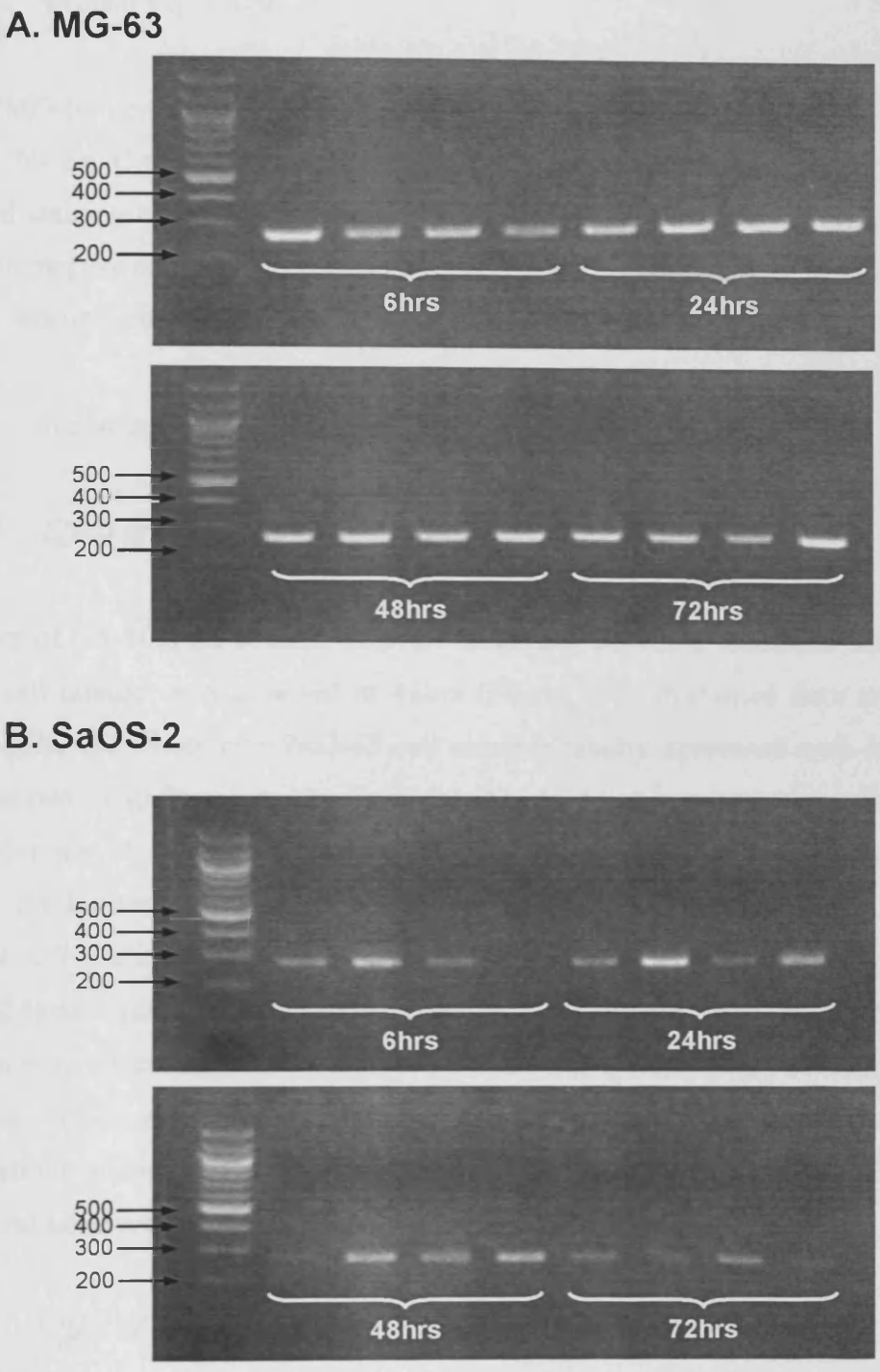

Figure 6.3. Expression of pcDNA3.1 vector (containing no insert) over 72hrs. Empty pcDNA3.1 vector was transfected into (A) MG-63 and (B) SaOS-2 cells. RNA was extracted at 6, 24, 48 and 72hrs for reverse transcription and amplification by 25 cycles of RT-PCR using primers that span the vector cloning site. Products were resolved on an agarose gel alongside a 100bp DNA ladder. Empty vector (246bp).

6.3.1.3 Protein expression

Neither MG-63 nor SaOS-2 cells transfected with pcDNA3.1 vector expressing the EAAT1 N- or C-terminal and stained for immunoreactivity to the V5 epitope displayed staining beyond that detected in the primary-negative control (not shown). In an attempt to enhance expression of the EAAT1 peptides, the use of sodium butyrate was investigated as a supplement to the transfection medium.

6.3.1.4 Induction of expression using sodium butyrate

6.3.1.4.1 Effect of sodium butyrate on viable adherent cell number

The effect of 0.5-100mM sodium butyrate treatment on viable adherent MG-63 and SaOS-2 cell number was assessed at 48hrs (Figure 6.4). Presented data are from a single experiment where n=3. MG-63 cell number rapidly decreased with increasing concentrations of sodium butyrate up to 10mM. At 10mM sodium butyrate, MG-63 cell number was 48 ± 0.7 % of control cells. At concentrations above 10mM sodium butyrate, no further decrease in MG-63 cell number was observed. SaOS-2 cell number at 0.5 and 2mM sodium butyrate was slightly increased to 107 ± 4.4 % and 114 ± 4.2 % of control cells respectively. SaOS-2 cell number then rapidly decreased at sodium butyrate concentrations between 2 and 10mM, with 10mM sodium butyrate decreasing viable adherent cell number to 15 ± 0.7 % of control cells. At concentrations above 10mM sodium butyrate, no further decrease in SaOS-2 cell number was observed.

6.3.1.4.2 Effect of 10mM sodium butyrate on pcDNA3.1 vector expression

MG-63 cell number was less affected by sodium butyrate toxicity than SaOS-2 cells. These cells were therefore transfected with pcDNA3.1 vector expressing EAAT1 N- or C-terminal for 48hrs in the presence of 0 and 10mM sodium butyrate. A concentration of 10mM sodium butyrate was chosen to maximise vector expression. Transfected cells were stained for the V5 epitope (Figure 6.5).

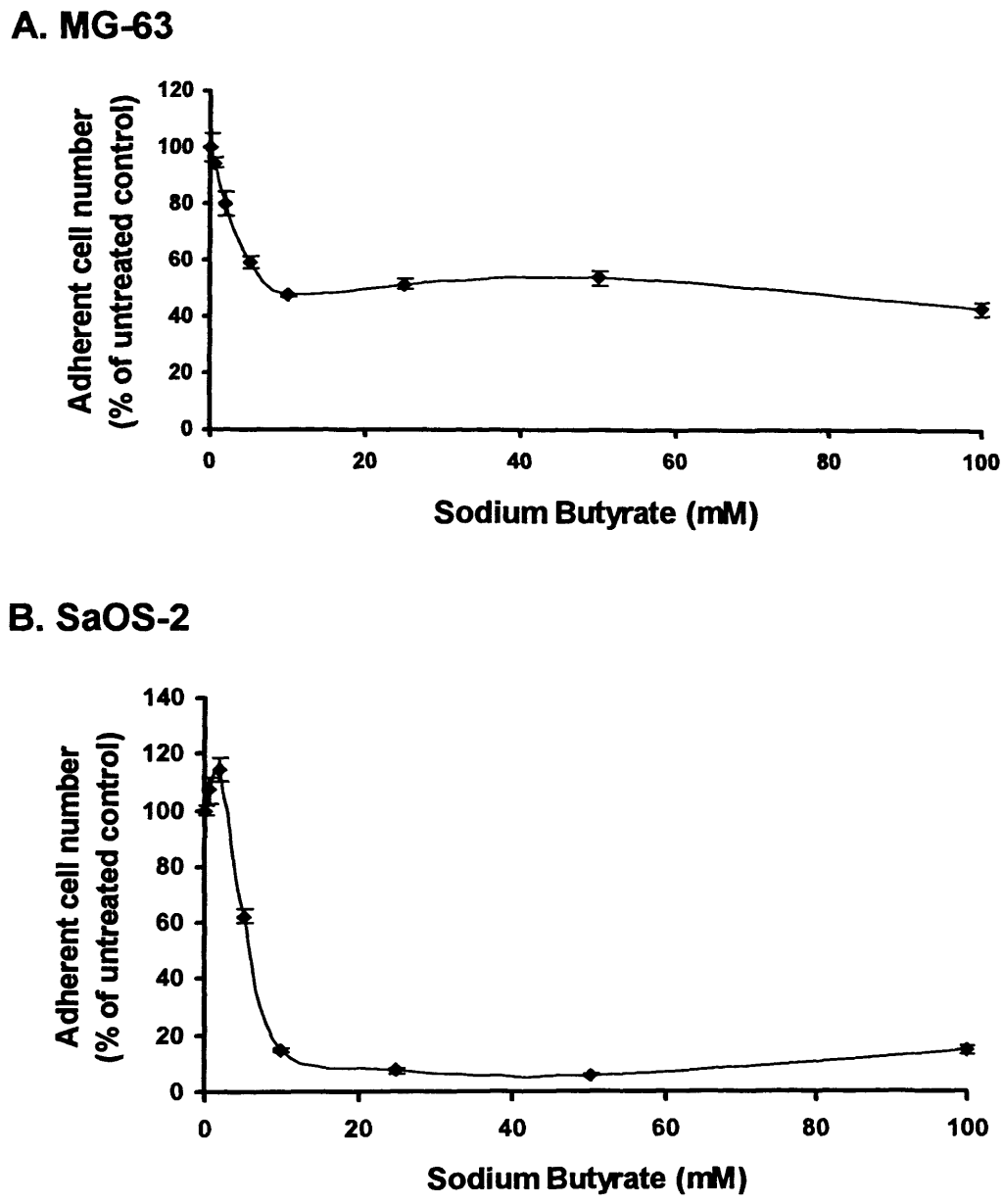

Figure 6.4. Effect of sodium butyrate on osteoblast viable cell number over 48hrs. MG-63 (A) and SaOS-2 (B) osteoblast-like cells were incubated with 0-100mM sodium butyrate for 48hrs. Adherent cell number was assayed by measuring LDH released upon total lysis of viable adherent cells and expressed as the mean percentage of LDH activity in viable adherent control cells (0mM sodium butyrate) ± S.E.M from a single experiment, n=3.

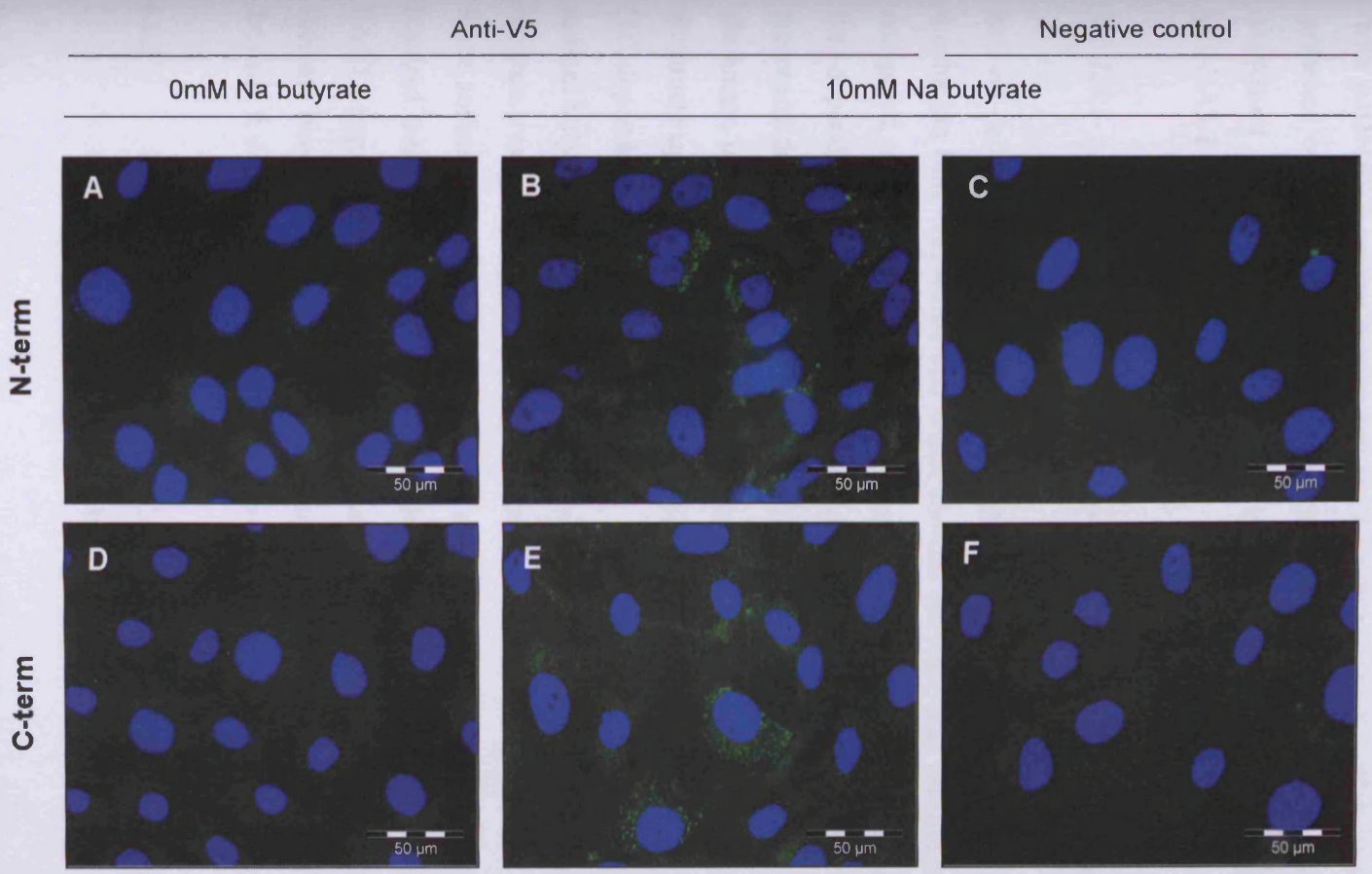

Figure 6.5. Immunoreactivity for the V5 epitope in MG-63 cells transfected with pcDNA3.1 vector containing EAAT1 intracellular domains. MG-63 cells were transfected with pcDNA3.1 vector containing EAAT1 N-terminal (A-C) and C-terminal (D-F) domains in the presence of 0 or 10mM sodium butyrate for 48hrs. Cells were immunostained for the V5 epitope tag on the expressed peptide (A,B,D,E). Transfected cells (C,F) were also probed with secondary antibody alone to determine levels of non-specific staining. Pictures were taken under 800ms exposure.

In the absence of sodium butyrate, no immunoreactivity for the V5 epitope above that detected in the primary-negative control was detected in MG-63 cells transfected with pcDNA3.1 vector expressing EAAT1 N- or C-terminal (Figure 6.5A,D). However, immunoreactivity for the V5 epitope was clearly detected in MG-63 cells transfected with pcDNA3.1 vector expressing EAAT1 N-terminal or C-terminal domains in the presence of 10mM sodium butyrate (Figure 6.5B,E), indicating that the peptide is expressed and that 10mM sodium butyrate does enhance expression from the pcDNA3.1 vector CMV promoter.

6.3.1.4.3 Effect of sodium butyrate on Na^+-dependent glutamate uptake

MG-63 cells were incubated with 10mM sodium butyrate for 8, 24 and 48hrs. Total incubation time was 48hrs and when sodium butyrate was removed prior to the 48hrs end-point, culture medium was replaced with fresh sodium butyrate-free medium. Na^+-dependent glutamate uptake was normalised to total cellular protein (mg) and presented data are from a single experiment where n=4 (Figure 6.6). Na^+-dependent glutamate uptake in sodium butyrate treated cells was compared to Na^+-dependent glutamate uptake in untreated cells at 48hrs.

Na^+-dependent glutamate uptake was significantly reduced in cells treated with sodium butyrate for 24 and 48hrs (one-way ANOVA $P<0.001$), however 8hrs sodium butyrate treatment did not affect glutamate uptake.

Since sodium butyrate treatment alone significantly reduced EAAT activity over the required treatment time of 48hrs, and the aim of these experiments was to modulate EAAT1 expression/activity using intracellular peptides, it was concluded that sodium butyrate treatment would significantly compromise interpretation of the experimental data and it was not used in any further experiments.

6.3.2 Effect of inhibition of EAAT1 intracellular interactions on Na^+-dependent glutamate uptake

Na^+-dependent glutamate uptake was measured in MG-63 and SaOS-2 osteoblast-like cells 48hrs post-transfection with empty pcDNA3.1 vector or the same vector expressing EAAT1 N-terminal, TM6-7 or C-terminal intracellular domains. Na^+-dependent glutamate uptake was also measured in untransfected cells under the same

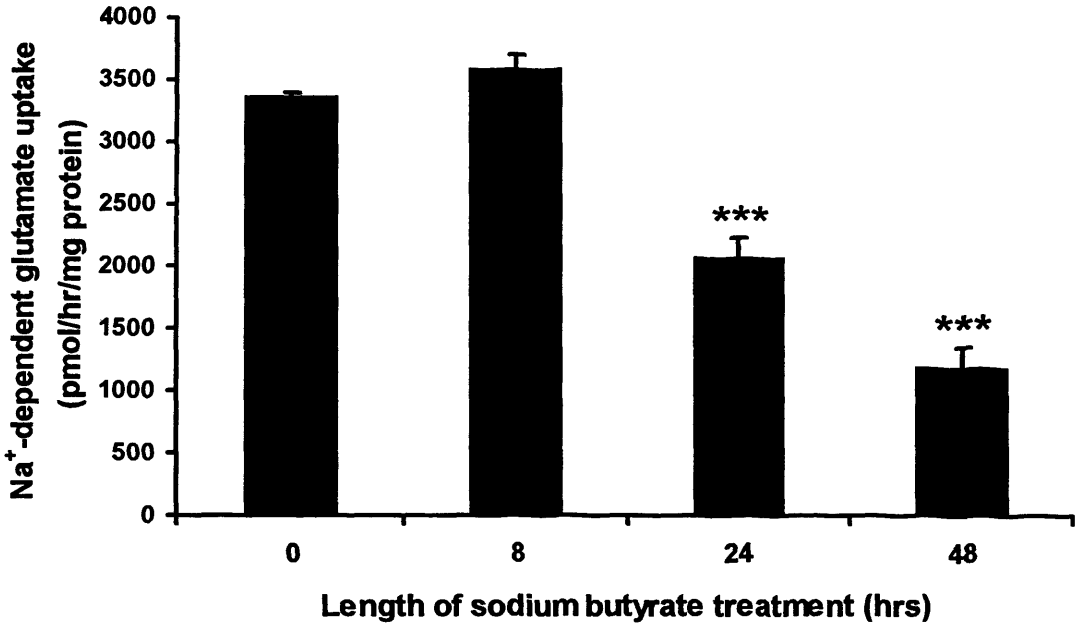

Figure 6.6. Effect of sodium butyrate on Na^+-dependent glutamate uptake in MG-63 cells over time. MG-63 cells were incubated with 10mM sodium butyrate and cultured for 48hrs; however medium was changed in replicate cultures at 8 and 24hrs and replaced with fresh medium. At 48hrs, cells were incubated with 10μM mix of radiolabelled and unlabelled glutamate at 37°C for 10 min in KRH buffer ± Na^+, followed by aspiration of the buffer and rinsing with cold KRH containing 1.5mM unlabelled glutamate. Na^+-dependent glutamate uptake was normalised to total cellular protein (mg). Values are mean ± S.E.M from a single experiment where n=4. MG-63 Na^+-dependent glutamate uptake was significantly reduced by 10mM sodium butyrate treatment for 24 and 48hrs (one-way ANOVA $P<0.001$). Significance values ***$P<0.001$.

conditions to determine the effects of the transfection procedure. Na^+-dependent glutamate uptake was normalised to total cellular protein (mg) and expressed as a percentage of empty vector control cells. Presented data are from three independent experiments where n=3.

6.3.2.1 MG-63

In transfected MG-63 cells, Na^+-dependent glutamate uptake was not significantly affected by expression of EAAT1 intracellular domains (Kruskal Wallis P=0.260) (Figure 6.7). Although not significant, a trend for increased glutamate uptake activity was observed in cells expressing EAAT1 N-terminal, TM6-7, and C-terminal intracellular domains to 140 ± 12.3 %, 144 ± 19.3 %, and 130 ± 14.8 % of empty vector controls respectively.

Na^+-dependent glutamate uptake was significantly decreased in empty vector control cells relative to untransfected cells (one-way ANOVA P=0.031).

6.3.2.2 SaOS-2

In transfected SaOS-2 cells, Na^+-dependent glutamate uptake was not significantly affected by expression of EAAT1 intracellular domains (Kruskal Wallis P=0.084) (Figure 6.8). Although not significant, a trend for decreased glutamate uptake activity was observed in cells expressing EAAT1 N-terminal, TM6-7, and C-terminal intracellular domains to 90 ± 5.7 %, 85 ± 5.0 %, and 95 ± 4.2 % of empty vector controls respectively.

Na^+-dependent glutamate uptake was significantly increased in empty vector control cells relative to untransfected cells (Kruskal Wallis P=0.001).

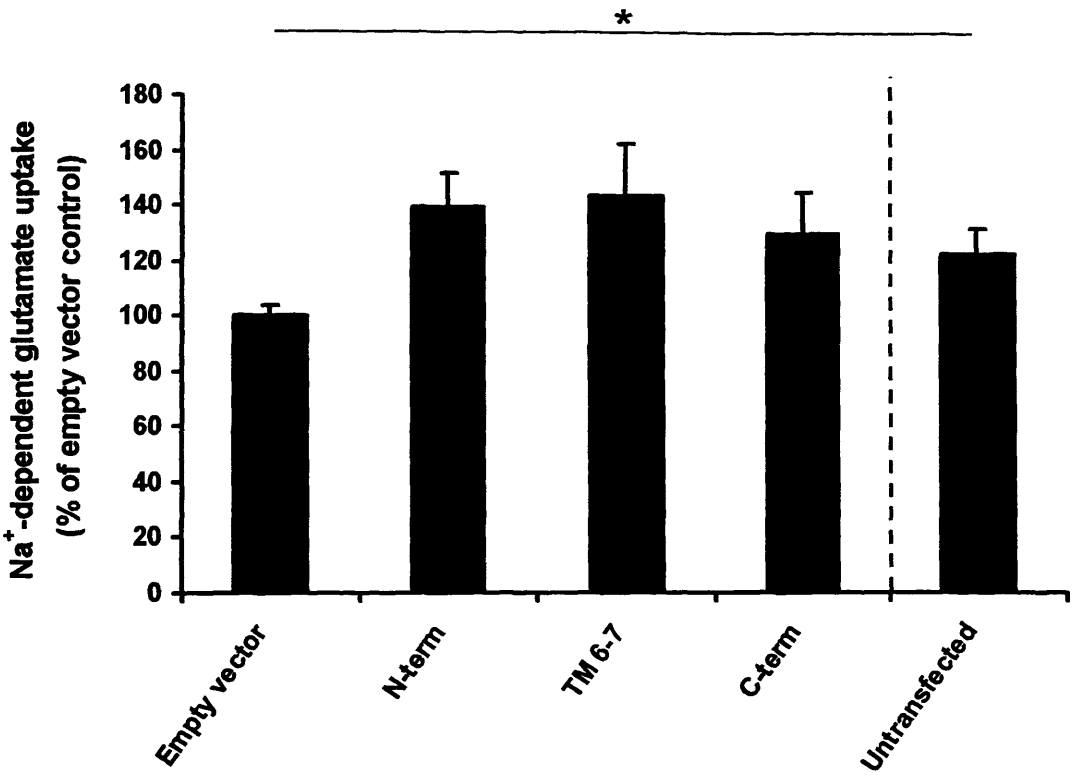

Figure 6.7. Effect of inhibition of EAAT1 intracellular interactions on Na^+-dependent glutamate uptake in MG-63 cells. MG-63 cells were transfected with empty pcDNA3.1 or pcDNA3.1 vector containing each EAAT1 intracellular domain for 48hrs. MG-63 cells were then incubated with 10μM mix of radiolabelled and unlabelled glutamate at 37°C for 10 min in KRH buffer ± Na^+, followed by aspiration of the buffer and rinsing with cold KRH containing 1.5mM unlabelled glutamate. Na^+-dependent glutamate uptake was normalised to total cellular protein (mg) and expressed as a percentage of empty vector control cells. Values are mean ± S.E.M from three independent experiments where n=3. Na^+-dependent glutamate uptake was not significantly affected by expression of EAAT1 intracellular domains (Kruskal Wallis P=0.260), however, Na^+-dependent glutamate uptake was significantly decreased by transfection with pcDNA3.1 relative to untransfected cells (one-way ANOVA P=0.031). Significance values *P<0.05.

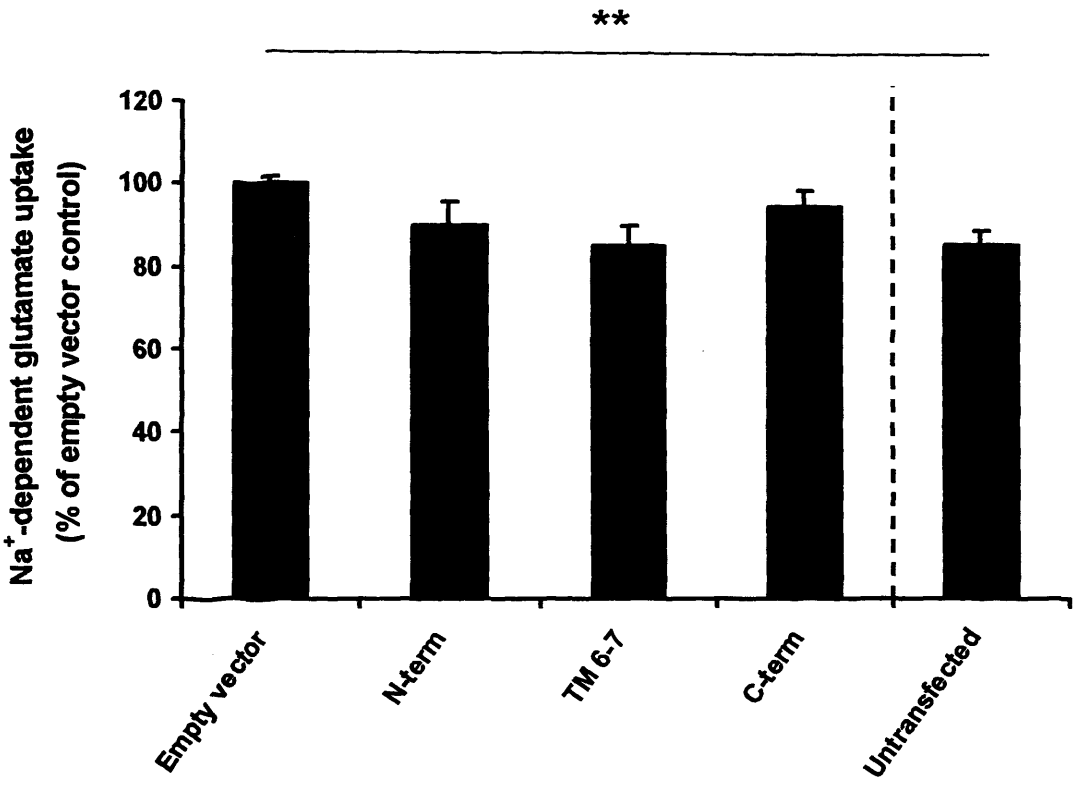

Figure 6.8. Effect of inhibition of EAAT1 intracellular interactions on Na^+-dependent glutamate uptake in SaOS-2 cells. SaOS-2 cells were transfected with empty pcDNA3.1 or pcDNA3.1 vector containing each EAAT1 intracellular domain for 48hrs. SaOS-2 cells were then incubated with 10μM mix of radiolabelled and unlabelled glutamate at 37°C for 10 min in KRH buffer ± Na^+, followed by aspiration of the buffer and rinsing with cold KRH containing 1.5mM unlabelled glutamate. Na^+-dependent glutamate uptake was normalised to total cellular protein (mg) and expressed as a percentage of empty vector control cells. Values are mean ± S.E.M from three independent experiments where n=3. Na^+-dependent glutamate uptake was not significantly affected by expression of EAAT1 intracellular domains (Kruskal Wallis P=0.084), however, Na^+-dependent glutamate uptake was significantly increased by transfection with pcDNA3.1 relative to untransfected cells (Kruskal Wallis P=0.001). Significance values $^{**}P<0.01$.

6.3.3 Effect of inhibition of EAAT1 intracellular interactions on cell number

MG-63 and SaOS-2 cells were transfected with empty pcDNA3.1 or pcDNA3.1 vector containing EAAT1 N-terminal, TM6-7, and C-terminal intracellular domains for 48hrs. 500μM glutamate was added to replicate cultures 24hrs post-transfection. Adherent cell number was assayed by measuring LDH released upon total lysis of viable adherent cells and expressed as a percentage of LDH activity of viable adherent control cells (empty vector, no glutamate). Presented data are from three independent experiments where n=3.

6.3.3.1 MG-63

In transfected MG-63 cells, cell number was significantly affected by expression of EAAT1 intracellular domains (Shierer Ray $P<0.001$) but not by 500μM glutamate (Shierer Ray $P=0.976$) and there was no interaction between the two factors (Shierer Ray $P=0.580$) (Figure 6.9). Post-hoc pair-wise comparisons (Mann Whitney U tests) revealed that, compared to empty vector controls at 500μM glutamate, cell number was significantly increased by transfection with pcDNA3.1 vector expressing EAAT1 C-terminal domain from 93 ± 3.8 % to 115 ± 3.5 % ($P=0.003$). Cell number was also increased by this treatment at 0μM glutamate to 109 ± 4.3 % of empty vector controls, however this did not reach statistical significance ($P=0.133$).

Transfection with pcDNA3.1 empty vector significantly decreased MG-63 cell number relative to untransfected cells (Shierer Ray $P<0.001$) and post-hoc comparisons (Mann Whitney U tests) revealed that this occurred at both 0μM and 500μM glutamate ($P<0.001$ and $P=0.008$ respectively).

6.3.3.2 SaOS-2

In transfected SaOS-2 cells, cell number was not significantly affected by expression of EAAT1 intracellular domains (Shierer Ray $P=0.123$) or by 500μM glutamate (Shierer Ray $P=0.455$) and there was no interaction between the two factors (Shierer Ray $P=0.837$) (Figure 6.10). Transfection with pcDNA3.1 had no significant effect on SaOS-2 cell number relative to untransfected cells (GLM $P=0.604$).

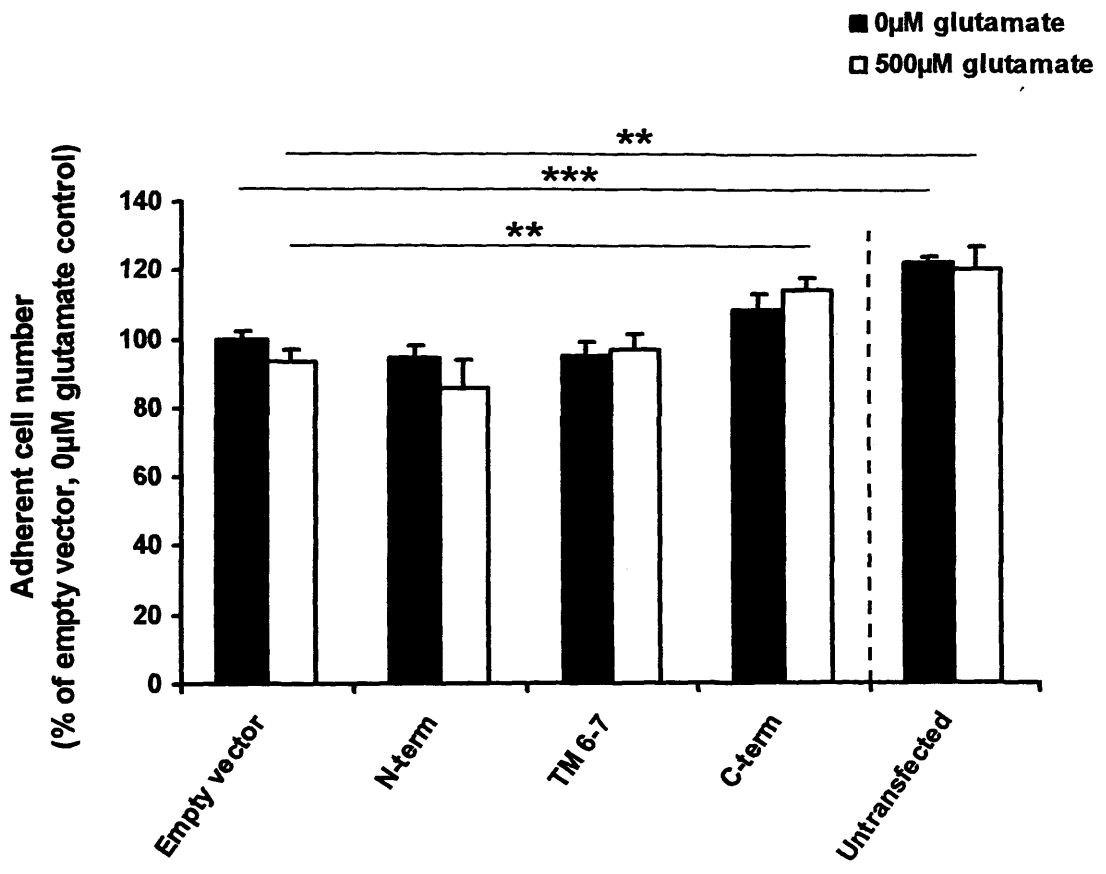

Figure 6.9. Effect of inhibition of EAAT1 intracellular interactions on MG-63 osteoblast-like cell number over 48hrs. MG-63 cells were transfected with empty pcDNA3.1 or pcDNA3.1 vector containing each EAAT1 intracellular domain for 48hrs. Adherent cell number was assayed by measuring LDH released upon total lysis of viable adherent cells and expressed as the mean percentage of LDH activity of viable adherent control cells (empty vector, no glutamate) ± S.E.M from three independent experiments, n=3. MG-63 cell number was significantly affected by expression of EAAT1 intracellular domains (Shierer Ray $P<0.001$), but not by glutamate concentration. Post-hoc pair-wise Mann Whitney U tests revealed that cell number was significantly increased in MG-63 cells transfected with pcDNA3.1 vector expressing EAAT1 C-terminal domain compared to empty vector controls at 500μM glutamate. Transfection with pcDNA3.1 significantly decreased MG-63 cell number relative to untransfected cells (Shierer Ray $P<0.001$). Significance values $^{**}P<0.01$, $^{***}P<0.001$.

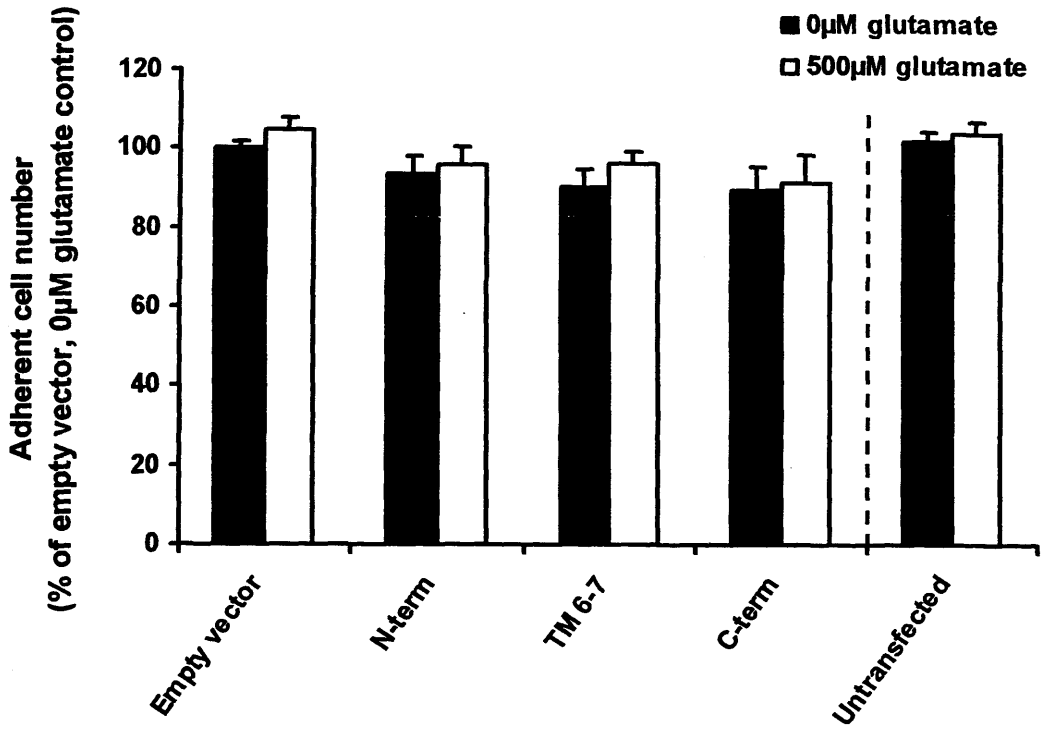

Figure 6.10. Effect of inhibition of EAAT1 intracellular interactions on SaOS-2 osteoblast-like cell number over 48hrs. SaOS-2 cells were transfected with empty pcDNA3.1 or pcDNA3.1 vector containing each EAAT1 intracellular domain for 48hrs. Adherent cell number was assayed by measuring LDH released upon total lysis of viable adherent cells and expressed as the mean percentage of LDH activity of viable adherent control cells (empty vector, no glutamate) ± S.E.M from three independent experiments, n=3. SaOS-2 cell number was not significantly affected by expression of EAAT1 intracellular domains or glutamate (Shierer Ray test). Empty vector transfection did not affect SaOS-2 cell number relative to untransfected cells (GLM).

6.3.4 Effect of inhibition of EAAT1 intracellular interactions on gene expression

MG-63 and SaOS-2 cells were transfected with empty pcDNA3.1 or pcDNA3.1 vector containing EAAT1 N-terminal, TM6-7, and C-terminal intracellular domains for 48hrs. 500μM glutamate was added to replicate cultures 24hrs post-transfection. Expression levels of osteocalcin, osteonectin, OPG and ALP were quantified by QRT-PCR and expressed as a percentage of gene expression in control cells (empty vector, no glutamate). Presented data are from three independent experiments where n=3.

6.3.4.1 Osteocalcin

6.3.4.1.1 MG-63

In transfected MG-63 cells, osteocalcin expression was significantly affected by expression of EAAT1 intracellular domains (GLM P=0.001) but not by 500μM glutamate (GLM P=0.480) and there was no interaction between the two factors (GLM P=0.458) (Figure 6.11A). Post-hoc comparisons (Tukey's tests) did not reveal any pair-wise significance between cells transfected with pcDNA3.1 expressing EAAT1 intracellular domains compared to empty vector control cells at the 5% level. However compared to empty vector control cells at 0μM glutamate, osteocalcin levels were increased in cells transfected with pcDNA3.1 vector containing EAAT1 N-terminal domain to 125 ± 13.6 % and decreased in cells transfected with pcDNA3.1 vector containing EAAT1 TM6-7 and C-terminal domain to 79 ± 7.9 % to 83 ± 9.7 % respectively. Transfection with pcDNA3.1 had no significant effect on MG-63 osteocalcin expression relative to untransfected cells (GLM with ranked data P=0.951).

6.3.4.1.2 SaOS-2

In transfected SaOS-2 cells, osteocalcin expression was significantly affected by expression of EAAT1 intracellular domains (GLM P=0.028) but not by 500μM glutamate (GLM P=0.656) and there was no interaction between the two factors (GLM P=0.578) (Figure 6.11B). Post-hoc comparisons (Tukey's tests) did not reveal

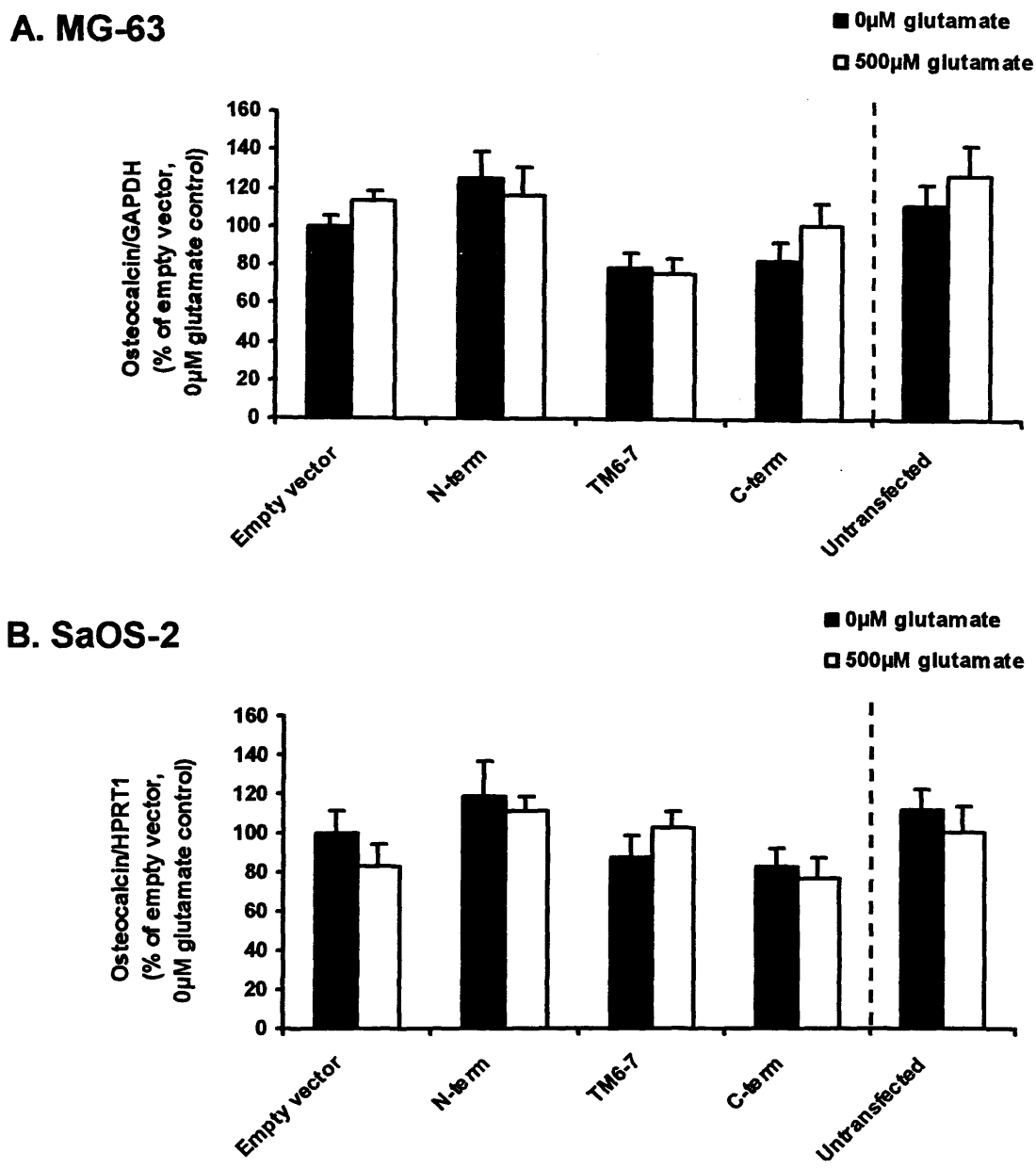

Figure 6.11. Effect of inhibition of EAAT1 intracellular interactions on osteocalcin mRNA expression in osteoblast-like cells at 48hrs post-transfection. Osteoblast-like cells (A, MG-63; B, SaOS-2) were transfected with empty pcDNA3.1 or pcDNA3.1 vector containing each EAAT1 intracellular domain for 48hrs and expression of mRNA for osteocalcin was assessed by QRT-PCR. Osteocalcin levels were normalised to housekeeping gene levels and expressed as the mean percentage change over control cells (empty vector, no glutamate) ± S.E.M from three independent experiments, n=3. MG-63 and SaOS-2 osteocalcin levels were significantly affected by expression of EAAT1 intracellular domains (GLM P=0.001 (MG-63) and P=0.028 (SaOS-2)), however no pair-wise Tukey's comparisons were statistically significant. Vector transfection did not affect osteocalcin expression relative to untransfected cells in MG-63 or SaOS-2 cells (GLM).

any pair-wise significance between groups transfected with the vector at the 5% level. However compared to empty vector control cells at 0μM glutamate, mean osteocalcin levels were decreased in cells expressing EAAT1 C-terminal domain at 0μM glutamate to 83 ± 9.7 % and compared to empty vector control cells at 500μM glutamate, mean osteocalcin levels were increased in cells expressing EAAT1 N-terminal domain at 500μM glutamate from 83 ± 11.0 % to 112 ± 7.5 %. Transfection with pcDNA3.1 had no significant effect on SaOS-2 osteocalcin expression relative to untransfected cells (GLM P=0.210).

6.3.4.2 Osteonectin

6.3.4.2.1 MG-63

In transfected MG-63 cells, osteonectin expression was not significantly affected by expression of EAAT1 intracellular domains (GLM with ranked data P=0.544) or by 500μM glutamate (GLM with ranked data P=0.557) and there was no interaction between the two factors (GLM with ranked data P=0.800) (Figure 6.12A). However, transfection with pcDNA3.1 empty vector resulted in an increase in osteonectin mRNA levels relative to untransfected cells (Shierer Ray P=0.003). Post-hoc pair-wise comparisons (Mann Whitney U tests) revealed pair-wise significance for this increase at 0μM (P=0.006) but not at 500μM glutamate (P=0.194).

6.3.4.2.2 SaOS-2

In transfected SaOS-2 cells, osteonectin expression was not significantly affected by expression of EAAT1 intracellular domains (GLM P=0.446) or by 500μM glutamate (GLM P=0.136) and there was no interaction between the two factors (GLM P=0.990) (Figure 6.12B). However, transfection with pcDNA3.1 resulted in a non-specific increase in osteonectin mRNA levels relative to untransfected cells (GLM with log data P=0.028). Post-hoc pair-wise comparisons (Tukey's tests) did not reveal pair-wise significance for this increase at 0μM (P=0.192) or 500μM glutamate (P=0.618).

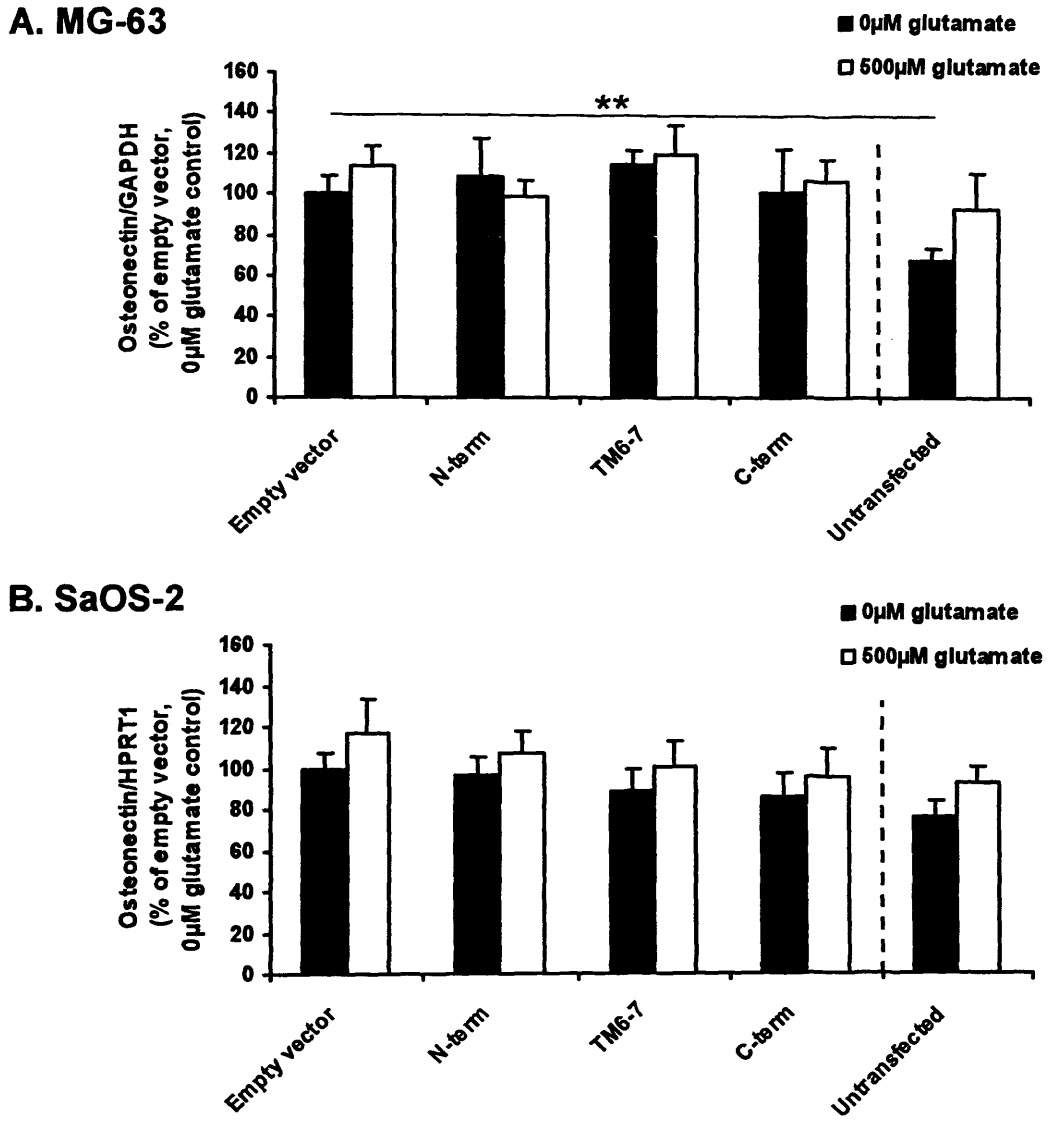

Figure 6.12. Effect of inhibition of EAAT1 intracellular interactions on osteonectin mRNA expression in osteoblast-like cells at 48hrs post-transfection. Osteoblast-like cells (A, MG-63; B, SaOS-2) were transfected with empty pcDNA3.1 or pcDNA3.1 vector containing each EAAT1 intracellular domain for 48hrs and expression of mRNA for osteonectin was assessed by QRT-PCR. Osteonectin levels were normalised to housekeeping gene levels and expressed as the mean percentage change over control cells (empty vector, no glutamate) ± S.E.M from three independent experiments, n=3. Osteonectin expression was not significantly affected by expression of EAAT1 intracellular domains or glutamate in MG-63 cells or SaOS-2 cells (GLM). Transfection with empty pcDNA3.1 significantly increased osteonectin expression relative to untransfected cells in both MG-63 and SaOS-2 cells (Shierer Ray test P=0.003 and GLM P=0.028 respectively). Pair-wise significance for this increase was only observed in MG-63 cells at 0μM glutamate. Significance values $**P<0.01$.

6.3.4.3 OPG

6.3.4.3.1 MG-63

In transfected MG-63 cells, OPG expression was not significantly affected by expression of EAAT1 intracellular domains (Shierer Ray P=0.290) or by 500μM glutamate (Shierer Ray P=0.496) and there was no interaction between the two factors (Shierer Ray P=0.890) (Figure 6.13A). However, transfection with pcDNA3.1 resulted in a non-specific increase in OPG mRNA relative to untransfected cells (GLM P<0.001) and post-hoc comparisons (Tukey's tests) revealed that this occurred at both 0μM and 500μM glutamate (P=0.018 and P=0.024 respectively).

6.3.4.3.2 SaOS-2

In transfected SaOS-2 cells, OPG expression was significantly affected by expression of EAAT1 intracellular domains (GLM with ranked data P=0.030) but not by 500μM glutamate (GLM with ranked data P=0.142) and there was no interaction between the two factors (GLM with ranked data P=0.392) (Figure 6.13B). Compared to empty vector control cells at 0μM glutamate, mean OPG expression was decreased in cells expressing EAAT1 N-terminal (P=0.267), TM6-7 (P=0.213), and C-terminal (P=0.192) domains, although post-hoc pair-wise comparisons (Tukey's tests) were not significant. Each peptide had different effects at 500μM glutamate.

Transfection with pcDNA3.1 resulted in a non-specific increase in OPG mRNA levels relative to untransfected cells (GLM with ranked data P<0.001). Post-hoc pair-wise comparisons (Tukey's tests) revealed pair-wise significance for this increase at 0μM (P<0.001), but not at 500μM glutamate (P=0.386). A significant effect of the interaction between transfection and glutamate was also apparent between untransfected and empty vector control cells (GLM with ranked data P=0.049). This reflects the increased OPG expression in response to 500μM glutamate observed in untransfected cells (Tukey's P=0.140) which is lost in empty vector transfected cells (Tukey's P=0.903) due to the non-specific increase in OPG expression as a result of transfection.

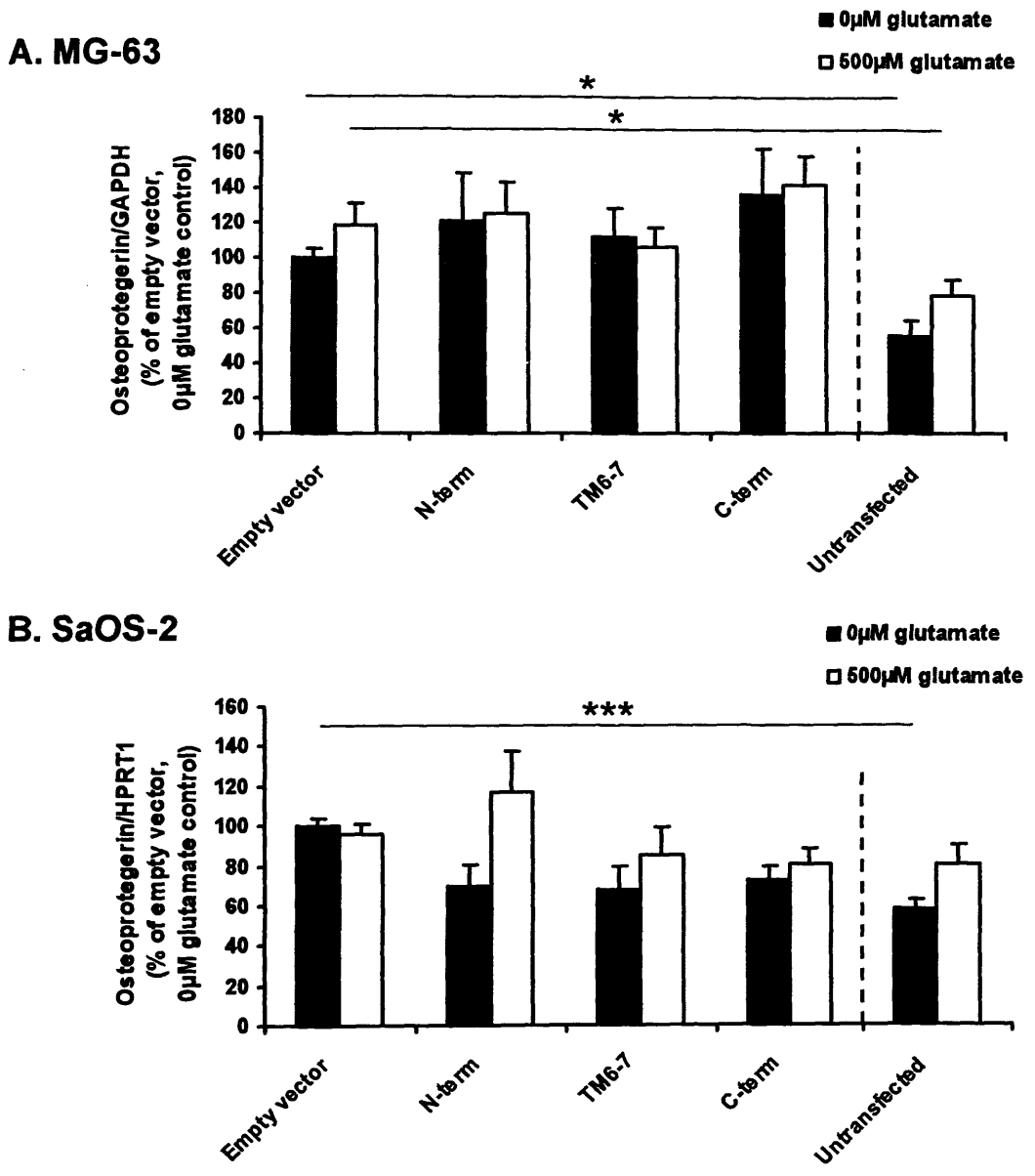

Figure 6.13. Effect of inhibition of EAAT1 intracellular interactions on osteoprotegerin (OPG) mRNA expression in osteoblast-like cells at 48hrs post-transfection. Osteoblast-like cells (A, MG-63; B, SaOS-2) were transfected with empty pcDNA3.1 or pcDNA3.1 vector containing each EAAT1 intracellular domain for 48hrs and expression of mRNA for OPG was assessed by QRT-PCR. OPG levels were normalised to housekeeping gene levels and expressed as the mean percentage change over control cells (empty vector, no glutamate) ± S.E.M from three independent experiments, n=3. MG-63 OPG expression was not significantly affected by EAAT1 intracellular domains or glutamate (Shierer Ray test). SaOS-2 OPG expression was significantly affected by expression of EAAT1 intracellular domains (GLM P=0.030), however no post-hoc Tukey's comparisons were significant. Transfection with pcDNA3.1 significantly increased OPG expression relative to untransfected cells (GLM P<0.001 (MG-63) and P<0.001 (SaOS-2)). Significance values *P<0.05, ***P<0.001.

6.3.4.4 ALP

6.3.4.4.1 MG-63

In transfected MG-63 cells, ALP expression was not significantly affected by expression of EAAT1 intracellular domains (GLM P=0.681) or by 500μM glutamate (GLM P=0.188) and there was no interaction between the two factors (GLM P=0.391) (Figure 6.14A). Transfection with pcDNA3.1 had no significant effect on MG-63 ALP expression relative to untransfected cells (GLM P=0.939). A general effect for 500μM glutamate increasing ALP expression was detectable when untransfected cells were compared with empty vector control cells (GLM P=0.044), however post-hoc comparisons (Tukey's tests) did not reveal any pair-wise significance.

6.3.4.4.2 SaOS-2

In transfected SaOS-2 cells, ALP expression was not significantly affected by expression of EAAT1 intracellular domains (GLM with log data P=0.090) or 500μM glutamate (GLM with log data P=0.368) and there was no interaction between the two factors (GLM with log data P=0.620) (Figure 6.14B). However, compared to empty vector control cells mean ALP expression was decreased in SaOS-2 cells transfected with pcDNA3.1 vector containing EAAT1 C-terminal domain at both glutamate concentrations, and by EAAT1 TM6-7 domain at 0μM glutamate.
Transfection with pcDNA3.1 had no significant effect on SaOS-2 ALP expression relative to untransfected cells (GLM P=0.095).

6.3.5 Effect of inhibition of EAAT1 intracellular interactions on ALP activity

SaOS-2 cells were transfected with empty pcDNA3.1 or pcDNA3.1 vector containing EAAT1 N-terminal, TM6-7, and C-terminal intracellular domains for 48hrs. 500μM glutamate was added to replicate cultures 24hrs post-transfection. ALP activity was measured colourimetrically and normalised to total cell number (total LDH activity within the adherent cell lysate). ALP activity is shown as the percentage of ALP

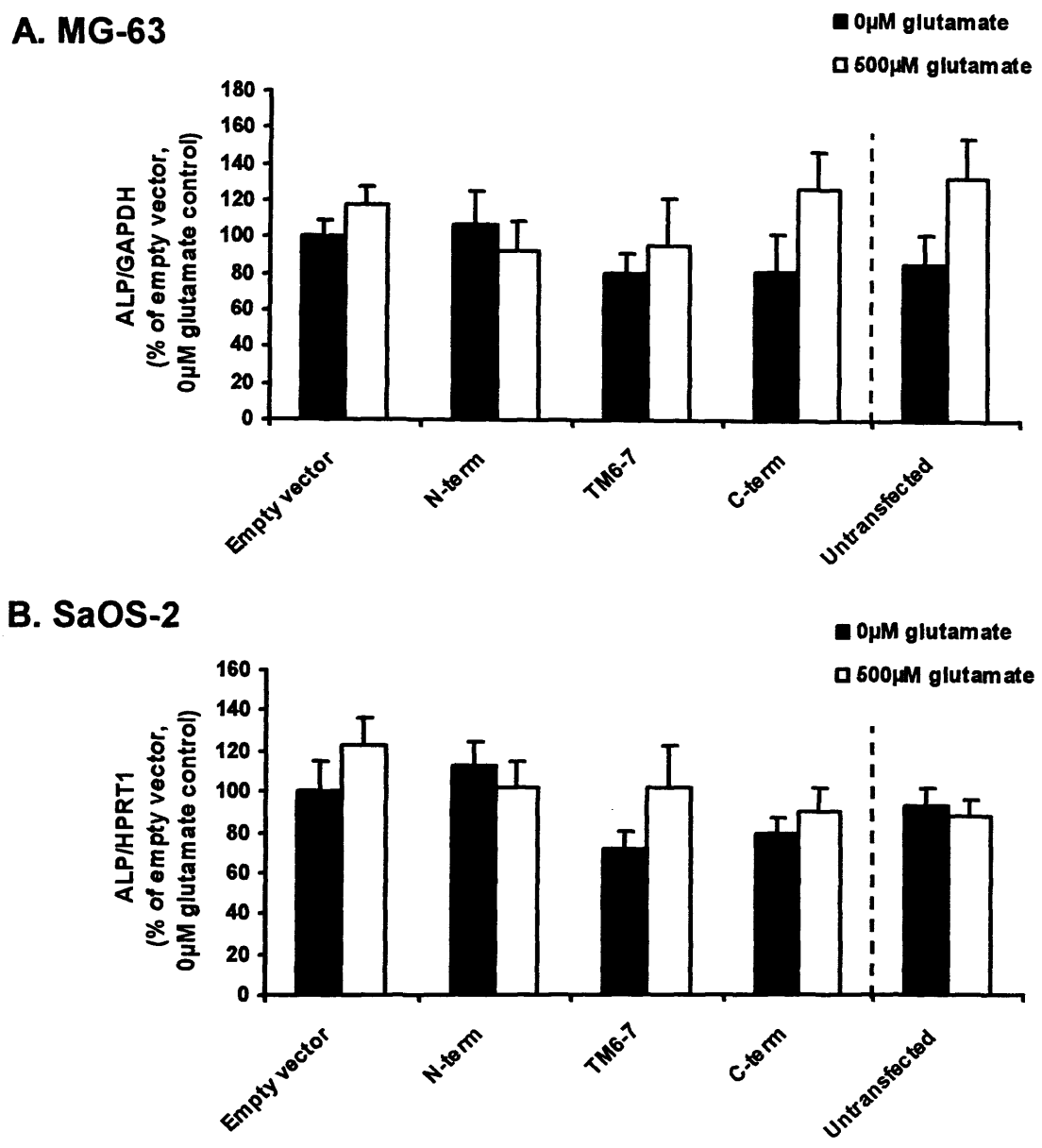

Figure 6.14. Effect of inhibition of EAAT1 intracellular interactions on ALP mRNA expression in osteoblast-like cells at 48hrs post-transfection. Osteoblast-like cells (A, MG-63; B, SaOS-2) were transfected with empty pcDNA3.1 or pcDNA3.1 vector containing each EAAT1 intracellular domain for 48hrs and expression of mRNA for ALP was assessed by QRT-PCR. ALP levels were normalised to housekeeping gene levels and expressed as the mean percentage change over control cells (empty vector, no glutamate) ± S.E.M from three independent experiments, n=3. ALP expression was not significantly affected by expression of EAAT1 intracellular domains or glutamate in MG-63 or SaOS-2 cells (GLM). Vector transfection did not affect ALP expression relative to untransfected cells in MG-63 or SaOS-2 cells (GLM).

activity of control cells (empty vector, no glutamate) (Figure 6.15). Presented data are from three independent experiments where n=3.

In transfected SaOS-2 cells, ALP activity was not significantly affected by expression of EAAT1 intracellular domains (Shierer Ray P=0.907), 500μM glutamate (Shierer Ray P=0.589) and there was no interaction between the two factors (Shierer Ray P=0.859). SaOS-2 ALP activity was also not significantly affected by transfection with pcDNA3.1 vector compared to untransfected cells (GLM P=0.333).

6.4 Discussion

6.4.1 Background

The intention of the experiments presented in this chapter was to introduce peptides into osteoblasts that mimic the sequences of EAAT1 that might be involved in protein-protein interactions within the cell. These experiments were carried out to determine whether this method of modulating of EAAT1 activity might enhance osteoblast bone-forming activity.

Transfection and expression of EAAT1 intracellular domains resulted in statistically significant effects upon MG-63 cell number, osteocalcin expression in both MG-63 and SaOS-2 cells and OPG expression in SaOS-2 cells. Expression of each peptide in osteoblast-like cells was detected at the mRNA level, however achieving detectable quantities of the peptide proved problematic.

Many of the identified interactions for EAAT1 and other members of the EAAT family have so far been shown to modulate EAAT localisation and/or glutamate transport activity; however there is also evidence to suggest that EAAT protein interactions can modulate the EAAT uncoupled anion conductance or lead to intracellular signalling events (Abe and Saito 2001; Marie et al. 2002; Fang et al. 2006). Competing peptides to EAAT1 intracellular domains therefore have the potential to target some, or all, of the activities of the glutamate transporter. Interestingly, the intracellular C-terminus has been shown to confer differences in chloride permeability between EAAT1 and EAAT2 in conjunction with other EAAT regions, suggesting that the C-terminus may associate with other intracellular domains

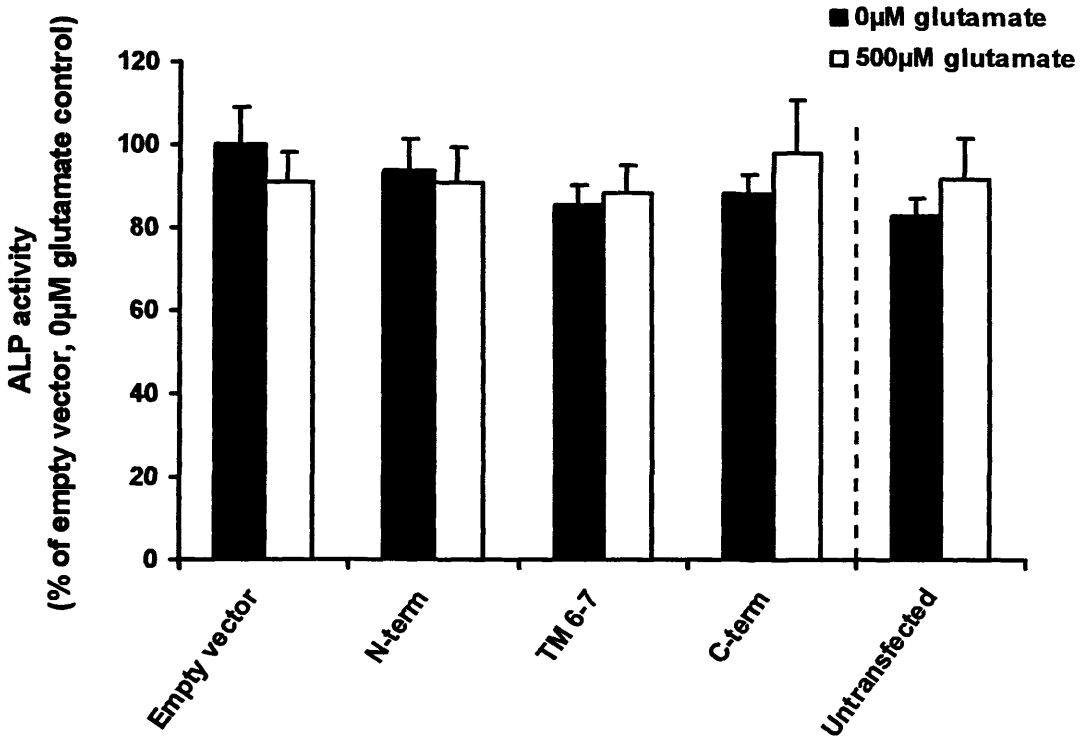

Figure 6.15. Effect of inhibition of EAAT1 intracellular interactions on SaOS-2 ALP activity over 48hrs. SaOS-2 cells were transfected with empty pcDNA3.1 or pcDNA3.1 vector containing each EAAT1 intracellular domain for 48hrs. ALP activity was measured colourimetrically and normalised to cell number (as measured by total cellular LDH activity). ALP activity is shown as the mean percentage of control cell ALP activity (empty vector, no glutamate) ± S.E.M from three independent experiments, n=3. SaOS-2 ALP activity was not significantly affected by expression of different EAAT1 intracellular domains, glutamate or the interaction between the two factors (Shierer Ray test). SaOS-2 ALP activity of empty vector control cells also did not display any significant non-specific effects compared to untransfected cells (GLM).

to influence the conformation of the anion pore (Mitrovic et al. 1998). Therefore, competing peptides to intracellular regions may also influence the conformation of the transporter.

Many of the studies that have identified proteins that interact with the EAATs have been carried out using brain tissue or CNS-derived cells, and it must be considered that post-translational regulation of EAATs might differ between cells of the CNS and osteoblasts. Only some of the identified EAAT-interacting proteins have also been shown to be expressed in osteoblasts (Table 6.1), such as NHERF1 (Schroeder et al. 2007) and ezrin (Khanna et al. 2001; Park et al. 2006). It is possible that other proteins of the same family or different proteins entirely, play a more prominent role in osteoblasts. For example, GFAP is an intermediate filament protein that interacts with the C-terminus of GLAST in pig and rat whole brain (Sullivan et al. 2007b). GFAP interacts with NHERF1 and ezrin to regulate the transport activity of the protein. GFAP is expressed in osteoblasts at low but constitutive levels (Kasantikul and Shuangshoti 1989; Chipoy et al. 2004), however the expression of another intermediate filament protein, vimentin, is high in pre-osteoblasts and regulated during differentiation (Lian et al. 2009). Furthermore, vimentin expression is upregulated in clonal SW982 synoviocytes following activation of iGluRs (McNearney et al. 2009). Vimentin also colocalises with NHERF1 in rat cochleal glial cells (Kanjhan et al. 2006) and siRNA mediated knockdown of vimentin in MG-63 osteoblast-like cells reduced Na^+-dependent glutamate uptake (Brakspear, Harper, Blain, Mason, unpublished).

The competing peptides expressed encompass large regions of the EAAT1 sequence, making it highly likely that more than a single protein-protein interaction or phosphorylation event was prevented. The intracellular N- and C-terminal amino acid sequences of EAAT1 display poor homology across the EAAT family, suggesting that these peptides will not compete for intracellular interactions with other EAAT subtypes. However, the class of PDZ domain binding motifs at the C-terminus of EAAT1 (ETKM) is shared by EAAT3 (TSQF) and EAAT4 (ESAM) (class II motifs) presenting the possibility that these transporters interact with proteins belonging to the same PDZ family. The TM6-7 sequence of EAAT1 is highly homologous across the EAAT family (homologies of 81% in EAAT2, 76% in EAAT3, 76% in EAAT4 and 71% in EAAT5) and therefore this peptide is likely to compete for intracellular interactions of this region with all EAATs expressed.

6.4.2 pcDNA3.1 as a tool for generating intracellular competing peptides against EAAT1 domains in osteoblasts

Our experiments have shown that transfected osteoblast-like cells express mRNA from pcDNA3.1 vector up to 72hrs post-transfection. However expression of the translated peptide could not be confirmed in the absence of the HDAC inhibitor sodium butyrate.

The sequences for EAAT1 N- and C-terminal domains were cloned in frame with the vector V5 and His tag epitopes. However, due to the small size of the peptides, western blotting was not attempted. Visualisation of the peptides by coomassie blue staining or silver staining following resolution of transfected cell lysate by sodium dodecyl sulphate-polyacrylamide gel electrophoresis (SDS-PAGE) (not shown) did not reveal bands of the appropriate molecular weight in either the presence or absence of sodium butyrate. Either these methods were not sensitive enough for the small size of the peptides or the peptides were expressed at very low levels.

Immunostaining for the V5 epitope did detect pcDNA3.1 vector expressing EAAT1 N- and C-terminal domains upon addition of 10mM sodium butyrate. However, sodium butyrate treatment considerably reduced MG-63 and SaOS-2 viability and reduced EAAT glutamate uptake activity in MG-63 cells. Sodium butyrate-induced cell death and inhibition of proliferation has been observed in other cell types, particularly cancer cell lines (Mandal and Kumar 1996; Mandal et al. 1997; Pajak et al. 2007). Interestingly, HDAC inhibitors have previously been shown to promote expression of GLT-1 and GLAST in rat primary astrocytes (Sheldon and Robinson 2007; Aguirre et al. 2008; Allritz et al. 2009) and increase glial glutamate uptake activity under toxic conditions (Wu et al. 2008).

Since sodium butyrate treatment inhibited EAAT activity in MG-63 cells, we were unable to use it to induce expression from the vector in experiments where the effect of the peptides on osteoblast phenotype was assessed. Since high levels of vector mRNA were detected in the absence of sodium butyrate, but anti-V5 immunostaining was not successful, it is likely that the peptides were expressed at very low levels. Thus large effects on the osteoblast phenotype were not expected but transfection of osteoblast-like cells with pcDNA3.1 expressing EAAT1 intracellular domains did result in significant effects upon cell number and gene expression indicative of the expression of functional peptides. Future optimisation of sodium butyrate

concentration and length of treatment may identify a set of conditions to maximise cell viability and peptide expression whilst maintaining EAAT activity.

Other methods to generate the competing peptides were considered. A synthetic peptide generated with a fluorophore tag would allow for detection of its accumulation within the cell; however synthesis of the long peptides used here was too costly. Cloning of the EAAT1 sequences into a bacterial expression vector followed by purification of the expressed peptide was also considered, and in retrospect, represented the most appropriate method to ensure generation of the peptide.

Direct peptide delivery into the cell would improve the experimental design of these studies since control cells transfected with the empty vector exhibited significant differences in EAAT activity, cell number and gene expression compared to untransfected cells. Since the empty vector does not contain a start codon and therefore cannot express a peptide, the non-specific effects observed must be the result of either the transfection agent or the foreign DNA. Some non-specific effects were also observed in osteoblasts transfected with the scrambled AON using Fugene HD transfection agent (section 5.4.2). Although AON non-specific effects were rarely statistically significant, the non-specific effects observed with the empty vector were. Thus, introduction of foreign DNA into osteoblast-like cells elicits significant non-specific effects, possibly due to the increased transcriptional activity of the vector or the immunogenicity of the plasmid DNA backbone, which has been observed in other cell types (Sato et al. 1996; Tudor et al. 2005).

6.4.3 Inhibition of EAAT1 intracellular interactions influences the osteoblast phenotype

6.4.3.1 Na^+-dependent glutamate uptake

Expression of pcDNA3.1 containing EAAT1 intracellular domains had no significant effects upon Na^+-dependent glutamate uptake in MG-63 and SaOS-2; however these findings were complicated by the effects of empty vector transfection. Transfection of MG-63 cells with pcDNA3.1 vector containing EAAT1 N-terminal, TM6-7, or C-terminal domains displayed a trend for increasing Na^+-dependent glutamate uptake, whereas transfection of SaOS-2 cells with pcDNA3.1 vector containing EAAT1 N-

terminal or TM6-7 domains displayed a trend for decreasing Na^+-dependent glutamate uptake. These findings suggest that the intracellular interactions of EAAT1 that regulate the activity of the transporter differ between the two cell lines, and that in general, the intracellular interactions of EAAT1 might act to slow the removal of extracellular glutamate in MG-63 cells but to accelerate its removal in SaOS-2 cells. A difference in the regulation of transport activity between the two cell lines is consistent with chapter 3 (Figure 3.15 and 3.16) where glutamate pre-incubation had contrasting effects on glutamate uptake activity without altering EAAT transcription. However, kinetic characterisation of K_M and V_{max} values for glutamate uptake under each experimental condition is necessary to determine the mechanisms responsible for these differential effects.

Surprisingly, inhibition of EAAT1 C-terminal intracellular interactions had the least effect on mean glutamate transport in both cell types. Most of the proteins identified to interact with the EAATs do so at the C-terminus and have a role in regulating the expression of the transporter at the plasma membrane (Table 6.1). It might therefore be expected that interruption of these interactions with EAAT1 in osteoblast-like cells would significantly influence glutamate transport activity. Many C-terminal interacting proteins identified for EAAT1 stabilise its expression at the cell surface (Lee et al. 2007; Sullivan et al. 2007b) suggesting that a loss of these interactions would decrease glutamate uptake activity. Interestingly, the EAAT1 C-terminal competing peptide increased mean Na^+-dependent glutamate uptake in MG-63 cells, suggesting that an inhibitory intracellular interaction was prevented. This is consistent with findings in retinal glia where a competing peptide identical to the extreme C-terminus of GLAST increased the affinity of the transporter for glutamate (Marie and Attwell 1999) and also correlates with the action of the septin GTPases which interact with the GLAST C-terminus and decrease glutamate transport activity (Kinoshita et al. 2004) and GTRAP3-18 which reduces the affinity of EAAC1 for glutamate via an interaction with the transporter C-terminus (Lin et al. 2001; Butchbach et al. 2003; Ruggiero et al. 2008). It is possible that the inhibition of EAAT1 C-terminal interactions did have a greater effect on glutamate uptake in MG-63 and SaOS-2 cells which could not be detected at only one concentration of glutamate, since interruption of proteins that stabilise cell-surface expression EAAT1 would affect the V_{max} of glutamate transport, and kinetic constants of uptake were not determined.

6.4.3.2 Cell number

Inhibiting EAAT1 intracellular interactions by competing peptides differentially affected adherent MG-63 and SaOS-2 cell number, which is unsurprising in light of the contrasting effects of these treatments on glutamate transport activity in the two cell lines.

At 500μM glutamate, cell number was significantly increased in MG-63 cells transfected with the EAAT1 C-terminal domain compared to empty vector controls. NMDA receptor activation has previously been implicated in the regulation of MC3T3-E1 osteoblast-like cell number (Fatokun et al. 2006) and the proliferation of neurons, cancer cells, chondrocyte-like cells and synovial fibroblasts (Contestabile 2000; Rzeski et al. 2001; Parada-Turska et al. 2006; Spitzer 2006; Piepoli et al. 2009), suggesting that the increase in MG-63 cell number in response to the EAAT1 C-terminal peptide might be the result of sustained high concentrations of extracellular glutamate available to activate receptors, possibly via decreased EAAT activity. Na^+-dependent glutamate uptake was not reduced in MG-63 cells expressing the EAAT1 C-terminal peptide, indicating that this explanation is unlikely, however the uptake kinetics of higher glutamate concentrations are not known.

A receptor-like function for the EAATs has been suggested whereby the transporter responds to glutamate binding by activating intracellular signalling events (Abe and Saito 2001; Mason 2004a). Such a function for EAAT1 might regulate cell proliferation in response to glutamate and be modulated in MG-63 cells by an intracellular protein that interacts with the EAAT1 C-terminal, and candidate proteins for such a function are shown in table 6.1. A receptor-like function for EAAT1 may also occur in response to activation of the uncoupled anion conductance of the transporter, which might be lost in cells expressing the EAAT1 C-terminal peptide due to inhibition of associations between the EAAT1 intracellular domains important for conformation of the anion pore (Mitrovic et al. 1998).

Transfection of SaOS-2 cells with the EAAT1 C-terminal domain had no effect on cell number, suggesting that either the peptides are not expressed at a high enough level to have a significant effect in SaOS-2 cells (where EAAT1 mRNA levels and the rate of glutamate transport is much greater than in MG-63 cells), or that the intracellular EAAT1 interactions differ between the two osteoblast-like cell lines.

6.4.3.3 Gene expression

Significant differences in gene expression were observed in MG-63 and SaOS-2 cells transfected with pcDNA3.1 vector expressing the competing peptides. These effects differed between the transfection groups suggesting that the peptides are expressed and functional within the cell.

Osteocalcin expression was significantly affected by expression of EAAT1 intracellular domains in both cell types. Compared to empty vector control cells, expression of the EAAT1 N-terminal domain slightly increased mean osteocalcin expression in MG-63 cells in the absence of glutamate, while a decrease was detected in MG-63 cells expressing the EAAT1 TM6-7 domain at both glutamate concentrations and the EAAT1 C-terminal domain at 0μM glutamate. Decreased osteocalcin expression may reflect an increased proliferative phenotype of MG-63 cells expressing the EAAT1 C-terminal domain.

In SaOS-2 cells, mean osteocalcin mRNA levels were also increased in cells expressing the EAAT1 N-terminal domain compared to empty vector control cells; however this was only apparent at 500μM glutamate. The EAAT1 C-terminal domain appeared to decrease SaOS-2 osteocalcin levels, though only in the absence of glutamate. While the expression pattern of osteocalcin in response to EAAT1 competing peptides was similar between the two cell types, the biggest effects observed were via EAAT1 TM6-7 and C-terminal domains in MG-63 and via EAAT1 N-terminal domain in SaOS-2.

SaOS-2 OPG expression was significantly decreased by expression of all three EAAT1 intracellular domains in the absence of exogenous glutamate and by EAAT1 TM6-7 and C-terminal domains in the presence of 500μM glutamate. 500μM glutamate increased mean OPG mRNA levels in untransfected SaOS-2 cells (shown here and Figure 4.10B) indicating a glutamate responsive signalling pathway leading to upregulated OPG expression. A reduction in OPG mRNA levels in cells expressing either the TM6-7 or C-terminal domain of EAAT1 at 500μM glutamate implicates the intracellular interactions of these regions in the signalling event. Since each EAAT1 peptide had a similar effect on OPG expression at 0μM glutamate in these cells, it is possible that these regions of EAAT1 are important for the tertiary structure of the protein, potentially implicating the anion pore of EAAT1 in this response (Mitrovic et al. 1998).

6.4.3.4 ALP activity

SaOS-2 ALP activity was not affected by expression of EAAT1 intracellular domains in either the presence or absence of glutamate, suggesting that intracellular interactions of these regions of EAAT1 are not important for the regulation of ALP activity in these cells. Consistent with this finding, competing peptides also had no significant effect on SaOS-2 ALP mRNA levels. Antagonists to NMDA and AMPA receptors have previously been shown to inhibit ALP activity in rat calvarial osteoblasts (Hinoi et al. 2003; Lin et al. 2008), suggesting that competing peptides to EAAT1 in SaOS-2 cells do not increase the level of glutamate available to act on NMDA/AMPA receptors, despite the decrease in mean Na^+-dependent glutamate uptake activity induced by transfection with pcDNA3.1 expressing these EAAT1 domains.

6.4.3.5 Inferences from these findings in osteoblast-like cells

Many differences were detected between the responses of the cell lines MG-63 and SaOS-2 to the transfection of pcDNA3.1 vector expressing EAAT1 competing peptides. This may suggest that EAAT1 interacts with different proteins in each cell line, with the inference that these differences reflect changes that occur during osteoblast differentiation. However, the EAAT expression profile differs between the two cell lines and is also likely to shape the response to EAAT1 competing peptides.
Interestingly, expression of EAAT1 competing peptides significantly affected osteocalcin expression in both cell lines and similar patterns of expression changes could be observed. This finding may indicate a common mechanism for EAAT1 mediated regulation of osteocalcin expression between the two cell lines, and therefore possibly throughout osteoblast differentiation.
Expression of EAAT1 TM6-7 and C-terminal peptides decreased MG-63 osteocalcin expression while the EAAT1 C-terminal peptide increased MG-63 cell number in response to 500μM glutamate, potentially implicating the intracellular interactions of these domains in the regulation of the osteoblast proliferative stage of maturation.

6.4.4 Peptides as a therapeutic tool in bone

There is increasing interest from the pharmaceutical industry in the development of peptide therapeutics. This follows improvements in manufacturing and large scale production methods; however synthesis of peptides remains costly and challenging in comparison to small molecule drugs. The advantages of peptide therapeutics are high activity, specificity and potency, low toxicity and they do not accumulate in tissues. Some examples of currently available peptide therapeutics are leuprolide acetate (Lupron) and goserelin acetate (Zoladex), which mimic gonadotropin-releasing hormone and are used for the treatment of advanced prostate cancer and endometriosis, exenatide (Byetta), which is an insulin secretagogue that is used for the treatment of type 2 diabetes, and enfuvirtide (Fuzeon) which mimics the fusion machinery of HIV-1 and therefore inhibits virus fusion.

Teriparatide (Forteo) was FDA approved in 2002 as a peptide therapeutic for the treatment of osteoporosis. Teriparatide is a recombinant peptide identical to the 34 N-terminal amino acids of human PTH, a major regulator of calcium and phosphate metabolism in bone and kidney. Teriparatide has a similar affinity for the PTH receptor as full-length PTH, and can therefore stimulate new bone formation when intermittently administered at a low dose (Dempster et al. 2001; Neer et al. 2001; Rubin and Bilezikian 2003; Sato et al. 2004). Since peptides have low stability *in vivo,* a short half-life and low oral bioavailability, teriparatide, and most other peptide therapeutics, are injected subcutaneously. The cost and difficult administration of these molecules makes it necessary that the therapeutic offers considerable benefits.

Another potential method for peptide delivery to bone is local application of the molecules in conjunction with an absorbable collagen sponge. A similar process is used in the application of rhBMP-2 and rhBMP-7 currently in clinical use for spinal fusion and the treatment of non-union fracture (section 1.2.1.5.2.1). This strategy has also been employed successfully to deliver synthetic peptides based on the sequence of BMP-2 (Choi et al. 2010) or osteopontin (Egusa et al. 2009) to rat calvarial defects.

6.4.4.1 Competitive peptides to EAAT1 as a therapeutic tool in bone

The peptide sequences of EAAT1 that have been investigated in this chapter are intracellular. The hydrophilic nature of peptides makes membrane transport

problematic and as a result, the majority of therapeutic peptide candidates target extracellular molecules. However, there is increasing interest in the use of cell penetrating peptides (CPPs) to deliver therapeutic molecules across the cell membrane. CPPs were discovered following the identification of sequences required for the cellular uptake of proteins such as the transcription-transactivating (Tat) protein of HIV-1 (Frankel and Pabo 1988). CPPs are short peptides that have either polycationic or amphipathic sequences and can be used to deliver a variety of different molecules into the cell including nucleic acids, large proteins, liposomes and small peptides (reviewed in (Heitz et al. 2009)). Use of CPPs in humans has reached clinical trial in some cases, for example phase II clinical trials of a CPP-based formulation of cyclosporine A (Psorban) for the topical treatment of psoriasis are currently underway (Rothbard et al. 2000; Price 2003).

CPPs have been used to transport proteins into rat and mouse calvarial osteoblasts *in vitro* (Dolgilevich et al. 2002; Sun et al. 2005) and represent a means of delivering the EAAT1 competing peptides into the cell, both *in vitro* and *in vivo* in conjunction with a collagen sponge. Local delivery of such a molecule for *in vivo* application would be necessary since the CPP would transport the peptide into cells indiscriminately, reducing the level of the therapeutic reaching bone and also leading to potential side effects since the glutamate signalling pathway functions in many central and peripheral tissues (reviewed in (Skerry and Genever 2001; Hinoi et al. 2004)). After generating a bacterial expression vector containing the EAAT1 sequences of interest in frame with a CPP sequence during the course of this PhD, time constraints prevented the purification and testing of these peptides in osteoblasts. Repeating the experiments presented in this chapter using a CPP-linked EAAT1 peptide would lead to a more reliable conclusion as to whether these molecules would be useful therapeutically, since the quantity of competing peptide within the cell could be defined and optimised and the effects of transfection could be avoided.

The intracellular N- and C-terminal domains of EAAT1 expressed within the cell lines were fairly long at ~50 amino acids. For therapeutic use the peptide would preferably be shorter in order to reduce the chance of any non-specific effects and also to reduce the costs associated with synthesis. Therefore, if any of the EAAT1 sequences investigated in this chapter were to be pursued as a therapeutic peptide, the region of the sequence conferring the activity would need to be identified.

The experiments presented in this chapter have shown that inhibition of EAAT1 C-terminal intracellular interactions can increase cell number of 'pre-osteoblast' MG-63 cells, which may be useful in the context of fracture repair since atrophic non-unions are typified by insufficient availability of bone forming cells, preventing normal bone healing from occurring (Megas 2005) (section 1.2.1.5.2). Expression of EAAT1 N-terminal competing peptides increased osteocalcin in both cell lines suggesting that this peptide may represent a means of increased osteoblast differentiation, relevant to diseases of low bone mineral density (BMD) such as osteoporosis. Furthermore, inhibition of EAAT1 intracellular interactions decreased OPG expression in SaOS-2 cells and a mechanism for reducing expression of OPG may have therapeutic application in fracture repair for the enhancement of bone remodelling and the replacement of the woven bone callus or the enhancement of osteoclast activity in diseases of high bone mass (section 1.2.1.1 and Table 1.1).

6.4.5 Summary

Expression of competing peptides to intracellular domains of EAAT1 was investigated in osteoblast-like cells to ascertain the importance of EAAT1 intracellular interactions in osteoblast proliferation and activity. In MG-63 cells, competing peptides to EAAT1 C-terminal domain significantly increased cell number at 500μM glutamate. Osteocalcin mRNA levels were affected similarly in both cell lines at 0 and 500μM glutamate with the EAAT1 N-terminal domain increasing expression and the EAAT1 TM6-7 and C-terminal domains decreasing expression. SaOS-2 OPG mRNA levels were significantly decreased by competing peptides to each EAAT1 intracellular domain at 0μM glutamate. Large differences in osteoblast glutamate transport were detected in response to expression of EAAT1 intracellular domains; however these were not significant due to the variances associated with the transient transfections. Thus, optimisation of peptide expression and increased replicates are necessary to further investigate these findings.

Peptide-specific significant effects were observed demonstrating that the peptides were expressed and functional and that intracellular interactions of EAAT1 modulate osteoblast cell number and gene expression.

Chapter 7: General discussion

7. General discussion

7.1 Background

New strategies to replace or repair traumatised or diseased bone is a major socioeconomic and clinical need in an ageing demographic. More than one million fractures occur in the UK each year and 5-10% of these experience problems in healing (Gaston and Simpson 2007). Furthermore, one in two women and one in five men over the age of 50 in the UK will fracture a bone as a result of osteoporosis (van Staa et al. 2001) and osteoporosis related fractures cost the health service an annual sum of over £1 billion (Torgensen 2001; PRODIGY 2006).

Glutamate was first linked to bone when a gene screening experiment designed to identify genes regulated following osteogenic mechanical loading of the rat ulna identified GLAST (Mason et al. 1997). GLAST (EAAT1) was constitutively expressed in osteocytes of control bone but absent in the loaded limb, implicating the transporter in the response of bone to mechanical load. Activation of ionotropic glutamate receptors can regulate the phenotype of osteoblasts and osteoclasts *in vitro* (Chenu et al. 1998; Peet et al. 1999; Itzstein et al. 2000; Hinoi et al. 2003; Ho et al. 2005) and bone mass *in vivo* (Burford et al. 2004; Lin et al. 2008; Skerry 2008). Mechanical loading plays a key role in the physiology of bone, allowing bone to functionally adapt to its environment (Lanyon 1996), however characterisation of the signalling events linking load to bone formation is incomplete. Identification and therapeutic exploitation of the mechanoresponse offers the opportunity to prevent and treat bone loss. This thesis has investigated the potential of targeting the glutamate signalling pathway in bone to this purpose. The hypothesis of this PhD was that inhibition of glutamate transporter activity in bone cells could be used to mimic mechanical stimulation and enhance osteoblast differentiation and/or bone forming activity, representing a new target for anabolic therapies in bone. The aims were to characterise EAAT expression and activity in human osteoblasts and to determine whether modulation of EAAT activity could enhance the osteoblast bone-forming phenotype *in vitro*. Potential therapeutic targeting of EAATs in bone for the treatment of osteoporosis or non-union fracture has been previously proposed (Mason et al. 1997; Mason 2004), but not comprehensively tested. EAATs are the gate-keepers of

the glutamate response and therefore offer the opportunity to modulate glutamate signalling without the potential side-effects associated with targeting particular glutamate receptor subtypes.

Since EAATs may exhibit multiple activities (glutamate uptake and release, glutamate gated Cl^- conductance and a receptor-like function) (reviewed in (Danbolt 2001; Mason 2004a)) in osteoblasts, the particular activity relevant to mechanically-induced bone formation is unknown. Therefore, each EAAT activity was inhibited in osteoblasts, and the effects on osteoblast activity assessed *in vitro*. This was done using broad range chemical EAAT inhibitors, antisense mediated EAAT1 exon skipping and competitive peptides to intracellular regions of EAAT1 thought to be involved in protein-protein interactions (illustrated in Figures 7.1 and 7.2).

7.2 EAATs are expressed and functional in human osteoblasts

Transcripts for EAATs 1-3 and two splice variants of EAAT1 (EAAT1a and EAAT1ex9skip) were detected in human bone, primary osteoblasts and osteoblast-like cell lines (MG-63 and SaOS-2) by RT-PCR. This confirms reports of the expression of EAATs 1-3 and EAAT1a in osteoblasts (Mason et al. 1997; Huggett et al. 2000; Huggett et al. 2002; Kalariti et al. 2004; Takarada et al. 2004; Kalariti et al. 2007); however this is the first report of EAAT1ex9skip expression in human bone tissue and osteoblasts.

We have quantified EAAT transcription in osteoblasts by QRT-PCR for the first time and shown that EAAT1 is expressed at higher levels than EAAT3 (~300-fold higher in MG-63 and ~50,000-fold higher in SaOS-2) while EAAT2 expression was too low to quantify accurately. Expression of EAATs 1 and 3 was confirmed in primary human osteoblasts and osteoblast-like cells by immunofluorescence, and functional EAAT expression was demonstrated by Na^+-dependent glutamate uptake into these cells. EAAT function has been previously demonstrated in rat calvarial osteoblasts (Takarada et al. 2004) but not in human osteoblasts. In human osteoblast-like cells, Na^+-dependent glutamate uptake was concentration dependent, sensitive to pharmacological EAAT inhibition (*t*-PDC, TBOA) and extracellular glutamate concentration (10-500μM). The role of extracellular glutamate in the regulation of EAAT activity has not been previously investigated in osteoblast-like cells.

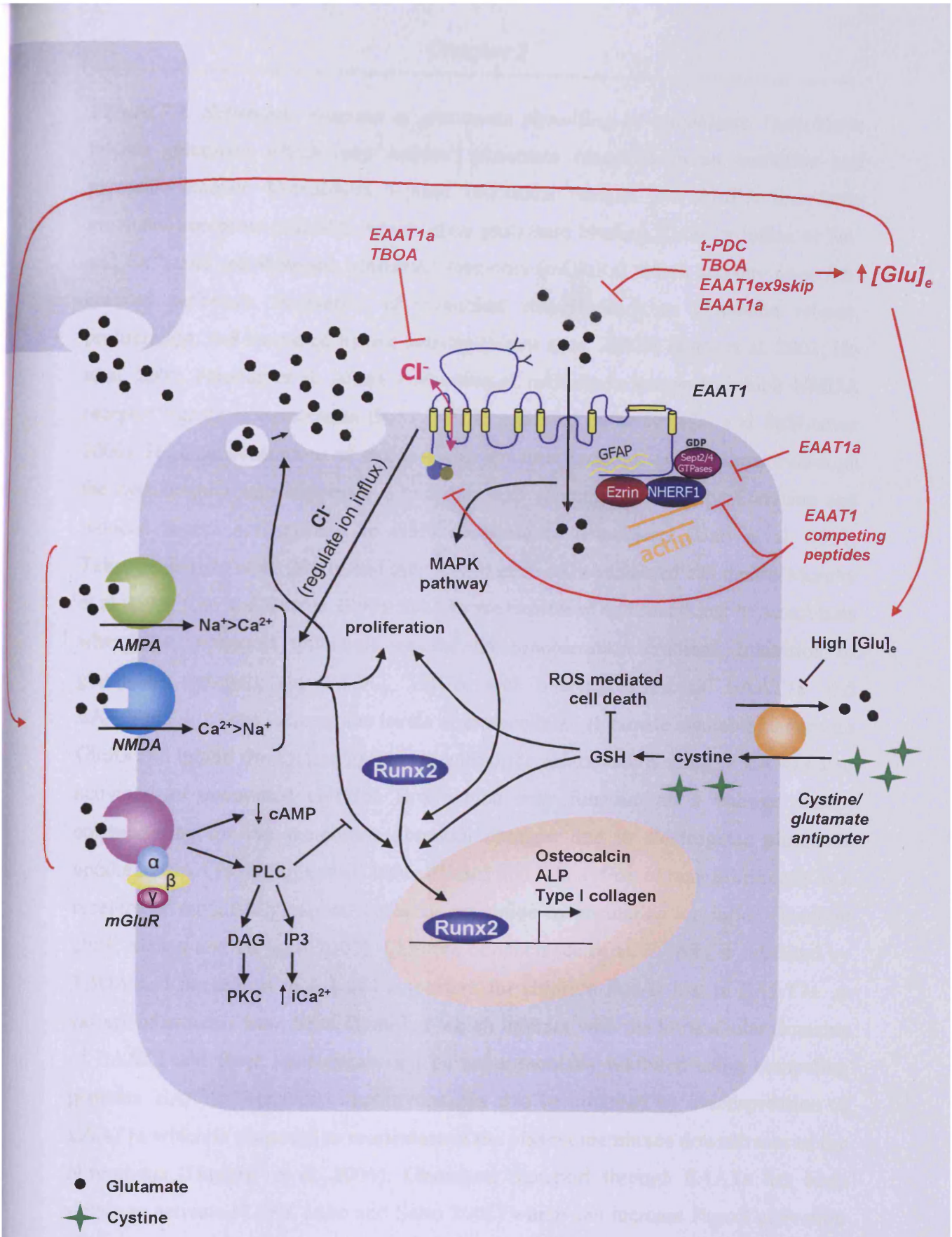
EAAT1a
TBOA
t-PDC
TBOA
EAAT1ex9skip
EAAT1a
↑[Glu]e
Cl-
EAAT1
GFAP
GDP
Sept2/4
GTPases
Ezrin
NHERF1
actin
EAAT1a
EAAT1
competing
peptides
Cl-
(regulate ion influx)
MAPK
pathway
AMPA
Na+>Ca2+
proliferation
High [Glu]e
ROS mediated
cell death
NMDA
Ca2+>Na+
GSH
cystine
Runx2
Cystine/
glutamate
antiporter
↓cAMP
α
β
γ
PLC
mGluR
Osteocalcin
ALP
Type I collagen
Runx2
DAG
IP3
PKC
↑iCa2+
Glutamate
Cystine

Figure 7.1. Schematic diagram of glutamate signalling in osteoblasts. Osteoblasts release glutamate which may activate glutamate receptors in an autocrine and paracrine manner. Osteoblasts express functional NMDA and AMPA ionotropic glutamate receptors (iGluRs), which upon glutamate binding allow an influx of Na^+ and Ca^{2+}, and metabotropic glutamate receptors (mGluRs) which activate G-protein coupled pathways. Activation of osteoblast iGluRs leads to glutamate release, proliferation, and increased Runx2 activity (Hinoi et al. 2002b; Hinoi et al. 2003; Ho et al. 2005; Fatokun et al. 2006). Activation of mGluRs is known to inhibit NMDA receptor signals in osteoblasts through PLC activated pathways (Gu and Publicover 2000). High concentrations of extracellular glutamate prevent cystine uptake through the cystine/glutamate antiporter which can lead to suppression of proliferation and reduced Runx2 activity due to GSH depletion in osteoblasts (Uno et al. 2007; Takarada-Iemata et al. 2010), and may also lead to ROS-mediated cell death (Murphy et al. 1989; Cho and Bannai 1990). EAATs are expressed and functional in osteoblasts where they transport glutamate against its concentration gradient. Inhibition of glutamate transport (by t-PDC, TBOA and overexpression of EAAT1a and EAAT1ex9skip) can increase the levels of extracellular glutamate available to activate GluRs and inhibit the cystine/glutamate antiporter. Glutamate binding to EAATs also activates an uncoupled chloride flux which may function as a voltage clamp, compensating for the membrane potential changes due to electrogenic glutamate uptake by EAATs (Billups et al. 1996; Eliasof and Jahr 1996), or may act directly as a receptor or modulate glutamate receptor activation by regulating ion influx (Danbolt 2001; Mason and Huggett 2002). Chloride conductance of all EAATs is inhibited by TBOA and the region of EAAT1 important for chloride flux is lost in EAAT1a. A variety of proteins have been identified which interact with the intracellular domains of EAAT1 and these interactions can be experimentally inhibited using competing peptides. EAAT1 C-terminal interactions can also be inhibited by overexpression of EAAT1a which is proposed to reorientate in the plasma membrane downstream of the N-terminus (Huggett et al. 2000). Glutamate transport through EAATs has been shown to activate MAPK (Abe and Saito 2001) which can increase Runx2 activation (Xiao et al. 2000). Phospholipase C (PLC), diacylglycerol (DAG), cyclic adenosine monophosphate (cAMP), protein kinase C (PKC), inositol triphosphate (IP3), alkaline phosphatase (ALP), reactive oxygen species (ROS), mitogen activated protein kinase (MAPK), excitatory amino acid transporter (EAAT), glutathione (GSH).

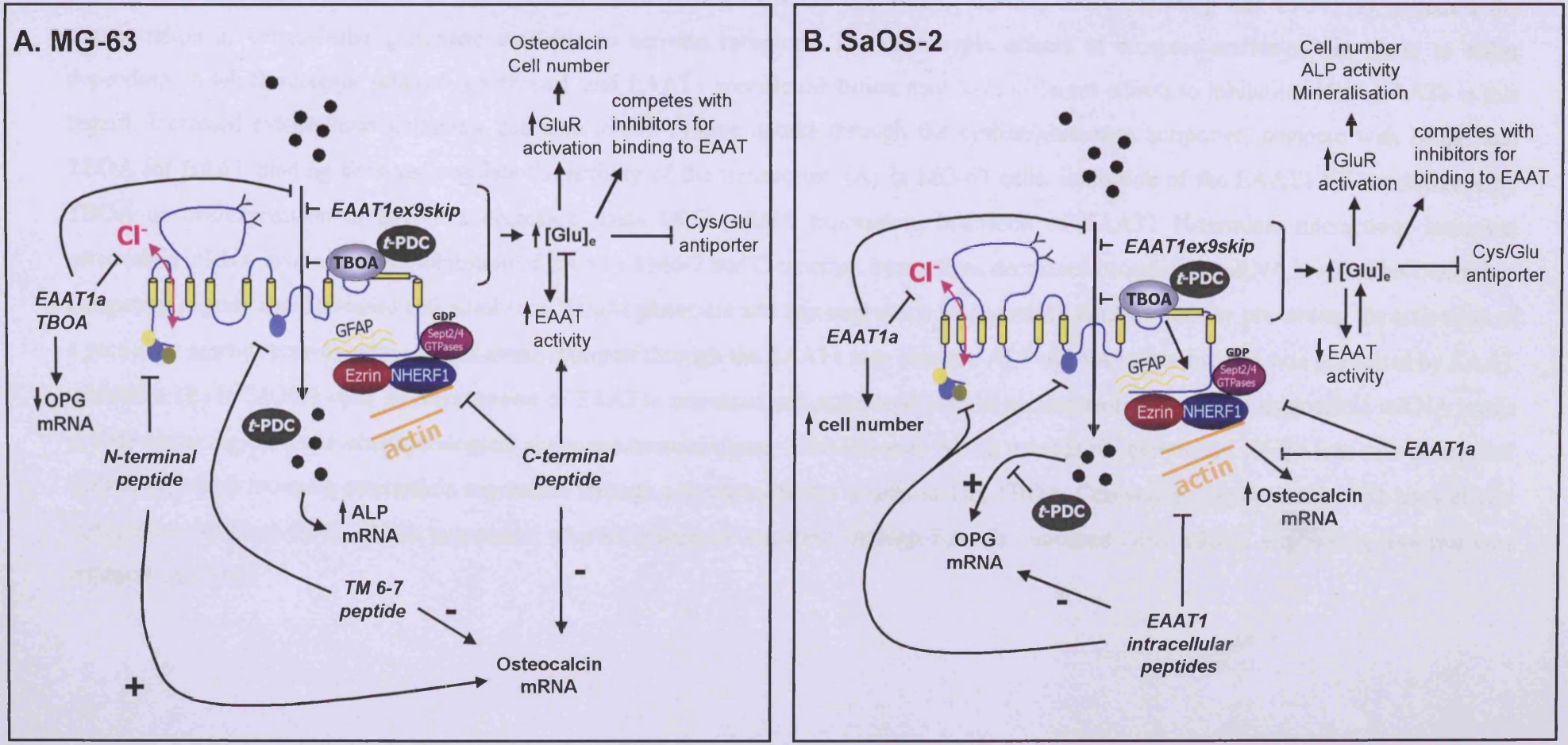
A. MG-63
Osteocalcin
Cell number
GluR activation
competes with inhibitors for binding to EAAT
EAAT1ex9skip
t-PDC
TBOA
[Glu]e
Cys/Glu antiporter
Cl-
EAAT1a
TBOA
GFAP
GDP
Sept2/4 GTPases
Ezrin
NHERF1
EAAT activity
OPG mRNA
actin
N-terminal peptide
t-PDC
C-terminal peptide
ALP mRNA
TM 6-7 peptide
Osteocalcin mRNA
B. SaOS-2
Cell number
ALP activity
Mineralisation
GluR activation
competes with inhibitors for binding to EAAT
EAAT1ex9skip
t-PDC
TBOA
[Glu]e
Cys/Glu antiporter
Cl-
EAAT1a
GFAP
GDP
Sept2/4 GTPases
Ezrin
NHERF1
EAAT activity
cell number
actin
EAAT1a
Osteocalcin mRNA
t-PDC
OPG mRNA
EAAT1 intracellular peptides

Figure 7.2. Diagram of the effects of modulating EAAT1 activity in osteoblast-like cells based on findings from this thesis. In both cell lines (MG-63 and SaOS-2), inhibition of glutamate transport through EAATs (by *t*-PDC, TBOA, EAAT1ex9skip and EAAT1a) increases the concentration of extracellular glutamate available to activate receptors. The phenotypic effects of receptor activation are likely to differ depending on which receptor subtype is activated, and EAAT1 specific inhibition may have different effects to inhibition of all EAATs in this regard. Increased extracellular glutamate can also inhibit cystine uptake through the cystine/glutamate antiporter, compete with *t*-PDC and TBOA for EAAT binding sites and regulate the activity of the transporter. (A) In MG-63 cells, inhibition of the EAAT1 Cl^- conductance by TBOA or overexpression of EAAT1a decreased mean OPG mRNA expression. Inhibition of EAAT1 N-terminal interactions increased osteocalcin mRNA levels whereas inhibition of EAAT1 TM6-7 and C-terminal interactions decreased osteocalcin mRNA levels. The C-terminal competing peptide also increased cell number at 500μM glutamate and this may occur via increased EAAT1 activity preventing the activation of a particular nearby receptor subtype. Glutamate transport through the EAATs may increase ALP mRNA levels and this was prevented by EAAT inhibitors. (B) In SaOS-2 cells, overexpression of EAAT1a increased cell number at 500μM glutamate and decreased osteocalcin mRNA levels at both physiological and pathophysiological glutamate concentrations. EAAT1a may inhibit osteocalcin expression via the loss of a C-terminal interaction which increases osteocalcin expression through a mechanism that is activated by TBOA. Competing peptides to EAAT1 intracellular interactions inhibited OPG mRNA expression whereas glutamate transport through EAATs increased OPG mRNA expression, and this was inhibited by *t*-PDC.

These studies indicate that EAAT1 is the dominant glutamate transporter in osteoblasts, demonstrating that regulation of EAAT1 expression in osteocytes in response to mechanical load (Mason et al. 1997) is likely to be physiologically relevant. Interestingly, the EAAT expression profile of osteoclasts (Table 1.4) reveals that these cells express EAAT2 and EAAT4 (Hinoi et al. 2007; Takarada and Yoneda 2008), in contrast to the predominant EAAT1 and EAAT3 expression of osteoblasts, though expression of EAAT4 has not been investigated in osteoblasts. This will aid cell-type specific targeting of the EAATs in bone. Cell-type specific EAAT expression patterns are present within the CNS and other peripheral tissues (Gegelashvili and Schousboe 1997; Danbolt 2001; Berger and Hediger 2006), demonstrating that the transporters exhibit broader functional roles than simply the maintenance of low concentrations of extracellular glutamate.

7.2.1 Novel characterisation of EAAT1 splice variants in bone

Characterisation of EAAT expression in bone has largely ignored the existence of multiple splice variants (section 5.1.1), with the exception of the EAAT1 splice variant EAAT1a (Huggett et al. 2000; Huggett et al. 2002). In the osteoblast cell lines studied, EAAT1a expression was very low, whilst levels of the dominant negative EAAT1ex9skip were much higher, comparable to levels detected in the brain (Vallejo-Illarramendi et al. 2005). Furthermore, the higher expression levels of EAAT1ex9skip relative to full-length EAAT1 in MG-63 (13% of full-length EAAT1 levels) compared to SaOS-2 cells (2% of full-length EAAT1 levels) suggests that this splice variant might be down-regulated during osteoblast maturation. This could be tested by analysing EAAT1 splicing during osteogenic differentiation of MSCs. A reduction in the expression of a dominant negative transporter would be expected to increase the cells capacity to transport glutamate, consistent with previous suggestions that osteoblasts acquire a more active glutamatergic signalling phenotype as they mature (Genever and Skerry 2001).

These are the first studies to utilise antisense mediated exon skipping techniques to overexpress the ratio of EAAT1 splice variant to full-length EAAT1 in bone cells, and we have shown that overexpression of EAAT1a and EAAT1ex9skip reduces Na^+-dependent uptake of 10μM glutamate in MG-63 and SaOS-2 cells. A reduction in glutamate transport in cells overexpressing EAAT1ex9skip is consistent with the

reported dominant negative role of this variant (Vallejo-Illarramendi et al. 2005). However EAAT1a was thought to be a functional transporter as only domains important for the glutamate-gated Cl^- conductance are absent (Mason, Huggett, Daniels, unpublished). The reduced glutamate transport activity in cells overexpressing EAAT1a either implicate EAAT1 exon 3 directly in the regulation of glutamate transport or reveal how loss of the Cl^- conductance of EAAT1 in osteoblasts, which normally compensates for the membrane potential changes due to electrogenic glutamate uptake by EAATs (Billups et al. 1996; Eliasof and Jahr 1996), can slow glutamate transport.

7.3 Regulation of EAAT activity modifies the osteoblast phenotype

The majority of glutamate signalling research within bone and other peripheral tissues has focused on the activity of the glutamate receptors. That the EAATs might also play a direct role in regulating the phenotype of bone cells has been hypothesised (Mason 2004a) and some studies have begun to investigate this theory, reporting that *t*-PDC prevents bone formation of calvarial osteoblasts *in vitro* (Taylor 2002). The experiments presented here have clearly shown that modulating EAAT activity at both physiological and pathophysiological glutamate concentrations can modify the osteoblast phenotype. Interestingly, some effects of EAAT modulation did not mimic exogenous glutamate treatment, providing evidence for the first time that specific transporter-mediated pathways might be active in osteoblasts, either through glutamate transport, chloride conductance or protein-protein interactions.

The main effects of the experimental modulations of EAAT activity in MG-63 and SaOS-2 osteoblast-like cells at physiological and pathophysiological concentrations of glutamate are summarised in tables 7.1 and 7.2 and Figure 7.2. Data from human primary osteoblasts are not included since these cells were not tested with every experimental treatment; but are discussed in the following sections where appropriate.

No exogenous glutamate was added to the medium to achieve the physiological concentration of glutamate (28μM in serum (Mally et al. 1996), 6μM in synovial fluid (Plaitakis et al. 1982; McNearney et al. 2000)) since it was known that osteoblasts spontaneously release glutamate (Genever and Skerry 2001). The pathophysiological concentration of glutamate chosen here (500μM) reflects the glutamate levels in the

Table 7.1. Summary of the effects of modulating EAAT activity at physiological glutamate concentrations on the osteoblast phenotype. Changes in expression/activity of MG-63 (black) and SaOS-2 (grey) are shown as increases (↑), decreases (↓) or no change (-) relative to respective controls (no inhibitor/scrambled AON/empty vector, 0μM glutamate). NT, not tested. Significance values *P<0.05, **P<0.01, ***P<0.001, n.s (not significant) by pair-wise post-hoc comparisons. Trends non-significant by post-hoc test but significant by ANOVA are indicated in brackets.

Transport — **Intracellular interactions**

Ion channel

	Ex9skip	*t*-PDC	TBOA	Ex3skip	C-term	TM6-7	N-term
Cell number	↓ * -	↑ n.s. ↑ ***	↑ n.s. ↑ *	- -	↑ n.s. -	- -	- -
Osteocalcin mRNA	↓ n.s. -	- ↑ n.s.	- ↑ *	↓ n.s. ↓ *	↓ n.s. (**) ↓ n.s. (*)	↓ n.s. (**) -	↑ n.s. (**) -
Osteonectin mRNA	- -	- -	↓ n.s. -	- -	- -	- -	- -
OPG mRNA	- ↑ n.s.	- -	↓ n.s. -	↓ n.s. -	↑ n.s. ↓ n.s. (*)	- ↓ n.s. (*)	- ↓ n.s. (*)
ALP mRNA	- ↑ n.s.	↓ n.s. -	- -	- -	- ↓ n.s.	- ↓ n.s.	- -
ALP activity	NT ↑ **	NT ↓ *	NT ↓ *	NT -	NT -	NT -	NT -
Mineralisation	NT NT	NT ↓ ***	NT ↓ ***	NT NT	NT NT	NT NT	NT NT

Table 7.2. Summary of the effects of modulating EAAT activity at pathophysiological glutamate concentrations on the osteoblast phenotype. Changes in expression/activity of MG-63 (black) and SaOS-2 (grey) are shown as increases (↑), decreases (↓) or no change (-) relative to respective controls (no inhibitor/scrambled AON/empty vector, 500μM glutamate). NT, not tested. Significance values $*P<0.05$, $**P<0.01$, $***P<0.001$, n.s (not significant) by pair-wise post-hoc comparisons. Trends non-significant by post-hoc test but significant by ANOVA are indicated in brackets.

Transport — **Intracellular interactions**

Ion channel

	Ex9skip	*t*-PDC	TBOA	Ex3skip	C-term	TM6-7	N-term
Cell number	-	↓ n.s. ↑ n.s.	↓ *	-	↑ **	-	-
	-	-	-	↑ **	-	-	-
Osteocalcin mRNA	- ↓ n.s.	-	-	- ↓ *	-	↓ n.s. (**)	- ↑ n.s. (*)
	-	-	-	-	-	-	-
Osteonectin mRNA	-	- ↑ n.s.	↓ *	-	-	-	-
	-	-	-	-	-	-	-
OPG mRNA	-	↓ n.s.	-	-	↑ n.s.	-	-
	-	↓ *	-	-	↓ n.s. (*)	-	-
ALP mRNA	- ↓ n.s.	↓ **	↓ *	-	-	-	-
	-	-	-	-	↓ n.s.	-	-
ALP activity	NT -	NT -	NT -	NT -	NT -	NT -	NT -
Mineralisation	NT NT	NT ↓ ***	NT ↓ ***	NT NT	NT NT	NT NT	NT NT

synovial fluid of patients with inflamed joints due to OA, RA and gout (McNearney et al. 2004) and are associated with peripheral pain (Carlton 2001) and inflammation (Flood et al. 2007).

The treatments have been categorised within the table by the EAAT activity influenced, however these are not rigid classifications (as shown in Table 7.3). For instance, TBOA and EAAT1ex9skip inhibit glutamate transport and may therefore prevent any intracellular interactions associated with the conformational changes that occur upon glutamate transport. Furthermore, EAAT1ex9skip lacks residues within exon 9 known to be important for glutamate binding (Figure 1.8) (Seal and Amara 1998; Zhang and Kanner 1999; Leighton et al. 2006), which may influence the glutamate gated Cl^- conductance. Therefore, explanations exist as to why findings are not consistent across the groups as they are categorised in tables 7.1 and 7.2. The pertinent findings from these data will now be discussed.

Table 7.3. Known and potential effects of experimental modulation of EAAT activity and specificity of these treatments to EAAT1. Each experimental modulation of EAAT activity is shown in conjunction with the EAAT activities that are known to be inhibited (Y), may be inhibited (?) or are unlikely to be influenced (N). EAAT1 specificity is also shown.

	Transport	Anion conductance	Intracellular interactions	EAAT1 specific
t-PDC	Y	N	?	N
TBOA	Y	Y	?	N
Ex3skip	Y	Y	Y	Y
Ex9skip	Y	?	?	Y
N-term peptide	N	N	Y	Y
TM 6-7 peptide	N	?	Y	N
C-term peptide	?	?	Y	?

7.3.1 Targeting of EAAT1 elicits different effects to targeting all EAATs in osteoblasts

Inhibition of glutamate transport in osteoblasts was achieved by chemical inhibitors (*t*-PDC and TBOA) and by overexpression of the dominant-negative EAAT1ex9skip. While *t*-PDC and TBOA inhibit transport through all expressed EAATs, the effects of

overexpressing EAAT1ex9skip is expected to be specific to EAAT1. This may explain why these treatments resulted in contrasting effects on the cell phenotype. In the absence of exogenous glutamate, overexpression of EAAT1ex9skip decreased MG-63 cell number and mean osteocalcin expression levels while increasing SaOS-2 ALP activity, whereas EAAT inhibitors increased MG-63 and SaOS-2 cell number, increased SaOS-2 osteocalcin expression and decreased SaOS-2 ALP activity (Table 7.1).

Such effects could be the result of differences in expression, activity or localisation of the EAAT subtypes expressed. Transcript levels for EAATs 1-3 in MG-63 and SaOS-2 cells decrease in magnitude in the order of EAAT1>EAAT3>EAAT2 (EAATs 4 and 5 were not investigated). EAAT inhibitor concentrations (100μM) were sufficient to inhibit all EAAT subtypes (Table 2.3), though with ~10-fold greater affinity for EAATs 2, 4 and 5 (*t*-PDC) or EAATs 2-5 (TBOA) compared to EAAT1. The low mRNA expression of EAAT 2 (unquantifiable levels) suggests that inhibitors may be influencing the osteoblast phenotype via EAATs 3, 4 or 5. Thus detailed investigation of EAATs 3-5 in osteoblasts may be warranted. This may be particularly relevant for MG-63 cells which express EAAT1 at only 300-fold higher levels than EAAT3 but it seems unlikely that inhibition of transport specifically through EAAT1 would yield different effects to inhibiting transport through all EAATs in SaOS-2 cells, given that EAAT1 expression is ~50,000-fold higher than EAAT3 and that both subtypes display similar affinities for L-glutamate in *Xenopus oocytes* and HEK293 cells (Arriza et al. 1994; Jensen and Brauner-Osborne 2004). Therefore a role for EAATs 4 and 5 should be investigated in SaOS-2 cells.

It is known that the uptake kinetics and glutamate gated Cl^- conductance can vary across the EAAT subtypes, as can post-translational regulation by phosphorylation and protein-protein interactions (reviewed in (Danbolt 2001)), indicating that each EAAT subtype might have differential functional roles. For example, glial EAATs (1 and 2) are responsible for the bulk of glutamate transport in the CNS (Danbolt 2001; O'Shea 2002; Kanai and Hediger 2004) whereas neuronal EAATs (3 and 4) are thought to have more specialised roles that are poorly characterised.

The localisation of different EAAT subtypes within the cell is tightly regulated (reviewed in (Danbolt 2001; Amara and Fontana 2002)). Inhibition of EAATs close to certain glutamate receptor subtypes will allow glutamate spill-over and receptor activation, modulating intracellular signalling events. For example glutamate uptake

through EAAT4 limits mGluR activation and signalling at purkinje neurons in the cerebellum (Wadiche and Jahr 2005). EAAT1 may be located close to a particular receptor subtype in osteoblasts such that overexpression of EAAT1ex9skip decreases glutamate uptake in the vicinity of this receptor leading to its activation and intracellular signalling regulating cell proliferation, ALP activity and osteocalcin expression. This would not be apparent with more general chemical inhibition of EAATs. Activation of NMDA receptors can modulate these effects in osteoblasts (Hinoi et al. 2003; Ho et al. 2005; Fatokun et al. 2006; Lin et al. 2008) but colocalisation of EAAT1 with NMDA receptors has not been investigated in bone cells or the CNS, and may be a useful area for future work. Interestingly, GLAST has been implicated in restricting the activation of mGluRs in neurons from murine hippocampal slices (Huang et al. 2004). Therefore EAAT1 may be located close to mGluRs in osteoblasts which are activated upon specific inhibition of glutamate uptake by EAAT1. Such mGluRs may directly signal to decrease cell number and increase ALP activity or they may inhibit activation of NMDA receptors which signal to increase cell number and decrease ALP activity under these conditions. Gu and Publicover have shown that NMDA currents in osteoblasts that were rapidly lost upon treatment with 100μM glutamate could be restored by blockade of mGluRs with MCPG, indicating that inhibitory cross talk occurs between mGluRs and NMDA receptors in osteoblasts (Gu and Publicover 2000).

The differing effects of chemical EAAT inhibitors and overexpression of EAAT1ex9skip in these cells may also be explained by differences in the mode and timing of inhibition. For instance, the inhibitors are likely to be most active at the point of treatment, whereas exon skipping becomes increasingly effective, and confluence-dependent changes in osteoblasts may affect the responses.

7.3.2 Modulation of EAAT activity regulates expression of osteocalcin in osteoblasts

Of all the transcripts quantified as markers of osteoblast activity, osteocalcin expression was most consistently affected by each method of EAAT modulation. Each experimental condition inhibited different EAAT activities, highlighting the possibility that osteocalcin expression might be regulated by more than one mechanism involving EAATs. Effects were cell type specific and since MG-63 cells

represent an early osteoblast phenotype and SaOS-2 cells display a late osteoblast phenotype this supports the theory that glutamate signalling is dependent on osteoblast maturation stage (discussed further in section 7.3.4).

7.3.2.1 MG-63 cells

Osteocalcin expression was significantly reduced in MG-63 cells following 24hr incubation with 500μM glutamate. Osteocalcin expression is regulated by the transcription factor Runx2 (Ducy and Karsenty 1995; Merriman et al. 1995) and 500μM glutamate also decreased human primary osteoblast Runx2 expression. Others have shown that high concentrations of extracellular glutamate, leading to inhibition of the cystine/glutamate antiporter, downregulates Runx2 activity due to a depletion of GSH early in osteoblast differentiation (Takarada-Iemata et al. 2010). This mechanism may explain the observed effects on osteocalcin in MG-63 cells, which exhibit a pre-osteoblast phenotype and on Runx2 in primary osteoblasts after 24hrs culture but not at 5 days.

Overexpression of EAAT1a and EAAT1ex9skip in MG-63 cells appeared to mimic the glutamate-induced down-regulation of osteocalcin expression. Overexpression of either splice variant decreased glutamate uptake, thus increasing the levels of extracellular glutamate, known to inhibit the cystine/glutamate antiporter leading to decreased osteocalcin expression through depletion of GSH (Takarada-Iemata et al. 2010). In support of this, EAATs and the antiporter colocalise in human corneal epithelium (Langford et al. 2010) and rat lens (Lim et al. 2005). However EAAT inhibitors alone, which also reduce glutamate uptake, did not mimic the glutamate-induced down-regulation of osteocalcin expression. It is possible that *t*-PDC and TBOA do not sustain their inhibitory activity over time or at the specific location of the antiporter and, in the case of *t*-PDC, accumulate intracellularly preventing the sustained inhibition of extracellular glutamate uptake. Inhibitors of the cystine/glutamate antiporter, such as homocysteic acid, could be used to test the hypothesis that the glutamate-induced down-regulation of osteocalcin and Runx2 in MG-63 and primary human osteoblasts is the result of reversal of the cystine/glutamate antiporter.

At physiological glutamate concentrations, mean MG-63 osteocalcin expression was increased by inhibition of EAAT1 N-terminal interactions but decreased by inhibition

of EAAT1 TM6-7 and C-terminal interactions. Each EAAT1 competing peptide increased mean uptake activity of 10μM glutamate, suggesting that these effects are not mediated by increased extracellular glutamate inhibiting the cystine/glutamate antiporter, although kinetic characterisation of the glutamate uptake saturation curves with each peptide is necessary to be certain of this. Therefore, an EAAT-mediated mechanism involving intracellular interactions with EAAT1 TM 6-7 and/or C-terminus may positively regulate the expression of osteocalcin. This is consistent with the observed decrease in osteocalcin expression when overexpressing either EAAT1 splice variant since intracellular interactions downstream of TM2 (EAAT1a) and at the C-terminus (EAAT1ex9skip) are likely to be altered.

These findings suggest that MG-63 osteocalcin expression may be regulated by both the effects of extracellular glutamate on the cystine/glutamate antiporter and by an EAAT1-mediated mechanism that is dependent on intracellular interactions of the protein but not dependent on the extracellular glutamate concentration.

7.3.2.2 SaOS-2 cells

SaOS-2 cells exhibit a late-osteoblast phenotype (Pautke et al. 2004; Shapira and Halabi 2009). SaOS-2 cells display low levels of Na^+-independent compared to Na^+-dependent glutamate transport (section 3.3.3.1.1), suggesting that in comparison to the EAATs, the cystine/glutamate antiporter does not play a major role in the uptake of 1-250μM extracellular glutamate in SaOS-2 cells. Inhibition of EAAT glutamate transport by *t*-PDC and TBOA at physiological glutamate concentrations increased SaOS-2 osteocalcin expression. In rat calvarial osteoblasts, NMDA receptor activation increases Runx2 activity and expression of osteocalcin (Hinoi et al. 2003; Lin et al. 2008), suggesting that in SaOS-2 cells, EAAT inhibition increases the level of extracellular glutamate available to activate NMDA receptors. However, 500μM glutamate alone and in combination with EAAT inhibitors had no effect on SaOS-2 osteocalcin expression, indicating that at physiological glutamate concentrations, there is a transporter-mediated effect on osteocalcin expression in these cells that is independent of extracellular glutamate.

Since TBOA caused the largest increase in SaOS-2 osteocalcin expression and is known to block the glutamate gated anion conductance of EAATs (Shimamoto et al. 1998; Seal et al. 2001; Ryan and Vandenberg 2002), this may suggest that the

chloride flux downregulates osteocalcin expression. However overexpression of EAAT1a, which lacks domains required for glutamate gated anion conductance, significantly decreased SaOS-2 osteocalcin expression. This suggests that the effect of TBOA may be due to inhibition of anion conductance of EAATs 2-5. Alternatively, the data are consistent with an intracellular interaction of EAAT1, lost in EAAT1a, therefore down-stream of the N-terminus that is activated upon binding of TBOA (but not *t*-PDC or glutamate), leading to increased osteocalcin expression. TBOA is non-transportable, unlike glutamate and *t*-PDC, and may remain bound extracellularly for longer, sustaining an intracellular interaction response that increases osteocalcin expression. Further evidence for this hypothesis is provided by inhibition of EAAT1 C-terminal intracellular interactions, which leads to decreased mean osteocalcin mRNA levels in SaOS-2 cells. Potential mediators of this response include ezrin, GFAP, NHERF1 and Sept2/4 which are known to bind to the C-terminus of EAAT1 (Table 6.1) (Kinoshita et al. 2004; Lee et al. 2007; Sullivan et al. 2007b).

This possible receptor-like function for EAATs leading to increased osteocalcin expression is potentially important in bone biology and the mechanism should be further investigated. There is some evidence linking EAAT activity with MAPK activation (Abe and Saito 2001; Marie et al. 2002) and MAPK activity has been associated with regulation of osteocalcin expression in MC3T3-E1 osteoblast-like cells, through direct phosphorylation of Runx2 (Xiao et al. 2000). EAAT activation of MAPK was dependent on glutamate transport (Abe and Saito 2001) or via an N-terminal EAAT interaction (Marie et al. 2002). This mechanism does not explain our data in SaOS-2 cells since increased osteocalcin expression was observed with TBOA which inhibits transport and preventing EAAT1 N-terminal interactions using competing peptides had no effect at physiological glutamate concentrations and increased mean osteocalcin levels at pathophysiological glutamate concentrations. To determine whether EAAT1 activation of MAPK activity is relevant to this response, SaOS-2 cells treated with TBOA in the presence and absence of competing peptides to EAAT1 intracellular domains could be analysed by western blotting for phosphorylated MAPK.

7.3.3 Modulation of EAAT activity may influence coupling of proliferation and differentiation in osteoblasts

Proliferation and differentiation towards a bone-forming phenotype are negatively coupled in osteoblasts (Lian and Stein 1995; Karsenty 2003) (Figure 4.18). The expression of genes associated with proliferation decreases as bone matrix genes are upregulated during osteoblast maturation (Malaval et al. 1999; Karsenty 2003; Lian and Stein 2003; Stein et al. 2004). Osteosarcoma cells such as MG-63 and SaOS-2 exhibit a dysregulation of sequential gene expression that normally occurs during osteoblast differentiation and the genes associated with each development stage are expressed simultaneously (Lian and Stein 1993). However the data presented here and discussed below indicate that modulation of EAAT activity may influence the coupling of proliferation and differentiation in osteoblast-like cells. Experiments with primary human osteoblasts at early and late differentiation stages did not validate all the findings in MG-63 and SaOS-2 cells; however insufficient experiments and replicates were carried out to comprehensively test this.

Further understanding of the regulatory mechanisms that govern the relationship between proliferation and differentiation in osteoblasts could provide valuable guidance for the diagnosis and targeted treatment of skeletal disorders such as bone cancers, where aberrations in this relationship have occurred. Furthermore, prolonging the proliferative stage of osteoblast development prior to differentiation may have application to fracture repair where it would be advantageous to ensure an adequate quantity of osteoblasts is available to fill the defect. The role of EAATs in regulating the coupling of osteoblast proliferation and differentiation should be further investigated by comprehensively determining the effects of EAAT modulation at each stage of primary osteoblast maturation (Figure 4.18).

7.3.3.1 MG-63 cells

At physiological glutamate concentrations, *t*-PDC and TBOA increased mean MG-63 cell number. It is not possible to say whether inhibitors increased proliferation or decreased apoptosis, particularly since glutamate signalling through ionotropic glutamate receptors is known to mediate both neural progenitor cell proliferation

(Haydar et al. 2000; Bai et al. 2003) and survival (Ikonomidou et al. 1999). However, EAAT inhibitors did not significantly affect human primary osteoblast cell death.

NMDA receptor activation causes proliferation of MC3T3-E1 osteoblast-like cells (Fatokun et al. 2006) as well as neuronal progenitor cells, cancer cells, chondrocyte-like cells and synovial fibroblasts (Contestabile 2000; Rzeski et al. 2001; Parada-Turska et al. 2006; Spitzer 2006; Piepoli et al. 2009). This suggests that EAAT inhibitors increase MG-63 cell number by increasing the concentration of extracellular glutamate available to activate NMDA receptors.

In contrast to the effects of *t*-PDC and TBOA, overexpression of EAAT1ex9skip (which specifically inhibits glutamate transport through EAAT1) decreased MG-63 cell number at physiological glutamate concentrations. Thus EAAT1 directly increases MG-63 cell number, independently of the extracellular glutamate concentration, possibly through localisation close to particular inhibitory glutamate receptor subtypes (section 7.3.1). Overexpression of EAAT1a did not decrease MG-63 cell number at physiological glutamate concentrations, indicating differences between the two splice variants in their mechanism of EAAT1 inhibition.

Pathophysiological glutamate concentrations (500μM) only increased cell number when added during the proliferative stage of osteoblast growth. For example, 500μM glutamate increased MG-63 cell number in experiments presented in chapter 4 but not in untransfected cells in chapters 5 or 6 where glutamate was added 24hrs later when cells were more confluent. Changes in components of the glutamate signalling system may occur as osteoblasts grow and mature (discussed further in section 7.3.4).

Loss of C-terminal interactions using competing peptides increased MG-63 cell number in the presence of 500μM glutamate indicating that the EAAT1 C-terminal may interact with other proteins within the cell directly to downregulate cell number. Alternatively, since loss of C-terminal intracellular interactions increased mean glutamate uptake activity in MG-63 cells, this may reduce the activation of nearby glutamate receptor subtypes that signal to inhibit the increase in cell number. The C-terminal competing peptide may also disrupt the conformation of the anion pore (Mitrovic et al. 1998). The glutamate-gated chloride conductance may negatively regulate proliferation under normal conditions by modulating ion entry following NMDA receptor activation. However, blocking the glutamate-gated chloride conductance of all EAATs using TBOA prevented the glutamate-induced increase in

MG-63 cell number, suggesting that the mechanism responsible may be specific to EAAT1.

7.3.3.2 SaOS-2 cells

EAAT inhibition by *t*-PDC and TBOA significantly increased SaOS-2 cell number, suggesting that reduced glutamate uptake increases the extracellular glutamate available to activate the NMDA receptors responsible for increasing cell number. EAAT inhibitors also decreased SaOS-2 ALP activity and mineralisation suggesting that these treatments may prolong the proliferation stage of osteoblast maturation, preventing the upregulation of genes associated with matrix maturation and mineralisation. Prolonging of the proliferation stage of osteoblast maturation has previously been observed in primary human and rat osteoblasts subjected dynamic cell stretching (Stanford et al. 1995a; Kaspar et al. 2000) and TGF-β (Lian and Stein 1993). Inconsistent with this however, is the increase in SaOS-2 osteocalcin expression, a marker of late osteoblasts, in response to TBOA and this may reflect the dysregulation of proliferation and differentiation in osteosarcoma cell lines.

In contrast, overexpression of EAAT1ex9skip (which specifically inhibits glutamate transport through EAAT1) increased SaOS-2 ALP activity at physiological glutamate concentrations. Thus specific inhibition of EAAT1 may drive osteoblast differentiation from the proliferative stage to the non-proliferating matrix maturation stage, inferring that EAAT1 activity specifically decreases ALP activity, independently of glutamate receptor activation by extracellular glutamate. Overexpression of EAAT1a did not have the same effects, again suggesting differences between the two splice variants.

Pathophysiological glutamate concentrations alone did not affect SaOS-2 cell number; however overexpression of EAAT1a increased SaOS-2 cell number at 500μM glutamate. Overexpression of EAAT1a decreased SaOS-2 glutamate uptake, suggesting that the increase in cell number may be due to increased activation of NMDA receptors. However, overexpression of EAAT1ex9skip, which inhibited SaOS-2 uptake of 10μM glutamate to a greater extent compared to overexpression of EAAT1a (Figure 5.9), had no effect on SaOS-2 cell number at pathophysiological glutamate concentrations. This suggests the existence of an alternative mechanism relating glutamate to cell number that is dependent upon regions of the EAAT1

protein lost in EAAT1a. EAAT1a is thought to reorient in the plasma membrane thus preventing any C-terminal intracellular interactions (Huggett et al. 2000). Consistent with this, loss of C-terminal interactions using competing peptides increased MG-63 cell number in the presence of 500μM glutamate.

7.3.4 Evidence for maturation-specific glutamatergic signalling in osteoblasts

Modulation of EAAT activity often differentially affected MG-63 and SaOS-2 cells, suggesting that cells with a pre-osteoblast phenotype (MG-63) respond differently to cells with a late osteoblast phenotype (SaOS-2). The confluence dependent effects of glutamate (discussed in section 7.3.3.1) and the differences in the short- and long-term effects of EAAT inhibitors on primary osteoblast ALP activity also support the theory that glutamate signalling may have different effects in osteoblasts depending on the maturation stage. The differentiation stage of osteoblasts is also known to regulate the response to 1,25-dihydroxyvitamin D_3 and PTH (Majeska and Rodan 1982; Isogai et al. 1996).

The effect of osteoblast differentiation stage on the response to glutamate and/or EAAT inhibitors may reflect altered levels of glutamate receptor/transporter expression, the expression of particular receptor/transporter subtypes, or differences in glutamate release or transporter activities. The evidence from this thesis and other publications to support this is discussed below.

This thesis has highlighted the differences between MG-63 and SaOS-2 cells in EAAT expression and activity, in the regulation of EAAT activity by extracellular glutamate, and the ratio of EAAT1 to its splice variant EAAT1ex9skip. Other studies have shown that total glutamate uptake decreases as rat calvarial osteoblasts mature in culture from 7 to 21 days (Takarada et al. 2004). This is in contrast to MG-63 and SaOS-2 cells which are thought to represent a pre- and late-osteoblast phenotype respectively, since SaOS-2 cells display greater total and Na^+-dependent glutamate uptake activity than MG-63 cells (section 3.3.3.1.1). These differences could be due to species or culture conditions.

In addition to the EAATs, osteoblast differentiation also alters glutamate release, receptor expression and the response to glutamate receptor activation and cystine/glutamate antiporter activity. For example, glutamate release increases during

maturation of MC3T3-E1 osteoblast-like cells (Genever and Skerry 2001). Although again this is in contrast to the maturation phenotypes of MG-63 and SaOS-2 cells since SaOS-2 cells exhibit lower rates of glutamate release (~3.7 nmoles/mg protein) than MG-63 cells (~7 nmoles/mg protein) (Genever and Skerry 2001). In rat calvarial osteoblasts, expression of NR1 mRNA remained constant over 7-28 days *in vitro*, whereas expression of NR2D mRNA was reduced by ~50% in osteoblasts cultured for 21 and 28 days compared to 7 days (Hinoi et al. 2003).

There appear to be two opposing mechanisms linking glutamate to osteoblast differentiation. Osteoblast differentiation of bone marrow stromal cells was prevented by high concentrations of glutamate which inhibit the cystine/glutamate antiporter and reduce GSH levels (Takarada-Iemata et al. 2010), whereas studies from Hinoi et al. demonstrate that NMDA receptor activation is associated with increased Runx2 and ALP activity of rat calvarial osteoblasts if added to the culture after the proliferative stage of maturation (Hinoi et al. 2003). These data suggest that high concentrations of glutamate can inhibit osteoblast differentiation of bone marrow stromal cells in association with GSH depletion but that glutamate signalling through specific glutamate receptors increases differentiation and bone forming activity of committed osteoblasts. These differences may reflect changes in the expression and activity of glutamate signalling components during maturation of osteoblasts, or the effects of different glutamate concentrations i.e. pathophysiological concentrations inhibit the cystine/glutamate antiporter whereas physiological concentrations activate glutamate receptors. The latter possibility is highly relevant to pathological situations associated with high glutamate concentrations such as OA, RA, gout (McNearney et al. 2004) and may be important in fresh bone fractures. Enhanced knowledge of maturation-stage dependent glutamate signalling in bone would be useful for the therapeutic targeting of EAATs or other glutamatergic signalling components in the treatment of bone disorders or fracture.

7.4 A role for EAATs in the regulation of bone remodelling?

The mechanisms that couple osteoblast and osteoclast activities in bone remodelling (section 1.2) are poorly understood but could be exploited therapeutically to inhibit bone resorption while simultaneously promoting bone formation. Osteoclast

differentiation and resorption is regulated by osteoblasts via the OPG/RANK/RANK-L system (section 1.1.1.2) (Yasuda et al. 1998a; Yasuda et al. 1998b) and the data in this thesis indicate that modulation of EAAT activity affects expression of OPG in SaOS-2 osteoblasts. Mean OPG mRNA levels were increased in SaOS-2 cells in response to 24hr incubation with 500μM glutamate and this was prevented by *t*-PDC. Thus glutamate uptake through the transporter may promote expression of OPG. A reduction in OPG mRNA levels in SaOS-2 cells expressing either the TM6-7 or C-terminal domain of EAAT1 at 500μM glutamate, or all three peptides at physiological glutamate levels, implicates these regions in the signalling event. Since each EAAT1 peptide had a similar effect on OPG expression in SaOS-2 cells, it is possible that the glutamate-induced increase in OPG expression requires the tertiary structure of EAAT1 protein, possibly to form the anion pore (Mitrovic et al. 1998). This is the first report linking the glutamate signalling pathway in bone to the regulation of OPG expression.

The role of glutamate in the processes that couple osteoblast and osteoclast activity is shown in Figure 7.3. Evidence is provided by expression of glutamatergic signalling components in each cell type (Table 1.3 and 1.4), activation of glutamate receptors that regulate osteoclast and osteoblast differentiation and activity (Chenu et al. 1998; Peet et al. 1999; Itzstein et al. 2000; Hinoi et al. 2003; Ho et al. 2005; Lin et al. 2008), glutamate release by both cell types (Genever and Skerry 2001; Morimoto et al. 2006) and the fact that inhibition of the cystine/glutamate antiporter inhibits differentiation of both osteoclasts (Hinoi et al. 2007) and osteoblasts (Takarada-Iemata et al. 2010). Modulation of EAAT activity *in vivo* will therefore affect multiple bone cell types and strategies to target cell type specific EAAT activity may need to be employed in further studies.

A role for osteoblast expressed EAATs in regulating the expression of OPG, and therefore the differentiation and activity of osteoclasts, could be further tested by specifically inhibiting SaOS-2 EAATs (by siRNA) in co-cultures of osteoblasts and pre-osteoclasts and analysing RANKL expression and osteoclast differentiation and activity.

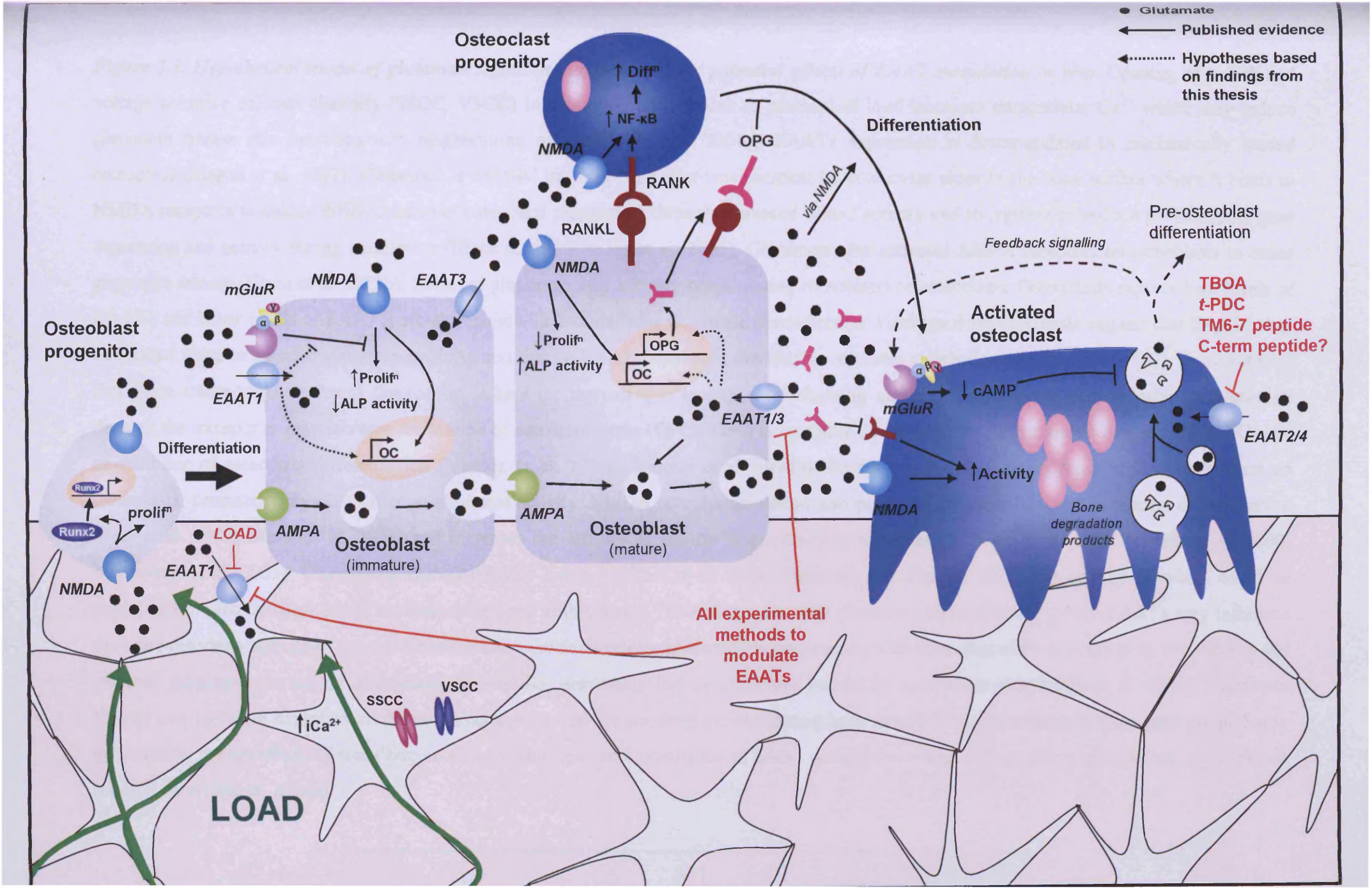
Glutamate
Published evidence
Hypotheses based on findings from this thesis
Osteoclast progenitor
↑ Diffⁿ
↑ NF-κB
NMDA
RANK
RANKL
OPG
Differentiation
via NMDA
Pre-osteoblast differentiation
Feedback signalling
TBOA
t-PDC
TM6-7 peptide
C-term peptide?
Activated osteoclast
mGluR
↓ cAMP
↑Activity
EAAT2/4
EAAT1/3
Bone degradation products
Osteoblast progenitor
EAAT1
↑Prolifⁿ
↓ALP activity
OC
Differentiation
Runx2
prolifⁿ
LOAD
AMPA
Osteoblast (immature)
Osteoblast (mature)
All experimental methods to modulate EAATs
SSCC
VSCC
↑iCa2+
LOAD

Figure 7.3. Hypothetical model of glutamate signalling in bone and the potential effects of EAAT modulation in vivo. Opening of stretch and voltage sensitive calcium channels (SSCC, VSCC) in osteocytes in response to mechanical load increases intracellular Ca^{2+} which may induce glutamate release into junctions with neighbouring osteocytes (Mason 2004a). EAAT1 expression is downregulated in mechanically loaded osteocytes (Mason et al. 1997). Glutamate is released into the bone microenvironment by osteocytes close to the bone surface where it binds to NMDA receptors to induce differentiation of osteoblast progenitors through increased Runx2 activity and to regulate osteoblast proliferation, gene expression and activity during maturation (Hinoi et al. 2003; Ho et al. 2005). Glutamate also activates AMPA receptors on osteoblasts to cause glutamate release (Hinoi et al. 2002b). Released glutamate may activate neighbouring osteoblasts or osteoclasts. Osteoblasts express high levels of EAAT1 and lower levels of EAAT3, which regulate the extracellular glutamate concentration. Findings from this thesis suggest that EAAT1 may be located close to specific inhibitory mGluRs and that an EAAT1-mediated mechanism regulates expression of osteocalcin (OC), demonstrating that these transporters represent therapeutic targets for increasing osteoblast bone-forming activity. Furthermore, accumulation of glutamate through the transporter may increase expression of osteoprotegerin (OPG). OPG is a soluble decoy receptor for osteoblast-expressed RANKL and an inhibitor of osteoclast differentiation (Yasuda et al. 1998a; Yasuda et al. 1998b). Binding of RANKL to its receptor RANK, present on osteoclasts, promotes osteoclast differentiation and activity. NMDA receptor activation also promotes NF-κB stimulated osteoclast differentiation (Peet et al. 1999; Merle et al. 2003) and increases the activity of mature bone-resorbing osteoclasts (Chenu et al. 1998; Itzstein et al. 2000; Mentaverri et al. 2003). Osteoclasts express EAATs 2 and 4 (Hinoi et al. 2007; Takarada and Yoneda 2008), the activity of which could be modulated *in vivo* by some of the methods developed in this thesis. Preventing osteoclast glutamate accumulation through EAATs may influence the bone-resorbing activity of the cell since mature osteoclasts release glutamate in conjunction with bone degradation products by transcytosis and released glutamate can act on autorgeulatory mGluRs, preventing further glutamate release by osteoclasts (Morimoto et al. 2006). Glutamate signals may therefore contribute to the mechanoresponse and the coupling process during bone remodelling. Alterations in bone mass are probably governed by the net effects of signalling on all bone cell types and modulation of EAAT activity *in vivo* is likely to affect multiple cell types. Figure adapted from (Mason 2004a).

7.5 Do EAATs play a role in regulating bone formation?

A role for glutamate in the regulation of bone mass has been highlighted by transgenic models lacking components of the signalling pathway, including VGLUT1$^{-/-}$ and bone specific NMDAR1 subunit knockouts, which display reduced bone mass (Hinoi et al. 2007; Skerry 2008). Furthermore, glutamate receptor activation has been implicated in osteoblast and osteoclast differentiation and activity (Chenu et al. 1998; Peet et al. 1999; Itzstein et al. 2000; Hinoi et al. 2003; Merle et al. 2003; Ho et al. 2005; Lin et al. 2008; Olkku and Mahonen 2008), and mechanical load, a potent osteogenic stimulus, can regulate expression of GLAST and glutamate receptors in bone *in vivo* (Mason et al. 1997; Ho et al. 2005; Szczesniak et al. 2005). These findings provide evidence that glutamate signalling regulates bone formation and remodelling and that modulation of the transporters can influence this.

The role of EAATs in the regulation of bone formation has not been comprehensively tested *in vitro* and the lack of an effect on bone growth in the GLAST knockout mouse has led some researchers to believe that GLAST activity does not play a major role in bone growth (Gray et al. 2001). However, redundancy amongst the transporters expressed was not taken into account, nor were the effects of modelling versus remodelling or the response to challenge (Chenu et al. 2001; Skerry et al. 2001). The studies presented in this thesis strongly suggest that EAAT activity in osteoblasts regulates the bone forming phenotype.

7.5.1 Could therapeutic modulation of EAATs enhance bone formation?

Inhibition of each EAAT activity has shown the potential to increase osteoblast cell number and/or bone-forming activity, demonstrating potential for therapeutic enhancement of bone mass. TBOA increased cell number and osteocalcin expression in SaOS-2 cells at physiological glutamate levels and increased ALP activity and mineralisation of primary human osteoblasts at pathophysiological glutamate concentrations. Overexpression of EAAT1a also increased cell number in SaOS-2 cells at 500μM glutamate and overexpression of EAAT1ex9skip increased SaOS-2 ALP activity in the absence of exogenous glutamate. Furthermore, competing peptides to EAAT1 C-terminal domain increased MG-63 cell number at 500μM

glutamate while inhibition of EAAT1 N-terminal interactions increased mean osteocalcin expression in MG-63 cells at 0μM glutamate and in SaOS-2 cells at 500μM glutamate.

These effects varied between different cell lines, time in culture (section 7.3.4) and glutamate concentration, indicating that therapeutic modulation of EAAT activity should be targeted to a particular osteoblast maturation stage and pathological state with respect to glutamate concentration.

Glutamate concentration is increased in inflamed joints (Lawand et al. 2000; McNearney et al. 2004) however the glutamate concentration that osteoblasts are exposed to at the defect site of a fresh or non-union fracture or in osteoporosis is currently unknown. Glutamate concentrations might be expected to increase during the initial inflammatory stage of fracture repair (section 1.2.1.5.1); however such concentrations may then dissipate under conditions of non-union. Therefore to define the most appropriate therapeutic strategy for targeting EAATs in bone, information regarding glutamate levels at the site of treatment is required. Alternatively, glutamate itself, or specific agonists, could be directly delivered with the therapeutic to achieve the appropriate conditions.

Whilst potential for therapeutic targeting of EAATs in bone has been revealed here, the data are complex and require further investigation. The data suggest that EAATs may finely tune the glutamate response in a manner that depends on osteoblast differentiation stage, EAAT subtype expression and localisation as well as which specific EAAT activity predominates. To further investigate the potential for EAAT modulation in bone repair, these experimental methodologies should be applied to a model of human primary osteoblast differentiation, to determine the appropriate maturation stage to target at physiological and pathophysiological glutamate concentrations, and then ultimately an *in vivo* model. The experiments here indicate that the primary outputs to measure in such *in vitro* studies are osteocalcin and OPG expression and ALP activity. The *in vivo* model chosen will depend on the dosing and delivery of a particular therapeutic agent but could comprise a rodent model of fracture repair or a model of post-menopausal bone loss in ovariectomised mice. However, effects *in vivo* are likely to differ from *in vitro* since modulation of glutamatergic signalling has the potential to affect each cell type in bone (illustrated in Figure 7.3) as well as other tissues and nerves.

7.5.1.1 Therapeutic strategies in bone

7.5.1.1.1 Non-union fracture

Atrophic non-unions are typified by insufficient availability of bone forming cells, preventing normal bone healing from occurring (Megas 2005) (section 1.2.1.5.2). Therefore, treatments to increase the number or activity of osteoblasts available to fill the defect would be advantageous.

Data from this thesis (section 7.5.1), demonstrates that inhibition of each EAAT activity can increase osteoblast cell number and/or bone-forming activity, suggesting that therapeutic targeting of EAATs may have application to fracture repair.

Local delivery of a therapeutic for fracture healing does not require chronic application, since there is no need for the activity to persist beyond the time required to achieve healing, therefore each of our methods to inhibit EAAT activity displays therapeutic potential. One method for site-specific delivery to bone is the application of the molecules incorporated in an absorbable collagen sponge. This process is currently used clinically in the application of rhBMP-2 and rhBMP-7 for spinal fusion and the treatment of non-union fracture (section 1.2.1.5.2.1), and is appropriate for the delivery of chemical EAAT inhibitors, AONs and competing peptides with CPP tags. Alternative delivery strategies include the direct injection of the molecules into the defect space or, with respect to AONs and peptides, the injection of viral vectors expressing the sequences. This method has the advantage of being non-surgical.

7.5.1.1.2 Osteoporosis

Osteoporosis is a disorder of uncoupled bone remodelling, where insufficient bone is formed in response to increased resorption (section 1.2.1.2). The majority of current therapeutics for osteoporosis target bone resorption and there is a pressing need for the development of anabolic bone agents. Methods that regulate EAATs to increase osteoblast bone forming activity may reflect potential therapies for osteoporosis. These include TBOA and competing peptides to the EAAT1 N-terminal domain which increased expression of osteocalcin at both physiological and pathophysiological glutamate concentrations, and overexpression of EAAT1ex9skip which increased SaOS-2 ALP activity at physiological glutamate levels.

Osteoporosis is a systemic disease and therefore requires systemic delivery of a therapeutic. Since glutamate signalling pathways are functional in several sites of the body besides the CNS and bone (reviewed in (Skerry and Genever 2001; Hinoi et al. 2004)), a targeted delivery strategy for EAAT modulation to mineralised tissues would need to be employed to avoid adverse systemic effects. One way to achieve this might be tagging the therapeutic to bisphosphonates (section 1.2.1.4) which selectively adsorb to mineral surfaces (Jung et al. 1973), thus forming a new type of drug that is both anabolic and anti-resorptive. However, linking the drug to targeting compounds would increase its size, thus potentially reducing its oral bioavailability, necessitating injection.

AONs could be delivered systemically by injecting into the blood and targeted to bone by viral vectors expressing the sequence under a bone specific promoter, such as the Runx2 or osteocalcin promoter. The promoter used would depend on the appropriate maturation stage of the osteoblast to target.

7.5.1.1.3 Osteolysis

Osteolysis is the most significant long-term complication associated with artificial joint replacement and is characterised by bone resorption leading to implant loosening and failure (reviewed in (Purdue et al. 2007)). Methods to improve the osteoconduction and osteoinduction of the implant, or to reduce the activity of osteoclasts in the vicinity of the implant, could prevent osteolysis and implant loosening

The data in this thesis shows that modulation of EAAT activity increases osteoblast cell number and markers of bone formation, strategies that could be osteoinductive. Furthermore, overexpression of EAAT1ex9skip and competing peptides to the EAAT1 C-terminal domain increased expression of OPG in SaOS-2 and MG-63 cells respectively. Since OPG inhibits osteoclast differentiation and activation, these molecules could prevent the bone resorption that typifies osteolysis.

Delivery of therapeutics for osteolysis could involve tethering peptides to the surface of the implant or incorporation into a bone void filler for revision surgeries.

7.5.1.1.4 Osteosclerosis

Sclerosing bone dysplasias are characterised by increased bone density (section 1.2.1.1), so methods to reduce osteoblast activity or increase osteoclast activity could be potential treatments for these diseases.

Our data shows that chemical EAAT inhibition reduces ALP activity and mineralisation of SaOS-2 cells, suggesting that these inhibitors may be exploited therapeutically to reduce bone formation. However, these effects were not apparent in primary osteoblasts.

SaOS-2 OPG expression was decreased by *t*-PDC and competing peptides to each EAAT1 intracellular domain tested. Methods to decrease OPG expression in osteoblasts could be used to increase osteoclast differentiation and activity and therefore increase bone resorption.

Osteosclerosis is a systemic disorder, and therefore presents the same problems of therapeutic targeting to bone as discussed with reference to osteoporosis (section 7.5.1.1.2). Furthermore, these disorders are characterised by genetic defects and as such would require chronic treatment, which may not be suited to application of the peptides which have a short half-life *in vivo*.

7.5.2 Non-bone therapeutic applications

7.5.2.1 Ectopic calcification

Ectopic calcification is the inappropriate mineralisation of soft tissues including kidney, cardiovascular tissues, skin and tendons (reviewed in (Giachelli 1999)). Therefore, although experiments designed to analyse the effects of EAAT inhibitors on mineralisation gave contradicting results in SaOS-2 and primary human osteoblasts, a consistent and considerable decrease in SaOS-2 mineralisation was detected. It may therefore be useful to investigate the activity of these inhibitors in conditions such as these, where mineralisation is undesirable.

7.5.2.2 Osteosarcoma

Osteosarcoma is the most common form of primary bone cancer and occurs primarily in developing bones. The MG-63 cell line used in these studies is osteosarcoma derived and overexpression of EAAT1ex9skip and chemical EAAT inhibition decreased MG-63 cell number at physiological and pathophysiological glutamate concentrations respectively. Methods to inhibit the growth of cancer cells are therapeutically advantageous and glutamate receptor antagonists are currently being investigated to this purpose (Rzeski et al. 2002). These studies indicate that targeting of EAATs in osteosarcoma may also represent a therapeutic strategy.

7.5.2.3 CNS pathologies

The methods developed here to characterise EAAT activity in osteoblasts may prove beneficial for the understanding, prevention and treatment of CNS pathologies such as ischemic brain damage (Kuwahara et al. 1992; Rossi et al. 2000), epilepsy (Meldrum 1994; Tanaka et al. 1997; Meldrum et al. 1999; Guo et al. 2010), ALS (Rothstein et al. 1995; Rothstein et al. 1996; Howland et al. 2002), Alzheimer's disease (Scott et al. 1995; Scott et al. 2002; Maragakis and Rothstein 2004) and Parkinson's disease (Blandini et al. 1996; Chase et al. 2000) which are characterised by a dysregulation of glutamatergic signalling. In the CNS, EAATs control the extracellular concentration of glutamate, preventing excitotoxicity and neuronal injury (Marcaggi and Attwell 2004). Trafficking of EAATs is poorly understood and competing peptides to EAAT1 may help identify interactions that are important for cell surface expression of the transporter in glial cells which undergo extensive cytoskeletal reorganisation during development and injury to the brain (Pekny and Nilsson 2005). SaOS-2 glutamate uptake was down-regulated following exposure to extracellular glutamate (Figure 3.16) with no alterations in EAAT transcription (Figure 3.3), and identification of the intracellular interactions important for this response may provide a target for maintaining glutamate transport under conditions of excitotoxic levels of glutamate in the CNS. Furthermore, characterisation of EAAT1 splicing following ischemia, or forced overexpression of the splice variants in glial cells *in vitro,* may be useful in the context of ischemic stroke injury. ATP levels drop in ischemia and the electrochemical gradients cannot be maintained, leading to reversed operation of

EAATs and glutamate release (Rossi et al. 2000), a major contributor to the neurotoxicity associated with stroke-induced ischemic brain damage (Kuwahara et al. 1992; Rossi et al. 2000). Inhibition of EAAT transport activity would prevent glutamate release under these conditions. We and others have shown that overexpression of EAAT1ex9skip inhibits glutamate uptake and Sullivan et al. detected EAAT1ex9skip expression in neurons and regions that are susceptible to damage in the hypoxic pig brain (Sullivan et al. 2007a), suggesting that EAAT1ex9skip expression may represent a protective mechanism.

7.6 Effects of modulating EAAT activity beyond the glutamate signalling pathway

The findings from this PhD have largely been discussed in the context of glutamate signalling; however it is likely that modulation of EAAT activity will have broader effects within the cell. Inhibition of EAAT uptake under conditions of high extracellular glutamate levels will reduce the intracellular accumulation of glutamate, reducing the driving force behind the cystine/glutamate antiporter, which has been shown to be important for osteoblast proliferation and differentiation (Iemata et al. 2007; Takarada-Iemata et al. 2010). In bone, such effects are likely to affect pre-osteoblasts since MG-63 cells displayed high levels of Na^+-independent glutamate uptake and decreased expression of osteocalcin in response to 500μM glutamate.

In addition, the intracellular glutamate concentration is regulated during osteoblast differentiation through the action of glutamine synthetase (GS) which converts glutamate to glutamine (Olkku and Mahonen 2008) and inhibition of osteoblast EAAT activity may disrupt this regulated control over intracellular glutamate concentration. During osteogenic differentiation of rat MSCs, GS activity declines rapidly at the onset of mineralisation and this change in activity is reflected by increased intracellular glutamate concentrations (Olkku and Mahonen 2008; Zheng and Quirion 2009). In our studies, inhibition of glutamate transport decreased mineralisation of SaOS-2 cells and this may occur as a consequence of reduced intracellular glutamate concentrations, consistent with these studies from Olkku and Mahonen. However a similar effect was not detectable in primary osteoblasts.

Evidence from the CNS suggests interplay between the glutamate signalling pathway and other signalling pathways that are present in bone such as IGF, adenosine and calcium (Gama et al. 2001; Ferre et al. 2002; Fuxe et al. 2003; Domenici et al. 2004; Ciruela et al. 2006). IGF has been implicated in mechanical load-induced osteogenesis (section 1.3) and adenosine and calcium receptors can also function in bone cells to influence bone formation (Dvorak and Riccardi 2004; Dvorak et al. 2004; Evans et al. 2006). Activation of PLC by PTH in rat femoral osteoblasts prevented calcium influx through NMDA receptors suggesting interplay between these two pathways in bone (Gu and Publicover 2000). Furthermore, the canonical Wnt signalling pathway negatively regulates the activity of GS in MG-63 cells, thus increasing the intracellular glutamate concentration (Olkku and Mahonen 2008). Therefore, the effects of modulating EAAT activity are complex and widespread.

7.7 Critique of the experimental approaches taken

MG-63 and SaOS-2 cell lines exhibit different maturational phenotypes and were purposely chosen to investigate whether EAAT modulation was more effective at a particular stage of osteoblast differentiation. Osteosarcoma-derived cells are commonly accepted and widely published as appropriate *in vitro* osteoblast models (Bilbe et al. 1996), however they lack the sequential gene expression that accompanies osteoblast differentiation (Lian and Stein 1993). Therefore it is necessary to confirm that the differences in the expression and activity of glutamate signalling components between these cell lines reflect the normal changes that occur during osteoblast differentiation. To do this, human primary osteoblasts were used, but proved too expensive to obtain adequate replicates. It would be informative to profile EAAT expression and activity as well as the effects of modulating EAAT activity in primary osteoblasts, preferably over maturation in culture. Primary osteoblasts from rodents are easier to obtain, however from a therapeutic perspective, showing proof of concept in human cells is more relevant than the same results in a non-human cell. Therefore, differentiating human osteoblasts should be used to answer the outstanding questions generated by this thesis.

These studies largely ignored the possibility that EAATs 4 and 5 might be expressed in osteoblasts since EAAT4 had not been detected in any peripheral tissue other than

placenta (Matthews et al. 1998) at the beginning of this PhD (Table 1.2) and expression of EAAT 5 is primarily restricted to the retina (Arriza et al. 1997; Pow and Barnett 2000). EAAT4 mRNA and protein expression have recently been demonstrated in osteoclasts (Hinoi et al. 2007; Takarada and Yoneda 2008) suggesting that this transporter might play a more active role in bone than was initially considered. EAAT5 mRNA was looked for and not detected in osteoclasts (Takarada and Yoneda 2008). It would be informative to quantify mRNA levels of EAATs 4 and 5 in human osteoblasts to determine more accurately the EAAT expression profile in these cells. Table 7.3 shows the experimental treatments utilised in this thesis which were not specific to EAAT1 and may therefore influence the activity of EAATs 4 and 5 should they be expressed in osteoblasts.

It is difficult to obtain an accurate view of the effects of altering EAAT activity in a system where glutamate is spontaneously released (Genever and Skerry 2001). Furthermore, the possibility exists that glutamate might also be released *in vitro* by medium displacement in osteoblasts due to its mechanoresponsiveness.

7.8 Future directions

7.8.1 Kinetic characterisation of glutamate uptake in cells overexpressing EAAT1 splice variants and competing peptides to EAAT1 intracellular domains

Overexpression of EAAT1 splice variants and competing peptides to EAAT1 intracellular domains altered Na^+-dependent uptake of 10μM glutamate in osteoblast-like cells. Kinetic characterisation of the Na^+-dependent glutamate uptake saturation curve in treated cells would further characterise the effect of the splice variants and competing peptides on EAAT1 activity. Such data would enhance our understanding of the transporter in all tissues where EAATs are expressed, particularly those where EAATs are known to be important in the pathogenesis of disease. Knowledge of the mechanisms regulating EAAT activity are poorly documented and very little is known regarding the physiological role of EAAT1a and EAAT1ex9skip. In our experiments, overexpression of EAAT1a reduced glutamate transport despite the variant retaining the regions of the protein important for glutamate binding and transport (Huggett et al.

2000) and evidence to suggest it is a functional transporter (Mason, Huggett, Daniels, unpublished). Therefore kinetic characterisation may help elucidate the importance of the ion channel domain, lost in EAAT1a, for glutamate uptake.

7.8.2 Is EAAT1 localised close to a particular receptor in osteoblasts and does this change during maturation?

EAAT localisation in the CNS can shape the synaptic event by regulating the local extracellular glutamate concentration available to activate glutamate receptors. Data from this thesis has suggested that inhibiting all EAATs may have different effects to inhibiting EAAT1 specifically and one explanation for this could be that EAAT1 is localised close to a particular receptor subtype that it important in the response of osteoblasts to glutamate. This hypothesis could be tested by immunofluorescent co-localisation of EAAT1 in osteoblasts with candidate glutamate receptor subtypes that are known to be expressed in osteoblasts (Table 1.3).

7.8.3 Does inhibition of EAATs sensitise osteoblasts to mechanical load?

The hypothesis behind this PhD was that inhibition of EAAT activity could mimic the osteogenic response of osteoblasts to mechanical load; however it is also possible that inhibition of EAAT activity actually primes the cells to be more responsive to mechanical load. It would be interesting to modulate EAAT activity in osteoblasts alone in a collagen gel, or in co-culture with osteocytes (Mason et al. 2008), subject to mechanical load and assess the effects on differentiation and bone-forming activity.

7.9 Concluding remarks

Glutamatergic signalling in bone is highly complex involving different receptors, transporters and various cell types. Its functional significance has been demonstrated in the literature and in this thesis. Many signalling pathways have been linked to load-induced bone formation and rather than any one factor that controls these events, it is probably an interplay of many signals. These data demonstrate that high-affinity glutamate transporters (EAATs) are expressed and functional in human osteoblasts

and that their modulation *in vitro* can affect osteoblast cell number and bone-forming activity. Furthermore, methods have been identified to therapeutically modulate EAAT activity *in vitro* that may have *in vivo* application for the treatment of traumatised or diseased bone.

Chapter 8: Bibliography

8. Bibliography

Aartsma-Rus A. and van Ommen G. J. (2007) Antisense-mediated exon skipping: a versatile tool with therapeutic and research applications. *RNA* **13,** 1609-1624.

Aartsma-Rus A., Kaman W. E., Weij R., den Dunnen J. T., van Ommen G. J. and van Deutekom J. C. (2006) Exploring the frontiers of therapeutic exon skipping for Duchenne muscular dystrophy by double targeting within one or multiple exons. *Mol Ther* **14,** 401-407.

Aartsma-Rus A., Janson A. A., Kaman W. E., Bremmer-Bout M., van Ommen G. J., den Dunnen J. T. and van Deutekom J. C. (2004) Antisense-induced multiexon skipping for Duchenne muscular dystrophy makes more sense. *Am J Hum Genet* **74,** 83-92.

Aartsma-Rus A., Fokkema I., Verschuuren J., Ginjaar I., van Deutekom J., van Ommen G. J. and den Dunnen J. T. (2009) Theoretic applicability of antisense-mediated exon skipping for Duchenne muscular dystrophy mutations. *Hum Mutat* **30,** 293-299.

Abdul M. and Hoosein N. (2005) N-methyl-D-aspartate receptor in human prostate cancer. *J Membr Biol* **205,** 125-128.

Abe K. and Saito H. (2001) Possible linkage between glutamate transporter and mitogen-activated protein kinase cascade in cultured rat cortical astrocytes. *J Neurochem* **76,** 217-223.

Adolph O., Koster S., Rath M., Georgieff M., Weigt H. U., Engele J., Senftleben U. and Fohr K. J. (2007) Rapid increase of glial glutamate uptake via blockade of the protein kinase A pathway. *Glia* **55,** 1699-1707.

Aguirre G., Rosas S., Lopez-Bayghen E. and Ortega A. (2008) Valproate-dependent transcriptional regulation of GLAST/EAAT1 expression: involvement of Ying-Yang 1. *Neurochem Int* **52,** 1322-1331.

Ajubi N. E., Klein-Nulend J., Alblas M. J., Burger E. H. and Nijweide P. J. (1999) Signal transduction pathways involved in fluid flow-induced PGE2 production by cultured osteocytes. *Am J Physiol* **276,** E171-178.

Allritz C., Bette S., Figiel M. and Engele J. (2009) Endothelin-1 reverses the histone deacetylase inhibitor-induced increase in glial glutamate transporter transcription without affecting histone acetylation levels. *Neurochem Int* **55,** 22-27.

Alter J., Lou F., Rabinowitz A., Yin H., Rosenfeld J., Wilton S. D., Partridge T. A. and Lu Q. L. (2006) Systemic delivery of morpholino oligonucleotide restores dystrophin expression bodywide and improves dystrophic pathology. *Nat Med* **12,** 175-177.

Amara S. G. and Fontana A. C. (2002) Excitatory amino acid transporters: keeping up with glutamate. *Neurochem Int* **41,** 313-318.

Apparsundaram S., Sung U., Price R. D. and Blakely R. D. (2001) Trafficking-dependent and -independent pathways of neurotransmitter transporter regulation differentially involving p38 mitogen-activated protein kinase revealed in studies of insulin modulation of norepinephrine transport in SK-N-SH cells. *J Pharmacol Exp Ther* **299,** 666-677.

Arbab A. S., Yocum G. T., Wilson L. B., Parwana A., Jordan E. K., Kalish H. and Frank J. A. (2004) Comparison of transfection agents in forming complexes with ferumoxides, cell labeling efficiency, and cellular viability. *Mol Imaging* **3,** 24-32.

Armour K. E. and Ralston S. H. (1998) Estrogen upregulates endothelial constitutive nitric oxide synthase expression in human osteoblast-like cells. *Endocrinology* **139,** 799-802.

Arriza J. L., Eliasof S., Kavanaugh M. P. and Amara S. G. (1997) Excitatory amino acid transporter 5, a retinal glutamate transporter coupled to a chloride conductance. *Proc Natl Acad Sci U S A* **94,** 4155-4160.

Arriza J. L., Fairman W. A., Wadiche J. I., Murdoch G. H., Kavanaugh M. P. and Amara S. G. (1994) Functional comparisons of three glutamate transporter subtypes cloned from human motor cortex. *J Neurosci* **14,** 5559-5569.

Aubin J. E., Liu F., Malaval L. and Gupta A. K. (1995) Osteoblast and chondroblast differentiation. *Bone* **17,** 77S-83S.

Bai F., Bergeron M. and Nelson D. L. (2003) Chronic AMPA receptor potentiator (LY451646) treatment increases cell proliferation in adult rat hippocampus. *Neuropharmacology* **44,** 1013-1021.

Bai G. and Lipton S. A. (1998) Aberrant RNA splicing in sporadic amyotrophic lateral sclerosis. *Neuron* **20,** 363-366.

Baik H. J., Huang Y., Washington J. M. and Zuo Z. (2009) Critical role of s465 in protein kinase C-increased rat glutamate transporter type 3 activity. *Int J Neurosci* **119,** 1419-1428.

Bain S. D. and Rubin C. T. (1990) Metabolic modulation of disuse osteopenia: endocrine-dependent site specificity of bone remodeling. *J Bone Miner Res* **5,** 1069-1075.

Baldock P. A., Sainsbury A., Couzens M., Enriquez R. F., Thomas G. P., Gardiner E. M. and Herzog H. (2002) Hypothalamic Y2 receptors regulate bone formation. *J Clin Invest* **109,** 915-921.

Balemans W., Van Den Ende J., Freire Paes-Alves A., Dikkers F. G., Willems P. J., Vanhoenacker F., de Almeida-Melo N., Alves C. F., Stratakis C. A., Hill S. C. and Van Hul W. (1999) Localization of the gene for sclerosteosis to the van Buchem disease-gene region on chromosome 17q12-q21. *Am J Hum Genet* **64,** 1661-1669.

Balemans W., Patel N., Ebeling M., Van Hul E., Wuyts W., Lacza C., Dioszegi M., Dikkers F. G., Hildering P., Willems P. J., Verheij J. B., Lindpaintner K., Vickery B., Foernzler D. and Van Hul W. (2002) Identification of a 52 kb deletion downstream of the SOST gene in patients with van Buchem disease. *J Med Genet* **39,** 91-97.

Balemans W., Ebeling M., Patel N., Van Hul E., Olson P., Dioszegi M., Lacza C., Wuyts W., Van Den Ende J., Willems P., Paes-Alves A. F., Hill S., Bueno M., Ramos F. J., Tacconi P., Dikkers F. G., Stratakis C., Lindpaintner K., Vickery B., Foernzler D. and Van Hul W. (2001) Increased bone density in sclerosteosis is due to the deficiency of a novel secreted protein (SOST). *Hum Mol Genet* **10,** 537-543.

Baltzer A. W., Lattermann C., Whalen J. D., Ghivizzani S., Wooley P., Krauspe R., Robbins P. D. and Evans C. H. (2000) Potential role of direct adenoviral gene transfer in enhancing fracture repair. *Clin Orthop Relat Res,* S120-125.

Bannai S. (1986) Exchange of cystine and glutamate across plasma membrane of human fibroblasts. *J Biol Chem* **261,** 2256-2263.

Bannai S. and Kitamura E. (1980) Transport interaction of L-cystine and L-glutamate in human diploid fibroblasts in culture. *J Biol Chem* **255,** 2372-2376.

Bannai S. and Kitamura E. (1981) Role of proton dissociation in the transport of cystine and glutamate in human diploid fibroblasts in culture. *J Biol Chem* **256,** 5770-5772.

Bannai S., Christensen H. N., Vadgama J. V., Ellory J. C., Englesberg E., Guidotti G. G., Gazzola G. C., Kilberg M. S., Lajtha A., Sacktor B. and et al. (1984) Amino acid transport systems. *Nature* **311,** 308.

Barbon A., Vallini I. and Barlati S. (2001) Genomic organization of the human GRIK2 gene and evidence for multiple splicing variants. *Gene* **274,** 187-197.

Bass B. L. (1995) RNA editing. An I for editing. *Curr Biol* **5,** 598-600.

Bassan M., Liu H., Madsen K. L., Armsen W., Zhou J., Desilva T., Chen W., Paradise A., Brasch M. A., Staudinger J., Gether U., Irwin N. and Rosenberg P. A. (2008) Interaction between the glutamate transporter GLT1b and the synaptic PDZ domain protein PICK1. *Eur J Neurosci* **27,** 66-82.

Bauman A. L., Apparsundaram S., Ramamoorthy S., Wadzinski B. E., Vaughan R. A. and Blakely R. D. (2000) Cocaine and antidepressant-sensitive biogenic amine transporters exist in regulated complexes with protein phosphatase 2A. *J Neurosci* **20,** 7571-7578.

Baylink D., Sipe J., Wergedal J. and Whittemore O. J. (1973) Vitamin D-enhanced osteocytic and osteoclastic bone resorption. *Am J Physiol* **224,** 1345-1357.

Beart P. M. and O'Shea R. D. (2007) Transporters for L-glutamate: an update on their molecular pharmacology and pathological involvement. *Br J Pharmacol* **150,** 5-17.

Begni B., Tremolizzo L., D'Orlando C., Bono M. S., Garofolo R., Longoni M. and Ferrarese C. (2005) Substrate-induced modulation of glutamate uptake in human platelets. *Br J Pharmacol* **145,** 792-799.

Beighton P. (1988) Sclerosteosis. *J Med Genet* **25,** 200-203.

Beighton P. and Hamersma H. (1979) Sclerosteosis in South Africa. *S Afr Med J* **55,** 783-788.

Beighton P., Durr L. and Hamersma H. (1976) The clinical features of sclerosteosis. A review of the manifestations in twenty-five affected individuals. *Ann Intern Med* **84,** 393-397.

Beighton P., Hamersma H. and Cremin B. J. (1979) Osteopetrosis in South Africa. The benign, lethal and intermediate forms. *S Afr Med J* **55,** 659-665.

Beighton P., Barnard A., Hamersma H. and van der Wouden A. (1984) The syndromic status of sclerosteosis and van Buchem disease. *Clin Genet* **25,** 175-181.

Belanger L. F. (1969) Osteocytic osteolysis. *Calcif Tissue Res* **4,** 1-12.

Bellido T., Ali A. A., Gubrij I., Plotkin L. I., Fu Q., O'Brien C. A., Manolagas S. C. and Jilka R. L. (2005) Chronic elevation of parathyroid hormone in mice reduces expression of sclerostin by osteocytes: a novel mechanism for hormonal control of osteoblastogenesis. *Endocrinology* **146,** 4577-4583.

Bendahan A., Armon A., Madani N., Kavanaugh M. P. and Kanner B. I. (2000) Arginine 447 plays a pivotal role in substrate interactions in a neuronal glutamate transporter. *J Biol Chem* **275,** 37436-37442.

Bendall A. J. and Abate-Shen C. (2000) Roles for Msx and Dlx homeoproteins in vertebrate development. *Gene* **247,** 17-31.

Bender A. S., Reichelt W. and Norenberg M. D. (2000) Characterization of cystine uptake in cultured astrocytes. *Neurochem Int* **37,** 269-276.

Benjamin A. M. and Quastel J. H. (1976) Cerebral Uptakes and Exchange Diffusion Invitro of L-Glutamates and D-Glutamates. *J. Neurochem.* **26,** 431-441.

Berger U. V. and Hediger M. A. (1998) Comparative analysis of glutamate transporter expression in rat brain using differential double in situ hybridization. *Anat Embryol (Berl)* **198,** 13-30.

Berger U. V. and Hediger M. A. (2006) Distribution of the glutamate transporters GLT-1 (SLC1A2) and GLAST (SLC1A3) in peripheral organs. *Anat Embryol (Berl)* **211,** 595-606.

Berger U. V., DeSilva T. M., Chen W. and Rosenberg P. A. (2005) Cellular and subcellular mRNA localization of glutamate transporter isoforms GLT1a and GLT1b in rat brain by in situ hybridization. *J Comp Neurol* **492,** 78-89.

Bernstein E. M. and Quick M. W. (1999) Regulation of gamma-aminobutyric acid (GABA) transporters by extracellular GABA. *J Biol Chem* **274,** 889-895.

Bhangu P. S. (2003) 'Pre-synaptic' vesicular glutamate release mechanisms in osteoblasts. *J Musculoskelet Neuronal Interact* **3,** 17-29.

Bhangu P. S., Genever P. G., Spencer G. J., Grewal T. S. and Skerry T. M. (2001) Evidence for targeted vesicular glutamate exocytosis in osteoblasts. *Bone* **29,** 16-23.

Bilbe G., Roberts E., Birch M. and Evans D. B. (1996) PCR phenotyping of cytokines, growth factors and their receptors and bone matrix proteins in human osteoblast-like cell lines. *Bone* **19,** 437-445.

Billiau A., Edy V. G., Heremans H., Van Damme J., Desmyter J., Georgiades J. A. and De Somer P. (1977) Human interferon: mass production in a newly established cell line, MG-63. *Antimicrob Agents Chemother* **12,** 11-15.

Billups B., Rossi D. and Attwell D. (1996) Anion conductance behavior of the glutamate uptake carrier in salamander retinal glial cells. *J Neurosci* **16,** 6722-6731.

Bjerggaard C., Fog J. U., Hastrup H., Madsen K., Loland C. J., Javitch J. A. and Gether U. (2004) Surface targeting of the dopamine transporter involves discrete epitopes in the distal C terminus but does not require canonical PDZ domain interactions. *J Neurosci* **24,** 7024-7036.

Bjurholm A., Kreicbergs A., Brodin E. and Schultzberg M. (1988a) Substance P- and CGRP-immunoreactive nerves in bone. *Peptides* **9,** 165-171.

Bjurholm A., Kreicbergs A., Dahlberg L. and Schultzberg M. (1990) The occurrence of neuropeptides at different stages of DBM-induced heterotopic bone formation. *Bone Miner* **10,** 95-107.

Bjurholm A., Kreicbergs A., Schultzberg M. and Lerner U. H. (1992) Neuroendocrine regulation of cyclic AMP formation in osteoblastic cell lines (UMR-106-01, ROS 17/2.8, MC3T3-E1, and Saos-2) and primary bone cells. *J Bone Miner Res* **7,** 1011-1019.

Bjurholm A., Kreicbergs A., Terenius L., Goldstein M. and Schultzberg M. (1988b) Neuropeptide Y-, tyrosine hydroxylase- and vasoactive intestinal polypeptide-immunoreactive nerves in bone and surrounding tissues. *J Auton Nerv Syst* **25,** 119-125.

Blackshaw S., Harpavat S., Trimarchi J., Cai L., Huang H., Kuo W. P., Weber G., Lee K., Fraioli R. E., Cho S. H., Yung R., Asch E., Ohno-Machado L., Wong W. H. and Cepko C. L. (2004) Genomic analysis of mouse retinal development. *PLoS Biol* **2,** E247.

Blair H. C., Teitelbaum S. L., Grosso L. E., Lacey D. L., Tan H. L., McCourt D. W. and Jeffrey J. J. (1993) Extracellular-matrix degradation at acid pH. Avian osteoclast acid collagenase isolation and characterization. *Biochem J* **290 (Pt 3),** 873-884.

Blandini F., Porter R. H. and Greenamyre J. T. (1996) Glutamate and Parkinson's disease. *Mol Neurobiol* **12,** 73-94.

Blitzblau R., Gupta S., Djali S., Robinson M. B. and Rosenberg P. A. (1996) The glutamate transport inhibitor L-trans-pyrrolidine-2,4-dicarboxylate indirectly evokes NMDA receptor mediated neurotoxicity in rat cortical cultures. *Eur J Neurosci* **8,** 1840-1852.

Bliziotes M., Eshleman A., Burt-Pichat B., Zhang X. W., Hashimoto J., Wiren K. and Chenu C. (2006) Serotonin transporter and receptor expression in osteocytic MLO-Y4 cells. *Bone* **39,** 1313-1321.

Bliziotes M. M., Eshleman A. J., Zhang X. W. and Wiren K. M. (2001) Neurotransmitter action in osteoblasts: expression of a functional system for serotonin receptor activation and reuptake. *Bone* **29,** 477-486.

Bollerslev J. and Andersen P. E., Jr. (1988) Radiological, biochemical and hereditary evidence of two types of autosomal dominant osteopetrosis. *Bone* **9,** 7-13.

Bonanno G. and Raiteri M. (1994) Release-regulating presynaptic heterocarriers. *Prog Neurobiol* **44,** 451-462.

Bonanno G., Pittaluga A., Fedele E., Fontana G. and Raiteri M. (1993) Glutamic acid and gamma-aminobutyric acid modulate each other's release through heterocarriers sited on the axon terminals of rat brain. *J Neurochem* **61,** 222-230.

Bonde C., Sarup A., Schousboe A., Gegelashvili G., Zimmer J. and Noraberg J. (2003) Neurotoxic and neuroprotective effects of the glutamate transporter inhibitor DL-threo-beta-benzyloxyaspartate (DL-TBOA) during physiological and ischemia-like conditions. *Neurochem Int* **43,** 371-380.

Bone H. G., Bolognese M. A., Yuen C. K., Kendler D. L., Wang H., Liu Y. and San Martin J. (2008) Effects of denosumab on bone mineral density and bone turnover in postmenopausal women. *J Clin Endocrinol Metab* **93,** 2149-2157.

Bonewald L. F. (1999) Establishment and characterization of an osteocyte-like cell line, MLO-Y4. *J Bone Miner Metab* **17,** 61-65.

Bonewald L. F. (2006) Mechanosensation and Transduction in Osteocytes. *Bonekey Osteovision* **3,** 7-15.

Borre L. and Kanner B. I. (2001) Coupled, but not uncoupled, fluxes in a neuronal glutamate transporter can be activated by lithium ions. *J Biol Chem* **276,** 40396-40401.

Borre L., Kavanaugh M. P. and Kanner B. I. (2002) Dynamic equilibrium between coupled and uncoupled modes of a neuronal glutamate transporter. *J Biol Chem* **277,** 13501-13507.

Bowe E. A. and Skerry T. M. (2005) Repetitions of mechanical loading potentiate bone cellular responses by a mechanism involving NMDA type glutamate receptors. *Journal of Bone and Mineral Research* **20,** S25-S25.

Brauner-Osborne H., Hermit M. B., Nielsen B., Krogsgaard-Larsen P. and Johansen T. N. (2000) A new structural class of subtype-selective inhibitor of cloned excitatory amino acid transporter, EAAT2. *Eur J Pharmacol* **406,** 41-44.

Bridges R. J. and Esslinger C. S. (2005) The excitatory amino acid transporters: pharmacological insights on substrate and inhibitor specificity of the EAAT subtypes. *Pharmacol Ther* **107,** 271-285.

Bridges R. J., Kavanaugh M. P. and Chamberlin A. R. (1999) A pharmacological review of competitive inhibitors and substrates of high-affinity, sodium-dependent glutamate transport in the central nervous system. *Curr Pharm Des* **5,** 363-379.

Bridges R. J., Stanley M. S., Anderson M. W., Cotman C. W. and Chamberlin A. R. (1991) Conformationally defined neurotransmitter analogues. Selective inhibition of glutamate uptake by one pyrrolidine-2,4-dicarboxylate diastereomer. *J Med Chem* **34,** 717-725.

Bridges R. J., Lovering F. E., Koch H., Cotman C. W. and Chamberlin A. R. (1994) A conformationally constrained competitive inhibitor of the sodium-dependent glutamate transporter in forebrain synaptosomes: L-anti-endo-3,4-methanopyrrolidine dicarboxylate. *Neurosci Lett* **174,** 193-197.

Brighton C. T., Adler S., Black J., Itada N. and Friedenberg Z. B. (1975) Cathodic oxygen consumption and electrically induced osteogenesis. *Clin Orthop Relat Res,* 277-282.

Brown J. P., Prince R. L., Deal C., Recker R. R., Kiel D. P., de Gregorio L. H., Hadji P., Hofbauer L. C., Alvaro-Gracia J. M., Wang H., Austin M., Wagman R. B., Newmark R., Libanati C., San Martin J. and Bone H. G. (2009) Comparison of the Effect of Denosumab and Alendronate on Bone Mineral Density and Biochemical Markers of Bone Turnover in Postmenopausal Women With Low Bone Mass: A Randomized, Blinded, Phase 3 Trial. *J Bone Miner Res,* 1-34.

Brunkow M. E., Gardner J. C., Van Ness J., Paeper B. W., Kovacevich B. R., Proll S., Skonier J. E., Zhao L., Sabo P. J., Fu Y., Alisch R. S., Gillett L., Colbert T., Tacconi P., Galas D., Hamersma H., Beighton P. and Mulligan J. (2001) Bone dysplasia sclerosteosis results from loss of the SOST gene product, a novel cystine knot-containing protein. *Am J Hum Genet* **68,** 577-589.

Buckwalter J. A., Glimcher M. J., Cooper R. R. and Recker R. (1996a) Bone biology. II: Formation, form, modeling, remodeling, and regulation of cell function. *Instr Course Lect* **45,** 387-399.

Buckwalter J. A., Glimcher M. J., Cooper R. R. and Recker R. (1996b) Bone biology. I: Structure, blood supply, cells, matrix, and mineralization. *Instr Course Lect* **45,** 371-386.

Bukowski D. M., Deneke S. M., Lawrence R. A. and Jenkinson S. G. (1995) A noninducible cystine transport system in rat alveolar type II cells. *Am J Physiol* **268,** L21-26.

Bullough P. (1992) *Atlas of orthapaedic pathology*, New York.

Burford J. H., Perrien D. S., Horner A., Bowe E. A., Notomi T., Suva L. J. and Skerry T. M. (2004) Glutamate signalling regulates skeletogenesis and bone growth. *Journal of Bone and Mineral Research* **19,** S212-S213.

Burger E. H. and Klein-Nulend J. (1999) Mechanotransduction in bone--role of the lacuno-canalicular network. *Faseb J* **13 Suppl,** S101-112.

Burgeson R. E. (1988) New collagens, new concepts. *Annu Rev Cell Biol* **4,** 551-577.

Burgess T. L., Qian Y., Kaufman S., Ring B. D., Van G., Capparelli C., Kelley M., Hsu H., Boyle W. J., Dunstan C. R., Hu S. and Lacey D. L. (1999) The ligand for osteoprotegerin (OPGL) directly activates mature osteoclasts. *J Cell Biol* **145,** 527-538.

Burnashev N., Monyer H., Seeburg P. H. and Sakmann B. (1992) Divalent ion permeability of AMPA receptor channels is dominated by the edited form of a single subunit. *Neuron* **8,** 189-198.

Burr D. B., Schaffler M. B. and Frederickson R. G. (1988) Composition of the cement line and its possible mechanical role as a local interface in human compact bone. *J Biomech* **21,** 939-945.

Burr D. B., Robling A. G. and Turner C. H. (2002) Effects of biomechanical stress on bones in animals. *Bone* **30,** 781-786.

Busse R. and Fleming I. (1998) Regulation of NO synthesis in endothelial cells. *Kidney Blood Press Res* **21,** 264-266.

Bustin S. A. (2000) Absolute quantification of mRNA using real-time reverse transcription polymerase chain reaction assays. *J Mol Endocrinol* **25,** 169-193.

Butchbach M. E., Guo H. and Lin C. L. (2003) Methyl-beta-cyclodextrin but not retinoic acid reduces EAAT3-mediated glutamate uptake and increases GTRAP3-18 expression. *J Neurochem* **84,** 891-894.

Calvo W. and Forteza-Vila J. (1969) On the development of bone marrow innervation in new-born rats as studied with silver impregnation and electron microscopy. *Am J Anat* **126,** 355-371.

Campbell J. M., Bacon T. A. and Wickstrom E. (1990) Oligodeoxynucleoside phosphorothioate stability in subcellular extracts, culture media, sera and cerebrospinal fluid. *J Biochem Biophys Methods* **20,** 259-267.

Campiani G., Fattorusso C., De Angelis M., Catalanotti B., Butini S., Fattorusso R., Fiorini I., Nacci V. and Novellino E. (2003) Neuronal high-affinity sodium-dependent glutamate transporters (EAATs): targets for the development of novel therapeutics against neurodegenerative diseases. *Curr Pharm Des* **9,** 599-625.

Canalis E. (1983) The hormonal and local regulation of bone formation. *Endocr Rev* **4,** 62-77.

Canalis E. (1993) Insulin like growth factors and the local regulation of bone formation. *Bone* **14,** 273-276.

Canalis E., McCarthy T. L. and Centrella M. (1989) The role of growth factors in skeletal remodeling. *Endocrinol Metab Clin North Am* **18,** 903-918.

Cancedda R., Castagnola P., Cancedda F. D., Dozin B. and Quarto R. (2000) Developmental control of chondrogenesis and osteogenesis. *Int J Dev Biol* **44,** 707-714.

Carlton S. M. (2001) Peripheral excitatory amino acids. *Curr Opin Pharmacol* **1,** 52-56.

Carrascosa J. M., Martinez P. and Nunez de Castro I. (1984) Nitrogen movement between host and tumor in mice inoculated with Ehrlich ascitic tumor cells. *Cancer Res* **44,** 3831-3835.

Carvelli L., Moron J. A., Kahlig K. M., Ferrer J. V., Sen N., Lechleiter J. D., Leeb-Lundberg L. M. F., Merrill G., Lafer E. M., Ballou L. M., Shippenberg T. S., Javitch J. A., Lin R. Z. and Galli A. (2002) PI 3-kinase regulation of dopamine uptake. *J. Neurochem.* **81,** 859-869.

Casado M., Zafra F., Aragon C. and Gimenez C. (1991) Activation of high-affinity uptake of glutamate by phorbol esters in primary glial cell cultures. *J Neurochem* **57,** 1185-1190.

Casado M., Bendahan A., Zafra F., Danbolt N. C., Aragon C., Gimenez C. and Kanner B. I. (1993) Phosphorylation and modulation of brain glutamate transporters by protein kinase C. *J Biol Chem* **268,** 27313-27317.

Chambers T. J. and Fuller K. (1985) Bone cells predispose bone surfaces to resorption by exposure of mineral to osteoclastic contact. *J Cell Sci* **76,** 155-165.

Chang K. H., Kim K. S. and Kim J. H. (1999) N-acetylcysteine increases the biosynthesis of recombinant EPO in apoptotic Chinese hamster ovary cells. *Free Radic Res* **30,** 85-91.

Chase T. N., Oh J. D. and Konitsiotis S. (2000) Antiparkinsonian and antidyskinetic activity of drugs targeting central glutamatergic mechanisms. *J Neurol* **247 Suppl 2,** II36-42.

Chaudhary L. R. and Avioli L. V. (1994) Dexamethasone regulates IL-1 beta and TNF-alpha-induced interleukin-8 production in human bone marrow stromal and osteoblast-like cells. *Calcif Tissue Int* **55,** 16-20.

Chellaiah M. A., Kizer N., Biswas R., Alvarez U., Strauss-Schoenberger J., Rifas L., Rittling S. R., Denhardt D. T. and Hruska K. A. (2003) Osteopontin deficiency produces osteoclast dysfunction due to reduced CD44 surface expression. *Mol Biol Cell* **14,** 173-189.

Chen J., Shapiro H. S. and Sodek J. (1992) Development expression of bone sialoprotein mRNA in rat mineralized connective tissues. *J Bone Miner Res* **7,** 987-997.

Chen J., McKee M. D., Nanci A. and Sodek J. (1994) Bone sialoprotein mRNA expression and ultrastructural localization in fetal porcine calvarial bone: comparisons with osteopontin. *Histochem J* **26,** 67-78.

Chen W., Aoki C., Mahadomrongkul V., Gruber C. E., Wang G. J., Blitzblau R., Irwin N. and Rosenberg P. A. (2002) Expression of a variant form of the glutamate transporter GLT1 in neuronal cultures and in neurons and astrocytes in the rat brain. *J Neurosci* **22,** 2142-2152.

Cheng C., Glover G., Banker G. and Amara S. G. (2002) A novel sorting motif in the glutamate transporter excitatory amino acid transporter 3 directs its targeting in Madin-Darby canine kidney cells and hippocampal neurons. *J Neurosci* **22,** 10643-10652.

Cheng M. Z., Zaman G., Rawlinson S. C., Suswillo R. F. and Lanyon L. E. (1996) Mechanical loading and sex hormone interactions in organ cultures of rat ulna. *J Bone Miner Res* **11,** 502-511.

Chenu C. (2002) Glutamatergic innervation in bone. *Microsc Res Tech* **58,** 70-76.

Chenu C. (2004) Role of innervation in the control of bone remodeling. *J Musculoskelet Neuronal Interact* **4,** 132-134.

Chenu C., Itzstein C. and Espinosa L. (2001) Absence of evidence is not evidence of absence. Redundancy blocks determination of cause and effect. *J Bone Miner Res* **16,** 1728-1729; author reply 1731-1722.

Chenu C., Serre C. M., Raynal C., Burt-Pichat B. and Delmas P. D. (1998) Glutamate receptors are expressed by bone cells and are involved in bone resorption. *Bone* **22,** 295-299.

Cherian P. P., Siller-Jackson A. J., Gu S., Wang X., Bonewald L. F., Sprague E. and Jiang J. X. (2005) Mechanical strain opens connexin 43 hemichannels in osteocytes: a novel mechanism for the release of prostaglandin. *Mol Biol Cell* **16,** 3100-3106.

Chien S., Li S. and Shyy Y. J. (1998) Effects of mechanical forces on signal transduction and gene expression in endothelial cells. *Hypertension* **31,** 162-169.

Chipoy C., Berreur M., Couillaud S., Pradal G., Vallette F., Colombeix C., Redini F., Heymann D. and Blanchard F. (2004) Downregulation of osteoblast markers and induction of the glial fibrillary acidic protein by oncostatin M in osteosarcoma cells require PKCdelta and STAT3. *J Bone Miner Res* **19,** 1850-1861.

Cho Y. and Bannai S. (1990) Uptake of glutamate and cysteine in C-6 glioma cells and in cultured astrocytes. *J Neurochem* **55,** 2091-2097.

Choi J. Y., Jung U. W., Kim C. S., Eom T. K., Kang E. J., Cho K. S., Kim C. K. and Choi S. H. (2010) The effects of newly formed synthetic peptide on bone regeneration in rat calvarial defects. *J Periodontal Implant Sci* **40,** 11-18.

Cholet N., Pellerin L., Magistretti P. J. and Hamel E. (2002) Similar perisynaptic glial localization for the Na+,K+-ATPase alpha 2 subunit and the glutamate transporters GLAST and GLT-1 in the rat somatosensory cortex. *Cereb Cortex* **12,** 515-525.

Chomczynski P. and Sacchi N. (1987) Single-step method of RNA isolation by acid guanidinium thiocyanate-phenol-chloroform extraction. *Anal Biochem* **162,** 156-159.

Chow J. W. and Chambers T. J. (1994) Indomethacin has distinct early and late actions on bone formation induced by mechanical stimulation. *Am J Physiol* **267,** E287-292.

Christiansen C., Christensen M. S., Larsen N. E. and Transbol I. B. (1982) Pathophysiological mechanisms of estrogen effect on bone metabolism. Dose-response relationships in early postmenopausal women. *J Clin Endocrinol Metab* **55,** 1124-1130.

Chung C. H., Golub E. E., Forbes E., Tokuoka T. and Shapiro I. M. (1992) Mechanism of action of beta-glycerophosphate on bone cell mineralization. *Calcif Tissue Int* **51,** 305-311.

Clements J. D. (1996) Transmitter timecourse in the synaptic cleft: its role in central synaptic function. *Trends Neurosci* **19,** 163-171.

Clezardin P., Malaval L., Ehrensperger A. S., Delmas P. D., Dechavanne M. and McGregor J. L. (1988) Complex formation of human thrombospondin with osteonectin. *Eur J Biochem* **175,** 275-284.

Cockett M. I., Bebbington C. R. and Yarranton G. T. (1990) High level expression of tissue inhibitor of metalloproteinases in Chinese hamster ovary cells using glutamine synthetase gene amplification. *Biotechnology (N Y)* **8,** 662-667.

Cohen M. M., Jr. (2006) The new bone biology: pathologic, molecular, and clinical correlates. *Am J Med Genet A* **140,** 2646-2706.

Collins C. L., Wasa M., Souba W. W. and Abcouwer S. F. (1998) Determinants of glutamine dependence and utilization by normal and tumor-derived breast cell lines. *J Cell Physiol* **176,** 166-178.

Colnot C., Lu C., Hu D. and Helms J. A. (2004) Distinguishing the contributions of the perichondrium, cartilage, and vascular endothelium to skeletal development. *Dev Biol* **269,** 55-69.

Colnot C. I. and Helms J. A. (2001) A molecular analysis of matrix remodeling and angiogenesis during long bone development. *Mech Dev* **100,** 245-250.

Connolly J. F. (1981) Selection, evaluation and indications for electrical stimulation of ununited fractures. *Clin Orthop Relat Res,* 39-53.

Conradt M. and Stoffel W. (1995) Functional analysis of the high affinity, Na(+)-dependent glutamate transporter GLAST-1 by site-directed mutagenesis. *J Biol Chem* **270,** 25207-25212.

Conradt M. and Stoffel W. (1997) Inhibition of the high-affinity brain glutamate transporter GLAST-1 via direct phosphorylation. *J Neurochem* **68,** 1244-1251.

Conradt M., Storck T. and Stoffel W. (1995) Localization of N-glycosylation sites and functional role of the carbohydrate units of GLAST-1, a cloned rat brain L-glutamate/L-aspartate transporter. *Eur J Biochem* **229,** 682-687.

Contestabile A. (2000) Roles of NMDA receptor activity and nitric oxide production in brain development. *Brain Res Brain Res Rev* **32,** 476-509.

Cooper A. J. and Kristal B. S. (1997) Multiple roles of glutathione in the central nervous system. *Biol Chem* **378,** 793-802.

Cooper L. F., Yliheikkila P. K., Felton D. A. and Whitson S. W. (1998) Spatiotemporal assessment of fetal bovine osteoblast culture differentiation indicates a role for BSP in promoting differentiation. *J Bone Miner Res* **13,** 620-632.

Corey J. L., Davidson N., Lester H. A., Brecha N. and Quick M. W. (1994) Protein kinase C modulates the activity of a cloned gamma-aminobutyric acid transporter expressed in Xenopus oocytes via regulated subcellular redistribution of the transporter. *J Biol Chem* **269,** 14759-14767.

Cox D. W. G., Headley M. H. and Watkins J. C. (1977) Actions of L-Homocysteate and D-Homocysteate in Rat Cns - Correlation between Low-Affinity Uptake and Time Courses of Excitation by Microelectrophoretically Applied L-Glutamate Analogs. *J. Neurochem.* **29,** 579-588.

Dagrenat D., Kempf, I. (2002) Treatment of nonunions, in *Practice of intramedullary locked, nails,* Vol. Chapter 6. Springer.

Danbolt N. C. (2001) Glutamate uptake. *Prog Neurobiol* **65,** 1-105.

Davie J. R. (2003) Inhibition of histone deacetylase activity by butyrate. *J Nutr* **133,** 2485S-2493S.

Davies P. F., Polacek D. C., Handen J. S., Helmke B. P. and DePaola N. (1999) A spatial approach to transcriptional profiling: mechanotransduction and the focal origin of atherosclerosis. *Trends Biotechnol* **17,** 347-351.

Davis K. E., Straff D. J., Weinstein E. A., Bannerman P. G., Correale D. M., Rothstein J. D. and Robinson M. B. (1998) Multiple signaling pathways regulate cell surface expression and activity of the excitatory amino acid carrier 1 subtype of Glu transporter in C6 glioma. *J Neurosci* **18,** 2475-2485.

Delaisse J. M., Ledent P. and Vaes G. (1991) Collagenolytic cysteine proteinases of bone tissue. Cathepsin B, (pro)cathepsin L and a cathepsin L-like 70 kDa proteinase. *Biochem J* **279 (Pt 1),** 167-174.

Delaisse J. M., Eeckhout Y., Neff L., Francois-Gillet C., Henriet P., Su Y., Vaes G. and Baron R. (1993) (Pro)collagenase (matrix metalloproteinase-1) is present in rodent osteoclasts and in the underlying bone-resorbing compartment. *J Cell Sci* **106 (Pt 4),** 1071-1082.

Delany A. M., Amling M., Priemel M., Howe C., Baron R. and Canalis E. (2000) Osteopenia and decreased bone formation in osteonectin-deficient mice. *J Clin Invest* **105,** 915-923.

Dempster D. W. (2006) Anatomy and functions of the adult skeleton, in *Primer of the metabolic bone diseases and disorders of mineral metabolism,* 6th Edition (Favus M. J., ed.), pp 7-11. American Society for Bone and Mineral Research, Washington DC.

Dempster D. W., Cosman F., Kurland E. S., Zhou H., Nieves J., Woelfert L., Shane E., Plavetic K., Muller R., Bilezikian J. and Lindsay R. (2001) Effects of daily treatment with parathyroid hormone on bone microarchitecture and turnover in patients with osteoporosis: a paired biopsy study. *J Bone Miner Res* **16,** 1846-1853.

Diamond J. S. and Jahr C. E. (1997) Transporters buffer synaptically released glutamate on a submillisecond time scale. *J Neurosci* **17,** 4672-4687.

Do S. H., Kamatchi G. L., Washington J. M. and Zuo Z. (2002) Effects of volatile anesthetics on glutamate transporter, excitatory amino acid transporter type 3: the role of protein kinase C. *Anesthesiology* **96,** 1492-1497.

Dolgilevich S., Zaidi N., Song J., Abe E., Moonga B. S. and Sun L. (2002) Transduction of TAT fusion proteins into osteoclasts and osteoblasts. *Biochem Biophys Res Commun* **299,** 505-509.

Donaldson C. L., Hulley S. B., Vogel J. M., Hattner R. S., Bayers J. H. and McMillan D. E. (1970) Effect of prolonged bed rest on bone mineral. *Metabolism* **19,** 1071-1084.

Dong H., O'Brien R. J., Fung E. T., Lanahan A. A., Worley P. F. and Huganir R. L. (1997) GRIP: a synaptic PDZ domain-containing protein that interacts with AMPA receptors. *Nature* **386,** 279-284.

Doolen S. and Zahniser N. R. (2001) Protein tyrosine kinase inhibitors alter human dopamine transporter activity in Xenopus oocytes. *J Pharmacol Exp Ther* **296,** 931-938.

Doty S. B. (1981) Morphological evidence of gap junctions between bone cells. *Calcif Tissue Int* **33,** 509-512.

Dowd L. A. and Robinson M. B. (1996) Rapid stimulation of EAAC1-mediated Na+-dependent L-glutamate transport activity in C6 glioma cells by phorbol ester. *J Neurochem* **67,** 508-516.

Driessen G. J., Gerritsen E. J., Fischer A., Fasth A., Hop W. C., Veys P., Porta F., Cant A., Steward C. G., Vossen J. M., Uckan D. and Friedrich W. (2003) Long-term outcome of haematopoietic stem cell transplantation in autosomal recessive osteopetrosis: an EBMT report. *Bone Marrow Transplant* **32,** 657-663.

Dringen R. (2000) Metabolism and functions of glutathione in brain. *Prog Neurobiol* **62,** 649-671.

Duan S., Anderson C. M., Stein B. A. and Swanson R. A. (1999) Glutamate induces rapid upregulation of astrocyte glutamate transport and cell-surface expression of GLAST. *J Neurosci* **19,** 10193-10200.

Ducy P. and Karsenty G. (1995) Two distinct osteoblast-specific cis-acting elements control expression of a mouse osteocalcin gene. *Mol Cell Biol* **15,** 1858-1869.

Ducy P., Zhang R., Geoffroy V., Ridall A. L. and Karsenty G. (1997) Osf2/Cbfa1: a transcriptional activator of osteoblast differentiation. *Cell* **89,** 747-754.

Ducy P., Amling M., Takeda S., Priemel M., Schilling A. F., Beil F. T., Shen J., Vinson C., Rueger J. M. and Karsenty G. (2000) Leptin inhibits bone formation through a hypothalamic relay: a central control of bone mass. *Cell* **100,** 197-207.

Duncan C. P. and Shim S. S. (1977) J. Edouard Samson Address: the autonomic nerve supply of bone. An experimental study of the intraosseous adrenergic nervi vasorum in the rabbit. *J Bone Joint Surg Br* **59,** 323-330.

Duncan R. L. (1995) Transduction of mechanical strain in bone. *ASGSB Bull* **8,** 49-62.

Duncan R. L. and Turner C. H. (1995) Mechanotransduction and the functional response of bone to mechanical strain. *Calcif Tissue Int* **57,** 344-358.

Dunckley M. G., Manoharan M., Villiet P., Eperon I. C. and Dickson G. (1998) Modification of splicing in the dystrophin gene in cultured Mdx muscle cells by antisense oligoribonucleotides. *Hum Mol Genet* **7,** 1083-1090.

Dunlop J., Lou Z., Zhang Y. and McIlvain H. B. (1999) Inducible expression and pharmacology of the human excitatory amino acid transporter 2 subtype of L-glutamate transporter. *Br J Pharmacol* **128,** 1485-1490.

Dunlop J., Grieve A., Damgaard I., Schousboe A. and Griffiths R. (1992) Sulphur-containing excitatory amino acid-evoked Ca(2+)-independent release of D-[3H]aspartate from cultured cerebellar granule cells: the role of glutamate receptor activation coupled to reversal of the acidic amino acid plasma membrane carrier. *Neuroscience* **50,** 107-115.

Eames B. F., de la Fuente L. and Helms J. A. (2003) Molecular ontogeny of the skeleton. *Birth Defects Res C Embryo Today* **69,** 93-101.

Edoff K., Hellman J., Persliden J. and Hildebrand C. (1997) The developmental skeletal growth in the rat foot is reduced after denervation. *Anat Embryol (Berl)* **195,** 531-538.

Eghbali-Fatourechi G. Z., Lamsam J., Fraser D., Nagel D., Riggs B. L. and Khosla S. (2005) Circulating osteoblast-lineage cells in humans. *N Engl J Med* **352,** 1959-1966.

Egusa H., Kaneda Y., Akashi Y., Hamada Y., Matsumoto T., Saeki M., Thakor D. K., Tabata Y., Matsuura N. and Yatani H. (2009) Enhanced bone regeneration via multimodal actions of synthetic peptide SVVYGLR on osteoprogenitors and osteoclasts. *Biomaterials* **30,** 4676-4686.

Ehrlich P. J. and Lanyon L. E. (2002) Mechanical strain and bone cell function: a review. *Osteoporos Int* **13,** 688-700.

Einhorn T. A. (1998) The cell and molecular biology of fracture healing. *Clin Orthop Relat Res,* S7-21.

Elefteriou F., Ahn J. D., Takeda S., Starbuck M., Yang X., Liu X., Kondo H., Richards W. G., Bannon T. W., Noda M., Clement K., Vaisse C. and Karsenty G. (2005) Leptin regulation of bone resorption by the sympathetic nervous system and CART. *Nature* **434,** 514-520.

Eliasof S. and Jahr C. E. (1996) Retinal glial cell glutamate transporter is coupled to an anionic conductance. *Proc Natl Acad Sci U S A* **93,** 4153-4158.

Erecinska M. and Silver I. A. (1990) Metabolism and role of glutamate in mammalian brain. *Prog Neurobiol* **35,** 245-296.

Eriksen E. F., Eghbali-Fatourechi G. Z. and Khosla S. (2007) Remodeling and vascular spaces in bone. *J Bone Miner Res* **22,** 1-6.

Erlebacher A., Filvaroff E. H., Gitelman S. E. and Derynck R. (1995) Toward a molecular understanding of skeletal development. *Cell* **80,** 371-378.

Eskandari S., Kreman M., Kavanaugh M. P., Wright E. M. and Zampighi G. A. (2000) Pentameric assembly of a neuronal glutamate transporter. *Proc Natl Acad Sci U S A* **97,** 8641-8646.

Espinosa L., Itzstein C., Cheynel H., Delmas P. D. and Chenu C. (1999) Active NMDA glutamate receptors are expressed by mammalian osteoclasts. *J Physiol* **518 (Pt 1),** 47-53.

Espinoza-Rojo M., Lopez-Bayghen E. and Ortega A. (2000) GLAST: gene expression regulation by phorbol esters. *Neuroreport* **11,** 2827-2832.

Estrada-Sanchez A. M., Camacho A., Montiel T. and Massieu L. (2007) Cerebellar granule neurons are more vulnerable to transient transport-mediated glutamate release than to glutamate uptake blockade. correlation with excitatory amino acids levels. *Neurochem Res* **32,** 423-432.

Evans C. H. (2010) Gene therapy for bone healing. *Expert Rev Mol Med* **12,** e18.

Faccio R., Grano M., Colucci S., Zallone A. Z., Quaranta V. and Pelletier A. J. (1998) Activation of alphav beta3 integrin on human osteoclast-like cells stimulates adhesion and migration in response to osteopontin. *Biochem Biophys Res Commun* **249,** 522-525.

Faccio R., Grano M., Colucci S., Villa A., Giannelli G., Quaranta V. and Zallone A. (2002) Localization and possible role of two different alpha v beta 3 integrin conformations in resting and resorbing osteoclasts. *J Cell Sci* **115,** 2919-2929.

Fairman W. A., Vandenberg R. J., Arriza J. L., Kavanaugh M. P. and Amara S. G. (1995) An excitatory amino-acid transporter with properties of a ligand-gated chloride channel. *Nature* **375,** 599-603.

Fallon M. D., Whyte M. P. and Teitelbaum S. L. (1980) Stereospecific inhibition of alkaline phosphatase by L-tetramisole prevents in vitro cartilage calcification. *Lab Invest* **43,** 489-494.

Fan M. Z., Matthews J. C., Etienne N. M., Stoll B., Lackeyram D. and Burrin D. G. (2004) Expression of apical membrane L-glutamate transporters in neonatal porcine epithelial cells along the small intestinal crypt-villus axis. *Am J Physiol Gastrointest Liver Physiol* **287,** G385-398.

Fang H., Huang Y. and Zuo Z. (2002) The different responses of rat glutamate transporter type 2 and its mutant (tyrosine 403 to histidine) activity to volatile anesthetics and activation of protein kinase C. *Brain Res* **953,** 255-264.

Fang H., Huang Y. and Zuo Z. (2006) Enhancement of substrate-gated Cl- currents via rat glutamate transporter EAAT4 by PMA. *Am J Physiol Cell Physiol* **290,** C1334-1340.

Fatokun A. A., Stone T. W. and Smith R. A. (2006) Hydrogen peroxide-induced oxidative stress in MC3T3-E1 cells: The effects of glutamate and protection by purines. *Bone* **39,** 542-551.

Felix R., Cecchini M. G. and Fleisch H. (1990) Macrophage colony stimulating factor restores in vivo bone resorption in the op/op osteopetrotic mouse. *Endocrinology* **127,** 2592-2594.

Feng J. Q., Huang H., Lu Y., Ye L., Xie Y., Tsutsui T. W., Kunieda T., Castranio T., Scott G., Bonewald L. B. and Mishina Y. (2003) The Dentin matrix protein 1 (Dmp1) is specifically expressed in mineralized, but not soft, tissues during development. *J Dent Res* **82,** 776-780.

Feng J. Q., Ward L. M., Liu S., Lu Y., Xie Y., Yuan B., Yu X., Rauch F., Davis S. I., Zhang S., Rios H., Drezner M. K., Quarles L. D., Bonewald L. F. and White K. E. (2006) Loss of DMP1 causes rickets and osteomalacia and identifies a role for osteocytes in mineral metabolism. *Nat Genet* **38,** 1310-1315.

Ferguson C., Alpern E., Miclau T. and Helms J. A. (1999) Does adult fracture repair recapitulate embryonic skeletal formation? *Mech Dev* **87,** 57-66.

Fletcher S., Honeyman K., Fall A. M., Harding P. L., Johnsen R. D., Steinhaus J. P., Moulton H. M., Iversen P. L. and Wilton S. D. (2007) Morpholino oligomer-mediated exon skipping averts the onset of dystrophic pathology in the mdx mouse. *Mol Ther* **15,** 1587-1592.

Flood S., Parri R., Williams A., Duance V. and Mason D. (2007) Modulation of interleukin-6 and matrix metalloproteinase 2 expression in human fibroblast-like synoviocytes by functional ionotropic glutamate receptors. *Arthritis Rheum* **56,** 2523-2534.

Flor P. J., Gomeza J., Tones M. A., Kuhn R., Pin J. P. and Knopfel T. (1996) The C-terminal domain of the mGluR1 metabotropic glutamate receptor affects sensitivity to agonists. *J Neurochem* **67,** 58-63.

Flowers J. M., Powell J. F., Leigh P. N., Andersen P. and Shaw C. E. (2001) Intron 7 retention and exon 9 skipping EAAT2 mRNA variants are not associated with amyotrophic lateral sclerosis. *Ann Neurol* **49,** 643-649.

Fogh J., Fogh J. M. and Orfeo T. (1977) One hundred and twenty-seven cultured human tumor cell lines producing tumors in nude mice. *J Natl Cancer Inst* **59,** 221-226.

Foreman M. A., Gu Y. C., Howl J. D., Jones S. and Publicover S. J. (2005) Group III metabotropic glutamate receptor activation inhibits Ca2+ influx and nitric oxide synthase activity in bone marrow stromal cells. *J. Cell. Physiol.* **204,** 704-713.

Fox S. W., Chambers T. J. and Chow J. W. (1996) Nitric oxide is an early mediator of the increase in bone formation by mechanical stimulation. *Am J Physiol* **270,** E955-960.

Frank O., Heim M., Jakob M., Barbero A., Schafer D., Bendik I., Dick W., Heberer M. and Martin I. (2002) Real-time quantitative RT-PCR analysis of human bone marrow stromal cells during osteogenic differentiation in vitro. *J Cell Biochem* **85,** 737-746.

Frankel A. D. and Pabo C. O. (1988) Cellular uptake of the tat protein from human immunodeficiency virus. *Cell* **55,** 1189-1193.

Fremeau R. T., Jr., Troyer M. D., Pahner I., Nygaard G. O., Tran C. H., Reimer R. J., Bellocchio E. E., Fortin D., Storm-Mathisen J. and Edwards R. H. (2001) The expression of vesicular glutamate transporters defines two classes of excitatory synapse. *Neuron* **31,** 247-260.

Fremeau R. T., Jr., Burman J., Qureshi T., Tran C. H., Proctor J., Johnson J., Zhang H., Sulzer D., Copenhagen D. R., Storm-Mathisen J., Reimer R. J., Chaudhry F. A. and Edwards R. H. (2002) The identification of vesicular glutamate transporter 3 suggests novel modes of signaling by glutamate. *Proc Natl Acad Sci U S A* **99,** 14488-14493.

Frost H. M. (1964) *Dynamics of bone remodeling,* pp 315-333, Boston, MA.

Fu D., Libson A., Miercke L. J., Weitzman C., Nollert P., Krucinski J. and Stroud R. M. (2000) Structure of a glycerol-conducting channel and the basis for its selectivity. *Science* **290,** 481-486.

Fuller K., Wong B., Fox S., Choi Y. and Chambers T. J. (1998) TRANCE is necessary and sufficient for osteoblast-mediated activation of bone resorption in osteoclasts. *J Exp Med* **188,** 997-1001.

Gallo V. and Ghiani C. A. (2000) Glutamate receptors in glia: new cells, new inputs and new functions. *Trends Pharmacol Sci* **21,** 252-258.

Gamboa C. and Ortega A. (2002) Insulin-like growth factor-1 increases activity and surface levels of the GLAST subtype of glutamate transporter. *Neurochem Int* **40,** 397-403.

Ganss B., Kim R. H. and Sodek J. (1999) Bone sialoprotein. *Crit Rev Oral Biol Med* **10,** 79-98.

Garlin A. B., Sinor A. D., Sinor J. D., Jee S. H., Grinspan J. B. and Robinson M. B. (1995) Pharmacology of sodium-dependent high-affinity L-[3H]glutamate transport in glial cultures. *J Neurochem* **64,** 2572-2580.

Gaston M. S. and Simpson A. H. (2007) Inhibition of fracture healing. *J Bone Joint Surg Br* **89,** 1553-1560.

Gebauer D., Mayr E., Orthner E. and Ryaby J. P. (2005) Low-intensity pulsed ultrasound: effects on nonunions. *Ultrasound Med Biol* **31,** 1391-1402.

Gebhardt F. M., Mitrovic A. D., Gilbert D. F., Vandenberg R. J., Lynch J. W. and Dodd P. R. (2010) Exon-skipping splice variants of excitatory amino acid transporter-2 (EAAT2) form heteromeric complexes with full-length EAAT2. *J Biol Chem.*

Gegelashvili G. and Schousboe A. (1998) Cellular distribution and kinetic properties of high-affinity glutamate transporters. *Brain Res Bull* **45,** 233-238.

Gegelashvili G., Civenni G., Racagni G., Danbolt N. C., Schousboe I. and Schousboe A. (1996) Glutamate receptor agonists up-regulate glutamate transporter GLAST in astrocytes. *Neuroreport* **8,** 261-265.

Gendreau S., Voswinkel S., Torres-Salazar D., Lang N., Heidtmann H., Detro-Dassen S., Schmalzing G., Hidalgo P. and Fahlke C. (2004) A trimeric quaternary structure is conserved in bacterial and human glutamate transporters. *J Biol Chem* **279,** 39505-39512.

Genever P. G. and Skerry T. M. (2001) Regulation of spontaneous glutamate release activity in osteoblastic cells and its role in differentiation and survival: evidence for intrinsic glutamatergic signaling in bone. *Faseb J* **15,** 1586-1588.

Genever P. G., Maxfield S. J., Kennovin G. D., Maltman J., Bowgen C. J., Raxworthy M. J. and Skerry T. M. (1999) Evidence for a novel glutamate-mediated signaling pathway in keratinocytes. *J Invest Dermatol* **112,** 337-342.

Georgescu H. I., Mendelow D. and Evans C. H. (1988) HIG-82: an established cell line from rabbit periarticular soft tissue, which retains the "activatable" phenotype. *In Vitro Cell Dev Biol* **24,** 1015-1022.

Gerber H. P., Vu T. H., Ryan A. M., Kowalski J., Werb Z. and Ferrara N. (1999) VEGF couples hypertrophic cartilage remodeling, ossification and angiogenesis during endochondral bone formation. *Nat Med* **5,** 623-628.

Gerstenfeld L. C., Cullinane D. M., Barnes G. L., Graves D. T. and Einhorn T. A. (2003) Fracture healing as a post-natal developmental process: molecular, spatial, and temporal aspects of its regulation. *J Cell Biochem* **88,** 873-884.

Giachelli C. M. (1999) Ectopic calcification: gathering hard facts about soft tissue mineralization. *Am J Pathol* **154,** 671-675.

Gilbert S. F. (2006) Intramembranous ossification, in *Developmental Biology,* 8th Edition, pp 420-421.

Gimble J. M., Robinson C. E., Wu X. and Kelly K. A. (1996) The function of adipocytes in the bone marrow stroma: an update. *Bone* **19,** 421-428.

Giraud-Guille M. M. (1988) Twisted plywood architecture of collagen fibrils in human compact bone osteons. *Calcif Tissue Int* **42,** 167-180.

Glass D. A., 2nd, Bialek P., Ahn J. D., Starbuck M., Patel M. S., Clevers H., Taketo M. M., Long F., McMahon A. P., Lang R. A. and Karsenty G. (2005) Canonical Wnt signaling in differentiated osteoblasts controls osteoclast differentiation. *Dev Cell* **8,** 751-764.

Glimcher M. J. and Katz E. P. (1965) Organization of Collagen in Bone - Role of Noncovalent Bonds in Relative Insolubility of Bone Collagen. *Journal of Ultrastructure Research* **12,** 705-&.

Glowacki J. and Lian J. B. (1987) Impaired recruitment and differentiation of osteoclast progenitors by osteocalcin-deplete bone implants. *Cell Differ* **21,** 247-254.

Goldberg G. (2004) Nutrition and Bone. *Women's Health Medicine* **1,** 25-29.

Gonzalez M. I. and Ortega A. (1997) Regulation of the Na+-dependent high affinity glutamate/aspartate transporter in cultured Bergmann glia by phorbol esters. *J Neurosci Res* **50,** 585-590.

Gonzalez M. I. and Ortega A. (2000) Regulation of high-affinity glutamate uptake activity in Bergmann glia cells by glutamate. *Brain Res* **866,** 73-81.

Gonzalez M. I., Lopez-Colom A. M. and Ortega A. (1999) Sodium-dependent glutamate transport in Muller glial cells: regulation by phorbol esters. *Brain Res* **831,** 140-145.

Gonzalez M. I., Kazanietz M. G. and Robinson M. B. (2002) Regulation of the neuronal glutamate transporter excitatory amino acid carrier-1 (EAAC1) by different protein kinase C subtypes. *Mol Pharmacol* **62,** 901-910.

Gonzalez M. I., Bannerman P. G. and Robinson M. B. (2003) Phorbol myristate acetate-dependent interaction of protein kinase Calpha and the neuronal glutamate transporter EAAC1. *J Neurosci* **23,** 5589-5593.

Gonzalez M. I., Susarla B. T. and Robinson M. B. (2005) Evidence that protein kinase Calpha interacts with and regulates the glial glutamate transporter GLT-1. *J Neurochem* **94,** 1180-1188.

Gordon J. A., Tye C. E., Sampaio A. V., Underhill T. M., Hunter G. K. and Goldberg H. A. (2007) Bone sialoprotein expression enhances osteoblast differentiation and matrix mineralization in vitro. *Bone* **41,** 462-473.

Goto T., Tsukuba T., Kiyoshima T., Nishimura Y., Kato K., Yamamoto K. and Tanaka T. (1993) Immunohistochemical localization of cathepsins B, D and L in the rat osteoclast. *Histochemistry* **99,** 411-414.

Gray C., Marie H., Arora M., Tanaka K., Boyde A., Jones S. and Attwell D. (2001) Glutamate does not play a major role in controlling bone growth. *J Bone Miner Res* **16,** 742-749.

Greenbaum M. A. and Kanat I. O. (1993) Current concepts in bone healing. Review of the literature. *J Am Podiatr Med Assoc* **83,** 123-129.

Gregor P., O'Hara B. F., Yang X. and Uhl G. R. (1993) Expression and novel subunit isoforms of glutamate receptor genes GluR5 and GluR6. *Neuroreport* **4,** 1343-1346.

Grewer C., Watzke N., Wiessner M. and Rauen T. (2000) Glutamate translocation of the neuronal glutamate transporter EAAC1 occurs within milliseconds. *Proc Natl Acad Sci U S A* **97,** 9706-9711.

Grewer C., Balani P., Weidenfeller C., Bartusel T., Tao Z. and Rauen T. (2005) Individual subunits of the glutamate transporter EAAC1 homotrimer function independently of each other. *Biochemistry* **44,** 11913-11923.

Griffiths R., Dunlop J., Gorman A., Senior J. and Grieve A. (1994) L-trans-pyrrolidine-2,4-dicarboxylate and cis-1-aminocyclobutane-1,3-dicarboxylate behave as transportable, competitive inhibitors of the high-affinity glutamate transporters. *Biochem Pharmacol* **47,** 267-274.

Grunewald M. and Kanner B. (1995) Conformational changes monitored on the glutamate transporter GLT-1 indicate the existence of two neurotransmitter-bound states. *J Biol Chem* **270,** 17017-17024.

Grunewald M. and Kanner B. I. (2000) The accessibility of a novel reentrant loop of the glutamate transporter GLT-1 is restricted by its substrate. *J Biol Chem* **275,** 9684-9689.

Grunewald M., Bendahan A. and Kanner B. I. (1998) Biotinylation of single cysteine mutants of the glutamate transporter GLT-1 from rat brain reveals its unusual topology. *Neuron* **21,** 623-632.

Grunewald R. A. (1993) Ascorbic acid in the brain. *Brain Res Brain Res Rev* **18,** 123-133.

Gu G., Mulari M., Peng Z., Hentunen T. A. and Vaananen H. K. (2005) Death of osteocytes turns off the inhibition of osteoclasts and triggers local bone resorption. *Biochem Biophys Res Commun* **335,** 1095-1101.

Gu Y. and Publicover S. J. (2000) Expression of functional metabotropic glutamate receptors in primary cultured rat osteoblasts. Cross-talk with N-methyl-D-aspartate receptors. *J Biol Chem* **275,** 34252-34259.

Gu Y., Genever P. G., Skerry T. M. and Publicover S. J. (2002) The NMDA type glutamate receptors expressed by primary rat osteoblasts have the same electrophysiological characteristics as neuronal receptors. *Calcif Tissue Int* **70,** 194-203.

Guillet B. A., Velly L. J., Canolle B., Masmejean F. M., Nieoullon A. L. and Pisano P. (2005) Differential regulation by protein kinases of activity and cell surface expression of glutamate transporters in neuron-enriched cultures. *Neurochem Int* **46,** 337-346.

Guiramand J., Martin A., de Jesus Ferreira M. C., Cohen-Solal C., Vignes M. and Recasens M. (2005) Gliotoxicity in hippocampal cultures is induced by transportable, but not by nontransportable, glutamate uptake inhibitors. *J Neurosci Res* **81,** 199-207.

Guo F., Sun F., Yu J. L., Wang Q. H., Tu D. Y., Mao X. Y., Liu R., Wu K. C., Xie N., Hao L. Y. and Cai J. Q. (2010) Abnormal expressions of glutamate transporters and metabotropic glutamate receptor 1 in the spontaneously epileptic rat hippocampus. *Brain Res Bull* **81,** 510-516.

Hagiwara T., Tanaka K., Takai S., Maeno-Hikichi Y., Mukainaka Y. and Wada K. (1996) Genomic organization, promoter analysis, and chromosomal localization of the gene for the mouse glial high-affinity glutamate transporter Slc1a3. *Genomics* **33,** 508-515.

Hall B. K. and Miyake T. (1992) The membranous skeleton: the role of cell condensations in vertebrate skeletogenesis. *Anat Embryol (Berl)* **186,** 107-124.

Hall B. K. and Miyake T. (2000) All for one and one for all: condensations and the initiation of skeletal development. *Bioessays* **22,** 138-147.

Hamersma H., Gardner J. and Beighton P. (2003) The natural history of sclerosteosis. *Clin Genet* **63,** 192-197.

Hara-Irie F., Amizuka N. and Ozawa H. (1996) Immunohistochemical and ultrastructural localization of CGRP-positive nerve fibers at the epiphyseal trabecules facing the growth plate of rat femurs. *Bone* **18,** 29-39.

Hartmann C. (2006) A Wnt canon orchestrating osteoblastogenesis. *Trends Cell Biol* **16,** 151-158.

Hauge E. M., Qvesel D., Eriksen E. F., Mosekilde L. and Melsen F. (2001) Cancellous bone remodeling occurs in specialized compartments lined by cells expressing osteoblastic markers. *J Bone Miner Res* **16,** 1575-1582.

Haugeto O., Ullensvang K., Levy L. M., Chaudhry F. A., Honore T., Nielsen M., Lehre K. P. and Danbolt N. C. (1996) Brain glutamate transporter proteins form homomultimers. *J Biol Chem* **271,** 27715-27722.

Hausen P. and Stein H. (1970) Ribonuclease H. An enzyme degrading the RNA moiety of DNA-RNA hybrids. *Eur J Biochem* **14,** 278-283.

Hayashi T., Yamada K., Esaki T., Kuzuya M., Satake S., Ishikawa T., Hidaka H. and Iguchi A. (1995) Estrogen increases endothelial nitric oxide by a receptor-mediated system. *Biochem Biophys Res Commun* **214,** 847-855.

Haydar T. F., Wang F., Schwartz M. L. and Rakic P. (2000) Differential modulation of proliferation in the neocortical ventricular and subventricular zones. *J Neurosci* **20,** 5764-5774.

Heckman J. D., Ryaby J. P., McCabe J., Frey J. J. and Kilcoyne R. F. (1994) Acceleration of tibial fracture-healing by non-invasive, low-intensity pulsed ultrasound. *J Bone Joint Surg Am* **76,** 26-34.

Heinegard D. and Oldberg A. (1989) Structure and biology of cartilage and bone matrix noncollagenous macromolecules. *FASEB J* **3,** 2042-2051.

Heitz F., Morris M. C. and Divita G. (2009) Twenty years of cell-penetrating peptides: from molecular mechanisms to therapeutics. *Br J Pharmacol* **157,** 195-206.

Henthorn P. S. and Whyte M. P. (1992) Missense mutations of the tissue-nonspecific alkaline phosphatase gene in hypophosphatasia. *Clin Chem* **38,** 2501-2505.

Herman M. A. and Jahr C. E. (2007) Extracellular glutamate concentration in hippocampal slice. *J Neurosci* **27,** 9736-9741.

Hert J., Sklenska A. and Liskova M. (1971) Reaction of bone to mechanical stimuli. 5. Effect of intermittent stress on the rabbit tibia after resection of the peripheral nerves. *Folia Morphol (Praha)* **19,** 378-387.

Herzog E., Bellenchi G. C., Gras C., Bernard V., Ravassard P., Bedet C., Gasnier B., Giros B. and El Mestikawy S. (2001) The existence of a second vesicular glutamate transporter specifies subpopulations of glutamatergic neurons. *J Neurosci* **21,** RC181.

Higuchi M., Single F. N., Kohler M., Sommer B., Sprengel R. and Seeburg P. H. (1993) RNA editing of AMPA receptor subunit GluR-B: a base-paired intron-exon structure determines position and efficiency. *Cell* **75,** 1361-1370.

Hill E. L. and Elde R. (1991) Distribution of CGRP-, VIP-, D beta H-, SP-, and NPY-immunoreactive nerves in the periosteum of the rat. *Cell Tissue Res* **264,** 469-480.

Himi T., Ikeda M., Yasuhara T. and Murota S. I. (2003) Oxidative neuronal death caused by glutamate uptake inhibition in cultured hippocampal neurons. *J Neurosci Res* **71,** 679-688.

Hinoi E., Fujimori S. and Yoneda Y. (2003) Modulation of cellular differentiation by N-methyl-D-aspartate receptors in osteoblasts. *Faseb J* **17,** 1532-1534.

Hinoi E., Fujimori S., Nakamura Y. and Yoneda Y. (2001) Group III metabotropic glutamate receptors in rat cultured calvarial osteoblasts. *Biochem Biophys Res Commun* **281,** 341-346.

Hinoi E., Fujimori S., Takemori A. and Yoneda Y. (2002a) Cell death by pyruvate deficiency in proliferative cultured calvarial osteoblasts. *Biochem Biophys Res Commun* **294,** 1177-1183.

Hinoi E., Wang L., Takemori A. and Yoneda Y. (2005a) Functional expression of particular isoforms of excitatory amino acid transporters by rodent cartilage. *Biochem Pharmacol* **70,** 70-81.

Hinoi E., Fujimori S., Takarada T., Taniura H. and Yoneda Y. (2002b) Facilitation of glutamate release by ionotropic glutamate receptors in osteoblasts. *Biochem Biophys Res Commun* **297,** 452-458.

Hinoi E., Takarada T., Ueshima T., Tsuchihashi Y. and Yoneda Y. (2004) Glutamate signaling in peripheral tissues. *Eur J Biochem* **271,** 1-13.

Hinoi E., Fujimori S., Takemori A., Kurabayashi H., Nakamura Y. and Yoneda Y. (2002c) Demonstration of expression of mRNA for particular AMPA and kainate receptor subunits in immature and mature cultured rat calvarial osteoblasts. *Brain Res* **943,** 112-116.

Hinoi E., Takarada T., Uno K., Inoue M., Murafuji Y. and Yoneda Y. (2007) Glutamate suppresses osteoclastogenesis through the cystine/glutamate antiporter. *Am J Pathol* **170,** 1277-1290.

Hinoi E., Ohashi R., Miyata S., Kato Y., Iemata M., Hojo H., Takarada T. and Yoneda Y. (2005b) Excitatory amino acid transporters expressed by synovial fibroblasts in rats with collagen-induced arthritis. *Biochem Pharmacol* **70,** 1744-1755.

Hirbec H., Perestenko O., Nishimune A., Meyer G., Nakanishi S., Henley J. M. and Dev K. K. (2002) The PDZ proteins PICK1, GRIP, and syntenin bind multiple glutamate receptor subtypes. Analysis of PDZ binding motifs. *J Biol Chem* **277,** 15221-15224.

Ho M. L., Tsai T. N., Chang J. K., Shao T. S., Jeng Y. R. and Hsu C. (2005) Down-regulation of N-methyl D-aspartate receptor in rat-modeled disuse osteopenia. *Osteoporos Int* **16,** 1780-1788.

Hoffman E. P. (2007) Skipping toward personalized molecular medicine. *N Engl J Med* **357,** 2719-2722.

Hohmann E. L. and Tashjian A. H., Jr. (1984) Functional receptors for vasoactive intestinal peptide on human osteosarcoma cells. *Endocrinology* **114,** 1321-1327.

Hohmann E. L., Elde R. P., Rysavy J. A., Einzig S. and Gebhard R. L. (1986) Innervation of periosteum and bone by sympathetic vasoactive intestinal peptide-containing nerve fibers. *Science* **232,** 868-871.

Holliday L. S., Welgus H. G., Fliszar C. J., Veith G. M., Jeffrey J. J. and Gluck S. L. (1997) Initiation of osteoclast bone resorption by interstitial collagenase. *J Biol Chem* **272,** 22053-22058.

Hollmann M. and Heinemann S. (1994) Cloned glutamate receptors. *Annu Rev Neurosci* **17,** 31-108.

Hollmann M., O'Shea-Greenfield A., Rogers S. W. and Heinemann S. (1989) Cloning by functional expression of a member of the glutamate receptor family. *Nature* **342,** 643-648.

Hollmann M., Boulter J., Maron C., Beasley L., Sullivan J., Pecht G. and Heinemann S. (1993) Zinc potentiates agonist-induced currents at certain splice variants of the NMDA receptor. *Neuron* **10,** 943-954.

Honig L. S., Chambliss D. D., Bigio E. H., Carroll S. L. and Elliott J. L. (2000) Glutamate transporter EAAT2 splice variants occur not only in ALS, but also in AD and controls. *Neurology* **55,** 1082-1088.

Horio Y., Hibino H., Inanobe A., Yamada M., Ishii M., Tada Y., Satoh E., Hata Y., Takai Y. and Kurachi Y. (1997) Clustering and enhanced activity of an inwardly rectifying potassium channel, Kir4.1, by an anchoring protein, PSD-95/SAP90. *J Biol Chem* **272,** 12885-12888.

Howell J. A., Matthews A. D., Swanson K. C., Harmon D. L. and Matthews J. C. (2001) Molecular identification of high-affinity glutamate transporters in sheep and cattle forestomach, intestine, liver, kidney, and pancreas. *J Anim Sci* **79,** 1329-1336.

Howland D. S., Liu J., She Y., Goad B., Maragakis N. J., Kim B., Erickson J., Kulik J., DeVito L., Psaltis G., DeGennaro L. J., Cleveland D. W. and Rothstein J. D. (2002) Focal loss of the glutamate transporter EAAT2 in a transgenic rat model of SOD1 mutant-mediated amyotrophic lateral sclerosis (ALS). *Proc Natl Acad Sci U S A* **99,** 1604-1609.

Hu H., Hilton M. J., Tu X., Yu K., Ornitz D. M. and Long F. (2005) Sequential roles of Hedgehog and Wnt signaling in osteoblast development. *Development* **132,** 49-60.

Huang L. F., Fukai N., Selby P. B., Olsen B. R. and Mundlos S. (1997) Mouse clavicular development: analysis of wild-type and cleidocranial dysplasia mutant mice. *Dev Dyn* **210,** 33-40.

Huang Y. H., Sinha S. R., Tanaka K., Rothstein J. D. and Bergles D. E. (2004) Astrocyte glutamate transporters regulate metabotropic glutamate receptor-mediated excitation of hippocampal interneurons. *J Neurosci* **24,** 4551-4559.

Huggett J., Vaughan-Thomas A. and Mason D. (2000) The open reading frame of the Na(+)-dependent glutamate transporter GLAST-1 is expressed in bone and a splice variant of this molecule is expressed in bone and brain. *FEBS Lett* **485,** 13-18.

Huggett J. F., Mustafa A., O'Neal L. and Mason D. J. (2002) The glutamate transporter GLAST-1 (EAAT-1) is expressed in the plasma membrane of osteocytes and is responsive to extracellular glutamate concentration. *Biochem Soc Trans* **30,** 890-893.

Hughes E. G., Maguire J. L., McMinn M. T., Scholz R. E. and Sutherland M. L. (2004) Loss of glial fibrillary acidic protein results in decreased glutamate transport and inhibition of PKA-induced EAAT2 cell surface trafficking. *Brain Res Mol Brain Res* **124,** 114-123.

Hukkanen M., Konttinen Y. T., Rees R. G., Gibson S. J., Santavirta S. and Polak J. M. (1992) Innervation of bone from healthy and arthritic rats by substance P and calcitonin gene related peptide containing sensory fibers. *J Rheumatol* **19,** 1252-1259.

Hukkanen M., Konttinen Y. T., Santavirta S., Paavolainen P., Gu X. H., Terenghi G. and Polak J. M. (1993) Rapid proliferation of calcitonin gene-related peptide-immunoreactive nerves during healing of rat tibial fracture suggests neural involvement in bone growth and remodelling. *Neuroscience* **54,** 969-979.

Hukkanen M., Konttinen Y. T., Santavirta S., Nordsletten L., Madsen J. E., Almaas R., Oestreicher A. B., Rootwelt T. and Polak J. M. (1995) Effect of sciatic nerve section on neural ingrowth into the rat tibial fracture callus. *Clin Orthop Relat Res,* 247-257.

Hunter G. K., Hauschka P. V., Poole A. R., Rosenberg L. C. and Goldberg H. A. (1996) Nucleation and inhibition of hydroxyapatite formation by mineralized tissue proteins. *Biochem J* **317 (Pt 1),** 59-64.

Hunziker E. B. (1994) Mechanism of longitudinal bone growth and its regulation by growth plate chondrocytes. *Microsc Res Tech* **28,** 505-519.

Hurtley S. M. and Helenius A. (1989) Protein oligomerization in the endoplasmic reticulum. *Annu Rev Cell Biol* **5,** 277-307.

Iemata M., Takarada T., Hinoi E., Taniura H. and Yoneda Y. (2007) Suppression by glutamate of proliferative activity through glutathione depletion mediated by the cystine/glutamate antiporter in mesenchymal C3H10T1/2 stem cells. *J Cell Physiol* **213,** 721-729.

Ihara H., Denhardt D. T., Furuya K., Yamashita T., Muguruma Y., Tsuji K., Hruska K. A., Higashio K., Enomoto S., Nifuji A., Rittling S. R. and Noda M. (2001) Parathyroid hormone-induced bone resorption does not occur in the absence of osteopontin. *J Biol Chem* **276,** 13065-13071.

Ikonomidou C., Bosch F., Miksa M., Bittigau P., Vockler J., Dikranian K., Tenkova T. I., Stefovska V., Turski L. and Olney J. W. (1999) Blockade of NMDA receptors and apoptotic neurodegeneration in the developing brain. *Science* **283,** 70-74.

Irie K., Hidehiro, O., Toshihiko, Y. (2000) The Histochemical and Cytochemical Changes from Formative to Resorptive Osteocytes. *Acta Histochem. Cytochem.* **33,** 385-391.

Ishijima M., Rittling S. R., Yamashita T., Tsuji K., Kurosawa H., Nifuji A., Denhardt D. T. and Noda M. (2001) Enhancement of osteoclastic bone resorption and suppression of osteoblastic bone formation in response to reduced mechanical stress do not occur in the absence of osteopontin. *J Exp Med* **193,** 399-404.

Isogai Y., Akatsu T., Ishizuya T., Yamaguchi A., Hori M., Takahashi N. and Suda T. (1996) Parathyroid hormone regulates osteoblast differentiation positively or negatively depending on the differentiation stages. *J Bone Miner Res* **11,** 1384-1393.

Itzstein C., Espinosa L., Delmas P. D. and Chenu C. (2000) Specific antagonists of NMDA receptors prevent osteoclast sealing zone formation required for bone resorption. *Biochem Biophys Res Commun* **268,** 201-209.

Itzstein C., Cheynel H., Burt-Pichat B., Merle B., Espinosa L., Delmas P. D. and Chenu C. (2001) Molecular identification of NMDA glutamate receptors expressed in bone cells. *J Cell Biochem* **82,** 134-144.

Iyama K., Ninomiya Y., Olsen B. R., Linsenmayer T. F., Trelstad R. L. and Hayashi M. (1991) Spatiotemporal pattern of type X collagen gene expression and collagen deposition in embryonic chick vertebrae undergoing endochondral ossification. *Anat Rec* **229,** 462-472.

Izumi Y., Shimamoto K., Benz A. M., Hammerman S. B., Olney J. W. and Zorumski C. F. (2002) Glutamate transporters and retinal excitotoxicity. *Glia* **39,** 58-68.

Jabaudon D., Shimamoto K., Yasuda-Kamatani Y., Scanziani M., Gahwiler B. H. and Gerber U. (1999) Inhibition of uptake unmasks rapid extracellular turnover of glutamate of nonvesicular origin. *Proc Natl Acad Sci U S A* **96,** 8733-8738.

Jackson M., Song W., Liu M. Y., Jin L., Dykes-Hoberg M., Lin C. I., Bowers W. J., Federoff H. J., Sternweis P. C. and Rothstein J. D. (2001) Modulation of the neuronal glutamate transporter EAAT4 by two interacting proteins. *Nature* **410,** 89-93.

Jande S. S. and Belanger L. F. (1973) The life cycle of the osteocyte. *Clin Orthop Relat Res,* 281-305.

Jean Y. H., Wen Z. H., Chang Y. C., Huang G. S., Lee H. S., Hsieh S. P. and Wong C. S. (2005) Increased concentrations of neuro-excitatory amino acids in rat anterior cruciate ligament-transected knee joint dialysates: a microdialysis study. *J Orthop Res* **23,** 569-575.

Jean Y. H., Wen Z. H., Chang Y. C., Hsieh S. P., Lin J. D., Tang C. C., Chen W. F., Chou A. K. and Wong C. S. (2008) Increase in excitatory amino acid concentration and transporters expression in osteoarthritic knees of anterior cruciate ligament transected rabbits. *Osteoarthritis Cartilage.*

Jee W. S. S. (1983) The Skeletal Tissues, in *Histology: cell and tissue biology,* 5th Edition (Weiss L., ed.), pp 206-254.

Jensen A. A. and Brauner-Osborne H. (2004) Pharmacological characterization of human excitatory amino acid transporters EAAT1, EAAT2 and EAAT3 in a fluorescence-based membrane potential assay. *Biochem Pharmacol* **67,** 2115-2127.

Johnell O. (1997) The socioeconomic burden of fractures: today and in the 21st century. *Am J Med* **103,** 20S-25S; discussion 25S-26S.

Johnson L. C. (1964) *Morphological analysis in pathology: the kinetics of disease and general biology of bone*, Vol. 550. Little, Brown and Company, Boston.

Johnston C. C., Jr., Lavy N., Lord T., Vellios F., Merritt A. D. and Deiss W. P., Jr. (1968) Osteopetrosis. A clinical, genetic, metabolic, and morphologic study of the dominantly inherited, benign form. *Medicine (Baltimore)* **47,** 149-167.

Johnston G. A. R. (1981) Glutamate uptake and its possible role in neurotransmitter inactivation, in *Roberts, P.J., Storm-Mathisen, J.* (Johnston G. A. R., ed.), pp 77-87. Wiley, Chichester, UK.

Jones H. H., Priest J. D., Hayes W. C., Tichenor C. C. and Nagel D. A. (1977) Humeral hypertrophy in response to exercise. *J Bone Joint Surg Am* **59,** 204-208.

Jones S. J. and Boyde A. (1976) Experimental study of changes in osteoblastic shape induced by calcitonin and parathyroid extract in an organ culture system. *Cell Tissue Res* **169,** 499-465.

Jukkola A., Risteli L., Melkko J. and Risteli J. (1993) Procollagen synthesis and extracellular matrix deposition in MG-63 osteosarcoma cells. *J Bone Miner Res* **8,** 651-657.

Jung A., Bisaz S. and Fleisch H. (1973) The binding of pyrophosphate and two diphosphonates by hydroxyapatite crystals. *Calcif Tissue Res* **11,** 269-280.

Kalandadze A., Wu Y. and Robinson M. B. (2002) Protein kinase C activation decreases cell surface expression of the GLT-1 subtype of glutamate transporter. Requirement of a carboxyl-terminal domain and partial dependence on serine 486. *J Biol Chem* **277,** 45741-45750.

Kalandadze A., Wu Y., Fournier K. and Robinson M. B. (2004) Identification of motifs involved in endoplasmic reticulum retention-forward trafficking of the GLT-1 subtype of glutamate transporter. *J Neurosci* **24,** 5183-5192.

Kalariti N., Lembessis P. and Koutsilieris M. (2004) Characterization of the glutametergic system in MG-63 osteoblast-like osteosarcoma cells. *Anticancer Res* **24,** 3923-3929.

Kalariti N., Lembessis P., Papageorgiou E., Pissimissis N. and Koutsilieris M. (2007) Regulation of the mGluR5, EAAT1 and GS expression by glucocorticoids in MG-63 osteoblast-like osteosarcoma cells. *J Musculoskelet Neuronal Interact* **7,** 113-118.

Kamioka H., Honjo T. and Takano-Yamamoto T. (2001) A three-dimensional distribution of osteocyte processes revealed by the combination of confocal laser scanning microscopy and differential interference contrast microscopy. *Bone* **28,** 145-149.

Kanai Y. and Hediger M. A. (1992) Primary structure and functional characterization of a high-affinity glutamate transporter. *Nature* **360,** 467-471.

Kanai Y. and Hediger M. A. (2004) The glutamate/neutral amino acid transporter family SLC1: molecular, physiological and pharmacological aspects. *Pflugers Arch* **447,** 469-479.

Kanai Y., Smith C. P. and Hediger M. A. (1993) A new family of neurotransmitter transporters: the high-affinity glutamate transporters. *FASEB J* **7,** 1450-1459.

Kanai Y., Bhide P. G., DiFiglia M. and Hediger M. A. (1995a) Neuronal high-affinity glutamate transport in the rat central nervous system. *Neuroreport* **6,** 2357-2362.

Kanai Y., Nussberger S., Romero M. F., Boron W. F., Hebert S. C. and Hediger M. A. (1995b) Electrogenic properties of the epithelial and neuronal high affinity glutamate transporter. *J Biol Chem* **270,** 16561-16568.

Kaneko T. and Fujiyama F. (2002) Complementary distribution of vesicular glutamate transporters in the central nervous system. *Neurosci Res* **42,** 243-250.

Kaneps A. J., Stover S. M. and Lane N. E. (1997) Changes in canine cortical and cancellous bone mechanical properties following immobilization and remobilization with exercise. *Bone* **21,** 419-423.

Kanis J., Oden A. and Johnell O. (2001) Acute and long-term increase in fracture risk after hospitalization for stroke. *Stroke* **32,** 702-706.

Kanjhan R., Hryciw D. H., Yun C. C., Bellingham M. C. and Poronnik P. (2006) Postnatal developmental expression of the PDZ scaffolds Na+ -H+ exchanger regulatory factors 1 and 2 in the rat cochlea. *Cell Tissue Res* **323,** 53-70.

Karsenty G. (1999) The genetic transformation of bone biology. *Genes Dev* **13,** 3037-3051.
Karsenty G. (2003) The complexities of skeletal biology. *Nature* **423,** 316-318.
Karsenty G. and Wagner E. F. (2002) Reaching a genetic and molecular understanding of skeletal development. *Dev Cell* **2,** 389-406.
Kasantikul V. and Shuangshoti S. (1989) Positivity to glial fibrillary acidic protein in bone, cartilage, and chordoma. *J Surg Oncol* **41,** 22-26.
Kaspar D., Seidl W., Neidlinger-Wilke C., Ignatius A. and Claes L. (2000) Dynamic cell stretching increases human osteoblast proliferation and CICP synthesis but decreases osteocalcin synthesis and alkaline phosphatase activity. *J Biomech* **33,** 45-51.
Kassem M., Risteli L., Mosekilde L., Melsen F. and Eriksen E. F. (1991a) Formation of osteoblast-like cells from human mononuclear bone marrow cultures. *APMIS* **99,** 269-274.
Kassem M., Mosekilde L., Rungby J., Mosekilde L., Melsen F. and Eriksen E. F. (1991b) Formation of osteoclasts and osteoblast-like cells in long-term human bone marrow cultures. *APMIS* **99,** 262-268.
Kato S., Negishi K., Mawatari K. and Kuo C. H. (1992) A mechanism for glutamate toxicity in the C6 glioma cells involving inhibition of cystine uptake leading to glutathione depletion. *Neuroscience* **48,** 903-914.
Kawakami H., Tanaka K., Nakayama T., Inoue K. and Nakamura S. (1994) Cloning and expression of a human glutamate transporter. *Biochem Biophys Res Commun* **199,** 171-176.
Keller H. and Kneissel M. (2005) SOST is a target gene for PTH in bone. *Bone* **37,** 148-158.
Khan S. A., Kanis J. A., Vasikaran S., Kline W. F., Matuszewski B. K., McCloskey E. V., Beneton M. N., Gertz B. J., Sciberras D. G., Holland S. D., Orgee J., Coombes G. M., Rogers S. R. and Porras A. G. (1997) Elimination and biochemical responses to intravenous alendronate in postmenopausal osteoporosis. *J Bone Miner Res* **12,** 1700-1707.
Khanna C., Khan J., Nguyen P., Prehn J., Caylor J., Yeung C., Trepel J., Meltzer P. and Helman L. (2001) Metastasis-associated differences in gene expression in a murine model of osteosarcoma. *Cancer Res* **61,** 3750-3759.
Kim E., Niethammer M., Rothschild A., Jan Y. N. and Sheng M. (1995) Clustering of Shaker-type K+ channels by interaction with a family of membrane-associated guanylate kinases. *Nature* **378,** 85-88.
Kinoshita N., Kimura K., Matsumoto N., Watanabe M., Fukaya M. and Ide C. (2004) Mammalian septin Sept2 modulates the activity of GLAST, a glutamate transporter in astrocytes. *Genes Cells* **9,** 1-14.
Kitayama S., Dohi T. and Uhl G. R. (1994) Phorbol esters alter functions of the expressed dopamine transporter. *Eur J Pharmacol* **268,** 115-119.
Klausner R. D. and Sitia R. (1990) Protein degradation in the endoplasmic reticulum. *Cell* **62,** 611-614.
Klein-Nulend J., Semeins C. M., Ajubi N. E., Nijweide P. J. and Burger E. H. (1995) Pulsating fluid flow increases nitric oxide (NO) synthesis by osteocytes but not periosteal fibroblasts--correlation with prostaglandin upregulation. *Biochem Biophys Res Commun* **217,** 640-648.
Klein-Nulend J., Helfrich M. H., Sterck J. G., MacPherson H., Joldersma M., Ralston S. H., Semeins C. M. and Burger E. H. (1998) Nitric oxide response to shear stress by human bone cell cultures is endothelial nitric oxide synthase dependent. *Biochem Biophys Res Commun* **250,** 108-114.
Koch H. P. and Larsson H. P. (2005) Small-scale molecular motions accomplish glutamate uptake in human glutamate transporters. *J Neurosci* **25,** 1730-1736.
Koch H. P., Kavanaugh M. P., Esslinger C. S., Zerangue N., Humphrey J. M., Amara S. G., Chamberlin A. R. and Bridges R. J. (1999) Differentiation of substrate and nonsubstrate inhibitors of the high-affinity, sodium-dependent glutamate transporters. *Mol Pharmacol* **56,** 1095-1104.
Kodama H., Nose M., Niida S. and Yamasaki A. (1991) Essential role of macrophage colony-stimulating factor in the osteoclast differentiation supported by stromal cells. *J Exp Med* **173,** 1291-1294.
Kohler M., Kornau H. C. and Seeburg P. H. (1994) The organization of the gene for the functionally dominant alpha-amino-3-hydroxy-5-methylisoxazole-4-propionic acid receptor subunit GluR-B. *J Biol Chem* **269,** 17367-17370.
Kohler M., Burnashev N., Sakmann B. and Seeburg P. H. (1993) Determinants of Ca2+ permeability in both TM1 and TM2 of high affinity kainate receptor channels: diversity by RNA editing. *Neuron* **10,** 491-500.
Kole R. and Sazani P. (2001) Antisense effects in the cell nucleus: modification of splicing. *Curr Opin Mol Ther* **3,** 229-234.

Komori T., Yagi H., Nomura S., Yamaguchi A., Sasaki K., Deguchi K., Shimizu Y., Bronson R. T., Gao Y. H., Inada M., Sato M., Okamoto R., Kitamura Y., Yoshiki S. and Kishimoto T. (1997) Targeted disruption of Cbfa1 results in a complete lack of bone formation owing to maturational arrest of osteoblasts. *Cell* **89,** 755-764.

Komuro H. and Rakic P. (1993) Modulation of neuronal migration by NMDA receptors. *Science* **260,** 95-97.

Kornau H. C., Schenker L. T., Kennedy M. B. and Seeburg P. H. (1995) Domain interaction between NMDA receptor subunits and the postsynaptic density protein PSD-95. *Science* **269,** 1737-1740.

Kugler P. (2004) Expression of glutamate transporters in rat cardiomyocytes and their localization in the T-tubular system. *J Histochem Cytochem* **52,** 1385-1392.

Kurata K., Heino T. J., Higaki H. and Vaananen H. K. (2006) Bone marrow cell differentiation induced by mechanically damaged osteocytes in 3D gel-embedded culture. *J Bone Miner Res* **21,** 616-625.

Kurreck J. (2003) Antisense technologies. Improvement through novel chemical modifications. *Eur J Biochem* **270,** 1628-1644.

Kuwahara O., Mitsumoto Y., Chiba K. and Mohri T. (1992) Characterization of D-aspartic acid uptake by rat hippocampal slices and effect of ischemic conditions. *J Neurochem* **59,** 616-621.

Lacey D. L., Timms E., Tan H. L., Kelley M. J., Dunstan C. R., Burgess T., Elliott R., Colombero A., Elliott G., Scully S., Hsu H., Sullivan J., Hawkins N., Davy E., Capparelli C., Eli A., Qian Y. X., Kaufman S., Sarosi I., Shalhoub V., Senaldi G., Guo J., Delaney J. and Boyle W. J. (1998) Osteoprotegerin ligand is a cytokine that regulates osteoclast differentiation and activation. *Cell* **93,** 165-176.

Lai M. D., Chen C. S., Yang C. R., Yuan S. Y., Tsai J. J., Tu C. F., Wang C. C., Yen M. C. and Lin C. C. (2009) An HDAC inhibitor enhances the antitumor activity of a CMV promoter-driven DNA vaccine. *Cancer Gene Ther* **17,** 203-211.

Laketic-Ljubojevic I., Suva L. J., Maathuis F. J., Sanders D. and Skerry T. M. (1999) Functional characterization of N-methyl-D-aspartic acid-gated channels in bone cells. *Bone* **25,** 631-637.

Lamoureux F., Baud'huin M., Duplomb L., Heymann D. and Redini F. (2007) Proteoglycans: key partners in bone cell biology. *Bioessays* **29,** 758-771.

Lampasso J. D., Marzec N., Margarone J., 3rd and Dziak R. (2002) Role of protein kinase C alpha in primary human osteoblast proliferation. *J Bone Miner Res* **17,** 1968-1976.

Lane T. F. and Sage E. H. (1994) The biology of SPARC, a protein that modulates cell-matrix interactions. *FASEB J* **8,** 163-173.

Lang T., LeBlanc A., Evans H., Lu Y., Genant H. and Yu A. (2004) Cortical and trabecular bone mineral loss from the spine and hip in long-duration spaceflight. *J Bone Miner Res* **19,** 1006-1012.

Langford M. P., Redmond P., Chanis R., Misra R. P. and Redens T. B. (2010) Glutamate, excitatory amino acid transporters, Xc- antiporter, glutamine synthetase, and gamma-glutamyltranspeptidase in human corneal epithelium. *Curr Eye Res* **35,** 202-211.

Lanyon L. E. (1996) Using functional loading to influence bone mass and architecture: objectives, mechanisms, and relationship with estrogen of the mechanically adaptive process in bone. *Bone* **18,** 37S-43S.

Lau C. L., Beart P. M. and O'Shea R. D. (2010) Transportable and non-transportable inhibitors of L-glutamate uptake produce astrocytic stellation and increase EAAT2 cell surface expression. *Neurochem Res* **35,** 735-742.

Laubach V. E., Garvey E. P. and Sherman P. A. (1996) High-level expression of human inducible nitric oxide synthase in Chinese hamster ovary cells and characterization of the purified enzyme. *Biochem Biophys Res Commun* **218,** 802-807.

Law R. M., Stafford A. and Quick M. W. (2000) Functional regulation of gamma-aminobutyric acid transporters by direct tyrosine phosphorylation. *J Biol Chem* **275,** 23986-23991.

Lawand N. B., McNearney T. and Westlund K. N. (2000) Amino acid release into the knee joint: key role in nociception and inflammation. *Pain* **86,** 69-74.

Lee A., O'Driscoll S., Pow D. V. and Poronnik P. (2008) Identification of glutamate transporter glast splice variants in hypoxic neonatal pig brain. *Proceedings of the Australian Physiological Society* **39,** 104P.

Lee A., Rayfield A., Hryciw D. H., Ma T. A., Wang D., Pow D., Broer S., Yun C. and Poronnik P. (2007) Na+-H+ exchanger regulatory factor 1 is a PDZ scaffold for the astroglial glutamate transporter GLAST. *Glia* **55,** 119-129.

Lee K., Jessop H., Suswillo R., Zaman G. and Lanyon L. (2003) Endocrinology: bone adaptation requires oestrogen receptor-alpha. *Nature* **424,** 389.

Lehre K. P., Davanger S. and Danbolt N. C. (1997) Localization of the glutamate transporter protein GLAST in rat retina. *Brain Res* **744,** 129-137.

Lehre K. P., Levy L. M., Ottersen O. P., Storm-Mathisen J. and Danbolt N. C. (1995) Differential expression of two glial glutamate transporters in the rat brain: quantitative and immunocytochemical observations. *J Neurosci* **15,** 1835-1853.

Leighton B. H., Seal R. P., Shimamoto K. and Amara S. G. (2002) A hydrophobic domain in glutamate transporters forms an extracellular helix associated with the permeation pathway for substrates. *J Biol Chem* **277,** 29847-29855.

Leighton B. H., Seal R. P., Watts S. D., Skyba M. O. and Amara S. G. (2006) Structural rearrangements at the translocation pore of the human glutamate transporter, EAAT1. *J Biol Chem* **281,** 29788-29796.

Levi G., Poce U. and Raiteri M. (1976) Uptake and exchange of GABA and glutamate in isolated nerve endings. *Adv Exp Med Biol* **69,** 273-289.

Lewiecki E. M., Miller P. D., McClung M. R., Cohen S. B., Bolognese M. A., Liu Y., Wang A., Siddhanti S. and Fitzpatrick L. A. (2007) Two-year treatment with denosumab (AMG 162) in a randomized phase 2 study of postmenopausal women with low BMD. *J Bone Miner Res* **22,** 1832-1841.

Li C. Y., Majeska R. J., Laudier D. M., Mann R. and Schaffler M. B. (2005a) High-dose risedronate treatment partially preserves cancellous bone mass and microarchitecture during long-term disuse. *Bone* **37,** 287-295.

Li C. Y., Price C., Delisser K., Nasser P., Laudier D., Clement M., Jepsen K. J. and Schaffler M. B. (2005b) Long-term disuse osteoporosis seems less sensitive to bisphosphonate treatment than other osteoporosis. *J Bone Miner Res* **20,** 117-124.

Li J., Ahmad T., Spetea M., Ahmed M. and Kreicbergs A. (2001) Bone reinnervation after fracture: a study in the rat. *J Bone Miner Res* **16,** 1505-1510.

Li X., Liu P., Liu W., Maye P., Zhang J., Zhang Y., Hurley M., Guo C., Boskey A., Sun L., Harris S. E., Rowe D. W., Ke H. Z. and Wu D. (2005c) Dkk2 has a role in terminal osteoblast differentiation and mineralized matrix formation. *Nat Genet* **37,** 945-952.

Li Z., Zhou Z., Saunders M. M. and Donahue H. J. (2006) Modulation of connexin43 alters expression of osteoblastic differentiation markers. *Am J Physiol Cell Physiol* **290,** C1248-1255.

Lian J. B. and Stein G. S. (1993) The developmental stages of osteoblast growth and differentiation exhibit selective responses of genes to growth factors (TGF beta 1) and hormones (vitamin D and glucocorticoids). *J Oral Implantol* **19,** 95-105; discussion 136-107.

Lian J. B. and Stein G. S. (1995) Development of the osteoblast phenotype: molecular mechanisms mediating osteoblast growth and differentiation. *Iowa Orthop J* **15,** 118-140.

Lian J. B. and Stein G. S. (2003) Runx2/Cbfa1: a multifunctional regulator of bone formation. *Curr Pharm Des* **9,** 2677-2685.

Lian N., Wang W., Li L., Elefteriou F. and Yang X. (2009) Vimentin inhibits ATF4-mediated osteocalcin transcription and osteoblast differentiation. *J Biol Chem.*

Lievremont M., Potus J. and Guillou B. (1982) Use of alizarin red S for histochemical staining of Ca2+ in the mouse; some parameters of the chemical reaction in vitro. *Acta Anat (Basel)* **114,** 268-280.

Lim J., Lam Y. C., Kistler J. and Donaldson P. J. (2005) Molecular characterization of the cystine/glutamate exchanger and the excitatory amino acid transporters in the rat lens. *Invest Ophthalmol Vis Sci* **46,** 2869-2877.

Lin C. I., Orlov I., Ruggiero A. M., Dykes-Hoberg M., Lee A., Jackson M. and Rothstein J. D. (2001) Modulation of the neuronal glutamate transporter EAAC1 by the interacting protein GTRAP3-18. *Nature* **410,** 84-88.

Lin C. L., Bristol L. A., Jin L., Dykes-Hoberg M., Crawford T., Clawson L. and Rothstein J. D. (1998) Aberrant RNA processing in a neurodegenerative disease: the cause for absent EAAT2, a glutamate transporter, in amyotrophic lateral sclerosis. *Neuron* **20,** 589-602.

Lin J. H. (1996) Bisphosphonates: a review of their pharmacokinetic properties. *Bone* **18,** 75-85.

Lin T. H., Yang R. S., Tang C. H., Wu M. Y. and Fu W. M. (2008) Regulation of the maturation of osteoblasts and osteoclastogenesis by glutamate. *Eur J Pharmacol.*

Lineweaver H. and Burk D. (1934) The Determination of Enzyme Dissociation Constants. *J. Am. Chem. Soc.* **56,** 658-666.

Lipton S. A. (2006) Paradigm shift in neuroprotection by NMDA receptor blockade: memantine and beyond. *Nat Rev Drug Discov* **5,** 160-170.

Lipton S. A., Choi Y. B., Pan Z. H., Lei S. Z., Chen H. S., Sucher N. J., Loscalzo J., Singel D. J. and Stamler J. S. (1993) A redox-based mechanism for the neuroprotective and neurodestructive effects of nitric oxide and related nitroso-compounds. *Nature* **364,** 626-632.

Liu X. S., Sajda P., Saha P. K., Wehrli F. W. and Guo X. E. (2006) Quantification of the roles of trabecular microarchitecture and trabecular type in determining the elastic modulus of human trabecular bone. *J Bone Miner Res* **21,** 1608-1617.

Liu X. S., Bevill G., Keaveny T. M., Sajda P. and Guo X. E. (2009) Micromechanical analyses of vertebral trabecular bone based on individual trabeculae segmentation of plates and rods. *J Biomech* **42,** 249-256.

Liu X. S., Sajda P., Saha P. K., Wehrli F. W., Bevill G., Keaveny T. M. and Guo X. E. (2008) Complete volumetric decomposition of individual trabecular plates and rods and its morphological correlations with anisotropic elastic moduli in human trabecular bone. *J Bone Miner Res* **23,** 223-235.

Lomeli H., Mosbacher J., Melcher T., Hoger T., Geiger J. R., Kuner T., Monyer H., Higuchi M., Bach A. and Seeburg P. H. (1994) Control of kinetic properties of AMPA receptor channels by nuclear RNA editing. *Science* **266,** 1709-1713.

Loots G. G., Kneissel M., Keller H., Baptist M., Chang J., Collette N. M., Ovcharenko D., Plajzer-Frick I. and Rubin E. M. (2005) Genomic deletion of a long-range bone enhancer misregulates sclerostin in Van Buchem disease. *Genome Res* **15,** 928-935.

Lopez-Bayghen E. and Ortega A. (2004) Glutamate-dependent transcriptional regulation of GLAST: role of PKC. *J Neurochem* **91,** 200-209.

Lopez-Bayghen E., Espinoza-Rojo M. and Ortega A. (2003) Glutamate down-regulates GLAST expression through AMPA receptors in Bergmann glial cells. *Brain Res Mol Brain Res* **115,** 1-9.

Lorenz-Depiereux B., Bastepe M., Benet-Pages A., Amyere M., Wagenstaller J., Muller-Barth U., Badenhoop K., Kaiser S. M., Rittmaster R. S., Shlossberg A. H., Olivares J. L., Loris C., Ramos F. J., Glorieux F., Vikkula M., Juppner H. and Strom T. M. (2006) DMP1 mutations in autosomal recessive hypophosphatemia implicate a bone matrix protein in the regulation of phosphate homeostasis. *Nat Genet* **38,** 1248-1250.

LoTurco J. J., Owens D. F., Heath M. J., Davis M. B. and Kriegstein A. R. (1995) GABA and glutamate depolarize cortical progenitor cells and inhibit DNA synthesis. *Neuron* **15,** 1287-1298.

Lundberg J. M., Hokfelt T., Schultzberg M., Uvnas-Wallensten K., Kohler C. and Said S. I. (1979) Occurrence of vasoactive intestinal polypeptide (VIP)-like immunoreactivity in certain cholinergic neurons of the cat: evidence from combined immunohistochemistry and acetylcholinesterase staining. *Neuroscience* **4,** 1539-1559.

Mach D. B., Rogers S. D., Sabino M. C., Luger N. M., Schwei M. J., Pomonis J. D., Keyser C. P., Clohisy D. R., Adams D. J., O'Leary P. and Mantyh P. W. (2002) Origins of skeletal pain: sensory and sympathetic innervation of the mouse femur. *Neuroscience* **113,** 155-166.

Macnab L. T. and Pow D. V. (2007a) Central nervous system expression of the exon 9 skipping form of the glutamate transporter GLAST. *Neuroreport* **18,** 741-745.

Macnab L. T. and Pow D. V. (2007b) Expression of the exon 9-skipping form of EAAT2 in astrocytes of rats. *Neuroscience* **150,** 705-711.

Macnab L. T., Williams S. M. and Pow D. V. (2006) Expression of the exon 3 skipping form of GLAST, GLAST1a, in brain and retina. *Neuroreport* **17,** 1867-1870.

Mahadomrongkul V., Aoki C. and Rosenberg P. A. (2002) THE GLUTAMATE TRANSPORTER GLT1B and PICK1 BOTH LOCALIZE TO PRE - AND POST - SYNAPTIC PROCESSES OF PYRAMIDAL NEURONS As WELL As ASTROCYTES OF INTACT ADULT RAT CEREBRAL CORTEX. *Society for Neuroscience Abstract Viewer and Itinerary Planner* **2002,** Abstract No. 44.47.

Majeska R. J. and Wuthier R. E. (1975) Studies on matrix vesicles isolated from chick epiphyseal cartilage. Association of pyrophosphatase and ATPase activities with alkaline phosphatase. *Biochim Biophys Acta* **391,** 51-60.

Majeska R. J. and Rodan G. A. (1982) The effect of 1,25(OH)2D3 on alkaline phosphatase in osteoblastic osteosarcoma cells. *J Biol Chem* **257,** 3362-3365.

Maki R., Robinson M. B. and Dichter M. A. (1994) The glutamate uptake inhibitor L-trans-pyrrolidine-2,4-dicarboxylate depresses excitatory synaptic transmission via a presynaptic mechanism in cultured hippocampal neurons. *J Neurosci* **14,** 6754-6762.

Malaval L., Liu F., Roche P. and Aubin J. E. (1999) Kinetics of osteoprogenitor proliferation and osteoblast differentiation in vitro. *J Cell Biochem* **74,** 616-627.

Mally J., Baranyi M. and Vizi E. S. (1996) Change in the concentrations of amino acids in CSF and serum of patients with essential tremor. *J Neural Transm* **103,** 555-560.

Mandal M. and Kumar R. (1996) Bcl-2 expression regulates sodium butyrate-induced apoptosis in human MCF-7 breast cancer cells. *Cell Growth Differ* **7,** 311-318.

Mandal M., Wu X. and Kumar R. (1997) Bcl-2 deregulation leads to inhibition of sodium butyrate-induced apoptosis in human colorectal carcinoma cells. *Carcinogenesis* **18,** 229-232.

Mangano R. M. and Schwarcz R. (1981) The human platelet as a model for the glutamatergic neuron: platelet uptake of L-glutamate. *J Neurochem* **36,** 1067-1076.

Mann C. J., Honeyman K., McClorey G., Fletcher S. and Wilton S. D. (2002) Improved antisense oligonucleotide induced exon skipping in the mdx mouse model of muscular dystrophy. *J Gene Med* **4,** 644-654.

Maragakis N. J. and Rothstein J. D. (2004) Glutamate transporters: animal models to neurologic disease. *Neurobiol Dis* **15,** 461-473.

Maravic M., Le Bihan C., Landais P. and Fardellone P. (2005) Incidence and cost of osteoporotic fractures in France during 2001. A methodological approach by the national hospital database. *Osteoporos Int* **16,** 1475-1480.

Marcaggi P. and Attwell D. (2004) Role of glial amino acid transporters in synaptic transmission and brain energetics. *Glia* **47,** 217-225.

Marie H. and Attwell D. (1999) C-terminal interactions modulate the affinity of GLAST glutamate transporters in salamander retinal glial cells. *J Physiol* **520 Pt 2,** 393-397.

Marie H., Billups D., Bedford F. K., Dumoulin A., Goyal R. K., Longmore G. D., Moss S. J. and Attwell D. (2002) The amino terminus of the glial glutamate transporter GLT-1 interacts with the LIM protein Ajuba. *Mol Cell Neurosci* **19,** 152-164.

Marks S. C., Jr. (1984) Congenital osteopetrotic mutations as probes of the origin, structure, and function of osteoclasts. *Clin Orthop Relat Res*, 239-263.

Martin T. J. and Sims N. A. (2005) Osteoclast-derived activity in the coupling of bone formation to resorption. *Trends Mol Med* **11,** 76-81.

Martinez-Lopez I., Garcia C., Barber T., Vina J. R. and Miralles V. J. (1998) The L-glutamate transporters GLAST (EAAT1) and GLT-1 (EAAT2): expression and regulation in rat lactating mammary gland. *Mol Membr Biol* **15,** 237-242.

Marx R. E. (2003) Pamidronate (Aredia) and zoledronate (Zometa) induced avascular necrosis of the jaws: a growing epidemic. *J Oral Maxillofac Surg* **61,** 1115-1117.

Marx R. E., Sawatari Y., Fortin M. and Broumand V. (2005) Bisphosphonate-induced exposed bone (osteonecrosis/osteopetrosis) of the jaws: risk factors, recognition, prevention, and treatment. *J Oral Maxillofac Surg* **63,** 1567-1575.

Mary S., Gomeza J., Prezeau L., Bockaert J. and Pin J. P. (1998) A cluster of basic residues in the carboxyl-terminal tail of the short metabotropic glutamate receptor 1 variants impairs their coupling to phospholipase C. *J Biol Chem* **273,** 425-432.

Mason D. J. (2004a) Glutamate signalling and its potential application to tissue engineering of bone. *Eur Cell Mater* **7,** 12-25; discussion 25-16.

Mason D. J. (2004b) The role of glutamate transporters in bone cell signalling. *J Musculoskelet Neuronal Interact* **4,** 128-131.

Mason D. J. and Huggett J. F. (2002) Glutamate transporters in bone. *J Musculoskelet Neuronal Interact* **2,** 406-414.

Mason D. J., Dillingham C. M., Evans B. A., Brakspear K. and Ralphs J. R. (2008) A 3D culture system to investigate osteocyte control of osteoblasts. *Bone* **42,** 23.

Mason D. J., Suva L. J., Genever P. G., Patton A. J., Steuckle S., Hillam R. A. and Skerry T. M. (1997) Mechanically regulated expression of a neural glutamate transporter in bone: a role for excitatory amino acids as osteotropic agents? *Bone* **20,** 199-205.

Masu M., Tanabe Y., Tsuchida K., Shigemoto R. and Nakanishi S. (1991) Sequence and expression of a metabotropic glutamate receptor. *Nature* **349,** 760-765.

Matsumoto Y., Enomoto T. and Masuko T. (1999) Identification of truncated human glutamate transporter. *Tohoku J Exp Med* **187,** 173-182.

Matthews J. C., Beveridge M. J., Malandro M. S., Rothstein J. D., Campbell-Thompson M., Verlander J. W., Kilberg M. S. and Novak D. A. (1998) Activity and protein localization of multiple glutamate transporters in gestation day 14 vs. day 20 rat placenta. *Am J Physiol* **274,** C603-614.

Mawatari K., Yasui Y., Sugitani K., Takadera T. and Kato S. (1996) Reactive oxygen species involved in the glutamate toxicity of C6 glioma cells via xc antiporter system. *Neuroscience* **73,** 201-208.

Mayeda A., Hayase Y., Inoue H., Ohtsuka E. and Ohshima Y. (1990) Surveying cis-acting sequences of pre-mRNA by adding antisense 2'-O-methyl oligoribonucleotides to a splicing reaction. *J Biochem* **108,** 399-405.

McClung M. R. (2006) Inhibition of RANKL as a treatment for osteoporosis: preclinical and early clinical studies. *Curr Osteoporos Rep* **4,** 28-33.

McCullumsmith R. E. and Meador-Woodruff J. H. (2002) Striatal excitatory amino acid transporter transcript expression in schizophrenia, bipolar disorder, and major depressive disorder. *Neuropsychopharmacology* **26,** 368-375.

McNearney T., Speegle D., Lawand N., Lisse J. and Westlund K. N. (2000) Excitatory amino acid profiles of synovial fluid from patients with arthritis. *J Rheumatol* **27,** 739-745.

McNearney T., Baethge B. A., Cao S., Alam R., Lisse J. R. and Westlund K. N. (2004) Excitatory amino acids, TNF-alpha, and chemokine levels in synovial fluids of patients with active arthropathies. *Clin Exp Immunol* **137,** 621-627.

McNearney T. A., Ma Y., Chen Y., Taglialatela G., Yin H., Zhang W. R. and Westlund K. N. (2009) A peripheral neuroimmune link: glutamate agonists upregulate NMDA NR1 receptor mRNA and protein, vimentin, TNF-alpha, and RANTES in cultured human synoviocytes. *Am J Physiol Regul Integr Comp Physiol* **298,** R584-598.

Megas P. (2005) Classification of non-union. *Injury* **36 Suppl 4,** S30-37.

Meister A. (1983) Transport and metabolism of glutathione and gamma-glutamyl amino acids. *Biochem Soc Trans* **11,** 793-794.

Meldrum B. S. (1994) The role of glutamate in epilepsy and other CNS disorders. *Neurology* **44,** S14-23.

Meldrum B. S., Akbar M. T. and Chapman A. G. (1999) Glutamate receptors and transporters in genetic and acquired models of epilepsy. *Epilepsy Res* **36,** 189-204.

Menniti F. S., Pagnozzi M. J., Butler P., Chenard B. L., Jaw-Tsai S. S. and Frost White W. (2000a) CP-101,606, an NR2B subunit selective NMDA receptor antagonist, inhibits NMDA and injury induced c-fos expression and cortical spreading depression in rodents. *Neuropharmacology* **39,** 1147-1155.

Menniti F. S., Chenard B. L., Collins M. B., Ducat M. F., Elliott M. L., Ewing F. E., Huang J. I., Kelly K. A., Lazzaro J. T., Pagnozzi M. J., Weeks J. L., Welch W. M. and White W. F. (2000b) Characterization of the binding site for a novel class of noncompetitive alpha-amino-3-hydroxy-5-methyl-4-isoxazolepropionic acid receptor antagonists. *Mol Pharmacol* **58,** 1310-1317.

Mentaverri R., Kamel S., Wattel A., Prouillet C., Sevenet N., Petit J. P., Tordjmann T. and Brazier M. (2003) Regulation of bone resorption and osteoclast survival by nitric oxide: possible involvement of NMDA-receptor. *J Cell Biochem* **88,** 1145-1156.

Menton D. N., Simmons D. J., Chang S. L. and Orr B. Y. (1984) From bone lining cell to osteocyte--an SEM study. *Anat Rec* **209,** 29-39.

Merle B., Itzstein C., Delmas P. D. and Chenu C. (2003) NMDA glutamate receptors are expressed by osteoclast precursors and involved in the regulation of osteoclastogenesis. *J Cell Biochem* **90,** 424-436.

Merriman H. L., van Wijnen A. J., Hiebert S., Bidwell J. P., Fey E., Lian J., Stein J. and Stein G. S. (1995) The tissue-specific nuclear matrix protein, NMP-2, is a member of the AML/CBF/PEBP2/runt domain transcription factor family: interactions with the osteocalcin gene promoter. *Biochemistry* **34,** 13125-13132.

Merry K., Dodds R., Littlewood A. and Gowen M. (1993) Expression of osteopontin mRNA by osteoclasts and osteoblasts in modelling adult human bone. *J Cell Sci* **104 (Pt 4),** 1013-1020.

Meyer T., Munch C., Knappenberger B., Liebau S., Volkel H. and Ludolph A. C. (1998) Alternative splicing of the glutamate transporter EAAT2 (GLT-1). *Neurosci Lett* **241,** 68-70.

Meyer T., Fromm A., Munch C., Schwalenstocker B., Fray A. E., Ince P. G., Stamm S., Gron G., Ludolph A. C. and Shaw P. J. (1999) The RNA of the glutamate transporter EAAT2 is variably spliced in amyotrophic lateral sclerosis and normal individuals. *J Neurol Sci* **170,** 45-50.

Miller P. D., Bolognese M. A., Lewiecki E. M., McClung M. R., Ding B., Austin M., Liu Y., San Martin J. and Amg Bone Loss Study G. (2008) Effect of denosumab on bone density and turnover in postmenopausal women with low bone mass after long-term continued, discontinued, and restarting of therapy: a randomized blinded phase 2 clinical trial. *Bone* **43,** 222-229.

Miller S. C., de Saint-Georges L., Bowman B. M. and Jee W. S. (1989) Bone lining cells: structure and function. *Scanning Microsc* **3,** 953-960; discussion 960-961.

Miller S. C., and Jee, W. S. S. (1992) Bone lining cells, in *Bone: bone metabolism and mineralization*, Vol. 4 (Hall B. K., ed.), pp 1-19, Boca Raton, FL.

Mitrovic A. D., Amara S. G., Johnston G. A. and Vandenberg R. J. (1998) Identification of functional domains of the human glutamate transporters EAAT1 and EAAT2. *J Biol Chem* **273,** 14698-14706.

Mizuno M., Imai T., Fujisawa R., Tani H. and Kuboki Y. (2000) Bone sialoprotein (BSP) is a crucial factor for the expression of osteoblastic phenotypes of bone marrow cells cultured on type I collagen matrix. *Calcif Tissue Int* **66,** 388-396.

Monaghan D. T., Bridges R. J. and Cotman C. W. (1989) The excitatory amino acid receptors: their classes, pharmacology, and distinct properties in the function of the central nervous system. *Annu Rev Pharmacol Toxicol* **29,** 365-402.

Morimoto R., Uehara S., Yatsushiro S., Juge N., Hua Z., Senoh S., Echigo N., Hayashi M., Mizoguchi T., Ninomiya T., Udagawa N., Omote H., Yamamoto A., Edwards R. H. and Moriyama Y. (2006) Secretion of L-glutamate from osteoclasts through transcytosis. *Embo J* **25,** 4175-4186.

Moss D. W., Eaton R. H., Smith J. K. and Whitby L. G. (1967) Association of inorganic-pyrophosphatase activity with human alkaline-phosphatase preparations. *Biochem J* **102,** 53-57.

Muir K. W. (2006) Glutamate-based therapeutic approaches: clinical trials with NMDA antagonists. *Curr Opin Pharmacol* **6,** 53-60.

Muir K. W. and Lees K. R. (1995) Clinical experience with excitatory amino acid antagonist drugs. *Stroke* **26,** 503-513.

Mulari M. T., Zhao H., Lakkakorpi P. T. and Vaananen H. K. (2003) Osteoclast ruffled border has distinct subdomains for secretion and degraded matrix uptake. *Traffic* **4,** 113-125.

Mullender M. G. and Huiskes R. (1995) Proposal for the regulatory mechanism of Wolff's law. *J Orthop Res* **13,** 503-512.

Munch C., Penndorf A., Schwalenstocker B., Troost D., Ludolph A. C., Ince P. and Meyer T. (2001) Impaired RNA splicing of 5'-regulatory sequences of the astroglial glutamate transporter EAAT2 in human astrocytoma. *J Neurol Neurosurg Psychiatry* **71,** 675-678.

Munch C., Ebstein M., Seefried U., Zhu B., Stamm S., Landwehrmeyer G. B., Ludolph A. C., Schwalenstocker B. and Meyer T. (2002) Alternative splicing of the 5'-sequences of the mouse EAAT2 glutamate transporter and expression in a transgenic model for amyotrophic lateral sclerosis. *J Neurochem* **82,** 594-603.

Munch C., Zhu B. G., Leven A., Stamm S., Einkorn H., Schwalenstocker B., Ludolph A. C., Riepe M. W. and Meyer T. (2003) Differential regulation of 5' splice variants of the glutamate transporter EAAT2 in an in vivo model of chemical hypoxia induced by 3-nitropropionic acid. *J Neurosci Res* **71,** 819-825.

Mundy G. R. (1999) *Bone Remodelling and its Disorders*. Martin Dunitz Ltd, London.

Mundy G. R., Chen D., Zhao M., Dallas S., Xu C. and Harris S. (2001) Growth regulatory factors and bone. *Rev Endocr Metab Disord* **2,** 105-115.

Munir M., Correale D. M. and Robinson M. B. (2000) Substrate-induced up-regulation of Na(+)-dependent glutamate transport activity. *Neurochem Int* **37,** 147-162.

Murata K., Mitsuoka K., Hirai T., Walz T., Agre P., Heymann J. B., Engel A. and Fujiyoshi Y. (2000) Structural determinants of water permeation through aquaporin-1. *Nature* **407,** 599-605.

Murphy T. H., Miyamoto M., Sastre A., Schnaar R. L. and Coyle J. T. (1989) Glutamate toxicity in a neuronal cell line involves inhibition of cystine transport leading to oxidative stress. *Neuron* **2,** 1547-1558.

Nagai M., Abe K., Okamoto K. and Itoyama Y. (1998) Identification of alternative splicing forms of GLT-1 mRNA in the spinal cord of amyotrophic lateral sclerosis patients. *Neurosci Lett* **244,** 165-168.

Nakagawa N., Kinosaki M., Yamaguchi K., Shima N., Yasuda H., Yano K., Morinaga T. and Higashio K. (1998) RANK is the essential signaling receptor for osteoclast differentiation factor in osteoclastogenesis. *Biochem Biophys Res Commun* **253,** 395-400.

Nakamura H. (2007) Morphology, Function, and Differentiation of Bone Cells. *J. Hard Tissue Biology* **16,** 15-22.

Nakanishi O., Ishikawa T. and Imamura Y. (1999) Modulation of formalin-evoked hyperalgesia by intrathecal N-type Ca channel and protein kinase C inhibitor in the rat. *Cell Mol Neurobiol* **19,** 191-197.

Nakashima K., Zhou X., Kunkel G., Zhang Z., Deng J. M., Behringer R. R. and de Crombrugghe B. (2002) The novel zinc finger-containing transcription factor osterix is required for osteoblast differentiation and bone formation. *Cell* **108,** 17-29.

Nakayama T., Kawakami H., Tanaka K. and Nakamura S. (1996) Expression of three glutamate transporter subtype mRNAs in human brain regions and peripheral tissues. *Brain Res Mol Brain Res* **36,** 189-192.

Nampei A., Hashimoto J., Hayashida K., Tsuboi H., Shi K., Tsuji I., Miyashita H., Yamada T., Matsukawa N., Matsumoto M., Morimoto S., Ogihara T., Ochi T. and Yoshikawa H. (2004) Matrix extracellular phosphoglycoprotein (MEPE) is highly expressed in osteocytes in human bone. *J Bone Miner Metab* **22,** 176-184.

Neer R. M., Arnaud C. D., Zanchetta J. R., Prince R., Gaich G. A., Reginster J. Y., Hodsman A. B., Eriksen E. F., Ish-Shalom S., Genant H. K., Wang O. and Mitlak B. H. (2001) Effect of parathyroid hormone (1-34) on fractures and bone mineral density in postmenopausal women with osteoporosis. *N Engl J Med* **344,** 1434-1441.

Nicholls D. and Attwell D. (1990) The release and uptake of excitatory amino acids. *Trends Pharmacol Sci* **11,** 462-468.

Noble B. S., Stevens H., Loveridge N. and Reeve J. (1997) Identification of apoptotic changes in osteocytes in normal and pathological human bone. *Bone* **20,** 273-282.

Noble B. S., Peet N., Stevens H. Y., Brabbs A., Mosley J. R., Reilly G. C., Reeve J., Skerry T. M. and Lanyon L. E. (2003) Mechanical loading: biphasic osteocyte survival and targeting of osteoclasts for bone destruction in rat cortical bone. *Am J Physiol Cell Physiol* **284,** C934-943.

O'Shea R. D. (2002) Roles and regulation of glutamate transporters in the central nervous system. *Clin Exp Pharmacol Physiol* **29,** 1018-1023.

O'Shea R. D., Fodera M. V., Aprico K., Dehnes Y., Danbolt N. C., Crawford D. and Beart P. M. (2002) Evaluation of drugs acting at glutamate transporters in organotypic hippocampal cultures: new evidence on substrates and blockers in excitotoxicity. *Neurochem Res* **27,** 5-13.

Obrenovitch T. P., Urenjak J., Zilkha E. and Jay T. M. (2000) Excitotoxicity in neurological disorders--the glutamate paradox. *Int J Dev Neurosci* **18,** 281-287.

Oishi K. and Yamaguchi M. (1994) Effect of phorbol 12-myristate 13-acetate on Ca2+-ATPase activity in rat liver nuclei. *J Cell Biochem* **55,** 168-172.

Oldberg A., Franzen A. and Heinegard D. (1986) Cloning and sequence analysis of rat bone sialoprotein (osteopontin) cDNA reveals an Arg-Gly-Asp cell-binding sequence. *Proc Natl Acad Sci U S A* **83,** 8819-8823.

Olkku A. and Mahonen A. (2008) Wnt and steroid pathways control glutamate signalling by regulating glutamine synthetase activity in osteoblastic cells. *Bone* **43,** 483-493.

Olsen B. R., Reginato A. M. and Wang W. (2000) Bone development. *Annu Rev Cell Dev Biol* **16,** 191-220.

Ominsky M. S., Vlasseros F., Jolette J., Smith S. Y., Stouch B., Doellgast G., Gong J., Gao Y., Cao J., Graham K., Tipton B., Cai J., Deshpande R., Zhou L., Hale M. D., Lightwood D. J., Henry A. J., Popplewell A. G., Moore A. R., Robinson M. K., Lacey D. L., Simonet W. S. and Paszty C. (2010) Two doses of sclerostin antibody in cynomolgus monkeys increases bone formation, bone mineral density, and bone strength. *J Bone Miner Res* **25,** 948-959.

Ominsky M. S., Warmongton, K.S., Asuncion, F.J., Tan, H.L., Grisanti, M.S., Geng, Z., Stephens, P., Henry, A., Lawson, A., Lightwood, D., Perkins, V., Kirby, P., Moore, A., Popplewell, A., Robinson, M., Li, X., Kostenuik, PJ., Simonet, W.S., Lacey, D.L., Paszty, C. (2006) Sclerostin monoclonal antibody treatment increases bone strength in osteopenic ovariectomized rats. *J. Bone Miner. Res.* **21.**

Otis T. S. and Jahr C. E. (1998) Anion currents and predicted glutamate flux through a neuronal glutamate transporter. *J Neurosci* **18,** 7099-7110.

Owen M. and Friedenstein A. J. (1988) Stromal stem cells: marrow-derived osteogenic precursors. *Ciba Found Symp* **136,** 42-60.

Pack E. P. (2001) Bone structure, in *Anatomy and Physiology*, pp 61-63. Wiley Publishing Inc., Hoboken, NJ.

Padhi D., Stouch, B., Jang, G. (2007) Anti-sclerostin antibody increases markers of bone formation in healthy postmenopausal women [abstract]. *J. Bone Miner. Res.* **22(Suppl. 1)**.

Pajak B., Orzechowski A. and Gajkowska B. (2007) Molecular basis of sodium butyrate-dependent proapoptotic activity in cancer cells. *Adv Med Sci* **52,** 83-88.

Palumbo C., Palazzini S. and Marotti G. (1990) Morphological study of intercellular junctions during osteocyte differentiation. *Bone* **11,** 401-406.

Pampena D. A., Robertson K. A., Litvinova O., Lajoie G., Goldberg H. A. and Hunter G. K. (2004) Inhibition of hydroxyapatite formation by osteopontin phosphopeptides. *Biochem J* **378,** 1083-1087.

Papapoulos S. E. and Cremers S. C. (2007) Prolonged bisphosphonate release after treatment in children. *N Engl J Med* **356,** 1075-1076.

Parada-Turska J., Rzeski W., Majdan M., Kandefer-Szerszen M. and Turski W. A. (2006) Effect of glutamate receptor antagonists and antirheumatic drugs on proliferation of synoviocytes in vitro. *Eur J Pharmacol* **535,** 95-97.

Pardridge W. M. (2003) Blood-brain barrier drug targeting: the future of brain drug development. *Mol Interv* **3,** 90-105, 151.

Parfitt A. M. (1977) The cellular basis of bone turnover and bone loss: a rebuttal of the osteocytic resorption--bone flow theory. *Clin Orthop Relat Res*, 236-247.

Parfitt A. M. (1983) The physiologic and clinical significance of bone histomorphometric data, in *Bone histomorphometry: techniques and interpretation* (Recker R. R., ed.), pp 143-223. CRC Press Inc, Boca Raton, FL.

Parfitt A. M. (1987) Bone remodeling and bone loss: understanding the pathophysiology of osteoporosis. *Clin Obstet Gynecol* **30,** 789-811.

Parfitt A. M. (1994) Osteonal and hemi-osteonal remodeling: the spatial and temporal framework for signal traffic in adult human bone. *J Cell Biochem* **55,** 273-286.

Parfitt A. M. (2000) The mechanism of coupling: a role for the vasculature. *Bone* **26,** 319-323.

Park H. R., Jung W. W., Bacchini P., Bertoni F., Kim Y. W. and Park Y. K. (2006) Ezrin in osteosarcoma: comparison between conventional high-grade and central low-grade osteosarcoma. *Pathol Res Pract* **202,** 509-515.

Patel M. S. and Elefteriou F. (2007) The new field of neuroskeletal biology. *Calcif Tissue Int* **80,** 337-347.

Patton A. J., Genever P. G., Birch M. A., Suva L. J. and Skerry T. M. (1998) Expression of an N-methyl-D-aspartate-type receptor by human and rat osteoblasts and osteoclasts suggests a novel glutamate signaling pathway in bone. *Bone* **22,** 645-649.

Pautke C., Schieker M., Tischer T., Kolk A., Neth P., Mutschler W. and Milz S. (2004) Characterization of osteosarcoma cell lines MG-63, Saos-2 and U-2 OS in comparison to human osteoblasts. *Anticancer Res* **24,** 3743-3748.

Pead M. J., Skerry T. M. and Lanyon L. E. (1988) Direct transformation from quiescence to bone formation in the adult periosteum following a single brief period of bone loading. *J Bone Miner Res* **3,** 647-656.

Peet N. M., Grabowski P. S., Laketic-Ljubojevic I. and Skerry T. M. (1999) The glutamate receptor antagonist MK801 modulates bone resorption in vitro by a mechanism predominantly involving osteoclast differentiation. *Faseb J* **13,** 2179-2185.

Pekny M. and Nilsson M. (2005) Astrocyte activation and reactive gliosis. *Glia* **50,** 427-434.

Perez J. L., Khatri L., Chang C., Srivastava S., Osten P. and Ziff E. B. (2001) PICK1 targets activated protein kinase Calpha to AMPA receptor clusters in spines of hippocampal neurons and reduces surface levels of the AMPA-type glutamate receptor subunit 2. *J Neurosci* **21,** 5417-5428.

Persson M., Brantefjord M., Hansson E. and Ronnback L. (2005) Lipopolysaccharide increases microglial GLT-1 expression and glutamate uptake capacity in vitro by a mechanism dependent on TNF-alpha. *Glia* **51,** 111-120.

Phieffer L. S. and Goulet J. A. (2006) Delayed unions of the tibia. *J Bone Joint Surg Am* **88,** 206-216.

Piekarski K. and Munro M. (1977) Transport mechanism operating between blood supply and osteocytes in long bones. *Nature* **269,** 80-82.

Piepoli T., Mennuni L., Zerbi S., Lanza M., Rovati L. C. and Caselli G. (2009) Glutamate signaling in chondrocytes and the potential involvement of NMDA receptors in cell proliferation and inflammatory gene expression. *Osteoarthritis Cartilage* **17,** 1076-1083.

Pin J. P. and Duvoisin R. (1995) The metabotropic glutamate receptors: structure and functions. *Neuropharmacology* **34,** 1-26.

Pin J. P., Waeber C., Prezeau L., Bockaert J. and Heinemann S. F. (1992) Alternative splicing generates metabotropic glutamate receptors inducing different patterns of calcium release in Xenopus oocytes. *Proc Natl Acad Sci U S A* **89,** 10331-10335.

Pines G., Zhang Y. and Kanner B. I. (1995) Glutamate 404 is involved in the substrate discrimination of GLT-1, a (Na+ + K+)-coupled glutamate transporter from rat brain. *J Biol Chem* **270,** 17093-17097.

Pines G., Danbolt N. C., Bjoras M., Zhang Y., Bendahan A., Eide L., Koepsell H., Storm-Mathisen J., Seeberg E. and Kanner B. I. (1992) Cloning and expression of a rat brain L-glutamate transporter. *Nature* **360,** 464-467.

Pitsillides A. A., Rawlinson S. C., Suswillo R. F., Bourrin S., Zaman G. and Lanyon L. E. (1995) Mechanical strain-induced NO production by bone cells: a possible role in adaptive bone (re)modeling? *FASEB J* **9,** 1614-1622.

Plaitakis A., Berl S. and Yahr M. D. (1982) Abnormal glutamate metabolism in an adult-onset degenerative neurological disorder. *Science* **216,** 193-196.

Poole K. E., van Bezooijen R. L., Loveridge N., Hamersma H., Papapoulos S. E., Lowik C. W. and Reeve J. (2005) Sclerostin is a delayed secreted product of osteocytes that inhibits bone formation. *FASEB J* **19,** 1842-1844.

Pow D. V. (2008) Detection of a biomarker of aberrant cells of neuroectodermal origin in a body fluid, G01N 33/53 (2006.01) Edition, AU.

Pow D. V. and Barnett N. L. (1999) Changing patterns of spatial buffering of glutamate in developing rat retinae are mediated by the Muller cell glutamate transporter GLAST. *Cell Tissue Res* **297,** 57-66.

Price P. A., Parthemore J. G. and Deftos L. J. (1980) New biochemical marker for bone metabolism. Measurement by radioimmunoassay of bone GLA protein in the plasma of normal subjects and patients with bone disease. *J Clin Invest* **66,** 878-883.

Price V. H. (2003) Therapy of alopecia areata: on the cusp and in the future. *J Investig Dermatol Symp Proc* **8,** 207-211.

Prockop D. J. (1997) Marrow stromal cells as stem cells for nonhematopoietic tissues. *Science* **276,** 71-74.

PRODIGY (2006) Osteoporosis.

Purdue P. E., Koulouvaris P., Potter H. G., Nestor B. J. and Sculco T. P. (2007) The cellular and molecular biology of periprosthetic osteolysis. *Clin Orthop Relat Res* **454,** 251-261.

Putchler H., Meloan, S., and Terry, M. S. (1969) On the history and mechanism of alizarin and alizarin red S stains for calcium. *J. Histochem. Cytochem* **17,** 110-124.

Raisz L. G. (1997) The osteoporosis revolution. *Ann Intern Med* **126,** 458-462.

Raisz L. G. (1999) Physiology and pathophysiology of bone remodeling. *Clin Chem* **45,** 1353-1358.

Raisz L. G. (2005) Pathogenesis of osteoporosis: concepts, conflicts, and prospects. *J Clin Invest* **115,** 3318-3325.

Ralphe J. C., Segar J. L., Schutte B. C. and Scholz T. D. (2004) Localization and function of the brain excitatory amino acid transporter type 1 in cardiac mitochondria. *J Mol Cell Cardiol* **37,** 33-41.

Rantakokko J., Uusitalo H., Jamsa T., Tuukkanen J., Aro H. T. and Vuorio E. (1999) Expression profiles of mRNAs for osteoblast and osteoclast proteins as indicators of bone loss in mouse immobilization osteopenia model. *J Bone Miner Res* **14,** 1934-1942.

Rauen T. and Kanner B. I. (1994) Localization of the glutamate transporter GLT-1 in rat and macaque monkey retinae. *Neurosci Lett* **169,** 137-140.

Rauen T., Rothstein J. D. and Wassle H. (1996) Differential expression of three glutamate transporter subtypes in the rat retina. *Cell Tissue Res* **286,** 325-336.

Rauen T., Wiessner M., Sullivan R., Lee A. and Pow D. V. (2004) A new GLT1 splice variant: cloning and immunolocalization of GLT1c in the mammalian retina and brain. *Neurochem Int* **45,** 1095-1106.

Rawlinson S. C., Mosley J. R., Suswillo R. F., Pitsillides A. A. and Lanyon L. E. (1995) Calvarial and limb bone cells in organ and monolayer culture do not show the same early responses to dynamic mechanical strain. *J Bone Miner Res* **10,** 1225-1232.

Re D. B., Boucraut J., Samuel D., Birman S., Kerkerian-Le Goff L. and Had-Aissouni L. (2003) Glutamate transport alteration triggers differentiation-state selective oxidative death of cultured astrocytes: a mechanism different from excitotoxicity depending on intracellular GSH contents. *J Neurochem* **85,** 1159-1170.

Re D. B., Nafia I., Melon C., Shimamoto K., Kerkerian-Le Goff L. and Had-Aissouni L. (2006) Glutamate leakage from a compartmentalized intracellular metabolic pool and activation of the lipoxygenase pathway mediate oxidative astrocyte death by reversed glutamate transport. *Glia* **54,** 47-57.

Reichelt W., Stabel-Burow J., Pannicke T., Weichert H. and Heinemann U. (1997) The glutathione level of retinal Muller glial cells is dependent on the high-affinity sodium-dependent uptake of glutamate. *Neuroscience* **77,** 1213-1224.

Reye P., Sullivan R., Fletcher E. L. and Pow D. V. (2002) Distribution of two splice variants of the glutamate transporter GLT1 in the retinas of humans, monkeys, rabbits, rats, cats, and chickens. *J Comp Neurol* **445,** 1-12.

Reynolds I. J. and Miller R. J. (1988) [3H]MK801 binding to the N-methyl-D-aspartate receptor reveals drug interactions with the zinc and magnesium binding sites. *J Pharmacol Exp Ther* **247,** 1025-1031.

Rezende A. A., Pizauro J. M., Ciancaglini P. and Leone F. A. (1994) Phosphodiesterase activity is a novel property of alkaline phosphatase from osseous plate. *Biochem J* **301 (Pt 2),** 517-522.

Riedel G., Platt B. and Micheau J. (2003) Glutamate receptor function in learning and memory. *Behav Brain Res* **140,** 1-47.

Riggs B. L., Khosla S. and Melton L. J., 3rd (1998) A unitary model for involutional osteoporosis: estrogen deficiency causes both type I and type II osteoporosis in postmenopausal women and contributes to bone loss in aging men. *J Bone Miner Res* **13,** 763-773.

Riggs B. L., Wahner H. W., Melton L. J., 3rd, Richelson L. S., Judd H. L. and Offord K. P. (1986) Rates of bone loss in the appendicular and axial skeletons of women. Evidence of substantial vertebral bone loss before menopause. *J Clin Invest* **77,** 1487-1491.

Roach H. I. and Shearer J. R. (1989) Cartilage resorption and endochondral bone formation during the development of long bones in chick embryos. *Bone Miner* **6,** 289-309.

Robey P. G., Young M. F., Fisher L. W. and McClain T. D. (1989) Thrombospondin is an osteoblast-derived component of mineralized extracellular matrix. *J Cell Biol* **108,** 719-727.

Robinson M. B., Hunter-Ensor M. and Sinor J. (1991) Pharmacologically distinct sodium-dependent L-[3H]glutamate transport processes in rat brain. *Brain Res* **544,** 196-202.

Robinson M. B., Sinor J. D., Dowd L. A. and Kerwin J. F., Jr. (1993) Subtypes of sodium-dependent high-affinity L-[3H]glutamate transport activity: pharmacologic specificity and regulation by sodium and potassium. *J Neurochem* **60,** 167-179.

Robison R. (1923) The possible significance of hexosephosphoric esters in ossification. *Biochem. J.* **17,** 286-293.

Robling A. G., Bellido T. and Turner C. H. (2006) Mechanical stimulation in vivo reduces osteocyte expression of sclerostin. *J Musculoskelet Neuronal Interact* **6,** 354.

Robling A. G., Hinant F. M., Burr D. B. and Turner C. H. (2002) Improved bone structure and strength after long-term mechanical loading is greatest if loading is separated into short bouts. *J Bone Miner Res* **17,** 1545-1554.

Rodan G. A. (1997) Bone mass homeostasis and bisphosphonate action. *Bone* **20,** 1-4.

Rosas S., Vargas M. A., Lopez-Bayghen E. and Ortega A. (2007) Glutamate-dependent transcriptional regulation of GLAST/EAAT1: a role for YY1. *J Neurochem* **101,** 1134-1144.

Rose T., Peng H., Shen H. C., Usas A., Kuroda R., Lill H., Fu F. H. and Huard J. (2003) The role of cell type in bone healing mediated by ex vivo gene therapy. *Langenbecks Arch Surg* **388,** 347-355.

Rosen C. J. and Bilezikian J. P. (2001) Clinical review 123: Anabolic therapy for osteoporosis. *J Clin Endocrinol Metab* **86,** 957-964.

Rossi D. J., Oshima T. and Attwell D. (2000) Glutamate release in severe brain ischaemia is mainly by reversed uptake. *Nature* **403,** 316-321.

Rothbard J. B., Garlington S., Lin Q., Kirschberg T., Kreider E., McGrane P. L., Wender P. A. and Khavari P. A. (2000) Conjugation of arginine oligomers to cyclosporin A facilitates topical delivery and inhibition of inflammation. *Nat Med* **6,** 1253-1257.

Rothstein J. D., Van Kammen M., Levey A. I., Martin L. J. and Kuncl R. W. (1995) Selective loss of glial glutamate transporter GLT-1 in amyotrophic lateral sclerosis. *Ann Neurol* **38,** 73-84.

Rothstein J. D., Martin L., Levey A. I., Dykes-Hoberg M., Jin L., Wu D., Nash N. and Kuncl R. W. (1994) Localization of neuronal and glial glutamate transporters. *Neuron* **13,** 713-725.

Rothstein J. D., Dykes-Hoberg M., Pardo C. A., Bristol L. A., Jin L., Kuncl R. W., Kanai Y., Hediger M. A., Wang Y., Schielke J. P. and Welty D. F. (1996) Knockout of glutamate transporters reveals a major role for astroglial transport in excitotoxicity and clearance of glutamate. *Neuron* **16,** 675-686.

Rothstein J. D., Patel S., Regan M. R., Haenggeli C., Huang Y. H., Bergles D. E., Jin L., Dykes Hoberg M., Vidensky S., Chung D. S., Toan S. V., Bruijn L. I., Su Z. Z., Gupta P. and Fisher P. B. (2005) Beta-lactam antibiotics offer neuroprotection by increasing glutamate transporter expression. *Nature* **433,** 73-77.

Rouleau M. F., Warshawsky H., Marks S. C., Jr. and Goltzman D. (1986) Calcitonin receptor binding as a marker of osteoclast heterogeneity in osteopetrotic rodents. *J Bone Miner Res* **1,** 543-553.

Rozyczka J. and Engele J. (2005) Multiple 5'-splice variants of the rat glutamate transporter-1. *Brain Res Mol Brain Res* **133,** 157-161.

Rubin C. T. and Lanyon L. E. (1984) Regulation of bone formation by applied dynamic loads. *J Bone Joint Surg Am* **66,** 397-402.

Rubin J., Murphy T. C., Zhu L., Roy E., Nanes M. S. and Fan X. (2003) Mechanical strain differentially regulates endothelial nitric-oxide synthase and receptor activator of nuclear kappa B ligand expression via ERK1/2 MAPK. *J Biol Chem* **278,** 34018-34025.

Rubin M. R. and Bilezikian J. P. (2003) The anabolic effects of parathyroid hormone therapy. *Clin Geriatr Med* **19,** 415-432.

Ruggiero A. M., Liu Y., Vidensky S., Maier S., Jung E., Farhan H., Robinson M. B., Sitte H. H. and Rothstein J. D. (2008) The endoplasmic reticulum exit of glutamate transporter is regulated by the inducible mammalian Yip6b/GTRAP3-18 protein. *J Biol Chem* **283,** 6175-6183.

Ruggiero S. L., Mehrotra B., Rosenberg T. J. and Engroff S. L. (2004) Osteonecrosis of the jaws associated with the use of bisphosphonates: a review of 63 cases. *J Oral Maxillofac Surg* **62,** 527-534.

Russell R. G. (2007) Bisphosphonates: mode of action and pharmacology. *Pediatrics* **119 Suppl 2,** S150-162.

Rutten S., Nolte P. A., Guit G. L., Bouman D. E. and Albers G. H. (2007) Use of low-intensity pulsed ultrasound for posttraumatic nonunions of the tibia: a review of patients treated in the Netherlands. *J Trauma* **62,** 902-908.

Ryan R. M. and Vandenberg R. J. (2002) Distinct conformational states mediate the transport and anion channel properties of the glutamate transporter EAAT-1. *J Biol Chem* **277,** 13494-13500.

Ryan R. M. and Vandenberg R. J. (2005) A channel in a transporter. *Clin Exp Pharmacol Physiol* **32,** 1-6.

Ryan R. M., Mitrovic A. D. and Vandenberg R. J. (2004) The chloride permeation pathway of a glutamate transporter and its proximity to the glutamate translocation pathway. *J Biol Chem* **279,** 20742-20751.

Rzeski W., Turski L. and Ikonomidou C. (2001) Glutamate antagonists limit tumor growth. *Proc Natl Acad Sci U S A* **98,** 6372-6377.

Rzeski W., Ikonomidou C. and Turski L. (2002) Glutamate antagonists limit tumor growth. *Biochem Pharmacol* **64,** 1195-1200.

Salter D. M., Wright M. O. and Millward-Sadler S. J. (2004) NMDA receptor expression and roles in human articular chondrocyte mechanotransduction. *Biorheology* **41,** 273-281.

Samuels A., Perry M. J. and Tobias J. H. (1999a) High-dose estrogen induces de novo medullary bone formation in female mice. *J Bone Miner Res* **14,** 178-186.

Samuels A., Perry M. J. and Tobias J. H. (1999b) High-dose estrogen-induced osteogenesis in the mouse is partially suppressed by indomethacin. *Bone* **25,** 675-680.

Samuels A., Perry M. J., Gibson R. L., Colley S. and Tobias J. H. (2001) Role of endothelial nitric oxide synthase in estrogen-induced osteogenesis. *Bone* **29,** 24-29.

Sanders J. L. and Stern P. H. (1996) Expression and phorbol ester-induced down-regulation of protein kinase C isozymes in osteoblasts. *J Bone Miner Res* **11,** 1862-1872.

Sands H., Gorey-Feret L. J., Cocuzza A. J., Hobbs F. W., Chidester D. and Trainor G. L. (1994) Biodistribution and metabolism of internally 3H-labeled oligonucleotides. I. Comparison of a phosphodiester and a phosphorothioate. *Mol Pharmacol* **45,** 932-943.

Sarantis M., Ballerini L., Miller B., Silver R. A., Edwards M. and Attwell D. (1993) Glutamate uptake from the synaptic cleft does not shape the decay of the non-NMDA component of the synaptic current. *Neuron* **11,** 541-549.

Sato H., Tamba M., Ishii T. and Bannai S. (1999) Cloning and expression of a plasma membrane cystine/glutamate exchange transporter composed of two distinct proteins. *J Biol Chem* **274,** 11455-11458.

Sato K., Adams R., Betz H. and Schloss P. (1995) Modulation of a recombinant glycine transporter (GLYT1b) by activation of protein kinase C. *J Neurochem* **65,** 1967-1973.

Sato M., Westmore M., Ma Y. L., Schmidt A., Zeng Q. Q., Glass E. V., Vahle J., Brommage R., Jerome C. P. and Turner C. H. (2004) Teriparatide [PTH(1-34)] strengthens the proximal femur of ovariectomized nonhuman primates despite increasing porosity. *J Bone Miner Res* **19,** 623-629.

Sato S., Hanada R., Kimura A., Abe T., Matsumoto T., Iwasaki M., Inose H., Ida T., Mieda M., Takeuchi Y., Fukumoto S., Fujita T., Kato S., Kangawa K., Kojima M., Shinomiya K. and Takeda S. (2007) Central control of bone remodeling by neuromedin U. *Nat Med* **13,** 1234-1240.

Sato Y., Roman M., Tighe H., Lee D., Corr M., Nguyen M. D., Silverman G. J., Lotz M., Carson D. A. and Raz E. (1996) Immunostimulatory DNA sequences necessary for effective intradermal gene immunization. *Science* **273,** 352-354.

Schafer M. K., Varoqui H., Defamie N., Weihe E. and Erickson J. D. (2002) Molecular cloning and functional identification of mouse vesicular glutamate transporter 3 and its expression in subsets of novel excitatory neurons. *J Biol Chem* **277,** 50734-50748.

Schaffler M. B., Burr D. B. and Frederickson R. G. (1987) Morphology of the osteonal cement line in human bone. *Anat Rec* **217,** 223-228.

Schagat T. and Kopish K. (2010) Optimize Transfection of Cultured Cells. Available from: http://www.promega.com/pubs/tpub_020.htm, [Internet] accessed 2010, September 6th.

Schmitt A., Asan E., Lesch K. P. and Kugler P. (2002) A splice variant of glutamate transporter GLT1/EAAT2 expressed in neurons: cloning and localization in rat nervous system. *Neuroscience* **109,** 45-61.

Schmitt A., Zink M., Petroianu G., May B., Braus D. F. and Henn F. A. (2003) Decreased gene expression of glial and neuronal glutamate transporters after chronic antipsychotic treatment in rat brain. *Neurosci Lett* **347,** 81-84.

Schneider A., Kalikin L. M., Mattos A. C., Keller E. T., Allen M. J., Pienta K. J. and McCauley L. K. (2005) Bone turnover mediates preferential localization of prostate cancer in the skeleton. *Endocrinology* **146,** 1727-1736.

Schniepp R., Kohler K., Ladewig T., Guenther E., Henke G., Palmada M., Boehmer C., Rothstein J. D., Broer S. and Lang F. (2004) Retinal colocalization and in vitro interaction of the glutamate transporter EAAT3 and the serum- and glucocorticoid-inducible kinase SGK1 [correction]. *Invest Ophthalmol Vis Sci* **45,** 1442-1449.

Schousboe A. and Divac I. (1979) Difference in glutamate uptake in astrocytes cultured from different brain regions. *Brain Res* **177,** 407-409.

Schroeder T. M., Nair A. K., Staggs R., Lamblin A. F. and Westendorf J. J. (2007) Gene profile analysis of osteoblast genes differentially regulated by histone deacetylase inhibitors. *BMC Genomics* **8,** 362.

Scott H. A., Gebhardt F. M., Mitrovic A. D., Vandenberg R. J. and Dodd P. R. (2010) Glutamate transporter variants reduce glutamate uptake in Alzheimer's disease. *Neurobiol Aging.*

Scott H. L., Tannenberg A. E. and Dodd P. R. (1995) Variant forms of neuronal glutamate transporter sites in Alzheimer's disease cerebral cortex. *J Neurochem* **64,** 2193-2202.

Scott H. L., Pow D. V., Tannenberg A. E. and Dodd P. R. (2002) Aberrant expression of the glutamate transporter excitatory amino acid transporter 1 (EAAT1) in Alzheimer's disease. *J Neurosci* **22,** RC206.

Seal R. P. and Amara S. G. (1998) A reentrant loop domain in the glutamate carrier EAAT1 participates in substrate binding and translocation. *Neuron* **21,** 1487-1498.

Seal R. P. and Amara S. G. (1999) Excitatory amino acid transporters: a family in flux. *Annu Rev Pharmacol Toxicol* **39,** 431-456.

Seal R. P., Leighton B. H. and Amara S. G. (2000) A model for the topology of excitatory amino acid transporters determined by the extracellular accessibility of substituted cysteines. *Neuron* **25,** 695-706.

Seal R. P., Shigeri Y., Eliasof S., Leighton B. H. and Amara S. G. (2001) Sulfhydryl modification of V449C in the glutamate transporter EAAT1 abolishes substrate transport but not the substrate-gated anion conductance. *Proc Natl Acad Sci U S A* **98,** 15324-15329.

Seeburg P. H. (1996) The role of RNA editing in controlling glutamate receptor channel properties. *J Neurochem* **66,** 1-5.

Seeburg P. H., Higuchi M. and Sprengel R. (1998) RNA editing of brain glutamate receptor channels: mechanism and physiology. *Brain Res Brain Res Rev* **26,** 217-229.

Seeman E. and Delmas P. D. (2006) Bone quality--the material and structural basis of bone strength and fragility. *N Engl J Med* **354,** 2250-2261.

Semenov M., Tamai K. and He X. (2005) SOST is a ligand for LRP5/LRP6 and a Wnt signaling inhibitor. *J Biol Chem* **280,** 26770-26775.

Semenov M. V. and He X. (2006) LRP5 mutations linked to high bone mass diseases cause reduced LRP5 binding and inhibition by SOST. *J Biol Chem* **281,** 38276-38284.

Serre C. M., Farlay D., Delmas P. D. and Chenu C. (1999) Evidence for a dense and intimate innervation of the bone tissue, including glutamate-containing fibers. *Bone* **25,** 623-629.

Shapira L. and Halabi A. (2009) Behavior of two osteoblast-like cell lines cultured on machined or rough titanium surfaces. *Clin Oral Implants Res* **20,** 50-55.

Sharma M. K., Seidlitz E. P. and Singh G. (2009) Cancer cells release glutamate via the cystine/glutamate antiporter. *Biochem Biophys Res Commun* **391,** 91-95.

Shashidharan P., Huntley G. W., Meyer T., Morrison J. H. and Plaitakis A. (1994) Neuron-specific human glutamate transporter: molecular cloning, characterization and expression in human brain. *Brain Res* **662,** 245-250.

Shayakul C., Kanai Y., Lee W. S., Brown D., Rothstein J. D. and Hediger M. A. (1997) Localization of the high-affinity glutamate transporter EAAC1 in rat kidney. *Am J Physiol* **273,** F1023-1029.

Sheldon A. L. and Robinson M. B. (2007) The role of glutamate transporters in neurodegenerative diseases and potential opportunities for intervention. *Neurochem Int* **51,** 333-355.

Sherman B. E. and Chole R. A. (2000) Sympathectomy, which induces membranous bone remodeling, has no effect on endochondral long bone remodeling in vivo. *J Bone Miner Res* **15,** 1354-1360.

Shigeri Y., Seal R. P. and Shimamoto K. (2004) Molecular pharmacology of glutamate transporters, EAATs and VGLUTs. *Brain Res Brain Res Rev* **45,** 250-265.

Shigeri Y., Shimamoto K., Yasuda-Kamatani Y., Seal R. P., Yumoto N., Nakajima T. and Amara S. G. (2001) Effects of threo-beta-hydroxyaspartate derivatives on excitatory amino acid transporters (EAAT4 and EAAT5). *J Neurochem* **79,** 297-302.

Shimamoto K., Shigeri Y., Yasuda-Kamatani Y., Lebrun B., Yumoto N. and Nakajima T. (2000) Syntheses of optically pure beta-hydroxyaspartate derivatives as glutamate transporter blockers. *Bioorg Med Chem Lett* **10,** 2407-2410.

Shimamoto K., Lebrun B., Yasuda-Kamatani Y., Sakaitani M., Shigeri Y., Yumoto N. and Nakajima T. (1998) DL-threo-beta-benzyloxyaspartate, a potent blocker of excitatory amino acid transporters. *Mol Pharmacol* **53,** 195-201.

Shimizu H., Julius M. A., Giarre M., Zheng Z., Brown A. M. and Kitajewski J. (1997) Transformation by Wnt family proteins correlates with regulation of beta-catenin. *Cell Growth Differ* **8,** 1349-1358.

Shinohe A., Hashimoto K., Nakamura K., Tsujii M., Iwata Y., Tsuchiya K. J., Sekine Y., Suda S., Suzuki K., Sugihara G., Matsuzaki H., Minabe Y., Sugiyama T., Kawai M., Iyo M., Takei N. and Mori N. (2006) Increased serum levels of glutamate in adult patients with autism. *Prog Neuropsychopharmacol Biol Psychiatry* **30,** 1472-1477.

Sierakowska H., Sambade M. J., Agrawal S. and Kole R. (1996) Repair of thalassemic human beta-globin mRNA in mammalian cells by antisense oligonucleotides. *Proc Natl Acad Sci U S A* **93,** 12840-12844.

Silverman S. L. and Landesberg R. (2009) Osteonecrosis of the jaw and the role of bisphosphonates: a critical review. *Am J Med* **122,** S33-45.

Simonet W. S., Lacey D. L., Dunstan C. R., Kelley M., Chang M. S., Luthy R., Nguyen H. Q., Wooden S., Bennett L., Boone T., Shimamoto G., DeRose M., Elliott R., Colombero A., Tan H. L., Trail G., Sullivan J., Davy E., Bucay N., Renshaw-Gegg L., Hughes T. M., Hill D., Pattison W., Campbell P., Sander S., Van G., Tarpley J., Derby P., Lee R. and Boyle W. J. (1997) Osteoprotegerin: a novel secreted protein involved in the regulation of bone density. *Cell* **89,** 309-319.

Skerry T., Genever P., Taylor A., Dobson K., Mason D. and Suva L. (2001) Absence of evidence is not evidence of absence. The shortcomings of the GLAST knockout mouse. *J Bone Miner Res* **16,** 1729-1730; author reply 1731-1722.

Skerry T. M. (1997) Mechanical loading and bone: what sort of exercise is beneficial to the skeleton? *Bone* **20,** 179-181.

Skerry T. M. (2002) Neurotransmitter functions in bone remodeling. *J Musculoskelet Neuronal Interact* **2,** 281.

Skerry T. M. (2008) The role of glutamate in the regulation of bone mass and architecture. *J Musculoskelet Neuronal Interact* **8,** 166-173.

Skerry T. M. and Genever P. G. (2001) Glutamate signalling in non-neuronal tissues. *Trends Pharmacol Sci* **22,** 174-181.

Skerry T. M., Bitensky L., Chayen J. and Lanyon L. E. (1989) Early strain-related changes in enzyme activity in osteocytes following bone loading in vivo. *J Bone Miner Res* **4,** 783-788.

Slotboom D. J., Konings W. N. and Lolkema J. S. (1999) Structural features of the glutamate transporter family. *Microbiol Mol Biol Rev* **63,** 293-307.

Slotboom D. J., Konings W. N. and Lolkema J. S. (2001a) Cysteine-scanning mutagenesis reveals a highly amphipathic, pore-lining membrane-spanning helix in the glutamate transporter GltT. *J Biol Chem* **276,** 10775-10781.

Slotboom D. J., Konings W. N. and Lolkema J. S. (2001b) Glutamate transporters combine transporter- and channel-like features. *Trends Biochem Sci* **26,** 534-539.

Smith C. P., Weremowicz S., Kanai Y., Stelzner M., Morton C. C. and Hediger M. A. (1994) Assignment of the gene coding for the human high-affinity glutamate transporter EAAC1 to 9p24: potential role in dicarboxylic aminoaciduria and neurodegenerative disorders. *Genomics* **20,** 335-336.

Smith E. L. and Gilligan C. (1996) Dose-response relationship between physical loading and mechanical competence of bone. *Bone* **18,** 455-505.

Smith J. W. (1960) Collagen fibre patterns in mammalian bone. *J Anat* **94,** 329-344.

Somerman M. J., Fisher L. W., Foster R. A. and Sauk J. J. (1988) Human bone sialoprotein I and II enhance fibroblast attachment in vitro. *Calcif Tissue Int* **43,** 50-53.

Sommer B., Keinanen K., Verdoorn T. A., Wisden W., Burnashev N., Herb A., Kohler M., Takagi T., Sakmann B. and Seeburg P. H. (1990) Flip and flop: a cell-specific functional switch in glutamate-operated channels of the CNS. *Science* **249,** 1580-1585.

Sommerfeldt D. W. and Rubin C. T. (2001) Biology of bone and how it orchestrates the form and function of the skeleton. *Eur Spine J* **10 Suppl 2,** S86-95.

Spencer G. J. and Genever P. G. (2003) Long-term potentiation in bone--a role for glutamate in strain-induced cellular memory? *BMC Cell Biol* **4,** 9.

Spencer G. J., Hitchcock I. S. and Genever P. G. (2004) Emerging neuroskeletal signalling pathways: a review. *FEBS Lett* **559,** 6-12.

Spencer G. J., Grewal T. S., Genever P. G. and Skerry T. M. (2001) Long-term potentiation in bone: A cellular basis of memory in osteoblasts? *Bone* **28,** S87-S87.

Spitzer N. C. (2006) Electrical activity in early neuronal development. *Nature* **444,** 707-712.

Staehling-Hampton K., Proll S., Paeper B. W., Zhao L., Charmley P., Brown A., Gardner J. C., Galas D., Schatzman R. C., Beighton P., Papapoulos S., Hamersma H. and Brunkow M. E. (2002) A 52-kb deletion in the SOST-MEOX1 intergenic region on 17q12-q21 is associated with van Buchem disease in the Dutch population. *Am J Med Genet* **110,** 144-152.

Stallcup W. B., Bulloch K. and Baetge E. E. (1979) Coupled transport of glutamate and sodium in a cerebellar nerve cell line. *J Neurochem* **32,** 57-65.

Standring S., ed. (2004) *Gray's Anatomy,* 39th Edition, pp 83-135. Elsevier, New York.

Stanford C. M., Morcuende J. A. and Brand R. A. (1995a) Proliferative and phenotypic responses of bone-like cells to mechanical deformation. *J Orthop Res* **13,** 664-670.

Stanford C. M., Jacobson P. A., Eanes E. D., Lembke L. A. and Midura R. J. (1995b) Rapidly forming apatitic mineral in an osteoblastic cell line (UMR 106-01 BSP). *J Biol Chem* **270,** 9420-9428.

Stauber M., Rapillard L., van Lenthe G. H., Zysset P. and Muller R. (2006) Importance of individual rods and plates in the assessment of bone quality and their contribution to bone stiffness. *J Bone Miner Res* **21,** 586-595.

Staudinger J., Lu J. and Olson E. N. (1997) Specific interaction of the PDZ domain protein PICK1 with the COOH terminus of protein kinase C-alpha. *J Biol Chem* **272,** 32019-32024.

Staudinger J., Zhou J., Burgess R., Elledge S. J. and Olson E. N. (1995) PICK1: a perinuclear binding protein and substrate for protein kinase C isolated by the yeast two-hybrid system. *J Cell Biol* **128,** 263-271.

Steffgen J., Koepsell H. and Schwarz W. (1991) Endogenous L-glutamate transport in oocytes of Xenopus laevis. *Biochim Biophys Acta* **1066,** 14-20.

Stein C. A. (2001) The experimental use of antisense oligonucleotides: a guide for the perplexed. *J Clin Invest* **108,** 641-644.

Stein G. S., Lian J. B., van Wijnen A. J., Stein J. L., Montecino M., Javed A., Zaidi S. K., Young D. W., Choi J. Y. and Pockwinse S. M. (2004) Runx2 control of organization, assembly and activity of the regulatory machinery for skeletal gene expression. *Oncogene* **23,** 4315-4329.

Steitz S. A., Speer M. Y., McKee M. D., Liaw L., Almeida M., Yang H. and Giachelli C. M. (2002) Osteopontin inhibits mineral deposition and promotes regression of ectopic calcification. *Am J Pathol* **161,** 2035-2046.

Stoffel W., Korner R., Wachtmann D. and Keller B. U. (2004) Functional analysis of glutamate transporters in excitatory synaptic transmission of GLAST1 and GLAST1/EAAC1 deficient mice. *Brain Res Mol Brain Res* **128,** 170-181.

Storck T., Schulte S., Hofmann K. and Stoffel W. (1992) Structure, expression, and functional analysis of a Na(+)-dependent glutamate/aspartate transporter from rat brain. *Proc Natl Acad Sci U S A* **89,** 10955-10959.

Strausberg R. L., Feingold E. A., Grouse L. H., Derge J. G., Klausner R. D., Collins F. S., Wagner L., Shenmen C. M., Schuler G. D., Altschul S. F., Zeeberg B., Buetow K. H., Schaefer C. F., Bhat N. K., Hopkins R. F., Jordan H., Moore T., Max S. I., Wang J., Hsieh F., Diatchenko L., Marusina K., Farmer A. A., Rubin G. M., Hong L., Stapleton M., Soares M. B., Bonaldo M. F., Casavant T. L., Scheetz T. E., Brownstein M. J., Usdin T. B., Toshiyuki S., Carninci P., Prange C., Raha S. S., Loquellano N. A., Peters G. J., Abramson R. D., Mullahy S. J., Bosak S. A., McEwan P. J., McKernan K. J., Malek J. A., Gunaratne P. H., Richards S., Worley K. C., Hale S., Garcia A. M., Gay L. J., Hulyk S. W., Villalon D. K., Muzny D. M., Sodergren E. J., Lu X., Gibbs R. A., Fahey J., Helton E., Ketteman M., Madan A., Rodrigues S., Sanchez A., Whiting M., Madan A., Young A. C., Shevchenko Y., Bouffard G. G., Blakesley R. W., Touchman J. W., Green E. D., Dickson M. C., Rodriguez A. C., Grimwood J., Schmutz J., Myers R. M., Butterfield Y. S., Krzywinski M. I., Skalska U., Smailus D. E., Schnerch A., Schein J. E., Jones S. J. and Marra M. A. (2002) Generation and initial analysis of more than 15,000 full-length human and mouse cDNA sequences. *Proc Natl Acad Sci U S A* **99,** 16899-16903.

Su X., Sun K., Cui F. Z. and Landis W. J. (2003) Organization of apatite crystals in human woven bone. *Bone* **32,** 150-162.

Su X. W., Feng Q. L., Cui F. Z. and Zhu X. D. (1997) Microstructure and micromechanical properties of the mid-diaphyses of human fetal femurs. *Connect Tissue Res* **36,** 271-286.

Suda T., Takahashi N. and Martin T. J. (1992) Modulation of osteoclast differentiation. *Endocr Rev* **13,** 66-80.

Sullivan R., Rauen T., Fischer F., Wiessner M., Grewer C., Bicho A. and Pow D. V. (2004) Cloning, transport properties, and differential localization of two splice variants of GLT-1 in the rat CNS: implications for CNS glutamate homeostasis. *Glia* **45,** 155-169.

Sullivan S. M., Macnab L. T., Bjorkman S. T., Colditz P. B. and Pow D. V. (2007a) GLAST1b, the exon-9 skipping form of the glutamate-aspartate transporter EAAT1 is a sensitive marker of neuronal dysfunction in the hypoxic brain. *Neuroscience* **149,** 434-445.

Sullivan S. M., Lee A., Bjorkman S. T., Miller S. M., Sullivan R. K., Poronnik P., Colditz P. B. and Pow D. V. (2007b) Cytoskeletal anchoring of GLAST determines susceptibility to brain damage: an identified role for GFAP. *J Biol Chem* **282,** 29414-29423.

Sun L., Blair H. C., Peng Y., Zaidi N., Adebanjo O. A., Wu X. B., Wu X. Y., Iqbal J., Epstein S., Abe E., Moonga B. S. and Zaidi M. (2005) Calcineurin regulates bone formation by the osteoblast. *Proc Natl Acad Sci U S A* **102,** 17130-17135.

Suzuki T., Higgins P. J. and Crawford D. R. (2000) Control selection for RNA quantitation. *Biotechniques* **29,** 332-337.

Szczesniak A. M., Gilbert R. W., Mukhida M. and Anderson G. I. (2005) Mechanical loading modulates glutamate receptor subunit expression in bone. *Bone* **37,** 63-73.

Szollar S. M., Martin E. M., Sartoris D. J., Parthemore J. G. and Deftos L. J. (1998) Bone mineral density and indexes of bone metabolism in spinal cord injury. *Am J Phys Med Rehabil* **77,** 28-35.

Takamori S., Rhee J. S., Rosenmund C. and Jahn R. (2000) Identification of a vesicular glutamate transporter that defines a glutamatergic phenotype in neurons. *Nature* **407,** 189-194.

Takamori S., Rhee J. S., Rosenmund C. and Jahn R. (2001) Identification of differentiation-associated brain-specific phosphate transporter as a second vesicular glutamate transporter (VGLUT2). *J Neurosci* **21,** RC182.

Takarada-Iemata M., Takarada T., Nakamura Y., Nakatani E., Hori O. and Yoneda Y. (2010) Glutamate preferentially suppresses osteoblastogenesis than adipogenesis through the cystine/glutamate antiporter in mesenchymal stem cells. *J Cell Physiol.*

Takarada T. and Yoneda Y. (2008) Pharmacological topics of bone metabolism: glutamate as a signal mediator in bone. *J Pharmacol Sci* **106,** 536-541.

Takarada T., Hinoi E., Fujimori S., Tsuchihashi Y., Ueshima T., Taniura H. and Yoneda Y. (2004) Accumulation of [3H] glutamate in cultured rat calvarial osteoblasts. *Biochem Pharmacol* **68,** 177-184.

Takeda S., Elefteriou F., Levasseur R., Liu X., Zhao L., Parker K. L., Armstrong D., Ducy P. and Karsenty G. (2002) Leptin regulates bone formation via the sympathetic nervous system. *Cell* **111,** 305-317.

Tanabe Y., Masu M., Ishii T., Shigemoto R. and Nakanishi S. (1992) A family of metabotropic glutamate receptors. *Neuron* **8,** 169-179.

Tanaka K. (1993) Cloning and expression of a glutamate transporter from mouse brain. *Neurosci Lett* **159,** 183-186.

Tanaka K., Watase K., Manabe T., Yamada K., Watanabe M., Takahashi K., Iwama H., Nishikawa T., Ichihara N., Kikuchi T., Okuyama S., Kawashima N., Hori S., Takimoto M. and Wada K. (1997) Epilepsy and exacerbation of brain injury in mice lacking the glutamate transporter GLT-1. *Science* **276,** 1699-1702.

Tani-Ishii N., Tsunoda A. and Umemoto T. (1997) Osteopontin antisense deoxyoligonucleotides inhibit bone resorption by mouse osteoclasts in vitro. *J Periodontal Res* **32,** 480-486.

Tao Z., Zhang Z. and Grewer C. (2006) Neutralization of the aspartic acid residue Asp-367, but not Asp-454, inhibits binding of Na+ to the glutamate-free form and cycling of the glutamate transporter EAAC1. *J Biol Chem* **281,** 10263-10272.

Tashjian A. H., Jr. and Gagel R. F. (2006) Teriparatide [human PTH(1-34)]: 2.5 years of experience on the use and safety of the drug for the treatment of osteoporosis. *J Bone Miner Res* **21,** 354-365.

Taylor A. F. (2002) Osteoblastic glutamate receptor function regulates bone formation and resorption. *J Musculoskelet Neuronal Interact* **2,** 285-290.

Termine J. D., Kleinman H. K., Whitson S. W., Conn K. M., McGarvey M. L. and Martin G. R. (1981) Osteonectin, a bone-specific protein linking mineral to collagen. *Cell* **26,** 99-105.

Tezuka T., Umemori H., Akiyama T., Nakanishi S. and Yamamoto T. (1999) PSD-95 promotes Fyn-mediated tyrosine phosphorylation of the N-methyl-D-aspartate receptor subunit NR2A. *Proc Natl Acad Sci U S A* **96,** 435-440.

Thellin O., Zorzi W., Lakaye B., De Borman B., Coumans B., Hennen G., Grisar T., Igout A. and Heinen E. (1999) Housekeeping genes as internal standards: use and limits. *J Biotechnol* **75,** 291-295.

Tobias J. H. and Compston J. E. (1999) Does estrogen stimulate osteoblast function in postmenopausal women? *Bone* **24,** 121-124.

Todd C. J., Freeman C. J., Camilleri-Ferrante C., Palmer C. R., Hyder A., Laxton C. E., Parker M. J., Payne B. V. and Rushton N. (1995) Differences in mortality after fracture of hip: the east Anglian audit. *BMJ* **310,** 904-908.

Torgensen D. J. e. a. (2001) The economics of fracture prevention, in *The effective management of osteoporosis* (Barlow D. H., ed.), pp 111-121. Aesculapius Medical Press, London.

Torres G. E., Sweeney A. L., Beaulieu J. M., Shashidharan P. and Caron M. G. (2004) Effect of torsinA on membrane proteins reveals a loss of function and a dominant-negative phenotype of the dystonia-associated DeltaE-torsinA mutant. *Proc Natl Acad Sci U S A* **101,** 15650-15655.

Torres G. E., Yao W. D., Mohn A. R., Quan H., Kim K. M., Levey A. I., Staudinger J. and Caron M. G. (2001) Functional interaction between monoamine plasma membrane transporters and the synaptic PDZ domain-containing protein PICK1. *Neuron* **30,** 121-134.

Tovar Y. R. L. B., Santa-Cruz L. D., Zepeda A. and Tapia R. (2009) Chronic elevation of extracellular glutamate due to transport blockade is innocuous for spinal motoneurons in vivo. *Neurochem Int* **54,** 186-191.

Trotti D., Peng J. B., Dunlop J. and Hediger M. A. (2001) Inhibition of the glutamate transporter EAAC1 expressed in Xenopus oocytes by phorbol esters. *Brain Res* **914,** 196-203.

Tudor D., Dubuquoy C., Gaboriau V., Lefevre F., Charley B. and Riffault S. (2005) TLR9 pathway is involved in adjuvant effects of plasmid DNA-based vaccines. *Vaccine* **23,** 1258-1264.

Turner C. H., Takano Y., Owan I. and Murrell G. A. (1996) Nitric oxide inhibitor L-NAME suppresses mechanically induced bone formation in rats. *Am J Physiol* **270,** E634-639.

Turner C. H., Robling A. G., Duncan R. L. and Burr D. B. (2002) Do bone cells behave like a neuronal network? *Calcif Tissue Int* **70,** 435-442.

Udagawa N., Takahashi N., Jimi E., Matsuzaki K., Tsurukai T., Itoh K., Nakagawa N., Yasuda H., Goto M., Tsuda E., Higashio K., Gillespie M. T., Martin T. J. and Suda T. (1999) Osteoblasts/stromal cells stimulate osteoclast activation through expression of osteoclast differentiation factor/RANKL but not macrophage colony-stimulating factor: receptor activator of NF-kappa B ligand. *Bone* **25,** 517-523.

Uematsu M., Ohara Y., Navas J. P., Nishida K., Murphy T. J., Alexander R. W., Nerem R. M. and Harrison D. G. (1995) Regulation of endothelial cell nitric oxide synthase mRNA expression by shear stress. *Am J Physiol* **269,** C1371-1378.

Uno K., Takarada T., Hinoi E. and Yoneda Y. (2007) Glutamate is a determinant of cellular proliferation through modulation of nuclear factor E2 p45-related factor-2 expression in osteoblastic MC3T3-E1 cells. *J Cell Physiol* **213,** 105-114.

Utsunomiya-Tate N., Endou H. and Kanai Y. (1997) Tissue specific variants of glutamate transporter GLT-1. *FEBS Lett* **416,** 312-316.

Vaananen H. K., Zhao H., Mulari M. and Halleen J. M. (2000) The cell biology of osteoclast function. *J Cell Sci* **113 (Pt 3),** 377-381.

Vaes G. (1988) Cellular biology and biochemical mechanism of bone resorption. A review of recent developments on the formation, activation, and mode of action of osteoclasts. *Clin Orthop Relat Res,* 239-271.

Vahle J. L., Long G. G., Sandusky G., Westmore M., Ma Y. L. and Sato M. (2004) Bone neoplasms in F344 rats given teriparatide [rhPTH(1-34)] are dependent on duration of treatment and dose. *Toxicol Pathol* **32,** 426-438.

Vallejo-Illarramendi A., Domercq M. and Matute C. (2005) A novel alternative splicing form of excitatory amino acid transporter 1 is a negative regulator of glutamate uptake. *J Neurochem* **95,** 341-348.

Valsamis H. A., Arora S. K., Labban B. and McFarlane S. I. (2006) Antiepileptic drugs and bone metabolism. *Nutr Metab (Lond)* **3,** 36.

van Bezooijen R. L., ten Dijke P., Papapoulos S. E. and Lowik C. W. (2005) SOST/sclerostin, an osteocyte-derived negative regulator of bone formation. *Cytokine Growth Factor Rev* **16,** 319-327.

van Bezooijen R. L., Roelen B. A., Visser A., van der Wee-Pals L., de Wilt E., Karperien M., Hamersma H., Papapoulos S. E., ten Dijke P. and Lowik C. W. (2004) Sclerostin is an osteocyte-expressed negative regulator of bone formation, but not a classical BMP antagonist. *J Exp Med* **199,** 805-814.

van Buchem F. S. (1971) Hyperostosis corticalis generalisata. Eight new cases. *Acta Med Scand* **189,** 257-267.

Van Buchem F. S., Hadders H. N., Hansen J. F. and Woldring M. G. (1962) Hyperostosis corticalis generalisata. Report of seven cases. *Am J Med* **33,** 387-397.

van Deutekom J. C., Bremmer-Bout M., Janson A. A., Ginjaar I. B., Baas F., den Dunnen J. T. and van Ommen G. J. (2001) Antisense-induced exon skipping restores dystrophin expression in DMD patient derived muscle cells. *Hum Mol Genet* **10,** 1547-1554.

van Deutekom J. C., Janson A. A., Ginjaar I. B., Frankhuizen W. S., Aartsma-Rus A., Bremmer-Bout M., den Dunnen J. T., Koop K., van der Kooi A. J., Goemans N. M., de Kimpe S. J., Ekhart P. F., Venneker E. H., Platenburg G. J., Verschuuren J. J. and van Ommen G. J. (2007) Local dystrophin restoration with antisense oligonucleotide PRO051. *N Engl J Med* **357,** 2677-2686.

Van Hul W., Vanhoenacker F., Balemans W., Janssens K. and De Schepper A. M. (2001) Molecular and radiological diagnosis of sclerosing bone dysplasias. *Eur J Radiol* **40,** 198-207.

Van Hul W., Balemans W., Van Hul E., Dikkers F. G., Obee H., Stokroos R. J., Hildering P., Vanhoenacker F., Van Camp G. and Willems P. J. (1998) Van Buchem disease (hyperostosis corticalis generalisata) maps to chromosome 17q12-q21. *Am J Hum Genet* **62,** 391-399.

van Ommen G. J., van Deutekom J. and Aartsma-Rus A. (2008) The therapeutic potential of antisense-mediated exon skipping. *Curr Opin Mol Ther* **10,** 140-149.

Van Slyke M. A. and Marks S. C., Jr. (1987) Failure of normal osteoclasts to resorb calcified cartilage from osteosclerotic (oc/oc) mice in vitro. *Bone* **8,** 39-44.

van Staa T. P., Dennison E. M., Leufkens H. G. and Cooper C. (2001) Epidemiology of fractures in England and Wales. *Bone* **29,** 517-522.

Vandenberg R. J., Mitrovic A. D. and Johnston G. A. (1998) Molecular basis for differential inhibition of glutamate transporter subtypes by zinc ions. *Mol Pharmacol* **54,** 189-196.

Vandenberg R. J., Arriza J. L., Amara S. G. and Kavanaugh M. P. (1995) Constitutive ion fluxes and substrate binding domains of human glutamate transporters. *J Biol Chem* **270,** 17668-17671.

Vandenbroucke, II, Vandesompele J., Paepe A. D. and Messiaen L. (2001) Quantification of splice variants using real-time PCR. *Nucleic Acids Res* **29,** E68-68.

Vandesompele J., De Preter K., Pattyn F., Poppe B., Van Roy N., De Paepe A. and Speleman F. (2002) Accurate normalization of real-time quantitative RT-PCR data by geometric averaging of multiple internal control genes. *Genome Biol* **3,** RESEARCH0034.

Vatsa A., Semeins C. M., Smit T. H. and Klein-Nulend J. (2008) Paxillin localisation in osteocytes--is it determined by the direction of loading? *Biochem Biophys Res Commun* **377,** 1019-1024.

Vaughan R. A., Huff R. A., Uhl G. R. and Kuhar M. J. (1997) Protein kinase C-mediated phosphorylation and functional regulation of dopamine transporters in striatal synaptosomes. *J Biol Chem* **272,** 15541-15546.

Venkatachalapathy S., Crowe J. and Gray A. (2007) Atypical presentation of varicella zoster in a patient on alemtuzumab. *Br J Haematol* **138,** 406.

Verdoorn T. A., Burnashev N., Monyer H., Seeburg P. H. and Sakmann B. (1991) Structural determinants of ion flow through recombinant glutamate receptor channels. *Science* **252,** 1715-1718.

Vestergaard P., Krogh K., Rejnmark L. and Mosekilde L. (1998) Fracture rates and risk factors for fractures in patients with spinal cord injury. *Spinal Cord* **36,** 790-796.

Volterra A., Bezzi P., Rizzini B. L., Trotti D., Ullensvang K., Danbolt N. C. and Racagni G. (1996) The competitive transport inhibitor L-trans-pyrrolidine-2, 4-dicarboxylate triggers excitotoxicity in rat cortical neuron-astrocyte co-cultures via glutamate release rather than uptake inhibition. *Eur J Neurosci* **8,** 2019-2028.

Wada S., Kojo T., Wang Y. H., Ando H., Nakanishi E., Zhang M., Fukuyama H. and Uchida Y. (2001) Effect of loading on the development of nerve fibers around oral implants in the dog mandible. *Clin Oral Implants Res* **12,** 219-224.

Wadiche J. I. and Kavanaugh M. P. (1998) Macroscopic and microscopic properties of a cloned glutamate transporter/chloride channel. *J Neurosci* **18,** 7650-7661.

Wadiche J. I. and Jahr C. E. (2005) Patterned expression of Purkinje cell glutamate transporters controls synaptic plasticity. *Nat Neurosci* **8,** 1329-1334.

Wadiche J. I., Amara S. G. and Kavanaugh M. P. (1995) Ion fluxes associated with excitatory amino acid transport. *Neuron* **15,** 721-728.

Wagenfeld A., Yeung C. H., Lehnert W., Nieschlag E. and Cooper T. G. (2002) Lack of glutamate transporter EAAC1 in the epididymis of infertile c-ros receptor tyrosine-kinase deficient mice. *J Androl* **23,** 772-782.

Wahle S. and Stoffel W. (1996) Membrane topology of the high-affinity L-glutamate transporter (GLAST-1) of the central nervous system. *J Cell Biol* **135,** 1867-1877.

Walker D. G. (1993) Bone resorption restored in osteopetrotic mice by transplants of normal bone marrow and spleen cells. 1975. *Clin Orthop Relat Res*, 4-6.

Wang C. M., Chen Y., DeVivo M. J. and Huang C. T. (2001) Epidemiology of extraspinal fractures associated with acute spinal cord injury. *Spinal Cord* **39,** 589-594.

Wang G. J., Chung H. J., Schnuer J., Pratt K., Zable A. C., Kavanaugh M. P. and Rosenberg P. A. (1998) High affinity glutamate transport in rat cortical neurons in culture. *Mol Pharmacol* **53,** 88-96.

Wang S. and Kool E. T. (1995) Relative stabilities of triple helices composed of combinations of DNA, RNA and 2'-O-methyl-RNA backbones: chimeric circular oligonucleotides as probes. *Nucleic Acids Res* **23,** 1157-1164.

Wang Z., Li W., Mitchell C. K. and Carter-Dawson L. (2003) Activation of protein kinase C reduces GLAST in the plasma membrane of rat Muller cells in primary culture. *Vis Neurosci* **20,** 611-619.

Waniewski R. A. and Martin D. L. (1984) Characterization of L-glutamic acid transport by glioma cells in culture: evidence for sodium-independent, chloride-dependent high affinity influx. *J Neurosci* **4,** 2237-2246.

Wark J. D. (1993) Osteoporosis: pathogenesis, diagnosis, prevention and management. *Baillieres Clin Endocrinol Metab* **7,** 151-181.

Warrington J. A., Nair A., Mahadevappa M. and Tsyganskaya M. (2000) Comparison of human adult and fetal expression and identification of 535 housekeeping/maintenance genes. *Physiol Genomics* **2,** 143-147.

Watanabe M., Robinson M. B., Kalandadze A. and Rothstein J. D. (2003) Gps1, interacting protein with GLT-1. *Society for Neuroscience Abstract Viewer and Itinerary Planner* **2003,** Abstract No. 372.316.

Watts N. B. (1999) Clinical utility of biochemical markers of bone remodeling. *Clin Chem* **45,** 1359-1368.

Weinbaum S., Cowin S. C. and Zeng Y. (1994) A model for the excitation of osteocytes by mechanical loading-induced bone fluid shear stresses. *J Biomech* **27,** 339-360.

Weinreb M., Rodan G. A. and Thompson D. D. (1989) Osteopenia in the immobilized rat hind limb is associated with increased bone resorption and decreased bone formation. *Bone* **10,** 187-194.

Westbroek I., van der Plas A., de Rooij K. E., Klein-Nulend J. and Nijweide P. J. (2001) Expression of serotonin receptors in bone. *J Biol Chem* **276,** 28961-28968.

Wetterwald A., Hoffstetter W., Cecchini M. G., Lanske B., Wagner C., Fleisch H. and Atkinson M. (1996) Characterization and cloning of the E11 antigen, a marker expressed by rat osteoblasts and osteocytes. *Bone* **18,** 125-132.

Wheeler D. D. (1987) Are there both low- and high-affinity glutamate transporters in rat cortical synaptosomes? *Neurochem Res* **12,** 667-680.

Whelan J. A., Russell N. B. and Whelan M. A. (2003) A method for the absolute quantification of cDNA using real-time PCR. *J Immunol Methods* **278,** 261-269.

Whyte M. P. (2002) Osteopetrosis, in *Connective tissue and its heritable disorders: medical, genetic, and molecular aspects,* 2nd Edition (Royce P. M., Steinman, B., ed.), pp 753-770. Wiley-Liss, Inc, New York.

Wilton S. D., Lloyd F., Carville K., Fletcher S., Honeyman K., Agrawal S. and Kole R. (1999) Specific removal of the nonsense mutation from the mdx dystrophin mRNA using antisense oligonucleotides. *Neuromuscul Disord* **9,** 330-338.

Wimalawansa S. J., De Marco G., Gangula P. and Yallampalli C. (1996) Nitric oxide donor alleviates ovariectomy-induced bone loss. *Bone* **18,** 301-304.

Winkler D. G., Sutherland M. K., Geoghegan J. C., Yu C., Hayes T., Skonier J. E., Shpektor D., Jonas M., Kovacevich B. R., Staehling-Hampton K., Appleby M., Brunkow M. E. and Latham J. A. (2003) Osteocyte control of bone formation via sclerostin, a novel BMP antagonist. *Embo J* **22,** 6267-6276.

Wisden W. and Seeburg P. H. (1993) Mammalian ionotropic glutamate receptors. *Curr Opin Neurobiol* **3,** 291-298.

Wronski T. J., Cintron M. and Dann L. M. (1988) Temporal relationship between bone loss and increased bone turnover in ovariectomized rats. *Calcif Tissue Int* **43,** 179-183.

Wu J. Y., Niu F. N., Huang R. and Xu Y. (2008) Enhancement of glutamate uptake in 1-methyl-4-phenylpyridinium-treated astrocytes by trichostatin A. *Neuroreport* **19,** 1209-1212.

Wucherpfennig A. L., Li Y. P., Stetler-Stevenson W. G., Rosenberg A. E. and Stashenko P. (1994) Expression of 92 kD type IV collagenase/gelatinase B in human osteoclasts. *J Bone Miner Res* **9,** 549-556.

Xiao G., Jiang D., Thomas P., Benson M. D., Guan K., Karsenty G. and Franceschi R. T. (2000) MAPK pathways activate and phosphorylate the osteoblast-specific transcription factor, Cbfa1. *J Biol Chem* **275,** 4453-4459.

Yamada K., Wada S., Watanabe M., Tanaka K., Wada K. and Inoue Y. (1997) Changes in expression and distribution of the glutamate transporter EAAT4 in developing mouse Purkinje cells. *Neurosci Res* **27,** 191-198.

Yamada Y., Chochi Y., Ko J. A., Sobue K. and Inui M. (1999) Activation of channel activity of the NMDA receptor-PSD-95 complex by guanylate kinase-associated protein (GKAP). *FEBS Lett* **458,** 295-298.

Yamate T., Mocharla H., Taguchi Y., Igietseme J. U., Manolagas S. C. and Abe E. (1997) Osteopontin expression by osteoclast and osteoblast progenitors in the murine bone marrow: demonstration of its requirement for osteoclastogenesis and its increase after ovariectomy. *Endocrinology* **138,** 3047-3055.

Yasuda H., Shima N., Nakagawa N., Mochizuki S. I., Yano K., Fujise N., Sato Y., Goto M., Yamaguchi K., Kuriyama M., Kanno T., Murakami A., Tsuda E., Morinaga T. and Higashio K. (1998a) Identity of osteoclastogenesis inhibitory factor (OCIF) and osteoprotegerin (OPG): a mechanism by which OPG/OCIF inhibits osteoclastogenesis in vitro. *Endocrinology* **139,** 1329-1337.

Yasuda H., Shima N., Nakagawa N., Yamaguchi K., Kinosaki M., Mochizuki S., Tomoyasu A., Yano K., Goto M., Murakami A., Tsuda E., Morinaga T., Higashio K., Udagawa N., Takahashi N. and Suda T. (1998b) Osteoclast differentiation factor is a ligand for osteoprotegerin/osteoclastogenesis-inhibitory factor and is identical to TRANCE/RANKL. *Proc Natl Acad Sci U S A* **95,** 3597-3602.

Yernool D., Boudker O., Jin Y. and Gouaux E. (2004) Structure of a glutamate transporter homologue from Pyrococcus horikoshii. *Nature* **431,** 811-818.

Yoneda Y., Kawajiri S., Hasegawa A., Kito F., Katano S., Takano E. and Mimura T. (2001) Synthesis of polyamine derivatives having non-hypotensive Ca2 +-permeable AMPA receptor antagonist activity. *Bioorg Med Chem Lett* **11,** 1261-1264.

Yoshitake H., Rittling S. R., Denhardt D. T. and Noda M. (1999) Osteopontin-deficient mice are resistant to ovariectomy-induced bone resorption. *Proc Natl Acad Sci U S A* **96,** 8156-8160.

Younger E. M. and Chapman M. W. (1989) Morbidity at bone graft donor sites. *J Orthop Trauma* **3,** 192-195.

Zahniser N. R. and Doolen S. (2001) Chronic and acute regulation of Na+/Cl- -dependent neurotransmitter transporters: drugs, substrates, presynaptic receptors, and signaling systems. *Pharmacol Ther* **92,** 21-55.

Zambonin Zallone A., Teti A. and Primavera M. V. (1984) Resorption of vital or devitalized bone by isolated osteoclasts in vitro. The role of lining cells. *Cell Tissue Res* **235,** 561-564.

Zamecnik P. C. and Stephenson M. L. (1978) Inhibition of Rous sarcoma virus replication and cell transformation by a specific oligodeoxynucleotide. *Proc Natl Acad Sci U S A* **75,** 280-284.

Zerangue N. and Kavanaugh M. P. (1996) Flux coupling in a neuronal glutamate transporter. *Nature* **383,** 634-637.

Zerwekh J. E., Ruml L. A., Gottschalk F. and Pak C. Y. (1998) The effects of twelve weeks of bed rest on bone histology, biochemical markers of bone turnover, and calcium homeostasis in eleven normal subjects. *J Bone Miner Res* **13,** 1594-1601.

Zhang Y. and Kanner B. I. (1999) Two serine residues of the glutamate transporter GLT-1 are crucial for coupling the fluxes of sodium and the neurotransmitter. *Proc Natl Acad Sci U S A* **96,** 1710-1715.

Zhao S., Zhang Y. K., Harris S., Ahuja S. S. and Bonewald L. F. (2002) MLO-Y4 osteocyte-like cells support osteoclast formation and activation. *J Bone Miner Res* **17,** 2068-2079.

Zheng W. H. and Quirion R. (2009) Glutamate acting on N-methyl-D-aspartate receptors attenuates insulin-like growth factor-1 receptor tyrosine phosphorylation and its survival signaling properties in rat hippocampal neurons. *J Biol Chem* **284,** 855-861.

Zhou J. and Sutherland M. L. (2004) Glutamate transporter cluster formation in astrocytic processes regulates glutamate uptake activity. *J Neurosci* **24,** 6301-6306.

Zhu M. Y., Blakely R. D., Apparsundaram S. and Ordway G. A. (1998) Down-regulation of the human norepinephrine transporter in intact 293-hNET cells exposed to desipramine. *J Neurochem* **70,** 1547-1555.

APPENDICES

9. Appendices

9.1 Solutions

9.1.1 General solutions

Phosphate Buffered Saline (PBS)

8g of Sodium Chloride (NaCl)
0.2g of Potassium Chloride (KCl)
1.44g of Sodium phosphate, dibasic, anhydrous (Na_2HPO_4)
0.24g of Potassium phosphate, monobasic, anhydrous (KH_2PO_4)
Dissolved in 800ml dH_2O and pH adjusted to 7.4 with 1M Hydrochloric acid.
Volume made up to 1L with dH_2O and solution sterilised by autoclaving.

4% Paraformaldehyde/PBS

4g paraformaldehyde was dissolved in 100ml PBS with heating. The pH was raised (to pH 7-8) by adding a few drops of 1N NaOH until the solution cleared. Solution was used fresh.

9.1.2 Molecular biology

LB agar

LB agar tablets (Sigma) were dissolved in dH_2O (50ml/tablet) by autoclaving twice. The solution was allowed to cool slightly before adding ampicillin to 100µg/ml, IPTG to 0.5mM and X-galactosidase to 40µg/ml. Agar was poured into 10cm plates and allowed to solidify aseptically. Plates stored at 4°C.

LB broth

LB broth tablets (Sigma) were dissolved in dH_2O (50ml/tablet) by autoclaving once. The solution was allowed to cool before adding ampicillin to 100µg/ml. Stored at 4°C.

Tris-Borate EDTA buffer (TBE)

10X TBE was obtained from Promega and diluted 1:10 in dH_2O.

9.1.3 Glutamate uptake

Krebs-Ringer-HEPES buffer (KRH)

Prepared fresh, volume adjusted to 1L and pH adjusted to 7.4. Filter sterilised and stored at 4°C.

Stock solution	Volume for 1 litre	Final concentration
NaCl, 1.25M (73.05 g/l)	100ml	125mM
KCl, 70mM (5.22 g/l)	50ml	3.5mM
$CaCl_2 \cdot 2H_20$, 30mM (4.41 g/l)	50ml	1.5mM
MgSO4, 24mM (2.89 g/l)	50ml	1.2mM
KH_2PO_4, 24mM (3.27 g/l)	50ml	1.2mM
HEPES, 1M, pH 7.4	10ml	10mM
D-glucose, 1M (180.2 g/l)	2ml	2mM

9.2 QRT-PCR standard curves and dissociation curves

9.2.1 Stratagene (Cardiff University)

9.2.1.1 Example standard curve

GAPDH

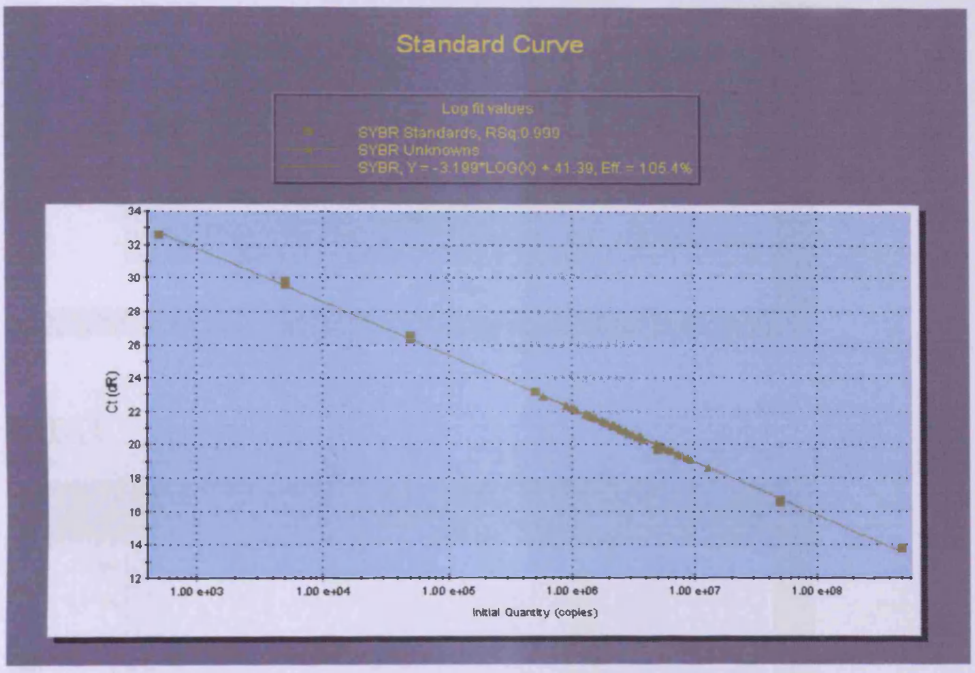

9.2.1.2 Dissociation curves

18S rRNA

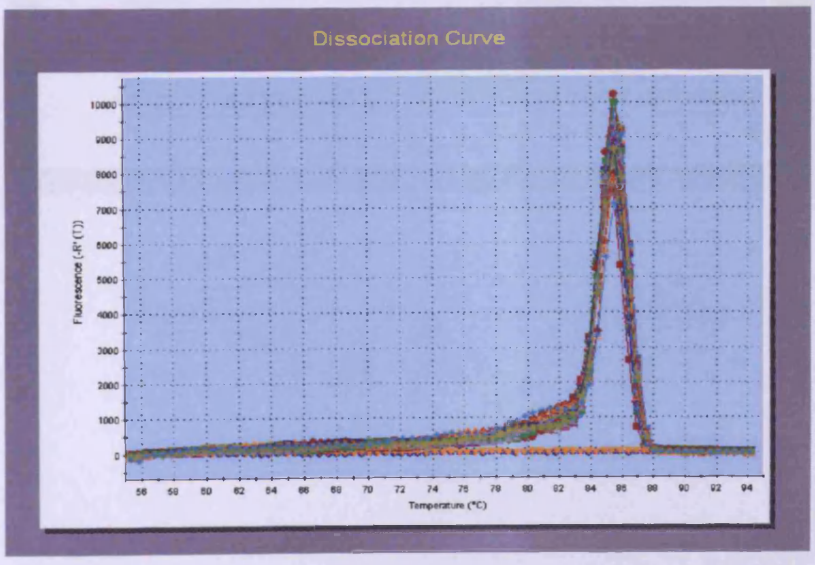

GAPDH

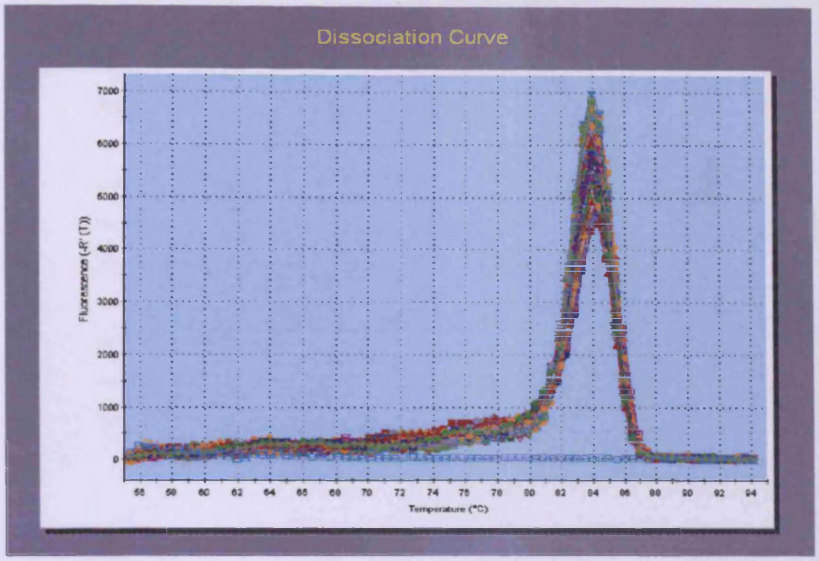
Dissociation Curve
Fluorescence (-R' (T))
Temperature (°C)

HPRT1

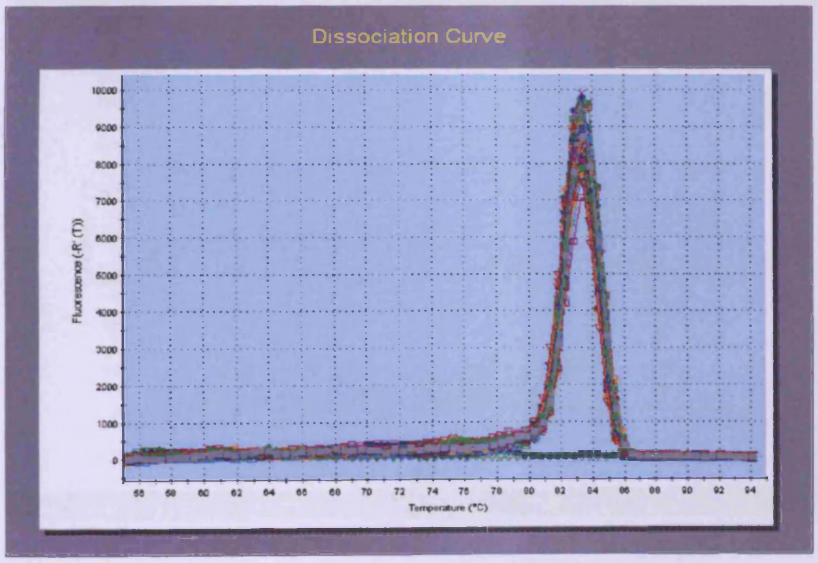
Dissociation Curve
Fluorescence (-R' (T))
Temperature (°C)

Osteocalcin

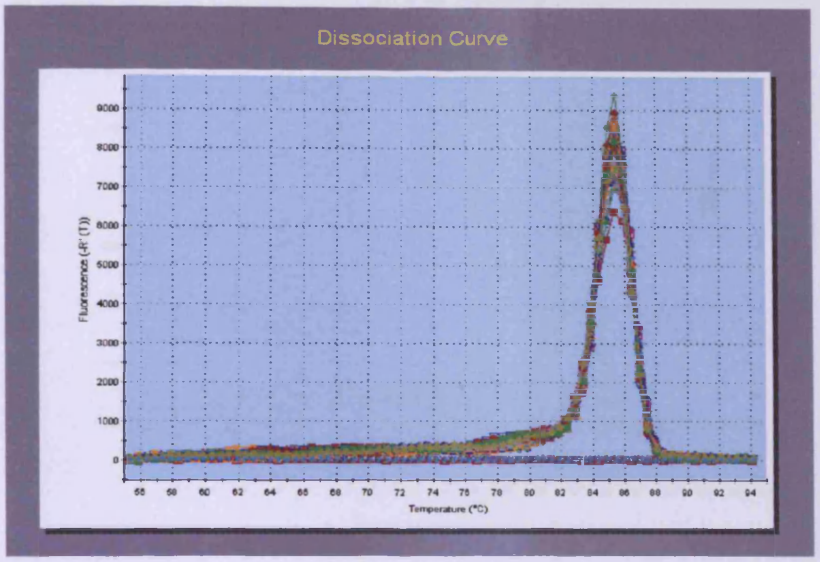

Osteonectin

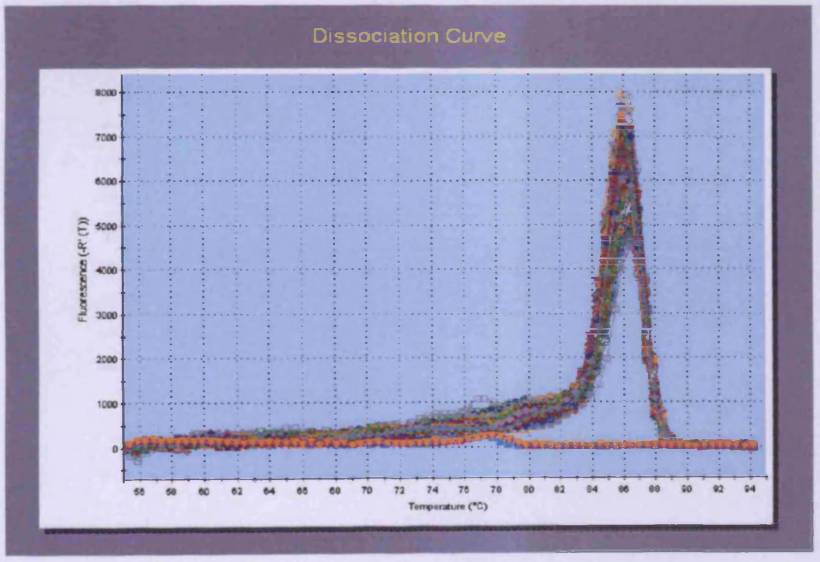

EAAT1 (+EAAT1ex9skip)

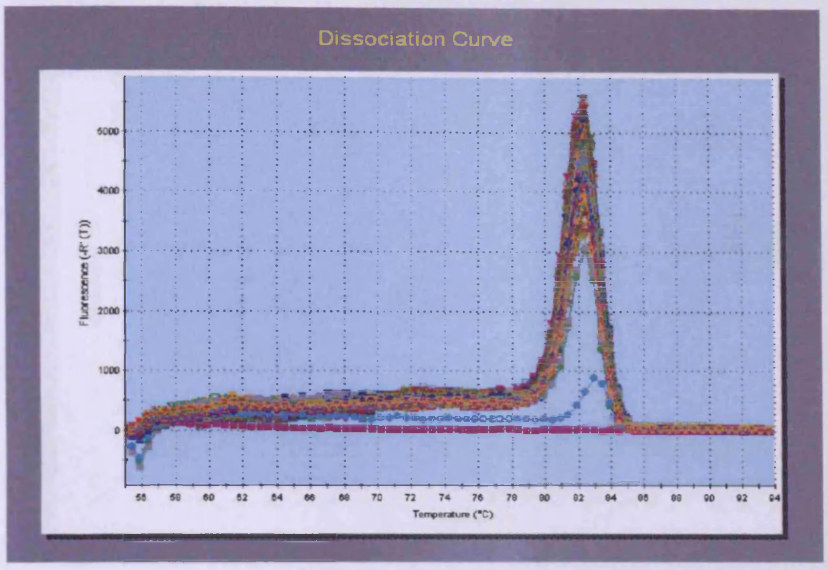

EAAT1ex9skip

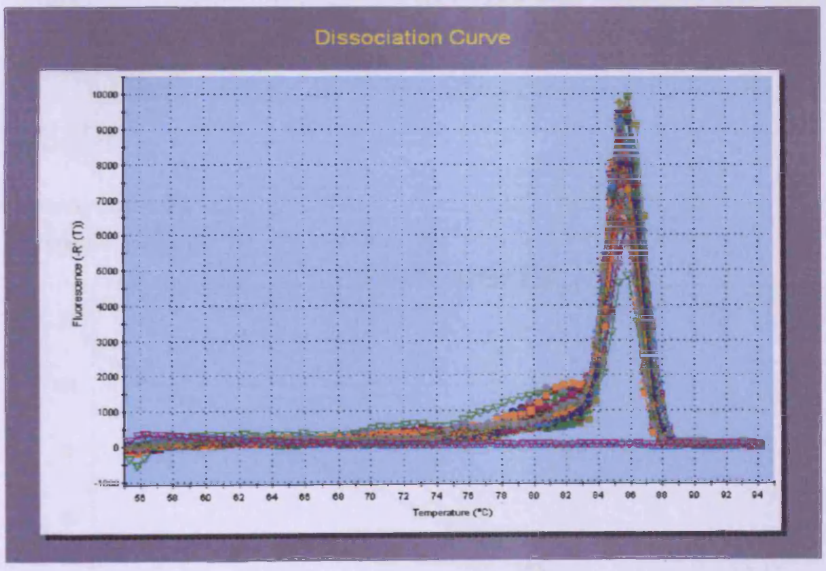

EAAT3

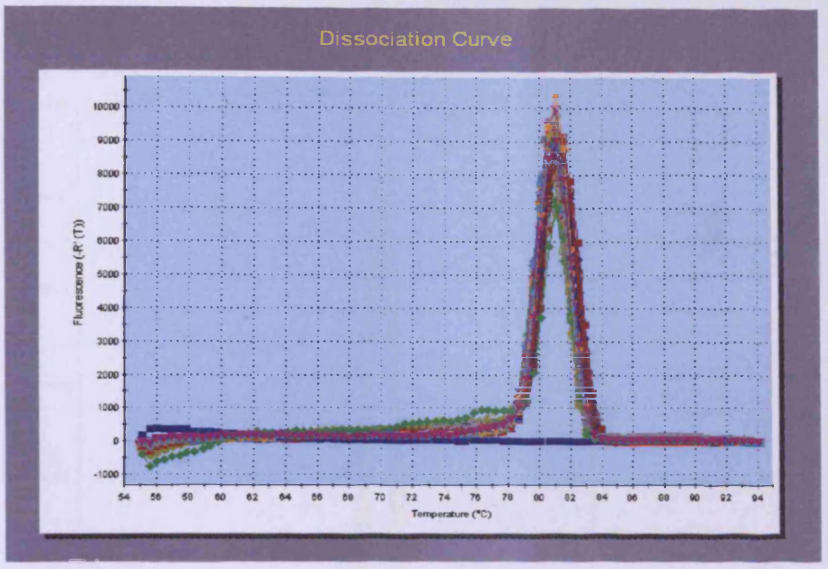

9.2.2 Applied Biosystems (Smith & Nephew Research Centre, York)

9.2.2.1 Example standard curve

GAPDH

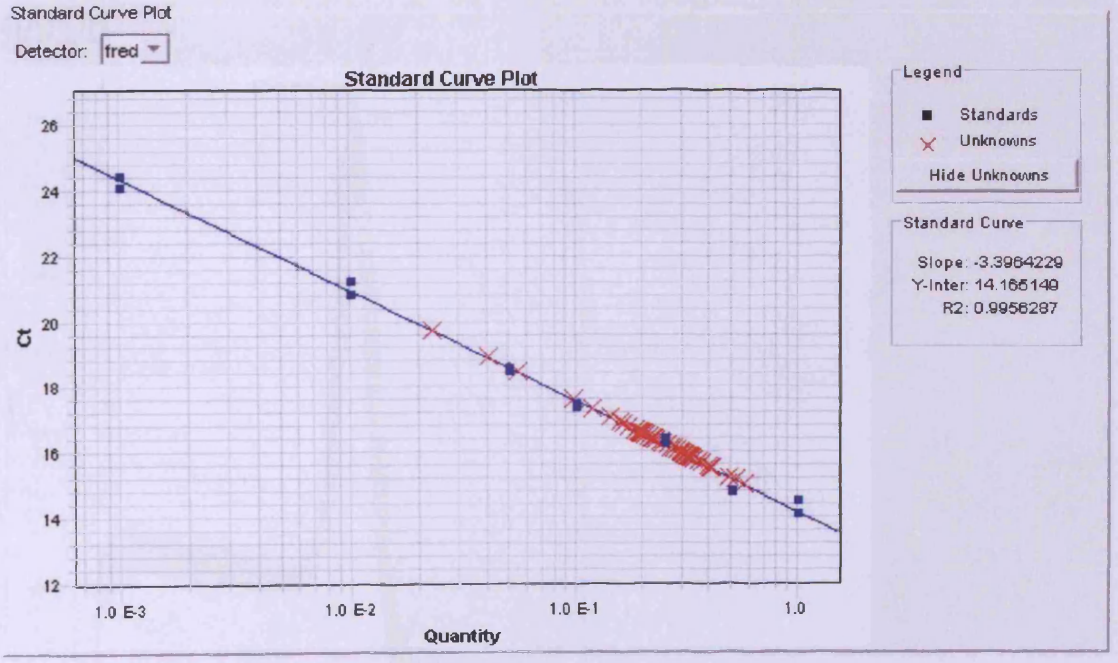

9.2.2.2 Dissociation curves

18S rRNA

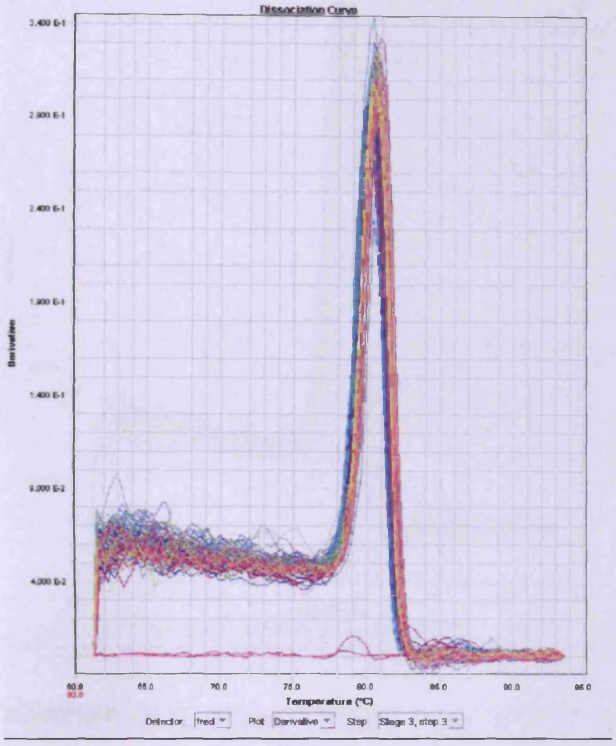

GAPDH

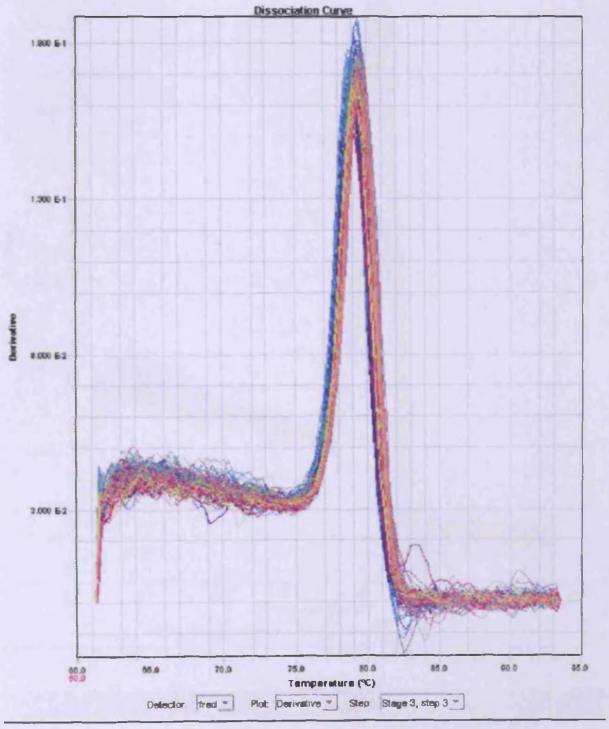

HPRT1

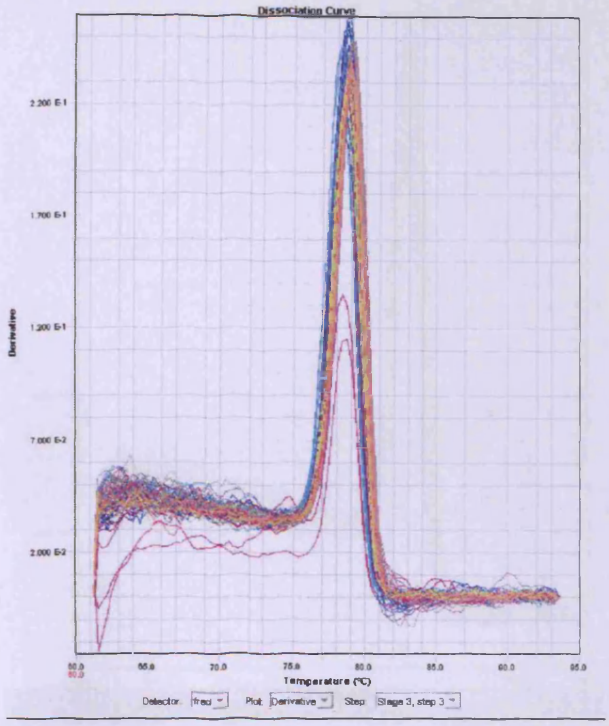

Osteocalcin

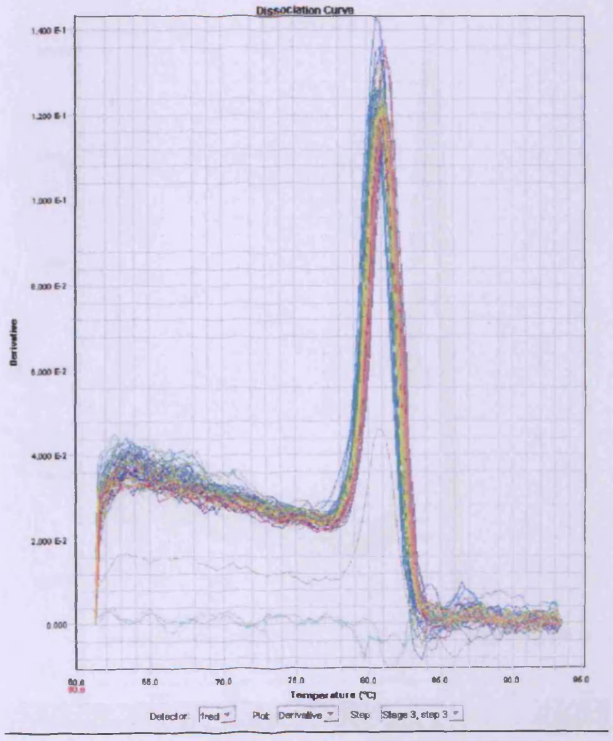

Osteonectin

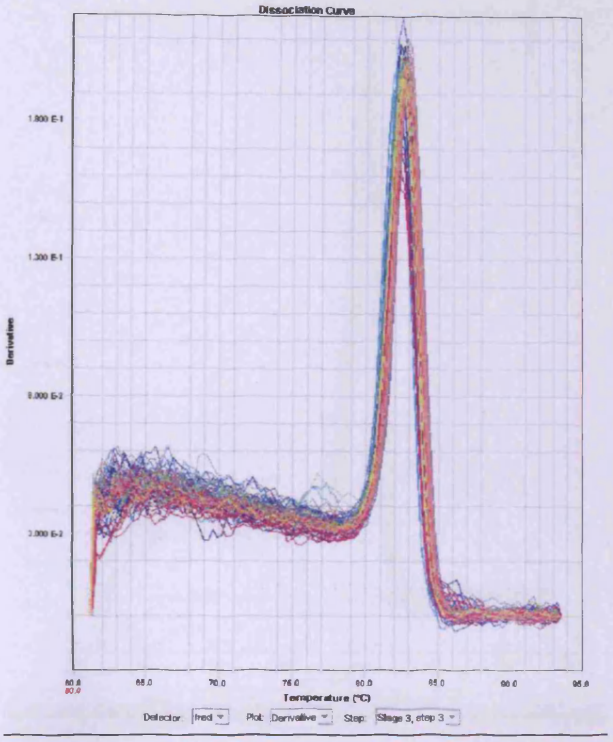

Alkaline phosphatase

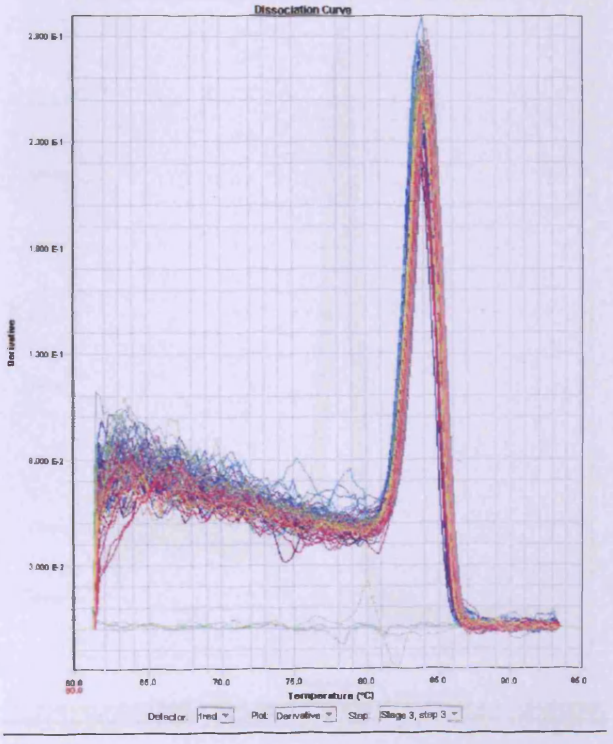

Osteoprotegerin

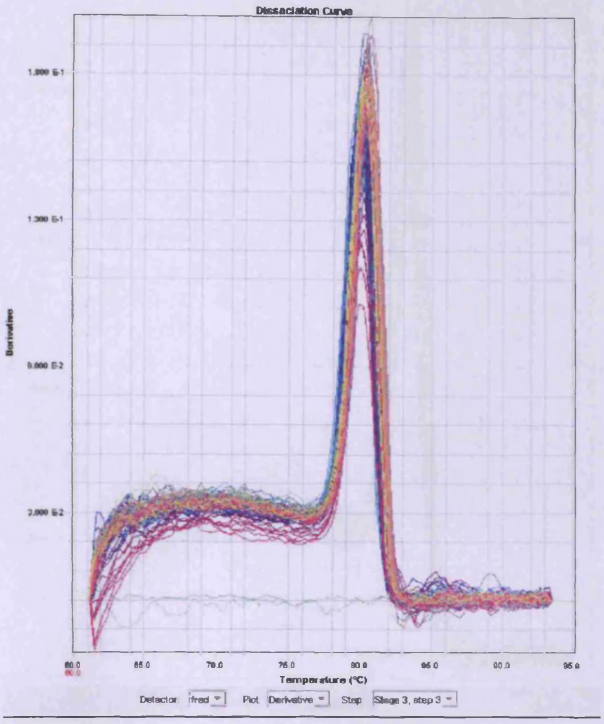

Runx2

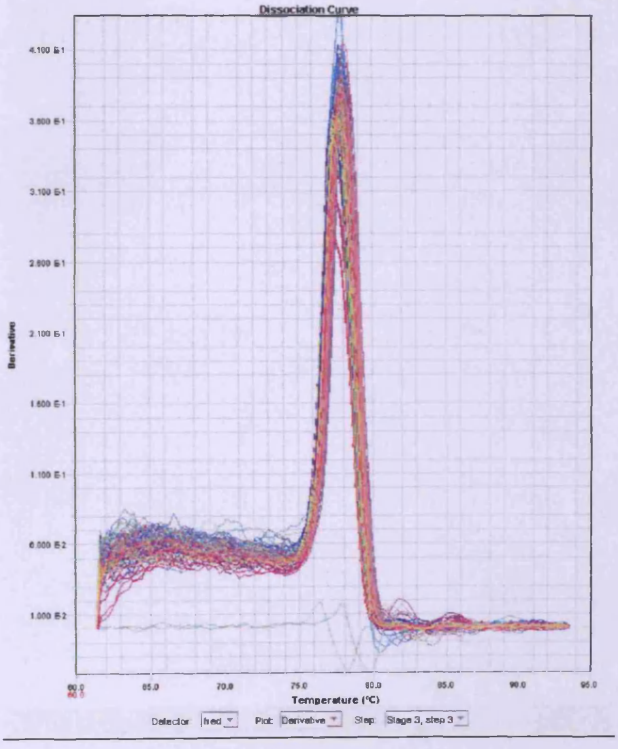

Type I collagen

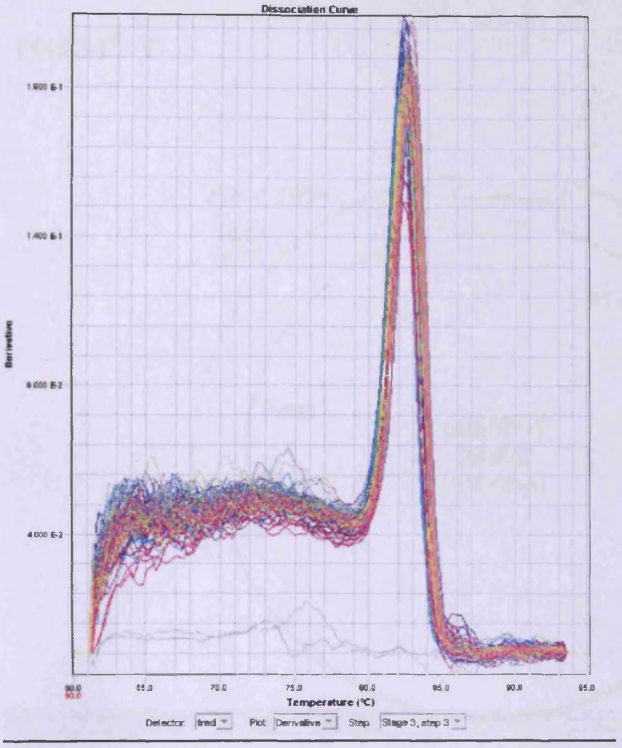

9.3 Vector maps and sequence reference points

PGEM®-T

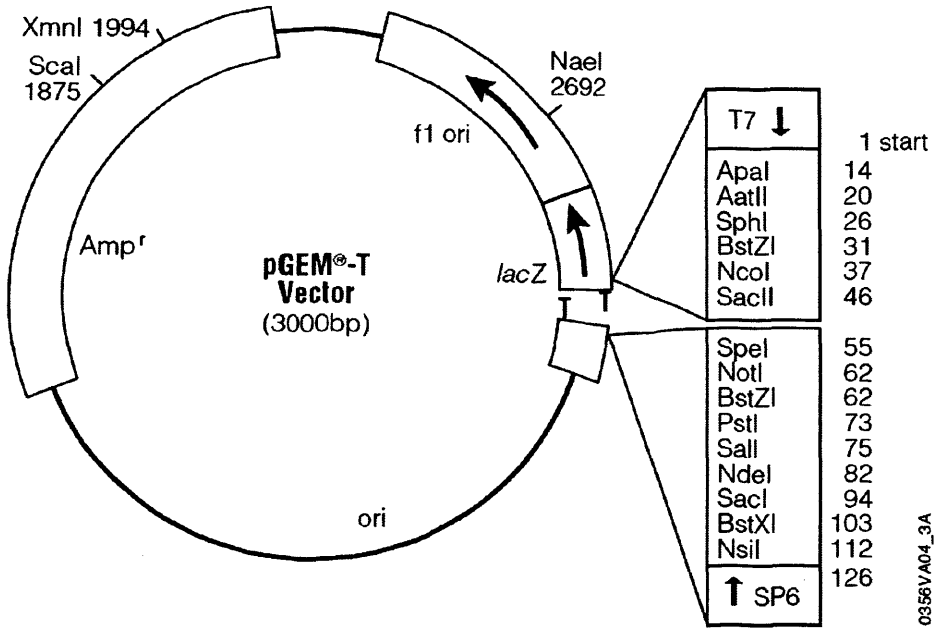

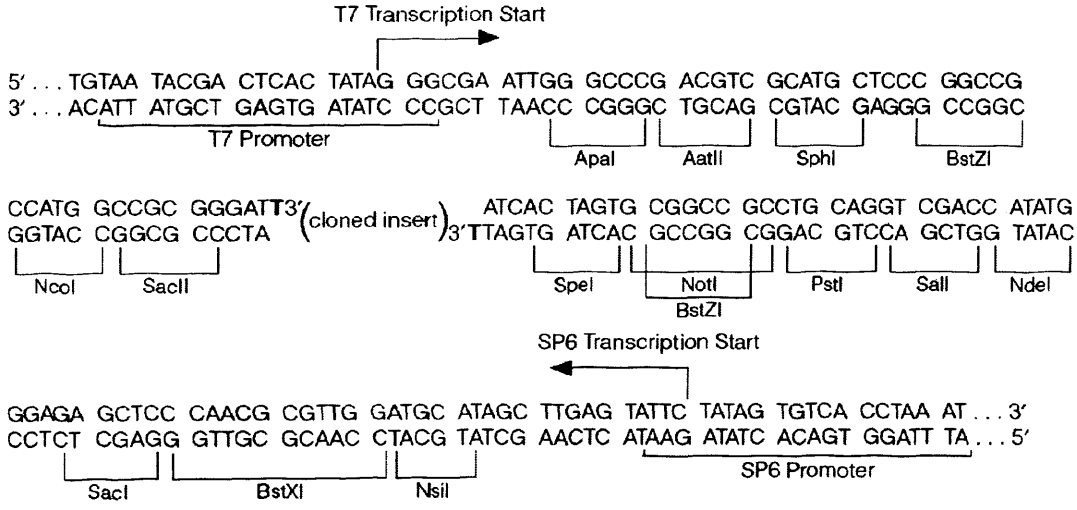

pcDNA3.1/V5-His©-TOPO®

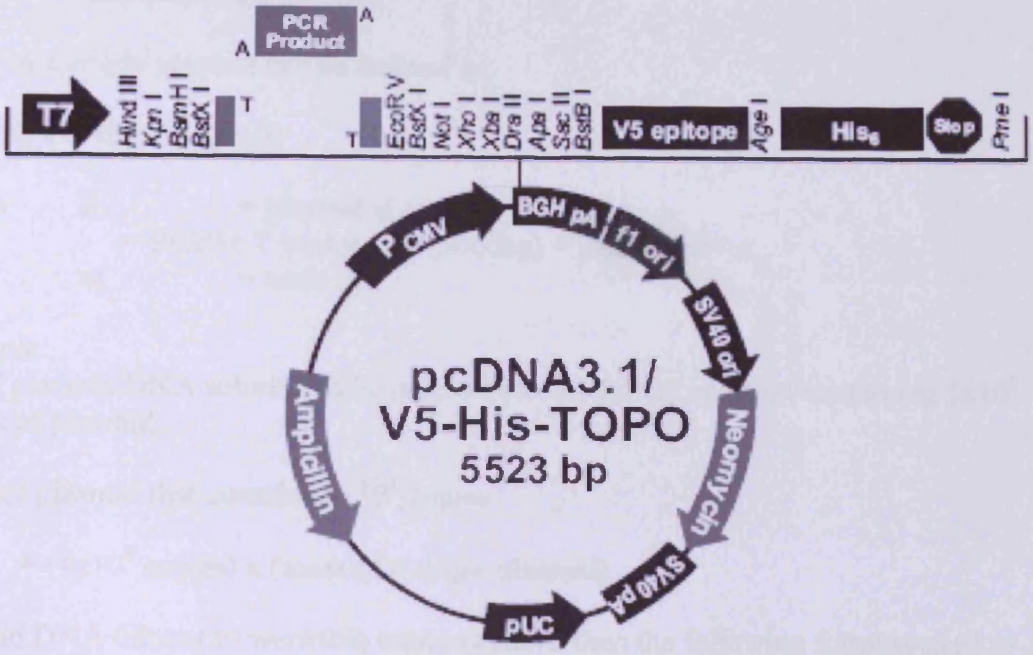

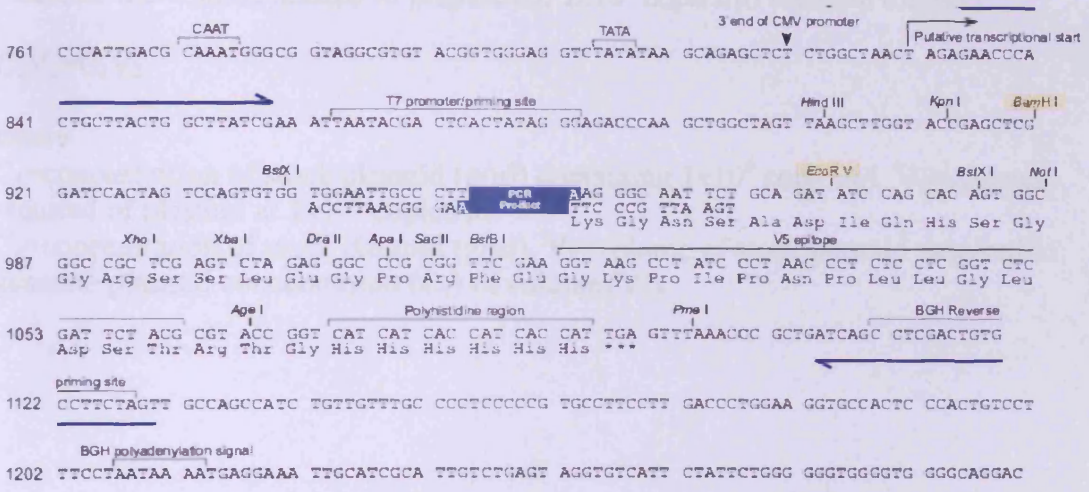

Vector primers (spanning the cloning site)

EAAT1 N- and C-terminal were cloned into pcDNA3.1 in frame with the vector V5 and His epitope tags. The nucleotide sequence of the EcoRV restriction site mutated during cloning of EAAT1 TM6-7 (loss of 2 nucleotides), taking the sequence out of frame of the V5 and His epitope tags, but having no effect on the translated sequence of the TM6-7 peptide and introducing new stop codons.

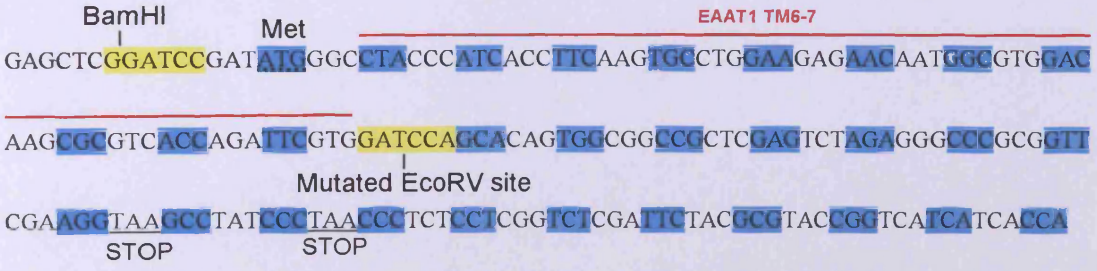

9.4 Generation of standard curves with plasmid DNA templates for absolute QRT-PCR

Mass of a single plasmid can be defined as;

$m = [n][1.096x10^{-21}(g/bp)]$

where n = plasmid size (bp)
= PGEM-T vector size (3000bp) + insert size.
m = mass (g)

Example:
1µl of plasmid DNA solution to be pipetted into each PCR reaction containing $1x10^8$ copies of plasmid.

Mass of plasmid that contains $1x10^8$ copies

= ($1x10^8$ copies) x (mass of a single plasmid)

Plasmid DNA diluted to workable concentrations then the following formula used to calculate the volume needed to prepare the $1x10^8$ copies/µl standard dilution.

$C_1V_1=C_2V_2$

where
C_1=concentration of stock plasmid (g/µl) containing $1x10^8$ copies/µl, V_2=volume required of plasmid at $1x10^8$ copies/µl.
C_2=concentration of stock plasmid (g/µl), V_2=volume of stock plasmid required to generate plasmid concentration (C_1) of volume (V_1).

9.5 Calculation of alkaline phosphatase activity

$$\text{Enzyme activity (nmoles/min/cell)} = \frac{V(\mu l) \times OD_{405nm}\ (cm^{-1}) \times 1000}{\varepsilon \times \text{incubation time (min)} \times \text{cell number (LDH } OD_{492nm})}$$

where ε is the molar extinction coefficient ($M^{-1}.cm^{-1}$) which for pNPP is 1.78×10^4 $M^{-1}.cm^{-1}$. OD_{405nm} (cm^{-1}) is the absorbance at 405nm divided by the light-path length (cm). V is the final assay volume, i.e. 225µl for a 96-well assay. OD_{492nm} is the absorbance of that sample at 492nm following incubation with components of Cytotox96 (Promega) to assay for cell number (normalised for sample volume across assays).

9.6 Time-course for glutamate uptake in SaOS-2 cells and primary human osteoblasts (NHOB2P9)

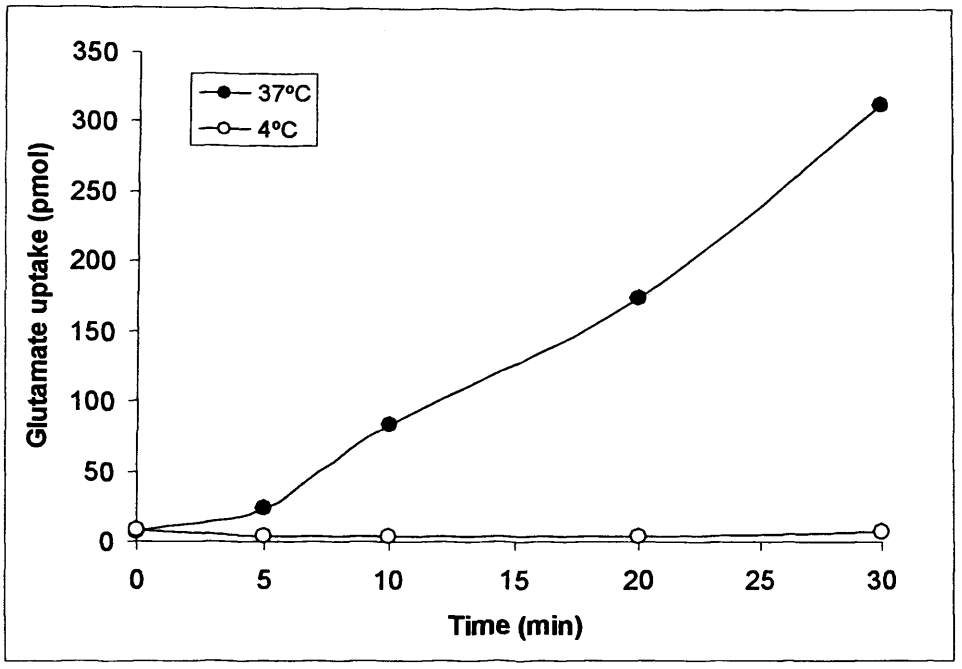

^{14}-C glutamate accumulation in SaOS-2 osteoblasts over time. Osteoblasts were incubated with 10μM mix of radiolabelled and unlabelled glutamate at 4 or 37°C for different periods of up to 30 min in KRH buffer, followed by aspiration of buffer and subsequent rinsing with buffer containing unlabeled glutamate at 1.5 mM. Values represent uptake (in pmol) from single wells at 37°C and 4°C.

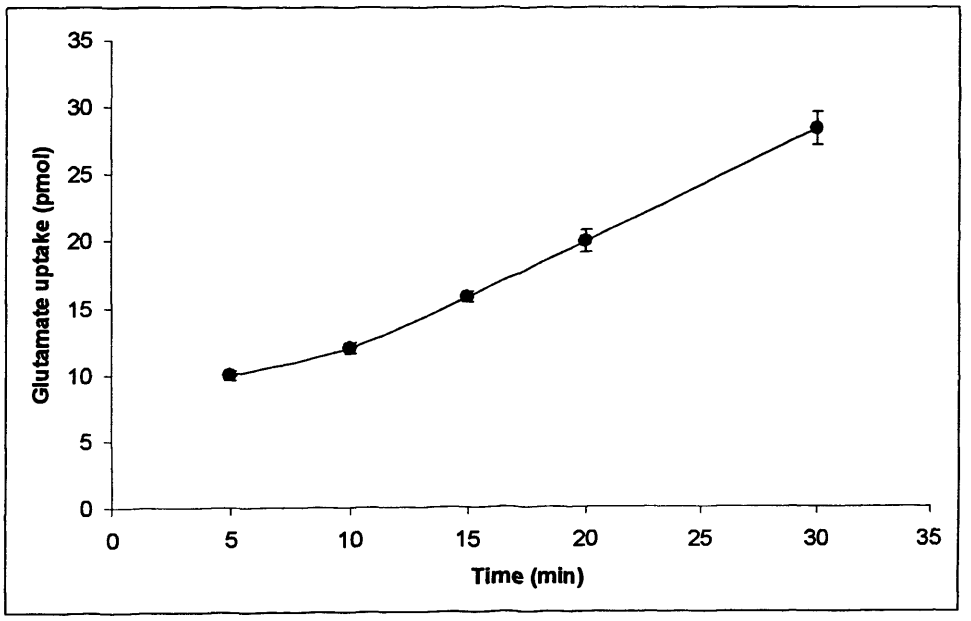

^{14}-C glutamate accumulation in primary human osteoblasts (NHOB2P9) over time. Osteoblasts were incubated with 10μM mix of radiolabelled and unlabelled glutamate at 37°C for different periods of up to 30 min in KRH buffer, followed by aspiration of buffer and subsequent rinsing with buffer containing unlabeled glutamate at 1.5 mM. Values represent uptake (in pmol) from 4 replicate wells at 37°C ± S.E.M.

9.7 Standard curve of alizarin red S dissolved in 5% perchloric acid

Absorbance was measured at 450nm

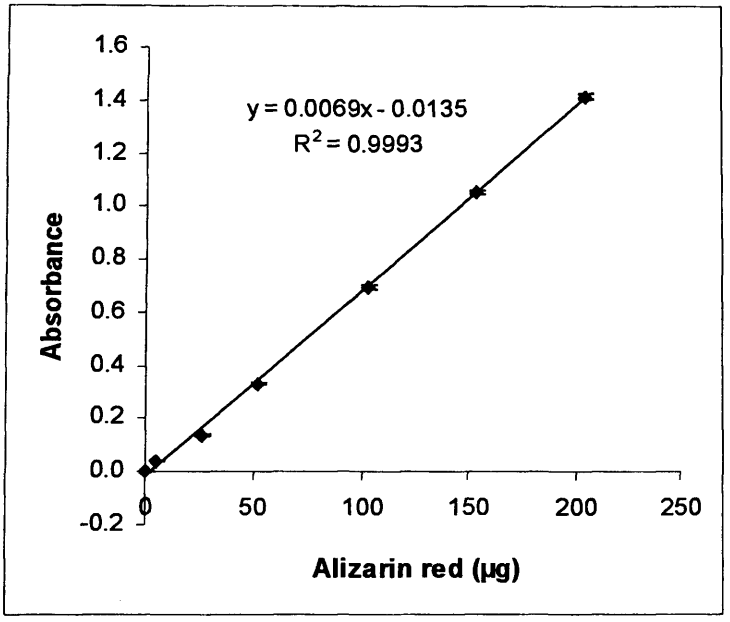

9.8 EAAT1 topology and amino acid sequence with the coding sequences for the amino acids cloned into pcDNA3.1/V5-His©-TOPO® underlined

The boxes above the sequence correspond to the transmembrane domains.

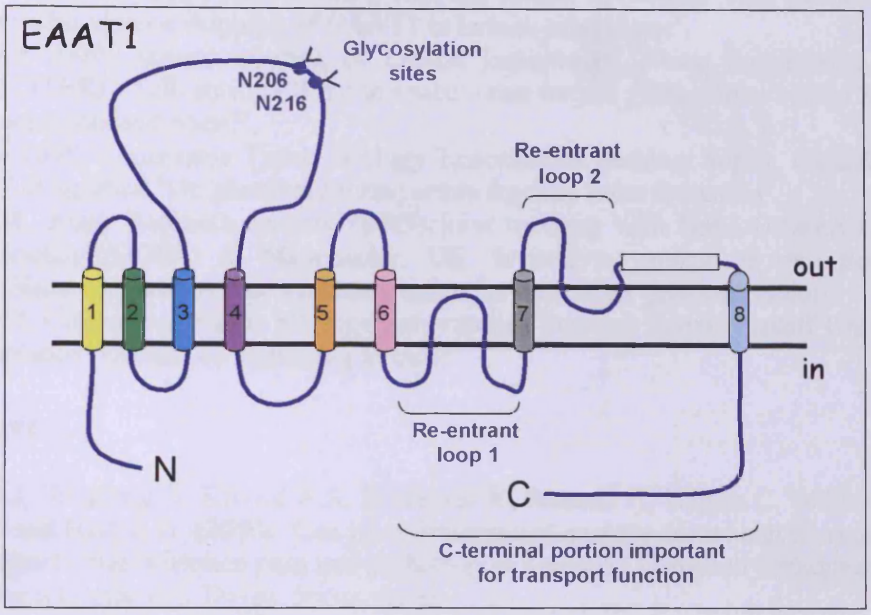


```
 1 MTKSNGEEPKMGGRMERFQQGVRKRTLLAKKKVQNITKEDVKSYLFRNAFVLLTVTAVIV

61 GTILGFTLRPYRMSYREVKYFSFPGELLMRMLQMLVLPLIISSLVTGMAALDSKASGKMG

121 MRAVVYYMTTTIIAVVIGIIIVIIIHPGKGTKENMHREGKIVRVTAADAFLDLIRNMFPP

181 NLVEACFKQFKTNYEKRSFKVPIQANETLVGAVINNVSEAMETLTRITEELVPVPGSVNG

241 VNALGLVVFSMCFGFVIGNMKEQGQALREFFDSLNEAIMRLVAVIMWYAPVGILFLIAGK

301 IVEMEDMGVIGGQLAMYTVTVIVGLLIHAVIVLPLLYFLVTRKNPWVFIGGLLQALITAL

361 GTSSSSATLPITFKCLEENNGVDKRVTRFVLPVGATINMDGTALYEALAAIFIAQVNNFE

421 LNFGQIITISITATAASIGAAGIPQAGLVTMVIVLTSVGLPTDDITLIIAVDWFLDRLRT

481 TTNVLGDSLGAGIVEHLSRHELKNRDVEMGNSVIEENEMKKPYQLIAQDNETEKPIDSET

541 KM
```

ORAL PRESENTATIONS

Speaker

July 2010, British Orthopaedic Research Society (BORS) annual meeting in Cardiff, UK. Invited to present a talk entitled 'Glutamate transporters: a new anabolic therapy in bone?'.

April 2010, RNA Cardiff joint meeting with the Bristol RNA club. Talk entitled 'Antisense-mediated exon skipping of EAAT1 in human osteoblasts'.

September 2009, Annual meeting of Cardiff Institute of Tissue Engineering and Repair (CITER). Talk entitled 'Lost in space – can we use glutamate to rescue mechanically compromised bone?'.

February 2009, Connective Tissue Biology Laboratories Seminar Series, Cardiff University. Talk entitled 'Do glutamate transporters regulate bone formation'.

June 2008, Bone Research Society (BRS) joint meeting with Bone Orthopaedic Research Society (BORS) in Manchester, UK. Invited to present an oral poster entitled 'Glutamate transporter inhibitors influence osteoblast gene expression'.

April 2008, Connective Tissue Biology Laboratories Seminar Series, Cardiff University. Talk entitled 'Glutamate signalling in bone'.

Co-author

Mason D.J, Whatling G, Kotwal R.S, Brakspear K, Roberts H, Wilson C, Williams R, Sultan J and Holt C.A. (2010). Can joint realignment surgery reveal mechanically regulated signals that influence pain and pathology in humans? European Orthopaedic Research Society meeting, Davos, Switzerland.

Mason D.J, Brakspear K, Wilson C, Williams R and Kotwal R. (2009). Expression of glutamate receptors and transporters in human subchondral bone in osteoarthritis. British Association of Knee Surgeons Annual Meeting, Edinburgh, UK. J Bone Joint Surg Br Proceedings; 92-B: 411.

Kotwal R.S, Brakspear K, Wilson C, Williams R and Mason D.J. (2009). Expression of glutamate receptors and transporters in human meniscus: correlation with anatomical locations, pain or pathology. British Association of Knee Surgeons Annual Meeting, Edinburgh, UK. J Bone Joint Surg Br Proceedings; 92-B: 411.

BOOK CHAPTERS

Mason D, Dillingham C, Evans B, Brakspear K, Jaen K and Ralphs J. (2009) Interactions between osteocytes and osteoblasts in a novel 3D co-culture system. 'Bio reconstruction de l'os a la peau' Group d'etude Os Sain et Pathologique Remodelage et Regeneration, University de Franche Comte. Published by Sauramps Medical, p35-40.

CONFERENCE ABSTRACTS AND POSTERS

Brakspear K, Parsons P and Mason D.J. (2010) Glutamate transporters: a new anabolic therapy in bone? British Orthopaedic Research Society (BORS) annual meeting in Cardiff, UK.

Kotwal, R.S., Brakspear, K., Roberts, H., Wilson, C., Williams, R., Sultan, J. and Mason, D.J. (2010) Is glutamatergic signalling mechanically–regulated in human subchondral bone? British Orthopaedic Research Society (BORS) annual meeting, Cardiff, UK.

Mason D, Brakspear K, Wilson C, Williams R and Kotwal R. (2010) Glutamatergic signals in human arthritis: A link between mechanical, nociceptive and pathological processes. *Bone.* (46):S76-76.

Mason D.J., Whatling G, Kotwal R.S., Brakspear K, Roberts H, Wilson C, Williams R, Sultan J and Holt C.A. (2010) Can joint realignment surgery reveal mechanically regulated signals that influence pain and pathology in humans? International conference on Orthopaedic Biomechanics, Clinical Applications and Surgery (OBCAS), London, UK. *Journal of Biomechanics*, 43(S1), S51(S-54).

Mason D.J., Brakspear K, Wilson C, Williams R and Kotwal R.S. (2010) Glutamate, a signal that links mechanical loading, pain and pathology in human arthritis. Proceedings of the 9th International Conference on Computer Methods in Biomechanics and Biomedical Engineering, Porto, Portugal.

Holt C.A., Brakspear K, Roberts H, Whatling G.M., Kotwal R.S., Wilson C, Williams R, Sultan J and Mason D.J. (2010) Correlating biomechanics and biological indicators of pathology for subjects undergoing High Tibial Osteotomy. International Union of Theoretical and Applied Mechanics (IUTAM) meeting, Belgium.

Mason D.J., Brakspear K, Wilson C, Williams R and Kotwal R.S. (2009) Glutamatergic signalling in the osteoarthritic knee. *Int. J. Exp. Pathol.* (91)2:A34-35

Brakspear K, Parsons P and Mason D.J. (2009). The role of glutamate transporters in osteoblast proliferation and activity. 2nd Joint Meeting of the Bone Research Society (BRS)/British Society for Matrix Biology, London, UK.

Mason D.J., Dillingham C.M., Evans B.A., Brakspear K, Jaen K and Ralphs J.R. (2009) Interactions between osteocytes and osteoblasts in a novel 3D co-culture system. ASBMR annual meeting, Denver, US. *J Bone Miner Res* 24 (Suppl 1).

Brakspear K, Parsons P and Mason D.J. (2009). Glutamate transporters function in osteoblasts to influence proliferation and activity. ASBMR annual meeting, Denver, US. *J Bone Miner Res* 24 (Suppl 1).

Kotwal R.S., Brakspear K, Wilson C, Williams R and Mason D.J. (2009) Expression of glutamate transporters in human meniscus: Correlation with anatomical location, pain or pathology. ORS Annual Meeting, Las Vegas, US.

Mason D.J., Brakspear K, Wilson C, Williams R and Kotwal R.S. (2009) Expression of glutamate receptors and transporters in human subchondral bone in osteoarthritis. ORS Annual Meeting, Las Vegas, US.

Mason D.J., Brakspear K, Wilson C, Williams R and Kotwal R.S. (2009) Expression of glutamate receptors and transporters in human subchondral bone in osteoarthritis. Knee Society Members Meeting, Boston, US.

Mason D.J., Dillingham C.M., Evans B.A., Brakspear K, Jaen K and Ralphs J.R. (2008) Interactions between osteocytes and osteoblasts in a novel 3D co-culture system. *Int. J. Exp. Pathol.* (90)2:A104-104

Brakspear K, Parsons P and Mason D.J. (2008). Glutamate Transporter inhibitors influence osteoblast gene expression and activity. *Int. J. Exp. Pathol.* (90)2:A107-108

Brakspear K, Parsons P and Mason D.J. (2008). Glutamate transporter inhibitors influence osteoblast gene expression. *Calcified Tissues Int.* (83)1:p1-33.

Mason D.J., Dillingham C.M., Evans B.A., Brakspear K and Ralphs J.R. (2008) A 3D culture system to investigate osteocyte control of osteoblasts. *Bone.* (42)S26-27.

PRIZES

September 2010, Annual meeting of Cardiff Institute of Tissue Engineering and Repair (CITER) and Arthritis Research UK Biomechanics and Bioengineering Centre in Gloucestershire, UK. Best poster: 'Glutamate transporters function in osteoblasts to influence proliferation and activity'

May 2009 and February 2008, Cardiff University School of Biosciences PhD Poster evening winner

April 2009, Cardiff University Speaking of Science Conference 2nd Prize. Title: 'Lost in Space – can we use glutamate to rescue mechanically compromised bone?'

June 2008, Bone Research Society (BRS) joint meeting with Bone Orthopaedic Research Society (BORS) in Manchester, UK. Best Oral poster presentation: 'Glutamate transporter inhibitors influence osteoblast gene expression'